IAEA-199

ATOMIC AND MOLECULAR DATA FOR FUSION

PROCEEDINGS OF AN ADVISORY GROUP MEETING
ON ATOMIC AND MOLECULAR DATA FOR FUSION
ORGANIZED BY THE
INTERNATIONAL ATOMIC ENERGY AGENCY
HELD AT THE UKAEA CULHAM LABORATORY
ABINGDON, UK, 1–5 NOVEMBER 1976

A TECHNICAL DOCUMENT ISSUED BY THE
INTERNATIONAL ATOMIC ENERGY AGENCY, VIENNA, 1977

ATOMIC AND MOLECULAR DATA FOR FUSION, IAEA, VIENNA, 1977

Printed by the IAEA in Austria
June 1977

PLEASE BE AWARE THAT
ALL OF THE MISSING PAGES IN THIS DOCUMENT
WERE ORIGINALLY BLANK

The IAEA does not maintain stocks of reports in this series. However, microfiche copies of these reports can be obtained from

INIS Microfiche Clearinghouse
International Atomic Energy Agency
Kärntner Ring 11
P.O. Box 590
A-1011 Vienna, Austria

on prepayment of US $0.65 or against one IAEA microfiche service coupon.

Foreword

The Advisory Group Meeting on Atomic and Molecular Data for Fusion was convened by the IAEA Nuclear Data Section at the UKAEA Culham Laboratory, UK, from 1-5 November 1976. This first international meeting on this topic was attended by 88 scientists, representing both the technical fusion and the academic atomic physics communities, from 18 countries and 2 international organizations.

Twenty one papers describing atomic and molecular data needs in fusion research and technology, and outlining national programmes and emphasis in this field were presented. Three comprehensive working group reports identifying requirements and availability of atomic collision data, atomic structure data, and surface interaction data in fusion research were produced by the participants.

The meeting recognized that the needs for atomic and molecular data for the development of fusion research and technology are so large that any one Member State cannot adequately fulfil these needs for the whole world. Thus, not only was it deemed necessary to coordinate the collection of the requirements and the acquisition of the required data on atomic and molecular processes, but also to create a network of data centres for the dissemination of these data to the fusion community. The meeting recommended the formation of an international network of data centres for the compilation and dissemination of atomic and molecular data required for fusion, and recommended that the IAEA Nuclear Data Section be given the responsibility to establish and coordinate this network.

Table of Contents

Session B: National Programmes and Emphasis

I. Meeting Summary

Experience with present-day fusion devices has shown a critical need for numerical data for the detailed understanding of the physical processes which occur in these devices. As the fusion research programs progress toward the design and construction of larger experimental devices, serving as prototype facilities for full-scale fusion reactors, the data requirements will become more severe as other physical processes become important and the required level of understanding becomes more advanced.

This meeting on atomic and molecular (A+M) data for fusion, convened by the IAEA and organized by the Nuclear Data Section, was the first international meeting on this topic. It was attended by 88 scientists, representing both the technical fusion and the academic atomic physics communities, from 18 countries and 2 international organizations. The opening address of the meeting was given by Sir Harry Massey.

The goals of the meeting were to identify specific data requirements, review the national programs, and agree on an international cooperative effort to compile and disseminate atomic and molecular data needed in fusion research and technology. The objectives achieved by this meeting were:

- to bring together experts in the field of fusion research knowledgeable in the requirements and availability of A+M data;
- to list specific A+M data needs, their accuracies and priorities;
- to identify the existence and availability of evaluated and compiled A+M data and compare them with the requirements;
- to identify and discuss measurements, calculations, and compilations required to satisfy the current and near term A+M data needs of fusion research; and
- to formulate specific recommendations on the IAEA programme and international cooperation in this field, and on the coordination of future activities.

To meet these objectives the meeting was organized around two sets of invited review papers covering the status of A+M data, their accuracies and priorities on one hand (Session A) and the national programmes and emphasis on the other (Session B) (Appendix I). The reviews which in themselves are timely technical reports, provided the basis for discussions and preparation of the conclusions and recommendations. The Agenda of the meeting is given in Appendix II, and the list of participants in Appendix III.

Following the presentation and discussion of the review and contributed papers in sessions A and B, which took the first two days of the meeting, four working groups met separately on the third and fourth days of the meeting to focus on three atomic and molecular data areas of importance to fusion research and technology, and on international cooperation in this field.

The four working groups

- on international cooperation,
- on atomic collision data,
- on atomic structure data, and
- on surface interaction data

formulated their conclusions and recommendations in the form of working group reports which were discussed in plenary session on the last day of the meeting. These reports are reproduced in their entirety in this summary report of the meeting.

In view of the significance of the overall objectives, achievements and recommendations of this meeting, and because of the interest of the review papers presented at this meeting to the fusion, atomic and astrophysics communities, the meeting strongly recommended that in addition to their dissemination through the IAEA report series, the proceedings of this meeting be published in one of the recognized physics journals having a wide circulation, e.g. Nuclear Fusion or Physics Reports.

REPORT OF THE WORKING GROUP ON INTERNATIONAL COOPERATION

Working Group Members

Arcipiani, Dr. B.
Barnett, Dr. C.F.
Decker, Dr. J.
Delcroix, Prof. J.L.
Ebel, Dr. G.
Hampel, Mr. V.
Harrison, Dr. M.F.A. (Chairman)
Johnston, Dr. P.
Lorenz, Mr. A.
Schmidt, Dr. J.J.
Suzuki, Prof. H.

Introduction

As outlined in the reports of the technical working groups, the needs for atomic and molecular data for the development of fusion research and technology are so large that it will be very difficult and costly for any one community to respond to these needs on a world-wide scale.

Thus, not only will it be necessary to coordinate the collection of the requirements and the acquisition of the required information on atomic and molecular data which are presently dispersed in the literature, but also to create a network for the dissemination of these data to the fusion community.

A. General Recommendations

A.1 Establishment of an A+M data centre network coordinated by the IAEA/NDS

The meeting supported the working group recommendation to form an international network of A+M data centres which will compile and disseminate bibliographic and numerical atomic and molecular data required for fusion. The cooperation between these centres should be coordinated by the new atomic and molecular data unit of the IAEA Nuclear Data Section. The centres which will initially form part of this network are listed in Appendix A. The objectives of the centres' cooperative activity should be to set up common operational procedures for the world-wide compilation, evaluation, exchange and dissemination of bibliographic and numerical A+M data required by the fusion community.

Member States participating in the activities of this network are urged to support the national data centres and to provide for the services of scientists to help compile A+M data and forward them to their respective

centre. Those Member States which do not have a national centre, are encouraged to provide similar support and forward their data to the international network through the nearest cooperating centre.

A.2 Formation of a network of Liaison Officers

In order to provide an efficient channel of communication between the various data producing and data using research groups, it is recommended that the IAEA form a network of liaison officers in all Member States concerned, so as to provide a link for the exchange of information between national centres, the IAEA/NDS and the research laboratories as well as for the coordination of experimental and theoretical research aimed at the determination of A+M data for fusion in different countries. These liaison officers should be key people in key national establishments or data centers conversant with the data requirements of fusion, and also be experienced in at least one of the basic A+M data fields.

Generally, it will be their responsibility to ensure that their national fusion establishments and universities coordinate their A+M activities effectively with the data centre network. Specifically, it will be their responsibility among others, to provide to the IAEA as well as to their national data centres pre-published new data and to identify data needs for inclusion in a bulletin to be published periodically by the IAEA (see Recommendation B.2.3 below).

A.3 Promotion of interaction between the technical fusion and academic physics communities

Recognizing on the one hand that many of the required data are unavailable, and on the other hand that numerous atomic physics groups in universities and laboratories all over the world have the capability to measure or calculate the required data, the meeting strongly recommends to the IAEA that it foster the interaction between the fusion, atomic physics and astrophysics communities in order to encourage the determination of A+M data for fusion.

B. Recommendations to the IAEA/NDS

B.1 General Objectives of the IAEA/NDS

In addition to the general tasks of establishing and coordinating the network of A+M data centres, the meeting recommended that IAEA/NDS give priority to the following objectives:

B.1.1 To compile and publish international computerized indexes to the literature on atomic and molecular collision, structure, and surface interaction data pertinent to fusion research;

B.1.2 To compile and disseminate in a quarterly bulletin newly measured and/or calculated A+M data and associated information;

B.1.3 To devise common formats for the compilation and exchange of bibliographic and numerical A+M data among the centre network; and

B.1.4 To develop standardized computer input and output formats for the systematic compilation and the dissemination of bibliographic and numerical A+M data.

B.2 Specific short-range tasks of the IAEA/NDS

B.2.1 Creation of an international bibliographic index for atomic collision data.

IAEA/NDS should coordinate the creation of an international computerized index of references to A+M collision data, with the assistance and input from the A+M data centre network, and the laboratories engaged in fusion research, and publish it by the end of 1978. This index should be patterned after the CINDA* index and should incorporate the techniques already developed by the IAEA/NDS and by the A+M data centres, and incorporate all existing compilations of A+M collision data references (see Appendix B), in particular the comprehensive bibliography compiled by the US/ORNL Controlled Fusion Atomic Data Center which covers the open literature for the period 1950-1976.

B.2.2 Consideration of Surface Interaction Data

Surface interaction problems play an important role in the development of fusion technology and there is a great need for the relevant data on surface interactions. The awareness of such data can be provided by a bibliographical index to the literature on surface interaction data as a first step and then finally by compilations and evaluations of the data themselves.

---

* CINDA is a computerized index to the literature on microscopic neutron data published by the IAEA on behalf of the neutron nuclear data centres' network.

It is therefore recommended that:

B.2.2.1 A bibliographical index be established covering the world-wide literature on surface interactions from which references to specific surface interaction data could be retrieved. In developing this bibliography the IAEA should make use of bibliographies compiled by existing centres, i.e. the Surface and Vacuum Physics Index in the Federal Republic of Germany, the bibliography on surface studies compiled for the T-20 design in the USSR, and the bibliographic data on surface interaction compiled by the Controlled Fusion Atomic Data Center at the Oak Ridge National Laboratory.

B.2.2.2 IAEA sponsor work on numerical data compilations and evaluations in those fields of surface interactions where such data are especially needed.

B.2.3 Publication of an International Bulletin on new A+M Measurements

During the conceptual design of plasma experiments and prototype reactors, a need often exists for atomic and molecular cross section data to aid in the adjusting and maximising of the various physical parameters. In addition, the interpretation of many diagnostic measurements depend on transition probabilities, photon wave-length identification, reaction rates, etc. Throughout the world, atomic scientists are actively engaged in the measurement and computation of atomic data directly related to fusion research. A crucial problem arises in transferring or communicating the current experimental or theoretical results to the international plasma physics community without costly delays. Usually 12-18 months elapse between the completion of an investigation and the publication of the results in a report or in the open literature.

To alleviate this problem it is recommended that IAEA/NDS compile, publish and distribute a quarterly bulletin on newly measured or calculated fusion-related A+M data. The bulletin would be compiled from input provided through the A+M Liaison Officers' network or directly from investigators in the Member States concerned. The bulletin should be patterned after the US "Atomic Data for Fusion" newsletter circulated by the ORNL Controlled Fusion Data Center and the US National Bureau of Standards, whose distribution is principally limited to the US laboratories. In addition, fusion workers are encouraged to communicate to the IAEA/NDS their current data needs which would be included in the quarterly bulletin. It is recommended that this bulletin be established immediately after IAEA/NDS obtains the required staff.

B.2.4 International A+M Data Meetings

B.2.4.1 The IAEA/NDS should convene Consultants' Meetings of representatives of A+M data centres participating in the international cooperation; the first such meeting should take place in 1977. The development of compilation and exchange formats for the international collaboration between the existing centres should be discussed at that meeting. This meeting should also stimulate the short-term efforts recommended by the first Advisory Group Meeting.

B.2.4.2 A second Advisory Group Meeting on Atomic and Molecular Data for Fusion should be held in 1978, to review the status of national and international activities, to identify new needs for atomic and molecular data and to recommend programmes for future work.

Appendix A

MEMBERS OF THE A+M DATA CENTRE NETWORK

Centre Code	Address	Head of Project or Centre
FR/Orsay	Laboratoire Physique des Plasmas Faculte des Sciences d'Orsay Batiment 212 F-91400 Orsay	Prof. J.L. Delcroix
FRG/ZAED	Zentralstelle fuer Atomkernenergie-Dokumentation Kernforschungszentrum D-7514 Eggenstein-Leopoldshafen	Dr. G. Ebel
FRG/Garching	Surface Physics Division Max Planck Institute for Plasma Physics D-8046 Garching bei Muenchen	Dr. H. Vernickel
IAEA/NDS	Nuclear Data Section International Atomic Energy Agency P.O. Box 590 A-1011 Vienna	Dr. J.J. Schmidt
JAP/Nagoya	Atomic Data Study Group Institute for Plasma Physics Nagoya University Nagoya 464, Japan	Prof. H. Suzuki
JAP/JAERI-A+M	Division of Physics Japan Atomic Energy Research Institute Tokai-Mura, Naka-gun Ibaraki-ken 319-11, Japan	Dr. T. Fuketa
UK/Belfast	Computer Centre Queens University Belfast, B17 1NN Northern Ireland, UK	Dr. F.J. Smith
US/NBS-AT	Data Centers on Atomic Transition Probabilities and Atomic Line Shapes and Shifts Optical Physics Division National Bureau of Standards Washington, D.C. 20234, USA	Dr. W.L. Wiese

Appendix A

Centre Code	Address	Head of Project or Centre
US/NBS-EL	Atomic Energy Levels Data Center Optical Physics Division National Bureau of Standards Washington, D.C. 20234, USA	Dr. W.C. Martin, Jr.
US/NBS-JILA	Atomic Collision Cross Section Information Center Joint Institute for Laboratory Astrophysics University of Colorado Boulder, Col. 80302, USA	Dr. E.C. Beaty
US/ORNL-CTR	Controlled Fusion Atomic Data Center Oak Ridge National Laboratory P.O. Box Y Oak Ridge, Tennessee 37830, USA	Dr. C.F. Barnett
USSR/Kurchatov	Institut Atomnoi Energii I.V. Kurchatova 46 Ulitsa Kurchatova Moscow, D-182, USSR	Dr. Yu.V. Martynenko

Appendix B

GENERAL DESCRIPTION OF THE PROPOSED BIBLIOGRAPHIC INDEX FOR A+M COLLISION DATA

1. Scope

This index should contain references to all publications on data measurements, calculations, evaluations and reviews of reactions between atoms, molecules, ions, electrons and photons, expressed in terms of cross sections and reaction rates. Excluded from the scope would be plasma-solid interactions, except in the few cases where these phenomena give information about single binary collision. This would also exclude atomic and molecular structure data as these data would require a more sophisticated format, such as spectroscopic notation.

2. Limits of coverage

The index should cover the properties of collisions between electrons, photons, atoms and molecules (including ions) in chemical systems composed of either pure hydrogen (including D and T), or of hydrogen (and/or D, T) plus one or two other elements, such as H+Mo or H+CO. The energy domain covered by the index should not be limited, but a simple specification of the energy or energy range of the referenced data should be given as qualitative information in the index.

3. Formats

The format of the bibliographic index for A+M data which is to be established by IAEA/NDS should integrate as far as possible the formats and information of existing A+M bibliographies, namely those of Dr. C.F. Barnett (US/ORNL), Prof. J.L. Delcroix (FR/Orsay), Dr. E.C. Beaty (US/ /NBS-JILA) and Prof. K. Takayanagi (JAP/Nagoya), and take advantage of the experience gained by these groups. The experience and the methods developed at the IAEA in the development of the CINDA index on neutron reaction data should also be used, recognising, however, the greater complexity of the problem in A+M data. A semi- quantitative description of the collision process according to its initial and final states, energy range, etc. is desirable. If possible, the indexing of any one collision should fit on one line of an appropriate computer print-out format to be sorted according to a number of desirable criteria.

4. Input to the bibliographic index

The input to the bibliographic index should come from the four centres mentioned in paragraph 3, but other centres, (e.g. USSR/Kurchatov, UK/Belfast, etc.) active in compilation, should also contribute to its input. The IAEA

should encourage all the contributing centres to computerize their bibliographies using the same format, and send tapes of their files to the IAEA centre. As an initial step the Orsay centre has proposed to collaborate in a joint effort among Western European Member States.

5. Nature of the analysed documents

The index should include references to publications in regular journals, books, review reports (like NBS reports), proceedings of major conferences in the A+M data field (i.e. ICPEAC* and ICAP**), and to theses if these are readily available, but not to internal reports which would be more or less covered by the proposed bulletin (see section B.2.3 of this Working Group Report).

6. Time-lag

Currently, the time lag between publication and input into the computer file of the France/Orsay bibliographic system varies from about 2 to 12 months because of a lack of man-power (the reading and extracting of information from the literature is made by highly trained scientists who are also pursuing research in the field). It is hoped that international cooperation and help from the IAEA/NDS could reduce this time-lag in the compilation of the international bibliographic index to about three months. In this respect it is recognized that the technical A+M literature from countries such as the USSR and Japan present particular language difficulties; it is therefore recommended that the IAEA/NDS ask the pertinent authorities in these Member States to help provide input to the international A+M data bibliographic index in the accepted English language input.

7. Up-dating

In addition to the regularly published editions of the international bibliographic index, users should have direct access to the computer file which is to be maintained by the IAEA. It is also desirable that the contributing A+M data centres provide IAEA/NDS with up-dates of their own files on magnetic tape every three months. These updates could also be in the form of listings which could be obtained by users directly from the centres. The publication of a supplement to the main issue of the index by the IAEA every six months could be investigated if considered to be economical.

---

* International Conference on the Physics of Electronic and Atomic Collisions.

** International Conference on Atomic Physics.

REPORT OF THE WORKING GROUP ON ATOMIC COLLISION DATA

Working Group Members

Baluja, Dr. K.L.
Brouillard, Dr. F.
Greenland, Dr. P.T.
Hogan, Dr. J.T. (Chairman)
Hvelplund, Mr. P.
Joachain, Prof. C.J.
McDowell, Prof. M.R.C.
McWhirter, Dr. R.W.P.
Ohtani, Dr. S.
Oepik, Dr. U.
Riviere, Dr. A.C.
Summers, Dr. H.
Tweed, Dr. R.S.

Introduction

Composition of the group

This working group is an ad hoc working group that was drawn from the body of meeting participants. The ad hoc nature of our group has resulted in certain areas receiving more attention than others, both for fusion problems and for the assessment of the adequacy of A+M data.

Sources of information available to the group

The following three reports, which survey the needs for A+M data in this field, have been written in the course of the past three years:

- US report of the panel on atomic, molecular and nuclear physics in CTR entitled "Atomic, Molecular and Nuclear Data Needs for CTR", ERDA-39, dated March 29, 1974.

- US report of the "Workshop of Theoretical Aspects of Atomic Physics in Controlled Thermonuclear Research", ERDA 76/106, September 1975.

- IAEA report INDC(NDS)-72/LNA entitled "Survey of Atomic and Molecular Data Needs for Fusion", by A. Lorenz, J. Phillips, J.J. Schmidt and J.R. Lemley, dated January 1976.

Emphasis given in this report to the fusion aspects

The present report complements the coverage given in the three cited reports: it introduces new needs in the area of neutral beam injection and covers some other areas with more detail than the previous reports. The areas of fusion applications that are specifically introduced are:

trapping cross-sections for neutral hydrogenic atoms on plasma impurities, cross-sections and rate coefficients needed for the particle and energy balance in tokamak discharge initiation and termination, scrape-off plasma, and divertor layer.

Emphasis given in this report to the A+M data needs

The authors of the present report take a significantly different view of the relative priorities of specific data needs in the plasma (spectroscopic) diagnostics and impurity radiation areas; here, the rate coefficients for collisional excitation and ionization are seen as the most important needs. The reference to specific groups and specific work is done to clarify the nature of the data needs. This is not meant to exclude other groups or other work, but rather to complement the descriptions given in the reports referred to above. In our final recommendation (paragraph B8) we propose the only practical scheme for making a realistic appraisal of the resources available to attack the problems that we have identified: specialist working parties should be established to make a detailed evaluation of available data and to set priorities for further work.

Accuracy considerations

The specification of existing conditions in CTR devices is often poor. For example, the chemical composition of the neutral heating beams that actually enter the plasma has not been determined. Conditions near the plasma edge cannot be measured with precision. The corresponding specifications of data needs must thus be given in broad terms: only approximate ranges of parameter values can be given and the accuracies required in some areas cannot yet be estimated. The accuracy to be aimed at for values of excitation rate coefficients (by electron collision) might reasonably be set at $\sim \pm 20\%$ (in a few cases better accuracy can be achieved) although there are indications at this time of very large disparities, in some cases as large as a factor of four. The achievement of this accuracy ($\pm$ 20%) is probably close to that aimed at for the most sophisticated quantum-mechanical computer codes currently being developed. Similarly, experimental techniques are such that only in the most careful work is this accuracy achieved. An accuracy of about $\pm$ 10% appears to be possible for ionization rate coefficients in the region of threshold experimental methods. Theoretical methods appear to be more suspect due particularly to the difficulty of taking account of exchange for threshold collisions.

A. Fusion Needs for A+M Collision Data

1. Beam Trapping

The fusion needs here are for cross-sections for charge exchange and for impact ionization of neutral hydrogenic atoms colliding with impurity ions in the plasma. The specific ions of interest can be grouped according to their source; for example, cross sections are needed for all states of ionization of particles from:

Walls (stainless steel):	Ni, Cr, Fe
Loosely bound light elements:	C, O
Limiters, guard plates:	W,Mo

The relevant energy ranges and required accuracies are further discussed in Review A1, "Atomic and Molecular Data Needs for CTR Beam Injection" by J.T. Hogan. Further analysis of the requirements taking into account negative ion processes are included below; attention is being drawn to the need for detailed understanding of elementary charge transfer and other processes.

The data needs for neutral beam trapping were discussed in Review A1. This review and the bulk of our recommendations have dealt with processes occurring within the plasma. The report INDC(NDS)-72/LNA by Lorenz et al. contains a thorough description of data needs for the neutral beam ion sources, extraction and acceleration systems, and for beam neutralization. We reproduce this information for completeness as Appendix A.

2. Needs for Plasma "Scrape-off" Data

There was no review dedicated to this subject, which covers three distinct areas: the plasma-wall interface in conventional tokamaks with material limiters, the initiation and termination phases of the tokamak discharge, and the processes which figure in the performance of divertor-tokamaks, such as DITE. This is in fact a newly developing field in fusion, although it requires data that were important to the stellerator work of ten years ago. An exhaustive specification of data needs in this area was not attempted, but rather some suggestions were made to increase the interaction among A+M physicists and those in the fusion area. The needs in this area will be strongly influenced by results of work on such surface-related processes as desorption (see the report of the Working Group on Surface Interactions).

Data on electron collisions with atoms, ions, and molecules, for atom-atom collisions and for recombination for both hydrogenic species and impurities are most urgently required for the calculation of the particle and energy balance. The conditions prevailing in the edge region of CTR devices can be characterized only approximately: the temperature is less than 50 eV, and the electron densities in the range of 10^{12}-10^{13} cm^{-3} have been measured in the near-limiter region of conventional tokamaks. The DITE divertor-tokamak is presently measuring changes effected by operation with a magnetic limiter. Conditions in the edge region in future devices are likely to involve higher temperatures and densities. Specific needs are considered in the listed Recommendations.

3. Plasma Impurities and Cooling

This working group considered some of the collisional processes needed for considerations of plasma impurities and cooling on the basis of the Review Paper A4, "Plasma Impurities and Cooling" by H.W. Drawin.

3.1 The data considered in this section are needed for a number of different purposes: the calculation of power loss due to radiation, the determination of impurity concentration, the electron temperature and density, and the ratios of radiation line intensities.

3.1.1 The calculation of the power loss due to radiation by impurity ions. This arises from three distinct processes, viz. line radiation, recombination radiation and bremsstrahlung. Of these, line radiation is by far the largest, especially in the phase of dynamic ionization before the steady-state is reached. The power must be summed over all the lines emitted by the ion, but fortunately only a small number contribute the great majority of the power and the rest can be taken account of by less accurate methods. The calculation of the total power loss requires a large number of different atomic coefficients. Of those that limit the accuracy of this calculation, they are, in the order of their importance:

- Collisional excitation rate coefficients from ground and metastable levels.
- Collisional ionization rate coefficients from ground and metastable levels.
- Recombination rate coefficients.

3.1.2 The determination of impurity concentration and the effective Z of the plasma from spectroscopic intensity measurements. This requires much the same data as for 3.1.1 above, but for a restricted set of lines. There is the same need to take account of metastable populations and state of ionization. Data on the excitation rate coefficients is the most important.

3.1.3 The determination of the electron temperature from the intensity ratio of suitable line pairs. Although largely superseded by laser scattering this method of estimating the electron temperature may offer advantages where, for example, it is important to check on departures from Maxwellian velocity distribution. The method depends on having good knowledge of the excitation rate coefficients for the chosen lines. Lithium-like and sodium-like lines are particularly suitable although only for the former has the method been developed in practice.

3.1.4 The determination of electron density from intensity ratios of suitable line pairs. Some ions such as Be-like ions have metastable levels with suitable radiative lifetimes to render certain line ratios sensitive to the ambient electron density. Such methods have been shown in principle to work, but have not been entirely successful in practice through lack of sufficiently accurate atomic data. Excitation rate coefficients, in particular for Be-like ions, are needed.

3.1.5 The ratios of the intensities of the satellite lines of resonance lines, particularly of He-like ions, provide valuable diagnostic possibilities for electron temperature and density. These satellites arise partly through dielectronic recombination and partly through inner shell excitation. Detailed rate coefficients for both processes are required.

3.2 The particular ions for which data are required cover a very wide range of elements and ionic charge. The need, therefore, is to make a selection on the basis of priorities, taking account firstly of the immediate straightforward needs of fusion, but also the limitations of present methods of evaluating this data so that a programme can be developed to improve its reliability. At the present time many of the most important quantities (such as the radiated power loss) can only be calculated with an accuracy amounting to a factor four or five. In the long term this is not

acceptable and there is therefore a need to improve the theoretical methods. The only satisfactory way of doing this is to develop a joint theoretical/experimental programme where new theories can be tested in the laboratory at various stages of its development. Such tests require, among other methods, spectroscopic measurements on low density plasmas such as those used in fusion research. Thus the cooperation of the fusion physics community is required in solving the problems in atomic physics. One way in which this could be attempted would be to make available a machine capable of producing low density, high temperature plasma (such as a tokamak) for spectroscopic studies. In such cooperative studies it would be essential to start by trying to understand the relatively simpler atomic systems (ions having few - less than five or six - orbital electrons). Detailed excitation studies of complex ions at this stage would certainly be counter-productive. (This is not to deny the need for spectral line classification of the lines of such ions - see report by the Working Group on Atomic Structure). In the meantime interim needs for excitation data on these complex ions can be met through use of the very simple g-formula or impact parameter methods with possibly some use of Coulomb-Born approximation. All this can lead to relatively large inaccuracies (up to a factor of 5).

3.3 To satisfy the requirements for plasma impurities and cooling data, there are needs for basic theoretical work that would enable the needed excitation and ionization rates, particularly near threshold, to be obtained for CTR materials by iso-electronic extrapolation. It is felt that a basic understanding of relatively simple systems should be produced at first. Spectroscopic studies on tokamaks are needed to complement the accuracy of direct A+M data for the rate processes important to the fusion problem. (Noble gas discharges have already been usefully employed to do this).

B. Recommendations

The recommendations are ordered according to the nature of the reactants and each have been assigned a priority, viz. (1) top priority, urgent; (2) medium priority, should be undertaken when possible; and (3) lower priority, needed but not immediately.

1. Charge Transfer

1.1 Theory

Although calculations are performed using a molecular orbital approach for energies up to $S_i^2 = 0.1$ (i.e. 2.5 keV for H^+ impact), there is no reliable theory that can be used quantitatively. At intermediate energies LCAO models with traveling orbitals

sometimes yield reasonable results. At higher energies the Born approximation or variants of it are used, but higher order terms are required. Fundamental theoretical investigation for simple systems is needed with priority 1.

1.2 Experiment

Results of relatively high accuracy for capture of electrons by wall ions (Fe^{n+}, Ni^{n+}, Cr^{n+}, etc.) with fast H^o, D^o, and possibly T^o are required for understanding the physics of beam injection. C and O are among the other interesting targets, and all states of ionization should be considered. Metastable states of the incident beam particles need to be considered, as well as other excited states. Injection with negative ions may raise further problems. Most such work will need to be carried out experimentally, but also to be supported by detailed theoretical calculations on simple systems to allow interpolation and isoelectronic extrapolation. Experimental work is already underway on a few such processes at the Oak Ridge National Laboratory, the FOM Institute of Atomic and Molecular Physics in the Netherlands, the Liebig-Universitaet Giessen in the Federal Republic of Germany, the Queen's University in Belfast, and the Université Catholique de Louvain in Belgium.

1.3 Further remarks on charge transfer

Among other places, theoretical studies of merit are being conducted at the University of Bordeaux, Stanford University, Queen's University at Belfast, and by the Indian Association for the Cultivation of Science in Calcutta. We believe that both theoretical and experimental work on these processes should begin with simple systems building on what is already known, and should be considered as priority 1. Theoretical investigations of high energy limits following recent work of Dettman and Leibfried in Germany and Shakeschaft and Spruch in the US, may be practical and should be given priority 2. Further work on bounds on transition probabilities, following Rapp and Storm and Shakeschaft and Spruch should be pursued.

It is important to note that total capture cross sections, including capture into excited states, are also required. At higher energies, capture by He^{++} produced in the basic thermonuclear reactions will be important, and data are required on all the above targets and beam particles at energies up to several MeV.

Low-energy charge transfer (below 1 keV) is important for the wall region, and investigations of capture from and into highly excited states needs further work (priority 2).

Charge transfer may also play an important role in the divertor channel and exhaust in actual CTR machines, for example acting as a pump for neutral impurities (priority 2).

2. Other Heavy Particle Processes

2.1 Ionization of fast neutral hydrogen by highly ionized particles

This is of great importance and little is known about this process. Theoretical methods are available to calculate total cross sections using distorted wave codes, which should be reliable down to 20 keV (equivalent proton energy) and are being developed, e.g. by the Royal Holloway College - Université Libre de Bruxelles collaboration. However, experimental work is also required, particularly at lower energies since it seems unlikely that accurate theory can soon be developed. This is also of first priority, though it should be stressed that the calculations will be lengthy and expensive.

2.2 Exitation in atom-atom and ion-atom collisions

We consider atom-atom and ion-atom direct inelastic processes of relatively low importance. Results are needed at low energies (below 50 eV) and some experimental groups may be able to tackle these problems. We need to know in more detail precisely what such reactions, including chemical reactions, are likely to be important in CTR work before we can assess the urgency for further investigations (priority 3).

2.3 Ion-ion reactions

Ion-ion reactions are generally expected to be unimportant unless a resonance process is involved. Identification of likely candidates depends on accurate knowledge of adiabatic molecular ion potentials.

2.4 Fundamental ion-atom processes

The data on reactions of H^+, He^+, and He^{++} on H and He are of fundamental importance in tokamak particle balance. They are perhaps less well-established than is commonly thought and critical evaluation of current data is required (priority 1).

3. Excitation of Positive Ions by Electron Impact

This process is of crucial importance both for understanding energy balance and for diagnostic purposes.

Recent advances in theoretical methods make use of large computers and are aimed at calculating excitation rate coefficients accurate to about ± 20%. Comparison between experimental measurements and preliminary results of these calculations are revealing disparities of up to factors of 4. The reasons for these disparities may be that either:

- the theory may be wrong;
- the experiment may be wrong;
- the method of analysing the data to make the comparison may be wrong.

These comparisons are being done for relatively simple ions (specifically Be-like) and we recommend strongly that efforts be confined to the understanding of these relatively simple ions before going on to apply these sophisticated computer methods to more complex atomic systems. Elementary theoretical methods, such as the Coulomb-Born approximation, are thought to be untrustworthy for excitation processes close to threshold, but distorted-wave and close-coupling treatments show promise. A fairly complete listing of the status of theoretical work in this area is attached (Appendix B, by D.M. Cochrane and R.W.P. McWhirter). The development of such new theoretical methods should be encouraged and we recommend that support be given to the major international collaboration in this field particularly between the groups at the Queen's University at Belfast, the Observatoire de Paris at Meudon, the University College London, the Université Libre de Bruxelles, the Royal Holloway College and groups in the USA and the USSR.

The theoretical collision work depends on the production of tractable, accurate wave-functions for the states involved. It may be possible to obtain these as a byproduct of the atomic structure work discussed by another Working Group. This should be given high priority (priority 1). The wave-function codes produced in this, or in other ways, must be developed to the point where the collision physicist can use these with ease.

We believe that, in this work on collisional excitation, comparisons must be made between theory and experiment as a check on the accuracy of the theory, which is the only conceivable means of evaluating the very large number of collisional rate coefficients that are required. Experimental checks on the calculated excitation rate coefficients and cross-sections are possible by two methods, viz.

- Quantitative plasma spectroscopy; and
- Crossed-beams experiments.

A listing of published work by both methods is attached as Appendix C. Many more such collisional processes need to be studied by these experimental methods. The former requires the provision of a powerful plasma source for spectroscopic studies. Currently, work is being developed or is established at the Maryland University, the Astrophysics Research Division Culham Laboratory, the US National Bureau of Standards in Washington, the Los Alamos Scientific Laboratory, and Bocham University. The work of all these groups is based on relatively high density theta-pinches but there is an important case for a low density tokamak plasma being used for this work. Another useful experimental check on the theory of collisional excitation is the measurement of radiative transition probabilities between relevant levels and their comparison with the values calculated using the wave-functions developed for the collision physics. Work using beam-foil spectroscopy is likely to prove very valuable in this connection.

Efforts should be directed to obtaining agreement between theory and experiment to within $\pm$ 20% at all energies but this is particularly important close to threshold. Data is required for ions in metastable levels as well as ground levels.

We consider this work on the simple ions (both the development of theoretical methods and the experimental comparisons) to be of the highest priority (priority 1). We recognize the ultimate importance of heavy impurities but there is no hope of understanding the more complex reactions with heavy metal ions until the simple systems are understood.

4. Ionization by Electron Impact

Cross-section values are needed up to two or three times threshold for ground level, metastable level and inner shell ionization for all ions of interest. In cases where it is important the contribution due to autoionization is also needed. Near threshold theoretical methods are unsatisfactory due particularly to the difficulty of taking account of exchange. Errors of up to a factor of 2 have been reported in the threshold region. For ground level and for autoionization near threshold experimental crossed beams methods have proved successful with reported accuracies of $\pm$ 10%. As these measurements have so far been limited to ions of charge one and two, there is an important need to extend this work to ions of higher charge. Measurements of ionization rate coefficients are also possible by time resolved plasma spectroscopy but with less accuracy. These measurements, however, cover ions in higher stages of ionization. We recommend the extension of this experimental work particularly with crossed beams. It is important also to encourage the development of theoretical methods of calculating cross sections for ionization close to threshold. Accuracies of $\pm$ 20% should be aimed at. This work also is of high priority (priority 1).

5. Electron-ion recombination processes

Impurities are expected to reach a condition of steady-state ionization balance in some of the plasma machines currently contemplated. Under these circumstances it is as important to have as good values for recombination rate coefficients as those for ionization. Three interrelated mechanisms of recombination have been identified as important in these circumstances:

- Radiative recombination
- Dielectronic recombination
- Collisional-radiative recombination.

Of these the first is a purely radiative process that may be calculated using the wave-functions discussed in the Atomic Structure Working Group's report. The other two mechanisms involve electron-ion collisions of the general nature of those discussed above in sections B.3 and B.4 of this report. The collisions that matter in recombination are those that involve high quantum levels of the recombining ion. Methods of calculating these rates have been developed but there are no significant experimental checks on them. Measurements on satellite lines promise to be valuable here and we recommend that these be done. At the same time these calculations and experiments form the basis for important diagnostic methods for plasma electron temperature and density through the observation of satellite lines.

6. Electron-Atom Collisions

Electron atom excitation and ionization processes are of importance in plasma formation and for diagnostic purposes. Both theoretical and experimental results accurate to about 10% are currently being achieved for simple systems, but little work has been done on heavy atoms. Relativistic effects are important for $Z > 20$, and can be treated with reasonable success up to $Z \approx 40$. Further work on fundamental theory of near-threshold ionization is required (priority 2), and further measurements of ionization cross sections for many elements at all energies are needed to check present empirical formulae. In view of the importance of the electron impact ionization of atomic hydrogen, a remeasurement and reassessment of the processes from ground and metastable states is required (priority 1).

7. Photon-Atom Collisions

The low-photon densities in non-laser induced plasmas imply that only single photon processes are important. Primarily attention should be devoted to photoionization of atoms and ions.

Further details are needed on photon energy spectra of current tokamaks and fusion devices before deciding which photo-ionization processes are likely to be important. Provided the wave function codes already mentioned are developed, there are no fundamental theoretical difficulties other than those involved in obtained accurate elastic scattering cross section from excited states of ions. We assess this work to be of priority 3.

Threshold photo-ionization cross sections should be first estimated by extrapolation of oscillator strength states.

8. Further Study

It seems to us essential that small specialist meetings on specific topics, e.g. charge-transfer, electron excitation of positive ions, tokamak spectroscopy etc. should be convened. These should review the current position in their field with respect to fusion applications and recommend priorities for further work. It would be most convenient to hold these as satellite meetings of established international conferences. They should be encouraged where necessary to set up small working parties to evaluate in a critical way the information in their field.

Appendix A

Extract from INDC(NDS)-72/LNA

Survey of Atomic and Molecular Data Needs for Fusion

A. Lorenz et al, January 1976, IAEA

For all indicated reactions the quantities which are of general interest are the reaction cross sections as a function of energy and the reaction rate coefficients as a function of plasma temperature. Additionally the atomic parameters for spontaneous photon emission and absorption processes are required for many of the indicated species.

Since all isotopes of hydrogen may be involved unless specifically stated, the symbol (H) is used to represent any of the isotopes H,D, or T. The symbol e is used for electrons, and the symbol X and Z may represent any other heavy particles.

PROBLEM AREAS	DATA NEEDS

1. INJECTION SYSTEMS

The designs of some fusion experiments and reactors require injection of neutral material into the plasma (core) either to raise its average temperature (plasma heating) or to supply the nuclear fuel.

Present injection techniques are restricted because little is known about the atomic and molecular collision processes which occur in the injection system. An understanding of the atomic and molecular physics of the hydrogen isotopes and of collision processes with other gases is necessary to provide data for the design of efficient sources of both positive and negative ions, for the efficient conversion of positive and negative ions to neutral atoms, and for efficient trapping of injected material in the fusion plasma.

The physical processes and data requirements which are encountered in injection systems are discussed under the following topics:

A. Plasma Heating by Injection of Beams of Neutral Particles.
   1) Ion Source
   2) Ion Extractor and Accelerator
   3) Ion Neutralization
   4) Trapping of Neutral Species in the Plasma

B. Plasma Heating by Injection of Particle Clusters.

C. Plasma Fueling
   1) Injection of Neutral Particles
   2) Injection of Particle Clusters
   3) Injection of Solid Fuel (Pellets)

At present it is not clear whether injection of neutral particles or particle clusters are likely to be useful methods for fueling a fusion reactor. Therefore the principal discussion of these topics occurs in connection with plasma heating. Both plasma heating and plasma fueling by means of neutral-particle injection involve the processes of ion-production, ion-neutralization and subsequent trapping of the neutral particles within the plasma. However the relative importance of the atomic and molecular processes which are involved might be very different depending on the energies and intensities of the beams which are required for the two purposes.

PROBLEM AREAS

DATA NEEDS

1A. Heating by Injection of Beams of Neutral Particles

1) Ion Source

The primary objective of the ion source is to produce a particular ion species by collisions of electrons with isotopes by hydrogen. These processes occur normally in competition with ion loss processes such as diffusion, ion recombination, and electron energy loss due to inelastic molecular collisions. In addition, impurities ($Z>1$) are produced as a result of the interaction of the ions and electrons with the walls and electrodes of the ion source. Together with the desired ion species these impurities may be introduced into the plasma, which they contaminate (see Impurities and Plasma Cooling below).

(i) Collisions between electrons and atomic and molecular complexes in various states of vibrational and electronic excitation

Production of positive ions - (typical processes)	$e + (H)_2 \longrightarrow (H)_2^+ + e + e$
	$e + (H)_2^+ \longrightarrow (H)^+ + (H) + e$
	$\longrightarrow (H)^+ + (H)^+ + e + e$
	$e + (H) \longrightarrow (H)^+ + e + e$
Production of negative ions - (typical processes)	$e + e + (H) \rightarrow (H)^- + e$
	$e + (H)_2 \rightarrow (H)^+ + (H)^- + e$

(ii) Some Processes affecting ion species

Ion-molecular reaction	$(H)_2^+ + (H)_2 \longrightarrow (H)_3^+ + (H)$
Association	$D + T \longrightarrow DT$
Recombination	$(H) + (H)^+ + \text{wall} \rightarrow (H)_2$

(iii) Electron energy loss processes

Atomic and molecular excitation	$e + (H) \longrightarrow (H)^* + e$
	$e + (H)_2 \longrightarrow (H)_2^* + e$
	$e + (H)_2 \longrightarrow (H) + (H)^* + e$
Electron-electron collisions	$e_{(\text{fast})} + e_{(\text{plasma})} \rightarrow (e+e)_{\text{thermal}}$

Electron recombination or detachment processes, which are the reverse reactions for production of positive or negative ions, respectively, except for the energy range involved

(iv) Interaction of ions with surfaces

- Reaction kinetics

  Some preliminary experiments show that the surfaces of the ion source walls play a dominant role in the production of $(H)^-$. A more precise knowledge of the reaction kinetics of $(H)_2^+$, $(H)^+$ and (H) particles interacting with surfaces contaminated by Cs, Mg, Na and Li in the energy range 5 - 500 eV. is required.

- Sputtering (see 2A and 2B)

- Charge exchange

- Charge exchange processes of hydrogen with impurities (e.g. Fe, Ni, Cr, Cu, C, W and Mo), which may enter the ionizing discharge due to sputtering from the walls and other surfaces.

PROBLEM AREAS

DATA NEEDS

2) Ion Extractor and Accelerator

Positive and negative ions extracted from the ion source are accelerated to energies ranging from ~ 10 keV to ~ 1 MeV. The ion beam is accelerated in a low density gas diffusing out of the ion source. In addition to the interaction of the accelerated ions with the gas, in which charge exchange, charge stripping, detachment and dissociation can occur, part of the beam interacts with metallic surfaces creating the attendant surface effects, such as sputtering and outgassing, thereby introducing additional impurities.

Secondary electrons, produced in the extractor and accelerator by particle impact and X-rays, can be accelerated back towards the ion source so that additional ion production takes place but at much higher electron energies; the production of X-rays by these electrons may introduce a significant hazzard to health. The presence of arcs in the extractor system introduces collisions with impurity atoms.

(i) Particle interaction in the beam. X is the neutralizer species.

Charge exchange $(H)^+ + X \longrightarrow (H) + (X)^+$

Ionization $(H) + X \longrightarrow (H)^+ + X + e$

Detachment $(H)^- + X \longrightarrow (H) + e + X$

Dissociation $(H)_2^+ + X \longrightarrow (H)^+ + (H) + Y$

(ii) Surface effects

$(H)^+$ + surface ⟶ radiation emission

$(H)^+$ + surface ⟶ electron emission

$(H)^+$ + surface ⟶ X-ray production

$(H)^+$ + surface ⟶ outgassing

$(H)^+$ + surface ⟶ sputtering

3) Ion Neutralization

a) Energetic neutral particles in the range 5 to 100 keV, which present injection concepts envisage, are most efficiently obtained by neutralization of accelerated positive ions in a gas cell.

(i) Production of neutrals from positive ions - typical processes:

Collisions with heavy species:

$$(H)^+ + X \longrightarrow (H) + X^+$$

$$(H)_2^+ + X \longrightarrow (H) + (H)^+ + X$$

Collisions with electrons:

$$(H)_2^+ + (X^+ + e) \longrightarrow (H) + (H)^+ + e + X^+$$

(ii) Some re-ionization processes:

$$(H) + X \longrightarrow (H)^+ + e + X$$

$$(H) + e \longrightarrow (H)^+ + e + e$$

b) In about five to ten years, however, larger experimental devices and prototype fusion reactors may require injected-particle energies ranging between 100 keV and 1 MeV. Several methods have been proposed to obtain intense atomic (H) beams in this energy range for heating and, possibly, fueling such devices. At these energies it will be more desirable to neutralize a beam of negative ions since the neutralizer efficiency is almost independent of ion energy and can be as high as 10 - 20 % in the case of a cesium-vapor-cell neutralizer. The following two methods have been proposed to obtain negative ions:

- use of a conventional positive ion source to produce a low-energy (1.5 keV) beam which is passed through an alkali vapor cell to form the required negative ions,
- development of a suitable negative ion source to produce the negative ions directly.

The negative ions are then accelerated to the desired energy and neutralized by stripping the excess electrons in a suitable target.

(iii) Formation of $(H)^-$ from positive ions and stripping of $(H)^-$ to form neutrals in gas or vapor cells.

- Interaction of $(H)_2^+$, $(H)^+$ ions with Cs, Na and Li in the energy region 0.5 - 5 keV. Little information is available for collisions of $(H)_2^+$ and $(H)_3^+$ ions in these vapors. Needed are the total cross sections, equilibrium fractions, and differential interaction cross sections to form $(H)^-$.
- No information is available concerning the cross section for the formation of D from D^+, D_2^+, and D_3^+ in target plasmas of either deuterium or Li. This may be a mechanism to produce 0.1 to 1 MeV D without resorting to the D^- cycle.
- Cross sections for the formation of (H) from $(H)^-$ collisions in gaseous targets of H_2, He, N_2, O_2, Ne, Ar and H_2O, in energy region between 50 and 300 keV.
- Peak fraction of (H) formed from $(H)^-$ in energy range 0.1 to 1 MeV.
- Formation of (H) from passage of $(H)^-$ through target plasma of deuterium or lithium in energy range 0.1 to 1 MeV.
- Stripping of $(H)^-$ in electromagnetic fields.

PROBLEM AREAS

c) Intense beams of ions cause the neutralizer target gas to become partially ionized so that charge-exchange (etc.) takes place in a plasma. Since "thick target" conditions may prevail in the neutralizer, cascading collisions are important. The balance between charge exchange and ion production are further complicated by the presence of excited atoms and molecules.

d) Trapping in the plasma core. After passing through the confining magnetic field, the injected (neutral) particles must be ionized before significant heating can occur. The importance of various ionization processes depends upon beam energy and plasma temperature.

DATA NEEDS

(iv) Charge exchange rates for (H), $(H)_2$ and $(H)_3$ in partially ionized neutralizer target gases are required.

(v) It is important to know the rate at which impurity atoms from the ion source enter the plasma confinement region. Required are cross sections for charge-exchange processes of C, N, O, Fe, Ta and Pt atoms with neutralizer gases over the energy range 5 to 100 keV and the rates for these processes in the environment of the neutralizing gas cell.

(vi) Typical trapping processes:

For beams < 50 keV:

$$\underline{(H)}_{(beam)} + (H)^+_{(plasma)} \longrightarrow (H)^+_{(trapped)} + (H).$$

At higher beam energies:

$$\underline{(H)}_{(beam)} + (H)^+_{(plasma)} \longrightarrow (H)^+_{(trapped)} + e + (H)^+.$$

(The underscores indicate energetic particles.)

(vii) Processes which result in trapping of heavy-ion impurities from the ion source within the plasma.

LIST OF REFERENCES TO CALCULATIONS OF CROSS-SECTIONS FOR THE EXCITATION OF POSITIVE IONS

Compiled by

D.M. Cochrane
and
R.W.P. McWhirter

Appleton Laboratory
Astrophysics Research Division
Culham

September 1976

Science Research Council
APPLETON LABORATORY
ASTROPHYSICS RESEARCH DIVISION

Culham Laboratory, Abingdon, Oxon OX14 3DB
Telephone Abingdon (0235) 21840 Telex No 83189

Your ref

Our ref RWPM/PR

Date 23 September 1976

Dear Colleague

Deirdre Cochrane and I have recently put together a list of references to theoretical calculations of excitation of positive ions (and some atoms) by electron impact. This information should be of interest to astrophysicists interested in the interpretation of spectra and to plasma physicists concerned with the problem of power loss from laboratory plasmas. We hope that you will find the enclosed list useful.

The chart covers all ions of all elements up to Molybdenum and gives access to the numbered foot notes on the accompanying list. Since some of the work is not published a list of the addresses of those contributing to the list is also enclosed. Please contact the addressees for information only when there is a genuine need for data. They too are busy people!

The material enclosed has been prepared with a minimum of editing. There has been no critical selection and a few of the people known to be working in the area did not respond to our enquiries. However, the general response was good and we believe the list will be a useful guide to the available data.

Since the charts were printed a number of additional references have been sent to us. You should therefore mark the following on the chart (the foot notes have been up-dated).

He I	21.1	He II	8.5
Be II	8.6	N II	2.10
O II	2.10	O III	2.10
Al XI	2.11	Cu I	21.1

Yours sincerely

R W P McWhirter

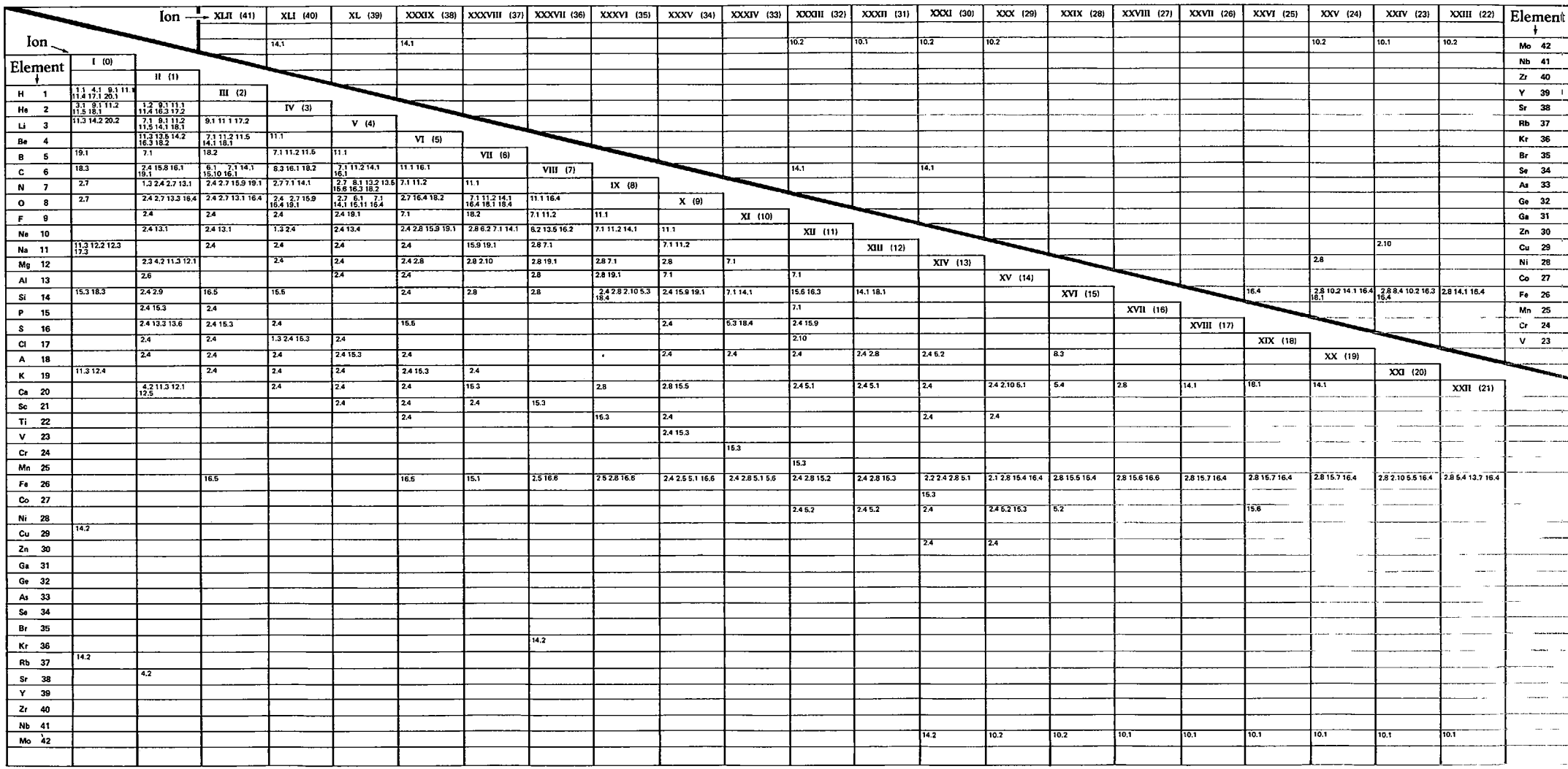
Ion
Element
I (0)
II (1)
III (2)
IV (3)
V (4)
VI (5)
VII (6)
VIII (7)
IX (8)
X (9)
XI (10)
XII (11)
XIII (12)
XIV (13)
XV (14)
XVI (15)
XVII (16)
XVIII (17)
XIX (18)
XX (19)
XXI (20)
XXII (21)
XLII (41)
XLI (40)
XL (39)
XXXIX (38)
XXXVIII (37)
XXXVII (36)
XXXVI (35)
XXXV (34)
XXXIV (33)
XXXIII (32)
XXXII (31)
XXXI (30)
XXX (29)
XXIX (28)
XXVIII (27)
XXVII (26)
XXVI (25)
XXV (24)
XXIV (23)
XXIII (22)
Element
H 1
He 2
Li 3
Be 4
B 5
C 6
N 7
O 8
F 9
Ne 10
Na 11
Mg 12
Al 13
Si 14
P 15
S 16
Cl 17
A 18
K 19
Ca 20
Sc 21
Ti 22
V 23
Cr 24
Mn 25
Fe 26
Co 27
Ni 28
Cu 29
Zn 30
Ga 31
Ge 32
As 33
Se 34
Br 35
Kr 36
Rb 37
Sr 38
Y 39
Zr 40
Nb 41
Mo 42
Mo 42
Nb 41
Zr 40
Y 39
Sr 38
Rb 37
Kr 36
Br 35
Se 34
As 33
Ge 32
Ga 31
Zn 30
Cu 29
Ni 28
Co 27
Fe 26
Mn 25
Cr 24
V 23

Reference Footnotes to Matrix

1. Dr Derek Banks

1.1 Highley-excited States $n \rightarrow n'$ transitions.
Percival I C and Richards D, 1975, Adv. in Atom and Molec.Phys. 11 + references therein.

1.2 The same techniques apply to He^+, etc, provided the ionisation level is not too extreme, as st. line paths are assumed for the incident electron.

1.3 The same techniques apply to all atoms provided only 1 electron is highly-excited. For $(n,\ell) \rightarrow (n',\ell')$ transitions we hope to have results within 12 months. Corrections are needed for low ℓ.

2. Dr Milan Blaha

2.1 Solar Phys. 3, 563 (1968). CB with and without exchange.
O Bely and M Blaha.

2.2 Solar Phys. 17, 99 (1971). CB without exchange. M Blaha.

2.3 Astron. Astrophys. 16, 437 (1972). CB without exchange. M Blaha.

2.4 Astron. Astrophys. 1, 42 (1969). DW with exchange. Transitions between fine-structure levels. M Blaha.

2.5 Phys.Rev.A 12, 1076 (1975). Univ. of Maryland Tech. Rep. TR 75-076 (1975).
CB without exchange. R U Datla, M Blaha and H-J Kunze.

2.6 Phys.Rev.A 11, 477 (1975). DW without exchange.
A W Allen, M Blaha, W W Jones, A Sanchez, H R Griem.

2.7 J Quant. Spectrosc. Radiat. Transfer 15, 1145 (1975).
DW without exchange. J Davis, P C Kepple, M Blaha.

2.8 Naval Research Lab. Memo. Rep. 3171 (1975).
DW with and without exchange. P C Kepple, J Davis, M Blaha.

2.9 Current work. DW without exchange. M Blaha.

2.10 Current work. DW with exchange. Transitions within the ground configuration. M Blaha, J Davis.

2.11 J.Ap.Phys. 47, 1426 (1976). Distorted wave calculation.
J Davis and K G Whitney.

3. Dr J van den Bos

3.1 Born-approximation, excited states: $2^1S, 3^1S, 4^1S, 2^1P, 3^1P, 4^1P, 3^1D, 4^1D, 4^1F$. Ref: Physica 42 (1969) 245-261.

4. Dr Alan Burgess

4.1 Current work. Multi-level close-coupling. R Poet.

4.2 Distorted wave. M Frank.

4.3 General methods, eg Bethe, ECIP, etc. B Christen-Dahlsgaard.

5. Dr Helen Mason All results - UCL Distorted wave program.

5.1 H E Mason (1975) Mon.Not.R.astr.Soc. 170, 651.

5.2 H E Mason. Calculations complete - no preprints yet (3/4 configurations).

5.3 H E Mason and A K Bhatia (Goddard Space Flight Center) (3 configurations) - Calculations complete.

5.4 H E Mason - Preprint available.

5.5 H E Mason - work planned.

5.6 H E Mason and H Nussbaumer - work planned (including configurations in n = 4 complex).

6. Professor Philip G Burke

6.1 Current work - Queens University Belfast. Electron collisions using R-matrix method and taking account of $2s^2\ ^1S\ 2s2p\ ^3P\ ^1P\ 2p^2\ ^3P\ ^1D\ ^1S$ levels. P G Burke, K A Berrington, P Dufton, A E Kingston. Also proton collisions for $2s2p^3P$ fine structure transitions.

6.2 Future work - otherwise as for 1 above.

7. Professor Alex Dalgarno

7.1 Exploration of relativistic effects using relativistic random phase approximation - He and Be isoelectronic sequences.
C D Lin, W Johnson, A Dalgarno.

8. Professor Ronald J W Henry

8.1 Have calculated - LSU noniterative integral equation method (NIEM) solution of close-coupling 5 levels. W L van Wyngaarden and R J W Henry. J.Phys.B.(June 1976).

8.2 Have calculated - NIEM 5 level close-coupling. W L van Wyngaarden and R J W Henry. Can.J.Phys. (1976).

8.3 Current work - NIEM 5 level close-coupling, including resonances.
J N Gau, J Callaway, R J W Henry.

8.4 Current and planned work - NIEM 5 level close-coupling, relativistic effects. J N Gau, J Callaway, R J W Henry.

8.5 He II Work completed 1s→2s and 1s→2p; NIEM close-coupling of 1s, 2s, 2p and pseudostates $\overline{3s}$ and $\overline{3p}$. R J W Henry and J J Matese, Phys.Rev.A (Oct 76).

8.6 Be II Current work 2s→2p; NIEM close-coupling of 2s, 2p and pseudo-states $\overline{3s}$, $\overline{3p}$, $\overline{3d}$. J J Matese and R J W Henry.

9. Professor C J Joachain

9.1 Electron excitation of H, He, He^+, Li^+, Li^{++}, using the Eikonal Born series theory and distorted wave methods. Incident electron energies $E \geq 50$ eV.

10. Dr M Klapisch

10.1 Current work - investigation of relativistic effects in Coulomb-Born approximation.

10.2 Beginning of work - use of R Matrix Package of Berrington, Burke et al. Comp.Phys. Com. 8, 149 (1974).

11. Professor M R C McDowell

11.1 DWPO I, II, III, published H,He^+. Rest unpublished.
McDowell, M R C, Morgan, L A, Myerscough, V P.

11.2 DWPO I,II. Results for H and He^+ published. For $3 \leq Z \leq 10$ in McDowell M.R.C., Morgan L.A., Myerscough V.P. and Scott T. Submitted to J.Phys.B.

11.3 DWPO I, II and Unitarised: Resonance transition;
Kennedy J, Myerscough V P and McDowell M R C. Submitted to J.Phys.B.

11.4 Close-Coupling-Pseudo-State-DW. Published H, He II in progress.
Callaway J, Morgan L A, McDowell M R C.

11.5 a. Simplified c.c.(equivalent exchange potentials).
Bransden B H, Joachain C J, McDowell M R C. In progress.

b. Double Distorted Wave.
K.L. Baluja, L.A. Morgan, M.R.C. McDowell. In progress.

12. Dr David L Moores

12.1 Scattering of electrons by Mg^+ and Ca^+; Burke code 2- and 3-state close coupling; H-Fock target wave functions with P G Burke. J.Phys.B 2, 161-73 (1970).

12.2 4-state close coupling "The scattering of electrons by Na Atoms" with D W Norcross. J.Phys.B 5, 1482-1505 (1972).

12.3 With D W Norcross and V B Sheorey. J.Phys.B.7, 371-5 (1974)
"Scattering from excited states of Na"

12.4 The scattering of electrons by K atoms.
J.Phys.B (in the press; proofs returned).

12.5 Current work; "IMPACT" with C Mendoza.

13. Dr Hannelore Saraph

13.1 Seaton M J, Roy.Astron.Soc.170, 1975, pp.475-86 (excitation of forbidden lines, CC,CI).

13.2 Hayes M, J.Phys.B.8, L8-11, 1975.

13.3 Pradhan A K, J.Phys.B.9, 1976, 433-443 (excitation of forbidden lines, CC, CI). Also: Pradhan, A K, Mon.Not.RAS, 1976, in press. Detailed resonance analysis for (O II) $^2D_{3/2}$-$^2D_{5/2}$, ^2D_y-^2P_y, and preliminary results for S II.

13.4 Jackson A and Pradhan A K, work nearing completion, CC, CI, resonance analysis.

13.5 Hayes M, work nearing completion, CC, DW, CI.

13.6 Pradhan A K, excitation of forbidden lines; work started CC, CI, DW.

13.7 Storey P, DW, CI, work near completion.

(CC: Close coupling, DW: Distorted wave, CI: Configuration interaction)

14. Dr David W Norcross

14.1 UCL DW Program, JILA version,
9 config. target (five LS terms) for He sequence ions,
11 config. target (14 LS terms) for Be sequence ions.

14.2 Model potential close-coupling.

15. Dr Harry Nussbaumer

15.1 Nussbaumer H, Osterbrook D E, 1970, Ap.J. 161, 811.

15.2 Flower D R, preprint available.

15.3 Flower D R, Pineau des Forêts G, 1973, Astron.Astrophys. 24, 181.
Nussbaumer H, 1973, Astron.Astrophys. 27, 303.
Flower D R, Nussbaumer H, 1974, Astron.Astrophys. 31, 353.
Nussbaumer H, A (forbidden) within $3s^23p^2$ (unpublished).

15.4 Flower D R, Jordan C, 1971, Astron.Astrophys. 14, 473.

15.5 Flower D R, Nussbaumer H, 1975, Astron.Astrophys. 42, 265.
Loulergue M, Nussbaumer H, unpublished.

15.6 Flower D R, 1971, J.Phys.B. 4, 697.
Loulergue M, Nussbaumer H, 1975, Astron.Astrophys., in press.

15.7 Loulergue M, Nussbaumer H, in connection with a study on solar active regions, H E Mason will study the Fe^{+1} $1 \geq 20$ for flare investigations. Fe^{+19} will be studied by either Mason or Loulergue and Nussbaumer.

15.8 Mühlethaler H P, in progress.

15.9 Flower D R, Nussbaumer H, 1975, Astron.Astrophys.(in press) or unpublished (N III, Ne VI).

15.10 Flower D R, Launay J M, 1973, Astron.Astrophys. 29, 321.

15.11 Malinovsky M, 1975, Astron.Astrophys. 43, 101.

16. Dr W Derek Robb

16.1 Current Work - R-matrix Close Coupling, CBO and DW, All levels from 1s, 2s and 2p with some n = 3 orbitals and CI - W D Robb, J B Mann and J M Peek.

16.2 Work Complete - Close-coupling, Coulomb Born with exchange (CBO) and Distorted Wave (DW) with exchange, lowest 5 levels, rates calculated - W D Robb, J B Mann and J M Peek.

16.3 Work Complete - Coulomb Born with exchange. All n = 2 levels and some n = 3 levels - J B Mann.

16.4 Future Work - R-matrix Close Coupling, CBO and DW - All lowest levels - W D Robb, J B Mann and J M Peek.

16.5 Work Completed - Close-coupling - R-matrix - Lowest levels CI where necessary - W D Robb.

16.6 Work Completed - Coulomb Born with exchange - Threshold to high energy - rates calculated - some CI. J B Mann.

17. Dr Mike J Roberts

17.1 Differential cross section for excitation of H. A classical path T-matrix approx. valid, at best, for high angle scattering only - No good for total x sections.

17.2 I intend to investigate the excitation of hydrogenic ions with similar technique.

17.3 Calculation of orientation parameters for excitation of optical levels.

18. Dr Aaron Temkin

18.1 Goddard program - distorted wave. Uses exchange approx. for exact initial stale wave function. Bhatia and Temkin (to be submitted for publication) (He isoelectronic ions).

18.2 Program being developed at Goddard - uses exchange approx. for 3 electron ions (as in 1) in distorted wave. M Ali (Howard Univ) and A K Bhatia.

18.3 Uses exchange approx. in distorted wave for arbitrary ion. Program being developed by M Pindzola (NRC fellow at Goddard) and A K Bhatia. Application currently being made to C, Si as indicated. Chief element of program is not to assume orthogonality of scattered orbital to bound orbitals!

18.4 Current work - UCL distorted wave computer programme. Work being done by A K Bhatia. In the case of Si IX and S XI with the collaboration of H E Mason.

19. Dr Eleonore Trefftz

19.1 B-like $2s^2 2p^2 P - 2s2p^2\ ^4P$, UCL Impact program, as exercise for using Impact; further aim: relativistic effects. E Trefftz, C W Dankwort.

20. Dr Donald G Truhlar

20.1 Planned work - Close coupling calculations. D G Truhlar and M E Riley.

20.2 Planned work - Close coupling calculations. D G Truhlar.

21. Prof Kenneth Smith

21.1 Current work - Multiconfiguration close-coupling approximation. K Smith and S J Wade.

Contributors' Addresses

1. Dr Derek Banks
Department of Applied Maths
Queen Mary College
Mile End Road
London E1 4NS

2. Dr Milan Blaha
Department of Physics & Astronomy
University of Maryland
College Park
Maryland 20742
USA

3. Dr J van den Bos
Faculty of Science
University of Nijmegen
Toernooiveld
Nijmegen
The Netherlands

4. Dr Alan Burgess
Dept of Applied Maths & Theoretical Physics
Silver Street
Cambridge CB3 9EW

5. Dr Helen E Mason
Dept of Applied Maths & Theoretical Physics
Silver Street
Cambridge CB3 9EW

6. Professor Philip G Burke
Dr Keith Berrington
Dr Arthur E Kingston
Dept of Applied Mathematics
Queens University Belfast BT7 1NN
N Ireland

7. Professor Alex Dalgarno
Center for Astrophysics
60 Garden Street
Cambridge
Massachusetts 02138
USA

8. Professor Ronald J W Henry
Department of Physics & Astronomy
Louisianna State University
Baton Rouge
Louisianna 70803
USA

9. Professor C J Joachain
Physique Théorique, Faculté des Sciences
Université Libre de Bruxelles
Campus de la Plaine, CP 227
boulevard du Triomphe
B- 1050 Bruxelles
Belgium

10. Dr M Klapisch
Racah Institute of Physics
Hebrew University
Jerusalem
Israel

11. Professor M R Coulter McDowell
Mathematics Department
Royal Holloway College
Egham Hill
Egham
Surrey TW20 0EX

12. Dr David L Moores
Dept of Physics and Astronomy
University College London
Gower Street
London WC1E 6BT

13. Dr Hannelore E Saraph
Dr Werner Eissner
Dr Gillian Peach
Professor M Seaton
Department of Physics & Astronomy
University College London
Gower Street
London WC1E 6BT

14. Dr David W Norcross
Joint Institute for Lab Astrophysics
University of Colorado
Boulder
Colorado 80309
USA

15. Dr Harry Nussbaumer
Eldgenossische Technische Hoschule Zurich
Gruppe fur Atom und Astrophysik
Gloriastrasse 35
Ch-8006 Zurich
Switzerland

16. Dr W Derek Robb
Group T-4 MS288
LASL P O Box 1663
Los Alamos
New Mexico 87544
USA

Contributors' Addresses (continued)

17. Dr Mike J Roberts
Department of Physics
University of Stirling
Stirling FK9 4LA
Scotland

18. Dr Aaron Temkin
NASA
Goddard Space Flight Center
Greenbelt
Maryland 20771
USA

19. Dr Eleonore Trefftz
Max Planck Institut fur Physik und
Postfach 40 12 12 Astrophysik
Föhringer Ring 6
D-8000 München 40
Germany

20. Dr Donald G Truhlar
Department of Chemistry
University of Minnesota
Minneapolis
Minnesota 55455
USA

21. Professor B H Bransden
University of Durham
Old Shire Hall
Durham DH1 3HP

22. Dr F Bely-Dubau
Dr J Dubau
Dr D Petrini
Observatoire de Nice
Le Mont Gros
06008 Nice
Cedex
France

23. Professor J Callaway
Department of Physics
Louisianna State University
Baton Rouge
Louisianna 70803
USA

24. Dr Jack Davis
Plasma Physics Division
Naval Research Laboratory
Washington DC 20375
USA

25. Mme M le Dourneuf
Section d'Astrophysique
Observatoire de Paris
92190 Meudon
France

26. Dr P Dufton
Dept of Applied Mathematics
Queens University
Belfast BT7 1NN
N Ireland

27. Dr David Flower
DAPHE
Observatoire de Paris
F92190 Meudon
France

28. Dr Michelle Loulergue
Section d'Astrophysique
Observatoire de Paris
92190 Meudon
France

29. Dr Monique Malinovsky
LPSP Boite Post No 10
91370 Verrières le Buisson
France

30 Dr J B Mann
Group T-4 MS288
LASL, P O Box 1663
Los Alamos
New Mexico 87544
USA

31. Dr R McCarroll
Laboratoire d'Astrophysique
Université de Bodeaux 1
33405 Talence
France

32. Dr J M Peek
Division 5641
Sandia Laboratories
Albuquerque
New Mexico 87106
USA

Contributors' Addresses (continued)

33. Professor Ian C Percival
Dept of Applied Mathematics
Queen Mary College
Mile End Road
London E1 4NS

34. Dr Henri Van Regemorter
Section d'Astrophysique
Observatoire de Paris
92190 Meudon
France

35. Dr Mike R H Rudge
Dept of Theoretical Physics
Queens University
Belfast BT7 1NN
N Ireland

36. Professor Kenneth Smith
Centre for Computer Studies
The University
Leeds LS2 9JT

37. Dr Vo Ky Lan
Section d'Astrophysique
Observatoire de Paris
92190 Meudon
France

References to Plasma Measurements and to Crossed Beam Measurements

A list of references to measurements of cross sections and rates for electron impact excitation in positive ions has been assembled. Those references appearing before December 1974 were obtained from the Bibliography of Low Energy Electron and Photon Cross Section Data by Lee J. Kieffer.* The remainder result from a search of the literature appearing between January 1975 and the middle of 1976. The references were not subject to critical selection, and it is possible that a few were overlooked.

The measurements may be divided into classes: plasma measurements and crossed beam measurements. The former are rate coefficient measurements made primarily in multiply ionized species. The crossed beam measurements are forethe excitation cross sections of spectral lines. In some instances, that type of cross section is used to obtain a level excitation cross section. With one notable and encouraging exception (ref. 15), the crossed beam measurements are for singly ionized species. Unfortunately, the two classes overlap for only one transition.

The accompanying chart presents the available data in a convenient form. It gives access to the numbered references on the list. Note that isoelectronic sequences follow diagonals.

---

* Lee J. Kieffer, Bibliography of Low Energy Electron and Photon Cross Section Data NBS Special Publication 426, U.S. Government Printing Office, Washington 1976.

Measurements of Cross Sections and Rates for Electron Impact Excitation in Positive Ions

Compiled by
W.L. Rowan, NBS, Washington, D.C.

Element	Ion									
	I (0)	II (1)	III (2)	IV (3)	V (4)	VI (5)	VII (6)	VIII (7)	IX (8)	X (9)
H 1		18,19,20,21,22								
He 2										
Li 3										
Be 4										
B 5										
C 6					5,9,12					
N 7	Neutrals Not Considered			8	1,11,15	5				
O 8					8	11	4,5			
F 9								5		
Ne 10		7	7	7	7	7	7,8,13	6,7,10,11	5	
Na 11										
Mg 12										
Al 13										
Si 14									8	
P 15										
S 16										
Cl 17										
A 18		26						2		
K 19										
Ca 20		23,25								
Sc 21										
Ti 22										
V 23										
Cr 24										
Mn 25										
Fe 26								3	3	3

For heavier elements, the following data sources are available:
Kr II → 26; Ba II → 14,16,24; Hg II → 17.

Plasma Measurements

1. B.C. Boland, F.C. Jahoda, T.J.L. Jones and R.W.P. McWhirter, J. Phys. B: Atom. Molec. Phys. 3, 1134 (1970)

2. R.U. Datla, H.J. Kunze, D. Petrini, Phys. Rev. A 6, 38 (1972)

3. R.U. Datla, M. Blaha, H.J. Kunze, Phys. Rev. A 12, 1076 (1975)

4. R.C. Elton and W.W. Koeppendoerfer, Phys. Rev. 160, 194 (1967)

5. W. Engelhardt, W. Koeppendoerfer, and J. Sommer, Phys. Rev. A 6, 1908 (1972)

6. G.N. Haddad and R.W.P. McWhirter, J. Phys. B: Atom. Molec. Phys. 6, 715 (1973)

7. Einar Hinnov, JOSA 56, 1179 (1966)
   - - - - - - , JOSA 57, 1392 (1966)

8. W.D. Johnston III and H.J. Kunze, Phys. Rev. A 4, 962 (1971)

9. H.J. Kunze, A.H. Gabriel, Hans R. Griem, Phys. Rev. 165, 267 (1968)

10. H.J. Kunze, Phys. Rev. A 4, 111 (1971)

11. H.J. Kunze and W.D. Johnston III, Phys. Rev. A 3, 1384 (1971)

12. A.N. Prasad and M.F. El-Menshawy, J. Phys. B 1, 471 (1968)

13. G. Tondello and R.W.P. McWhirter, J. Phys. B: Atom. Molec. Phys. 4, 715 (1971)

Crossed Beam Measurements

14. F.M. Bacon and J.W. Hooper, Phys. Rev. 178, 182 (1969)

15. J.N. Bradbury, T.E. Sharp, B. Mass and R.N. Varney, Nuclear Instruments and Methods 110, 75 (1973)

16. D.H. Crandall, P.O. Taylor, and G.H. Dunn Phys. Rev. A 10, 141 (1974)

17. D.H. Crandall, R.A. Phaneuf, Gordon H. Dunn, Phys. Rev. A 11, 1223 (1975)

18. N.R. Daly and R.E. Powell, Phys. Rev. Lett. 19, 1165 (1967)

19. D.F. Dance, M.F.A. Harrison, and A.C.H. Smith, Proc. R. Soc. Lond. A 290, 74 (1966)

20. A.I. Dashchenko, I.P. Zapesochnyi, A.I. Imre, V.S. Bukstich F.F. Danch, V.A. Kelman, Sov. Phys. JETP, USSR (English Translation) 40, 249 (1974)

21. A.I. Dashchenko, I.P. Zapesochnyi, A.I. Imre, JETP Letters USSRS (English Translation) 19, 137 (1975)

22. K.T. Dolder and B. Peart, J. Phys. B 6, 2415 (1973)

23. V.A. Kelman and A.I. Imre, Optics and Spectroscopy USA 38, 709 (1975)

24. M.O. Pace and J.W. Hooper, Phys. Rev. A 7, 2033 (1973)

25. P.O. Taylor and G.H. Dunn, Phys. Rev. A 8, 2304 (1973)

26. I.P. Zapesochnyi, A.I. Imre, A.I. Dashchenko, V.S. Vukstich, F.F. Danch and V.A. Kelman, Sov. Phys. JETP USSR (English Translation) 36, 1056 (1973)

REPORT OF THE WORKING GROUP ON THE REQUIREMENTS OF ATOMIC STRUCTURE DATA

Working Group Members

Bromage, Mr. G.E.
Drawin, Dr. H.W. (Chairman)
Fawcett, Mr. B.C.
Martinson, Prof. I.
Wiese, Dr. W.L.

Introduction

The working group has examined the status of atomic structure data with respect to the needs of Thermonuclear Fusion Research Programs. It is evident that there are major gaps in the data and that many immediate, as well as long term, needs exist: we focused especially on the very serious implications of heavy ion impurities in high-temperature plasmas, for example, radiative energy losses, which have been well described in the literature (see e.g. Review Paper A4). We deliberately excluded from discussion molecular structure problems, which may become important in the future. The subject has been subdivided into the following four data areas:

Wavelengths and energy levels,
Atomic transition probabilities,
Line shapes,
Radiative excitation, ionization and recombination processes.

For each of these categories we addressed three topics, namely:

Data requirements and justifications.
Assessment of the existing data compilations.
Recommendations to IAEA.

A. Data Requirements and Justification

1. Wavelength Data and Energy Levels

Data required	Reasons
1.1 Identification of the most intense lines in the spectra of elements heavier than nickel, in all stages of ionization, for all elements used as wall and limiter materials in fusion devices.	Wavelengths of these lines, mostly not yet available are needed for basic identification of presence and ionization states of impurities.

Data required	Reasons
1.2 Identification of the spectra of highly ionized impurity elements in spectral regions conveniently accessible to experiments, including forbidden lines.	Important for diagnostic purposes, for example via measurement of Doppler widths of lines in the visible or near ultraviolet.
1.3 Detailed identification of spectra arising from transitions involving the most important configurations, for all impurity elements encountered in fusion research.	Detailed knowledge provides valuable support for wave functions calculations and hence for calculations of oscillator strengths and excitation cross-section.
1.4 Attention should also be paid to the following more specific points:	
i) wavelengths of K and L x-ray transitions of highly ionized impurity elements as a function of ion charge state	Needed for independent determination of stage of ionization of impurities.
ii) wavelengths of dielectronic-recombination "satellite" lines	Needed especially for diagnostics, and partly for plasma modelling.
iii) energy levels for autoionizing states	
iv) ionization energies	
2. Atomic Transition Probabilities	
2.1 Determination of the atomic transition probabilities of resonance and other prominent lines for highly ionized species of all those elements used as wall and limiter materials in fusion devices.	Needed for presently used approaches to the heavy ion impurity problem, both for measurements of impurity concentrations as well as modelling of the radiative power losses.
2.2 Determination of atomic transition probabilities of light element impurities (C,N,O) with high accuracy (5-10%) and covering essentially the complete spectrum.	Required (a) to select most suitable lines for impurity diagnostics, including spatial and temporal distributions of species in plasma, (b) to obtain detailed modelling of impurities for plasma energy balance, e.g. for laser and electron beam-induced high density plasmas ("laser fusion").
2.3 Atomic transition probabilities of medium to high accuracy (10-25%) for medium atomic weight elements used as wall materials (Cr,Fe,Ni).	Similar to above, e.g. for diagnostics (including applications of the branching ratio technique), plasma modelling, determination of impurity levels and radiative power losses of plasmas deviating from corona regime, to check theory regarding target wavefunctions.

Data required	Reasons
2.4 Determination of autoionization probabilities.	Knowledge is required for calculation of dielectronic recombination coefficients, ionization balance, radiation energy losses, and plasma modelling.
2.5 Atomic transition probabilities for forbidden lines of highly ionized species with relatively long as well as short wavelengths.	(a) Needed for selecting suitable lines for Doppler ion temperature diagnostics, (b) also required for plasma modelling (e.g. in calculating the population densities of excited levels of ions having metastable levels and hence in predicting their spectra, power loss, etc.)
3. Line Shapes	
3.1 Line profiles, especially Stark broadening parameters.	Plasma diagnostics; solution of radiative transfer problems, especially for high density plasma; plasma modelling.
3.2 Influence of strong magnetic and electric fields on line profiles, emission spectra, and dielectronic recombination.	Plasma diagnostics; solution of radiative transfer problems, especially for high density plasma; plasma modelling.
4. Radiative Excitation, Ionization and Recombination Processes	
4.1 Influence of radiation fields on atomic structure, photon excitation and ionization processes.	Ionization processes in the presence of strong laser radiation fields; plasma modelling.
4.2 Recombination mechanisms: i) radiative ii) dielectronic iii) collisional-radiative	Plasma modelling, energy loss calculations, plasma diagnostics (e.g. satellite lines). Special attention should be given to the influence of strong magnetic fields on the recombination coefficients, and especially on the dielectronic recombination coefficients.

B. Assessment of Data Compilations as Compared to Requirements

In the field of wavelengths and atomic energy data compilations the following principal tabulations are available:

- Atomic Energy Levels, Vols. 1,2,3, published by the NBS, Washington, 1949, 1952, 1959, and supplements on CI - CVI, NI - NVII, OI, HI, DI, TI, SiI - SiIV. Also, a new series of NBS compilations appearing in J. Phys. Chem. Ref. Data: FeI - FeXXVI, CrI - CrXXIV, (MnI - MnXXV in preparation).

- Revised Multiplet Tables, published by the NBS, Washington, 1945.

- Atomic and ionic emission lines below 2000 A, H through Kr, by R.L. Kelly and I.J. Palumbo, Naval Research Laboratory, Washington, 1973.

- Wavelengths and Classifications of Emission Lines, Z 28, by B.C. Fawcett, Atomic Data and Nuclear Data Tables, 16, (1975) 135-164.

Other useful publications are:

- Bibliographies on atomic energy levels and spectra, through June 1975, by NBS, Washington.

- Critical bibliography by Prof. Edlen, Lund University, published in the book "Beam-Foil Spectroscopy", I.A. Sellin and D.J. Pegg, Eds., Plenum Press, 1976.

- Atomic Energy Levels and Grotrian Diagrams, Vol. I, H through P XV by S. Bashkin and J.O. Stoner, Jr., North-Holland, Amsterdam, 1975.

In the field of atomic transition probabilities the following principal tabulations are available:

- Atomic Transition Probabilities Vol. I (H through Ne), Vol. II (Na through Ca) published by NBS, Washington, 1966 and 1969, and supplements on Sc, Ti.

These tabulations are being complemented by the NBS bibliographies on Atomic Transition Probabilities, NBS Spec. Publ. 320, and Supplements I and II. In the field of Line Shapes Data the following principal tabulation exists: Spectral Line Broadening by Plasmas, by H.R. Griem, Academic

Press, 1974. This book is complemented by the NBS - bibliography on Atomic Line Shapes and Shifts, NBS - Spec. Publ. 366, and Supplş. I and II (1972, 1974, 1975). For the other subject areas no critical data compilations exist. However, original work in the field of dielectronic recombination is being done in several laboratories (see e.g. Review Paper A4).

It is the opinion of the members of the Working Group that with respect to the requirements for Fusion Research the aforementioned compilations contain the following serious shortcomings:

- The three major atomic energy data compilations are rather incomplete with respect to the highly ionized heavy atoms. Furthermore, the compilation of Bashkin and Stoner only deals with the light elements up to phosphorus, and that of Kelly and Palumbo goes up to krypton and deals only with wavelengths in the vacuum ultra-violet region. These later compilations rely to a large part on the earlier mentioned atomic energy level compilations.

- Similarly, in the field of atomic transition probabilities the two major compilations are seriously deficient on highly ionized species. Most of the data on such ions have been obtained since then.

- On the subject of line shapes, the book of Griem only contains data for neutral and singly ionized species.

C. Recommendations to IAEA

On the basis of the assessments in Secs. A. and B. the members of the Working Group recommend that experimental and theoretical work on atomic structure centered on highly ionized species of heavy element impurities, as well as the updating and extension of compilations, should be given very high priority. Specifically:

1. Level structure of highly ionized systems

We recommend continued and increased efforts for their investigation. This should be pursued through theoretical calculations and especially through spectroscopic studies of highly ionized plasmas generated for instance in Tokamaks, theta-pinches, laser-produced plasmas, vacuum sparks, and beam foil sources. In particular, a more complete description of atomic energy levels is desirable, which should include the percentage composition of the levels.

2. Wave length compilations

Actual situations require substantial improvement. The description of atomic energy levels in terms of their composition as adopted by the National Bureau of Standards should become standard for the sake of easy comparison of data from different sources.

3. Radial parts of the wavefunctions

We recommend their tabulation further; Slater radial integrals computed by Hartree-Fock methods should be tabulated along with empirically adjusted Slater integrals for use by theoretical groups calculating atomic quantities like transition probabilities and cross-sections. Work of this kind needs accurate wavefunctions and term compositions. It is often of interest to study many members of the same iso-electronic sequence, up to high degrees of ionization. The radial parts of the wavefunctions are needed in simple parametric form to permit easy calculation of radial integrals. Since the tabulation of multiconfiguration wavefunctions for all systems of interest is likely to be costly and typographically impossible, it would be desirable to have available programs ready for use to produce the data requirements.

4. Determination of atomic transition probabilities

In this area the most promising approaches for determining data - primarily theoretical calculations and beam foil spectroscopy - should be vigorously applied. Advanced calculational methods should provide the bulk of the data, with experimental work providing mainly key check points. Since the experiments have not yet reached the area of very highly ionized species of primary interest for fusion plasma diagnostics, special efforts should be made to proceed in this direction. Also, full use should be made of systematic trends and regularities in atomic oscillator strengths. It is very desirable that the data have high accuracy, approaching the 10% level.

5. Compilation of atomic transition probabilities

Their compilations urgently need to be updated and extended to include all ionic species of interest to the fusion research programme. Especially important is an update of the tabulations of the principal light element impurities C, N, O, Al and Si.

6. Line shapes

Theoretical and experimental work should be concentrated on two specific subjects:

6.1 Determination of Stark broadening parameters for highly ionized species, which are especially needed for high-density plasmas generated by lasers.

6.2 Influence of strong magnetic and turbulent electric fields on the profiles of Doppler broadened lines used for ion temperature measurements in lower density plasmas.

7. Stark broadening

Critical data compilations of relevant parameters should be initiated as soon as a significant body of data becomes available.

8. Recombination processes

In this field work should be concentrated on the following four areas:

8.1 Measurement of the intensities and wavelengths of satellite lines due to dielectronic recombination.

8.2 Calculation of recombination rate coefficients, including dielectronic recombination, and their experimental verification.

8.3 As soon as sufficient data are available, a critical compilation should be undertaken.

8.4 Further studies of autoionization, dielectronic and collisional radiative recombination to high Rydberg states in the presence of intense magnetic fields.

REPORT OF THE WORKING GROUP ON SURFACE INTERACTION DATA FOR FUSION DEVICES

Working Group Members

Anderson, Dr. H.H.
Boschi, Dr. A.
Bottiger, Mr. J.
Erents, Dr. S.K.
Krebs, Prof. K.H.
Martinez, Dr. J.
Martynenko, Dr. Yu.V.
McCracken, Dr. G.M. (Chairman)
Nakai, Dr. Y.
Navinsek, Dr. B.
Pocs, Dr. L.
Riccato, Dr. A.
Vernickel, Dr. H.
Waelbroeck, Dr. F.
Watkins, Dr. J.

Introduction

Plasmas in magnetic containment devices are confined for relatively short times so that in any practical system the material walls surrounding the plasma will be subjected to bombardment by energetic ions and atoms, ultraviolet radiation and neutrons. The flux of these particles to the wall will result in the release of impurities into the plasma by a number of mechanisms. These impurities are known to have a deleterious effect on the plasma resulting most importantly in large energy losses by radiation. The input information which is required for surface interaction studies is the flux and energy distribution of the particles to the wall. Such studies aim to provide the fluxes and energies (and other relevant parameters) of the impurities re-entering the plasma. These data can then be used together with data on atomic reaction rates to estimate the concentrations of impurities in the plasma and hence the energy loss rates from the plasma. The data required from the surface physicist is thus dependent on the fluxes arriving at the walls and on the parameters which are relevant to the atomic collision processes of the impurity flux from the wall. Because these different areas are so interdependent, a number of iterative stages will obviously be required before it is clear what are the most important mechanisms for impurity production, and therefore what accuracies are required. Although some estimates of particle fluxes to the wall in reactors may be made on rather general grounds, particle fluxes in contemporary plasma containment devices are not well known.

The present working party has considered the role of surfaces primarily from the point of view of the effects of impurities and of plasma recycling. An equally important aspect is the erosion and radiation damage, which may affect the mechanical integrity of the first wall.

There are both immediate and long term needs for the understanding of first wall interactions. We have considered the materials which are of primary importance and also studied the underlying physics of the surface interaction concerned.

A. Particle Surface Interactions

There are many particle surface interactions which may be relevant to the problems of controlled fusion and these have been outlined in a number of different reports. In our review of the interactions of importance we have relied to a large extent on the Review Paper A2 prepared for the advisory group meeting by Dr. H. Vernickel. In his paper he discusses the role which these processes play in the different types of plasma containment devices. We list below the processes, the energy ranges of the primary particles, and the parameters most of interest. The fluxes of particles to the wall in reactors have been summarized in the proceedings of an earlier IAEA workshop.* Note that hydrogen is used as shorthand for all the hydrogen isotopes.

1. Reflection of hydrogen and helium

Primary energy: 10 eV to 10 keV

Data to be measured: reflection coefficient, energy and angular distributions, charge state, excitation state

Important parameters: angle of incidence, surface structure

2. Accommodation of hydrogen atoms

Primary energy: 1 eV to 100 eV

Data to be measured: accommodation coefficient

3. Trapping of hydrogen and helium

Primary energy: 100 eV to 100 keV (hydrogen), 3.5 MeV (helium)

Data to be measured: trapping coefficient

Important parameters: angle of incidence, temperature, dose, influence of radiation damage

---

* Nuclear Fusion, Special Supplement on Fusion Reactor Design Problems, p. 472, 1974.

4. Detrapping processes for hydrogen and helium

These processes concern thermal and beam induced desorption of trapped gas

Primary energy: 10 eV to 100 keV

Data to be measured: detrapping cross-sections, energy distribution

Important parameters: angle of incidence, target temperature, influence of radiation damage

5. Sputtering by hydrogen, helium, and "impurities"

Energy: from threshold to 100 keV

Data to be measured: yields, angular and energy distribution of sputtered material, chemical composition of sputtered material

Important parameters: angle of incidence, temperature for multi-component surfaces

6. Blistering by hydrogen and helium

Energy: 1 keV to 100 keV (hydrogen) or 3,5 MeV (helium)

Data to be measured: critical dose

Important parameters: energy and angular distributions of incident particles (simultaneous He and H bombardment, see also discussion on synergistic effects)

Most important aspect: does blistering or exfoliation contribute to wall erosion for high dose bombardment, and if so, under what conditions? Yields, size of particles, and composition

7. Desorption by ions (hydrogen, helium, impurities)

Primary energy: from threshold to $\sim$ 100 keV

Data to be measured: cross-section, charge state, excitation state, energy distribution

Important parameters: angle of incidence, surface damage, surface composition

8. Desorption by electrons

Primary energy: from threshold to 100 keV

Data to be measured: cross-section, charge state, excitation state

Important parameters: surface damage, surface composition

9. Desorption by photons

Energy: 5 eV to 100 keV

Data to be measured: cross-section, charge state

Important parameter: surface damage

10. Chemical reactions of hydrogen atoms and ions

Data to be measured: reaction probability

Important parameters: energy of hydrogen atom, surface temperature, effect of surface contamination, flux density of incident particles

11. Secondary electron emission due to ions and electrons

Primary energy: 10 eV to 100 keV

Data to be measured: coefficients

Important parameters: angle of incidence, surface composition

12. Arcing

Little direct evidence of arcing has been published, but both unipolar and power arcs may play a role in the region outside limiters and at divertor targets

13. Energy loss

Energy loss for hydrogen and helium are necessary for theoretical predictions and interpolations concerning the earlier points 1, 2, 4, 5, 6 and 11.

B. Surface Materials of Interest

Since there are so many different criteria determining the wall material it is not always possible to specify the ideal material from the point of view of the surface interactions. Some decoupling of the two requirements for surface interactions and structural materials may be obtained by use of surface coatings or liners. The materials of interest fall into five broad categories.

1. Stainless steels and Inconels

These are of particular interest as being the constructional materials of present generation and the next generation machines, e.g. P.L.T., T.F.T.R., T.10, T.20, J.E.T., J.T.60. The most commonly used alloys are stainless steels 304L and 316LN and Inconel 600 and 625.

2. Refractory materials e.g. Mo, Nb, V, W and alloys

These are used in present machines as limiters and may possibly be used in high temperature commercial reactors. However, the high atomic number (z), particularly of tungsten, and high cost are disadvantages.

3. Low z materials e.g. C, SiC, B_4C, Al_2O_3, Be, BeO, BN

These materials may reduce the total radiation because of their low atomic number and some have been used in tokamaks already with encouraging results. However, chemical effects leading to impurities have been shown to be serious in some cases, e.g. carbon.

4. Trapping materials

In applications where large fluxes of ions have to be pumped, e.g. in divertors, metals which react chemically with hydrogen are being used. Exemples are Ti, Zr.

5. Coatings

This heading covers the use of thin coatings of materials on top of structural materials. These coatings may either be of the materials mentioned above, e.g. low z materials, or of thin metal films. The latter are of interest because in practical devices thin films are produced in the course of operation due to evaporation, sputtering, etc. The wall of many plasma containment devices has been observed to be covered with a layer of molybdenum from the limiter.

C. Characterization of Surfaces

Many of the surface properties of interest are very sensitive to the surface conditions, in particular to surface composition and structure. Thus the importance of surface characterization is emphasized. Three aspects of the problem, can be considered.

1. The source of the materials

Since the composition and structure, particularly of alloys, can vary with manufacturer, a common source of these materials for investigations of surface properties would be very valuable. It is suggested that this might be coordinated through the designers of large machines e.g. T.F.T.R., J.E.T., and T.20 and J.T.60.

2. Surface preparation

The cleaning techniques, both liquid chemical cleaning and discharge cleaning, have an important bearing on the surface composition and hence on surface properties. Discharge cleaning techniques are still at a very empirical stage and the development of these techniques is important. In particular, direct measurements of the efficiency of different techniques and their comparison, is an important element in the surface interaction program. The importance of working on materials characteristic of real plasma devices is emphasized, and efforts should be made to characterize the wall materials in machines after discharge cleaning and operation in order that surface interaction data may be obtained on relevant technological surfaces as well as pure materials.

3. Measurement of composition and structure

The direct measurement of composition and structure of the surfaces on which surface interactions are being studied is important. It was noted that surface composition and structure will change during bombardment by ion beams. This can be particularly important in the case of multi-component alloys where preferential sputtering can take place. Thus the composition may depend on the bombardment dose rate and possibly on the rate of replacement of the preferentially sputtered material from the bulk by thermal or radiation enhanced diffusion.

D. Accuracies

Because of the strongly interactive nature of the plasma and wall processes and the many approximations used in the simulation of the wall, it was not considered possible to give estimates of the accuracies required from computer modelling. Ultimately it is hoped to undertake sensitivity analysis using computer modelling which would allow accuracies to be specified.

Accuracies which should be obtainable experimentally were discussed and the following estimates suggested:

- Particle reflection coefficients (backscattering) $\pm$ 20%
- Energy reflection coefficients $\pm$ 20%

- Sputtering yields
  - when measured for a particular sample of defined preparation and composition ± 10%
  - for materials of the same nominal composition in different laboratories within a factor of 2

It is noted however, that although absolute yields will change due to variations in binding energy the trends with parameters such as energy and angle of incidence should be reproducible to within ± 20%.

- Secondary Electron Emission ± 20%
- Desorption cross-sections ± 50%

An extension of the range of parameters investigated as outlined in Section A, and a more thorough understanding of the fundamental processes are considered to be more important than more accurate measurements.

E. Priorities

The working group did not undertake to formulate a detailed list of priorities. Since there had been a previous study by consultants to the IAEA who included it, their recommendations are listed in Appendix A. It is clear that priorities are to some extent subjective and they will change as new ideas and methods of operation arise. To take an obvious example, if a satisfactory low z wall material is developed, no further data on heavy metals will be required, except for neutral injection. However, within these limitations there were some broad areas in which it was felt that emphasis was required:

- Measurements at low energies < 3 keV
- Data on materials used in next generation machines e.g. stainless steels and inconels as in Section C
- Data on desorption processes and cleaning methods relative to the removal of surface impurities by ions, electrons and photons.

F. Data Compilation and Evaluation

Three stages in theprocess can be distinguished

- Bibliography
- Data compilation
- Data evaluation

Only two attempts to collect data were identified by the working group, these were:

- the Vacuum and Surface Physics Index produced by the IPP Garching, FRG, which produces a monthly bibliography covering the field of interest to fusion, within the wider vacuum field. This is carried out in collaboration with the ZAED and the IUVSTA.* No compilation or evaluation of data is attempted but computer-aided literature searches can be undertaken.

- the Controlled Fusion Atomic Data Centre at ORNL. This annotated bibliographical file includes surface interaction data as well as gas phase atomic collisions. Difficulties have been found in attempting to evaluate surface data since little attention has been paid to surface characterization. Data compilation in some areas of surface interactions have been undertaken.

It was considered that, although many difficulties in evaluating data occur in some areas of surface interactions, data compilation should be relatively straightforward. In particular data for low energy, light ion interactions is relatively limited and so the task of compilation will not be overwhelming. Such a compilation would make clear the extent of scatter of the data and the areas where more data are required. The following surface interactions were those considered to be ones in which it would be possible and useful to carry out compilation and evaluation:

- Sputtering
- Backscattering coefficients
- Desorption cross-sections by ions, electrons and photons
- Thermal desorption of adsorbed gases and release of implanted gas
- Secondary electron emission by ions and electrons
- Stopping power measurements and ranges
- Chemical interaction yields by ions and atoms

Computerization of the data, as in the atomic physics field, should be examined.

G. Special Areas of Surface Interactions

A number of special problems arise in particular techniques. These were not discussed in detail but note was taken that in some cases additional surface data might be required for a full understanding.

---

* IUVSTA = International Union for Vacuum Science Technique and Applications.

1. Pellet injection

It is clear that if pellet injection is used as a method of refuelling plasmas the process of ablation will require investigation. A qualitative idea of the processes involved is probably best acquired by direct observation of ablation in plasmas. However, fundamental data on sputtering and secondary electron emission from solid hydrogen surfaces will be required.

2. Heating techniques

Both r.f. heating and neutral injection may give rise to local particle fluxes and energies much higher than observed in ohmically heated plasmas. In our assessment of the energy range of interest in different phenomena we have tried to include these effects. However, more detailed information on the fluxes and energies to be expected would be valuable. Heavy metal impurities in the beam could be important.

3. Cold gas blanket and gas puffing

The special conditions at the wall, which will be of interest, have not been adequately assessed. They might include recombination phenomena and diffusion into the bulk materials.

H. Conclusions

1. Survey of surface interactions, tabulation of relevant parameters, priorities

Surface interactions of importance in fusion have been surveyed and the processes, energies and other parameters of interest have been tabulated. Assessment of priority areas has been included. Another evaluation of priorities has been examined and there is general agreement with its conclusions.

2. Characterization of surfaces

One of the major problems in assessing surface interaction data is the one of adequately characterizing the surface and proposals have been put forward as to how this situation can be improved. Emphasis has been put on using materials of direct relevance to the fusion programme and on the use of well defined and relevant surface preparation techniques. However, further understanding of the fundamental physics is also required in many areas.

3. Data compilation and evaluation

Despite the difficulties, there are some areas of surface interaction where the underlying physics is well enough understood to make data compilation and evaluation a worthwhile exercise. These areas include sputtering, backscattering, secondary electron emission (by ions and electrons), energy loss measurements, desorption cross-sections (by electrons and ions) and chemical interaction yields. In other areas which include blistering, arcing and synergistic effects, the underlying physics is not well enough understood to make compilation or evaluation very fruitful at the present stage. However, properly annoted bibliographies in these areas are required.

I. Recommendations

It is recommended that

1. The two data centres at present preparing bibliographies in the area of surface interactions (and others if they exist) discuss ways in which the work may be coordinated and possibly integrated. That the IAEA consider playing a role in the dissemination of the bibliographies produced.

2. That compilation and evaluation of data in the field of surface interactions for fusion be initiated by the IAEA starting with the specific areas identified as being suitable.

3. Further assessments of needs and priorities in the surface interaction field should be carried out at regular intervals.

Priority List of Surface Interactions of Importance in Fusion Devices

From the recommendations of a panel of consultants to the IAEA Vienna, November 1975. The indicated priorities and urgencies were estimated by three consultants.

The consultants listed a number of surface effect processes of importance to fusion. Each was rated on its priority and when the information might be available.

Priority: High → 1 Urgency: Near term (0-2 years) → 1
Medium → 2 Medium term (2-4 years) → 2
Low → 3 Long term (4 years) → 3

Process			Priority	Urgency
1.	Sputtering:	(a) Physical; liberation of material due to beam of particles	1,1,1	2,2.5,3
		(b) Chemical; non-momentum transfer	1,1,1	2,2,2.5
2.	Desorption; release of gas by			
		(a) Ions	1,2,2	2,2,3
		(b) Electrons	2,3,3	1,1,3
		(c) Photons	2,2,3	2,3,3
		(d) Thermal effects	1,2,2	1.5,2,3
3.	Blistering by	(a) Alphas (b) Hydrogen isotopes	1.5,2,3	1,3,3
4.	Backscattering		1,2,2	2,2,2
5.	Trapping and release of implanted H and H_2		2,2,2	2,2,2
6.	Pellet refuelling; interaction of ions and electrons with solid H_2		2,2,2	2,3,3
7.	Impurity control; gettering, baking, discharge cleaning		1,1,1	1,2,1
8.	Chemical reactions; as atomic hydrogen on low z materials		1,2,2	2,2,3
9.	Combined effects; as erosion rates of blistering plus large thermal effects		1,1.5,2	3,3,3

Advisory Group Meeting on Atomic and Molecular Data for Fusion

REVIEW TOPICS AND REVIEWERS

Introductory Papers

1. Overall Appraisal of A+M Data for Fusion, Present and Future (M.F.A. Harrison)
2. Proposed IAEA Programme on A+M Data for Fusion (J.J. Schmidt and A. Lorenz, IAEA)

A. Data Needs, Priorities and Accuracies

1. Beam Injection (J.T. Hogan, ORNL, US)
2. Plasma Surface Interaction (H. Vernickel, IPP, FRG)
3. Plasma Modelling (M.L. Watkins, Culham Laboratory, UK)
4. Plasma Impurities and Cooling (H.W. Drawin, Fontenay-aux-Roses, France)
5. Plasma Diagnostics (R.W.P. McWhirter, ARD(SRC) Culham Laboratory, UK)

B. National Programmes and Emphasis

1. France (J.L. Delcroix, Centre d'Orsay)
2. Federal Republic of Germany (F. Waelbroeck, KFA Juelich)
3. Japan (H. Suzuki, Nagoya University, Nagoya)
4. USSR (Yu.V. Martynenko, Kurchatov Institute, Moscow)
5. United Kingdom (M.F.A. Harrison, Culham Laboratory)
6. United States (C.F. Barnett, ORNL)

IAEA Advisory Group Meeting on

Atomic and Molecular Data for Fusion

Culham Laboratory, 1-5 November 1976

Meeting Agenda

Monday, 1 November

- Opening of the meeting
- Welcome on behalf of IAEA: J.J. Schmidt
- Welcome on behalf of Culham: R.S. Pease
- Opening address: Sir Harry Massey
- Meeting organization: A. Lorenz
  - Meeting schedule and organization
  - Appointment of session chairmen and working group chairmen

First presentation session: C.F. Barnett, chairman

- First introductory paper
  "The Role of Atomic and Molecular Processes in Fusion Research", M.F.A. Harrison
- Second introductory paper
  "Proposed IAEA Programme on A+M Data for Fusion", J.J. Schmidt
- Review Paper A1
  "Data Needs, Priorities and Accuracies for Beam Injection", J.T. Hogan
- Review Paper A2
  "Data Needs, Priorities and Accuracies for Plasma Surface Interactions", H. Vernickel
- 1st Contributed Paper to topic A2
  "Blistering of Stainless Steel by He^+ Ions", B. Navinsek
- 2nd Contributed Paper to topic A2
  "Investigation of Sputtering and Secondary Ion Yield from Metals under Bombardment of Noble Gases", H. Krebs
- Review Paper A3
  "Data Needs, Priorities and Accuracies for Plasma Modelling", M.L. Watkins

- First Contributed Paper to topics A3 and A4
  "Survey on the Scattering of Electron by Atoms", C. Joachain

- Panel Discussion of Technical Objectives
  (Drs. Barnett, Afrosimov, Hogan, McCracken and Drawin, panelists and Dr. Harrison, moderator)

Tuesday, 2 November

- Review Paper A4
  "Data Needs, Priorities and Accuracies in Considerations of Plasma Impurities and Cooling", H.W. Drawin

- Second Contributed Paper to topics A3 and A4
  "Cross Section Data Including Atoms and Ions in the Highly Excited Rydberg States", S. Ohtani

- Review Paper A5
  "Data Needs, Priorities and Accuracies for Plasma Diagnostics", R.W.P. McWhirter

- 1st Contributed Paper to topic A5
  "Techniques for the Calculation of Atomic Data Required for Plasma Diagnostics", H.E. Saraph.

- 2nd Contributed Paper to topic A5
  "Measurements of Atomic Transition Probabilities in Highly Ionized Atoms by Fast Ion Beams", I. Martinson

Second presentation session: H. Suzuki

- Review Paper B1
  "National Programmes and Emphasis in France", J.L. Delcroix

- Review Paper B2
  "National Programmes and Emphasis in the Federal Republic of Germany", F. Waelbroeck

- Review Paper B3
  "National Programmes and Emphasis in Japan", H. Suzuki

- Contributed Paper to topic B3
  "Activities on Atomic and Molecular Data in JAERI", Y. Nakai (JAERI)

- Review Paper B4
  "National Programmes and Emphasis in the USSR", Yu.V. Martynenko

- Review Paper B5
  "National Programmes and Emphasis in the United Kingdom"
  M.F.A. Harrison

- Contributed Paper to topic B5
  "(Storage and Retrieval of Bibliographic and Numerical Atomic and Molecular Data at the Queen's University in Belfast)",
  F.J. Smith

- Review Paper B6
  "National Programmes and Emphasis in the USA", C.F. Barnett

- Contributed Paper to topic B6
  "Atomic Physics Program of the Division of Physical Research of ERDA", J.V. Martinez

- Contributed Paper to topic B6
  "Atomic Data Compilation and Evaluation Programmes at NBS",
  W.L. Wiese

- Contributed Paper to topic B6
  "Activities of the Management Research Project at the Lawrence Livermore Laboratory", V. Hampel

- Panel Discussion of Technical Objectives
  (same panelists and moderator as on Monday) and
  organization of working groups

Wednesday, 3 November

- Working group meetings throughout the day

Thursday, 4 November

- Working group meetings. Working groups to finalize their draft reports

- Culham laboratory tour

Friday, 5 November

- Plenary Session: Discussion and Approval of Working Group Reports

IAEA ADVISORY GROUP MEETING ON ATOMIC AND MOLECULAR DATA FOR FUSION

CULHAM LABORATORY, 1-5 NOVEMBER 1976

LIST OF PARTICIPANTS

BOLDEMAN, MR. J.W.
AAEC RESEARCH ESTABLISHMENT
PRIVATE MAIL BAG
SUTHERLAND, N.S.W. 2232
AUSTRALIA

+

JOACHAIN, PROF. C.J.
PHYSIQUE THEORETIQUE
UNIVERSITE LIBRE DE BRUXELLES
CAMPUS DE LA PALINE
CODE POSTALE 227
B-1050 BRUXELLES

+

BOETTIGER, MR. J.
PHYSICAL INSTITUTE
UNIVERSITY OF AARHUS
DK-8000 AARHUS
DENMARK

+

DRAWIN, DR. H.W.
CENTRE D'ETUDES NUCLEAIRES
B.P. NO.6
F-92260 FONTENAY AUX ROSES

+

KREBS, PROF. K.H.
PHYSICS SECTION
APPLIED MASS SPECTROMETRY BRANCH
HUMBOLDT UNIVERSITY
DDR-104 BERLIN
GERMAN DEMOCRATIC REPUBLIC

+

RICCATO, DR. A.
FACHBEREICH PHYSIK
UNIVERSITAET MARBURG
RENTHOF 5
D-355 MARBURG L

+

WAELBROECK, DR. F.
KERNFORSCHUNGSANLAGE JUELICH
G.M.B.H.
POSTFACH 1913
D-5170 JUELICH

+

ARCIPIANI, DR. B.
C.N.E.N.
VIALE REGINA MARGHERITA 125
I-00198 ROMA

+

OHTANI, DR. S.
INSTITUTE FOR PLASMA PHYSICS
NAGOYA UNIVERSITY
NAGOYA, JAPAN

EDER, DR. O.J.
OESTERREICHISCHE STUDIENGES.
FUER ATOMENERGIE
FORSCHUNGSZENTRUM SEIBERSDORF
A-2444 SEIBERSDORF

+

ALCOCK, DR. J.
DIVISION OF PHYSICS
NATIONAL RESEARCH COUNCIL
MONTREAL ROAD
OTTAWA, ONTARIO
K1A 0R6 CANADA

+

HVELPLUND, MR. P.
PHYSICAL INSTITUTE
UNIVERSITY OF AARHUS
DK-8000 AARHUS
DENMARK

+

TWEED, DR. R.
LABORATOIRE DES COLLISIONS
ELECTRONIQUES ET ATOMIQUES
FACULTE DES SCIENCES
UNIVERSITE DE BREST
F-29200 BREST

+

EBEL, DR. G.
ZENTRALSTELLE FUER
ATOMKERNENERGIE-DOKUMENTATION
KERNFORSCHUNGSZENTRUM
D-7514 EGGENSTEIN-LEOPOLDSHAFEN

+

STOECKLIN, PROF. DR.
INSTITUT FUER RADIOCHEMIE
KERNFORSCHUNGSANLAGE JUELICH
POSTFACH 365
D-517 JUELICH

+

POCS, DR. L.
CENTRAL RESEARCH INSTITUTE FOR
PHYSICS
P.O. BOX 49
H-1525 BUDAPEST 114, HUNGARY

+

BOSCHI, DR. A.
C.N.E.N.
VIALE REGINA MARGHERITA 125
I-00198 ROMA

+

SUZUKI, PROF. H.
DEPARTMENT OF PHYSICS
FACULTY OF SCIENCE & TECHNOLOGY
SOPHIA UNIVERSITY
CHIYODA-KU, KIOICHO 7
TOKYO 102, JAPAN

BROUILLARD, DR. F.
UNIVERSITE DE LOUVAIN
INSTITUT DE PHYSIQUE
B-1348 LOUVAIN-LA-NEUVE
BELGIQUE

+

ANDERSEN, DR. H.H.
INSTITUTE OF PHYSICS
UNIVERSITY OF AARHUS
AARHUS
DENMARK

+

DELCROIX, DR. J.L.
LABORATOIRE PHYSIQUE DES PLASMAS
FACULTE DES SCIENCES D'ORSAY
BATIMENT 212
F-91400 ORSAY

+

WERKOFF, DR. F.
CENTRE D'ETUDES NUCLEAIRES
B.P. NO.6
F-92260 FONTENAY AUX ROSES

+

LOTZ, DR. W.
MAX-PLANCK-INSTITUT
FUER PLASMAPHYSIK
D-8046 GARCHING BEI MUENCHEN

+

VERNICKEL, DR. H.
MAX-PLANCK-INSTITUT
FUER PLASMAPHYSIK
D-8046 GARCHING BEI MUENCHEN

+

SHVARTS, DR. D.
N.R.C.N.
P.O. BOX 9001
8490-BEER SHEVA
ISRAEL

+

NAKAI, DR. Y.
DIVISION OF PHYSICS
JAPAN ATOMIC ENERGY RESEARCH
INSTITUTE
TOKAI-MURA, NAKA-GUN
IBARAKI-KEN 319-11, JAPAN

+

DE HEER, DR. F.J.
INSTITUTE FOR ATOMIC AND
MOLECULAR PHYSICS
KRUISLAAN 407
AMSTERDAM (WGM)
THE NETHERLANDS

MARTINSON, PROF. I.
ATOMIC SPECTROSCOPY SECTION
PHYSICS DEPARTMENT
UNIVERSITY OF LUND
SOELVEGATAN 14 B
S-223 62 LUND, SWEDEN

+

BALUJA, DR. K.L.
ROYAL HOLLOWAY COLLEGE
EGHAM HILL
EGHAM, SURREY TW20 OEX
UNITED KINGDOM

+

BRIGGS, DR. J.S.
U.K. ATOMIC ENERGY AUTHORITY
ATOMIC ENERGY RESEARCH
ESTABLISHMENT
HARWELL, DIDCOT.OXON. OX11 ORA
UNITED KINGDOM

+

CARRUTHERS, DR. R.
CULHAM LABORATORY
U.K. A.E.A.
ABINGDON, OXON. OX14 3DB
ENGLAND

+

EISSNER, DR. W.
DEPT. OF PHYSICS AND ASTRONOMY
UNIVERSITY COLLEGE LONDON
GOWER STREET
LONDON WC1E 6BT
UNITED KINGDOM

+

GREEN, DR. T.S.
CULHAM LABORATORY
U.K. A.E.A.
ABINGDON, OXON. OX14 3DB
ENGLAND

+

HARRISON, DR. M.F.A.
CULHAM LABORATORY
U.K. A.E.A.
ABINGDON, OXON. OX14 3DB
ENGLAND

+

HUBLET, DR. M.C.
CULHAM LABORATORY
U.K. A.E.A.
ABINGDON, OXON. OX14 3DB
ENGLAND

+

MARTIN, DR. A.R.
CULHAM LABORATORY
U.K. A.E.A.
ABINGDON, OXON. OX14 3DB
ENGLAND

+

MCDOWELL, PROF. M.R.C.
DEPT. OF APPLIED MATHEMATICS
ROYAL HOLLOWAY COLLEGE
EGHAM HILL
EGHAM, SURREY TW20 OEX
UNITED KINGDOM

+

OTTLEY, DR. T.
DEPARTMENT OF PHYSICS
THE UNIVERSITY
SOUTHAMPTON SO9 5NH
UNITED KINGDOM

WIEDLING, DR. TOR
AB ATOMENERGI
STUDSVIK
FACK
S-611 01 NYKOEPING 1

+

BELL, DR. K.L.
DEPT. OF APPLIED MATHEMATICS
AND THEORETICAL PHYSICS
THE QUEEN'S UNIVERSITY
BELFAST BT7 1NN NORTHERN IRELAND
UNITED KINGDOM

+

BROMAGE, DR. G.E.
SCIENCE RESEARCH COUNCIL
APPLETON LABORATORY
ASTROPHYSICS RESEARCH DIV.
CULHAM, OXFORDSH. OX14 3DB
UNITED KINGDOM

+

CARTER, PROF. G.
DEPARTMENT OF ELECTRICAL
ENGINEERING
THE UNIVERSITY OF SALFORD
SALFORD 5, LANCASHIRE
ENGLAND

+

FAWCETT, DR. B.C.
SCIENCE RESEARCH COUNCIL
APPLETON LABORATORY
ASTROPHYSICS RESEARCH DIV.
CULHAM, OXFORDSH. OX14 3DB
UNITED KINGDOM

+

GREENLAND, DR.P.T.
THE DARESBURY LABORATORY
DARESBURY WARRINGTON
CHESHIRE WA4 4AD
UNITED KINGDOM

+

HEDDLE, PROF. D.W.O.
DEPARTMENT OF PHYSICS
ROYAL HOLLOWAY COLLEGE
EGHAM HILL
EGHAM, SURREY TW20 OEX
UNITED KINGDOM

+

JONES, DR. E.M.
CULHAM LABORATORY
U.K. A.E.A.
ABINGDON, OXON. OX14 3DB
ENGLAND

+

MASSEY, SIR HARRY
THE ROYAL SOCIETY
6 CARLTON HOUSE TERRACE
LONDON SW1Y 5AC
ENGLAND

+

MCWHIRTER, DR. R.W.P.
SCIENCE RESEARCH COUNCIL
APPLETON LABORATORY
ASTROPHYSICS RESEARCH DIV.
CULHAM, OXFORD OX14 3DB
ENGLAND

+

PEASE, DR. R.S.
CULHAM LABORATORY
U.K. A.E.A.
ABINGDON, OXON. OX14 3DB
ENGLAND

MARTYNENKO, DR. YU. V.
INSTITUT ATOMNOI ENERGII
I.V. KURCHATOVA
46 ULITSA KURCHATOVA
MOSCOW D-182, U.S.S.R.

+

BOTTCHER, DR. C.
THE DARESBURY LABORATORY
DARESBURY WARRINGTON
CHESHIRE WA4 4AD
UNITED KINGDOM

+

BROOK, DR. E.
CULHAM LABORATORY
U.K. A.E.A.
ABINGDON, OXON. OX14 3DB
ENGLAND

+

DOLDER, PROF. K.T.
DEPARTMENT OF ATOMIC PHYSICS
SCHOOL OF PHYSICS
NEWCASTLE UPON TYNE
NE1 7RU
ENGLAND

+

GILBODY, PROF. H.B.
DEVELOPMENT OF PURE AND
APPLIED PHYSICS
QUEENS UNIVERSITY
BELFAST 7
NORTHERN IRELAND BT7 1NN, U.K.

+

HARBOUR, DR. P.J.
CULHAM LABORATORY
U.K. A.E.A.
ABINGDON, OXON. OX14 3DB
ENGLAND

+

HOTSTON, DR. E.
CULHAM LABORATORY
U.K. A.E.A.
ABINGDON, OXON. OX14 3DB
ENGLAND

+

LANG, DR. J.
SCIENCE RESEARCH COUNCIL
APPLETON LABORATORY
ASTROPHYSICS RESEARCH DIV.
CULHAM, OXFORDSH. OX14 3DB
UNITED KINGDOM

+

MCCRACKEN, DR. G.M.
CULHAM LABORATORY
U.K. A.E.A.
ABINGDON, OXON. OX14 3DB
ENGLAND

+

OEPIK, DR. U.
DEPT. OF APPLIED MATHEMATICS
AND THEORETICAL PHYSICS
THE QUEEN'S UNIVERSITY
BELFAST BT7 1NN NORTHERN IRELAND
UNITED KINGDOM

+

PEJCEV, MR. V.
DEPARTMENT OF PHYSICS
THE UNIVERSITY
SOUTHAMPTON SO9 5NH
UNITED KINGDOM

POSPIESZCZYK, DR. A.
CULHAM LABORATORY
U.K. A.E.A.
ABINGDON, OXON. OX14 3DB
ENGLAND

+

ROSS, DR. K.J.
PHYSICS DEPARTMENT
UNIVERSITY OF SOUTHAMPTON
SOUTHAMPTON SO9 5NH
UNITED KINGDOM

+

SERIES, PROF. G.W.
DEPARTMENT OF PHYSICS
UNIVERSITY OF READING
READING RG6 2AF, BERKSHIRE
UNITED KINGDOM

+

STEPHENS, DR. K.G.
DEPARTMENT OF ELECTRICAL
ENGINEERING
UNIVERSITY OF SURREY
GUILDFORD, SURREY GU2 5XH
UNITED KINGDOM

+

TAIT, DR. J.H.
U.K. ATOMIC ENERGY AUTHORITY
ATOMIC ENERGY RESEARCH
ESTABLISHMENT
HARWELL, DIDCOT.OXON. OX11 ORA
UNITED KINGDOM

+

WHITE, DR. M.
DEPARTMENT OF PHYSICS
THE UNIVERSITY
SOUTHAMPTON SO9 5NH
UNITED KINGDOM

+

BARNETT, DR. C.F.
HOLIFIELD NATIONAL LABORATORY
P.O.BOX Y
OAK RIDGE, TENNESSEE 37830
U.S.A.

+

HOGAN, DR. J.T.
BLDG. 9201-2, MS 2
OAK RIDGE NATIONAL LABORATORY
P.O. BOX Y
OAK RIDGE, TN 37830
U.S.A.

+

NAVINSEK, DR. B.
INSTITUT JOSEF STEFAN
P.O. BOX 199-4
YU-61001 LJUBLJANA

+

JOHNSTON, DR. P.
NEA NEUTRON DATA COMPILATION
CENTRE
B.P. NO.9
F-91190 - GIF-SUR-YVETTE

RIVIERE, DR. A.C.
CULHAM LABORATORY
U.K. A.E.A.
ABINGDON, OXON. OX14 3DB
ENGLAND

+

ROWLANDS, MR. J.L.
ROOM 220
BUILDING 821
AEE WINFRITH
DORCHESTER, DORSET
UNITED KINGDOM

+

SMITH, DR. A.C.H.
UNIVERSITY COLLEGE
GOWER STREET
LONDON WC1
ENGLAND

+

STRONG, DR. R.
DEPARTMENT OF PHYSICS
UNIVERSITY OF SUSSEX
BRIGHTON BN1 9QH
UNITED KINGDOM

+

TAYLOR, DR. A.J.
U.K. ATOMIC ENERGY AUTHORITY
ATOMIC ENERGY RESEARCH
ESTABLISHMENT
HARWELL, DIDCOT.OXON. OX11 ORA
UNITED KINGDOM

+

WOODING, DR. E.
ROYAL HOLLOWAY COLLEGE
EGHAM HILL
EGHAM, SURREY TW20 0EX
UNITED KINGDOM

+

DECKER, DR. J.
DIVISION OF MAGNETIC
FUSION ENERGY
ENERGY RES. & DEVELOP. ADMIN.
WASHINGTON, D.C. 20545
U.S.A.

+

MARTINEZ, DR. J.
NUCLEAR SCIENCE
DIVISION OF PHYSICAL RESEARCH
U.S. ENERGY RES.& DEVELOP.ADMIN.
WASHINGTON, D. C. 20545
U.S.A.

+

LORENZ, MR. A.
NUCLEAR DATA SECTION
IAEA

+

ROSE, DR. B.
NUCLEAR PHYSICS DIV., HANGAR 8
ATOMIC ENERGY RESEARCH
ESTABLISHMENT
HARWELL,DIDCOT,OXON. OX11 ORA
UNITED KINGDOM

+

SARAPH, DR. H.E.
DEPT. OF PHYSICS AND ASTRONOMY
UNIVERSITY COLLEGE LONDON
GOWER STREET
LONDON WC1E 6BT
ENGLAND

+

SMITH, DR. F.J.
COMPUTER CENTRE
QUEEN'S UNIVERSITY
BELFAST, B17 1NN
NORTHERN IRELAND
UNITED KINGDOM

+

SUMMERS, DR. H.P.
DEPT. OF APPLIED MATHEMATICS
AND THEORETICAL PHYSICS
UNIVERSITY OF CAMBRIDGE
SILVER STREET
CAMBRIDGE, ENGLAND

+

WATKINS, DR. M.L.
CULHAM LABORATORY
U.K. A.E.A.
ABINGDON, OXON. OX14 3DB
ENGLAND

+

WOODRUFF, DR. P.R.
CULHAM LABORATORY
U.K. A.E.A.
ABINGDON, OXON. OX14 3DB
ENGLAND

+

HAMPEL, MR. V.
LAWRENCE LIVERMORE LABORATORY
L-380
P.O. BOX 808
LIVERMORE, CALIFORNIA 94550
U.S.A.

+

WIESE, DR. W.L.
NATIONAL BUREAU OF STANDARDS
WASHINGTON, D.C. 20234
U.S.A.

+

SCHMIDT, DR. J.J.
NUCLEAR DATA SECTION
IAEA

+

ADDRESS OF WELCOME

Dr R S Pease
DIRECTOR

Euratom-UKAEA Association for Fusion Research, Culham Laboratory
Abingdon, Oxfordshire OX14 3DB, UK.

My first task is to welcome the IAEA Advisory Group Meeting to Culham and to make sure that those attending are comfortable and happy and have an interesting and instructive week. It is naturally a great pleasure for me to see so many distinguished colleagues and friends from overseas.

I must confess to a certain element of responsibility for the negotiations that have led to this conference. The position is that fusion experiments are, as a matter of routine, now reaching electron temperatures of $10M^{o}K$ and maintaining these for confinement times of 1s, the product of density and confinement time, $n\tau$, being greater than 10^{12} $cm^{-3}s$. A rich crop of impurities species is found and these impurities have a significant effect on the plasmas. Perhaps the simplest process is the radiation of appreciable amounts of energy, but there are many subtle effects of significance which I hope will be explored. Appreciable amounts of data are required in order to predict what will happen for each impurity species: data on spectra, ionization rates by electrons as well as by photons and other ions, recombination rates (both two- and three-body), charge exchange and so forth. Moreover, data for negative ions and some molecular species are likely to be

of importance.

To put the problems in perspective we should note that for fusion reactions to occur it is necessary to have a region of hot, fully ionized gas but between this region and the laboratory environment there must exist cooler regions. The situation is somewhat analogous to the D, E and F layers between the earth and the solar corona. These cooler regions are present in the throat of divertors, or close to surfaces in magnetic confinement experiments. An alternative route to fusion power may be via laser compression and such experiments pose a new range of atomic physics problems related to both high temperature and high density. With such a wide range of plasma environments and contaminants it is likely that some 5,000 atomic and molecular species are involved.

To many in the fusion community it seemed that some form of central data bank would be of great value to our work. To date we have relied upon the valuable compilations provided by C W Allen, S Brown and C F Barnett, but something more extensive is required to handle 5,000 species. For many years the I.A.E.A. have provided a central service for the dissemination of neutron data and it was natural for us to approach them with our problems. As a consequence, approval has been obtained for the formation of a section of the I.A.E.A. to deal with atomic and molecular data for fusion. This section is under the direction of Dr. J J Schmidt and it is the purpose of this Advisory Group Meeting to provide Dr Schmidt and his colleagues in Vienna with a good basis for planning and executing the first stages of this data service.

At present there exists a great breadth of both experimental and theoretical knowledge of atomic and molecular processes per se. Also workers in ionospherics, astrophysics and solar physics have accumulated extensive data, much of it relevant to fusion. Such data should be presented to the fusion

researcher in a form related to the particular problems of fusion. To achieve these aims the specialist skills in data bank handling and critical assessment developed by Dr. Schmidt and his colleagues will be of great value.

There is one matter of special significance: with 5,000 species and several different processes for each specie, the task of simply collating experimental data is both enormously expensive and time-consuming; moreover it is very inelegant. It is now over 60 years since quantum mechanics were first applied to atomic systems and we must by now be able to do a great deal with the aid of theoretical estimates. A central point of guidance is required, namely what can be done by theory, especially in relation to extrapolation and interpolation. In my view, the service that the I.A.E.A. can provide will turn crucially on the ability to use and critically underline the theoretical formulae. I am therefore particularly grateful to Sir Harrie Massey for taking an interest in this work and coming down to the conference.

Let me conclude by reiterating how pleased we are to see you, and what an interesting and important job there is to be done, and I hope you will enjoy the week as much as I am sure my colleagues from Culham will.

INTRODUCTORY PAPERS

Introductory Paper 1

The Role of Atomic and Molecular Processes in Fusion Research

M F A Harrison

Euratom-UKAEA Association for Fusion Research, Culham Laboratory
Abingdon, Oxfordshire OX14 3DB, UK.

Abstract

This paper considers the relevance of atomic and molecular processes to research into controlled nuclear fusion and in particular their effects upon the magnetically confined plasma in Tokamak experiments and conceptual Tokamak reactors. The relative significance of collective phenomena and of single particle collisions to both plasma heating and loss processes are discussed and the pertinent principles of plasma refuelling and plasma diagnostics are outlined. The methods by which atomic and molecular data are applied to these problems, the contributing effects of surface interactions and the consequent implications upon the accuracy and the type of data needed are described in a qualitative manner. Whilst particular atomic and molecular processes are not discussed in detail, sufficient information is given of the physical environments of Tokamak devices for significant processes to be self evident.

1. INTRODUCTION

For two decades research into sources of controlled thermonuclear energy has been a major factor in stimulating studies of atomic and molecular processes. Nevertheless the diverse and changing aspects of fusion research make it difficult for workers outside the field to keep abreast with its needs for atomic and molecular data. Thus a major aim of this paper is to discuss present day fusion devices and envisaged reactor systems from the standpoint of atomic and molecular processes. There are four potentially suitable fusion reactions embracing the lighter elements, but the process,

$$D + T \rightarrow {}^{4}He\ (3.52\ MeV) + n\ (14.06\ MeV),$$

reaches significant rates of reaction at the lowest temperature, namely 4 to 5 keV, and the neutrons from this process are likely to be the main source of power in early fusion reactors. At this temperature the D-T mixture is a fully ionized plasma and most of the alpha particles will be confined within the reactor depositing their energy as they slow down, firstly to the electrons and secondly to the ions. The neutrons will pass into a lithium blanket where tritium will be bred. The predominant reaction is exothermic, namely,

$$^{6}Li + n \rightarrow {}^{4}He + T + 4.80\ MeV,$$

so that the total neutron energy per fusion collision is about 19 MeV. The neutron energy will be converted into heat and some of the thermal energy must be fed back into the plasma to maintain its energy density $(3nk(T_e + T_i)/2)$. Here n and T are the density and temperature of the plasma and the subscripts e and i refer to electrons and ions. At reactor temperatures the main energy loss process is bremsstrahlung radiation due to free-free collisions between electrons and ions and the plasma must be confined for a time τ_c before the time integrated energy from the fusion reaction exceeds this loss. The assumptions of 30 to 40% for the thermal conversion plus feed back efficiencies, $n_e = n_i = n$, $T_e = T_i = T$ and the ionic charge Z = 1, leads to the well known Lawson Criterion for breakeven conditions, namely, $n\tau_c = 10^{14}\ cm^{-3}s$ and T = 10 to 15 keV.

The methods which presently seem most appropriate to produce these conditions are, (a) magnetically confined plasmas and (b) laser-driven, compressively heated, pellet systems. The magnetically confined plasmas

consist of either open ended systems (mirror devices) or closed line systems (toroidal devices); they may be subdivided into low β and high β systems where $\beta = 2\ nkT/(B^2/8\pi)$ is the ratio of kinetic pressure of the plasma to the pressure of the confining magnetic field B. Various reactor concepts arising from these basic approaches have recently been reviewed by Ribe [1]. Although no uniquely suitable route to a reactor has yet been established, the Tokamak is presently viewed with particular favour and is the predominant subject for plasma physics research and reactor systems studies. It is moreover a system which is rather sensitive to atomic and molecular processes and is described here in some detail to provide a framework against which such processes can be assessed. In addition, a detailed consideration of the Tokamak and its ancillary equipment will identify most of the atomic and molecular processes presently relevant to fusion.

We may start by a broad classification of processes. Firstly there are those essential to the operation of the fusion device. These relate to:- (a) energy and particle losses from the plasma; (b) the introduction of impurities other than hydrogen isotopes and the elimination of such impurities; (c) damage to the confining vessel and recycling of contaminants; (d) heating of the plasma via energy feedback mechanisms and (e) refuelling of the plasma. Secondly there are important peripheral needs for atomic and molecular data and these relate largely to diagnostic requirements such as spectroscopy and to probes which operate with either emitted or transmitted particles. Atomic collision processes associated with the development of lasers are not regarded as pertinent to this paper but they are nevertheless very important aspects of present and future fusion research.

It should be stressed that a full understanding of fusion devices can only come from interactive assessments of fields such as surface processes, free-free and free-bound collisions coupled to plasma collective phenomena.

2. TOKAMAK EXPERIMENTS AND REACTOR CONCEPTS

2.1 General characteristics

The Tokamak is a diffuse toroidal pinch device; it has closed magnetic field lines and low β. The plasma is formed into a ring of major radius R and minor radius r as is shown schematically in Figure 1. A current I_ϕ is induced to flow in the plasma in the toroidal direction and this current generates a poloidal magnetic field B_θ which contains the plasma pressure. Invoking the pressure ratio β_θ and using units of G, A

and cm, we have,

$$2nkT = \frac{\beta_\theta B_\theta^2}{8\pi} = \frac{\beta_\theta I_\phi^2}{200\ \pi\ r^2} \quad .$$

A plasma subject solely to a poloidal magnetic field is unstable and so a toroidal magnetic field B_ϕ is applied parallel to the axis of plasma by means of external windings. The field lines resulting from B_θ and B_ϕ form helices around the axis of the plasma as is shown by the arrow in Figure 1. These helices define the orbits of the guiding centres of the confined particles.

The general conception of the device and its operating procedure can also be understood from Figure 1. The vacuum vessel of minor radius, a, passes through a symmetrically distributed set of toroidal field windings used to generate B_ϕ (only two of these coils are shown). After this field is switched on, gas is introduced into the torus and pre-ionized by a pulsed or RF discharge. The ionized gas is confined by the B_ϕ field and forms an electron conducting ring which serves as the secondary winding of a transformer to whose primary a large pulsed current is now fed. The current I_ϕ is thus induced to flow in the plasma with two results, firstly it generates the poloidal B_θ magnetic field and secondly it heats the plasma because the driven electrons collide with and so heat the ions. This Ohmic heating power density is given by $P_\Omega = \eta j^2$ where η is the plasma resistivity and j is the current density (here in A cm^{-2}). Following Spitzer [2] we have,

$$P_\Omega = 5.2 \times 10^4\ j^2\ Z\ \chi\ \ell n\ \Lambda\ (T_e)^{-3/2}\ (\text{ergs}\ s^{-1}\ cm^{-3}) \qquad (1)$$

where Λ is the ratio of the Debye shielding length to the minimum impact parameter for electron - ion Coulomb collisions (10 to 20 in fusion plasmas) and T_e is in eV. The dimensionless factor χ allows for non-classical collective effects which increase η above the classical "Spitzer" value and Z is the ionic charge in units of e.

The confinement time is finite and so energy and also particles are continuously lost from the plasma. In a closed system the only losses of charged particles can be from radial diffusion of electrons and ions across the magnetic field. This also results in the loss of the energy carried by particles. Photon losses arise from the emission of bremsstrahlung radiation from the bulk plasma and from line radiation emitted by any atoms or non-stripped ions present. Plasmas in low β devices are optically thin and so

most of the emitted photons can reach the walls. Particle losses also occur due to neutralisation of the plasma ions, predominantly through charge exchange collisions of H^+ on H (or of their isotopes). For most processes the vacuum wall can be regarded as a sink for photons and for particle energy and charge (but not necessarily for neutral particles). Thus boundary conditions are imposed upon the plasma which, coupled with the finite size and axial symmetry of the plasma and with plasma current criteria for stability result in profiles of temperature, density and current that are peaked on the axis of the torus. An example of typical profiles for a present day device are shown in Figure 2, they are taken from the calculations of Hogan and Clarke [3] for the ORMAK Tokamak at Oak Ridge. T_e falls more steeply than n_e and of course $T_e > T_i$ is a necessary requirement for Ohmic heating. Peak values of T_e in most present day devices are about 1 keV and those of n_e about 2 to 4.10^{13} cm^{-3}. I_ϕ ranges from 100 to 250 kA, and the B_ϕ fields are in the region of 20 to 40 kG.

2.2 Limiters and divertors

The plasma radius is restricted to a minor radius $r < a$ by an orfice plate termed a "limiter" (r presently ranges from 10 to 25 cm). On account of the helical nature of the particle orbits the limiter need not completely encircle the plasma and is often formed by a rod which projects into and skims off the outside of the plasma (in a manner anologous to turning by a lathe). In more sophisticated experiments and in reactor concepts the limiter action is performed magnetically by external windings that oppose and annul the B_θ field at one or two azimuthal positions so that all field lines within a surface defined by r_s are closed and all field lines outside r_s intersect the vacuum vessel. The open field lines are directed into specially shaped differentially pumped regions of the vacuum vessel where the unconfined plasma can be neutralised and its products pumped away. The surface defined by r_s is termed the 'separatrix' and the unconfined plasma is termed the "scrape-off" plasma. In Figure 1 a torus with a single neutral point poloidal divertor is sketched out and the separatrix indicated. The advantages of the magnetic limiter/divertor concept are firstly that plasma diffusing radially outwards across the separatrix is directed into the divertor and hence does not impact upon the walls and so cause the release of atoms or molecules of impurities. Secondly such neutral species near to the torus walls (and this could include in a reactor the helium from neutralised alpha particles) will, in principle, be ionized in the scrape-off plasma and swept into the

divertor region rather than pass over the separatrix and into the high temperature confined plasma. An alternative divertor concept is the bundle or non-axisymmetric toroidal divertor. In this concept some of the lines of the B_ϕ field are bulged outwards, directed into a divertor region and then back into the torus; the DITE device at Culham utilizes this approach.

2.3 Atomic scale lengths, impurity ions and recycling

Present day Tokamaks are sized to comply with the characteristic lengths of plasma processes. The equivalent scale lengths of atomic processes are in general appreciably larger and this discrepancy has a bearing upon the performance of the device. As an example let us consider the fate of H_2 molecules present near to the torus wall. Most of these molecules will be ionized by electron impact in the outer region of the plasma giving rise to H_2^+ ions which have essentially the same thermal energy as their parent molecules. The orbits of these H_2^+ ions will follow the magnetic field lines and, unless directed into a divertor, the molecular ions will be dissociated by further electron impact $\left[H_2^+ + e \rightarrow H^+ + H + e\right]$ giving rise to H atoms with appreciable kinetic energies ($\gtrsim$ 5 eV). These H atoms released near the walls can penetrate the plasma to a significant depth before being ionized mainly by electron impact and to a lesser extent by charge exchange. The scale length for the electron impact ionization process $\left[H + e \rightarrow H^+ + e + e\right]$ can be expressed as $\langle v_H \rangle / n_e \langle \sigma_H(v_e) v_e \rangle$ where $\sigma(v_e)$ is the ionization cross section and the brackets denote averaging over the velocity distributions. In the outer region of present day plasmas this length is about 10 cm and is hence comparable to r. A typical consequence can be seen in Figure 2 where the profile of the neutral H density, n_o, calculated in [3] is shown. The presence of these H atoms in the higher temperature regions of the plasma causes neutralisation of protons through charge exchange $\left[H + H^+_{(T_i)} \rightarrow H^+ + H_{(T_i)}\right]$ and so fast H atoms are produced with velocities corresponding to T_i. These fast atoms formed within the plasma have even larger scale lengths and can reach the walls even in quite dense plasmas. Impact of fast H atoms on the walls causes sputtering of high Z metallic wall material and, together with energy transported by charged particles and photons to the walls, causes emission of any occluded H_2 or other impurity gases such as O_2 and CO from the walls. The release of molecules such as H_2 can have a yield of several molecules per incident atom so that a recycling process can be set up. Even when the device has a divertor (for example DITE) the scrape-off plasma is relatively

thin ($\gtrsim$ 5 cm) so that the inward neutral atom flux will not be greatly attenuated in present day devices. The over-riding reason for these dimensional inadequacies is economy in size due to the high cost and long building time associated with large volume and high intensity magnetic fields. In reactors, r must become several metres so these particular problems of charge exchange will be less significant. However in the higher temperature plasmas of reactors the power losses due to bremsstrahlung radiation (insignificant at present) will be dominant; these are proportional to Z^2 and so the presence of even small numbers of impurity ions with $Z > 1$ will make significant demands upon heating power.

2.4 Plasma heating

Criteria for plasma confinement together with technical and economic restraints all impose limitations upon the power available from Ohmic heating. One such is that the ratio of plasma to poloidal magnetic field pressures must not exceed the aspect ratio $A = R/r$. Since

$$\beta_\theta = \frac{R}{r} = \frac{400\ nkT}{\pi\ j^2\ r^2}$$

and $r \gtrsim a$, it follows from equation (1), when allowance [4] is made for realistic radial distributions of j, n and T and for non-classical effects, that,

$$T \lesssim 9.2.10^8\ A\ \frac{I_\phi^{\,2}}{na^2} \quad . \quad (eV)$$

Thus the temperature is both density and geometry dependent. A second stability constraint is related to the pitch of the resultant field lines arising from B_θ and B_ϕ (shown by the arrow in Figure 1). The ratio of this pitch to the circumference of the plasma ($2\pi R$) should be greater than about 2 to 3 at the edge ($r \gtrsim a$) of the plasma and a "stability margin", q, is defined as

$$q(a) = \frac{a}{R}\ \frac{B_\phi}{B_\theta} = \frac{5\ B_\phi}{\pi\ R}\ \frac{1}{j}$$

For commercially viable reactor systems B_ϕ is some 50 to 100 kG and R is 10 m to 15 m, (1 to 2 m in present day experiments) so that j lies in region 50 to 100 A cm^{-2} in reactors and is about 100 to 250 A cm^{-2} in present day experiments. The magnitudes of the magnetic field and the minor radius of a reactor must of course be adequate for the confinement

of alpha particles so that these can eventually heat the plasma. The aspect ratio is about 3 to 5 and for reactors, $I_\phi \gtrsim 6$ to 20 MA is conceived of, and present experiments operate at some 0.1 to 1.0 MA.

The consequence of these various constraints is that Ohmic heating alone will not raise the plasma temperature above some 3 keV which is not adequate to produce effective alpha particle heating. Thus it is necessary to provide additional heating before either the energy and particles of the plasma are lost or the pulsed current in the transformer primary has decayed. Three methods of heating are being considered; (a) to feed in RF power and so heat the electrons, (b) to perturb the B_ϕ field and so compress the plasma and (c) to feed in high energy particles which must be neutral in order to pass through the confining magnetic field. Neutral beam injection is presently the most favoured approach and the concept is illustrated in Figure 1. Molecular hydrogen (deuterium and maybe D_2-T_2 mixtures in reactors) is ionized in a source and the emerging beam containing H^+, H_2^+ and H_3^+ accelerated to some 50 to 100 keV and then passed through a gas target. Collisions such as charge exchange with the target gas (see Section 4) produce substantial numbers of fast neutral atoms which then traverse the magnetic field and enter the plasma. These injected atoms (H_{in}) are ionized predominantly in collisions with the plasma protons, the processes being charge exchange and proton impact ionization $\left[H_{(in)} + H^+_{(T_i)} \rightarrow H^+_{(in)} + e + H^+_{(T_i)}\right]$. The resultant fast ions are trapped within the magnetic field and give up their energy to both electrons and plasma ions as they slow down. The optimum beam energy and atomic species are discussed in [4 and 5] and the atomic processes relevant to injection are considered in Section 4 of this paper. Beam power requirements are formidable and lie in the MW range.

2.5 The effective ion charge

The presence of impurity ions affects plasma heating because the resistivity depends upon the effective ionic charge, $\eta \propto Z_{eff}/T_e^{3/2}$. The toroidal loop voltage is $V = j\eta\, 2\pi R$ and the Ohmic power density is $(j\eta)^2/\eta \propto (V/2\pi R)^2\, T_e^{3/2}/Z_{eff}$. Thus the electron temperature depends upon the ability of the external circuits to sustain either V or j . The effective charge can be expressed as,

$$Z_{eff} = \frac{1 + \sum_{ii} (n_{ii}/n_i) Z^2_{ii}}{1 + \sum_{ii} (n_{ii}/n_i) Z_i},$$

where n_{ii} and Z_{ii} are the density and charge of the impurity ions and the

summation is over all available charge states. Thus it can be seen that small concentrations of impurities, such as fully stripped oxygen where $Z_{ii}^2 = 64$, can substantially effect Ohmic heating. This is even more marked for high Z impurities such as metallic ions (Fe, Mo, W in present devices, Nb, V and other neutron compatible elements in reactors) which, although not fully stripped, can be very highly ionized with $T_e \gtrsim 10$ keV.

2.6 Trapping of impurity ions

Another property of ions with atomic mass M_{ii} and charge Z_{ii} greater than the plasma ions, i.e. $Z_{ii} > 1$, $M_{ii} > 1$ or (2 and 3), is that such ions will generally diffuse inwards against the radial density gradient of plasma [6]. Thus impurities move inwards becoming more highly charged as they reach regions of smaller r and higher T_e and n_e. Low Z elements such as C and O become fully stripped and, unless gradients in T_e prohibit this inward diffusion, become trapped on the axis of the toroid. The same mechanism is also likely to drive He^{++} onto the axis as alpha particles from fusion reactions cool and their energy approaches T_i. Thus a fusion reactor is liable to fill up with unreactive burnt fuel and so a continuously operating device is difficult to envisage although re-distribution of He^{++} ions through effects such as plasma turbulence may mitigate against this problem.

Tokamak reactor concepts [1] envisage the following generalised type of operational cycle; (a) pre-ionization of the neutral D-T mixture, (b) Ohmic heating, (c) neutral injection heating, (d) fusion burn with alpha particle heating, possibly augmented by neutral injection and some form of refuelling and finally (e) controlled release of a cooled confined plasma by combinations of magnet field perturbation and injection of impurities followed by exhaust of its neutral products. Reactor cycles range from 600 to 6,000s duration. Present day experiments embrace only (a) and (b) and last about 0.1 to 0.3s.

2.7 Refuelling

Refuelling of fusion devices is probably the least well developed subject. The introduction of fuel should not perturb conditions necessary for plasma stability nor the thermonuclear reaction rates. Thus the fuel should penetrate the plasma and become ionized near to the poloidal axis. Compared to reactor dimensions the mean free path for ionization of thermal energy D-T molecules within the plasma is small and so fast neutral injection has been considered. However unless the injection energy

is very high the particle range is still insufficient to reach the axis of a reactor ($r \gtrsim 3$ m). For example 50 keV protons have a range of some 50 cm in a plasma with $n \gtrsim 10^{14}$ cm^{-3}. Thus neutral atom beam energies in the MeV range are considered although such beams require significant fractions of reactor output power. An alternative suggestion is to fire in high velocity pellets of frozen D-T. Once inside the plasma these pellets are bombarded by electrons and ions and rapidly ablate. A dense atmosphere of D-T mixture is formed around the pellet in which incident particles are slowed down. Equilibrium conditions should be reached when the energy carried by the incident particles to the pellet surface maintains this atmosphere at plasma pressure (which will be $\gtrsim 15$ atm within a reactor) against losses into the plasma. Provided the pellet velocity is sufficiently high it may penetrate deeply into the plasma and hopefully release most of its fuel near to the axis. Atomic processes are obviously of considerable importance and relate to interactions and ranges of 10 keV electrons, deuterons and tritions incident upon the high density D_2 - T_2 atmosphere. The problem is further complicated because the lack of spherical symmetry of the magnetic field will probably cause the pellet atmosphere to expand rapidly in the toroidal direction and so reduce the penetration depth of the pellet.

3. ATOMIC PROCESSES WITHIN THE TOKAMAK PLASMA

3.1 Energy balance

Energy balance in the plasma is maintained by both collective plasma interactions and by atomic collision processes. The collective processes are:-

(a) Convective transport; which comprises the energy carried by the particles as they diffuse radially across the magnetic field due to the gradient in plasma density. The ions are less well confined than the electrons and, since both must move together to maintain charge neutrality, it is the electrons which control the rate of this diffusion process.

(b) Thermal conduction transport; both electrons and ions transport energy radially across the magnetic field due to the radial gradient in their temperatures.

(c) Electron-ion energy transfer; since the electrons are generally at a higher temperature than the ions they transfer energy to the latter by

the process of electron-ion Coulomb collisions and without external sources of energy they would cool so that T_e approaches T_i.

(d) The electrons gain energy from Ohmic heating as defined in equation (1). Other forms of heating either by particle injection or by alpha particles from the fusion reaction are not considered here, but both interact in a similar manner to the role of the electrons in (c), see Section 4.

The predominant free-free radiation loss processes at reactor temperatures is bremsstrahlung radiation. However at temperatures in excess of 20 keV, synchrotron radiation emitted by the electrons orbiting in the magnetic field can become dominant for low density and low β plasmas. The effects of atomic processes upon the plasma are conveniently considered through their contributions to both the above particle and energy losses.

3.2 Electron collisions

The balance between the plasma processes and electron collision processes during the Ohmic heating phase can be expressed, as for example in [7], by considering the power flow per unit length, p(r), within a thin toroidal shell of minor radius r and thickness dr,

$$\frac{p(r)}{2\pi r dr} = \frac{1.6 \times 10^{-12}}{r} \frac{d}{dt}\left(\frac{3}{2} n_e T_e\right)$$

$$= \frac{1.6 \times 10^{-12}}{r} \frac{\partial}{\partial r}\left(\frac{3}{2} r D T_e \frac{\partial n_e}{\partial r} + n_e r D \frac{T_e}{(T_e + T_i)} \frac{\partial T_e}{\partial r}\right)$$

$$\left[\text{——— (a) ———}\right] + \left[\text{——— (b) ———}\right]$$

$$- 2.4 \times 10^{-9} \frac{n_e^2 Z^2 \ell n \Lambda}{M} \frac{(T_e - T_i)}{T_e^{3/2}} + 5.34 \times 10^4 \frac{Z \chi j^2 \ell n \Lambda}{T_e^{3/2}}$$

$$- \left[\text{————————(c)————————}\right] + \left[\text{—— Ohmic Heating ——}\right]$$

$$- 1.54 \times 10^{-25} n_e n_i Z^2 T_e^{\frac{1}{2}} - P_e$$

$$- \left[\text{—— bremsstrahlung ——}\right] - \left[\text{atomic processes}\right] \qquad (2)$$

In equation (2) the power is in ergs s^{-1} cm^{-3}, T_e is in eV, n_e, n_i are in cm^{-3} and M the atomic mass of the ions is in AMU. The ionic charge Z = 1 for hydrogenous plasmas and the electron density n_e arises predominantly from

electron-proton ion pairs, i.e. $n_e \approx Zn_i$. Bremsstrahlung radiation in all wavelengths by impurity ions of density n_{ii} is proportional to $n_e\, n_{ii}\, Z^2$ and so contributions from each species of impurity ion must be summated and appropriately introduced into equation (2). D is the diffusion coefficient for the toroidal plasma and for the plasma regions somewhat away from the axis is often expressed as

$$D = 0.84 \times 10^{-5} \frac{C\, nZ\, \ell n\, \Lambda}{B_\theta^{\,2}} \quad \frac{(T_e + T_i)}{T_e^{\,3/2}} \quad . \quad (cm^2\ s^{-1})$$

Here the dimentionless parameter C accounts for non-classical effects and B_θ is in Gauss. All the terms on the right hand side of equation (2) are functions of r and so must be integrated from r = 0 to a to yield the total energy lost.

The plasmas in Tokamaks are optically thin and the values of n_e and T_e are such that radiative decay rates for bound-bound and free-bound transitions generally exceed the rates for electron collisions. Consequently conditions tend to those of coronal equilibrium [8 and 9] and the ratio of populations of two levels n and m can be expressed as

$$\frac{N_n}{N_m} = \frac{n_e\, S_{mn}}{A_n}$$

where S_{mn} is the collision rate coefficient for the transition from level m to level n and A_n is the total Einstein transition probability for level n. Further, in ionization processes it is generally possible to neglect ionization from all states except the ground state, thus the ratio of populations, x, of two ionization states is,

$$\frac{x_{(i+1)}}{x_i} = \frac{S_i}{\alpha_{(i+1)}} = \frac{\Sigma \langle \sigma(v_e) v_e \rangle}{\Sigma \langle q(v_e) v_e \rangle} \quad .$$

Here S_i is the electron impact ionization coefficient for the ground state of i to whatever levels of the ion (i + 1) are populated and $\alpha_{(i+1)}$ is the total recombination coefficient from the higher ion state.

For a pure hydrogen plasma at $n_e \approx 10^{14}$ cm^{-3} and $T_e \approx 10$ keV, so the loss term P_e is insignificant because the ionization rate coefficient is about 2×10^{-8} for the process $[e + H \rightarrow e + e + H^+]$ whereas the

sum of two body recombination [$e + H^+ \rightarrow H + h\nu$] and collisional-radiative recombination [10] is $\sim 10^{-15}$ cm^3 s^{-1}. Thus the hydrogen is fully ionized and loses negligible energy from line radiation. Hydrogen has the metastable state H(2S) whose lifetime is appreciably longer than electron-atom collision relaxation time but this will be quenched by both the $\underline{B} \times \underline{V}$ Lorentz field and any other small electric fields within the plasma. The coronal conditions will also be violated by some higher excited states but the overall effect is negligible. Thus if P_e is to be a significant loss term its contributions must arise largely from excitation of impurity ions with smaller contributions from ionization and recombination radiation.

The elements O and C are fairly common contaminants in fusion experiments, their concentrations lie in the range 0.1 to 5%. In addition small concentrations of heavy metals such as Mo and W arise from plasma impact upon the limiter and Fe,Cr etc are produced by sputtering of the stainless steel torus walls by high energy charge exchange atoms. Impurity atoms (or molecules) released near to the wall drift into the cooler periphery of the plasma and become ionized by electron impact. The drift time by diffusion of these ions from a localised region of n_e, T_e is much larger than electron-impact relaxation times so that ionization proceeds to higher states by cascading electron impacts but from the groundstate of each ionization state. Thus at any radial position r an equilibrium concentration of highly ionized impurities is approached, characteristic of the n_e, T_e conditions of this position [9 and 11]. This concept was an underlying premise of early spectroscopic measurements of electron temperature by observation of impurity line radiation. Such measurement is now carried out by Thompson scattering of laser light but the Doppler broadening of line radiation is sometimes used to measure the temperature of the impurities. The overall intensities of line radiation are presently the main diagnostic route to determining the concentrations of impurities. The highly charged ions diffuse preferentially towards the toroidal axis [6] unless steep gradients in T_e reverse this transport. Thus the core of the plasma becomes populated with fully stripped O and C and also metallic impurity ions approaching some 20 to 30 times ionized.

If the ionization and recombination coefficients are known, then the distributions of ion states can be found from the ratio $x_{(i+1)}/x_i$ as a function of electron temperature. The total two body recombination rates for multi-electron impurity ions are appreciably enhanced over the two body

radiative rates by the process of di-electronic recombination and, as an example, calculations of $\alpha(T_e)$ and $S(T_e)$ by Summers [13] for oxygen is shown in Figure 3. These particular data are for an electron density of 10^{12} cm^{-3}. The ion state population is also shown as a function of T_e and it can be seen that, except for fully stripped O^{8+}, each ion state is confined to a limited range of temperatures. Thus in the Tokamak, where T_e is a function of r, the ion states are distributed throughout the plasma like so many toroidal onion skins. Each species is radiating due to electron excitation and its concentration is a balance between ionization and recombination into and out of adjacent ion states, recombination also giving rise to photons. The atomic processes are drains upon the electron energy and must be represented in the term P_e. For a fully confined plasma and a constant amount of neutral impurity (initial density n_{oi}), the ion concentration in state i (denoted by subscript i) at any time t during the plasma cycle is given by $n_{oi}\, x_i$ where Burton and Wilson [12] express x_i as,

$$x_i = \beta_i \exp - (n_e\, S'_i t) - \beta_{(i-1)} \exp - (n_e\, S'_{(i-1)} t) + \gamma_i \ .$$

Here $S'_i = S_i + \alpha_i + \alpha_{(i+1)}$ and $\beta_i = 1 - \sum_{o}^{i} \gamma_i$.

γ_i is the equilibrium value of x_i at $t = \infty$ given by

$$\frac{\gamma_i}{\gamma_{(i+1)}} = \frac{\alpha_{(i+1)}}{S_i} \ .$$

The intensity of emitted radiation of any line of wavelength λ is

$$I_\lambda = C_\lambda\, n_e\, x_i \ .$$

Here C_λ is the excitation rate for the particular line from the ground-state of the ion. Thus the total energy loss due to line radiation from an ion state i is found from the summation $\Sigma\, I_\lambda\, h\nu$ over all transitions integrated over time and over the plasma radius r. In practical conditions the analysis may have to allow for the possibility of a continuous input of impurities by some form of re-cycling and it should also account for redistribution of ion densities by diffusion within the plasma. Helium-like and beryllium-like impurity ions have metastable states whose lifetimes are not affected by the fields within the plasma and in such cases the total

rate processes should also take account of the concentration of ions in metastable states [11].

Results of an analysis [3] of the power flow across the minor radius of the plasma based on the principles of equation (2) for the ORMAK Tokamak is shown in Figure 4. Here the relative contributions of the various loss process can be seen and, even with modest concentrations of oxygen and carbon impurities, the energy loss due to line radiation dominates near to the periphery of the plasma. The energy is transported to this region mainly by convection. However the cooling of electrons by radiation can in some ways be regarded as beneficial because it reduces the energy carried to the walls by convected charged particles and so may reduce recycling. Fully and partially stripped ions in the core of the plasma are emitting bremsstrahlung radiation which may be used as a temperature control mechanism in reactors. In addition, the presence of some high Z impurities may be necessary in order to reduce the effects of "collisionless instabilities" and in some reactor concepts impurities such as argon are introduced together with D-T during refuelling. Hence there is also interest in atomic data for the inert gases.

3.3 Heavy particle collisions

Energy losses for ions can be considered in a similar manner to those for electrons [7], namely,

$$\frac{p_i(r)}{2\pi r dr} = 1.6 \times 10^{-12} \frac{d}{dt} \left(\frac{3}{2} n_i T_i\right)$$

$$= \frac{1.6 \times 10^{-12}}{r} \frac{\partial}{\partial r} \left(\frac{3}{2} r D T_i \frac{\partial n_i}{\partial r} + \kappa \frac{\partial T_i}{\partial r}\right)$$

$$+ 2.4 \times 10^{-9} \frac{n_i^2 Z^2 \ell n \Lambda}{M} \frac{(T_e - T_i)}{T^{3/2}} - P_i$$

where the classical ion thermal conductivity can be expressed as

$$\kappa = \frac{10^{-9} M^{\frac{1}{2}} n_i^2 \ell n \Lambda}{B_\phi^2 T_i^{\frac{1}{2}}} \cdot \quad (cm^{-1} s^{-1}) \quad .$$

If fast alpha particle collisions are neglected, then the reaction rates $\langle \sigma(v_i) v_i \rangle$ contributing to P_i are only significant if the cross sections are large because of the relatively low velocities of the plasma ions. Thus ion-ion excitation and ionization processes do not contribute significantly

and the dominant reaction in present day devices is, symmetrical charge exchange with any neutral H present in the plasma. The analysis for ORMAK [3] has also been extended to ions and is shown as an example of typical conditions in Figure 5. Again convection and conduction predominate in transporting energy from the core but energy is carried from the outer regions and lost to the walls by fast neutral atoms. The electron and ion power terms P_e and P_i in equations (2) and (3) are coupled because the fast neutral atoms may be re-ionized by electron impact before they leave the plasma. Alternatively, recycling terms can be introduced, see for example [7], by accounting for the release of impurity atoms or molecules and of cold H_2 from the walls due to atom impact and energy loading. These neutral particles are then assumed to enter the plasma and be ionised by electron impact. The energies of atoms formed by charge exchange deep within the plasma are well characterized by the proton temperature T_i. If the distributions of n_o and n_e can be estimated and the probability for electron impact re-ionization accounted for, then the energy distribution of the flux of emerging atoms can be used to determine the proton temperature. This is a much used diagnostic technique for measuring T_i in present devices.

H atoms produced in collisions of protons with impurity ions can be neglected as a source of energy loss but collisions of impurity ions with any H atoms present are likely to be a powerful source of impurity ion recombination. As an example the process $\left[O^{8+} + H \rightarrow O^{7+} \ (n = 8) + H\right]$ has zero energy defect and is likely to have a relatively large cross section for the production of excited O^{7+} even though the effects of curve crossing may make the interaction favour levels other than n = 8. This contention is supported, all be it for lower Z and for H_2 molecules, by the work of Crandall et al [14]. Indeed an approximate assessment based on the roughly comparably process $\left[He^{++} + H \rightarrow He^{+} \ (n = 2) + H^{+}\right]$ indicates that 1% of H atoms could produce 30 times more O^{7+} than arises from electron-ion recombination when $T_e \approx T_i \approx 600$ eV and greatly more at higher temperatures. The reverse reaction $\left[O^{7+*} + H^{+} \rightarrow O^{8+} + H\right]$ is negligible because the spontaneous decay rates for O^{7+*} are very much larger than ion-ion collision rates.

The larger dimensions of a reactor (and possibly the introduction of efficient divertors) will greatly diminish the significance of reactions between plasma protons and slow H and other impurity atoms released from the walls. Nevertheless comparable reactions will take place within the

atmosphere of any injected fuel pellets. Ion-atom charge exchange and ion-atom ionization, all be it at energies above 50 keV, are essential processes for the heating (and beam fuelling) of plasmas by neutral injection and are now discussed.

4. NEUTRAL INJECTION

4.1 Beam heating and trapping

Sweetman [4] has extended the principles illustrated in Section 2 and by equations (2) and (3) to a pure hydrogen plasma and determined the power needed to bridge the gap between Ohmic and trapped alpha particle heating in order to achieve a critical temperature T_c at which the plasma becomes self heating. His results are shown for a reactor sized device in Figure 6 and for an experimental device in Figure 7. It is worthy of note that for present experiments the balance at T_c lies predominantly between diffusion losses and alpha particle heating whereas for a reactor the bremsstrahlung losses exceed those of diffusion. The actual power calculated to bridge the gap (for the experimental device) is shown in Figure 8; it reaches about 110 kW at $T \approx 10$ keV but of course will be sensitive to impurities which are not allowed for in the analysis. Alpha particle production by fusion reactions requires that the plasma ions be heated; thus the injection system should be optimised to heat ions rather than electrons. The rate of energy transfered to the plasma electrons by a trapped ion (injected as an atom) with energy E_{in} and atomic mass M_{in} is, for $v_e >> v_{in}$,

$$\frac{1}{E_{in}} \frac{d E_{in}}{dt} = - 3.3 \times 10^{-9} \frac{n Z^2 \ell n \Lambda}{M_{in} T_e^{3/2}} \cdot \quad (s^{-1})$$

The rate of energy transfer to the plasma ions is approximately

$$\frac{1}{E_{in}} \frac{d E_{in}}{dt} \simeq 1.8 \times 10^{-7} \frac{M^{\frac{1}{2}}}{M_P} \frac{Z^2 \ell \Lambda}{E_{in}^{3/2}}, \quad (s^{-1})$$

where M_P is the mean mass of the plasma ions (i.e. either a D-T mixture or $M_P = 1$ in present hydrogen experiments).

Thus the ratio to be optimised is,

$$\frac{\text{Transfer rate to ions}}{\text{Transfer rate to electrons}} = \frac{56}{M_P} \left(\frac{M_{in} T_e}{E_{in}} \right)^{3/2}$$

Hence the energy transfer ratio is enhanced if heavy atoms are injected but unfortunately impurity radiation losses are likely to restrict the choice of atomic species to H or D. Further the optimum injection energy for H atoms is related to the electron temperature of the plasma. It is also necessary to consider the time τ_h available for heating. If the available beam power is high then it is possible for $\tau_h < \tau_c$ (τ_c is the energy confinement time) and the injected energy goes only into heating the plasma. At lower beam power $\tau_h >> \tau_c$ and all the energy losses have to be overcome; so although the beam power is less a greater total energy is required. In present day devices, beams of up to 1 MW operating for 1 to 10s are considered feasible.

Injected atoms must be ionized and trapped in order that their energy be transferred to the plasma. The attenuation of the atom beam at a depth ℓ within the plasma is thus given by,

$$I = I_o\, e^{-n\,\sigma'\ell} = I_o\, e^{-\frac{n\ell}{d}} ,$$

where d is a characteristic ($\exp^{-1}$ folding) plasma target thickness. For the condition $v_e > v_{in} > v_i$ the thickness can be expressed as,

$$d = \frac{1}{\sigma'} = \frac{1}{\sigma_x(v_{in}) + \sigma_i(v_{in}) + \langle\sigma(v_e)v_e/v_{in}\rangle} .$$

Here $\sigma_x(v_{in})$ and $\sigma_i(v_{in})$ are respectively the cross sections for charge exchange and ionization in collisions between injected atoms and plasma ions. The cross sections together with the "averaged electron ionization term" ($\langle\sigma(v_e)\, v_e/v_{in}\rangle$) are shown in Figure 9. Charge exchange is the predominant atomic process in trapping when $E_{in} \lesssim 50$ keV and proton impact ionization (perhaps a more illustrative terminology is H stripping on H^+) becomes dominant at higher injection energies. Trapping in high temperature plasmas by electron ionization is a minor contribution. The regime of lower injection energy is unattractive because of the unavoidable production of charge exchange atoms which are not confined and so bombard the torus walls, thus it is the higher energy regime which offers most promise. The maximum useable injection energy is a balance between the need for the trapping length ℓ to be encompassed within a reasonble distance along the toroidal axis (as sketched for a tangentially injected beam in Figure 1) and

the maximum beam velocity and operating time that are available from the injection system due to technological constraints.

4.2 Beam production

The preceding discussion has considered only a beam of H atoms or D atoms at the same velocity. These atoms must first be accelerated up to injection velocities. The most practical method appears to be to ionize neutral gas, from a beam of electrostatically accelerated ions and then to neutralise this beam by atomic collisions in a gas target. The atoms of interest arise from molecular gases so that the efflux from the ion source comprises a mixture of H^+, H_2^+ and some H_3^+ as well as appreciable numbers of thermal H_2 and H atoms. Each ion species is accelerated through the same potential difference and so has a different velocity. The atomic processes for both ion neutralisation and fast atom trapping within the plasma are dependent upon particle velocity and this fact must be allowed for in the mixed species ion beam. In this context the different velocities of hydrogen and its isotopes are important and the differences in the molecular properties of D_2, DT and T_2 must be taken into account. The technical problems associated with the high energy transported by the beam and also the large potentials needed on the accelerating electrodes are severe and so sources that are rich in H^+ or D^+ are desirable in order to minimise the acceleration potentials.

In principle, all ion sources presently regarded as suitable for injection comprise a hot filament emitting electrons into a discharge chamber filled with molecular gas. A low temperature plasma is thus produced within the chamber and this plasma diffuses to a multi-aperture plate through which beamlets of ions are extracted by an external, accelerating electric field. Some sources also have a magnetic field so arranged as to restrict electron motion to the discharge chamber anode thereby decreasing ion diffusion and enhancing the time that ions are exposed to electron impact. The relevant physical parameters within the source are the density of neutral molecular gas n_{ms}, the ion residence time τ_{rs}, the current density of electrons emitted from the filament j_f and the plasma density n_{es}, n_{is} of electron-ion pairs within the source. Plasma temperatures T_{es} are usually low ($\lesssim$ 10 eV) so that ionization is often regarded as arising mainly from the current of electrons accelerated across the potential difference which exists between the cathode and the plasma of such discharges. However plasma instabilities might increase T_{es}

so that ionization could then arise from electrons in the bulk of the plasma. The most important atomic and molecular processes are $[e + H_2 \rightarrow e + e + H_2^+]$ and $[e + H_2^+ \rightarrow e + H + H^+]$, these yield firstly H_2^+ and then H^+ from cascading collisions. The lower temperature electrons will tend to dissociate H_2, namely $[e + H_2 \rightarrow e + H + H]$, and the ionization process $[e + H \rightarrow e + e + H^+]$ also contributes. The species H_3^+ arises most likely from $[H_2^+ + H_2 \rightarrow H_3^+ + H]$. A collection of relevant data (as far as it is presently available) has been prepared by Martin [15]. It is the objective of the source designer to adjust the parameters of the plasma and molecular gas feed to optimise the H^+ yield. However here attention is drawn to the problems encountered in providing relevant atomic and molecular data due to the uncertainties in the vibrational excitation states of the molecular species within the source and the dramatic effect of such excitation upon molecular rate processes at low electron energies.

4.3 Ion beam neutralisation

The ions beam accelerated from the source must be neutalised by atomic collision processes. Some neutralisation of the beam occurs in the ionized gas leaving the source (less than 50% of the molecular gas being ionized within the discharge chamber) and this gas forms the neutraliser target in present day injectors. It is an unfortunate but evident fact of nature that the conditions optimal for trapping within the toroidal plasma are generally unfavourable for ion neutralisation within a gas target. Thus relatively few of the ions extracted from the source are neutralised at the higher beam energies. The principle difference between the gas neutraliser and the toroidal plasma is that the former has a much more readily controlled density and is likely to present thicker target conditions so that the atom fractions will approach their equilibrium values.

So high are the energy requirements of neutral injection that in future concepts some form of ion energy recovery will be essential. A typical concept is illustrated in Figure 10. Ions are accelerated to potential U_{in} and passed into a gas cell, of "thick" target conditions so that equilibrium fractions are produced. The neutral component of the beam then passes on into the fusion device. The remaining ions leave the gas cell but are decelerated back to source potential (except for a small potential difference ΔU_{in} needed to collect the ions). These decelerated ions are collected in a dump chamber so that the ideal power requirements are $U_{in}\ I_{in}$ for the neutral beam but only $\Delta U_{in}\ I_{in}^+$ for the ion beam.

Beam neutralisation has been considered in some detail by Riviere [16, Appendix 3]. For H^+ or D^+ beams into molecular gas targets the equilibrium fraction arises mainly from the simple balance between charge exchange and ionization i.e. $D^+ \rightarrow D$ and $D \rightarrow D^+$. It should be stressed however that the injection beam powers are very large, for example 0.5 A cm^{-2} at say 100 keV, so that the target gas will become ionized and collisions between the injected beam and the target plasma electrons and ions must be taken into account. The target plasma will generally have a low temperature and so the assumption $v_{et} \approx v_{in}$ is valid, where v_{et} is the electron-ion collision velocity in the centre of mass of the atomic system. The effect of electron collisions for D^+ beams are significant because $v_{et} \approx 3 \times 10^8$ $cms^{-1} \equiv 25$ eV for 100 keV D^+ and so is above the threshold for $[e + D \rightarrow e + e + D^+]$. The resultant electron impact ionization reduces somewhat the yield of D at the higher injection energies.

Conditions for a D_2^+ or H_2^+ beam in H_2 targets are substantially different. There are many more channels for heavy particle collisions, for example $D_2^+ \rightarrow D_2$, $D_2 \rightarrow D_2^+$ and $D_2^+ \rightarrow (D^+ + D)$ together with the subsequent collisions of D^+ and D. However attention is drawn to the electron impact dissociation of H_2^+ or D_2^+ which here is of considerable importance due to the low threshold and large cross section of the reaction especially because the molecular ions are vibrationally excited. Calculated neutral fractions from D^+ assuming that the H_2 gas target is fully ionized [16] are shown in Figure 11. The beneficial effect of electron collisions can be seen especially at high ion beam energies. For a more precise analysis the ion-ion interactions should also be added, namely $(D_2^+ + D^+)$ and $(D_2^+ + D_2^+)$ both of which will produce dissociation.

The low yield of atoms from high energy positive ions has directed attention towards the possible use of D^- as the parent ion species from which a D atom beam can be produced by stripping in ion-molecule collisions, such as $[D^- + H_2 \rightarrow D + e + H_2]$ and, for an ionized gas target, by $[D^- + e \rightarrow D + e + e]$. The cross sections for these processes are substantial even at high injection energies. The power efficiency of the neutraliser may be defined as

$$\eta_o = \frac{\text{Power in atom beam leaving neutraliser}}{\text{Power in ion beam entering}}$$

and Riviere [16] has evaluated η_o for D^+, D_2^+, D_3^+ and D^- parent beam ions. The results are shown in Figure 12 for both neutral and fully ionized

targets and they demonstrate the superiority of D^- beams at high energies. However, effects of ion-ion recombination with the H^+ and H_2^+ ions within the ionized hydrogen targets, i.e. $\left[D^- + H^+ \rightarrow D + H\right]$ and $\left[D^- + H_2^+ \rightarrow D + H_2^*\right]$ should be added in order to provide a more complete analysis.

4.4 Negative ion beams

There are unfortunately problems associated with the use of H^- and D^- parent ions, namely the low yields available from ion sources. In brief, H^- is produced in electron bombardment gas sources by processes such as $\left[e + H_2 \rightarrow H^+ + H^-\right]$ and $\left[e + H_2 \rightarrow e + H + H$ followed by $e + H \rightarrow H^-\right]$ all of which require low energy electrons. To transport large fluxes of such electrons throughout the discharge chamber it is necessary to compensate the electron space charge so that an equivalent charge density of positive ions must also be present. Thus the H^- yield is greatly attenuated by the very powerful process of ion-ion recombination. A solution may lie in the production of H^- or D^- at ceasiated surfaces [17] but more conventional routes lie in the use of a positive ion sources which fire their beams into alkali metal vapour targets so that H^- or D^- ions are produced by double electron capture processes such as $\left[D^+ + Cs \rightarrow D^- + Cs^{++}\right]$. The parent D^+ and D_2^+ beams would be at low energy (say 2 keV) in order to optimise the double electron capture processes and so the high injection beam energies would be achieved by subsequent acceleration of the emerging D^- ions. If the ceasium target becomes ionized such processes as $\left[D^- + Cs^+ \rightarrow D + Cs\right]$ will reduce the D^- yield.

4.5 The effect of plasma impurity ions

The presence of impurity ions must also be taken into account. Obviously the injected beam should not contain significant fractions of high Z impurities, but here we consider only the effects upon the trapping of the neutral beam by impurity ions confined within the toroidal plasma itself. Trapping via processes such as $\left[H + O^{x+} \rightarrow H^+ + O^{(x-1)+*}\right]$ must be added to the $(H + H^+)$ process previously discussed. Charge exchange collisions with highly charged impurity ions involve electron capture into fairly high excited levels and so at any injection energy there is always a level lying close to energy resonance. Thus the charge exchange cross sections are likely to vary only slightly with incident beam energy and so will appreciably exceed (possibly by a factor 5 to 10) at high injection energies those for $(H + H^+)$ and $(D + D^+)$. This can be inferred from data [14] for $(C^{x+} + H_2)$ and $(O^{x+} + H_2)$. Small concentrations of highly charged impurity

ions within the toroidal plasma can therefore contribute powerfully to trapping. The distribution of trapped beam energy across the minor radius, r, of the plasma may therefore differ appreciably from that needed for effective heating if the radial distributions of the atom-impurity ion trapping rates differ from those of the atom-proton trapping rates. Thus it is necessary to assess if collective plasma processes will redistribute the trapped beam ions and so provide acceptable profiles of energy deposited within the plasma.

5. DIAGNOSTICS

Measurement of parameters such as n,T and the local values of B and of the electric fields within the torus are greatly complicated by the large fluxes of particles present and by the high magnetic fields. In addition, the dynamic nature of the plasma calls for good resolution in both time and space. Mechanical devices cannot be placed in regions of high n and T and so external observations are made which rely on the fluxes of photons and neutral particles emitted from the torus. Conversely, electromagnetic radiation or neutral particles can be beamed through the plasma whose properties are inferred from both scattering and attenuation of the beams. Very high energy beams of massive ions can penetrate the magnetic fields and 250 keV beams of Tl^+ have been used to measure n_e by the ionization process $\left[e + Tl^+ \rightarrow e + e + Tl^{2+}\right]$ and the local electric fields by the deflection of the ion trajectories within them.

The present discussion is restricted to atomic rather than free-free processes and within these limits one of the most common diagnostic techniques is the observation of line radiation emitted by both neutral hydrogen and impurity ions. The intensity of emitted photons is dependent upon the integral of the excitation rates for the selected transition within the field of view of the spectrometer. Collimation restricts the view to a chord across the torus along which the spatial and temporal distributions of n_e and T_e can be determined by Thompson scattering of laser light. Taking note of the considerations for the "onion skin" type of radial distributions of emitting species outlined in Section 3.2 it is possible to determine average line densities of ions if the rate coefficients are known. The radial distribution of these line densities and hence the presence of "onion skins" can be inferred by spectroscopic observation along several parallel chords progressively displaced from the toroidal axis. The interpretation depends upon knowledge of the atomic cross sections for

ionization, excitation and neutralization (the term is used specifically to include both electron recombination and any contributing H atom collisions) as well as the radial density and energy distribution functions of the electrons coupled to the assumption of plasma symmetry around the poloidal axis.

To achieve fast time resolution it is desirable to observe strong transitions with the proviso that for highly charged ions the strong resonance lines lie in X-ray regions and hence may be difficult to detect and resolve. If a finite amount of low Z impurity is present then, for devices with long confinement times, a particular ion species may well become 'burnt-out' as the ions become fully stripped. For high Z metallic ions a limit to the state of ionization will be reached depending on T_e at the core of the plasma as discussed in [11]. Hence the time dependence of spectral intensities is a useful guide to conditions pertaining within the plasma.

The principles underlying particle beam diagnostics are evident from Sections 3 and 4. Information on line averaged values of ion density and temperature can be inferred by measuring the attenuation of fast neutral atom beams fired through the plasma. It may also be possible to study the non-radiating fully stripped ions due to the photons emitted subsequent to charge exchange collisions with beam atoms. Alternatively the fluxes of emitted H atoms produced by charge exchange with slow H within the plasma yield information about the energy of the plasma ions and are used to determine T_i. However, re-ionization by electron impact in the larger and denser devices envisaged over the next decade will reduce the value of emitted atom probes. Then T_i will probably be measured by the scattering of long wavelength laser light. Atom probe data must of course be unfolded in an appropriate manner and its interpretation is subject to uncertainties in the plasma characteristics comparable to those for photon data. Much remains to be developed in the diagnostic field, there is a particular lack of data in the regions of lower temperature and density near to the torus walls. Here plasma conditions must be determined before the problems of recycling and divertor operation can be adequately assessed.

6. GENERAL COMMENTS ON ATOMIC DATA

In considering the relative importance of atomic and molecular data it is useful to maintain a simple overall view of the Tokamak problems. Firstly energy losses from line radiation of low Z impurities (C and O) are

quite high in present devices. However, longer confinement times are expected for future devices and so such impurities may well become fully stripped so that line radiation will only be emitted during the time taken for the low Z impurity to become stripped. Thus the possibility of continuous inputs of impurity particles from the walls and their attenuation by ionization and diversion in the scrape-off plasma are therefore significant source terms for the time integrated losses due to bremsstrahlung radiation. The rate processes for neutral O_2, CO, O and C as well as metallic atoms are therefore important. In this context the importance of surface effects cannot be overstressed, in particular the degree of vibrational excitation of any desorbed molecules may have substantial effects upon the magnitude of their ionization cross sections and the velocities of their dissociation fragments. The velocity and hence scale length of neutral atoms is of prime importance in determining the characteristics of the scrape-off plasma.

High Z impurities present different problems. These do not become fully stripped and their contributions to bremsstrahlung losses are dependent upon the charge state reached. Thus the processes of ionization and dielectronic recombination remain significant throughout the operating phase of the plasma. The total power lost will be sensitive to the distribution of ion charge states throughout the total volume of the plasma. It should also be noted that high Z impurities may be deliberately fed into a reactor to increase Z_{eff} and damp out collisionless instabilities.

The parameters relevant to energy losses are total excitation rates, total ionization rates from the ground state and total recombination rates. Detailed structure in the cross sections are generally not important because of the averaging effects of the electron energy distributions. This does not imply that resonance-like effects are negligible as is evident from the significance of dielectronic recombination. The accuracy needed for atomic data should be related to the accuracy of plasma modelling, both are uncertain at the present. There is but limited experimental atomic data because the atomic species of interest are either highly charged ions or neutral atoms that are difficult to study. Thus a carefully selected and balanced programme of theory and measurement is needed. The ionization balance and excitation rates in plasma modelling are often determined using combinations of semi-empirical cross sections and simple recombination models so that some uncertainties exist especially for high Z impurities where large extrapolations must be made [see the discussion in 11]. Such

extrapolation calls for characteristic excitation and ionization energies for various electronic shells and these data are presently of interest for plasma modelling of high Z impurities. Interpretation of spectroscopic data requires accurate knowledge of the excitation rates of a particular line as well as the total rates of processes which determine the density of the emitting ionic species. Branching ratios and oscillator strengths are clearly of importance in this area. However, again there are grounds for compromise between the accuracy of the atomic data and the uncertainties in the unfolding procedure for the plasma parameters.

Data needed for fast atomic beam processes are slightly different. Here it is generally the cross sections that must be known and many are already well established. However ion-ion collisions which will occur during beam neutralisation and energy recovery in future devices are in general not known. Data for collision processes between atoms and highly charged impurity ions are also lacking and are of interest in the energy range 0.5 keV up to 250 keV. It must be stressed that neutral injection systems will cost almost as much as the toroidal confinement systems in future Tokamaks and so injector problems are of major economic significance.

A full understanding of ion source performance calls for detailed knowledge of the various molecular break-up patterns and dissociation energies of H_2^+ and D_3^+ etc. However it is unlikely that source development will be delayed by lack of such data because many of the present problems are either technological or relate to the transport physics of intense ion beams. In this area it should again be stressed that particle-surface interactions and the release of secondary neutral and charged particles are of considerable importance in the production of low temperature plasmas in ion sources and the acceleration and transport of the ion beams. Neither should such processes be overlooked in the low temperature, "pre-ionization" discharge phase within the Tokamak torus itself. Impurities released at this time may well be trapped throughout the subsequent confinement phases so the problem is of appreciable significance. Indeed there are several proposals for the controlled filling of Tokamaks so that their initial plasmas do not interact strongly with the torus walls; for example laser ionization of injected pellets of frozen H_2 or D-T.

7. CONCLUSION

In this paper an attempt has been made to outline in simple terms the physical environments within the Tokamak fusion device. Other fusion

concepts such as high β theta-pinch and laser pellet devices present different atomic and molecular problems. In the theta-pinch the plasma densities are much larger and heating is by shock effects, but whilst the roles of atomic and molecular processes must be re-assessed, they will not differ widely from the principles discussed here. On the other hand, the laser concept is a case of limiting high density where photon collisions (generally negligible in the optically thin plasma of the Tokamak) become of paramount importance. However conditions in the outer regions of the ablating pellet of a laser device can be compared to the pellet refuelling problems of a Tokamak without the complications imposed by magnetic fields.

Provision of adequate data presents a considerable challenge to workers in atomic, molecular and surface physics. Many reactions are difficult to study either experimentally or theoretically but fortunately these constraints do not necessarily occur simultaneously. For example the electron impact excitation rates for highly ionized ions are probably more amenable to theoretical than to experimental treatment whereas the reverse will be true for low energy ($\sim$ 100 eV) molecular ion-ion collisions such as ($H_2^+ + H_e^+$). Simplifications also arise due to considerations of isoelectronic and isotropic sequences and the principles of detailed balancing may be invoked if one side of a reaction equation is the easier to observe. Nevertheless the problems remain formidable and much data are needed before a full understanding of fusion devices can be obtained.

REFERENCES

[1] RIBE, F.L., Rev. Mod. Phys. 47 (1975) 7.

[2] SPITZER, L. "Physics of fully ionized gases", Interscience Publishers, New York (1962).

[3] HOGAN, J.T. and CLARKE, J.F., Journ. Nucl. Materials, 53 (1974) 1.

[4] SWEETMAN, D.R. Nucl. Fusion 13 (1973) 157.

[5] SWEETMAN, D.R. "Neutral injection and heating of toroidal reactors" (Sweetman, D.R. Ed.) Culham Laboratory Rep. CLM-R112 (1971).

[6] TAYLOR, J.B. "Fusion reactor design problems" (Proc. IAEA Workshop at Culham, United Kingdom) IAEA, Vienna (1974) 403.

[7] HOTSTON, E., Culham Laboratory Rep. CLM-P 449 (1976), to be published in Nuclear Fusion.

[8] WOOLEY, R.V.D.R. and ALLEN, C.W., Mon. Not. Roy. Astr. Soc., 108 (1948) 292.

[9] WILSON, R., J. Quant. Spectrosc. Radiat. Transfer. 2 (1962) 477.

[10] BATES, D.R., KINGSTON, A.E. and McWHIRTER, R.W.P., Proc. Roy. Soc. A, 267 (1962) 297.

[11] HINNOV, E., Plasma Physics Laboratory, Princeton, Rep. MATT-777 (1970).

[12] BURTON, W.M. and WILSON, R., Proc. Phys. Soc. 78 (1961) 1416,

[13] SUMMERS, H.P., Appleton Laboratory, Rep. IM 367 (1974).

[14] CRANDALL, D.H. and KOCHER, D.C., "Atomic data for fusion", Oak Ridge Newsletters, 1 3 (1975) 12 and 1 6 (1975) 11.

[15] MARTIN, A.R., Culham Laboratory Rep. CLM-R157 (1976).

[16] RIVIERE, A.C., "Neutral injection heating of toroidal reactors" Appendix 3, (Sweetman, D.R. Ed.) Culham Laboratory Rep. CLM-R112 (1977).

[17] BELCHENKO, Yu.I., DIMOV, G.I. and DUDNIKOV, V.G., Proc. 2nd Symp. "Ion sources and formation of ion beams" (Berkeley VIII-1,1974).

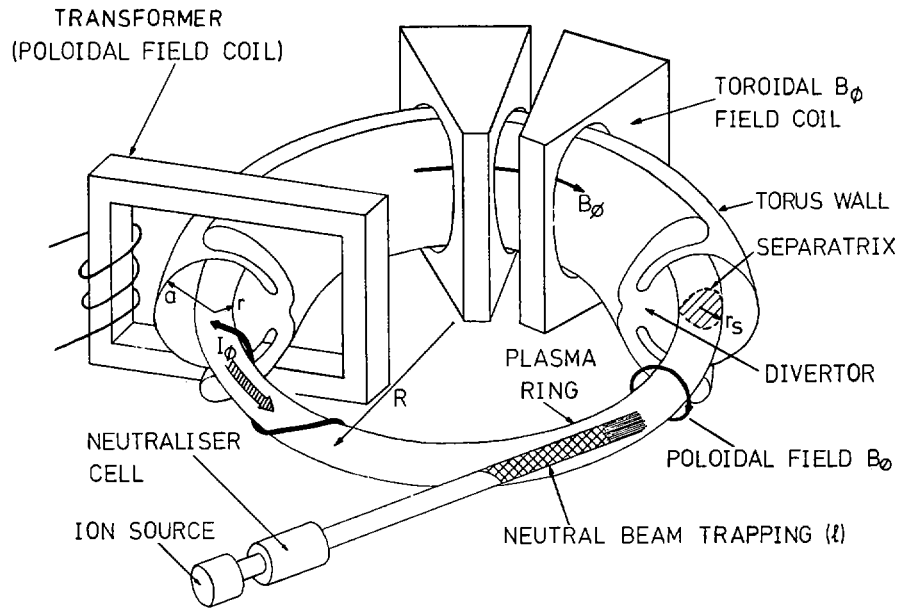

FIG. 1. Schematic diagram of a Tokamak plasma. The torus is shaped for a single neutral point poloidal divertor and the plasma heated by neutral beam injection.

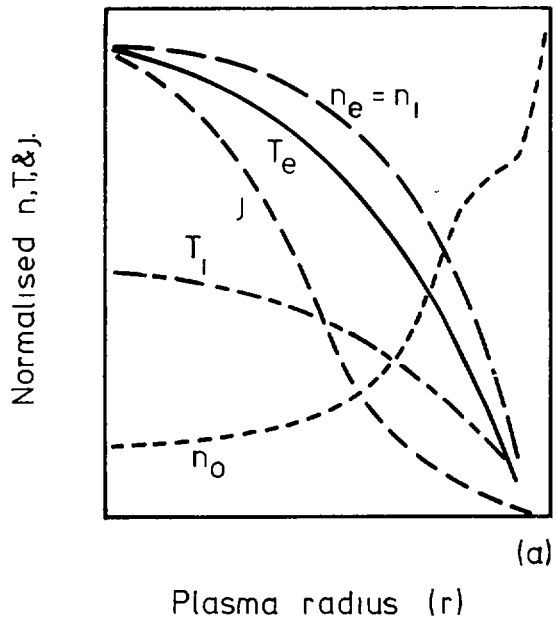

FIG. 2. Radial profiles of plasma parameters. Calculated by Hogan and Clarke [3] for the ORMAK Tokamak at Oak Ridge. Plasma parameters are: a = 22 cm, R = 80 cm, I_ϕ ranges from 60 to 275 kA, and at r = 0, n_e is 1 to 3 x 10^{13} cm^{-3}, T_e is 400 to 1000 eV and T_i is 200 to 400 eV.

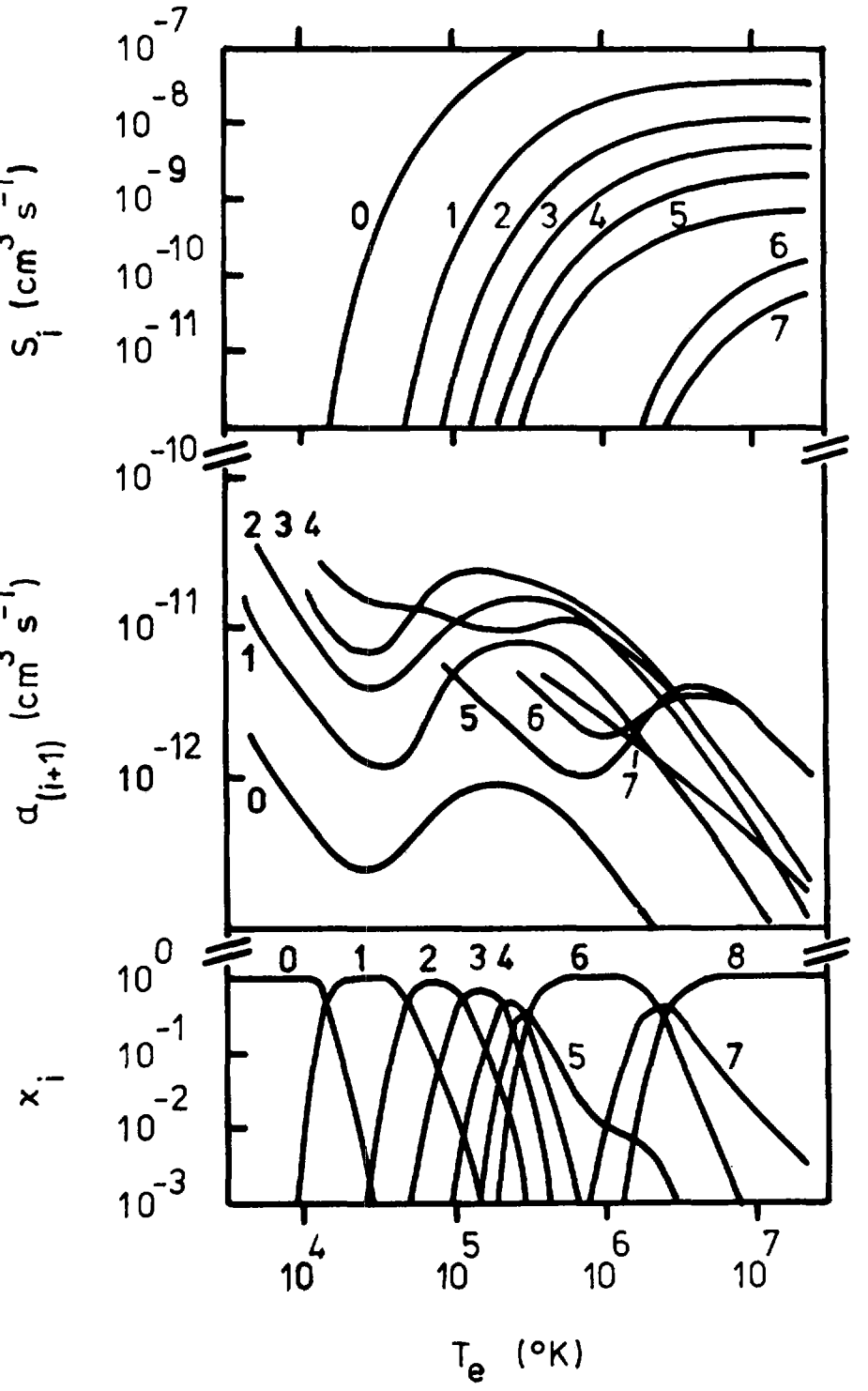

FIG. 3. Ionization coefficients $S_i(T_e)$, collisional dielectronic recombination coefficients $\alpha_{(i+1)}(T_e)$ and ionization state populations χ_i calculated by Summers [13] for oxygen ions and $n_e = 10^{12}$ cm^{-3}. Curves for each ion state i are shown.

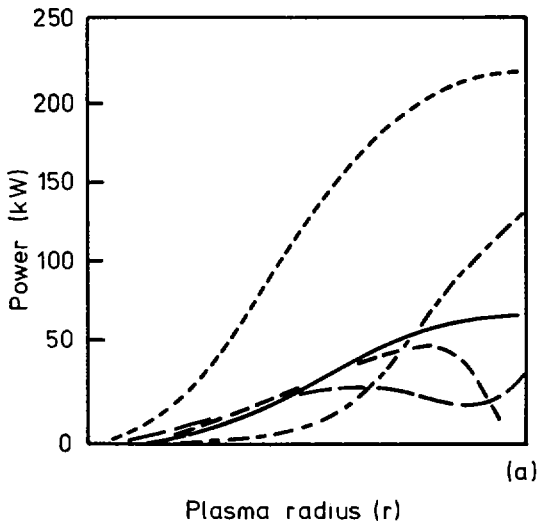

FIG. 4 Integrated radial power flow associated with electrons calculated for I_ϕ = 120 kA in ORMAK by Hogan and Clarke [3] The plasma modelling used is similar to that defined by equation (2). The curves are identified as follows :- ——— electron-ion energy transfer (term c in equation 2), – – – convective transport (term a), ——— thermal conduction transport (term b) and — – — the power losses P_e arising from atomic processes (assumed here to be entirely due to line radiation)

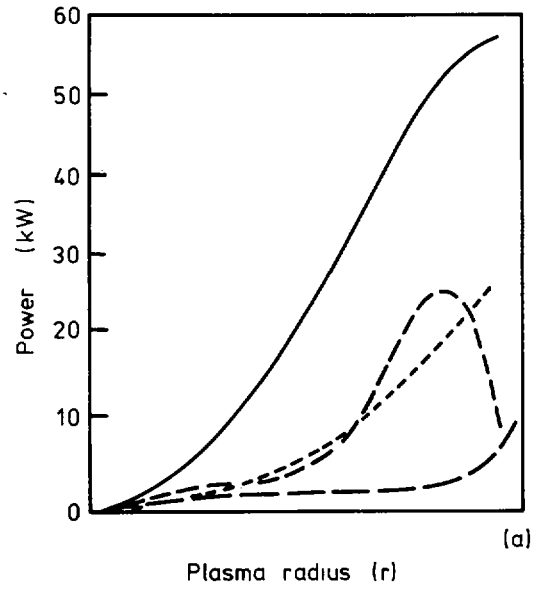

FIG. 5 Integrated radial power flow associated with ions [3]. Curve – – – shows charge exchange (P_i) and the other curves are as in FIG. 4; the plasma model is based on similar lines to equation (3).

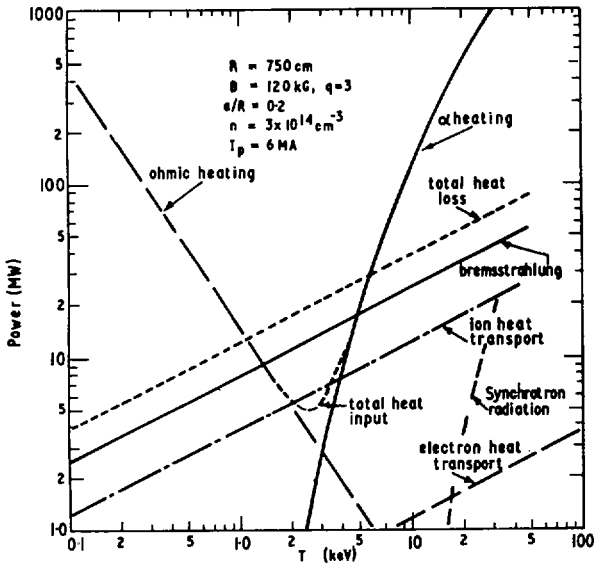

FIG. 6 Power balance - reactor case calculated by Sweetman [6] Parameters typical of those used for reactor design studies at Culham have been used. For this graph neo-classical heat losses are assumed.

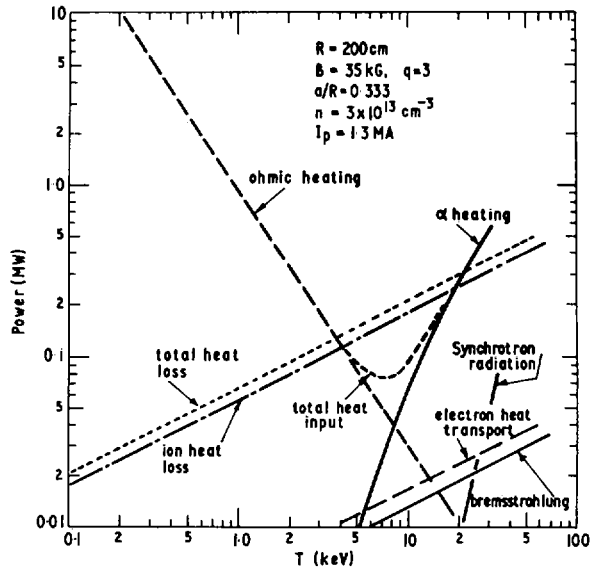

FIG. 7 Power balance - ignition experiment [4]. This case corresponds to the minimum plasma current that could give ignition at a reasonable temperature and assumes neo-classical losses.

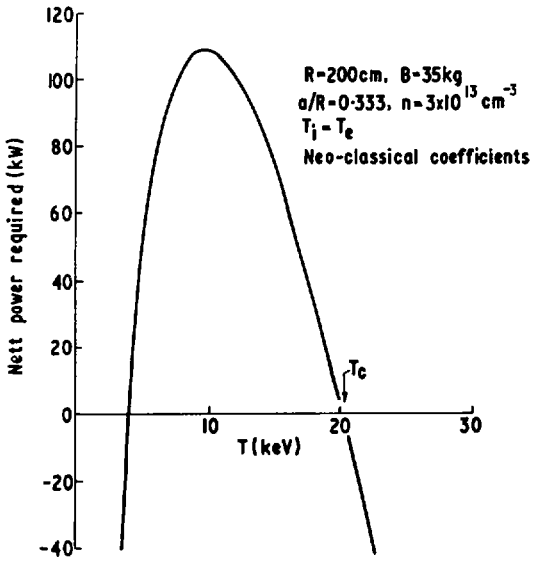

FIG. 8. Net power required to maintain the plasma at a temperature T calculated in [4] for a minimum ignition case. The critical temperature at which the plasma becomes self-sustaining is shown.

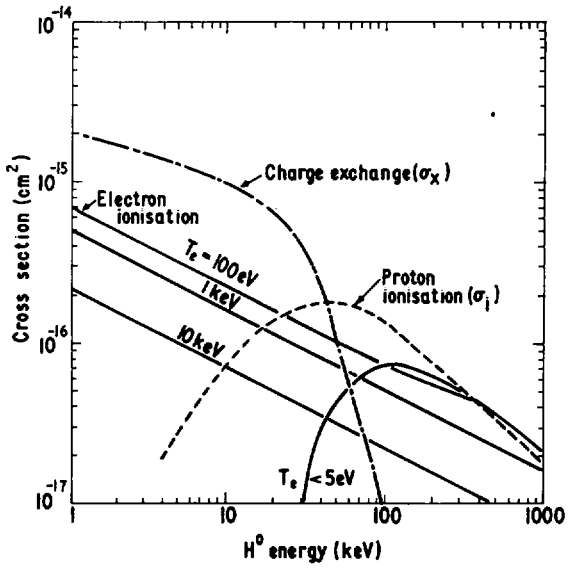

FIG 9. The separated cross-sections for ionization of the injected neutral beam versus energy. In the case of electron ionization, when $v_e > v_{in} < \delta(v_e)\ v_e/v_{in} >$ is shown for a Maxwellian electron-velocity distribution at temperature T_e; for $v_e < v_o$ the cross-section δ_e is shown for the velocity v_{in}.

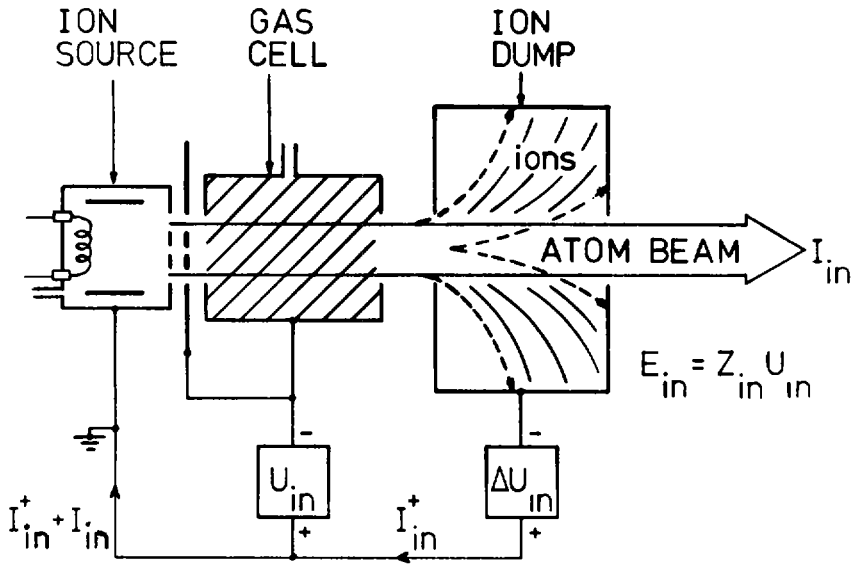

FIG. 10. Scheme for a neutral beam injector with ion energy recovery. If no beam power losses in the neutraliser cell are assumed, then power expended in the ion beam is only $\Delta U_{in}\ I^+_{in}$, where as neutral beam power is $U_{in}\ I_{in}$ and the neutral particle energy is E_{in}.

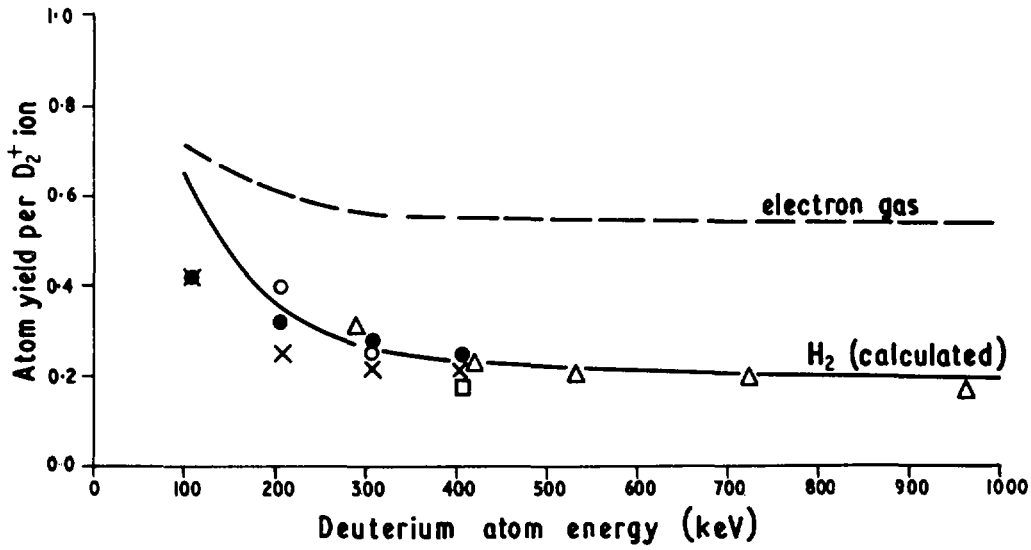

FIG. 11. Atom yield per incident D_2^+ ion for optimum target thickness calculated by Riviere [16], experimental data for H_2O, Mg, Zn, Li and Hg vapour targets are shown as well as the effects of dissociation by electron collisions in a fully ionized target.

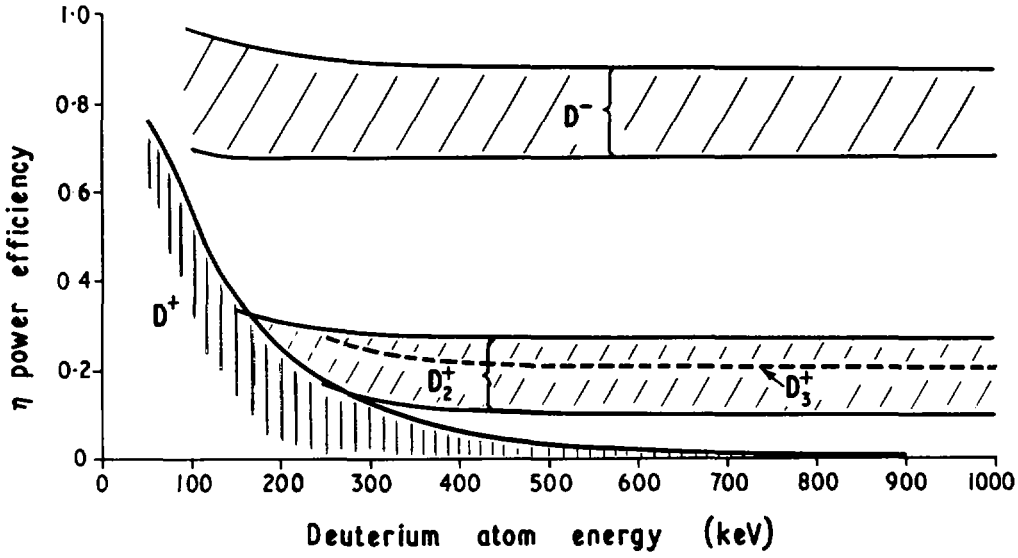

FIG. 12. Power efficiency for atom production from D^+, D_2^+, D_3^+ and D^- beams. Hatched area indicates variation with degree of ionization of target. Ionization reduces η_o for D^+ and increases η_o for D_2^+ and D^- ions.

PROPOSED IAEA PROGRAMME ON A+M DATA FOR FUSION

J.J. Schmidt and A. Lorenz
Nuclear Data Section
International Atomic Energy Agency

Abstract

After an outline of the major functions of the IAEA Nuclear Data Section (IAEA/NDS) as an international data centre a short description is given of the past development and future plans of the new IAEA/NDS programme on atomic and molecular (A+M) data for fusion. This programme is designed to coordinate the international cooperation in the assessment, determination, compilation and evaluation of A+M data and their dissemination to the scientific community concerned.

1. Introduction

The establishment of an international neutron data exchange activity twelve years ago by the IAEA, formed the basis for the international centre for nuclear data operated today by the IAEA Nuclear Data Section (IAEA/NDS).

Situated at the cross-roads of international atomic energy activities, IAEA/NDS has always been in a unique position, being exposed to all aspects of nuclear technology. Although initiated primarily to satisfy neutron cross section data requirements for the development of thermal and fast fission reactors, the IAEA nuclear data programme, reflecting the growth and emphasis of national and international nuclear programmes during the last decade, has expanded its original scope in the last few years to include all nuclear data. Today, in addition to neutron nuclear data required mainly by nuclear energy oriented programmes, the IAEA/NDS programme scope includes nuclear structure and reaction data to support the continuous development of improved and sophisticated nuclear methods and techniques, and atomic and molecular (A+M) data required in the field of plasma physics and fusion technology.

Today IAEA/NDS provides cost-free data centre services to scientists in approximately fifty IAEA Member States, with an emphasis on the developing countries, and in coordination with other regional and national centres it cooperates in the systematic world-wide collection, compilation, and dissemination of all nuclear data. As such, this centre has been developing an

awareness of the needs for all nuclear data in all pertinent aspects of science and technology in all parts of the world, and forms a focal point for the activities of all nuclear data centres.

Before introducing the Agency's new programme on A+M data for fusion, I would like to outline in some detail those major data centre functions which IAEA/NDS has assumed for nuclear data and which, from 1977 onwards, it is supposed to assume also for A+M data.

2. Functions of IAEA/NDS as a Data Centre

In its approach to the overall problem of data centre operation, the IAEA/NDS programme has been centered around three major functions: assessment, identifying what has to be done, coordination, how it is to be done, and finally service, which comprises the data centre's compilation and dissemination functions.

Assessment of data status and needs

In addition to the day-to-day growth of the awareness of data needs and data adequacy, IAEA/NDS has pursued a number of well-defined activities whose primary objective has been the assessment of data status and needs. These consist of conducting surveys of specific nuclear data requirements and identifying their priorities in context of a given field of application, and reviewing the adequacy of existing data and assessing their availability. Four independent means are used by IAEA/NDS to achieve this:

- scientific meetings;
- reviews of data status and applications;
- data evaluations; and
- the maintenance of a world-wide request list for nuclear data.

Coordination and Organization

A data centre, having the scientific scope, technical versatility and geographic coverage as IAEA/NDS, cannot perform its tasks satisfactorily on its own, without the support and guidance of an advisory committee, and the cooperation of other regional and national nuclear data centres and committees. At the same time, IAEA/NDS being an integral part of the IAEA, is in an advantageous position to foster in a systematic way the experimental and theoretical determination of the required nuclear data by organizing and coordinating research programmes, granting research assistance in the form of contracts, supplying target and sample materials in support of regional or national nuclear data programmes, and by holding training courses and seminars.

Services: Data compilation and dissemination

Data Centre services can vary, according to need and available resources, from a basic referral service to broad scope and in-depth compilation, analysis, evaluation and dissemination centre services. The latter are typical functions of an Information Analysis Center (IAC). Of the services provided by IAEA/NDS, data center services for neutron nuclear data include practically all IAC functions, while those for nuclear structure and decay data are restricted to referral and dissemination of general information.

3. The A+M data programme of IAEA/NDS past development

At its Fifth Meeting in Tokyo in November 1974, the International Fusion Research Council (IFRC) brought out the vital importance and need for a coordinated world-wide A+M data service to ensure the successful development of fusion technology. It recommended that the IAEA perform a survey of existing A+M data activities and consider adding A+M data for fusion to the scope of its existing nuclear data programme.

It was considered appropriate that the IAEA assume this new responsibility as

- its membership includes all countries with fusion research programmes;
- fusion research and technology forms part of the Agency's programme;
- nuclear data for fusion is already included in the IAEA/NDS programme; and
- IAEA/NDS is already experienced in international data compilation and dissemination.

In response to the IFRC recommendation, the following steps were taken by the IAEA. IAEA/NDS performed a first survey of the needs and availability of A+M data for fusion published as INDC(NDS)-72 in January 1976. In July 1975 it convened a Consultants Meeting of A+M data experts to advise the IAEA on the size and scope of its future A+M data programme.

On this basis, and with the support of the Agency's International Nuclear Data Committee (INDC), IAEA approved the establishment of an A+M data for fusion programme for a trial period of two years (1977/78). Upon a recommendation by INDC agreed by IFRC a joint IFRC/INDC Subcommitte on A+M data for fusion was formed with the major responsibilities to review the progress and achievements of the IAEA A+M data programme during the trial period and to advise the IAEA at the end of 1978 on the future of the programme.

Plans for 1977-78

From the beginning of 1977 professional and support staff will be available to IAEA/NDS to form a new NDS unit on A+M data for fusion and to pursue the A+M data programme. The scope of the work during the trial period will be oriented towards identifying and meeting important needs expressed by the fusion community and in particular by this meeting. The work will comprize the following main tasks:

- to compile and publish an international computerized index to the literature on A+M data;
- to compile A+M data of specific importance to current fusion research;
- to start establishing a data centre network for the systematic compilation, exchange and dissemination of available A+M data required for fusion; and
- to start formulating standardized computer input and output formats for the storage and retrieval of bibliographic and numerical A+M data.

Provided that the continuation of the programme is recommended by the joint IFRC/INDC Subcommittee at the end of 1978 it is foreseen that the aforementioned tasks be continued by IAEA/NDS as a regular long-term programme and that IAEA/NDS be the international centre for A+M data for fusion.

Annual meetings are planned to assess the current needs and status of A+M data for fusion to coordinate the cooperation of the A+M data centres and to determine the directions of future work.

4. Importance of this meeting

The importance of this meeting lies in the fact that it brings together plasma physics and fusion experts, experimental and theoretical atomic physicists and scientists working in atomic data compilation and evaluation. It is precisely these three major categories of scientists who will have to cooperate in the future in order to meet the A+M data requirements of fusion research and technology. It is hoped that the meeting will foster and initiate such cooperation.

Furthermore this meeting will present for the first time a review of national A+M data programmes with respect to fusion and is supposed to deepen our present understanding of A+M data needs, priorities and accuracies for beam injection, surface interactions, plasma modelling, plasma impurities and cooling, and plasma diagnostics. The results, conclusions and recommendations of this meeting incorporated in the reports from the working groups will therefore be very important in determining scope, emphasis and priorities of the IAEA A+M data programme.

A. DATA NEEDS, PRIORITIES AND ACCURACIES

Review Paper A1

ATOMIC AND MOLECULAR DATA NEEDS, PRIORITIES, AND ACCURACIES FOR TOKAMAK BEAM INJECTION*

J. T. Hogan
Oak Ridge National Laboratory, Oak Ridge, Tennessee 37830

1. BACKGROUND

The tokamak magnetic geometry possesses satisfactory confinement properties[1] and will form the basis for many large, new experiments in the next few years.[2,3] The aim of all of these experiments is to explore the physics of hot, dense plasmas in conditions near to those for which significant thermonuclear energy production is a possibility. Some experiments, such as the Tokamak Fusion Test Reactor, at the Princeton Plasma Physics Laboratory, may even attain breakeven, with energy produced from D-T fusion reactions equalling the energy input needed to sustain the plasma against losses.

It is a common assumption that some sort of external heating mechanism will be required to achieve high plasma temperature. While various forms of radio frequency and other wave heating techniques are being studied, the dominant emphasis is being placed on heating by the injection of energetic beams of neutral hydrogenic particles. We will first discuss the processes which are important to an understanding of the neutral beam injection process in a tokamak, and then discuss those areas for which atomic and molecular data are particularly needed. We conclude with an assessment of the accuracies required and with some estimation of the priorities which ought to be assigned.

2. NEUTRAL BEAM INJECTION: BASIC PROCESSES AND PARAMETERS

To describe the influence of atomic and molecular processes on the plasma physics of neutral beam injection, we will begin with a concise discussion of the injection and thermalization process.

---

*Research sponsored by the Energy Research and Development Administration under contract with Union Carbide Corporation.

We will restrict the discussion to events occurring after the accelerated ion beam has been neutralized and enters the plasma chamber. Figure 1 (from Rome et al.[4]) shows the tokamak geometry and a typical incident neutral beam. The neutral particles are trapped in the plasma by charge transfer with plasma ions, by electron impact ionization, or by impact ionization on the plasma ions. Once charged, these energetic injected particles are confined by the tokamak magnetic field. For the case of injection nearly tangential to the magnetic field shown in Fig. 1, the particles follow trajectories which also lie nearly along the fields. However, a projection of their orbits onto a plane perpendicular to the toroidal axis shows that there are important drift motions for these ions: their orbits are displaced outward from the axis of symmetry for particles injected nearly parallel to the plasma current, inward for those particles which are nearly anti-parallel. By calculating this resulting drift after trapping, and averaging the densities of these fast ions over the tokamak radial flux surfaces, the deposition of fast ions is finally characterized by the function H(r) shown in Fig. 1: it is the normalized density of deposited fast ions as a function of plasma minor radius. Various radial deposition profiles are shown as a function of a/λ. a is the plasma minor radius, λ the mean free path against trapping by all the processes mentioned. That is,

$$\frac{a}{\lambda} \equiv \int (n_e \langle\sigma_e V_e\rangle + n_H \sigma_X V_o + n_Z \sigma_{XZ} V_o + n_H \sigma_i V_o + n_Z \sigma_{iZ} V_o) ds \qquad (1)$$

$n_{e,H,Z}$: spatial densities of electrons, hydrogenic ions, and other (impurity) species.

V_o: velocity of the injected neutral atoms.

$\langle\sigma_e V_e\rangle$: electron impact ionization rate averaged over the electron distribution.

$\sigma_{X,XZ}$: charge exchange cross section for beam atoms with hydrogenic and other (impurity) species.

$\sigma_{i,iZ}$: ionization cross section for impact of beam atoms upon hydrogenic and other (impurity) species.

The integral is taken along the path of the beam from entrance to a point on the vacuum chamber wall opposite the injector.

Once deposited, these energetic ions undergo interaction with the background confined plasma. While many possible collective thermalization processes have been considered[5] the model of successive distant binary encounters, as described by the Fokker-Planck drift-kinetic equation[6] is thought to be accurate. The injected fast neutrals, now fast ions, thus transfer momentum and energy to the plasma and finally join the background, increasing the plasma number density. Calculations with the Fokker-Planck equation yield estimates for these processes which are consistent with the rates observed in a number of present experiments.[7-11]

The chief effect of contemporary injection experiments is to transfer energy to the background plasma, and thus to heat it to temperatures impossible to obtain by ohmic heating alone. The beam particle input is small by comparison with the particle sources on the walls and aperture limiters. The momentum input is minimized by pairing injectors in the directions parallel and anti-parallel to the current, or by injecting nearly perpendicular to the current.

The energy input to the plasma is characterized by the ratio of the so-called critical energy of the thermalizing ion, below which energy transfer occurs chiefly to the more massive positive ion species, to the electron temperature. This ratio is:

$$\frac{E_c}{T_e} \equiv 14.6 \frac{A}{A_i^{2/3}} \left[\sum_{k=1}^{N} n_k Z_k^2 / A_k \right]^{2/3} \Big/ n_e^{2/3} \qquad (2)$$

where

A, A_k: atomic masses of the beam and k^{th} species of positive ion, respectively

T_e: electron temperature

E_c: 'critical' energy

n_k: density of k^{th} species of positive ion

Z_k: ionic charge of the k^{th} species of positive ion

N: number of positive ion charge species.

This ratio depends upon the radial distributions of electron temperature, charge, and ion density.

In some present experiments the bean energy transfer to the plasma is degraded by charge exchange of the thermalizing ions with residual low-energy hydrogenic neutrals in the plasma. While the ratio of hydrogenic neutral/hydrogenic ion densities is typically 10^{-5}, the resonance charge exchange cross section is large enough to produce a significant loss of beam ions during the time (of order 10 milliseconds) required for thermalization.

Figure 2 shows a typical computed distribution of fast ions in velocity space. (This is a solution of the Fokker-Planck equation.) There is an empty region in the space of particles traveling counter to the current. This so-called 'loss region' is characterized by particle drift orbits whose spatial trajectories cause them to leave the machine and strike the wall. Perpendicular injection, such as is done on the TFR experiment,[10] also produces such a 'loss region,' especially at low plasma current. The rate at which the beam ions are lost through this gap in velocity space is characterized by the rate of diffusion in the angle made by the ion velocity with the magnetic field. This 'pitch angle diffusion' rate is proportional to the rate of momentum exchange with the background electrons, and is directly proportional to the plasma 'mean ionic charge,'

$$Z_{eff} \equiv \sum_{k=1}^{N} n_k Z_k^2 / n_e \qquad (3)$$

where the other terms have already been defined and n_e is the electron density. Again, the sum is to be taken over the N species of positive ions in the plasma.

Once the energy is transferred to the plasma, the considerations of plasma cooling by impurities to be discussed elsewhere in these proceedings will apply.

In summary, then, the neutral injection process in tokamaks requires knowledge of the deposition process (and the quantities in Eq. 1), the energy exchange process (quantities in Eq. 2), and momentum exchange (quantities in Eq. 3).

The cross sections and the rate coefficient needed for Eq. (1) are obvious examples of atomic data needs. The charge transfer and impact ionization cross sections are needed for quite a large number of species, and over a fairly wide range of energies. (We will discuss specific instances later.) The quantities needed for the critical energy and pitch angle diffusion processes (Eqs. 2 and 3) are also needed for plasma diagnostics and for estimates of plasma cooling due to impurity ions. One wishes to ascertain, largely from spectroscopy, the chemical composition (i.e., the n_k) and charge state distribution (i.e., Z_k) for the positive ion species in the plasma. The needs here are typically for identification of strong resonance lines, for transition probabilities and for shifts of K and L lines for highly ionized heavy metals. Estimates of the plasma cooling processes will require knowledge of the dielectronic and radiative recombination rates for the impurity ions. These topics will be discussed elsewhere in these proceedings.

Since these latter processes are important to the overall plasma energy balance, and are not unique to the neutral injection process, we will focus on the deposition cross sections in our discussion of atomic data needs.

In Table 1 we list the characteristics of present neutral beam injection experiments which are important to the atomic and molecular physics processes to be discussed.

Table 1. Neutral Injection Parameters for Present Experiments

Experiment	Injected[a] Species	Plasma[b] Species	Neutral Injection Energy[c] (keV)	Minor Radius (cm)
Cleo tokamak[d] (Culham Laboratory)	H^0	H^+	22.5	18
ORMAK[e] (ORNL)	H^0	H+,D+,O,Fe	25	23
Adiabatic toroidal compressor (ATC)[f] (PPPL)	D^0	H+,D+,O,Fe	15	17
TFR[g] (Fontenay-aux-Roses)	D^0	H+,D+,O,Fe,M_o	39	20
T-11[h] (Kurchatov Institute)	H^0	H^+	20	22

[a] H^0, D^0, and He^0 are all commonly injected.

[b] In present experimental devices the chemical composition is somewhat uncertain. Various devices have reported or suspected significant concentrations of C, O, Fe, M_o, W, N_i, N, Cr, Hg, P_t, Cu. In addition such gases as He, N_e, Ar, K_r, and X_e have been 'puffed' at very low energies into tokamak discharges as diagnostics and A_ℓ and S_c films have been sublimated by a laser burst and injected into the plasma in a controlled way to study the resulting diffusion [see footnote (i)]. The ATC device employed T_i gettering to reduce the impurity content. While the impurity concentrations were notably diminished [see footnote (j)] some traces of T_i appeared as a result.

[c] We quote the highest energy components. The presence of various molecular species in the ion source causes the appearance of lower energy injected atoms at fractions of the full energy. The energy spectrum is a characteristic of the source used on each experiment, but the bulk of the power is transmitted by the full and half energy components.

[d] J. G. Cordey et al., Nucl. Fusion 14, 441 (1974).

[e] W. R. Wing et al., Proceedings of the Fifth IAEA Conference on Plasma Physics and Controlled Nuclear Fusion Research, Tokyo, 1974.

[f] R. A. Ellis, Jr., et al., Nucl. Fusion 16, 524 (1976).

[g] Equipe TFR, Report EUR-CEA-FC-834, Fontenay-aux-Roses, 1976, also to be presented at Sixth IAEA Conference, Berchtesgaden, 1976.

[h] V. S. Mukhavatov et al., private communication.

[i] S. A. Cohen, J. L. Cecchi, and E. S. Marmar, Phys. Rev. Lett. 35, 1507 (1975).

[j] P. E. Scott, C. C. Daughney, and R. A. Ellis, Jr., Nucl. Fusion 15, 431 (1975).

In Table 2 we list the relevant injection parameters for some of the nearer term planned injection experiments.

In Table 3 we note the injection parameters planned for large tokamak experiments, to be operating circa 1980. [2]

Finally, we note that studies of fusion reactor power plants have been made[12] and that neutral beam energies of 180–200 keV D^0 are foreseen for D-T reactor operation. We note also that these reactor systems will contain an appreciable alpha particle residue from D-T reactions, so that there is an inevitable 'impurity' present in these systems. The minor radii of these devices are typically foreseen to be ~2 m.

Table 2. Neutral Injection Parameters for Near-Term Planned Experiments

Experiment	Injected Species[a]	Plasma Species[b]	Neutral Injection Energy (keV)	Minor Radius[c] (cm)
PLT (PPPL)	H^0	H^+, D^+	40	45
ORMAK Upgrade (ORNL)	H^0	H^+, D^+	40	30
Doublet III (GA)	H^0	H^+, D^+	80	45[d]
DITE (Culham)	H^0	H^+, D^+	30	27
TFR 600 (Fontenay-aux-Roses)	D^0	H^+, D^+	40	20
PDX (PPPL)	H^0	H^+, D^+	40	45

[a]Others, such as He, may be tried.

[b]The same impurities as noted in Table 1 are likely to be present.

[c]Again, as with Table 1, some distribution of lower energies is expected depending on the source.

[d]Doublet III has a vertical dimension 135 cm.

Table 3. Neutral Injection Parameters for Planned Experiments Circa 1980

Device	Injected Species[a]	Plasma Species[b]	Neutral Injection Energy (keV)	Minor Radius[c] (cm)
TFTR (PPPL)	H^0,D^0	H^0,D^0,T^0	120	85
JET (EURATOM)	H^0,D^0	H^0,D^0,T^0	80,160	125
JT-60 (JAERI)	H^0,D^0	H^0,D^0,T^0	50–100	100
T-10M (Kurchatov)	H^0,D^0	H^0,D^0,T^0	?	75

[a]Proposals for a counterstreaming ion torus (see footnote d) employ T^0 injection. In addition, there has been discussion of injecting D^0 into He^3.

[b]The impurity concentrations noted in Table 1 may be expected.

[c]The designers hope to optimize the beams in these large systems, so that most of the beam current is carried in the highest energy component.

[d]D. J. Jassby, Nucl. Fusion 16, 15 (1976).

3. BEAM TRAPPING

Making reference once more to Fig. 1, we note that beam deposition may be characterized by the ratio a/λ. Further, the deposition profile ceases to be peaked in the center and becomes flat for $a/\lambda \sim 4$. In present tokamaks the energy confinement is better in the center of the device than at the edge; thus, the peaked profiles in Fig. 1 will produce an efficient plasma heating, while those peaked outwardly will produce poor heating. Not only that, but such outwardly peaked profiles will also produce a stronger interaction with the wall, as we will discuss. Thus we choose $a/\lambda \sim 4$ as representing the lower limit of adequate beam penetration; larger values of a are deemed unsuitable.

The cross sections needed in Eq. (1) are not known for impurity trapping for the energies of interest. Since the sizes and injection energies of many large experiments with injection energy/nucleon ≥40 keV were predicated on the assumption that hydrogenic ion impact ionization was the dominant trapping process,[13] we will consider the consequences suggested by Girard et al. [14] of a different assumption. Assuming that the Born approximation is valid at these relatively low energies and that the impurity ion impact ionization cross section simply scales as Z^2 times the hydrogenic cross section, then

$$\left(\frac{a}{\lambda}\right)_{\substack{\text{impact}\\ \text{ionization}}} = \int ds\ (n_H + n_Z Z^2)\ \sigma_H$$

where the conventions are the same as for Eq. (1). Using the definition given by Eq. (3), the local trapping rate is proportional to $n_e\ Z_{eff}\ \sigma_H$. In Fig. 3 we see a 'universal curve'[15] which embodies these assumptions. The figure shows the locus of points which satisfy $\frac{a}{\lambda} = 4$ as a function of the product of minor radius and central electron density, Z_{eff} and the energy/nucleon. For all the experiments in Table 1 the range of central electron density is $2 \cdot 10^{13}\ cm^{-3} \leq n_e \leq 10^{14}\ cm^{-3}$ while $2 \leq Z_{eff} \leq 12$. Thus, most of the points for present experiments would lie below the curve, indicating adequate penetration. The near-term experiments listed in Table 2 become marginal, however, and the 1980-era experiments very clearly lack adequate penetration if the Born approximation assumptions are valid.

The status of the present and near-term experiments relies on assumptions made about the hitherto unknown charge transfer cross sections. They are assumed not to depend on impurities in Fig. 3 (the dotted line shows the locus of $a/\lambda = 4$ if this cross section is to be enhanced by Z_{eff} along with the impact ionization cross section).

As an example of the dynamic consequences of having $a/\lambda > 4$, we present a computational study of the TFTR device. The computer model has been described in Refs. 16–18. We assume as before that $\sigma_{iZ} \propto Z^2 \sigma_i$. The initial plasma state is shown in Fig. 4a, $T_{e,i}(0) = 4$ keV, plasma isolated from the wall. We suppose that 12 MW of D^0 neutrals are injected, with 40% of the particles at 120 keV, 40% at 60 keV, and 20% at 40 keV. The plasma is assumed to have 2% oxygen impurity relative to the proton density, distributed uniformly in radius. The hydrogenic plasma ions are initially assumed to be T^+. (As the beam injection proceeds the plasma becomes a D-T mixture.) As the 120 keV D^+ ions thermalize, they produce direct thermonuclear reactions by interacting with the background fuel ions. Thus, a 'breakeven' experiment may be envisaged in which the thermonuclear energy production is derived only from reactions between the beam and the background plasma.[10] Such an experiment would be relatively insensitive to the deleterious effects of impurities on the plasma energy balance in general, providing only that the beam ions can be deposited in the center of the plasma. In Figs. 4a-d we see the interrelation of impurity trapping of the beam and the subsequent dynamics. As the beam ions thermalize, the plasma is heated and resulting hot charge exchange neutrals leave the plasma to produce some impurities by sputtering. As these impurities (assumed to be Fe, as seen in Fig. 4c) enter the plasma, they decrease the mean free path against impact ionization. This, in turn, traps the beam farther to the outside, in a region of higher neutral density. The combination of edge heating and high neutral density at the edge produces an even stronger charge exchange bombardment of the wall, more sputtering, and a cascade in which the beam is effectively excluded from the plasma (Fig. 4d). The ratio of fusion energy production to beam energy input is ~0.35 in this case, and ~2 MJ of neutron energy is produced.

This beam deposition instability has been examined by a number of workers[20–23] and serves as an excellent example of the need for atomic data. To assess the likelihood of this cascade one needs the cross sections for charge transfer and impact ionization for the injection of H^0, D^0 (and perhaps T^0) into a hydrogenic plasma (electrons, H^+, T^+, D^+ and impurity ions). The energy ranges of interest are given in the tables. We should note also that the D-T cross section for 0–150 keV could perhaps be known more accurately.[24]

4. ACCURACY AND PRIORITIES

We first of all note that the beam density deposited along the chord in Fig. 1 is proportional to $e^{-\int ds/\lambda}$. Thus, all the relevant cross sections appear in an exponent. We note also that the calculations we have employed to suggest the importance of the beam deposition instability are model-dependent. Thus, if the dielectronic recombination rates were better known we might as well have concluded that photon emission carried the energy from the plasma, not charge exchange. Then the sputtering rates would be much lower and the cascading process might not occur at all. In this event, however, photo-electron stimulated desorption might produce enough light impurities from the wall to cause the same instability.

Thus, we may rather arbitrarily assign an overall estimate of 10% to the accuracy with which these charge transfer and impact ionization cross sections should be known. We must know the magnitude of the cross section as well as the dependence on charge for the spectrum of energies characteristic of each device.

The tables list quite a number of possible impurity ions to study for the relevant energy ranges. We should begin to order them by the following remarks.

1. The wall material of all the experiments is stainless steel; the limiter which all use, or will use, contains M_o or W.
2. Oxygen and carbon are ubiquitous light elements.
3. Novel wall or limiter materials are now being tried, or are planned for the future. Pyrolytic C, SiC, and B_4C have all been examined in tokamak experiments.

Cross-section measurements are needed for this problem to assess the importance of this cascade process: the information is needed so that one can decide whether more stringent conditions ought to be imposed on the vacuum system and/or wall and limiter materials.

REFERENCES

1. L. A. Artsimovich, Nucl. Fusion 12, 215 (1975) and H. P. Furth, Nucl. Fusion 15, 487 (1975).
2. Third "World Survey of Major Facilities in Controlled Fusion Research," special supplement to Nucl. Fusion (1976).
3. Large Tokamak Experiments, compiled by A. H. Spano, Nucl. Fusion 15, 909 (1975).
4. J. A. Rome, J. D. Callen, and J. F. Clarke, Nucl. Fusion 14, 141 (1974).
5. H. L. Berk et al., Nucl. Fusion 15 819 (1975).
6. J. G. Cordey and W.F.G. Core, Phys. Fluids 17, 1626 (1974).
7. J. G. Cordey et al., Nucl. Fusion 14, 441 (1974).
8. W. R. Wing et al., Proceedings of the Fifth IAEA Conference on Plasma Physics and Controlled Nuclear Fusion Research, Tokyo, 1974.
9. R. A. Ellis, Jr., et al., Nucl. Fusion 16, 524 (1976).
10. Equipe TFR, Report EUR-CEA-FC-834, Fontenay-aux-Roses, 1976; also to be presented at Sixth IAEA Conference, Beschtesgaden, 1976.
11. V. S. Mukhavatov et al., private communication.
12. J. W. Davis and G. L. Kulcinskii, Nucl. Fusion 16, 355 (1976).
13. A. C. Riviere, Nucl. Fusion 11, 363 (1971); D. R. Sweetman, Nucl. Fusion 13, 157 (1973)
14. J. P. Girard, D. A. Marty, and P. Moriette, Proceedings of the Fifth IAEA Conference on Plasma Physics and Controlled Nuclear Fusion, Tokyo, 1974.
15. H. C. Howe, Jr., private communication.
16. M. M. Widner and R. A. Dory, Bull. Am. Phys. Soc. 11 (1970); also Oak Ridge National Laboratory TM-3498 (1971).
17. J. T. Hogan, "Multifluid Tokamak Transport Models, Methods of Computational Physics," Vol. 16, Applications to Controlled Fusion Research.
18. J. K. Munro et al., Oak Ridge National Laboratory Report ORNL-TM-5262 (1976).

19. J. M. Dawson, H. P. Furth, and F. H. Terney, Phys. Rev. Lett. 26, 1156 (1971).

20. J. G. Cordey, W. G. F. Core, and J. Sheffield, Nucl. Fusion 15, 755 (1975).

21. H. P. Furth, private communication, and D. E. Post et al., Princeton Plasma Physics Laboratory Report MATT-1261 (1976).

22. R. W. Conn, M. Khelladi, and J. Kesner, J. Nucl. Mater. (to appear); also University of Wisconsin Report UWFDM-136 (1976).

23. J. T. Hogan and H. C. Howe, Jr., J. Nucl. Mater. (to appear); also Oak Ridge National Laboratory Report ORNL-TM-5361 (1976).

24. Leona Stewart and G. M. Hale, The T(d,n) ^{4}He and T(t,2n) Cross Sections at Low Energies, Los Alamos Scientific Laboratory Internal Report, LA-5878-MS (1975).

FIGURE CAPTIONS

Fig. 1. Geometry of neutral beam injection into a torus. At upper left, a top view showing the incident neutral beam. At upper right, a cross section of the torus, showing injected ion drift trajectories. Lower, typical radial deposition profiles for injection along (co-) and anti-parallel (counter-) to the plasma heating current.

Fig. 2. The density of fast ions at the magnetic axis of the torus, shown here in velocity space $v_{\|}$ is the component of velocity parallel to the toroidal magnetic field, $v_{\perp}$ is normal to the field. The heating current is assumed to be in the same direction as the magnetic field, so that the overall number of counter-injected ions is smaller than the number of co-injected ions. [See H(0) for co- and counter-injection in Fig. 1.] Particles in the loss region have drift orbits with radii larger than the plasma minor radius, and so are lost before they thermalize.

Fig. 3. Maximum products of plasma electron density and plasma minor radius allowed for beam penetration, as a function of energy/nucleon of the injected species, with Z_{eff} as a parameter. These curves are made with the assumption that the impact ionization cross section is enhanced by Z_{eff}.

Fig. 4. A computational study of TFTR. Figure 4a shows the time evolution of the electron and fuel ion (D-T) temperature profiles from t = 0 to 300 milliseconds. The edge trapping of the beam produces strong ion heating at the edge, in a region where the neutral atom density is highest. The resulting increased charge exchange flux produces impurities (assumed to be Fe in this example, Fig. 4c). The electron density evolves as shown in Fig. 4b, with new electrons being produced by the stripping of impurities. Figure 4d shows the evolution in time of the beam deposition profile, H(r). The initially peaked profile proceeds to become peaked toward the edge during the heating phase.

Figure 1

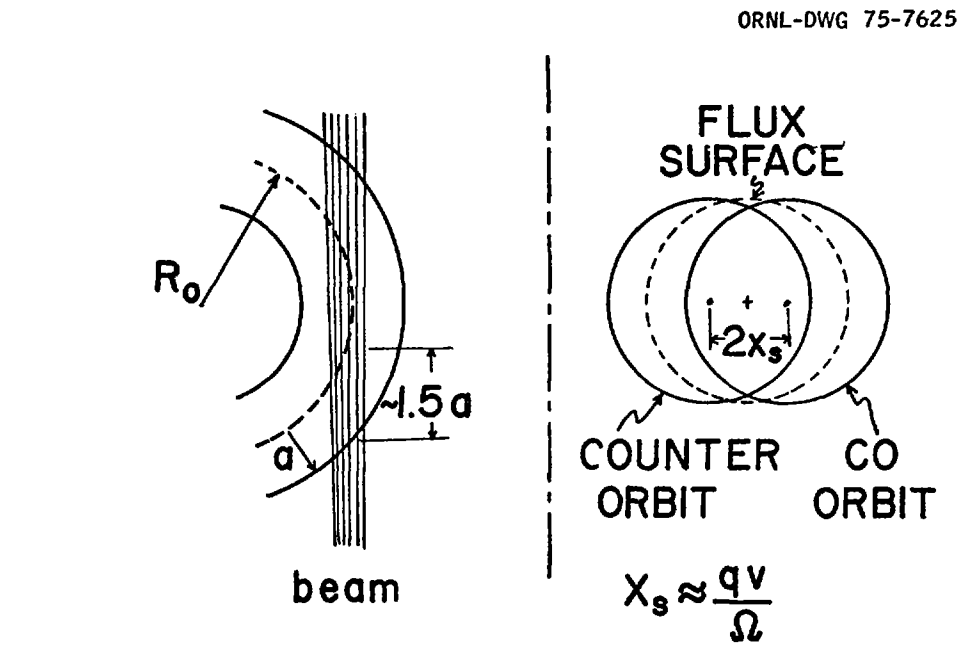
ORNL-DWG 75-7625
R_0
~1.5a
a
beam
FLUX SURFACE
$2x_s$
COUNTER ORBIT
CO ORBIT
$X_s \approx \frac{qv}{\Omega}$
$\dot{n}_f(r) = \frac{I_B/e}{(2\pi R_0)(\pi a^2)} H(r) = \frac{d\dot{N}/dr}{\text{DRIFT SURFACE AREA}}$
COINJECTION
$a/\lambda_0 = 1$, 99 %
$a/\lambda_0 = 2$, 99 %
$a/\lambda_0 = 4$, 99 %
$a/\lambda_0 = 8$, 98 %
COUNTERINJECTION
$R_B = 68.5$ cm
$a/\lambda_0 = 1$, 92 %
$a/\lambda_0 = 2$, 86 %
$a/\lambda_0 = 8$, 55 %
$a/\lambda_0 = 4$, 74 %
$\langle H(r,\theta) \rangle_\theta$
r/a
r/a

Figure 2

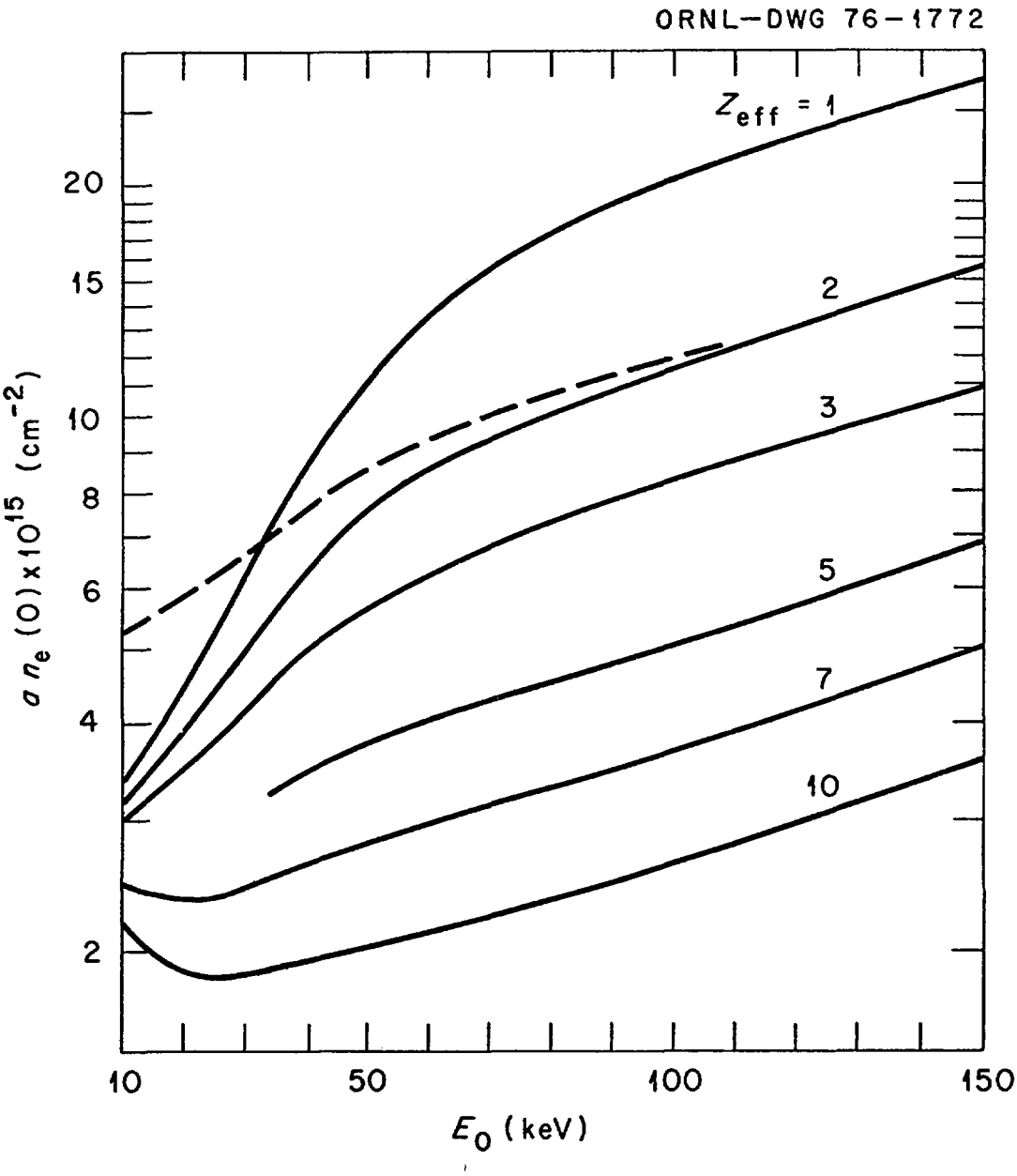
ORNL-DWG 76-1772
Z_{eff} = 1
2
3
5
7
10
20
15
10
8
6
4
2
$\sigma n_e(0) \times 10^{15}$ (cm^{-2})
10
50
100
150
E_0 (keV)

Figure 3

$F(V_{\parallel}, V_{\perp}, R=0)$ ORMAK

RADIAL FOKKER PLANCK TRANSPORT CODE

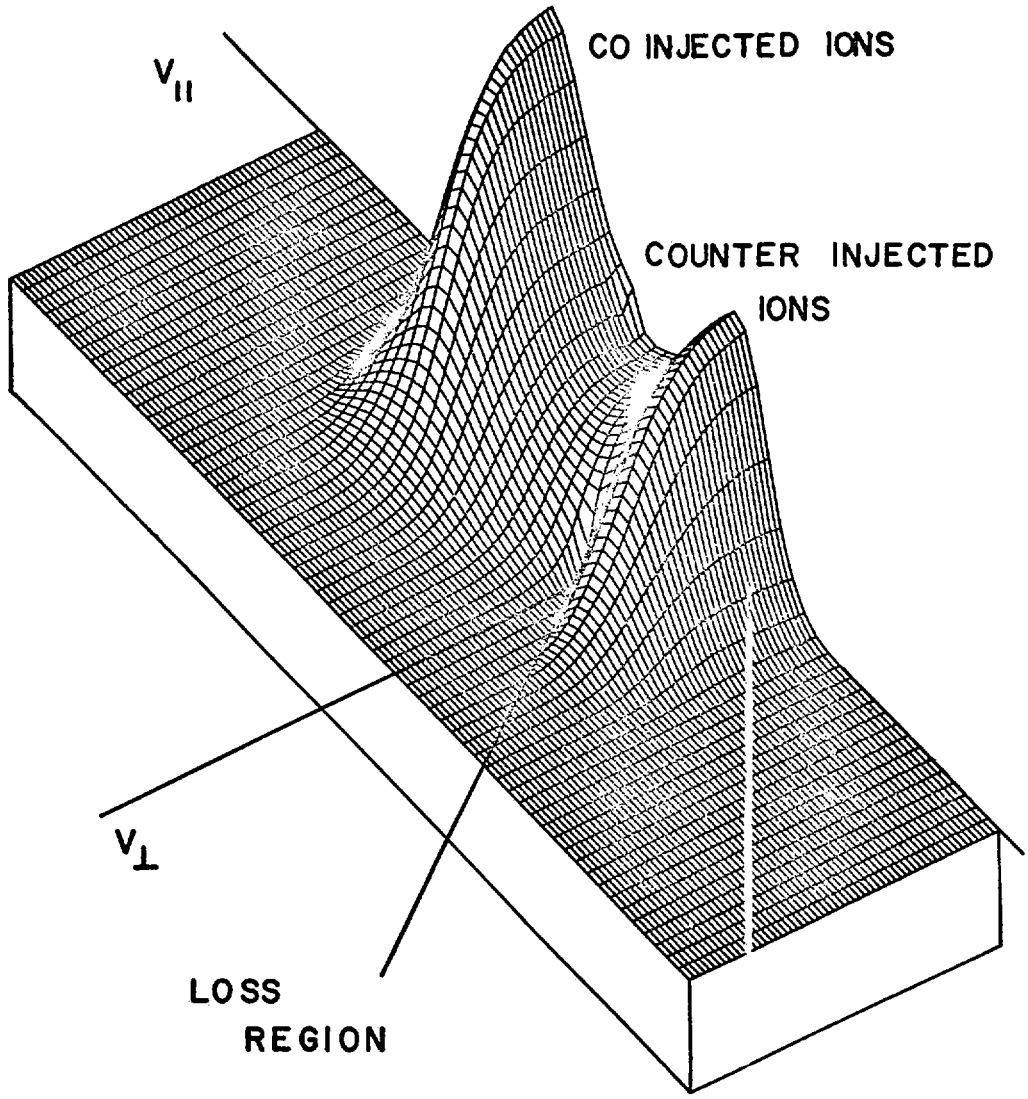

Figure 4

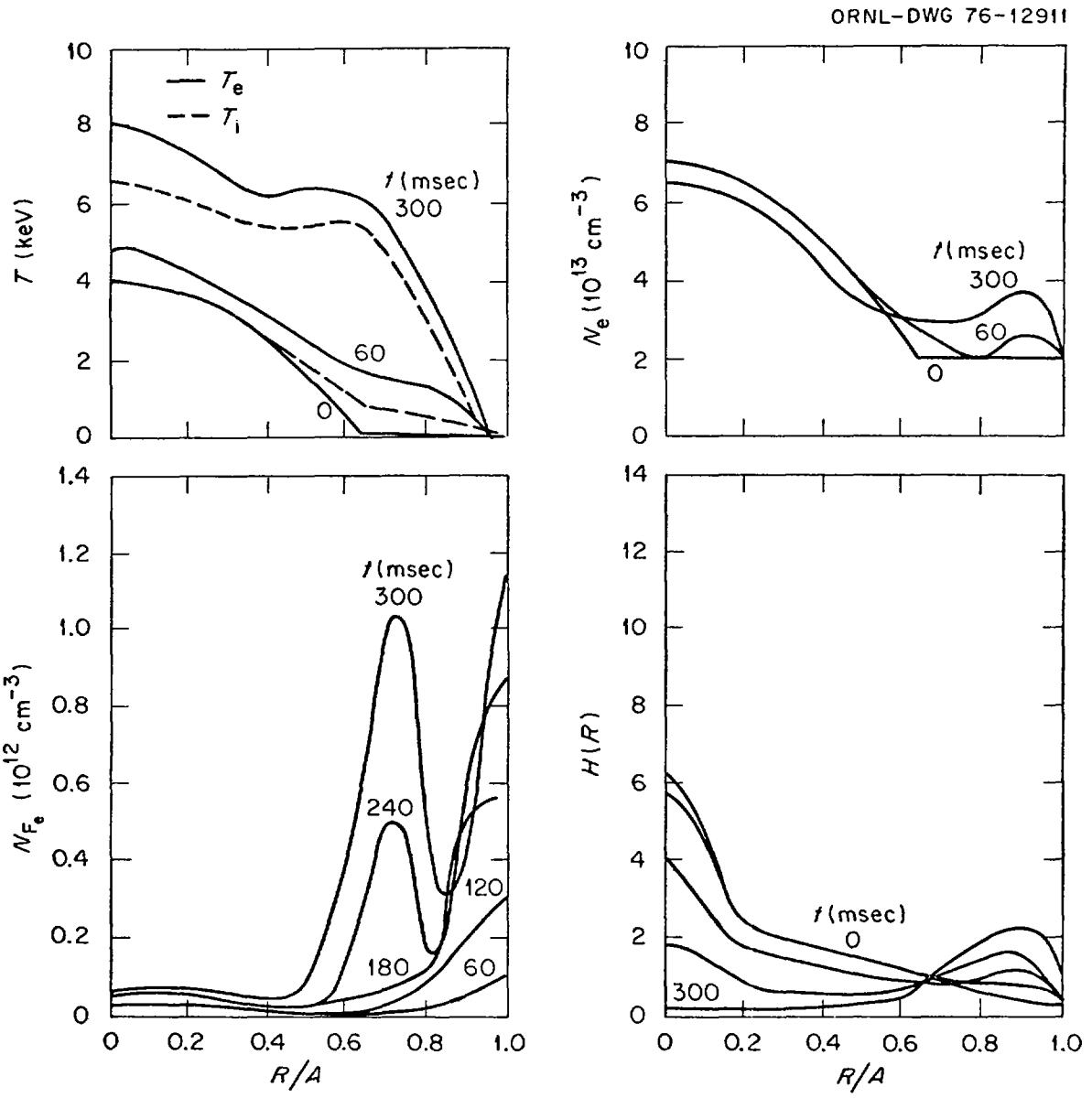
ORNL-DWG 76-12911
T_e
T_i
T (keV)
t (msec)
300
60
0
N_e (10^{13} cm^{-3})
N_{F_e} (10^{12} cm^{-3})
240
120
180
H(R)
R/A

Atomic and Molecular Data for Fusion

A2. Data Needs for Plasma Surface Interaction

H.Vernickel

Max-Planck-Institut für Plasmaphysik, EURATOM Association
D-8046 Garching/München, Germany

Abstract

Requirements for data on surface phenomena important for plasma surface interactions are given. These include yields for sputtering by light ions, data on reflection and trapping of hydrogen, information about blistering and yields for desorption of adsorbed gases by ions, electrons and photons. The importance of plasma surface interaction is explained, the data requirements for the different types of plasma machines and reactors are outlined. After a short description of the present state of knowledge of the individual processes a discussion of possible synergistic effects is presented. They are shown to be important but without dramatic consequences according to our present knowledge.

1. Introduction

The present contribution contains the data requirements for plasma surface interaction (PSI). I shall restrict myself to atomic and molecular data of the surface processes occurring during PSI. The discussion of radiation damage in the first wall and of macroscopic properties, e.g. the resistance to thermal shocks, is not the topic of this paper.

Plasma physics of the boundary layer, including the behaviour of impurities, is very important for PSI. Atomic data needed in that context, as cross sections for charge exchange, for ionization etc., will, however, not be tretated here. They will be contained in contributions A3 and A4.

Only approximate statements about the data needed can be made, since PSI is not yet understood in detail. Rather broad limits on the parameter ranges of interest have therefore to be given.

In the next chapter the importance of PSI for fusion research will be explained. In this context we shall also deal with the desired accuracy of the data.

In the third chapter the data needs for the different lines will be more precisely defined; in the fourth section a short outline of the present state of knowledge will be given. An estimate on possible nonlinear superpositions and synergistic effects will be attempted in the fifth chapter.

The final chapter summarizes the date requirements in tabular form. This then also states which data, in the authors opinion,should be included in a data collection.

Many review papers on plasma wall interaction have appeared in recent years, some of which are quoted as ref.[1] to [12],two conferences have been devoted to this topic [13, 14]. Many aspects are treated in more detail in these papers.

In quoting literature, review papers are preferred. Otherwise those papers are being quoted which best illustrate a given point or which simply happen to be familiar to the present author. No attempt has been made to be complete or historically correct.

2. Plasma Surface Interaction (PSI)

The first wall is, depending on its condition, a source or a sink of particles or both; it is always a sink of energy. The interaction between plasma and wall therefore influences the composition, the density and the temperature profiles of the plasma at least in the boundary layer; the processes occurring at the wall determine the boundary conditions for the plasma. In present-day tokamaks the discharge lasts typically ten times the particle confinement time, i.e. the reemission of particles from the wall is very important.

From this it follows that

- PSI is important for understanding the discharge.

This would even be true, if only hydrogen[1)] would be involved in this interaction. However, added to this is an inflow of impurities released from the wall by PSI. (Impurities for the plasma are all elements except hydrogen.)

Impurities increase radiation losses, dilute the fuel and increase the collision frequency due to their larger charge. The latter has different consequences for the plasma, desriable ones as well as undesirable ones [5,15], which cannot be discussed here. At any rate, radiation losses set an upper limit for the tolerable concentration of impurities [16]. This may lead to short burning cycles of a reactor [17]. We see:

- PSI is important because of the release of impurities.

This release of atoms from the wall also leads to wall erosion. Now estimates show this erosion to be fairly tolerable if the particle and energy fluxes to the wall are uniformly distributed [18]. The lifetime of the first wall in this case is primarily determined by neutron induced radiation damage. (Older calculations of severe wall erosion even for uniform

---

1) The term "hydrogen" is used for all hydrogen isotopes.

wall bombardment [19] have been estimates of upper limits for reactors of a neutron wall load of 13 MW/m^2. In more recent designs the wall load has been decreased by roughly a factor of ten.) Nevertheless, erosion still has to be regarded as a severe problem. On the one hand there are special parts that receive a larger than average load, limiters in present-day machines and possibly divertor plates in reactors, on the other hand there is always the possibility of a locally increased interaction, as we have seen, for instance,in TFR, where the plasma burnt holes into the liner [20]. As a third point we see therefore:

- PSI is important because of the wall erosion caused by it.

In order to get a better understanding of the processes occurring, it is important to measure density and temperature profiles in the boundary layer, to compare them with theoretical predictions, and to determine the state of the surface, all of this in the most advanced plasma machines.

A basis for the interpretation of these measurements is a knowledge of cross sections and yields of the individual processes, i.e. knowledge of the atomic and molecular data of the surface processes. Their discussion forms the main body of the present paper.

These data and the observations in plasma machines, in which usually several processes occur simultaneously, are connected by theoretical models. Simple particle balance equations, as are often used for discussions of PSI (see for example, [2,3,7] and literature quoted therein) give only a rough survey. More complicated models are necessary, which, however, can only be handled with the aid of complex numerical codes. These codes, e.g. [21,22] provide no analytical solutions, therefore general statements about the necessary accuracy of the data are not possible. In general an accuracy of a factor of 2 should be sufficient in the present state of affairs. There are, however, cases in which higher precision is necessary. It may, for instance, occur during the ignition

phase that the radiated power almost compensates the heating power. A factor of 2 in impurity concentration then determines whether the impurities can be completely ionized, in which case radiation decreases or whether the discharge is quenched. We conclude:

- It would be desirable that the data are accurate to 20%. Taking into account that accuracy is only meaningful to the extent that the data refer to a known and reproducible surface state and the difficulties of determining the influence of several uncertain parameters on the data, it would seem premature to require more than a factor of 2 in accuracy.

It may be pointed out here that in present-day machines we usually deal with undefined "technical" surfaces. The clean-surface data therefore have to be supplemented by data from well defined technical surfaces. Data from less well defined technical surfaces can at times be useful, since they at least outline the range in which data may vary (see, for example, photo desorption!)

Better understanding of PSI will primarily contribute to improved predictions of the discharge in new machines. It may also help in the selection of proper materials, although it should be noted that there are many different requirements on the material properties of the first wall of a reactor [17], such as resistance against neutron radiation damage, compatibility with thermal shocks, with high temperature operation, availability and many others. Separation of the two functions: mechanical structure and surface facing the plasma, for instance by coating the first wall or by placing a curtain in front ot it, as proposed in [23] would give more freedom in the design.

3. PSI in the various machines, data requirements

A general survey of the important processes may be obtained from the matrix in Fig.1. Here the "matrix elements" name the processes connecting the fluxes from plasma to the wall (upper line) with the fluxes from the wall to the plasma (left row).

Evaporation is only important if plasma energy is deposited at a small area in a short time [10,11]. There are numerous collections of heats of evaporation and vapour pressure.

In some reactor designs the first wall is protected by low Z curtains or bumpers which are cooled only by radiation. In that case rates of evaporation or sublimation have to be known since they limit the permissible temperature and hence the thermal wall load. In what follows the different lines will be treated separately.

3.1 Stationary and quasi-stationary toroidal machines

These are primarily tokamaks but the same effects occur in low and high beta stellaraotrs if the burning phase is sufficiently long.

PSI depends very much on the properties of the boundary layer. It is hoped to influence it favorably by either incorporating divertors and thus shifting the main PSI to separate chambers or by having a cold gas blanket. With the latter the plasma is surrounded by a dense layer of cold plasma or neutral gas, such that ions, electrons and neutrals leaving the plasma are slowed down below the threshold for sputtering or desorption before reaching the wall. Both of these schemes are under investigation but no definite answers as to their operation in a reactor are possible at this time.

3.1.1. Reactors (with clean walls)

We assume that after some time of continuous operation the walls will be atomically clean. Then backscattering,

reemission and sputtering remain, while desorption from surfaces may still be of some importance during start-up after venting. If the wall material exhibits large hydrogen solubility, desorption of adsorbed hydrogen during temperature excursions of the wall may occur.

> It is sometimes discussed if diffusion of gas, dissolved in technical materials, might not be a long lasting source for impurities at the surface. This would be of importance if a surface coverage were maintained such that the desorption is comparable with the rate of sputtering. For simplicity let us only consider hydrogen bombardment, in which case we can simply compare the yields for sputtering S with the yields for desorption Nq(N is the number density at the surface q the cross section for desorption). Since S is of the order of 10^{-2}, desorption is important if $Nq \gtrsim 10^{-2}$. In the worst case diffusion supplies continuously the concentration, where both effects are equal. Now let the hydrogen flux be $10^{15}/cm^2$, the initial gas concentration in the wall material 10^{-3} and the wall thickness 1 cm, then the supply lasts for 50 days. In reality outdiffusion drops exponentially. If in the beginning desorption is larger than assumed here it dominates initially but gets less important than sputtering in a shorter time. If desorption is less than sputtering from the outset it lasts long, but may be neglected compared with sputtering. This is not in contradiction with the observations in [24], where the outgassing yield in radiation environment decreased considerably after desorption of 10^4 monolayers.

More important processes are:

Reflection and reemission of hydrogen(and helium). These processes are important for the so-called recycling and for wall bombardment with energetic charge exchange neutrals. We need the coefficient of reflection, the energy and angular distribution of the reflected particles and their charge state. For primary energies above 10 keV fluxes to the wall should be small and the reflection coefficients also gets small,hence data on reflection are primarily needed for energies below this limit.

Reflected particles retain part of their initial energy. Those not reflected initially come to rest in the solid. They either become permanently trapped or are subsequently released. The released particles also contribute to recycling. If the

primary energy gets low (10 to 100 eV) penetration into the solid ceases, there is only energy exchange between particle and wall. This accommodation is important for a cold gas blanket. This means that the processes discussed here have to be studied down to very small energies.

Trapping, especially for primary energies below 10 keV is especially important for possible "pumping divertor plates" or similar divertor pumps [25,26].

The other important field is erosion by sputtering and blistering. Sputtering occurs by bombardment with hydrogen, helium and with impurities heated in the plasma (carbon, oxygen, wall material). We are interested in data covering the energy range between sputtering threshold and a few keV for the impurities, about 100 keV (the injection energy) for hydrogen and up to 3,5 MeV (the energy at which alphas are born) for helium. Of course, the number of alphas hitting the wall with the full energy is unknown. For a particular beam driven machine it has been estimated that about 20 % of the alphas are on uncontained orbits and hit the wall with full energy [27].

This point is especially important for the other erosion mechanisms, blistering and exfoliation. They have to be investigated in the same energy range as sputtering.

3.1.2 Present-day machines

Conditions in present-day tokamaks (and stellarators) are quite different. The walls are not clean, on the contrary we have to expect at least several monolayers of foreign material.

These layers are not removed during a discharge to any appreciable extent. Even in a relatively dirty discharge the impurity content in the plasma corresponds to only a small fraction ξ of a monolayer at the wall. This fraction is given by (for one kind of impurity)

$$\xi = \frac{n_e}{N_s} \cdot \frac{r}{2} \cdot \frac{Z_{eff}^{-1}}{Z^2-Z}$$

where n_e is the electron density in the plasma; N_s the number density in the surface monolayer, r the minor radius, Z_{eff} the effective Z and Z the charge number of the impurity. ζ usually amounts to a few percent. At the end of the discharge impurities are redeposited (or implanted at the wall) only a small fraction is pumped. The interval between shots of 5 to 10 minutes, furthermore, is sufficiently long for readsorption even with, for tokamaks, relatively good vacua of 10^{-5} to 10^{-6} Pa (10^{-7} to 10^{-8} torr).

This being the case, desorption and chemical interactions with adsorbed layers are important. At present they certainly dominate sputtering of the base material. This certainly will also be true in the next generation of machines, probably for the next 10 years.

The data needed are the following:

Cross sections for desorption by photons for photon energies of a few eV into the 100 keV X-ray region. Cross sections as well as fluxes (the photons originating from "run-away electrons") should get small in that region. Some authors suggest [28,29] that photodesorption could be the main source for the early impurities in tokamaks.

Desorption by electrons (EID-electron induced desorption), again allowing for run-aways, should be investigated in the same energy range.

In the energy range between threshold (if such exists) and several keV desorption by ion bombardment (also termed sputtering of adsorbed layers) is another important area. Especially desorption by hydrogen and helium should be investigated.

Finally, for the sake of completeness thermal desorption should be mentioned. This now is a field well covered in the literature, which may be supplemented by data on technically relevant situations.

In divertor experiments the problem of installing sufficient pumping speed in the divertor chambers arises. Therefore the use of trapping divertor plates has been discussed [30]. Here trapping probabilities especially at energies below 1 keV and factors influencing them are important.

3.1.3 Materials

Definite statements about the best materials cannot be made at this time. On the contrary it appears useful to keep the field open, at least in order to clarify the physics of the different effects. Certain priorities should, however, be mentioned:

The stainless steels and nickel rich alloys (Inconel etc.) are the most important construction materials. This will be true for the foreseeable future. Limiters are often fabricated from molybdenum or tungsten. The use of low-Z materials (graphite, SiC, B_4C but also Al_2O_3) is being contemplated. Ti and Cr is of interest for trapping divertor plates.

3.2 Other fusion devices

3.2.1 Mirrors

The plasma in mirror machines is positively charged and expels impurities /31/, and so the impurity problem seems to be non-existent. But charge exchange losses play a role. Therefore reflection and reemission are important. Due to the high energies in mirrors, the interesting energies extend into the 100 keV range. Wall erosion may be caused by hydrogen and helium bombardment. The fluxes to be expected are discussed in [31].

A new problem arises with the direct energy converters: A possible deterioration of voltage holding due to particle bombardment [32]. However, this will not be considered as "atomic data". Also the importance of secondary electron emission due to ion bombardment in the direct converters is pointed out in [32]. The energy range again goes up to about 100 keV.

3.2.2 Pinches

In reactors the processes of PSI will basically be similar to those described for the Tokamak. Due to the short

burning cycle the problem of impurity accumulation will be less severe. Wall erosion will be dominated by the plasma impinging on the wall at the end of the pulse, unless the establishment of a cold gas blanket [33] proves feasible.

Because of the compression or shock heating the wall has to be covered by an insulating layer. Its decomposition by bombardment with electrons or UV-photons ("electron or photon sputtering") might occur, but probably the chemical attack by atomic hydrogen is the more serious process. Also the dielectric strength and other bulk properties have to be considered. For a review of surface problems in pinche-reactors see [34].

In present-day pinch experiments the duration of the discharge is shorter than the average flight time of particles between plasma and wall (10 μs compared with 0.1 ms for typical dimensions). Therefore one expects no influence of PSI on the plasma. But it occurs during the ignition phase, as indicated by oxygen impurities and also by strong gas exchange between plasma and wall [35].

3.2.3 Inertial Confinement

In this scheme the problems of mechanical and thermal shocks are severe. New atomic surface data, not discussed so far, do not seem to be required.

4. Surface processes, a short review

4.1 Backscattering, trapping, release

Light ions (hydrogen, helium) impinging on a solid are either backscattered with a fraction of their primary energy or they come initially to rest in the solid. Diffusivity and solubility as well as the rate at which the implanted surface layer is sputtered then determines their subsequent behaviour.

4.1.1. Backscattering [36]

Theory: In the parameter range of interest for PSI we have multiple scattering. Furthermore, the screening of the

nuclear charge by the core electrons has to be taken into account. The simple model of one binary collision with Rutherford cross section, successful at higher energies, is no longer valid. Calculations are either based on Boltzmann transport theory [37] or on computer simulation. Especially calculations based on the MARLOWE program are often quoted [38].

Experiment: In recent years backscattering coefficients R for several ion-target combinations have been measured [39-41]. Agreement with calculated values is usually good, Fig.2. The energy scale in Fig.2 is Lindhards reduced energy [42] given by

$$\varepsilon = 32{,}5 \frac{M_2}{M_1+M_2} \frac{(Z_1^{2/3}+Z_2^{2/3})^{-1/2}}{Z_1 Z_2} E$$

(M_1, Z_1 and M_2, Z_2 are atomic mass and charge of the incident ion and target atom, E the energy of the incident atom in keV). It would appear that the theoretical curve in Fig.2 predicts the reflection coefficients correctly to within a factor of two for $\varepsilon > 1$. Why the data for D→Mo [43] at low ε deviate so markedly is not clear. It is evident that experiments at $10^{-2} < \varepsilon < 1$ are badly needed. This is roughly the 100 eV range the range in which probably a large part of the recycling takes place. The experimental difficulties of measuring neutral hydrogen at these energies are the reason for the lack of data.

Particle reflection coefficients (and the sometimes measured energy reflection coefficient) are integral quantities. One really would like to know the differential reflection coefficient $r(E, E_o, \theta, \theta_o, 1)$ indicating the probability that a particle impinging with E_o, θ_o is reflected into the energy and angular interval around E, θ and leaves the surface with charge state 1.

Only few measurements exist on angular distributions [41]. The majority of the reflected atoms seem to obey a cosine

distribution,only for those with energies close to E_o some forward scattering has been observed.

The charge state of the reflected hydrogen is an important parameter for PSI. It is roughly indicated by Fig.3, taken from [44]. Deviations from this universal curve for different materials and different surfaces are observed especially below 10 keV. However, as a rule of thumb one may say that more than 90 % of the backscattered particles are neutral.

4.1.2 Release

The emission of atoms originally implanted in the solid is termed release[2)]. The release may take place by diffusion to the surface and subsequent desorption or by sputtering or on blistering. Most of the released particles will be neutral. If thermal desorption takes place, which is certainly the dominating effect with hot wall, molecules will be desorbed [10]. To what extent "gas-sputtering" or desorption by ion bombardment, in which cases one would expect atoms to be released, contributes with room temperature walls is not yet clear.

4.1.3 Trapping

In general trapping is high at low dose (close to 1-R) and decreases as saturation of the surface layer whose depth corresponds to the ion range is approached. In saturation gas concentration may be 10 to 50 % and the amount of trapped gas is then often a multiple of the gas in the plasma.

If diffusivity is sufficiently large, trapping stays high even for high doses, the implanted gas then diffuses into the interior of the solid. This is the case for the hydride forming metals in appropriate temperature ranges.

A survey of the literature on these effects can be found in [45]; new material is contained in [14] and [46]. In general

---

2) Some authors use different definitions

it can be said that in the range below 1 keV there is considerable uncertainty, attributed to unresolved influences of surface layers.

4.2 Sputtering

Physical sputtering is the removal of atoms as a result of collision cascades, created by the primary ion (or atom).

The literature on the topic is large, most of it can be found by consulting the reviews [1,45,47,48,49,50].

The sputtering yield for the light ions has its maximum around a few keV. The lower the Z of the target material the lower is the energy at which the maximum occurs, Fig.4 [51].

For energies below 10keV and for light ions the results available for stainless steel are collected in Fig.5 /from[12]). Only two papers [52,53] containing data on the angular distribution and none on energy distribution of material sputtered by hydrogen seem to exist. Extrapolation from the results with heavier noble gases is hardly possible, since the mean transferred energy is much smaller than in the usual case with $M_1 \approx M_2$.

Since yields and other quantities may depend on the surface structure which changes considerably over a long period [54], it is important that experiments be conducted with a sufficiently high dose.

Concerning the erosion by impurities, extrapolation from noble gas sputtering can serve as a good first approximation.

If volatile compounds are formed between the implanted atoms and those of the solid, erosion increases owing to this chemical sputtering. The enhanced sputtering of graphite on hydrogen bombardment at higher temperature, Fig.6, is explained by this effect, namely by CH_4 formation [55]. The yields are much larger than in normal chemical reactions between atomic hydrogen and graphite!

Here, a word should be added about neutron sputtering. Since 14 MeV neutron fluxes available at present are rather small, all experiments measuring yields are plagued with the

problems of detecting minute amounts of sputtered material. This may explain why erroneously large yields have,been quoted several times. In a recent review [56], it is shown that, in general, yields are below 10^{-4}. This has been confirmed by several papers in [14]. Thus neutron sputtering does not present a danger in fusion.

4.3 Blistering

With an electron microscope one observes the formation of little bubbles inside the solid if gas concentrations of 5 to 10% are reached and if solubility is low. At higher concentrations, usually after a dose of 10^{17} to $10^{18} cm^{-2}$, one observes the formation of blisters or the exfoliation of the surface. For a review see [57]. If this were to occur repeatedly the consequent wall erosion would be much larger than that due to sputtering.

Fortunately, according to recent results this is not the case, at least not for some materials. Rather does blistering disapear after one deckeldicke (thickness of the cover of the blisters) is sputtering away. After bombardment with a broad energy distribution, and this is the relevant case, blistering is much less apparent.

Overall it can be said that blistering is much less dangerous than had previously been thought. Nevertheless, it is important to confirm this by further investigations with other materials, high doses at high energy and broad energy distribution.

4.4 Desorption

4.4.1 Desorption by ions (sputtering of adsorbates)

Sputtering of the adsorbates is a standard method in surface physics for cleaning surfaces. Nevertheless, hardly any cross sections or yields for this process are available in the literature. For deuterium bombardment large desorption yields of the order of unity have been observed at 5 keV for

technical surfaces and much larger yields for condensed water or carbon dioxide [58]. The desorption of oxygen from Ni due to He-bombardment has been studied in [59]. Cross sections of several $10^{-17}cm^2$ have been determined for energies between 500 and 1500 eV. (Additional literature on the topic is quoted in [59]). An interesting observation is that the energy dependence of the yield for bombardment with the heavier noble gases, e.g. Ne, is similar to that for sputtering of the base material while for He the desorption yield increases with decreasing energy (in the above mentioned range) in contrast to the sputtering yield. This could mean that sputtering of adsorbed layers at low ion energies is much more important than has hitherto been assumed.

More data and improved theoretical understanding are badly needed.

4.4.2 Desorption by electrons (EID)

Desorption by electrons as an interesting physical process and a useful tool in surface physics has been extensively studied. For reviews see for example [60,61,62,63]. Often only parameter dependences have been studied, but some cross-sections can be found in the literature. In general they are around $10^{-18}cm^2$ or less for electron energies around 100 eV and as such they are considerably smaller than for dissociation in the gas phase. For technical surfaces larger cross-sections have been reported [64]. Again, there is lack of data for well defined technical surfaces as well as for higher electron energies.

4.4.3 Desorption by photons

The yields for the desorption of monolayers on clean metals by UV photons [65] are around 10^{-7}. At technical surfaces of stainless steel they are four orders of magnitude larger, see Fig.7 [66], although the dependence on wave length is very similar. It has been suggested that the desorption

is from a layer of semiconducting chromium oxide since for semiconductors the yields are similar.

In several recent papers photo desorption by 20 to 50 keV X-rays has been observed [67]. Yields of about 6×10^{-4} (mainly O_2, CO_2 and CO from SS) have been determined for 20 keV photons. Considering that the photon fluxes (see [28]) together with the yields quoted would yield all impurities observed in the early stages of for example ST tokamak, it follows that only limited data exist for an important effect!

4.5 Chemical effects on the surface

Chemical reactions on the metal surfaces between (atomic) hydrogen and adsorbed carbon and oxygen, readsorption of radicals of hydrocarbons, of OH etc. could be quite important in PSI in present machines. Little is known about these rather complex phenomena. The problem has been reviewed in [68,69]. Also reactions between atomic hydrogen and carbon or oxygen containing materials are important; several papers in [14] deal with these effects.

4.6 Other effects

In this chapter, a few additonal effects are listed, which, for reasons mentioned below, seem to be of lesser importance at the moment.

4.6.1 Emission of secondary electrons

Nearly all interactions discussed above are connected with emission of secondary electrons. These electrons influence space charge in front of the wall and possibly electronic heat conduction to a divertor. The literature on secondary emission is extensive (for a recent review of ion-induced secondary electrons see [45]), and no immediate need for additional data is apparent at the moment. This could change should more attention be focussed on space charge and heat conduction to divertors than is done at present.

4.6.2 Reflection of photons

Reflection of synchrotron radiation is of interest for the energy balance in reactors. In the wavelength region concerned, namely the millimeter and submillimeter ranges, reflectivity from metals is high. It has not been investigated if that is still true for surfaces roughened by ion bombardment. Since the surface structures on eroded surfaces are mostly in the micrometer range, no large influence is expected.

4.6.3 "Sputtering" of insulators by photons and electrons

Removal of atoms by photon and electron bombardment is well known for ionic crystals and for organic substances. Whether it also occurs with more strongly bound insulators such as Al_2O_3, which could be considered for lining the inside wall of theta pinches, is doubtful, but no definite evidence is known to the author.

5. Nonlinear superposition of effects (synergistic effects), Nonlinearities

Estimates of PSI are rather uncertain at present owing to lack of knowledge of particle and energy fluxes to the wall, even if the atomic data were available and wall conditions were well defined. But there is still another question: Are the effects linearly dependent on dose and flux and more important, can the total effect be described as a linear superposition of the individual effects if the different radiations are impinging at the same time with considerable intensity? The answer to this question is pure speculation, and in part the problem involves parameter ranges inaccessible at this time. One should therefore always be prepared for unpleasant surprises. Nevertheless, an answer will be attempted.

5.1 Nonlinear dependences from flux

Collision cascades, initiated by impact of ions or atoms on a solid last less than 10^{-12} s [70]. Their linear dimensions on the surface are of the order of a few tens of Å. Superposition of two cascades from independent surface encounters which could lead to nonlinear effects can therefore be excluded. Furthermore, cascades created by the light ions are so "thin" that thermal spike phenomena, known from heavy ion sputtering [71] do not occur. The same should be true of sputtering by light molecules, which means that hydrogen molecules sputter with the same efficiency as two atoms of the same velocity. Similarly, electronic excitations and collision cascades of two independent primary encounters will never interfere in metals. The latter could be different in insulators, where electronic excitations can persist for a considerable time.

Another possibility for a flux dependence is due to changes in surface temperature. This is covered by measuring the temperature dependence of the processes, with two exceptions: influence of temperature gradients and influence of sudden changes in heat conductivity during blistering. With sufficiently high beam power the latter could lead to evaporation of the blister covers [54,72].

If diffusivity is such that there is competition between injection and diffusion, the critical dose for blistering becomes flux dependent.

5.2 Nonlinear dependences on dose

The surface seems to acquire some kind of equilibrium structure after sputtering of a layer of about ten times the deckeldicke [54]. Prior to this transient phenomena are to be expected for all effects depending on surface structure. For reactor applications it is important that data be determined for large doses, a requirement fortunately often satisfied for values of sputtering in the literature.

5.3 Nonlinear superposition of different effects

Neutron radiation damage influences many material properties. This, however, should not be the case for the surface effects, since in the surface layer radiation damage due to ion bombardment usually dominates. This can easily be seen from the following argument: The primary event in radiation damage is the displacement of an atom, the number of displacements being proportional to energy deposited in nuclear motion. Sputtering on the other hand is proportional to the energy deposited in nuclear motion in the uppermost atom layers. Thus sputtering events and number of displacements are proportional. Now yields for neutron sputtering are at least a factor 10^2 below those for sputtering by light ions. The flux of hydrogen ions (plus charge exchange neutrals) should be at least of the same order of magnitude as that of neutrons, even with fairly efficient divertors. From this it follows that, to a distance of the range of the ions below the surface, the ions and atoms create orders of magnitude more displacements than the neutrons. Influence of neutron radiation damage on the effects due to fast atom bombardment can therefore be excluded, while influence on other surface effects is only possible if there is no bombardment with fast atoms, as in the case of a cold gas blanket.

Influence of ion induced radiation damage on adsorption and desorption is probable since sorption energies depend on atomic surface defects (although an older attempt at detecting it [73] has been without success).

Trapping of hydrogen and helium is largely increased by radiation damage [74].

High energy helium blistering may be influenced by hydrogen sputtering if the latter contributes to forming an equilibrium surface structure, hydrogen blistering may be influenced by helium bombardment due to increased trapping.

5.4 Cyclic loads

Fusion reactors will be pulsed although the estimated pulse length varies by many orders of magnitude. Mechanical stability under the resulting cyclic loads is a problem in itself. In addition, there could be an influence on blistering. With hot walls, diffusion processes in the interval between pulses could influence trapping and the formation of surface structures. No investigations of these problems exist.

5.5 Conclusions on synergistic effects

Several sources of possible synergistic effects have been identified, others have been excluded and still others certainly have not been thought of. These effects are important since they may change the numerical values of the A & M data. But it is felt by the present author that so far there are no indications for any catastrophes.

6. List of surface A & M data, parameter ranges, materials

Reflection of hydrogen and helium

Primary energy: 100 eV to 10 keV
Data to be measured: reflection coefficient, energy and angular distributions, charge state
Important parameters: angle of incidence, surface structure.

Accommodation

Primary energy: 1 eV to 100 eV
Data to be measured: accommodation coefficient

Trapping of hydrogen (and helium)

Primary energy: 100 eV to 100 keV
Data to be measured: trapping coefficient
Important parameters: angle of incidence, temperature, dose, influence of radiation damage.

Sputtering by hydrogen, helium (and "impurities")

Energy: threshold to 20 keV

Data to be measured: yields, angular and energy distribution of sputtered material, chemical composition of sputtered material

Important parameters: angle of incidence, temperature

Blistering by hydrogen and helium

Energy: 1 keV to 100 keV (hydrogen) or 3,5 MeV (helium)

Data to be measured: critical dose

Important parameters: energy and angular distributions of incident particles (synchronons He and H bombardment, see also discussion on synergistic effects)

Most important aspect: Does blistering or exfoliation contribute to wall erosion for high dose bombardment, and if so, under what conditions?

Desorption by ions (hydrogen, helium, impurities)

Primary energy: threshold to several keV

Data to be measured: yields, charge state

Important parameter: angle of incidence, surface damage

Desorption by electrons

Primary energy: threshold to 100 keV

Data to be measured: yields, charge state

Important parameter: surface damage

Desorption by photons

Energy: 5 eV to 100 keV

Data to be measured: cross section, charge state

Important parameter: surface damage

Chemical reactions of atomic hydrogen

Data to be measured: reaction probability,

Important parameter: energy of hydrogen atom

Materials of first priority:

Stainless steels

Nickel base alloys

Mo

Graphite

Al_2O_3

(SiC, B_4C)

Getters

Acknowledgement

I am indebted to many colleagues, especially R.Behrisch, D.Düchs, E.Taglauer, H.Verbeek for stimulating discussions and useful suggestions.

Literature

/1/ Behrisch, R., "Fusion-first wall problems", Materials Problems in Energy Production (Stein, Ch., Ed.) Academic Press, New York 1976 (in print).

/2/ Scherzer, B.M.U., J.Vac.Sci.Tech. 13 (1976) 420

/3/ Behrisch, R., Kadomtsev, B.B., Plasma Phys.Contr.Nucl. Fusion Research 1974 (Proc.Conf.Tokyo 1974) II, IAEA Vienna (1975) 229

/4/ Meade, D.M., Proc.Int.Conf.Radiation Test Facilities for the CTR Surface and Materials Programm (Argonne 1975) ANL/CTR-75-4 (1975)46

/5/ Cohen,S.A., J.Vac.Tech.13 (1976)449

/6/ Behrisch,R., Kadomtsev,B.B., Nucl.Fusion, Special Suppl. 1974 (Proc.Workshop Fusion Reactor Design Problems, Culham 1974)451

/7/ McCracken,G.M., Ref./6/, 471

/8/ Kaminsky,M., Proc.Int.Summer Institute of Surface Science, University of Milwaukee 1975, to be publ.

/9/ Kaminsky,M., Proc.Int.Working Sessions on Fusion Reactor Technology (Oak Ridge 1971), ORNL Conf.-710624 (1971)86

/10/ Vernickel,H., Course on the Stationary and Quasi-Stationary Toroidal Reactors (Proc.Int.School Fusion Reactor Techn., Erice 1972) EUR 4999e, Luxembourg (1973) 303

/11/ Behrisch,R., Nucl.Fusion 12 (1972) 695

/12/ Behrisch,R., Tokamak Reactors for Breakeven (Proc.Int. Summer School, Erice 1976), Luxembourg, to be publ.

/13/ Conf.on Surface Effects in Controlled Fusion, Argonne 1974, Proceedings published in J.Nucl.Mat.53 (1974)

/14/ Int.Conf.on Surface Effects in Controlled Fusion Devices, San Francisco 1976, Proc.to be publ.in J.Nucl.Mat.

/15/ Vershkov, V.A., Mirnov,S.V., Nucl.Fusion 14 (1974) 383

/16/ Meade,D., Nucl.Fusion 14 (1974) 289

/17/ Düchs,D., Haas,G., Pfirsch,D., Vernickel,H.,J.Nucl. Mat.53 (1974) 102

/18/ Vernickel,H., Proc.First Topical Meeting on the Technology of controlled Nuclear Fusion (San Diego 1974), USAEC CONF-740402-PS (Hopkins,G.R.,Ed)II (1974)347

/19/ Vernickel,H., Nucl.Fusion 12 (1972)386

/20/ Rebut,P.H. et al., J.Nucl.Mat.53 (1974)16

/21/ Düchs,D.F., Furth, H.P.,Rutherford,P.H., Plasma Physics and Contr.Nucl.Fusion Res. 1971 (Proc.Conf.Madison 1971) I,IAEA Wien (1971) 369

/22/ Hotston, E.S.,McCracken, G.M.,UKEA Rep.CLM-P455 (1976)

/23/ Kulcinski,G.L.,Conn, R.W., Lang G., Nucl.Fusion 15 (1975)327

/24/ Dobrozemsky, R.,J.Vac.Sci.Tech.13 (1976) 467

/25/ McCracken,G.M.,Erents,S.K., Nuclear Fusion Reactors (Proc.Conf.Culham 1969),BNES (1970) 353

/26/ Kulcinski,G.L.,Conn,R.W., ref. /18/,I.,38

/27/ Conn, R.W., ref. /14/

/28/ Hinnov, E.,J.Nucl.Mat. 53 (1974) 9

/29/ Ginot,P., ref. /14/

/30/ Allgeyer,R., et.al.Proc.6th Sympl.Engn.Problems in Fusion Research, San Diego (1975)

/31/ Moir,R.W., ref./14/

/32/ Moir,R.W.,Barr,W.L.,Miley,G.H.,J.Nucl.Mat. 53 (1974) 86

/33/ Oliphant, T.A.,Gryczkowski,G.E., Kammash, T., Nucl.Fusion 16 (1976) 263

/34/ Clinard,F.W., Jr. et al.,Proc.High-Beta Pulsed Reactor Workshop (Leningrad 1975), in print

/35/ Engelhardt,W., Köppendörfer,W., Münich,M., Sommer, J., Proc.7th Europ.Conf.Contr.Fusion and Plasma Phys. (Lausanne 1975) 50

/36/ Verbeek,H., "Backscattering of light ions from solid surfaces", Radiation Effects on Solid Surfaces (Kaminsky, M.,Ed.) Adv.in Chemistry Series, in print

/37/ Weissmann,R., Sigmund,P., Rad.Eff. 19 (1973) 7

/38/ Oen,O.S., Robinson,M.T., Nuclear Instr.Meth. 132 (1976) 647

/39/ Eckstein,W., Matschke,F.E.P., Verbeek,H., ref /14/

/40/ Sidenius,G., Lenskjaer T., Nucl.Instr.Meth. 132 (1976)679

/41/ Verbeek,H., J.Appl.Phys.46 (1975) 2981

/42/ Lindhard,J., Scharff,M., Schiøtt,H., Mat.Fys.Medd.33 (1963) No 14

/43/ Braganza,C., Carter,G., Farrell,G., Nuclear Instr.Meth. 132 (1976) 679

/44/ Behrisch,R. et al., Atomic Collisions in Solids (Proc. Conf.Oak Ridge 1973)I, Plenum Publ.Corp.New York (1975) 315

/45/ McCracken,G.M.,Rep.Prog.Phys. 38 (1975) 241

/46/ Bohdansky,J., Roth,J., Poschenrieder, W.P., Inst.Phys. Conf.Ser.28 (1976) 7

/47/ Andersen,H.H., Phys.of Ionized Gases 1974 (Proc.Conf. Rovinj 1974,Vujnovic, V.Ed.) 361

/48/ Oechsner,H., Appl.Phys.8 (1975) 185

/49/ Carter,G., Colligon,J.S., Ion Bombardment of Solids, Heinemann, London 1968

/50/ Behrisch,R., Erg.d.Exakten Naturw. 35 (1964) 295

/51/ Bohdansky,J., Roth,J., Sinha,M.K., Proc.9th Symp. Fusion Tech.(Garmisch 1976), to be publ.

/52/ Summers, A.J.,Freeman,N.J.,Daly,N.R., J.Appl.Phys.42 (1971),4774

/53/ Finfgeld,C.R.,Report ORO-3557-15 (1976)

/54/ Behrisch,R., Risch,M., Roth,J.,Scherzer,B.M.U.,ref.51

/55/ Roth,J., Bohdansky,J., Poschenrieder,W.,Sinha,M.K., ref. /14/.

/56/ Behrisch,R., Nucl.Instr.Methods 132 (1976) 293

/57/ Roth,J., Instr.Phys.Conf.Series 28 (1976) 280

/58/ McCrakcen; G.M.,Vacuum 24 (1975) 463

/59/ Taglauer,E., Marin,G., Heiland,W., Beitat, U., Surf.Sci., in print

/60/ Madey,T.E., Yates,J.Y.,Jr., J.Vac.Sci.Tech.8 (1971) 525

/61/ Menzel,D., Surface Sci.47 (1975) 370

/62/ Lichtman,D., CRC Crit.Rev.Solid State Sci.4 (1974) 395

/63/ Menzel,D., "Desorption phenomena", Interactions on Metal Surfaces (Gomer,R. Ed) Springer Berlin (1975) 101

/64/ Redhead,P.A., Hobson, J.P., Kornelsen,E.V., The Physical Basis of Ultrahigh Vacuum, Chapman and Hall, London 1968

/65/ Kronauer, P., Menzel,D., Adsorption-Desorption Phenomena (Ricca,F., Ed) Academic Press, London (1972) 313

/66/ Fabel,G.W., Cox, S.M.,Lichtman, D., Surf.Sci.40 (1973)571

/67/ Brumbach, S.,Kaminsky,M., Proc. 6th Symp.Engn.Problems in Fusion Research, San Diego (1975) 1135; J.Nucl.Mat., in print; J.Appl.Phys. 47 (1976) 2844

/68/ Poschenrieder,W.P., Proc. 5th Italian Vacuum Congress Perugia (1975), in print

/69/ Gruen,D.M., "Chemical effects of plasma interactions with thermonuclear reactor surfaces", The Chemistry of Fusion Technology, (Gruen,D.M., Ed), Plenum Press, New York (1972) 215

[70] Oen,O.S., Robinson, M.T., J.Appl.Phys. 46 (1975) 5069

[71] Andersen,H.H., Bay,H.L., J.Appl.Phys.45 (1974) 953

[72] Risch, M., private Comm.

[73] Vernickel,H., Transactions 3rd Int.Vac.Congr. (Stuttgart 1965)II, Pergamon Press (1967) 709

[74] Erents, S.K., Proc.8th Symp.Fusion Technology (Noordwijkerhout 1974), EUR 5182 e, Luxembourg, (1974)895

[75] v.Seefeld, H., Schmidl,H., Behrisch,R., Scherzer,B.M.U., ref.[14]

[76] Oechsner,H., Thesis University of Würzburg 1963

[77] Rosenberg,J., Wehner,G.K., J.Appl.Phys. 35 (1964) 1842

[78] Roth,J., Bohdansky,J., Hofer,W.O., Kirschner,J., to be publ.

[79] Behrisch,R., et al.J.Nucl.Mat.60 (1976) 321

[80] Cohen,S., Report MATT-1171, Princeton 1975.

Note added in proof: More literature related to the topic of this talk may be found in the Proceeding of the Internat. Symposium on Plasma Wall Interaction, Jülich (Germany) Oct. 76, to be publ. by Commission of the European Communities.

Figure captions

Fig.1 Matrix of the surface effects important in plasma surface interaction. The matrix element name the processes connecting the fluxes from the plasma to the wall (upper line) with the fluxes from the wall to the plasma (left row).

Fig.2 Particle reflection coefficients as determined by different authors compared with theory.
○ H→SS, □ D→SS, ▽ H→Nb (annealed), ▽ H→Nb (bef.ann.), ◇ D→Nb (bef.ann.) /39/; • H→SS, ▼ H→Nb, ▲ H→Cu, ⊷ H→Al, ⊷ H→Mo, ⊷ H→Ag, ⊷ H→Ta, ⊷ H→Au /40/; +H→Zr, × H→Ti /51/; ⊗ D→Mo /43/; — — — [38].

Fig.3 Fraction of charged particles for backscattering of H from different materials as function of the energy of emerging particles. Normal incidence, angle of emergence 30° to the surface normal. From [44].

Fig.4 Sputtering yields for different materials in dependence on proton energy. All values are taken of normal incidence and target temperatures between 50°C and 150°C. From [51].

Fig.5 Sputtering yields for normal incidence of different ions on Fe, Ni, SS 304 and SS 316 as measured by different authors [51,75-79]. Also included are values extrapolated by S.A.Cohen [80]. From [12]

Fig.6 Temperature dependence of the sputtering yield (per atom) of pyrolytic graphite with hydrogen ions for different energies. From [55].

Fig.7 Yields for photodesorption from SS according to [66].

From Plasma / To Plasma	Hydrogen (fuel)	Helium	Impurities	Electrons	Photons	Neutrons	Heat
Hydrogen	Backscattering Reemission	Desorption	Desorption	EID (Electron impact)	Photo-desorption	-	Desorption
Helium	-	Backscattering Reemission	-	-	-	-	Detrapping
Impurities	Sputtering Ion induced desorption Blistering			EID Sputtering 1)	Photo-desorption	[Neutron Sputtering]	Desorption Evaporation
Electrons	Ion Induced Secondary Electrons			Secondary Emission	Photo-electron Emission	-	(Thermionic Emission)
Photons	-	-	-	-	Reflection	-	-

FIG.I

Note: - indicates "no contribution to PSI"

[..] means: of lesser importance, if any

1) Only with insulators, if at all

Figure 2

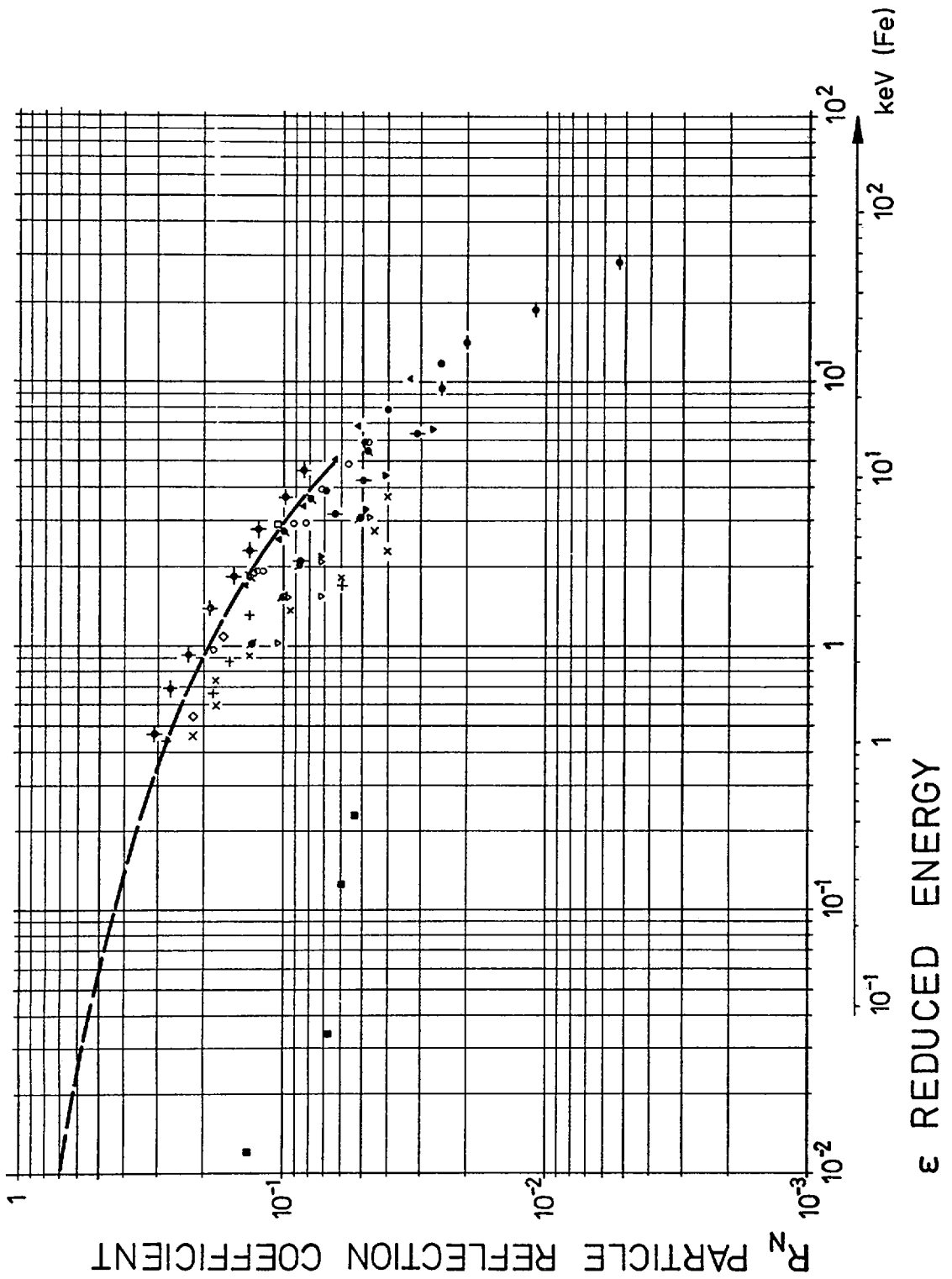
R_N PARTICLE REFLECTION COEFFICIENT
1
10^{-1}
10^{-2}
10^{-3}
10^{-2}
10^{-1}
1
10^{1}
10^{2}
keV (Fe)
10^{2}
10^{1}
1
10^{-1}
ε REDUCED ENERGY

Figure 3

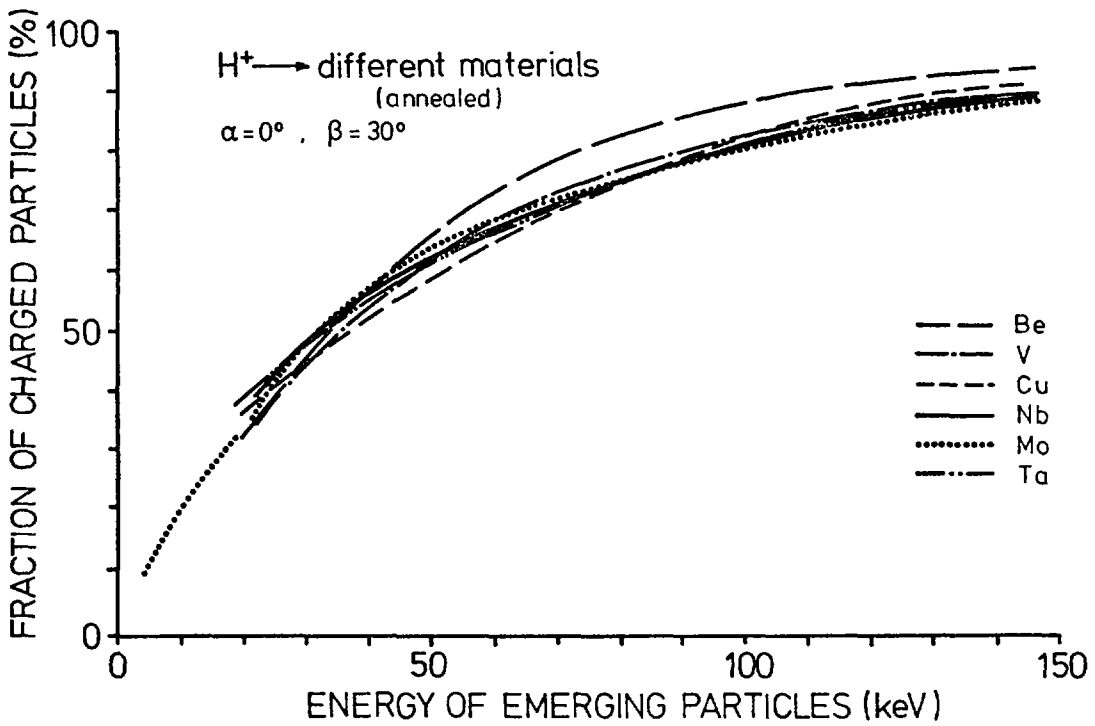
FRACTION OF CHARGED PARTICLES (%)
100
50
0
0
50
100
150
ENERGY OF EMERGING PARTICLES (keV)
H+ → different materials
(annealed)
α = 0° , β = 30°
Be
V
Cu
Nb
Mo
Ta

Figure 4

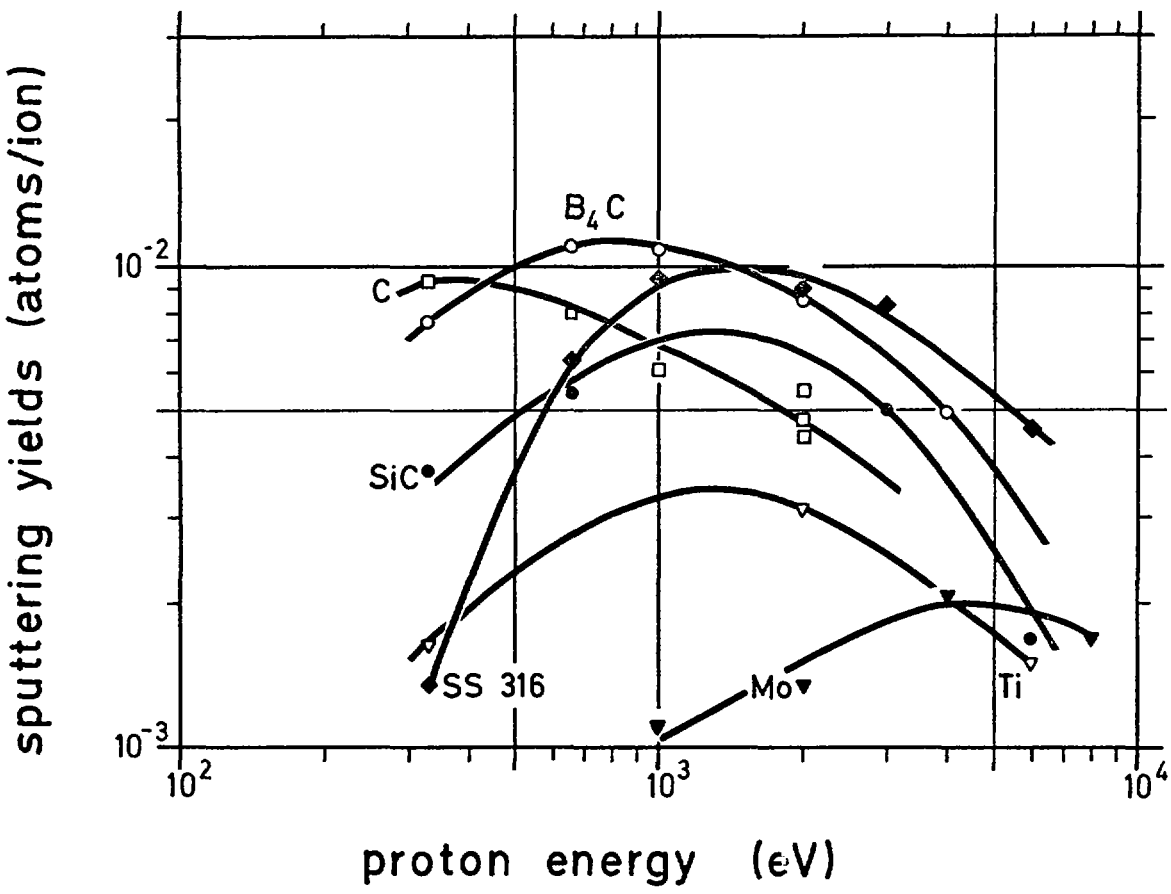
sputtering yields (atoms/ion)
10^{-2}
10^{-3}
B_4C
C
SiC
SS 316
Mo
Ti
10^2
10^3
10^4
proton energy (eV)

Figure 5

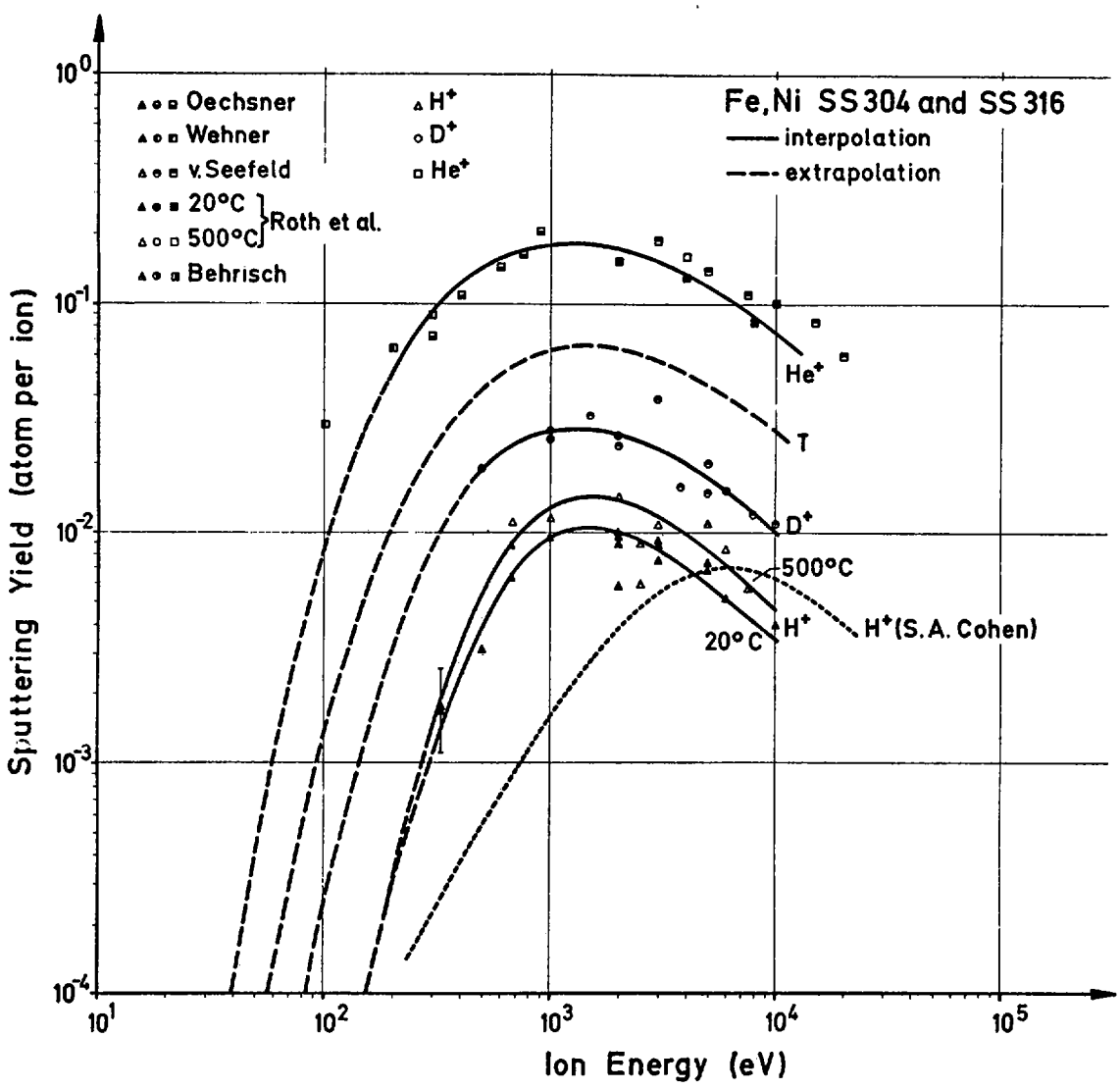
Fe,Ni SS304 and SS316
interpolation
extrapolation
Oechsner
Wehner
v.Seefeld
20°C
500°C
Behrisch
Roth et al.
H+
D+
He+
He+
T
D+
500°C
H+
20°C
H+(S.A. Cohen)
Sputtering Yield (atom per ion)
Ion Energy (eV)
10^0
10^-1
10^-2
10^-3
10^-4
10^1
10^2
10^3
10^4
10^5

Figure 6

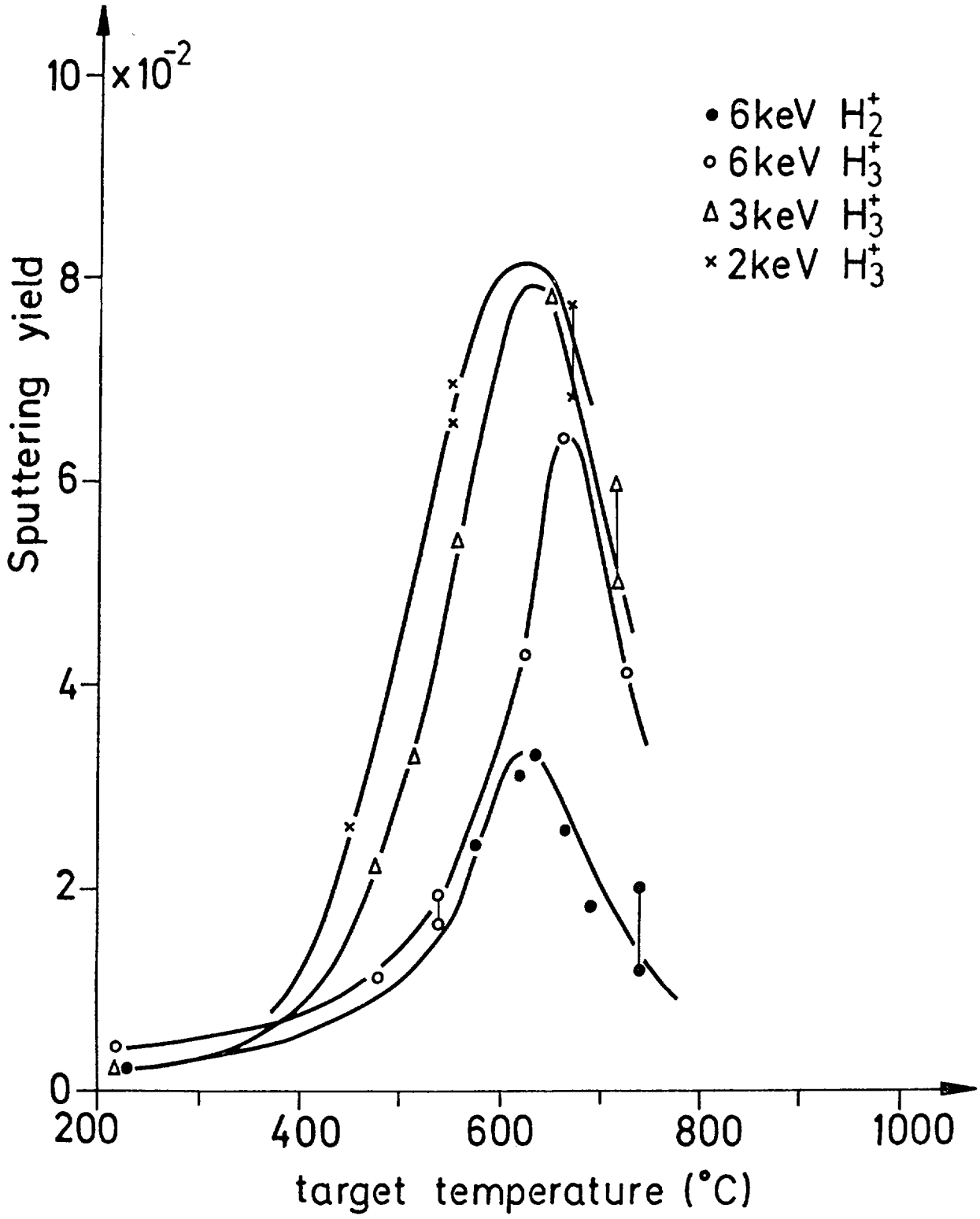
10
x10⁻²
8
6
4
2
0
Sputtering yield
• 6keV H₂⁺
∘ 6keV H₃⁺
Δ 3keV H₃⁺
× 2keV H₃⁺
200
400
600
800
1000
target temperature (°C)

Figure 7

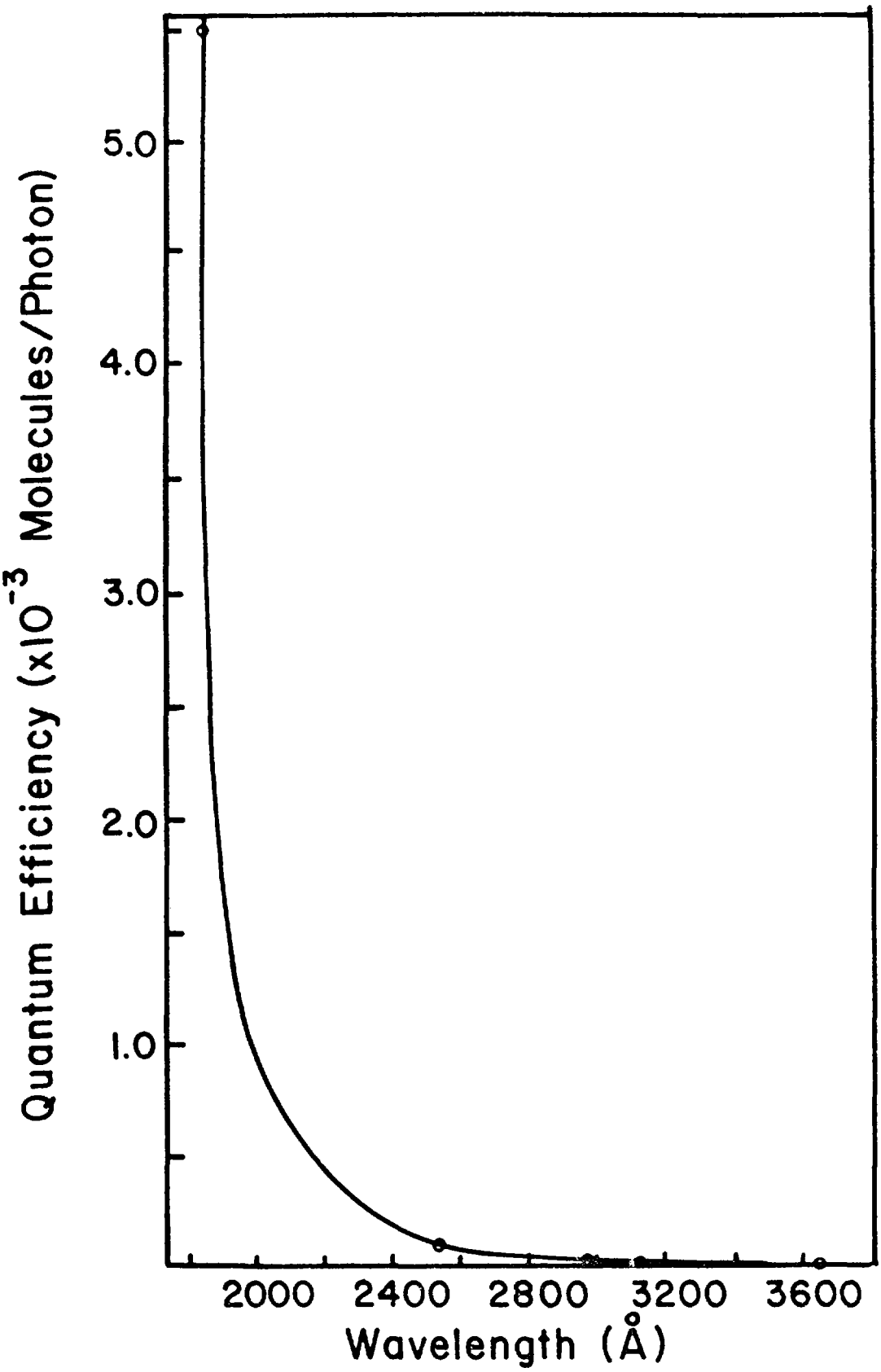
Quantum Efficiency (x10^{-3} Molecules/Photon)
5.0
4.0
3.0
2.0
1.0
2000
2400
2800
3200
3600
Wavelength (Å)

BLISTERING OF STAINLESS STEELS BY He^+ ION BOMBARDMENT*

B. Navinšek and A. Žabkar
J. Stefan Institute, University of Ljubljana, Ljubljana, Yugoslavia

Abstract

BLISTERING OF STAINLESS STEELS BY He^+ ION BOMBARDMENT

The surface erosion and blistering produced by high dose 6 and 10 keV He^+ ion bombardment in PROKRON 11 spec. and PROKRON 12 stainless steels have been studied using optical microscopy, scanning electron microsopy and the high resolution replica technique. The total ion dose was varied from 5.10^{17} to 10^{19} ions/cm^2 and the irradiation temperature was varied from room temperature to 650°C.

The results show that the influence of surface pre-treatments on the topography to be developed under low-energy He^+ bombardment is much greater for stainless steels than for other pure metals used for the first wall in fusion reactor. Only a few widely dispersed blisters of diameter 0.2–0.5μm were found on stainless steel samples bombarded at room temperature, some of which were attached at inclusions and various precipitates, while larger areas of the bombarded spot remained unaffected. The ion micro-erosion effect – on the few 100 Å scale – was observed all over the irradiated samples. The roughness of this "background" increased with target temperature. At 650°C blisters and "background" structure have similar diameters, while the height variations are larger than the diameter of surface features. Surface structure depends strongly on grain orientation and on the thermal treatment before ireadiation.

INTRODUCTION

It has been known for some time that the most promissing materials for the first wall in a thermonuclear fusion reactor are various stainless steels and nickel based alloys (316, 304 L, LS 1, PE 16, inconels, Hastelloys) and low Z-materials (C, SiC, B_4C, TiC). Therefore great interest has been shown in the last few years in studies on

* This work was supported by the International Atomic Energy Agency, Vienna, Austria under the Contract No 1761/RB, 1975

these materials materials related to the operating conditions, where the walls of the vacuum vessel are bombarded with energetic electrons, atoms, neutrons, photons and also with light ions having mean energies of 0.5 to 100 keV. It has already been shown that intense ion bombardment with currents between 10^{13} and 10^{18} ion/cm^2.sec induces penetration of ions, trapping, precipitation and coalescence, bubble formation, blistering, reemission and sputtering in the wall material [1—4]. The understanding of these processes and the collection of data relating to the individual processes are of importance in the evaluation of the interaction of a hot plasma with the surrounding walls.

Most of the experimental work on blistering has been done on niobium, molybdenum, vanadium and little on stainless steels [5]. Recently SiC, carbon, aluminium, SAP and ceramic coatings were also investigated. Blistering has been observed for the first time in situ using a scanning electron microscope mechanically coupled to the beam line of a 450 keV accelerator [6]. To have a better overall view of studies of blistering on stainless steels, the experimental conditions used by other authors are given in Table I. Only a few investigations were made in the low energy region, e.g., between 5 and 20 keV, and at high doses, e.g., between 5.10^{18} and 10^{20} ions/cm^2, where one should expect maximum surface changes. The development of the blistering process could also be clearly detected and identified under these experimental conditions. The target temperature is one of the most important parameters effecting the radiation blistering process. (the temperature region 20 to 700° C is the general range of interest for blistering investigations).

It should be pointed out that for Type 304 stainless steel, the blistering erosion rate increases with decreasing projectile energy [10], having a value of 0.5 atoms/ion at 500 keV He^+ and 450° C and value of 3 atoms/ion at 100 keV He^+ and 450° C. These yields are 3 times smaller at 550° C, which shows that the erosion yield goes through a maximum in the temperature range of about 400—500° C The blistering erosion rate for 304 stainless steel (at 100 keV He^+ bombardment to a dose of 3.10^{18} ions/cm^2; ~ 3 atoms/ion) is in fact nearly two orders of magnitude larger than the estimated sputtering yield. Finally, very irregular surface features, blister skin exfoliation and various types of holes are generally observed at elevated temperatures, where (depending on the target material) the erosion yield, remission of implanted gas and range profiles are remarkably changed.

Until now, however, most of the blistering work has been done with He^+ ions of relatively high energies. At energies below 20 keV sputtering predominates, which must induce large surface changes (increase of erosion rate with decreasing ion energy!) and therefore influences the development of blistering remarkably. One should also consider the threshold energy for blister appearance, the critical ion dose and especially the temperature dependence of the whole phenomena. This is the reason why we started our investigations of blistering on stainless steels by high dose He^+ ion bombardment in the energy range from 2 — 15 keV.

TABLE I. BLISTERING STUDIES ON STAINLESS STEELS (Experimental conditions used by other authors)

St.Steel	Ions	Energy (keV)	Ion dose (ions/cm^2)	Target temp. ^{o}C	Reference
304 L	He^+	0.1 – 1.4	$10^{12} - 10^{15}$	20 to 920	Picroux and Vook [7]
304	H^+	5	$0.5 - 9.9 \times 10^{19}$	20	Behrisch and Kadomtsev [1]
4301	D^+,He^+	15	$10^{17} - 10^{19}$	27 and 343	Verbeek and Eckstein [8]
302	H^+	20	$0.1 - 2 \times 10^{20}$	75 to 150	Wilson, Thomas and Bauer [16]
302	D^+	20			Panitz [9]
304	He^+	100 – 1500	$0.62 - 6.2 \times 10^{18}$	200 to 600	Das and Kaminsky [10,5]
316	H^+ He^+	150, 300	$0.4 - 2 \times 10^{19}$	– 170 to 700	Thomas and Bauer [11–13]
316	H^+	750 – 1050		20 to 500	Keefer and Pard [14], Keefer [15]

EXPERIMENTAL

Experimental conditions are given in the form of a table (Table II) based on the Das and Kaminsky list of major parameters that can affect radiation blistering [5]. Such a presentation of experimental condition here and in general could perhaps be useful for anybody who wants to take some data from an article, and especially in comparing results obtained under similar experimental conditions by different authors.

A standard ion bombardment apparatus using a B–A Type of ion source (He^+ beam of 30μA) was used for irradiation [17]. This apparatus has attached an "Ion Bombardment and Temperature Control Microprogrammer", to be used for cycling experiments in plasma–wall interaction [18]. Targets can be heated in a simple oven (up to 1100°C) or can be located in another system on a tungsten ribbon, the temperature of which is controlled by a Control Logic M 8080 Microcomputer. The ion source is switched on when the target reaches T_{max} (20 – 2000°C adjustable). Then the target is bombarded at preselected parameters of the ion source during the time t_{hold} (0 – 1000 sec. adj.) or $t_{hold} + t_{rest}$ (0–2000 sec. adj.). At the end of the cycle the ion source is switched off and the target remains at a preselected T_{rest} (20 – 1000°C adj.). The heating rate at the beginning of the cycle is from 10 – 150°C/sec. Using this microprogrammer, such an ion bombardment experiment can be continuously repeated and the number of cycles will be shown on the digital display. An ion integrator is connected to the system, so that we can observed not only the ion dose for one cycle, but also the total ion dose at each moment of the bombardment. One should only add that the microprogrammer can be used universally for many kinds of experiment, but especially for simulation of recycling of a fusion experiment and for all kinds of thermal desorption studies.

TABLE II. EXPERIMENTAL CONDITIONS FOR BLISTERING STUDIES ON ST.STEELS

A.1. Projectile – Related Parameters	
A.1. Type of projectile	He^+ ions
A.2. Projectile energy	6 and 10 keV
A.3. Total ion dose	$5.10^{17} - 10^{19}$ ions/cm^2
A.4. Dose rate	$10^{14} - 10^{15}$ ions/cm^{2}sec.
A.5. Angle of incidence of projectile	normal incidence
B. Target – Related Parameters	
B.1. Type of targets:	a) St.Steel – Prokron 11 spec. Composition (%): Cr–18, Ni–10, Ti–0.5–1, Si–0.7, C–0.1, Fe–bal (similar to 304) b) St.Steel – Prokron 12 Composition (%): Cr–17.5, Ni–12.5, Mo–2.0, Mg–1.5, Si–0.5, C–0.1, Fe–bal (similar to 316) Pretreatment for both targets: annealing for 2 hours at 1000°C in vacuo.
B.2. Target temperature	20 – 650°C
B.3. Target microstructure	
a) grain size	20 – 100 μm
b) initial defect density	not investigated
c) effects of precipitates	not investigated
B.4. Crystallographic orientation of irradiated surface	polycrystalline samples
B.5. Target surface finish	a) mechanically polished only b) electrolytically polished only (deep removal) c) annealed and then electrolytically polished (deep removal) d) mechanically polished, annealed and then electrolytically polished (normal removal)
C. Parameters Affected by Target–Projectile Combination	
C.1. Solubility of projectile in target	not investigated
C.2. Critical ion dose for blister appearance	at 20°C: $2-5 \times 10^{18}$ ions/cm^2 at 630°C: $< 10^{18}$ ions/cm^2

The preparation of samples (thermal treatment, surface finish) has in principle a large influence on the topography obtained after low energy He^+ ion bombardment. Therefore, we made high resolution replices (C–Pt, 20Å resolution) on the prepared samples before irradiation. Most of the targets were electrolytically polished in a mixture of 200 ccm methanol +50 ccm perchloric acid at 14 V and 40 mA/cm^2 (polishing time 5–6 minutes). It was difficult to keep the electrical parameters constant but a perfect surface finish, observed by a scanning electron microscope, was obtained even with slight variations in voltage and current density.

RESULTS

The initial surface structure of stainless steels plays an important role in low energy He^+ ion bombardment ($E < 10$ keV), where the mean range is in the region of 100 – 500 Å. In this energy region the sputtering yield has a maximum, e.g., for stainless steel [1] : 0.2 atoms/ion for 6 keV He^+ and 0.17 atoms/ion for 10 keV He^+. Therefore we did not look only for blister appearance, but also for blistering erosion rate and changes of surface topography, to be demonstrated by the "background surface structure" observed in all our pictures of irradiated samples. Such ion–bombardment induced surface changes on solid surfaces have recently been reviewed by the author [19].

It is well known that mechanical and thermal treatments and mechanical and electrolytic polishing produce a high density of dislocations, grain boundaries, twins, inclusions and precipitates in stainless steels. All these surface features, including, artefacts, can enhance the growth of gas bubbles, decrease the helium bubble mobility and greatly influence the formation of blisters. Therefore we made a precise surface characterization of each sample before ion irradiation. Fig. 1 shows three surface structures of unirradiated annealed (2 hours at 1000°C in a vacuum of 10^{-5} torr) and electrolytically polished stainless steel samples (PROKRON 12). When we looked at these samples in a scanning electron microscope at a magnification of 10000x they were perfectly shiny and only a few large inclusions were visible. Microscopically small surface features were identified only by high resolution replicas. All polished surfaces were in general slightly etched (Fig. 1a/B, 1b/C and 1b/D) or were covered with well developed round flat etch pits – 200 to 1000 Å in diameter – having different diameters and a distribution on differently oriented grains (Fig. 1c/1, 1c/2 and 1c/3). Through the relatively large ion erosion effect when such initial surfaces were bombarded with 10 keV He^+ ions and doses higher than 10^{18} ions/cm^2, microscopically small surface features were eroded away, and only one type of precipitate, shown as black dots on the grain 3 of Fig. 1c, remained unaffected. These precipitates are probably small carbide inclusions and can also be seen on bombarded samples (Fig. 2a).

Using the replica technique, we found on both PROKRON stainless steels only a few widely dispersed dome shaped blisters when bombarded at room temperature with 6 keV He^+ and ion doses from 1 to 5.10^{18} ions/cm^2 [20]. Blisters of diameter 0.15 – 0.20 μm were in many cases found in small groups and attached to the inclusions, grain boundaries (Fig. 2a/B) and recrystallization twins (Fig. 2b/T). The diameter of the blisters varied with different grain orientation, the largest observed being approx. 0.6 μm in diameter. Many inclusions were found on bombarded surfaces (Fig. 2a/I) and one must be careful in distinguishing between blisters and inclusions, especially if they are similar in size.

Rough calculation showed that radiation blistering erosion is always present in such experiments. Such an effect is shown in Fig. 2b/E on a blister cover. It should be pointed out that under the same bombardment conditions, the erosion effect was found only on some grains, these having a "background" structure on Fig. 2b more rough than these e.g. on Fig. 2a, between inclusions. Investigations of a large number of samples showed that such a structure depends very much on the initial surface of the sample and on the target temperature.

On stainless steel surfaces bombarded at room temperature, we found not only an inhomogeneous distribution of blisters and a strong dependence on the orientation of grains, but also, in many cases, that the blisters transcended grain boundaries. It is only an impression that there are small differences in orientation of grains and that therefore grain boundaries are in fact very flat contrary to the deep grain boundaries in

Mo annealed to high temperatures [3,8]. In such a structure a blister could transcend the grain boundary (see Fig. 2a and Fig. 2b).

With respect to the inhomogeneity of blisters at room temperature, it should be pointed out that all these samples were annealed 2 hours at 1000°C and that a thick top layer of approx. 200 μm was removed by the electrolytic polishing technique. It is difficult to believe that this surface preparation could leave such an inhomogeneous distribution of strain on the surface and would therefore be the reason for the observed inhomogeneous distribution of blisters in stainless steels.

Helium implantation (10 keV) in stainless steels at elevated temperatures in general causes drastic changes in the bombarded surfaces. Fig. 3 shows an optical micrograph (a) and an electron micrograph–replica (b) of a sample implanted with an ion dose of 10^{19} ions/cm^2 at 630°C. The surface looks to be properly ion etched with average dimensions of 0.1 μm [19]. The topography of some grains was remarkably more flat and Fig. 4a shows small dome shaped blisters, some of them well separated, of a diameter 700–800 Å. Coalescence of two, three or more blisters can be clearly identified. We succeeded in bending the foil of the replica in an electron microscope so it was possible to observe surface roughness from the profile. The roughness of the bombarded area wasbelow 500 Å, and therefore contrast was relatively poor. It is believed that such surface features can only be seen and resolved using high resolution replica and transmission electron microscopy.

Large separate blisters were not found on these hot implanted samples. Some inclusions and bands were seen, but all of them were not affected by the bombardment, even though the surroundings was heavily roughened (Fig. 4b). This is an indication that these inclusions are probably hard nitrides or carbides, and also that the bands must have a structure different from the matrix.

One should conclude from these results that 6 and 10 keV H^+ ion implantation at room temperature on the investigated stainless steels produces only a few blisters, inhomogeneous in size and in distribution. "Background" structure remains practically smooth, even at the largest ion doses of 10^{19} ions/cm^2. Slight ion erosion effect can be seen on same blister covers. At elevated temperatures, sputtering predominates and the radiation blistering erosion rate increases. This is probably due to the thin blister skin (few 100 Å), the low penetration of He^+ ions and large swelling effect. Surfaces become homogeneously covered with blisters and clusters of blisters – surfaces become "rough" – and it seems that at temperatures between 500 and 650°C, the surfaces reach an equilibrium. This can be probably determined by the maximum erosion rate, flattening of the surface by sputtering, appearance of new blisters and the reemission of the already trapped gas.

ACKNOWLEDGEMENTS

The authors would like to thank Mrs. M. Peternel and Mrs. Z. Škraba for preparing targets and their skilful technical assistance during the experimental work and the preparation of the manuscript.

REFERENCES

[1] BEHRISCH,R., KADOMTSEV,B.B., in Plasma Physics and Controled Nuclear Fusion Research (Proc. 5th Int.Conf. Tokyo 1974) 2, IAEA, Vienna (1975) 229.
[2] SCHERZER,B.M.U., J.Vac.Sci.Tech. 13, (1976) 420.
[3] ERENTS,S.K., McCRACKEN,G.M., Rad. Effects 18 (1973) 191.
[4] ROTH,J., Institute of Physics, Conf.Ser. No 28, Ch. 7 (1976) 280.
[5] DAS,S.K., KAMINSKY,M., Proc. Symposium on Radiation Effects on Solid Surfaces, Chicago 1975 (ACS Meeting, Advances in Chemistry series), to be published.
[6] THOMAS,G.J., BAUER,W., Proc.Conf. Surface Effects in Controlled Fusion Devices, San Francisco (February 1976), to be published in the J.Nucl.Materials.
[7] PICROUX,S.T., VOOK,F.L., J.Nucl.Mat. 53 (1974) 246.
[8] VERBEEK,H., ECKERSTEIN,W., in Application of Ion Beams to Metals (Proc. Int. Conf. Albuquerque, 1973), (PICRAUX,S.T., EERNISSE,E.P., VOOK,F.L., Eds.), Plenum, New York (1974) 597.
[9] PANITZ,J.A., J.Vac.Sci.Tech. 11 (1974) 206.
[10] DAS,S.K., KAMINSKY,M., J.Nucl.Mat. 53 (1974) 115.
[11] THOMAS,G.J., BAUER,W., J.Nucl.Mat. 53 (1974) 134.
[12] BAUER,W., THOMAS,G.J., J.Nucl.Mat. 53 (1974) 127.
[13] BAUER,W., THOMAS,G.J., J.Nucl.Mat. 47 (1973) 241.
[14] KEEFER,D.W., PARD,A.G., Rad.Effects 22 (1974) 181.
[15] KEEFER,D.W., Rad. Effects 24 (1975) 29.
[16] WILSON,K.L., THOMAS,G.J., BAUER,W., Trans.Am.Nucl.Soc. 22 (1975) 36.
[17] NAVINŠEK,B., ŽABKAR,A., Proc. of Contributed Papers (8th Int. Summer School and Sympl. on the Physics of Ionized Gases, Dubrovnik, 1967), J.Stefan Institute, Ljubljana (1976) 256.
[18] NAVINŠEK,B., MILAVC,Z., DIVJAK,S., TASIČ,J., KEBER,M., J.Stefan Institute, Report, DP–994, Ljubljana June 1976.
[19] NAVINŠEK,B., Progress in Surface Science 7 (1976) 49.
[20] NAVINŠEK,B., ŽABKAR,A., Proc. of Contributed Papers (8th Int. Summer School and Symp. on the Physics of Ionized Gases, Dubrovnik 1976), J.Stefan Institute, Ljubljana (1976) 260.

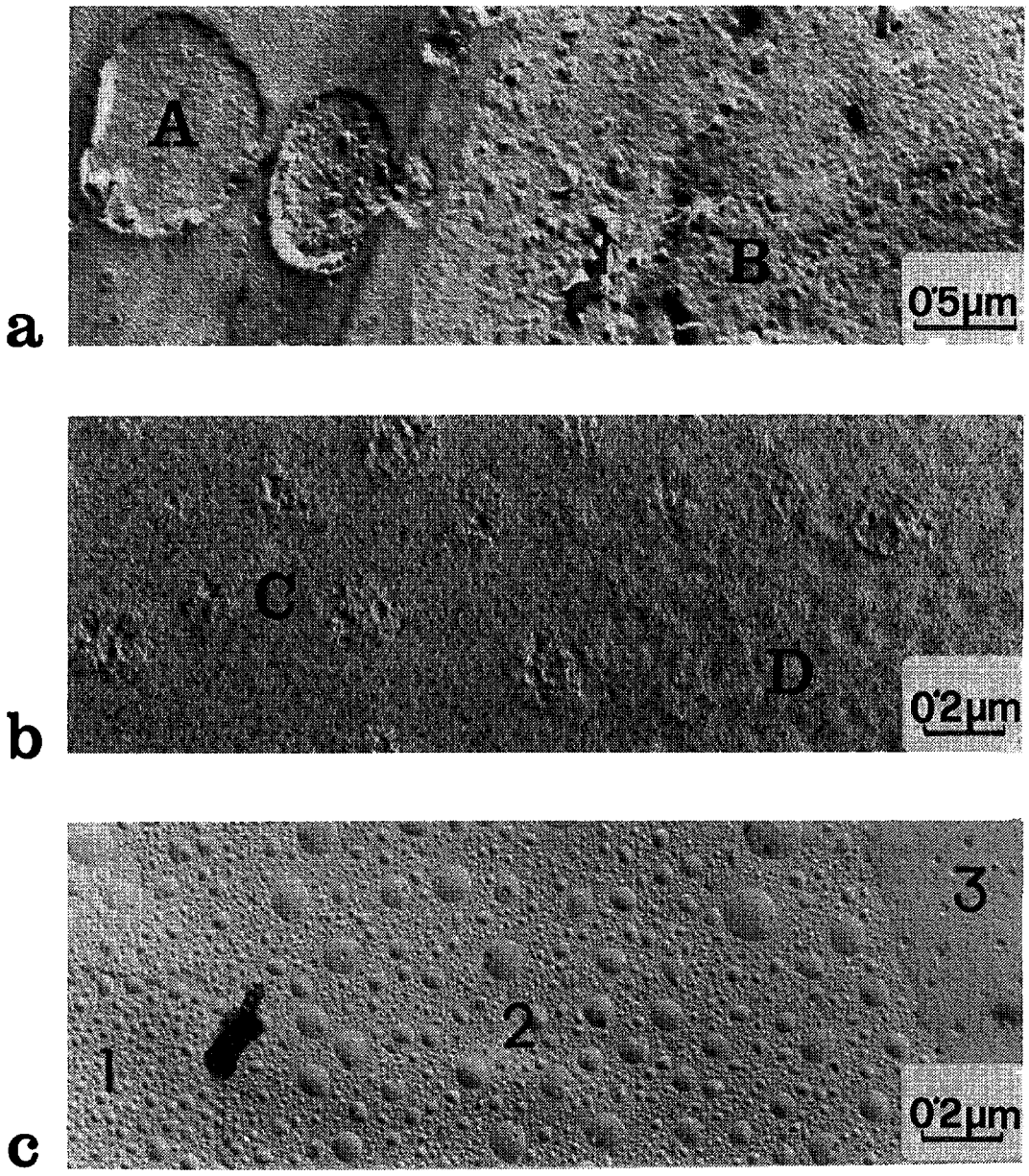

Fig. 1 Surface structures of unirradiated annealed and electrolytically polished stainless steel (PROKRON 12) under slightly different polishing conditions.

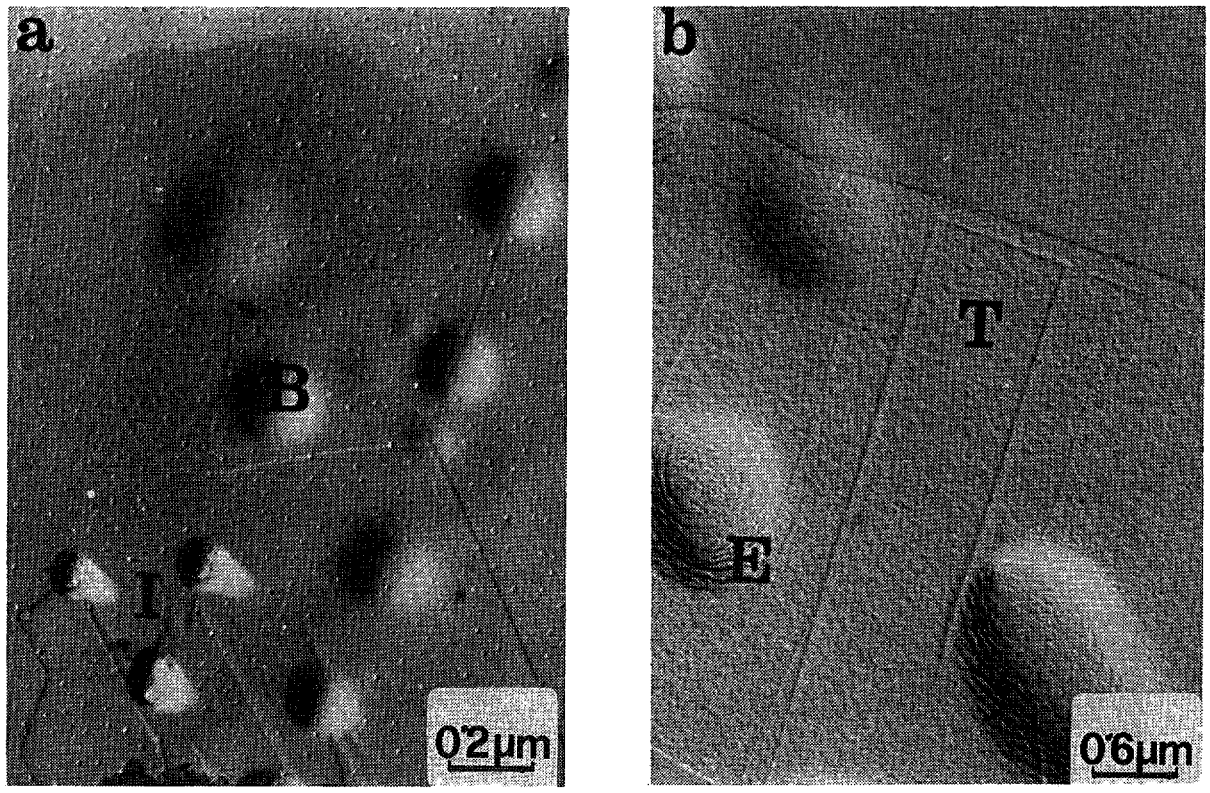

Fig. 2 Stainless steel (PROKRON 12) bombarded with 6 keV He^+ ions at room temperature, B – blisters, I – inclusions, E – erosion effect, T – twin.

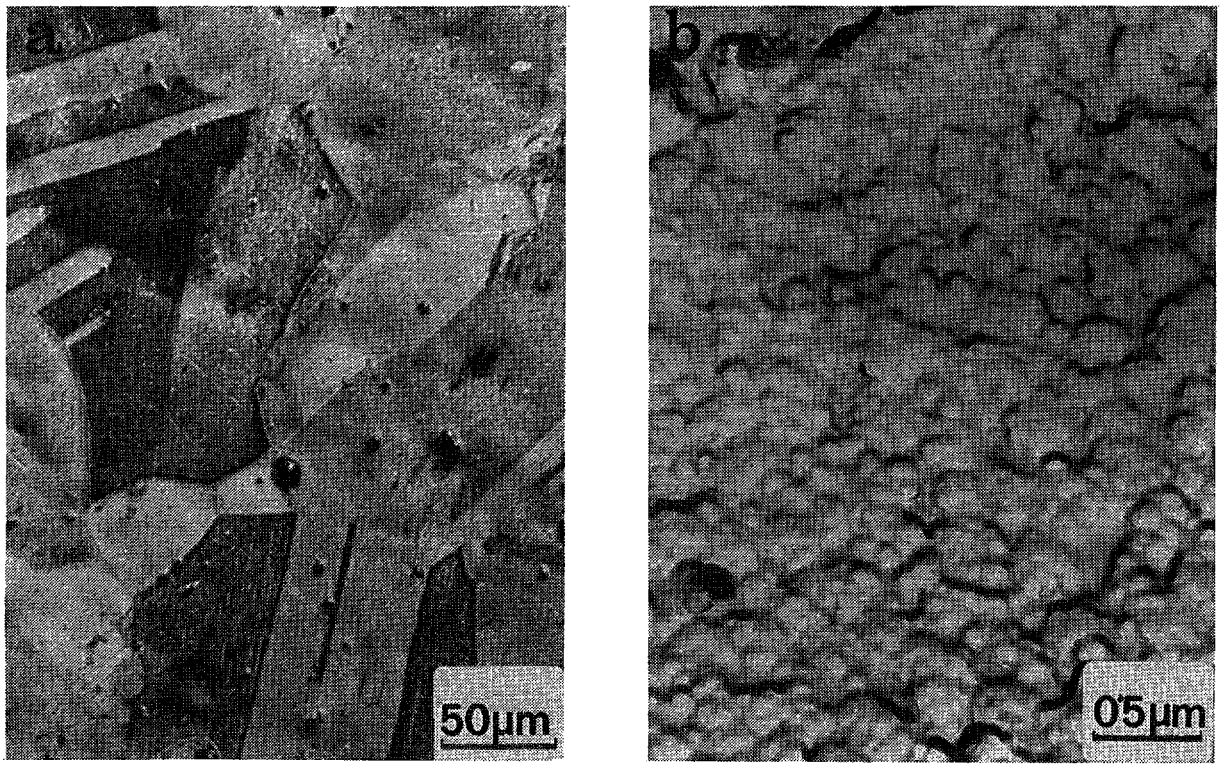

Fig. 3 Stainless steel (PROKRON 12) implanted with 10 keV He^+ ions at 630°C, a – optical micrograph, b – replica.

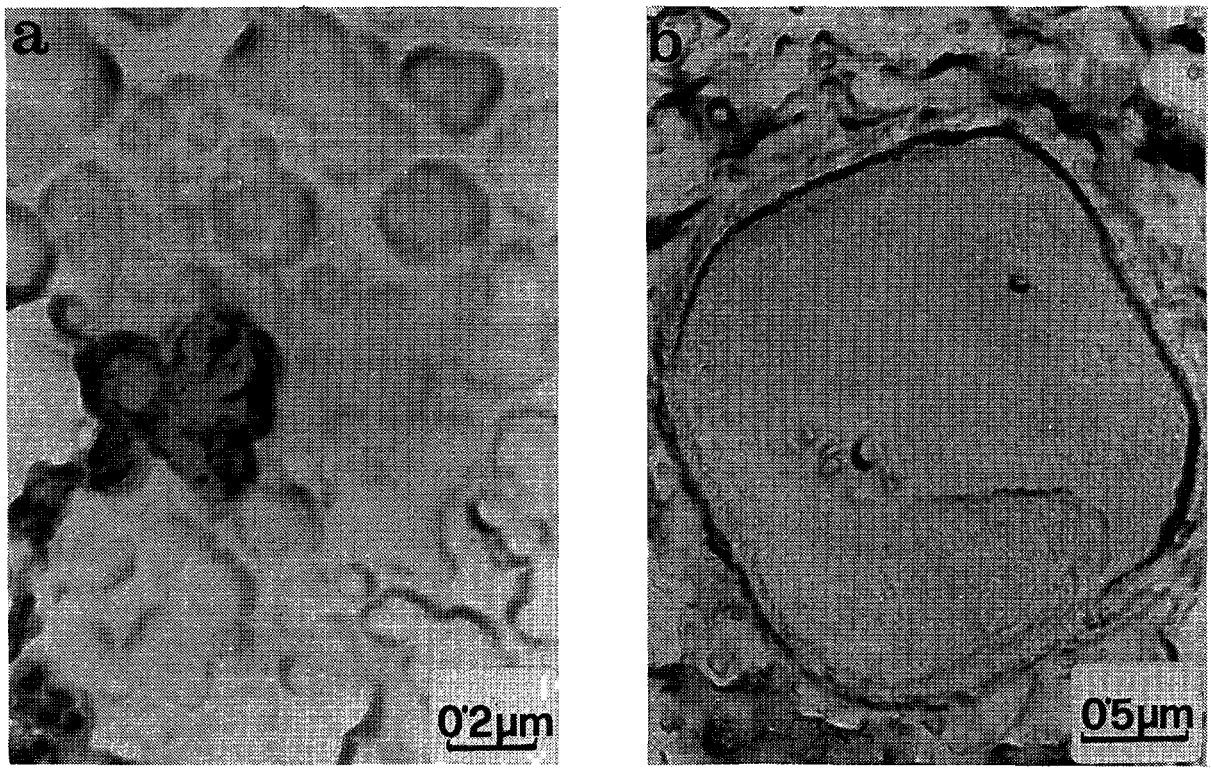

Fig. 4 Dome shaped blisters (a) and large inclusion (b) on stainless steel bombarded with 10 keV He^+ ions and ion dose of 10^{19} ions/cm^2 at 630°C.

INVESTIGATIONS ON SPUTTERING AND SECONDARY ION YIELD FROM METALS UNDER BOMBARDMENT OF NOBLE GASES IN THE ENERGY RANGE 5 - 25 keV

Karl Heinz Krebs

Department of Physics, Humboldt-University, Berlin, GDR

In the last years we were interested in the measurement of the positive ionization efficiency

$$R^+ = S^+/S \qquad (1)$$

with S^+ - positive secondary ion yield,

S - sputtering yield.

Therefore we constructed an apparatus which allows to measure these yields as a function of any parameters /1/. Fig.1 shows the principle of the equipment.

The generation system for the mass-selected energy-homogeneous ion beam consists of gas inlet, ion source, accelerating and focussing optics and the deflection magnet. This beam is focussed on the rotatable target, which is arranged in a vessel in which the pressure and the gas composition are variable by means of a gas inlet system. The detection of the integral positive SI-yield happens by means of a spherical collector around the target. By means of an ion optics a part of the secondary ions can enter a $\pi/2\sqrt{2}$-cylindrical condenser for energy analysis. Combined with a 60° deflecting magnet a mass analysis of the secondary ions is possible. The ions are detected by means of an ion-electron-converter.

The current density of the mass-selected primary ion beam was 0,75 mA/cm^2 in the case of 12 keV $^{40}Ar^+$ ions. In the target chamber an oil-free vacuum of $1 \cdot 10^{-6}$ torr was attained. Therefore we work with a dynamically clean surface, proved by means of the density dependence of the secondary ion yield (fig.2).

But it is well-known that the yield measured under dynamical conditions is always any percents higher than that at static conditions.

By means of polarity reversal of the deflecting magnetic field it is possible to focus the primary ion beam on the opposite output of the magnet chamber. Here is coupled a vacuum vessel with target houlder for investigations about sputtering. The sputtering yield can be measured by means of the well-known

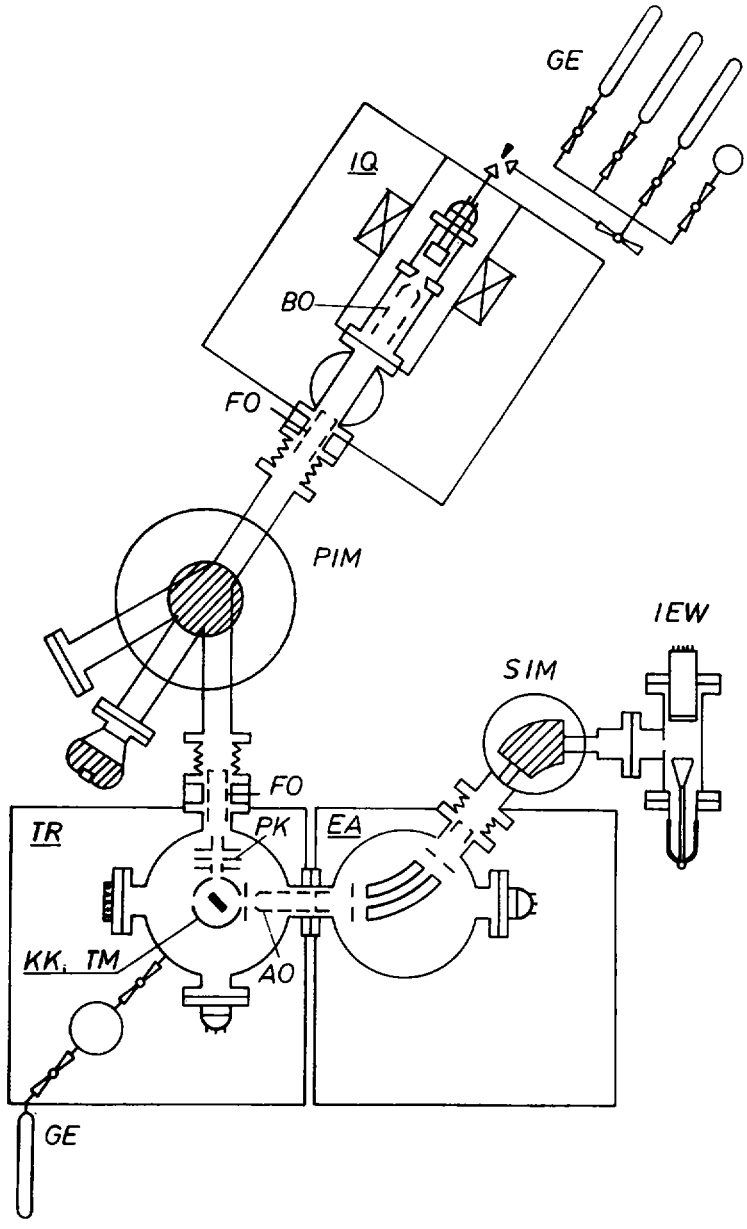

Fig.1
Apparatus for measurement of positive secondary ion emission /1/

weight-loss method or the frequency variation of a quartz crystal. Also it is possible to measure the so-called (integral) sputtering efficiency, introduced by SIGMUND /2/ by means of a thermal particle detector /3/ and the angular distribution of the sputtering efficiency by means of a specific thermal particle detector /4/ shown in fig.3.

By holding the target in position on a copper block K, which is in thermal contact with the target chamber via the thin mica foil G, the temperature of the target is prevented from raising consi-

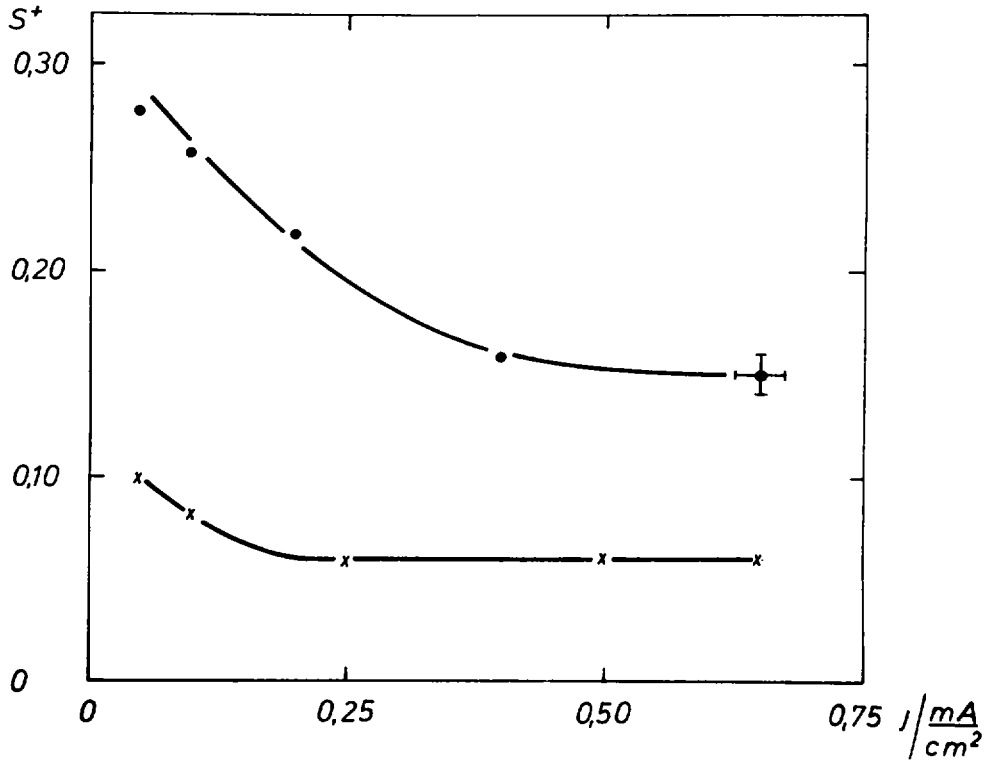

Fig.2
$S^+ = f(j)$ for 12 keV $^{40}Ar^+$ on Mo (xxx) and Al (●●●) /1/

derably owing to the ion bombardment. For suppressing the secondary electrons, two permanet magnets M generate a magnetic field of $2 \cdot 10^{-2}$ T parallel to the target surface at the ion impact point. The particle detector is mounted on a rotatable holder, the position of which can be set with an accuracy of 0.5°. The particles emitted from the target surface which pass through the dia-

phragm B reach the collector A_1 and heat it. The collector is made of Al foil 20 µm thick. The rise in temperature was recorded with a voltage signal by means of a glazed thermistor Th in a Wheatstone bridge circuit. For the detector used it was proved, that for powers $\leq$ 200 µW the measuring signal is proportional to the intensity and to the energy of the incident ions. Indepently of the ion type a calibration constant of 210 V/W with a standard deviation of 3 % was found for a thermistor resistance of 5 kΩ. The time constant was 39 sec.

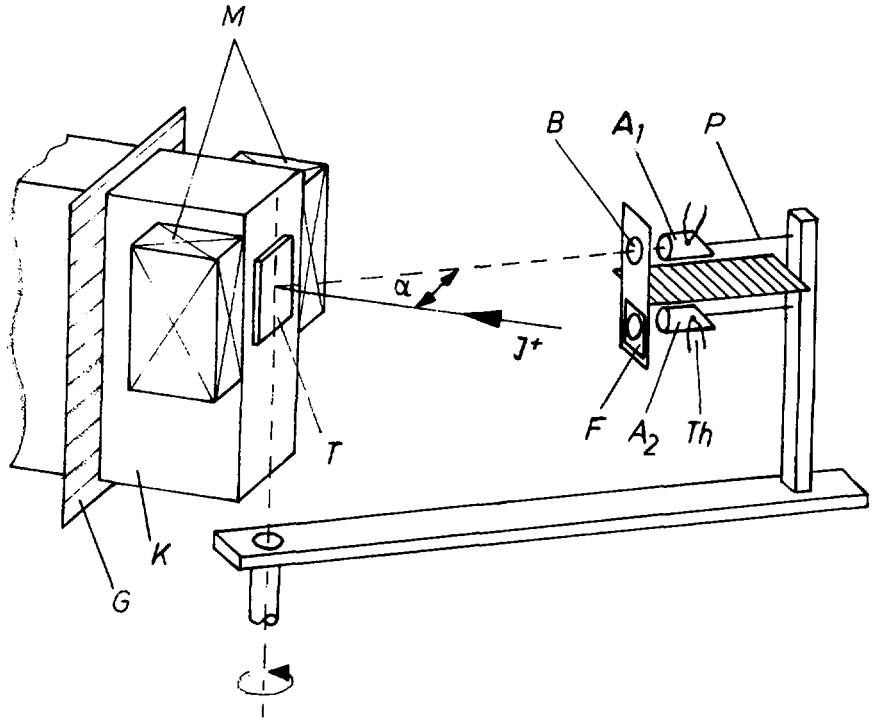

Fig.3
Experimental set-up for measuring the angular distribution of sputtering efficiency /4/

For measuring the integral sputtering efficiency a similar fixed arranged detector is used, which detects the hemispherical emission.

By sputtering efficiency is meant the part γ of the primary ion energy E_0 which leaves the solid again in the form of kinetic

energy of atomic particles, i.e. sputtered target atoms and molecules and reflected primary ions:

$$\gamma \cdot E_o = S \cdot \overline{E}_S + R \cdot \overline{E}_R \qquad (2)$$

with R - reflection coefficient and
$\overline{E}_S, \overline{E}_R$ - average energies of the sputtered resp. reflected particles.

The size of the two right-hand terms depends on the mass ratio $\mu = M_2/M_1$ in such a manner /5/ that for $\mu \lesssim 1$ the first term dominates, the opposite holds true for $\mu \gg 1$ (M_1, M_2 - mass numbers of primary ion resp. target atom).

Under the condition $\mu \lesssim 1$ the reflection term is negligible, and so it is possible to find from eq.2 the average energy of the sputtered particles (inclusively the secondary ions)

$$\overline{E}_S = \frac{\gamma E_o}{S} \qquad (3)$$

In the table are shown the measured resp. computed values for the normal bombardment of 13 element targets with $^{40}Ar^+$ ions with an energy of 12 keV /6/.

Element	Z	γ[%]	S	S^+	$\bar{E}_S$/eV	R^+	
Mg	12	1,45	2,8	0,094	62	0,034	
Al	13	1,45	1,4	0,11	124	0,079	
Si	14	1,15	0,8	0,015	172	0,019	
Ti	22	1,50	0,9	0,042	200	0,047	
Mn	25	1,80	5,5	0,018*	39	0,0033	*nach Beske /7/
Fe	26	2,0	2,4	0,025	100	0,010	
Co	27	2,2	3,3	0,017	80	0,0052	
Ni	28	2,2	3,5	0,035	75	0,010	
Cu	29	2,2	6,7	0,023	39	0,0034	
Zn	30	2,75	16,8	0,024	20	0,0014	
Ge	32	2,5	3,8	0,016	79	0,0042	
Mo	42	—	1,6	0,048	—	0,030	
Ta	73	—	1,4	0,06	—	0,043	

The targets were mechanically and chemically purified polycrystals with exception of Si and Ge, which were (111)-orientated monocrystals. The S^+-values are corrected by secondary mass analysis, the S^+-value for Mn is estimated from BESKE /7/.

Because the condition $\mu \lesssim 1$ is not valid, the γ- and $\overline{E_S}$-values for Mo and Ta are not computable.

By means of the computed values of R^+ and $\overline{E_S}$ it is possible to prove the fitness of the theoretical assumption by SCHROEER et al. /8/

$$R^+ = S^+/S = \frac{A^2}{(I-\phi)^2} \left[\frac{\bar{v}\,\hbar}{a(I-\phi)}\right]^n \qquad (4)$$

with A - binding energy of a surface atom,
I - ionization potential of the free atom,
ϕ - work function of the target material,
$\bar{v}$ - average velocity of the emitted atom ,
a - thickness of the region above the surface, in which the ionization of the atoms take place.

Under the assumption that the energy distribution N(E) of the emitted particles is proportional to E^{-2} for $A \leq E \leq T$
with T - maximum energy which can transferred to a target atom in a single collison,
and zero for the other energies, by means of eq.3 the average velocity $\bar{v}$ of the emitted atoms is calculated to

$$\bar{v} = 2\left(\frac{2\gamma E_0}{Sm_2}\right)^{1/2} \left(\ln \frac{T}{A}\right)^{-1/2} \qquad (5)$$

By use of the table values for A /9/, I and ϕ/10/ and the computed $\bar{v}$ one can plot

$$R^+ \frac{(I-\phi)^2}{A^2} = f\left[\frac{\bar{v}\,\hbar}{(I-\phi)}\right] \qquad (6)$$

and determine n and a (fig.4).

The least-square analysis yields $n = 1.2 \pm 0.3$ and $a = 0.6$ Å

This is in a good agreement with the statements of RÜDENAUER et al. /11/.

In fig.4 the values of Mg and Zn deviate remarkably from the calculate straight line. The reason could be in the reaction of these unnoble elements with the oxygen in the target chamber. It is well-known /12,13/ that oxygen has a strong influence on the secondary ion emission. As well the binding energy A as the work function ϕ can be influenced by oxygen covering the surface. If we take the

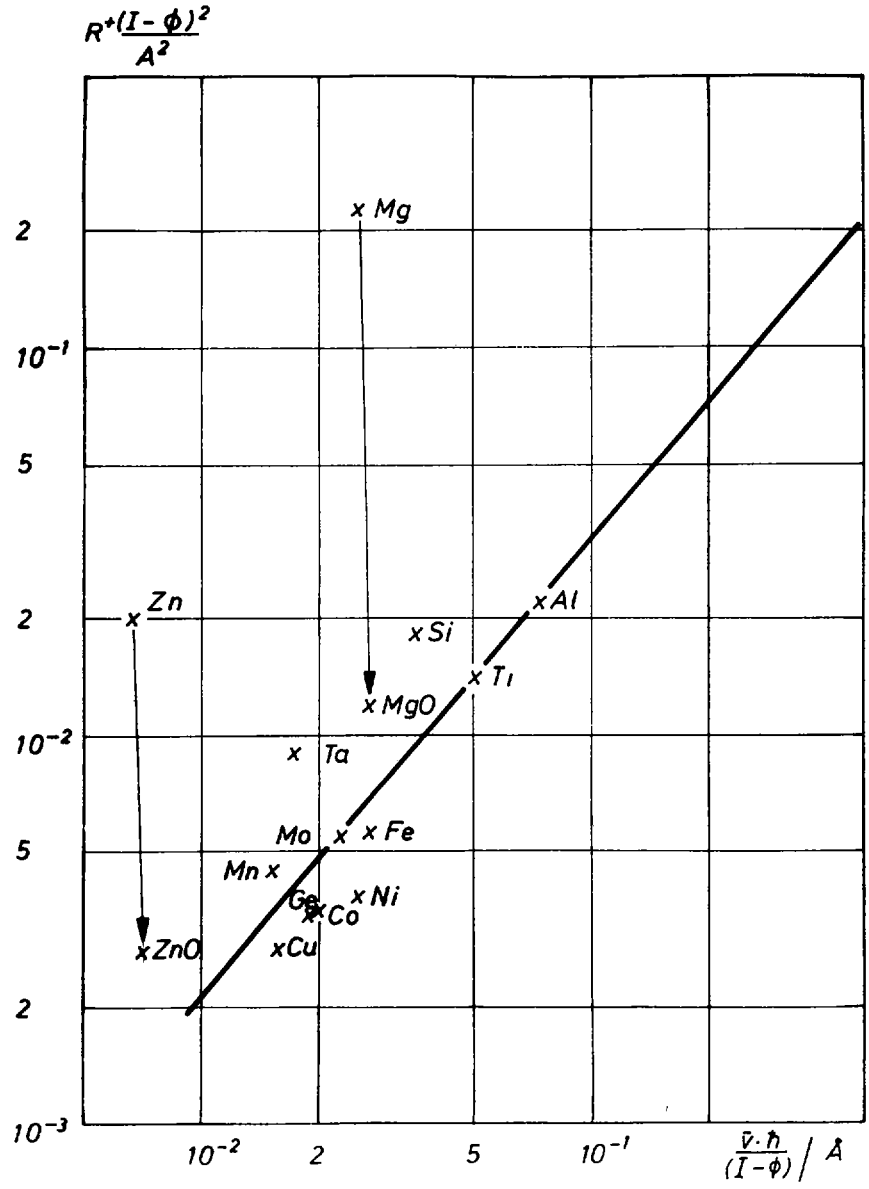

Fig.4
Data analysis according to eq.6 /6/

binding energy of the oxides in eq.6 the deviations are smaller.

The reported measurements were execute by my coworkers Dr.Düsterhöft, Mr.Hildebrandt, Dr.Rogaschewski and Dr.Manns in the Applied Mass Spectrometry Group of the Physics Department of the Berlin Humboldt-University.

LITERATURE

/1/ H.DÜSTERHÖFT, R.MANNS and S.ROGASCHEWSKI, Exp.Techn.Phys., (in press)

/2/ P.SIGMUND, Can.J.Phys. 46, 731 (1968)

/3/ D.HILDEBRANDT and R.MANNS, to be published

/4/ D.HILDEBRANDT and R.MANNS, Rad.Eff.,(in press)

/5/ J.BØTTIGER, J.A.DAVIES, P.SIGMUND and K.WINTERBON, Rad.Eff. 11, 69 (1971)

/6/ H.DÜSTERHÖFT, R.MANNS and D.HILDEBRANDT, phys.stat.sol.(a) 36, K93 (1976)

/7/ H.E.BESKE, Z.Naturf. 22a, 459 (1967)

/8/ J.SCHROEER, T.RHODIN and R.BRADLEY, Surf.Sci. 34, 571 (1973)

/9/ C.KITTEL, Einführung in die Festkörperphysik, Akademische Verlagsgesellschaft Geest & Portig, Leipzig, 1973, p. 128

/10/ D'ANS und LAX, Taschenbuch für Chemiker und Physiker, 1970, vol.III, p.248

/11/ F.G.RÜDENAUER, W.STEIGER and R.PORTENSCHLAG, Microchim.Acta 5, 421 (1974)

/12/ G.BLAISE and M.BERNHEIM, Surf.Sci. 47, 324 (1975)

/13/ A.BENNINGHOVEN, Surf.Sci. 53, 596 (1975)

DATA NEEDS, PRIORITIES AND ACCURACIES FOR PLASMA MODELLING

M L Watkins

UKAEA Culham Laboratory, Abingdon, Oxfordshire, England
(Euratom/UKAEA Fusion Association)

Abstract

To determine the needs, priorities and accuracies of the atomic and molecular physics data required for plasma modelling the rôle of these data in computer simulations of magnetically confined plasmas is reviewed. The models approximate atomic and molecular reactions in many different ways. Multi-dimensional calculations concerned with the equilibrium and stability of a plasma-magnetic field configuration assume the plasma to consist of fully ionised hydrogen ions and electrons in the magnetohydrodynamic approximation: the effect of atomic and molecular reactions is minimal. Zero (spatial) dimensional calculations of the break-down phase of gas discharges assume the gas to consist of atomic and molecular hydrogen, electrons and impurity ions such as oxygen, carbon, iron, tungsten and molybdenum: the effect of plasma motion is minimal. Between these extremes are classes of computations such as the one (spatial) dimension transport calculations which attempt to establish a realistic balance between the behaviour of ions, atoms and molecules in an established discharge. The limitations and inadequacies of present data and models for atomic and molecular processes are illustrated by several specific calculations. The results of these calculations permit identification of the areas where improved models and data for the atomic and molecular reactions are required.

1. Introduction

To determine the needs, priorities and accuracies of the atomic and molecular physics data required in computer simulations of plasmas it is necessary to examine the models that are used, to illustrate the effect of atomic and molecular reactions on these models and to identify those areas of the models where improvements are necessary. In particular, I shall concentrate on the detailed behaviour of magnetically confined plasmas in present and future generation experiments. I shall exclude discussions of both inertial confinement systems and the extrapolation of either confinement system to reactor conditions. In such extrapolations the detailed behaviour of the discharge gas is taken (at present) to be of secondary importance.

I review the general rôle of atomic and molecular processes in the computer simulation of plasmas. The limitations and inadequacies of present data and models for these processes are illustrated by the results of several specific calculations. The particle and energy balance of low Z-number species (which include hydrogen atoms and molecules) is examined by means of the zero (spatial) dimensional models used to simulate the break-down phase of gas discharges. In these calculations the effect of plasma motion is taken to be minimal. The transport properties of low Z-number species in an established discharge are examined by means of a one (spatial) dimensional model. These calculations may also be used to determine the energy balance of a plasma which is heated by an injected beam of energetic neutral particles and cooled by radiation losses associated with impurity ions that enter the discharge as a result of plasma-wall interactions.

The results of these calculations permit the identification of the areas sensitive to the data used for the atomic and molecular processes. The improvement of the data and the models is discussed.

2. Computational models for magnetically confined plasmas

A convenient categorisation of computational models for magnetically confined plasmas is illustrated in Table I. The categories are not necessarily mutually exclusive: stability calculations may utilise the energy principle [1] or may use a time-dependent model [2] which follows the temporal evolution of the system from a given equilibrium configuration.

All types of calculations illustrated in Table I can be very demanding on both computer storage and time. Vlasov and particle codes [3] require to follow the behaviour of a large number (often in excess of 10^6) of particles (or pseudo-particles) under the influence of defined force-laws which may be externally applied. The demand on computer storage from Fokker-Planck models [4] arises from the need to represent the distribution functions for different ion and electron species in a multi-dimensional phase space. It is usual to follow the temporal behaviour of the distribution functions on grid points on a finite-difference mesh mapped onto the spatial and velocity axes of the phase space. A similar demand on computer storage applies to multi-(spatial) dimensional magnetohydrodynamic codes [5] which follow the temporal behaviour, equilibrium or stability of plasma in given (or self-consistent) magnetic field configurations.

In all cases the models simulate phenomena which occur on grossly different timescales and often much computer time is needed to follow the highest frequencies to times characteristic of the longest timescales. For example, magnetohydrodynamic calculations often require to follow the fast timescales associated with magnetosonic modes along magnetic field lines, while interest is in the much slower phenomena associated with gross plasma motion across the magnetic field.

As a result of the large demands these codes have on the resources of present-day computers the description of atomic and molecular processes are often minimal. The extension of the models to incorporate the effects of complex geometries has resulted in the simplification of the physics content of the basic model. At best, collision frequencies may be enhanced by the effective charge,

$$Z_{eff} = \sum_{i \neq e} n_i Z_i^2 / n_e \qquad (1)$$

of a plasma which contains different ions of density, n_i, and charge state, Z_i,

and electrons of density n_e. At worst, transport coefficients, such as electrical conductivity, are given constant values.

An adequate description of a magnetically confined plasma will require a hybrid code. For example, even if a plasma is assumed to be described by a magnetohydrodynamic model, a two-dimensional equilibrium configuration that is calculated to satisfy pressure balance at any given time will be subject to diffusion, heating and other entropy-generating processes. These processes will modify the plasma-magnetic field parameters and lead by adiabatic re-adjustment to a new equilibrium configuration at a slightly later time. At each stage the configuration would have to be tested for stability.

It is appropriate to consider as a hybrid simulation the coupling of a one (spatial) dimensional transport model [6] to a zero (spatial) dimensional model [7] for atomic and molecular physics processes. One-dimensional transport calculations include approximate models which apply to slow time-scales typical of cross-field particle and energy diffusion times rather than detailed wave motion which can set up equilibrium along magnetic field lines. In this respect the model is inferior to those used in magnetohydrodynamic calculations, but can contain modes of particle localisation that are not included in the magnetohydrodynamic approximation. These modes include the enhancement of diffusion as the result of trapped particles [8]. The atomic and molecular physics data supplied to these calculations is illustrated in Figure 1. Both equilibrium and non-equilibrium models are used. In the case of low to intermediate Z-value elements the rate equations for the ground and ionised states may be solved. This approach is used for elements up to oxygen and includes the special case of hydrogen atoms. For intermediate to high-Z elements an equilibrium situation is often assumed to exist and the interaction with the transport model is through the supply of the ionisation state and the radiation losses. This model is used typically for impurity ions such as iron, tungsten and molybdenum.

In the remainder of this paper hybrid models are used to investigate the behaviour of plasma confined in the tokamak configuration (Figure 2). Specific calculations applicable to present [9] and future [10] generation experiments (Tables II and III) illustrate the importance of accurate representations of the atomic and molecular processes.

3. Particle and energy balance of low Z-value species

The particle and energy balance of low Z-value species in the low temperature regions of a discharge is examined by the zero-dimension models of partially ionised plasmas used to simulate the first phase of the current rise [7]. These break-down calculations are important for the next generation of large tokamak since the requirements placed on the ohmic heating system to establish a plasma discharge are very much more severe than in present generation devices [11].

The calculations follow the build-up of plasma (hydrogen ions and electrons) which occupies a volume, V_o, in a vessel of total volume, V_1 (Figure 3). Initially, the volume V_1 is filled with molecular hydrogen gas, H_2^o. The molecular volume, $V(H_2)$ is calculated with time and decreases as the electron and ion temperatures increase and the importance of H_2^o and H_2^+ diminishes. The models are described by the reactions indicated in Table IV. The cross-sections for each reaction are theoretical estimates and uncertainties may be particularly important at low temperatures ($\lesssim$ 10 eV).

During the first stage of the discharge break-down phase (for timescales less than 1 ms in present generation tokamak and 10 ms in future generation tokamak) the dominant energy loss mechanisms result from atomic physics processes. These are volume effects and so a zero (spatial) dimensional model is appropriate. Figure 4 indicates that a balance is established over the first 10 ms of a large tokamak between the large ohmic input power, the atomic and molecular reactions and charge exchange losses. Transport processes associated with charged particles have little effect on either the particle or energy balance.

The production of a highly ionised, current carrying plasma is particularly sensitive to the concentration of impurity ions. In particular, the radiation associated with a 5% concentration of oxygen impurity (Figure 5) extends the timescale over which reactions involving atomic and molecular hydrogen are of importance. The volt seconds required for breakdown is thus increased and indeed breakdown might not even be accomplished.

At the end of the first stage of discharge break-down the transport properties of charged particles become important.

4. Transport properties of low Z-number species

The simplest models that illustrate the transport properties of hydrogen atoms and ions, electrons and impurity ions are the one-dimensional models [6] applicable to pure plasmas (hydrogen ions and electrons) to which have been added transport models [12] for atomic hydrogen and impurity ions. One-dimensional plasma diffusion codes [6] are used widely to model the temporal behaviour of plasma and poloidal magnetic field in axisymmetric, toroidal, plasma containment devices of the tokamak type (Figure 2). The theoretical models [13] incorporate averaging over the toroidal and poloidal co-ordinates with the result that the plasma-magnetic field configuration is described by a set of essentially conservative equations in the single spatial co-ordinate, r, the distance from the minor axis of the torus. The dependent variables typically represent the electron (or hydrogen ion) and impurity ion density, n_e and n_z, the electron and total ion pressure, p_e and p_i, and the poloidal component of the magnetic field, B_θ. The toroidal component of the magnetic field, B_ϕ, is considered to be sufficiently large to be unaffected by the plasma (low-β approximation) and only enters the calculation through its effect on the transport coefficients.

The model is completed by the specification of the radial particle and heat fluxes, the toroidal electric field and any additional source terms. In general, these expressions are complex functions of the dependent variables and theoretical models are often incompatible with experiment. For example, the predictions of neoclassical theory [6] (applicable to low density, high temperature discharges in a tokamak configuration) are that narrow, almost linear density profiles are coupled with much broader thermal distributions (Figure 6). These distributions are very different from those observed experimentally (Figure 7), which indicate that the energy balance is dominated by electron thermal conduction and recycling of particles rather than by ion thermal conduction and radiation as predicted numerically. It is necessary to introduce anomalous diffusion fluxes for the electrons so as to decrease the particle and electron energy confinement times. As a result, a species of recycled particles is necessary to maintain the particle content of the torus.

Detailed calculations of the effect of a neutral gas component have been performed by many authors [6,12] and take into account the production of hot

neutrals as a result of charge exchange with the background ion population. Particle codes can be used to follow the behaviour of neutral atoms and molecules. The particles are emitted from a boundary and are assumed to follow straight-line trajectories until they are annihilated or change their energy by ionisation and charge exchange processes. In this way the energy of neutral particles can cascade to higher values. A maximum upper limit to the number of permissible charge exchange neutrals is set by computer resources.

Simpler analytic models for the neutrals are sometimes used [14] to represent the diffusion of neutrals in a slab geometry according to exponential decay laws. For example, the neutrals can be separated into two species according to temperature: the cold neutrals with temperature less than 10 eV for which a penetration length, L_c, is assumed

$$L_c = \frac{V_{th,c}/\sqrt{3}}{n_e[\langle\sigma v\rangle_{CX} + \langle\sigma v\rangle_I]} \tag{2}$$

and a population of charge exchange neutrals which have the local ion temperature and for which a modified penetration length, L_h, is assumed

$$L_h = \left[\frac{\langle\sigma v\rangle_{CX}}{\langle\sigma v\rangle_I}\right]^{\frac{1}{2}} \frac{V_{th,h}/\sqrt{3}}{n_e[\langle\sigma v\rangle_{CX} + \langle\sigma v\rangle_I]} \tag{3}$$

These assumptions may be valid for future generation tokamak which would be impermeable to neutrals. In this model the essential features of the neutral particles are emphasised: the particle content is maintained, there exists a species of fast charge exchange neutrals which can sample the high temperature regions of the discharge and there exist energy loss mechanisms as a result of charge exchange, ionisation and line radiation following the excitation of neutral atoms.

With this model for the neutral particles and anomalous diffusion losses for the electrons, closer agreement with the experimental plasma profiles is obtained (Figure 8) [15].

5. Energy balance with high Z-number impurity species

Although it is possible to use a non-equilibrium method to study the energy balance of low Z-number impurities, an equilibrium model is necessary in practice to determine the mean state of ionisation and radiation properties of high Z-number impurities. A coronal model [16] based upon rate coefficients which balance collisional ionisation and dielectronic and radiative recombination [17] is used to determine the equilibrium properties of oxygen and iron. This model can be extended to incorporate the properties of other impurity ions, such as molybdenum and tungsten.

An important effect in the energy balance in the presence of high Z-number impurities involves the interaction of high energy neutral beams with impurity ions produced by wall sputtering. The formation of an impurity barrier near the wall of a large tokamak has been observed in numerical simulations [18] which use a number of different models for the plasma transport. This impurity barrier has a disastrous effect on the use of neutral beam injection as a mechanism for heating the plasma above temperatures obtained by ohmic heating methods.

In the case of energetic neutral particles required to heat future generation experiments to near fusion temperatures, the process of thermalisation of the fast ions produced on magnetic surfaces must be described by a Fokker-Planck model [4]. These models will obtain the correct spatial variation of plasma and magnetic field from magnetohydrodynamic or diffusion models of the plasma and will be able to describe the slowing-down process of fast ions.

However, the essential features of the impurity-beam instability are exhibited by a simple model for the deposition profile of the beam particles. Provided that the energies of the fast neutrals are sufficiently high $E_f > 2 \times 10^4 A_f$ eV (where A_f is the atomic mass of the fast neutrals), the number $n_f(r,t)drdt$ of fast neutrals that are deposited in the radial interval $r \to r + dr$ and the time interval $t \to t + dt$ is given by [19].

$$n_f(r,t) = \left[\frac{I_f}{q_f L} n_e(r)\right]\left[\exp\left\{\int_0^{x=r} \frac{n_e}{L}(x)dx\right\} + \exp\left\{-\int_0^{x=r} \frac{n_e}{L}(x)dx\right\}\right]\exp\left\{-\int_0^{x=a} \frac{n_e}{L}(x)dx\right\} \quad (4)$$

where I_f and q_f are respectively the neutral beam equivalent current and charge, and n_e is the electron number density. For sufficiently high energies the penetration "length" [20]:

$$L = 5.5 \times 10^{14} \frac{E_f}{A_f} \frac{\sin\delta}{Z_{eff}(r)} \quad \left[m^{-2}\right] \quad (5)$$

is a measure of the penetration of the beam and is affected by the effective charge, Z_{eff}, and the angle, δ, at which the beam is inclined to the magnetic field. The penetration length, L, is an approximation to the inverse cross-section for beam capture, given more precisely [21]

$$L^{-1} \approx \langle\sigma_{Total}\rangle = \frac{\langle\sigma_I V_e\rangle}{V} + \frac{n_i}{n_e}\langle\sigma_{CX}\rangle + Z_{eff}\langle\sigma_P\rangle \quad (6)$$

$\langle\sigma_{Total}\rangle$ is a function of the cross-sections for hydrogen ionisation by electrons $\langle\sigma_I\rangle$ and protons $\langle\sigma_p\rangle$ and charge exchange, $\langle\sigma_{CX}\rangle$. The proton ionisation curve has been increased by a factor Z_{eff} to account for the impact of the beam on impurity ions (Figure 9) [22]. V_e and V are respectively the electron thermal and beam speeds.

A simple model [20] for the birth profile, S(r,t) of slow ions that result from ionisation and instantaneous slowing down of the fast beam particles and the appropriation of the fractions of the beam energy to the electrons (f_e) and the ions (f_i) is also used.

$$S(r,t) = \frac{n_f(r,t)}{4\pi^2 r R}$$

$$f_i = \left[1 + 0.34X^{1.2}\right]^{-1}, \quad f_e = 1 - f_i \quad (7)$$

$$X = \left[\frac{A_i^{2/3}}{14.6A_f}\right]\frac{E_f}{T_e}$$

(R is the major radius of the torus and A_i is the atomic mass of the plasma ions).

The results of these calculations will be dependent on the surface phenomena occurring on the limiter and the vacuum chamber walls. In general, the boundary represents the sources for recycled particles of all kinds: hydrogen atoms and molecules to fuel the discharge and impurity ions which can terminate the discharge. Both cold neutral particles and impurity ions absorbed on the walls can be emitted by an efflux of plasma and impurity ions, neutral particles and, perhaps, photons. Four mechanisms for the influx of recycled particles may be visualised. Energetic atoms can be created as a result of back scattering from lattice atoms. Low energy neutral molecules will diffuse from the surface with energies characteristic of the surface. Layers of absorbed gas may be desorbed by energetic neutrals. Impurity ions may be sputtered as a result of surface bombardment by energetic neutrals and ions.

The models for this behaviour that are actually used in simulation codes are much simpler. For example, in the case of the break-down calculations cold hydrogen is recycled for all loss processes. In the case of transport calculations, impurity sputtering is also considered. The data used for the sputtering coefficients is often a fit to experimental results [23]. Uncertainty in the experimental results at low energies requires an extrapolation of the curve to the theoretical energy below which sputtering does not occur (Figure 10).

This model exhibits the greater attenuation experienced by high energy neutral beams injected into an impure plasma. These beams are stopped in the edge layer and give further sputtering, so increasing the barrier. The final result is a radiation cooled plasma rather than one that is beam heated (Figure 11).

The beam-impurity instability may be eliminated by using smaller values of the sputtering coefficients (so as to simulate a honeycomb wall structure) so that the influx of impurity ions is greatly reduced. An alternative solution has been proposed [24] which produces a hot central core of plasma isolated from the outer wall (or limiter) by a warm plasma ($\sim$ 20 - 50 eV). The warm blanket is sufficiently cold to prevent sputtering of impurities by plasma ions (threshold for sputtering $\sim$ 60 eV for stainless steel) and yet sufficiently hot to ionise an appreciable fraction of the incoming neutral particles. This solution is based upon the possibility that a stable mode of operation could be achieved with a balance between the ohmic input power ($\sigma E^2 \sim T_e^{3/2}$) and the radiation losses (Figure 12). This is not possible if the classical model for radiation were to be used [25].

The plasma is separated into two regions by virtue of the radiation model having a maximum at an electron temperature, T_1 ($\sim$ 100 eV for iron and 20 eV for oxygen). The central hot core is ohmically heated to above the temperature, T_1, when the impurities affect the energy balance to a lesser extent, and an outer warm region is established in which a balance between the ohmic input and the radiation losses is achieved (Figure 13).

Unfortunately, the configuration achieved is unstable, with the hot central core showing a great affinity to carry more current. The outer edge is cooled further by radiation losses until the temperature is so low ($\lesssim$ 20 eV) that little ionisation of recycled neutrals occurs and many charge exchange neutrals are created. These neutrals can sample the hot central core and produce increased sputtering. (This effect would also be observed if the temperature profile had been modified by means of cold

gas injection to cool the outer edge).

However, a more stable situation may be achieved by enhancement of the diffusion of energy from the hot central core (to simulate anomalous processes that may occur when large temperature gradients are established) or by heating the outer edge regions with low energy neutral beams (Figure 13).

6. Summary

Numerical simulations of the break-down and evolutionary stages of tokamak discharges indicate the complex interaction that exists between the transport properties of ionised gases and the atomic and molecular processes. It is necessary to improve the transport models for all particle species. Additionally, it is necessary to improve the model for the atomic and molecular processes to include increased accuracy in:

(a) radiation losses for low Z-number particles at low temperatures ($T_e \lesssim 10$ eV),
(b) radiation losses for intermediate to high Z-number particles for all temperatures (C,O,F$_e$,M$_o$,W),
(c) the trapping of neutral injection beams in impure plasmas,
(d) the recycling conditions of all particles (and also, perhaps, radiation) from the limiter and wall.

Preliminary data associated with theoretical models for (a),(b) and (c) above is available and should be ratified by experiment if possible to an accuracy of 10%. The boundary conditions associated with the recycling of atoms, molecules and ions are of paramount importance to both the build-up and evolutionary stages of the discharge. It is essential that greatly improved models be developed to describe the phenomena occurring at the surface of limiters and walls.

Acknowledgements

The author would like to acknowledge valuable discussions with many of his colleagues especially, J A Reynolds, A Gibson, D Marty and B J Green.

References

[1] GRIMM, R.C., et al., "Computations of the Magnetohydrodynamic Spectrum in Axisymmetric Confinement Systems" in Methods in Computational Physics, Vol. 16 (KILLEEN, J., et al., Eds), Academic Press, New York (1976).
[2] SYKES, A., WESSON, J.A., Nucl. Fus. 14 (1974) 645.
[3] NIELSON, C.W., "Particle Code Models for the Vlasov Equation" in Methods in Computational Physics, Vol. 16 (KILLEEN, J., et al., Eds), Academic Press, New York (1976).
[4] KILLEEN, J., et al., "The Solution of the Kinetic Equations for a Multispecies Plasma", in Methods in Computational Physics, Vol. 16 (KILLEEN, J., et al., Eds), Academic Press, New York (1976).
[5] ROBERTS, K.V., POTTER, D.E., "Magnetohydrodynamic Calculations", Ch. 9, Methods in Computational Physics, Vol. 9 (ALDER, B., et al., Eds), Academic Press, New York (1970).
[6] DNESTROVSKII, Y.N., et al., 4th Europ. Conf. Contr. Fus. Plasma Physics (Proc. Conf. Rome, 1970) 1 (1970) 17.
DORY, R.A., WIDNER, M.M., Bull. Am. Phys. Soc. Ser. II, No. 11 (1970) 1418.
DÜCHS, D.F., Bull. Am. Phys. Soc. Ser. II, No. 11 (1970) 1488.
DÜCHS, D.F., et al., 4th Int. Conf. Plasma Physics Contr. Nucl. Fus. Res. (Proc. Conf. Madison, 1971) 1 (1971) 369.
HOGAN, J.T., et al., Phys. Rev. Lett. 36A, 3 (1971) 217.

KEEPING, P.M., et al., 5th Europ. Conf. Contr. Fus. Plasma Physics (Proc. Conf. Grenoble, 1972) 1 (1972) 38.
WATKINS, M.L., et al., "ICARUS - A One-Dimensional Plasma Diffusion Code", in Methods in Computational Physics, Vol. 16 (KILLEEN, J., et al., Eds), Academic Press, New York (1976).
[7] GIRARD, J.P., Fontenay-aux-Roses Rep. EUR-CEA-FC 538 (1970).
HAWRYLUK, R.J., SCHMIDT, J.A., Princeton Plasma Physics Laboratory Rep. MATT-1201 (1976).
JET Design Phase Rep. EUR-JET R8 (To be published) (1976).
[8] KADOMTSEV, B.B., POGUTSE, O.P., Nucl. Fus. 11 (1971) 67.
[9] DIMOCK, D., et al., 4th Int. Conf. Plasma Physics Contr. Nucl. Fus. Res. (Proc. Conf. Madison, 1971) 1 (1971) 451.
[10] The JET Project Design Proposal, Rep. EUR-JET R5 (Report EUR 5516e) (1975).
[11] MEADE, D.M., Nucl. Fus. 14 (1974) 289.
[12] GREENSPAN, E., Nucl. Fus. 14 (1974) 771.
PARSONS, C., MEDLEY, S., Plasma Phys. 16 (1974) 267.
HOGAN, J.T., "Multifluid Tokamak Transport Models" in Methods in Computational Physics, Vol. 16 (KILLEEN, J., et al., Eds), Academic Press, New York (1976).
[13] HAZELTINE, R.D., et al., Phys. Fluids 16 (1973) 1645.
[14] PODESTA, G., ENGELMANN, F., 3rd Int. Symp. Toroidal Plasma Confinement (Proc. Conf. Garching, 1973) (1973) C9.
[15] WATKINS, M.L., Bull. Am. Phys. Soc. Ser. II, 20 (10) (1975) 1329.
[16] BRETON, C., et al., Fontenay-aux-Roses Rep. EUR-CEA-FC-822 (1976).
[17] SUMMERS, H.P., Appleton Laboratory Rep. IM 367 (1974).
[18] CONN, R.W., et al., University of Wisconsin Rep. UWFDM-136 (1975).
HOGAN, J., HOWE, H.C., Bull. Am. Phys. Soc. Ser. II, 20 (10) (1975) 1228.
POST, D.E., et al., Bull. Am. Phys. Soc., Ser. II, 20 (10) (1975) 1346.
The JET Project Design Proposal Rep. EUR-JET R5 (Rep. EUR 5516e) (1975).
[19] RIVIERE, A.C., Nucl. Fus. 11 (1971) 363.
[20] SWEETMAN, D.R., Nucl. Fus. 13 (1973) 157.
[21] EQUIPE TFR, 3rd Int. Mtg. on Heating Tor. Plasmas (Proc. Conf. Grenoble, 1976) (To be published) (1976).
[22] MORIETTE, P., 7th Symp. Phys. Ionised Gases (Proc. Conf. Rovinj, 1974)(1974) 43.
FREEMAN, R.L., JONES, E.M., Culham Laboratory Rep. CLM-R 137 (1974).
[23] BEHRISCH, R., Nucl. Fus. 12 (1972) 695.
HOTSTON, E.S., McCRACKEN, G.M., Private Communication (1976).
[24] GIBSON, A., et al., Bull. Am. Phys. Soc. (To be published) (1976).
[25] MOSHER, D., Naval Research Laboratory Rep. NRL-MR-2563 (1973).

TABLE I

Computer models for plasma simulations

1. Vlasov and Particle models.
2. Fokker-Planck models
3. Time-dependent models
   (a) Magnetohydrodynamic approximation - fast timescales
   (b) Diffusion approximation - slow timescales
   (c) Rate models for atomic and molecular processes
4. Time-independent models
   (a) Equilibrium
   (b) Stability
   (c) Steady state radiation models for atomic and molecular processes
5. Hybrid models

TABLE II

Present generation tokamak (ST)

Major Radius	1.09 m
Minor Radius	0.14 m
Toroidal field	3.7 T
Toroidal current	60 kA
Typical mean electron density	2×10^{19} m^{-3}
Typical mean electron temperature	0.76 keV
Timescale	$\lesssim$ 100 ms

TABLE III

Future generation tokamak (JET)

Major Radius	2.93 m
Minor Radius	1.28 m
Toroidal field	3 T
Toroidal current	3 MA
Typical mean electron density	5×10^{19}
Typical mean electron temperature	$\gtrsim$ 2 keV
Timescale	$\gtrsim$ 1 s

TABLE IV

Atomic and molecular physics reactions used in break-down models

Dissociation of H_2^+

$$H_2^+ + e^- \rightarrow H^+ + H^o + e^-$$
$$H_2^+ + e^- \rightarrow 2H^+ + 2e^-$$

Atomic Ionisation

$$H^o + e^- \rightarrow H^+ + 2e^-$$

Molecular Ionisation

$$H_2^o + e^- \rightarrow H_2^+ + 2e^-$$

Recombination

$$H_2^+ + e^- \rightarrow H_2^o \rightarrow 2H^o$$

Molecular Dissociation

$$H_2^o + e^- \rightarrow 2H^o + e^-$$

Charge Exchange

$$H^o + \bar{H}^+ \rightarrow \bar{H}^o + H^+$$

Excitation

$$H_2^o + e^- \rightarrow H_2^{o(*)} + e^-$$
$$H_2^+ + e^- \rightarrow H_2^{+(*)} + e^- \rightarrow H^+ + H^o + e^-$$
$$H^o + e^- \rightarrow H^{o(*)} + e^-$$

(-) represents a fast particle

(*) represents an excited state

Figure Captions

Figure 1 Atomic and Molecular Data for plasma simulations.

Figure 2 Schematic diagram of tokamak torus.

Figure 3 Schematic diagram of domain of interest for plasma build-up calculations.

Figure 4 Energy balance during plasma build-up in a large tokamak (3×10^{-4} Torr H^o).

Figure 5 Energy balance during plasma build-up in a large tokamak (3×10^{-4} Torr H^o + 5% oxygen).

Figure 6 Radial profiles of particle density, n, electron temperature, T_e, and ion temperature, T_i, for conditions applicable to a low density discharge in a small tokamak (ST) at 60 ms as given by the code, ICARUS (-), and that of Düchs (+,0,Δ), using the neoclassical diffusion model [6].

Figure 7 Radial profiles of particle density, n, electron temperature, T_e, and ion temperature, T_i, for conditions applicable to a high density discharge in a small tokamak (ST) at 35 ms [9].

Figure 8 Radial profiles of particle density, n, electron temperature, T_e, and ion temperature, T_i, for conditions applicable to a high density discharge in a small tokamak (ST) at 35 ms using the code ICARUS, anomalous electron losses (200 x Pfirsch-Schlüter) and a simple neutral recycling model [14].

Figure 9 Cross-section for the capture of a neutral beam with energy E_f/A_f (eV) as given by
(a) Equation (6) with $n_i/n_e = 0.5$, $Z_{eff} = 4$ [21,22]
(b) Equation (5) with $Z^i_{eff} = 1$ [20]
(c) Equation (5) with $Z_{eff} = 4$ [20].

Figure 10 Sputtering yield of 304 SS by H^+ ions (Atoms released per incident ion) as a function of the energy of the incident ion.

Figure 11 Temporal variation of the spatially averaged electron temperature in a large tokamak with (a) anomalous electron losses (10 x Pseudoclassical) and (b) additional neutral beam heating (4 MW, 70 keV beam from 0.5s).

Figure 12 Impurity radiation losses for ion as given by models of Mosher [25] and Breton et al [16]. The Ohmic input at constant electric field ($\sigma E^2 \sim T_e^{3/2}$) is also indicated.

Figure 13 Radial profiles of the electron temperature for conditions applicable to a large tokamak with (a) anomalous electron losses (10 x Pseudoclassical), (b) additional enhancement of electron thermal conductivity in regions of large ∇T_e and (c) additional neutral beam heating (4 MW, 25 keV beam).

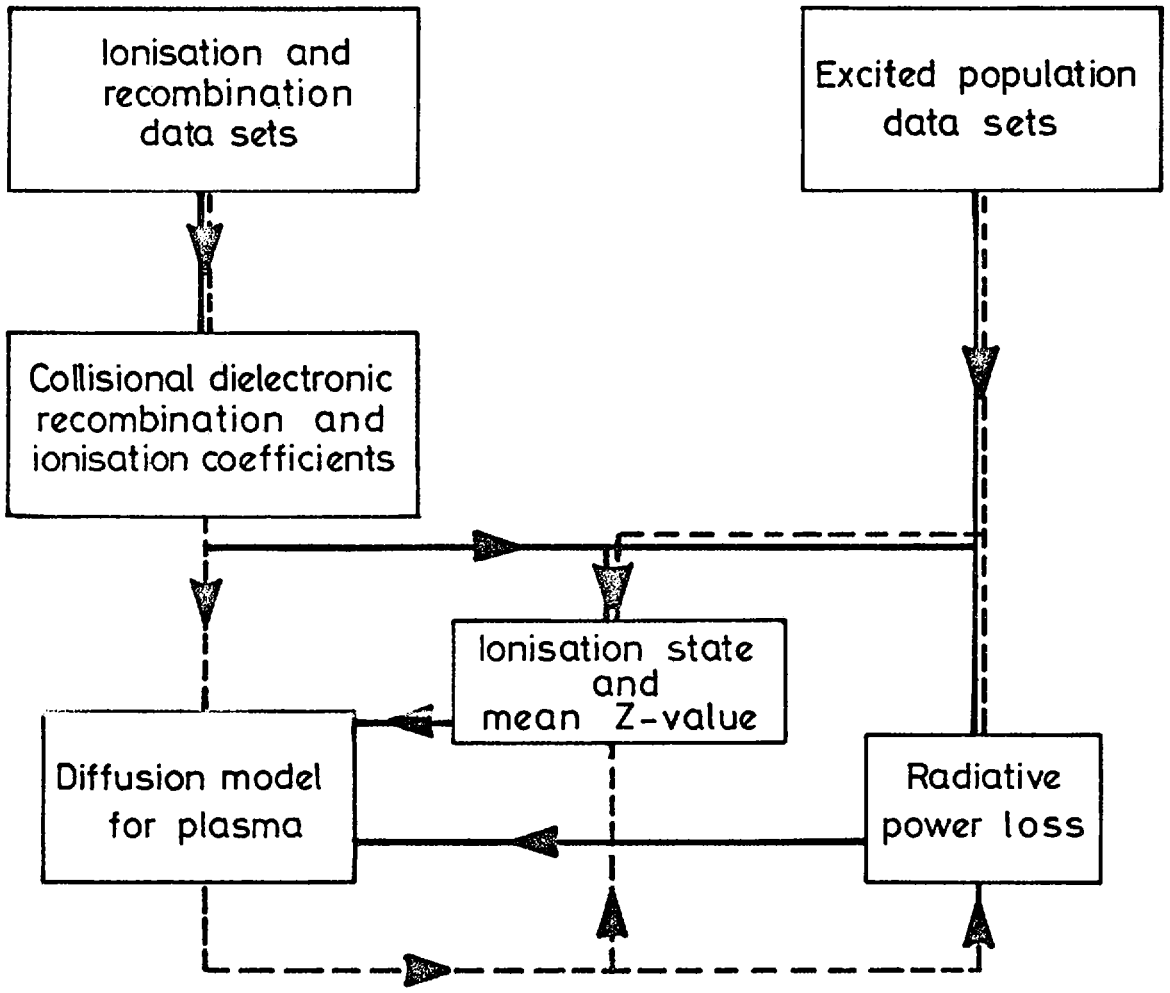
Ionisation and recombination data sets
Excited population data sets
Collisional dielectronic recombination and ionisation coefficients
Ionisation state and mean Z-value
Diffusion model for plasma
Radiative power loss
Equilibrium model for atomic and molecular processes
Non-equilibrium model for atomic and molecular processes

Figure 1

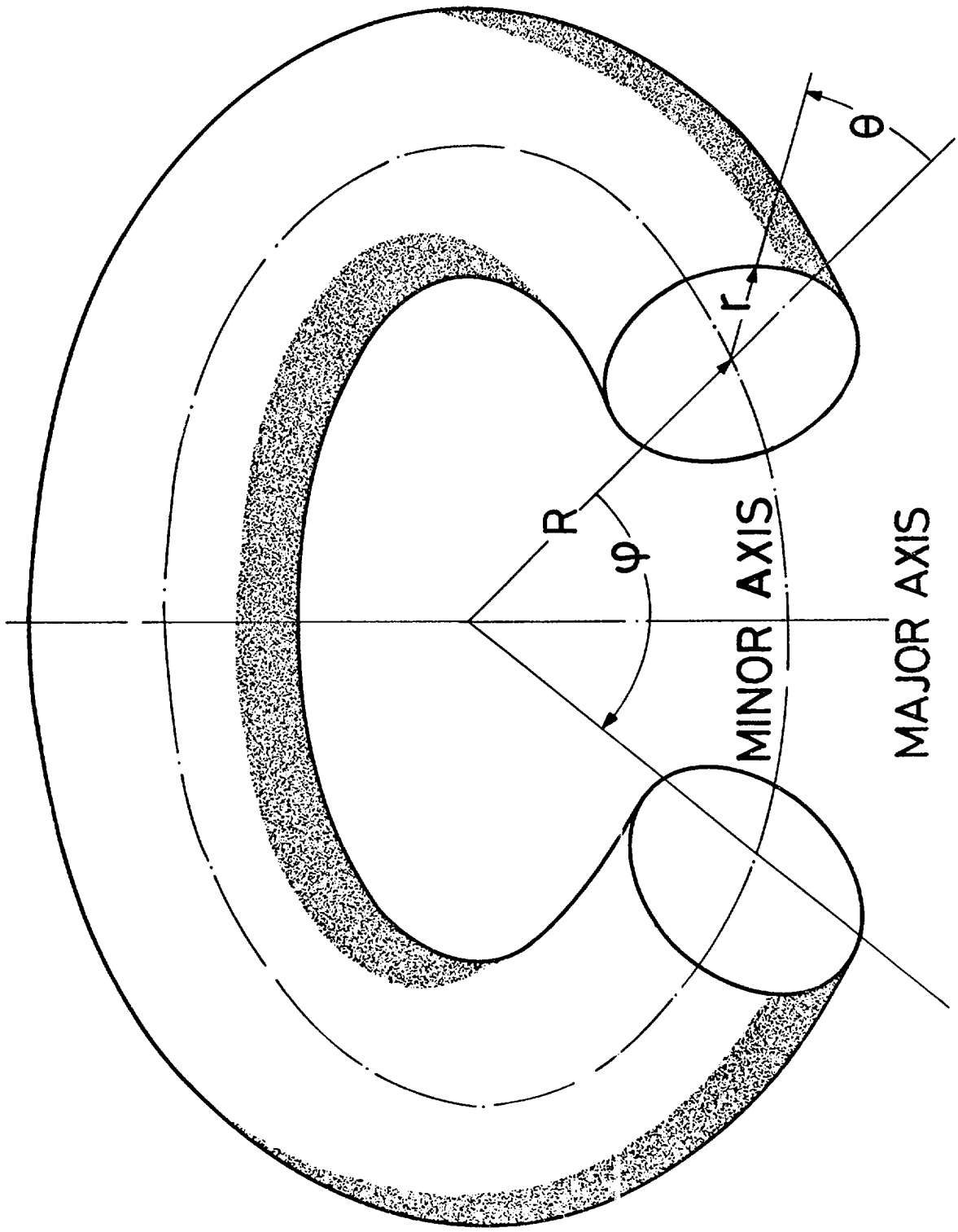

Figure 2

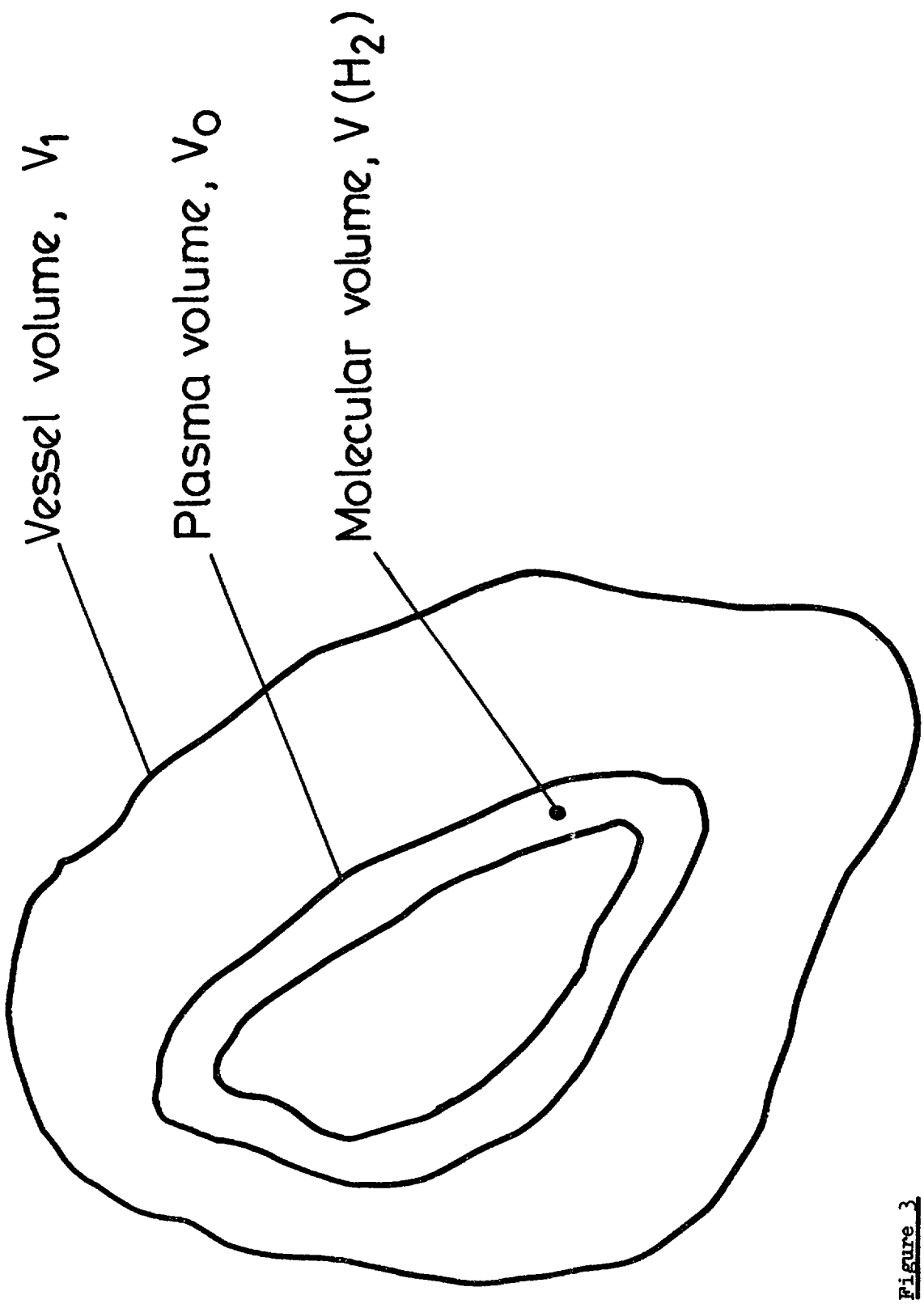

Figure 3

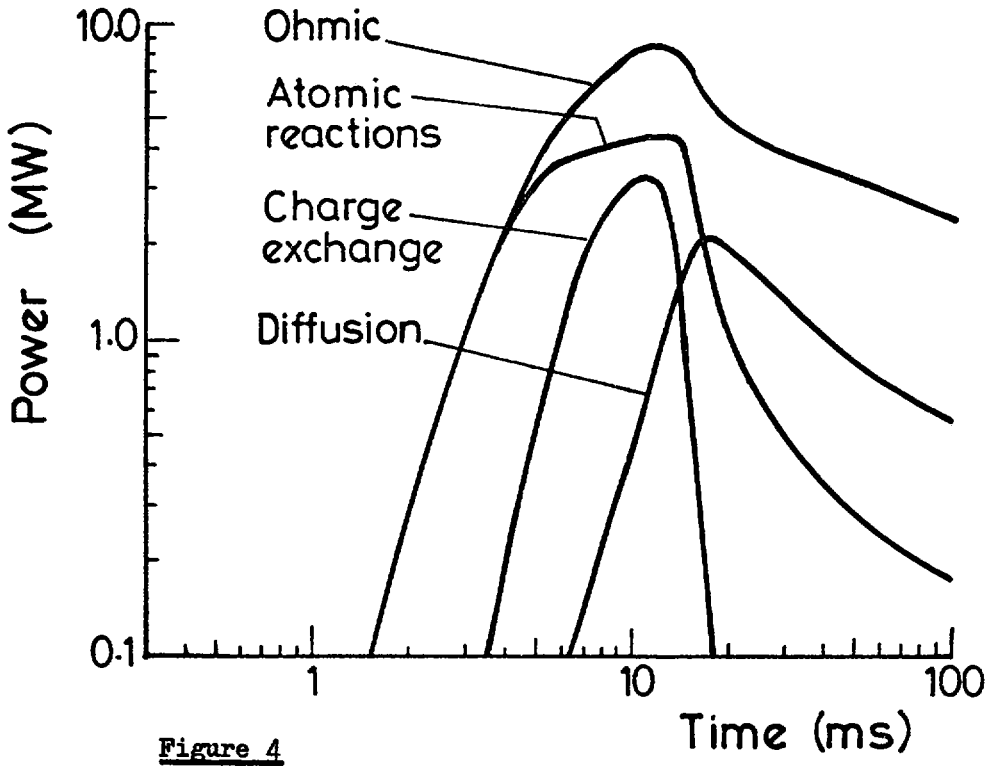

Figure 4

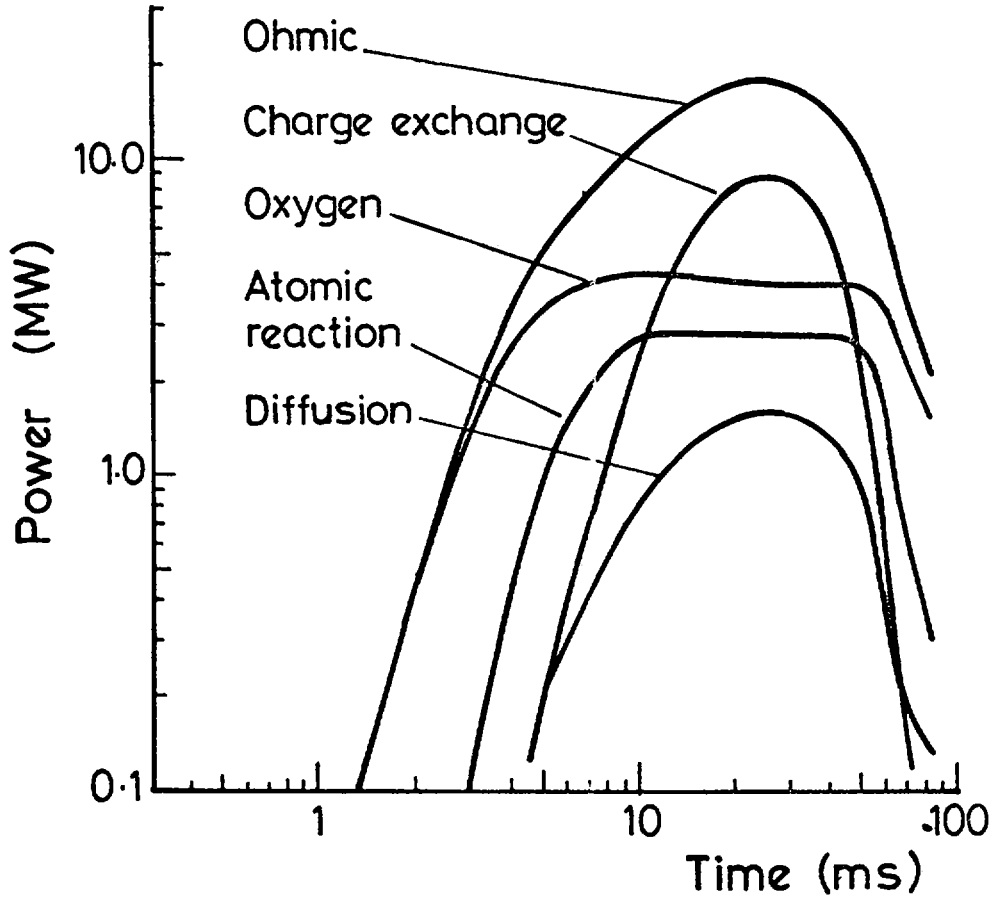

Figure 5

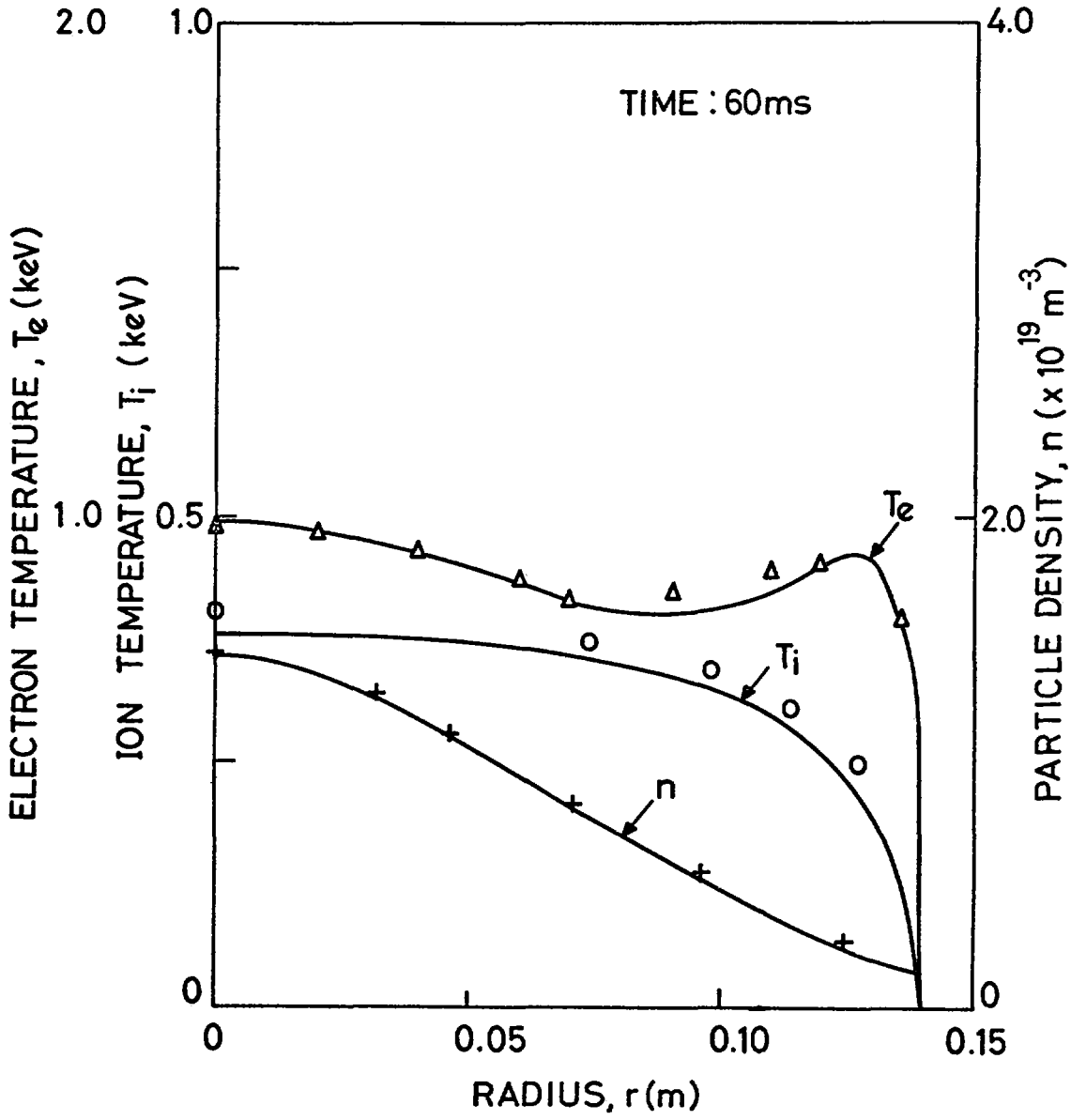
TIME : 60ms
ELECTRON TEMPERATURE , T_e (keV)
ION TEMPERATURE, T_i (keV)
PARTICLE DENSITY, n ($\times 10^{19}$ m^{-3})
RADIUS, r (m)
Te
Ti
n
2.0
1.0
0
0.5
1.0
4.0
2.0
0
0.05
0.10
0.15

Figure 6

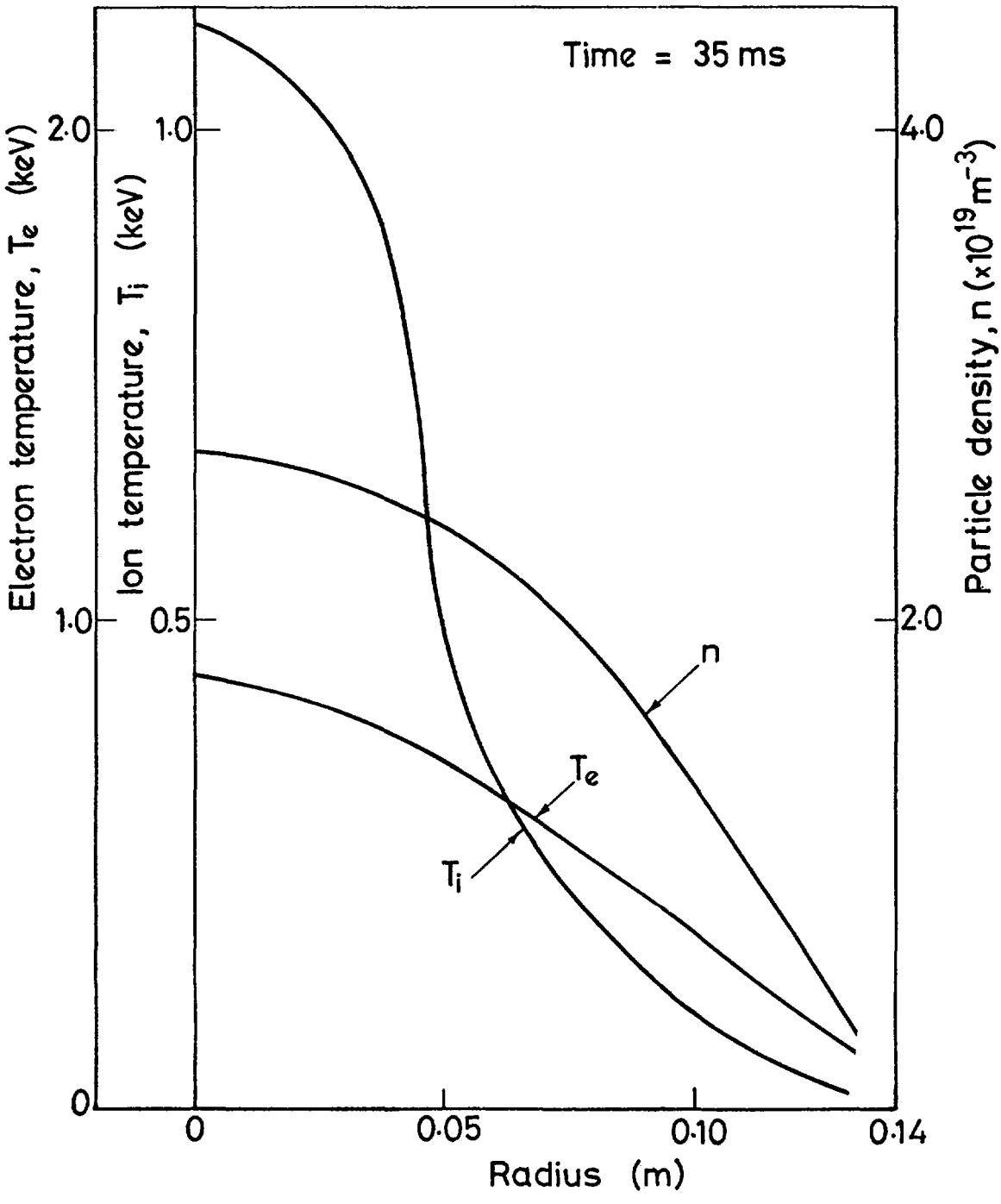
Time = 35 ms
Electron temperature, T_e (keV)
Ion temperature, T_i (keV)
Particle density, n ($\times 10^{19}$ m^{-3})
2·0
1·0
0
1·0
0·5
4·0
2·0
n
T_e
T_i
0
0·05
0·10
0·14
Radius (m)

Figure 7

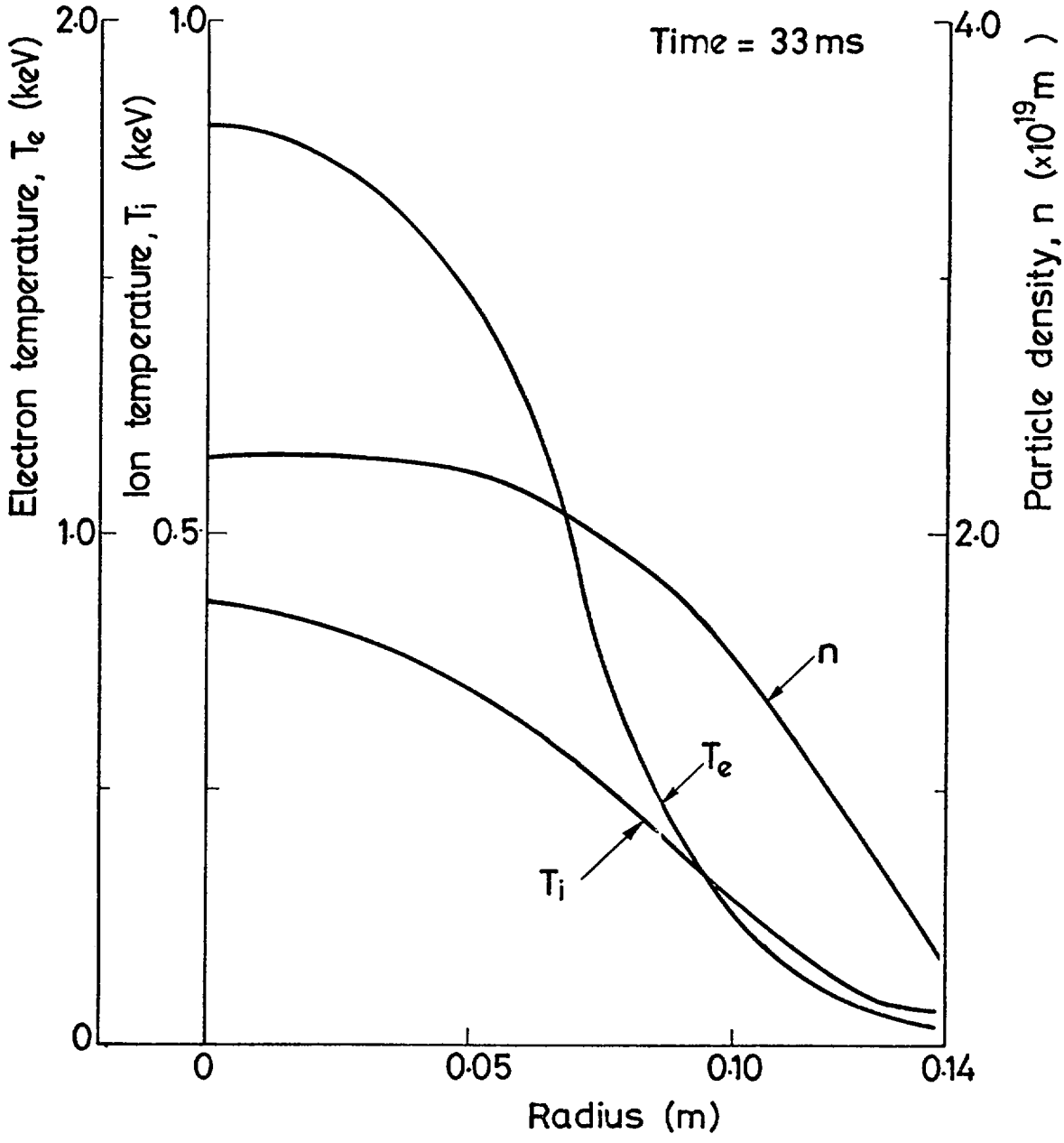
Time = 33 ms
Electron temperature, T_e (keV)
Ion temperature, T_i (keV)
Particle density, n ($\times 10^{19}$m^{-3})
2·0
1·0
0
1·0
0·5
4·0
2·0
n
T_e
T_i
0
0·05
0·10
0·14
Radius (m)

Figure 8

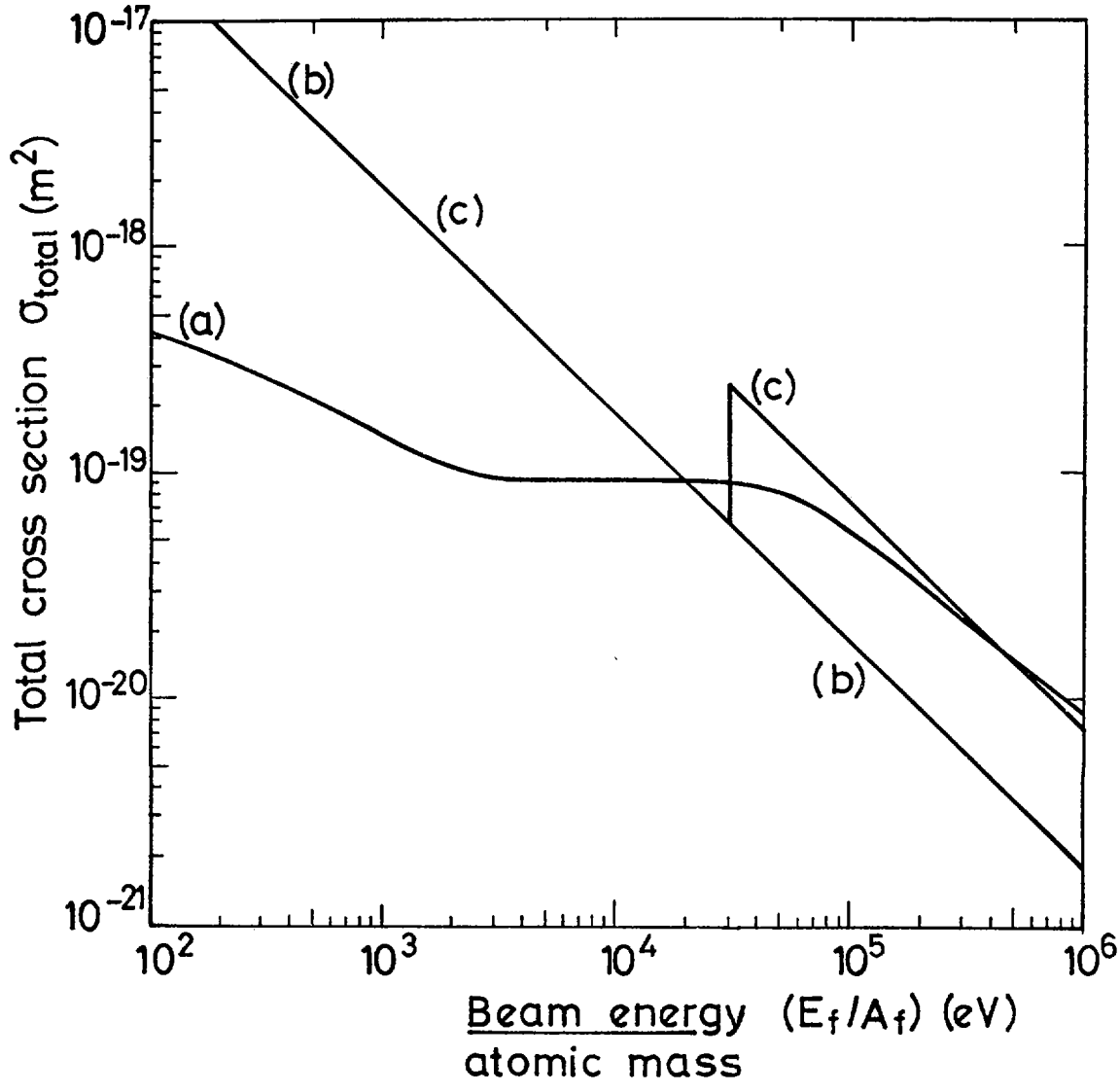
Total cross section σ_{total} (m^2)
10^{-17}
10^{-18}
10^{-19}
10^{-20}
10^{-21}
(a)
(b)
(c)
(c)
(b)
10^2
10^3
10^4
10^5
10^6
Beam energy (E_f/A_f) (eV)
atomic mass

Figure 9

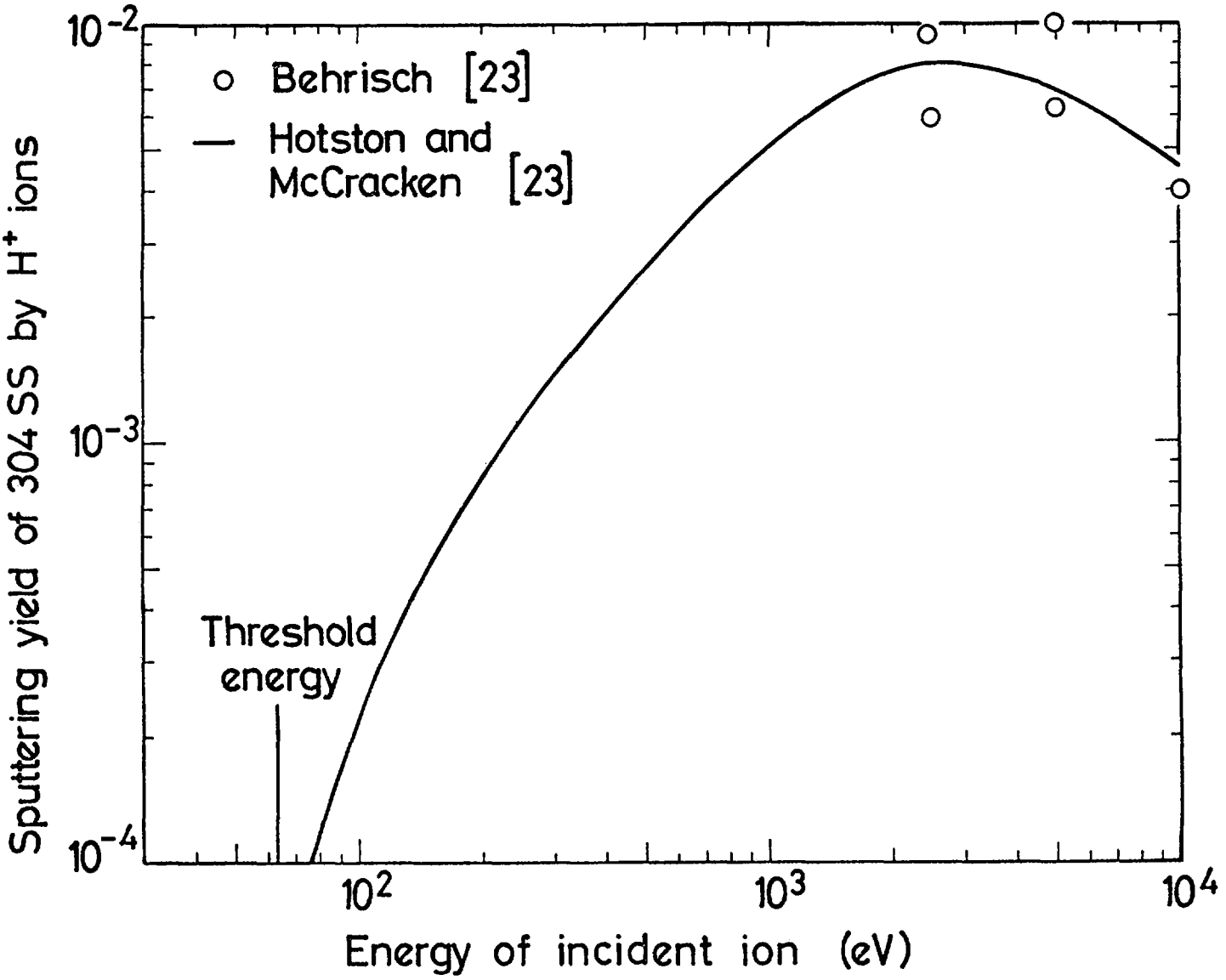
Behrisch [23]
Hotston and McCracken [23]
Threshold energy
Sputtering yield of 304 SS by H+ ions
Energy of incident ion (eV)
10-2
10-3
10-4
10²
10³
10⁴

Figure 10

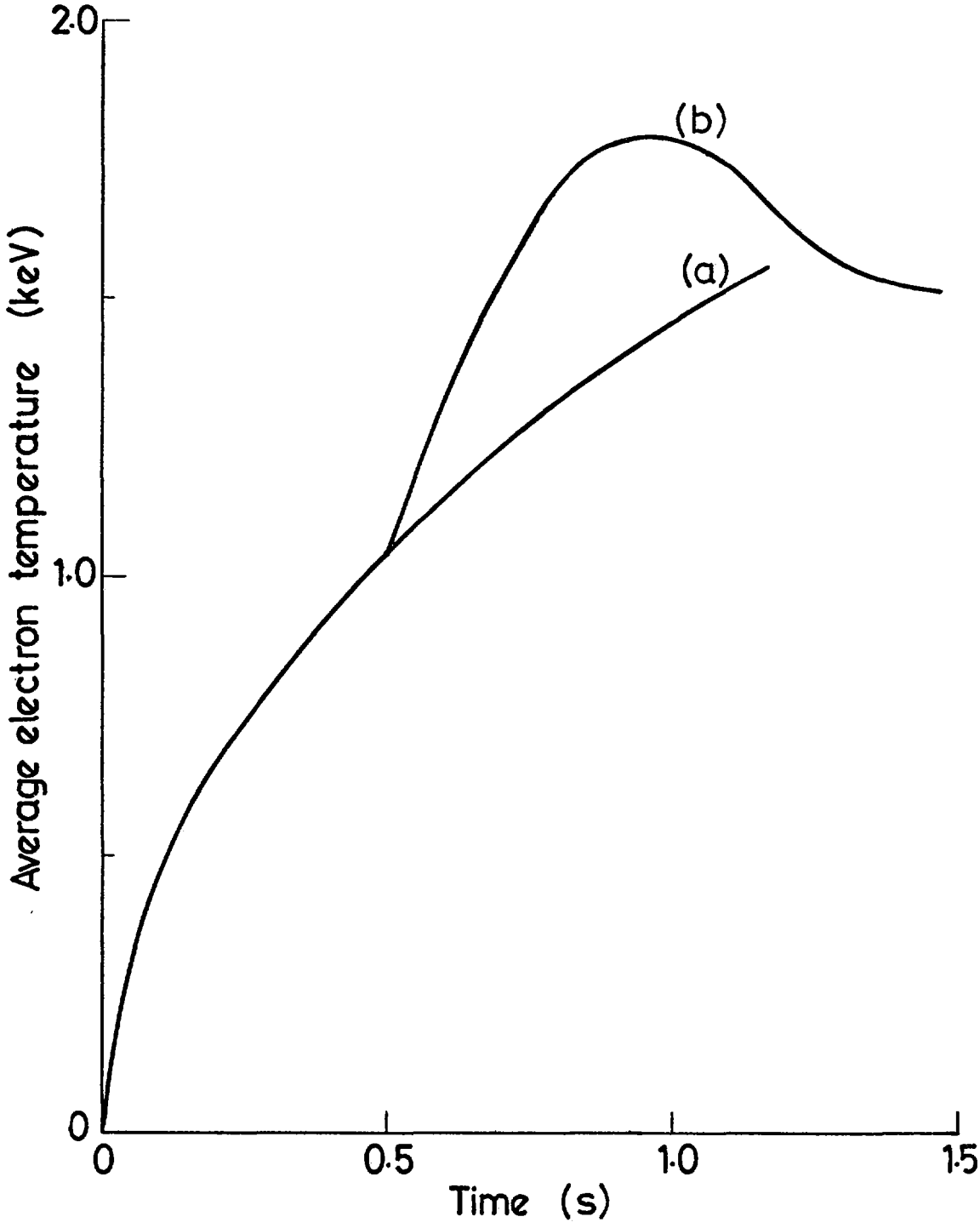

Figure 11

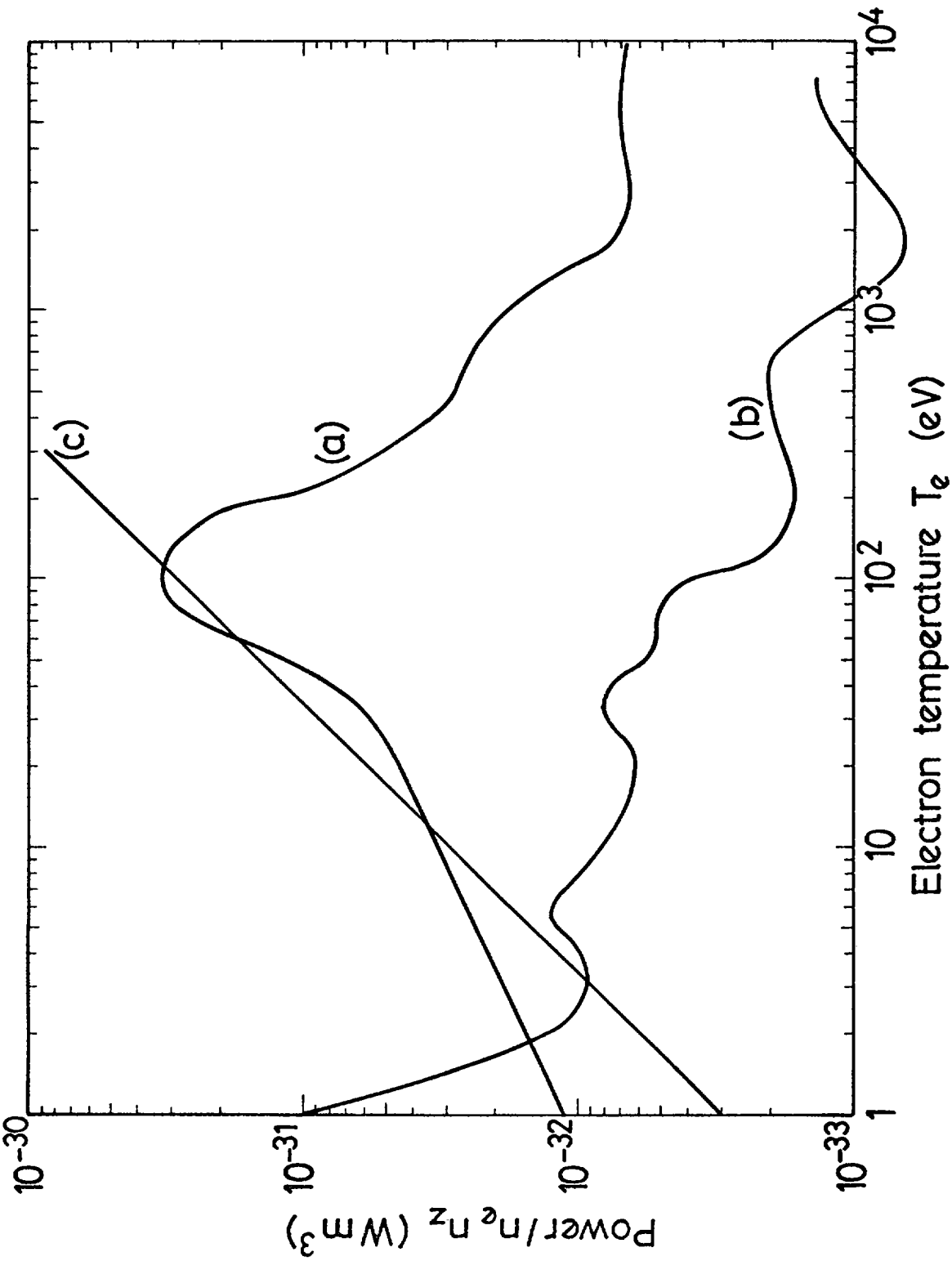
Power/n_e n_z ($W m^3$)
10^{-30}
10^{-31}
10^{-32}
10^{-33}
1
10
10^2
10^3
10^4
Electron temperature T_e (eV)
(a)
(b)
(c)

Figure 12

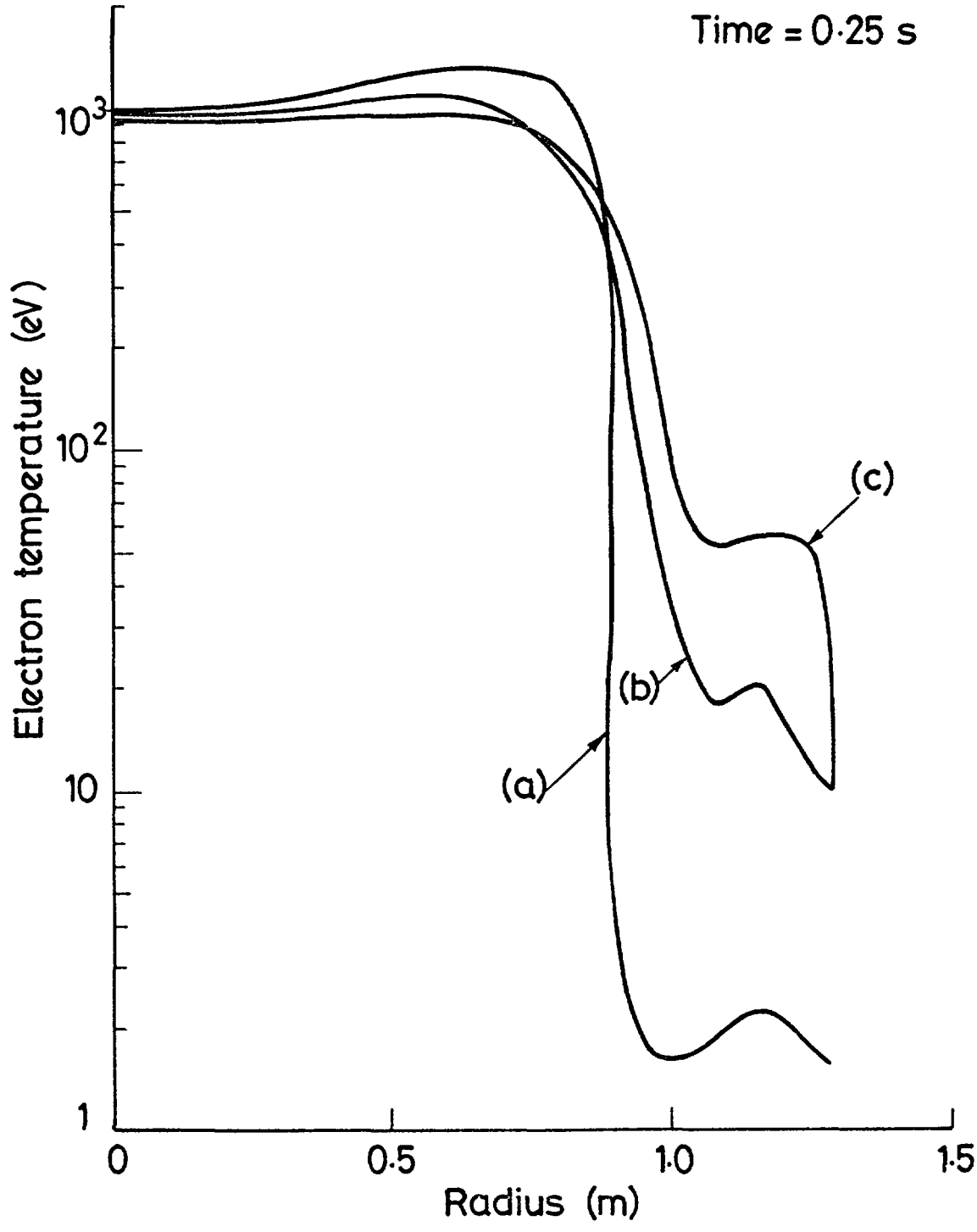
Time = 0·25 s
Electron temperature (eV)
10³
10²
10
1
0
0·5
1·0
1·5
Radius (m)
(a)
(b)
(c)

Figure 13

PLASMA IMPURITIES AND COOLING

DRAWIN H.W.

ABSTRACT

In high-temperature low-density plasmas radiation cooling by impurity atoms can be an important energy loss mechanism, since the radiation is not reabsorbed. In a brief historical survey it is shown that the problem is not new but was discussed since the first beginning of controlled thermonuclear fusion research.It is then shown how radiation losses enter into the general power balance equation of a plasma containing impurities. The equations for the different types of radiation losses are given as a function of the atomic quantities. In a special section simplifications due to the corona model assumption are discussed. It follows a detailed survey of the results obtained by several authors for the ionization balance and power losses of impurity elements observed in present high-temperature plasma machines used in CTR, especially in TOKAMAKS. In the conclusion a survey is given of the atomic datae which experimentalists and theorists need for current research on impurities in fusion-like plasmas.

1. HISTORICAL

Since the first beginning of controlled thermonuclear fusion research, plasma impurities and radiation cooling have played an important role in the overall energy balance of the created high-temperature plasmas. It has in fact very early been recognized that the impurity problem must be solved satisfactorily in "fusion-like" plasmas when one wants to achieve controlled thermonuclear fusion in a true fusion device. Energy loss due to radiation cooling is not a recent discovery, however, it becomes now much more serious, since present plasma machines yield such high plasma temperatures that the enhanced energy loss by highly stripped impurity atoms may become one of the dominant loss mechanism. Before discussing the atomic physics as far as radiation cooling is concerned it may be instructive to give a brief historical review in order to show how the impurity problem has evolved during the past.

The probably first mentioning of the energy loss due to impurity ions in a fusion device is by POST [1]. In connection with the calculation of the power P_b radiated by bremsstrahlung (p. 344 in [1]) he concludes : "Because "of the Z^2 dependence of P_b, it is apparent that the presence of even a "small amount of ionized high-Z elements could greatly increase the radiated "power density. It follows that high purity is a prime requirement for the "plasma of a fusion reactor. For this and other reasons utmost attention "must be paid to the role of the material walls of the reactor in introducing "impurities through bombardment and heating effects which might otherwise be "considered unimportant". In Post's article nothing is said about line radiation and magnetic radiation, both obviously assumed to be unimportant at that time.

It is worth mentioning that the LAWSON criterion [2] formulated in 1957 is based on the sole assumption that the nuclear reaction power (multiplied by an efficiency coefficient η) must be balanced by the power losses due to plasma diffusion and bremsstrahlung of a clean D-D or D-T plasma. Admitting impurities which significantly contribute to the general energy loss will change the LAWSON criterion for both the temperature and the value of $n\tau$ (n being the plasma particle density and τ the particle confinement time).

In his talk "peaceful uses of fusion" given at the Geneva conference in 1958, E. TELLER [3] discussed the difficulties encountered in obtaining

a fusion plasma. He said : "Another difficulty that is quite generally en-
"countered is connected with impurities. The presence of impurities leads to
"increased bremsstrahlung radiation and the consequent rapid loss of energy
"from the plasma. At temperatures low compared with ignition temperature, these
"losses are often aggravated by radiation from incompletely ionized atoms.
"These partially ionized systems are usually not in Saha equilibrium, since
"of the four possible processes, collisional ionization, radiative electron
"capture, recombination by triple collisions and ionization by photons, only
"the first two occur. This somewhat involved problem... has led to the reco-
"gnition that heating must be carried out rapidly, particularly in the low
"temperature regions. If neutral atoms are knocked off the walls, these cause
"an energy loss by an additional mechanism : They can neutralize fast plasma
"ions by charge exchange and these fast neutral particles can cross the
"magnetic barrier and reach the wall. Here they can knock out more neutral
"particles and a loss mechanism can be built up".

TELLER's talk gives the first indication that (line) radiation of incompletely stripped atoms may lead to additional radiation losses and that plasma-wall interaction is the key problem of the impurity level in a plasma. If one particle knocks off more than one wall atom, contamination will occur exponentially with time. No such effect has still been observed, except in certain cases in which fast H-atoms liberate adsorbed and absorbed H-atoms which led to a rapid increase of plasma density.

In the ZETA machine also described at the Geneva conference highly ionized C,N,O and probably Al impurities have been detected (BUTT et al.[4]). THOMPSON [5] commented these results in the following manner ; "In the tem-
"perature estimates made so far, we have considered the radiation loss by
"unionized deterium, but have made no allowance for the energy loss by brems-
"strahlung and by radiation from impurities present. The first of these is
"negligible,..., but the second is more serious". It follows a quantitative estimate of the radiation losses which leads to the conclusion : "Hence,
"if the concentration of aluminium rises much above 1% it constitutes a
"serious source of energy". In THOMPSON's paper the importance of energy due to line radiation of impurities is now fully recognized.

Impurity radiation is not only important relative to radiation cooling. Line radiation from impurities represents a diagnostic tool which has since the very beginning of thermonuclear research successfully been applied

in order to determine temperature and/or densities and to observe the macroscopic stability behavior of plasmas. In this context may be mentioned the papers by TUCK [6], GOLOVIN et al. [7], DOLGOV-SAVELIEV et al. [8], AYMAR et al.,[9] , ANDREOLETTI et al.[10], HARDING et al, [11], LUKYANOV and SINITSIN [12], SPITZER [13], BURNETT et al.[14].

The first quantitative treatment of the energy loss due to the radiation of impurities in a high-temperature hydrogen plasma is due to KNORR [15] who calculated the relaxation times of highly ionized impurities to reach a stationary state population and the power radiated by oxygen and calcium impurities. KNORR concludes : "The plasma loses most of the energy due to bound-"bound radiation.... Let us assume that the plasma contains 1 Ca-atom per 10^4 "hydrogen atoms. At 10^6 K and an electron density of 10^{15} cm^{-3}, the hydrogen "radiates approximately 10^6 erg cm^{-3} sec^{-1}, the calcium impurities $7 \cdot 10^7$ erg "cm^{-3} sec^{-1}."

The guide lines for the calculation of radiation losses from high-temperature plasmas have been traced by POST [16] with the assumption that the astrophysical corona model can be applied to this kind of laboratory plasmas. POST treates losses in stationary and in transient plasmas. There one reads : "One way to visualize the radiation loss situation during a "transient build-up of the plasma is first to recognize that many stages of "ionization will be passed through as the final state is approached. But "between each suceessive ionization event many collisional excitations may "occur, each of which results in a loss of energy. Thus, one can consider "that successively to strip a given high Z atom up to a highly ionized state "will require an inevitable energy "fee " in excitation radiation losses. "This fee may be much larger than the sum of the ionization energies. More-"over, after this fee has been paid, if the ion does not become completely "stripped, further energetic "operating expenses" must be borne to support "the continued excitation radiation losses. If the impurity ion escapes to "the wall of the vacuum chamber, is there neutralized and returns afresh, "a new fee must be paid for each round trip".

At that time appeared many spectroscopic papers. Only a few may be mentioned : JONES and WILSON [17] described the spectroscopic studies of ion energies in ZETA. They observed lines originating from Ar VIII, Kr VIII, Ne VI, O VI, see also the papers by HOBBS et al. [18] , HEARN et al.[19] , BURTON and WILSON [20], and HOBBS and ROSE [21] . Similar measurements were made on the SCEPTRE - machine,see HUGUES and WILLIAMS [22] , WILLIAMS and

KAUFMAN [23] , on Z-pinches (CURZON et al. [24] , LUK'IANOV and SINITSYN [25]), on θ-pinches (GRIEM et al. [26] , KOLB [27]). Considerable spectroscopic work on impurity radiation has been performed on the Princeton C-STELLARATOR (see e.g. HINNOV [28], HIRSCHBERG [29] , HINNOV [30]) and on the Fontenay-aux-Roses T.A. 2000 machine (BRETON, et al. [31]).

Although impurity measurements continued to be made at the end of the sixties and during the early seventies (see e.g. DÜCHS and GRIEM [32] , LOTZ [33], HINNOV [34], DECROISETTE and PIAR [35], BRETON and YA'AKOBI [36]) it seems that radiation cooling due to the presence of impurities was not considered as a limiting factor on the way to higher plasma performances, compared with the obstacles encountered in connection with plasma turbulence and plasma instability. In this context it is worth mentioning that plasma loss experiments made on the ZETA machine by BURTON et al. [37] led apparently to the conclusion that "plasma loss is responsable for the major part "of the energy loss at high energies per unit mass.... The plasma loss is "associated with an excess resistance.... Measurements of the electric fields, "..., yield mass motion of the plasma with the required velocities and fre-"quencies to account for the plasma loss by a random-walk process..." (BOHM diffusion). Strong plasma loss leads to an increased plasma-wall interaction, and thus to an increased contamination. At the Salzburg-1962 Conference ARTSIMOVICH [38] described this situation with the phrases : "The production of sufficiently pure hydrogen or deuterium plasma is itself "a difficult task since, due to interaction with the walls of the vacuum "chamber, the bunches of hot plasma very rapidly become contaminated with "impurity atoms and ions which are absorbed on the surface of the walls-"resulting in very high radiation losses. For example, in experiments with "toroidal plasma rings, there are intense flashes of radiation from impuri-"ties, even after prolonged vacuum conditioning. This is one of the basic "factors preventing a rise in plasma temperature in experiments of this kind. "Very serious difficulties arise merely in the attempt to study the proper-"ties of the plasma in such annular columns, since in this case we are con-"fronted with a characteristic uncertainly principle, by which the purity of "the experimental conditions is in irreconciable opposition to the use of "diagnostic methods."

It seems that during the past ten years the development of plasma instabilities was considered as the main obstacle on the way to fusion plasmas which have at least to satisfy the LAWSON criterion $n\tau \cong 10^{14}$ cm^{-3} sec.

In 1966, ECKART and KEILHACKER [39] summarized this in the phrase (transl. from german) : "Thus, the present experiments serve to investigate the two "most important conditions for realizing controlled nuclear fusion, namely "the heating of a plasma to very high temperatures and the stable plasma con- "finement during a sufficiently long time".

During the past ten years great progress has been made in stabilizing the plasma columns and to work with wall materials conditioned to be less sensitive to plasma bombardment . During the mid-seventies, ion temperatures of $1 \cdot 10^6$ to $2 \cdot 10^7$ K (kT = 0.1 keV to 2 keV) could be realized in TOKOMAK machines, the temperatures in θ-pinches are still higher. However, although relatively stable, these high-temperature plasmas (especially the low-density plasmas in magnetically confined systems) are not free of impurities. In the contrary, present plasmas contain so highly ionized impurity atoms that approximately 50% of the ohmic input power is conveyed out by impurity radiation. Radiation cooling is again considered - as 20 years ago - as an energy loss mechanism which must be considered as a very serious one on the way towards fusion. The situation is still aggravated by the fact that classically the diffusion flux vector of the impurities points towards the plasma center and that the highly ionized impurity atoms might thus concentrate in the plasma core and will leave it only through plasma instabilities, if the plasma confinement is only limited by collisions (i.e. by classical diffusion), see e.g. S.I. BRAGINSKII, Rev. Plasma Physics 1 (1965) 205. At present, this point is still investigated and needs definite confirmation by experiments. If the highly ionized atoms are kept in the plasma core, radiation cooling due to impurities will be one of the dominant energy loss mechanisms as long as the plasma is contaminated by too a high concentration of impurity atoms. (By the way, due to our present knowledge the impurity flux problem also applies to the α-particles (He-ions) produced in a fusion plasma. The α-particles stay in the plasma and lead to increasing contamination in a continuous working machine).

2. THE NEED OF ATOMIC DATAE.

In connection with the impurity problem and radiation cooling of high-temperature plasmas atomic datae are needed for the following purposes:

- a. Energy loss measurements, especially in the vacuum ultra-violet and (soft) X-ray region. One must know the wavelengths of the most important spectral lines responsable for the energy losses. For calibration purposes

of radiation detectors it is desirable to know for selected transitions the branching ratios (ratios of Einstein coefficients).

- b. For diagnostic purposes (determination of the impurity level of specific impurities, of ion temperature and of mass motions) one needs the wavelengths of prominent lines belonging to the different ions. This is an "a priori" condition for spectroscopical diagnostic measurements. Further are needed excitation and ionization cross-sections and the rate coefficients for autoionization, radiative and dielectronic recombination as a function of electron energy. For special transitions the cross-sections for ion collisions should be useful in the near future . Further are needed the oscillators strengths (or Einstein coefficients) for the most prominent lines used for the diagnostics and the determination of the desired plasma parameters.

- c. For energy balance calculations and theoretical studies of the kinetics of impurity atoms and ions one needs the energy levels of the various ions present, the ionization energies, the cross-sections for excitation, ionization, autoionization, radiative and dielectric recombination. In this context it is worth mentioning that the impurity ions affect the electrical conductivity, i.e. the ohmic power. Due to the Z^2 dependence of the electron-ion Coulomb cross-section, impurities increase the plasma resistivity and, thus, the ohmic heating efficiency.

At present our knowledge of the mentioned atomic datae is bad. Many wavelengths of highly ionized heavy atoms are only known "approximately". The same holds for the energy levels. Precise datae especially for dielectronic recombination do practically not exist. The ionization cross-sections are assumed to be known with a precision of approximately ± 30% for most of the impurity ions of interest. For the excitation cross-sections the situation is much worse. It is generally believed that they are known within a factor of two, i.e. their precision is $^{+100}_{-50}$ %. (This is a supposition which has not yet been checked experimentally). For the oscillator strengths the situation seems to be better.

As the cross-sections and Einstein coefficients enter linearly in the energy balance it is extremely important to know these quantities for the most prominent transitions with a precision better than a factor two.

Before discussing specific cases, let us look how atomic physics enters the general kinetic equations which permit to get an overall view of the role played by the impurities in the energy balance of plasmas.

3. FUNDAMENTAL KINETIC EQUATIONS.

In order to determine plasma impurities from measurements and to calculate cooling rates due to impurity radiation, one needs an appropriate collisional-radiative model which describes the essential kinetic properties of a plasma in a realistic manner. A powerful treatment is via the statistical approach which consists in considering the different momenta of the velocity-integrated Boltzmann equations. When the velocity distribution functions are not known one has to solve the Boltzmann equations as a function of velocity.

In the following we distinguish different chemical species by subscript cripts $k,\ell,\ldots$, and excited bound states by a second subscript $h,i,j,\ldots$ Especially electrons are characterized by subscript "e". Different ionization stages of the same chemical element are distinguished by the ion charge numbers $z-1$, z, $z+1,\ldots$, which appear as superscripts. Further, $\underset{\sim}{w}$ is the velocity vector, $\langle \underset{\sim}{w} \rangle = (1/n) \int \underset{\sim}{w}\, n(\underset{\sim}{w})\, d\underset{\sim}{w}$ is the mean velocity vector with respect to the laboratory system, n is the number density.

We have the following statistical rate equations for a chemical element k in charge state z and in the bound state i (see also DRAWIN [40]) :

- for the rate of change of particle density $n^z_{k,i}$:

$$\frac{dn^z_{k,i}}{dt} \equiv \frac{\partial n_{k,i}}{\partial t} + \underset{\sim}{\nabla} \cdot (n^z_{k,i} \langle \underset{\sim}{w}^z_{k,i} \rangle) = \left[\frac{\partial n^z_{k,i}}{\partial t} \right]_{\substack{\text{collision} \\ \text{radiation}}} \qquad (1)$$

- for the rate of change of momentum $n^z_{k,i}\, m_k \langle w^z_{k,i} \rangle$:

$$\frac{\partial (n^z_{k,i}\, m_k \langle \underset{\sim}{w}^z_{k,i} \rangle)}{\partial t} + \underset{\sim}{\nabla} \cdot (n^z_{k,i}\, m_k \langle \underset{\sim}{w}^z_{k,i}\, \underset{\sim}{w}^z_{k,i} \rangle) - n^z_{k,i} \underset{\sim}{F}^z_{k,i}$$

$$= \left[\frac{\partial (n^z_{k,i} m_k \langle \underset{\sim}{w}^z_{k,i} \rangle)}{\partial t} \right]_{\substack{\text{collision} \\ \text{radiation}}} \qquad (2)$$

where

$$n^z_{k,i}\, \underset{\sim}{F}^z_{k,i} = n^z_{k,i}\, ze_o \left[\underset{\sim}{E} + \frac{1}{c} (\underset{\sim}{w}^z_{k,i} \times \underset{\sim}{B}) \right] \qquad (3)$$

is the generalized Lorentz force ($\underset{\sim}{E}$ = electric field strength, $\underset{\sim}{B}$ = magnetic induction, ze_o = electric charge of the particle considered).

• for the rate of change of kinetic energy $n^z_{k,i}\,\frac{1}{2}m^z_k\,\langle \underset{\sim}{w}^{z\,2}_{k,i}\rangle$:

$$\frac{\partial}{\partial t}(n^z_{k,i}\,\tfrac{1}{2}m^z_k\,\langle \underset{\sim}{w}^{z\,2}_{k,i}\rangle) + \underset{\sim}{\nabla}\cdot(n^z_{k,i}m^z_k\,\langle \underset{\sim}{w}^{z\,2}_{k,i}\,\underset{\sim}{w}^z_{k,i}\rangle) - n^z_{k,i}\underset{\sim}{F}^z_{k,i}\cdot\langle \underset{\sim}{w}^z_{k,i}\rangle$$

$$= \left[\frac{\partial n^z_{k,i}(1/2)m^z_k\,\langle \underset{\sim}{w}^{z\,2}_{k,i}\rangle}{\partial t}\right]_{\substack{\text{collision}\\ \text{radiation}}} \qquad (4)$$

• for the rate of change of internal (excitation) energy $E^z_{k,1i}$:

$$\frac{d}{dt}(n^z_{k,i}E^z_{k,i}) \equiv \frac{\partial n^z_{k,i}E^z_{k,i}}{\partial t} + \underset{\sim}{\nabla}\cdot(n^z_{k,i}E^z_{k,i}\,\langle \underset{\sim}{w}^z_{k,i}\rangle) = \left[\frac{\partial n^z_{k,i}\,E^z_{k,i}}{\partial t}\right]_{\substack{\text{collision}\\ \text{radiation}}} \qquad (5)$$

To these equations we have to add the corresponding ones for the electron gas. We have especially for the

• rate of change of energy density of the electrons:

$$\frac{\partial}{\partial t}\,(n_e\,\frac{1}{2}\,m_e\langle \underset{\sim}{w}^2_e\rangle) + \underset{\sim}{\nabla}\cdot\,(n_e\,\frac{1}{2}\,m_e\langle \underset{\sim}{w}_e\underset{\sim}{w}_e\rangle) - n_e\underset{\sim}{F}_e\cdot\langle \underset{\sim}{w}_e\rangle \qquad (6)$$

$$= \left[\frac{\partial n_e(1/2)\,m_e\,\langle \underset{\sim}{w}^2_e\rangle}{\partial t}\right]_{\substack{\text{collision}\\ \text{radiation}}}$$

Here, m is the particle mass, and $E^z_{k,i}$ denotes the internal energy of chemical species k of charge state z and in the (excited) state i, relative to the ground state of the atom. For $z > 1$, one has therefore to add to the usual excitation energy the ionization energies for all states smaller than z. This may be demonstrated by the following reactions in connection with Fig.1.

(i) Radiative recombination of a singly ionized atom with an electron is energetically submitted to the following condition, symbolically :

$$A^1_1\,(\tfrac{3}{2}\,kT^1 + E^1_1) + e^-(E) \rightarrow A^o_i\,(\tfrac{3}{2}\,kT^o + E^o_i) + h\nu$$

where the photon energy is given by $h\nu = E^1_1 - E^o_i + E$. In words : a singly ionized atom ($z = 1$) in the ground level ($i = 1$) has a mean kinetic energy of $(3/2)kT^1$ and the internal energy E^1_1 which equals the ionization energy of the neutral atom. This ion recombines with an electron of kinetic energy E. After recombination into the excited level i the ion species have lost the kinetic energy of amount $(3/2)\,kT^1_1 + E^1_1$ and the electrons the

translational energy E, since both the ion and the electron have disappeared. On the other hand, after recombination there appear two new "particles", namely the neutral atom of kinetic energy (3/2) kT^o and of internal energy E_i^o, and a photon. Therefore, the exact energy relation for the photons is $h\nu = E_l^1 - E_i^o + E + \frac{3}{2} k(T^1 - T^o)$. With the assumption that the recombination process does not change the translational energy of the heavy particles one obtains the above given relation for the photon $h\nu$ and which is generally applied in all calculations.

(ii) Three-body collisional recombination of a two-fold ionized atom is energetically described by

$$A_l^{2+}(\tfrac{3}{2} kT^2 + E_l^2) + e^-(E) + e^-(E') \rightarrow A_i^+(\tfrac{3}{2} kT^1 + E_i^1) + e^-(E' + \Delta E)$$

The excess energy $\Delta E = E_l^2 - E_i^1 + E$ is imparted to the electron which has not recombined (under the condition that $T^2 = T^1$). The energy difference $E_l^2 - E_i^1$ is equal to the ionization energy of the singly ionized atom in level i.

If follows from this, that potential or internal energy is only contained in heavy particles. When internal energy is given to electrons, the latter are heated. On the other hand, electrons can lose kinetic energy to the profit of an increase of internal energy of the heavy particles (e.g. excitation or ionization).

When we adopt this convention it follows that summation of the Eqs. (4) and (5) yields the rate equation for the total energy density of the particles i of chemical species k in charge state z. Summing the Eqs. (4) and (5) over all values z,k,i yields the rate equation for the energy density contained in *all* heavy particles. Adding to these the electron energy equation (6) yields the rate of change of the total energy density of the plasma. The diffusion term of Eqs. (4) and (6) contains the contributions to the usual or "contact heat conductivity". The so-called "reaction heat conductivity" is contained in the diffusion term of equations of type (5). Energy losses due to bound-bound radiation are contained in the collisional-radiative terms of Eq. (5), losses due to free-bound radiation are contained in the collisional-radiative terms of both equations (5) and (6), and losses due to bremsstrahlung are entirely contained in the collisional-radiative term of the Eq. (6), see also Eq. (35).

The term $n_e \underset{\sim}{F}_e \cdot \langle \underset{\sim}{w}_e \rangle$ represents the power density furnished to the electron gas due to externally applied fields. This term accounts for the ohmic input power. In present TOKAMAK machines one now applies energetic neutral particle beams for additional heating. When the heating process is due to direct "heavy particle-heavy particle" interaction, the transfer rate of energy must be accounted for in the collisonal-radiative terms of Eqs. (4) and (5), Eq. (4) yields the increase of translational energy, Eq. (5) the increase of internal energy. When the injected beam particles act primarily on the electrons, the additional processes leading to heating of the electron gas are accounted for by additional terms in the collisional-radiative term of the electron energy equation (6). For reasons of simplicity it is practical to add the additional heating terms to the term describing the ohmic input power and to reserve the collisional-radiative terms only for processes directly connected to plasma particles proper. It should be pointed out however, that this procedure may be admissible as long as the additionally injected particles do not sensitively increase the total number density and do not directly influence the excitation and ionization of the impurities of the plasma. In the opposite case, the additional heating must be included in the corresponding collisional-radiative terms.

We still mention that the condition of quasi-neutrality requires that the relation

$$n_e = \sum_{z,k,i} z\, n^z_{k,i} \tag{7}$$

is fulfilled. Further, every ionization process $z \rightarrow z+1$ creates a particle of type $z+1$ and destroys a particle of type z. The opposite applies to recombination. It follows from this that summation of all Eqs. (1) yields for a monatomic gas

$$\sum_{z,k,i} \left[\frac{\partial n^z_{k,i}}{\partial t} \right]_{\substack{\text{collision} \\ \text{radiation}}} = 0 \tag{8}$$

Thus the conservation equation for the number density of heavy particles becomes

$$\sum_{z,k,i} \left[\frac{\partial n^z_{k,i}}{\partial t} + \underset{\sim}{\nabla} \cdot \left(n^z_{k,i} \langle \underset{\sim}{w}^z_{k,i} \rangle \right) \right] = 0 \tag{9}$$

whereas the conservation equation for n_e is given by

$$\frac{dn_e}{dt} \equiv \frac{\partial n_e}{\partial t} + \underset{\sim}{\nabla}.(n_e \langle \underset{\sim}{w}_e \rangle) = \left[\frac{\partial n_e}{\partial t} \right]_{\substack{\text{collision} \\ \text{radiation}}} \tag{10}$$

The electrons are furnished by the main gas (e.g. hydrogen or deuterium) and by the impurity atoms. We thus have :

$$\frac{\partial n_e}{\partial t} + \underset{\sim}{\nabla}.(n_e \langle \underset{\sim}{w}_e \rangle) = \left[\frac{\partial n_e}{\partial t} \right]^{\text{main gas}}_{\substack{\text{collision} \\ \text{radiation}}} + \left[\frac{\partial n_e}{\partial t} \right]^{\text{impurity}}_{\substack{\text{collision} \\ \text{radiation}}} \tag{11}$$

The impurity level can be considered as low when the number of "impurity electrons" is small compared to the number of electrons delivered by the main gas, i.e. :

$$\boxed{n_e^{\text{impurity}} \ll n_e^{\text{main gas}}} \tag{12}$$

In present TOKAMAK machines, this is not always a strong inequality. This means that impurities can determine to a large extent the collisional-radiative kinetics. The degree of impurity is often defined by the "effective" ion charge number z_{eff} defined by

$$\boxed{z_{eff} = \frac{\sum_{z,k,i} z^2 n^z_{k,i}}{\sum_{z,k,i} z\, n^z_{k,i}} = \frac{\sum_{z,k,i} z^2 n^z_{k,i}}{n_e}} \tag{13}$$

This quantity intervenes directly in the equation for the electrical conductivity. For a pure hydrogen or deuterium plasma $z_{eff} = 1$ holds. In present TOKAMAK machines one finds z_{eff} ranging from approximately one to 8-10.

In order to separate first the different macroscopic effects contained in the terms on the r.-h.-s. of the Eqs. (4) (5) (6) we introduce the *total mass average velocity relative to the laboratory system by the equation*

$$\underset{\sim}{v}_o(r,t) = \frac{1}{\rho} \left(\sum_{z,k,i} n^z_{k,i}\, m^z_k\, \underset{\sim}{w}^z_{k,i} + n_e m_e \underset{\sim}{w}_e \right) \tag{14}$$

where the total mass density is defined by

$$\rho = \sum_{z,k,i} n^z_{k,i}\, m^z_k + n_e m_e \tag{15}$$

We further introduce the "*peculiar velocity*" by

$$\underset{\sim}{V}(r,t) = \underset{\sim}{w}(r,t) - \underset{\sim}{v}_o(r,t) \tag{16}$$

$\underset{\sim}{w}$ is a velocity vector relative to the laboratory system, $\underset{\sim}{V}$ the velocity vector relative to the mass average velocity $\underset{\sim}{v}_o$ of the whole plasma. Especially for the electrons :

$$\underset{\sim}{V}_e(r,t) = \underset{\sim}{w}_e(r,t) - \underset{\sim}{v}_o(r,t) \tag{17}$$

For a stable plasma column, terms associated with a temporal variation of $\underset{\sim}{v}_o$ become equal to zero. Introducing $\underset{\sim}{w}_e$ from Eq. (17) into the electron energy equation (6) yields for the first term on the ℓ.-h.-s. the expression

$$\frac{\partial}{\partial t}(n_e \frac{1}{2} m_e \langle \underset{\sim}{w}_e^2 \rangle) = \frac{\partial}{\partial t} [\frac{1}{2} n_e m_e v_o^2 + \frac{1}{2} n_e m_e \langle V_e^2 \rangle + n_e m_e \underset{\sim}{v}_o \cdot \langle \underset{\sim}{V}_e \rangle] \tag{18}$$

In the paranthesis of the r.-h.-s., the first term represents the electron energy density associated with the macroscopic (bulk) velocity of the whole plasma. According to that what has been said before, the time derivative of this quantity will assumed to be zero (stable plasma column). The next term represents the internal translational energy density of the electron gas relative to a system moving with $\underset{\sim}{v}_o$. For a Maxwellian velocity distribution one has

$$\frac{1}{2} n_e m_e \langle V_e^2 \rangle = n_e \frac{3}{2} kT_e \tag{19}$$

i.e., the time derivative of the second term measures the temporal variation of the electron pressure. The last term in the parenthesis is associated with momentum transfer between the electron gas and the ensemble of the plasma. In the following this term will also be put equal to zero. In any case, summed over all species, this term is equal to zero because of the fact that the mass average diffusion velocity with respect to $\underset{\sim}{v}_o$ is zero :

$$\sum_{z,k,i} n_{k,i}^z m_k^z \langle \underset{\sim}{V}_{k,i}^z \rangle + n_e m_e \langle \underset{\sim}{V}_e \rangle = 0 \tag{20}$$

In the same manner we can proceed with Eqs. (4) and (5) when substituting $\underset{\sim}{w}_{k,i}^z$ by the corresponding relations of type (16).

The first term of the electron energy equation (6) therefore reduces to

$$\frac{\partial}{\partial t}\left(n_e \frac{1}{2} m_e \langle \underset{\sim}{w}_e^2 \rangle\right) = \frac{\partial}{\partial t}\left(\frac{3}{2} n_e kT_e\right) = \frac{\partial \bar{E}_e^{tr}}{\partial t} \tag{21}$$

where we have put $\bar{E}_e^{tr} = (3/2)\, n_e kT_e$ for the mean energy density of the electron gas. In quite the same manner we can proceed with the diffusion term on the ℓ.-h.-s. of Eq. (6). One ends up with the following electron energy equation relative to a coordinate frame moving with $\underset{\sim}{v}_o$:

$$\frac{\partial \bar{E}_e^{tr}}{\partial t} + \underset{\sim}{\nabla} \cdot \underset{\sim}{q}_e^{tr} = \Omega_e + \left[\frac{\partial n_e (1/2) m_e \langle \underset{\sim}{v}_e^2 \rangle}{\partial t}\right]_{\substack{\text{collision} \\ \text{radiation}}} \tag{22}$$

where we have introduced the *electron heat flux vector* by

$$\underset{\sim}{q}_e^{tr} = \frac{1}{2} n_e m_e \langle v_e^2 \underset{\sim}{v}_e \rangle \tag{23}$$

and the ohmic (or external) input power per unit volume by

$$\Omega_e = n_e \underset{\sim}{F}_e (\langle \underset{\sim}{w}_e \rangle - \underset{\sim}{v}_o) = n_e \underset{\sim}{F}_e \cdot \langle \underset{\sim}{v}_d \rangle \tag{24}$$

where $\langle \underset{\sim}{v}_d \rangle$ is the mean electron drift velocity relative to $\underset{\sim}{v}_o$.

We proceed in the same manner with the Eqs. (4) and (5) and obtain after summation over z,k and i - for the rate of **change** of *translational energy of the heavy particles*, relative to the coordinate frame moving with $\underset{\sim}{v}_o$, the relation

$$\frac{\partial \bar{E}_h^{tr}}{\partial t} + \underset{\sim}{\nabla} \cdot \underset{\sim}{q}_h^{tr} = \Omega_h + \sum_{z,k,i} \left[\frac{\partial n_{k,i}^z (1/2) m_k^z \langle v_{k,i}^{z\,2} \rangle}{\partial t}\right]_{\substack{\text{collision} \\ \text{radiation}}} \tag{25}$$

where we have introduced the following abbreviations :

$$\bar{E}_h^{tr} = \sum_{z,k,i} \frac{3}{2} n_{k,i}^z kT_{k,i}^z \tag{26}$$

$$\underset{\sim}{q}_h^{tr} = \sum_{z,k,i} \frac{1}{2} n_{k,i}^z m_k^z \langle v_{k,i}^{z\,2} \underset{\sim}{v}_{k,i}^z \rangle \tag{27}$$

$$\Omega_h = \sum_{z,k,i} n_{k,i}^z \underset{\sim}{F}_{k,i}^z \cdot \langle \underset{\sim}{v}_{k,i}^z \rangle \tag{28}$$

$\underset{\sim}{q}_h^{tr}$ is the heat flux vector associated to translational energy of the heavy particles.

With the same assumptions as above one finds as equation which describes the rate of change of *internal energy*

$$\frac{\partial \bar{E}_h^{int}}{\partial t} + \underset{\sim}{\nabla} \cdot \underset{\sim}{q}_h^{int} = \sum_{z,k,i} \left[\frac{\partial n_{k,i}^z \, E_{k,i}^z}{\partial t} \right]_{\substack{\text{collision} \\ \text{radiation}}} \tag{29}$$

where we have introduced the *internal energy density* by

$$\bar{E}_h^{int} = \sum_{z,k,i} n_{k,i}^z \, E_{k,i}^z \tag{30}$$

and the *heat flux vector for the transport of internal energy* (reaction heat conductivity) by

$$\underset{\sim}{q}_h^{int} = \sum_{z,k,i} n_{k,i}^z \, E_{k,i}^z \, \langle \underset{\sim}{V}_{k,i}^z \rangle \tag{31}$$

Summing up the Eqs. (22), (25) and (29) yields the relation which describes the *rate of change of the energy density of the whole plasma*. With the abreviations

$$\bar{E} = \bar{E}_e^{tr} + \bar{E}_h^{tr} + \bar{E}_h^{int} \tag{32}$$

$$\underset{\sim}{q} = \underset{\sim}{q}_e^{tr} + \underset{\sim}{q}_h^{tr} + \underset{\sim}{q}_h^{int} \tag{33}$$

$$\Omega_{ext} = \Omega_e + \Omega_h \tag{34}$$

follows

$$\begin{aligned} \frac{\partial \bar{E}}{\partial t} + \underset{\sim}{\nabla} \cdot \underset{\sim}{q} = \Omega_{ext} &+ \left[\frac{\partial n_e (1/2) m_e \langle \underset{\sim}{V}_e^2 \rangle}{\partial t} \right]_{\substack{\text{coll.} \\ \text{rad.}}} \\ &+ \sum_{z,k,i} \left[\frac{\partial n_{k,i}^z (1/2) \, m_k^z \, \langle \underset{\sim}{V}_{k,i}^{z\,2} \rangle}{\partial t} \right]_{\substack{\text{coll.} \\ \text{rad.}}} \\ &+ \sum_{z,k,i} \left[\frac{\partial n_{k,i}^z \, E_{k,i}^z}{\partial t} \right]_{\substack{\text{coll.} \\ \text{rad.}}} \end{aligned} \tag{35}$$

It is worth mentioning that the term $\underset{\sim}{\nabla}.\underset{\sim}{q}$ contains several contributions, since $n = n(r,t)$, $\underset{\sim}{V} = \underset{\sim}{V}(r,t)$ and $\langle \underset{\sim}{V}^2 \rangle = \langle \underset{\sim}{V}^2(r,t) \rangle$. For magnetically confined plasmas, the calculation of $\underset{\sim}{V}$ is a difficult task and shall not be discussed here. In general two different effects contribute to the $\underset{\sim}{\nabla}.\underset{\sim}{q}$, namely "ordinary density diffusion" due to a density gradient and the so-called "thermo-diffusion" due to a temperature gradient. Eq. (33) shows that three different types of energies contribute to the global heat conduction. For further details, the reader is refered to the articles of FINKELNBURG and MAECKER [41] and DRAWIN [42][43] .

In order to obtain the radiation losses as a function of the atomic parameters in the collisional-radiative terms of Eq.(35) we need a collisional-radiative model which permits to express the three last terms on the r.-h.-s. of Eq. (35) by atomic processes. This shall be developed now.

The Eq. (35) can be interpreted in the following sense : ohmic external heating is used to change the thermal plus internal energy density and to compensate energy losses due to thermal diffusion and collisional-radiative processes. Both elastic and inelastic (superelastic) collisions contribute to the collisional-radiative terms which will therefore be decomposed in two parts:

$$\left[\frac{\partial n_e (1/2) m_e \langle V_e^2 \rangle}{\partial t}\right]_{\substack{\text{coll.} \\ \text{rad.}}} + \sum_{z,k,i} \left[\frac{\partial n_{k,i}^z (1/2) m_k^z \langle V_{k,i}^{z\,2} \rangle}{\partial t}\right]_{\substack{\text{coll.} \\ \text{rad.}}}$$

$$+ \sum_{z,k,i} \left[\frac{\partial n_{k,i}^z E_{k,i}^z}{\partial t}\right]_{\substack{\text{coll.} \\ \text{rad.}}} = \Phi_{el} + \psi_{inel} \qquad (36)$$

where Φ_{el} accounts for elastic and ψ_{inel} for inelastic, superelastic, and radiative processes.

The elastic processes simply account for energy transfer between electrons and heavy particles due to elastic collisions. In a coordinate frame moving with $\underset{\sim}{v}_o$ one obtains for the electronic part of Φ_{el} the relation

$$\Phi_{el,e} = -n_e \sum_{z,k,i} \frac{2m_e}{m_k^z} \nu_{e,ki}^z \frac{3}{2} k(T_e - T_{k,i}^z) \qquad (36a)$$

where $T^z_{k,i}$ is the temperature associated with particles of type z,k,i ; $\nu^z_{e,ki}$ is the average frequency of elastic collisions between electrons and the heavy particles. Eq. (32) describes the exchange of thermal energy between electrons and heavy particles, leading to a loss of the electrons. The same amount of energy is given to the heavy particles (h) and appears in the contribution to Φ_{el} with a positive sign :

$$\Phi_{el,h} = + n_e \sum_{z,k,i} \frac{2m_e}{m^z_k} \nu^z_{e,k,i} \frac{3}{2} k(T_e - T^z_{k,i}) = - \Phi_{el,e} \qquad (36b)$$

Thus, $\Phi_{el} = \Phi_{el,e} + \Phi_{el,h} = 0$ which simply means that collisions alone cannot change the total energy density, they can only redistribute the energy amongst the different species.

For the inelastic, superelastic and radiative processes, the following collisional-radiative processes shall be taken into account. Symbols below and above the arrows denote rate coefficients. The following reactions apply to "usual" and "autoionizing" states.

a. electronic ionization and three-body collisional recombination :

$$A^z(i) + e^- \underset{Q^{z+1}_i}{\overset{S^z_i}{\rightleftarrows}} A^{z+1}(1) + e^- + e^- \qquad (37)$$

b. electronic excitation and de-excitation

$$A^z(i) + e^- \underset{F^z_{ij}}{\overset{C^z_{ji}}{\rightleftarrows}} A^z(j) + e^- \qquad (38)$$

c. Spontaneous emission, induced emission and photoexcitation due to radiative absorption

$$\left.\begin{aligned} A^{(z)}(i) + h\nu_{ij} &\xleftarrow{A^z_{ij}} A^z(j) \\ A^z(i) + 2h\nu_{ij} &\longleftarrow A^z(j) + h\nu_{ij} \\ A^z(i) + h\nu_{ij} &\xrightarrow{1 - \Lambda^z_{ij} A^z_{ij}} A^z(j) \end{aligned}\right\} \qquad (39)$$

The effective radiative de-excitation rate is $\Lambda^z_{ij} A^z_{ij} n^z_j$, where A^z_{ij} is the Einstein coefficient for spontaneous de-excitation $j \to i$ and Λ^z_{ij} the optical escape factor for this transition. The Λ^z_{ij} can be estimated according to a procedure given by HOLSTEIN [44] or DRAWIN and EMARD [45] and in which intervenes the equation of radiative transfer. For completely optically thin transitions (no reabsortion) $\Lambda^z_{ij} = 1$ holds. When all radiation is reabsorbed one has $\Lambda^z_{ij} = 0$.

d. radiative recombination, stimulated recombination and photoionization.

These processes can symbolically be described by

$$\left.\begin{array}{l} A^z(i) + h\nu \xleftarrow{R^{z+1}_i} A^{z+1}(1) + e^- \\ A^z(i) + 2h\nu \longleftarrow A^{z+1}(1) + e^- + h\nu \\ A^z(i) + h\nu \xrightarrow{1-\Lambda^{z+1}_i R^{z+1}_i} A^{z+1}(1) + e^- \end{array}\right\} \qquad (40)$$

The effective two-body recombination rate into level i is $\Lambda^{z+1}_i R^{z+1}_i n^{z+1}_1 n_e$, where Λ^{z+1}_i is the optical escape factor for bound-free radiation of the i-th continuum. It can be estimated according to a procedure given by DRAWIN and EMARD [45] . R^{z+1}_i is the recombination coefficient for the i-th continuum.

e. dielectronic recombination.

This effect is de-composed into two individual reactions, namely excitation of an ion simultaneously with electron capture into an autoionizing state of the formed doubly excited particle, and radiative decay of one of the two excited electrons ; symbolically :

$$A^{z+1}(1) + e^- \underset{\mathcal{A}^z_{k,1i}}{\overset{\varphi^{z+1}_k}{\rightleftarrows}} A^z(i) \xrightarrow{\mathcal{P}^z_{k,hi}} A^z(h) + h\nu \qquad (41)$$

For all levels i lying below the usual(or simple)ionization energy of the corresponding ion the rate coefficients are zero. The energies involved are $E^z_{k,i} - E^{z+1}_{k,1}$ for the passage from $A^{z+1}(1)$ to $A^z(i)$ This energy is taken from the electrons. The photon energy involved is given by

$E^z_{k,i} - E^z_{k,h} = h\nu$ (with $i > h$) for the passage from a state above to a state below the ionization limit. The dielectronic recombination rate is proportional to the branching ratio $\mathcal{A}^z_{k,hi} / (\mathcal{A}^z_{k,hi} + \mathcal{A}^z_{k,1i})$. $\mathcal{A}^z_{k,1i}$ is the rate coefficient for auto-ionization.

f. inelastic electron-ion collisions leading to bremsstrahlung (free-free radiation).

$$A^z + e^- + \{^{\text{kinetic}}_{\text{energy}}\} \rightarrow A^z + e^- + h\nu \qquad (42)$$

We neglect absorption and inverse bremsstrahlung.

In our model we neglect collisions with protons or deuterons and any other type of collision between impurity particles.

The source term Ψ_{inel} of Eq. (36) can now be expressed as a function of the rate coefficients, the particle densities and the excitation (ionization) energy of the individual levels. When one writes down all terms one sees that all collision terms cancel each other. This shall be demonstrated for the excitation – de-excitation processes due to electronic collisions : The electrons lose the following energy per unit volume and unit time :

$$\left[\begin{matrix} \text{Energy} \\ \text{loss rate} \end{matrix} \right] = - \sum_z \sum_k \left[\sum_{i,j} (C^z_{k,ij} n^z_{k,i} n_e - F^z_{k,ij} n^z_{k,j} n_e)(E^z_{k,1j} - E^z_{k,1i}) \right]$$

The same amount of energy is gained by the heavy particles as internal energy. The overall balance due to these processes is thus zero. Only radiation processes contribute to Ψ_{inel} which may be put into the following form (synchrotron radiation omitted):

$$\Psi_{inel} = - P^{rad} = - P^{f-f} - P^{f-b} - P^{b-b} - P^{diel} \qquad (43)$$

where $P^{f-f}, P^{f-b}, P^{b-b}$ and P^{diel} denote the power densities of free-free, free-bound, bound-bound, and dielectric recombination respectively. One has the following expressions :

$$P^{f-f} = \frac{32\pi^2 e_o^6 (kT_e)^{1/2}}{3\sqrt{3}\, c^3 (2\pi m_e)^{3/2}} \sum_z \sum_k \sum_i n_e z^2 n^z_{k,i} \qquad (44)$$

$$P^{f-b} = \sum_z \sum_k \sum_i \Lambda^z_{k,i} R^z_{k,i} n^z_{k,1} n_e (E^{z-1}_{k,i} + \beta^{z-1}_{k,i} kT_e) \quad (45)$$

$$P^{b-b} = \sum_z \sum_k \sum_{i,j} \Lambda^z_{k,ij} A^z_{k,ij} n^z_{k,j} (E^z_{k,j} - E^z_{k,i}) \quad (46)$$

$$P^{diel} = \sum_z \sum_k \sum_{k,i} \mathcal{D}^z_{k,hi} n^z_{k,i} (E^z_{k,i} - E^z_{k,h}) \quad (47)$$

where the summation over z begins with z=0(neutrals) and ends with z = Z, Z being the charge number of the bare nuclei. The coefficient $\beta^{z-1}_{k,i}$ is of order unity, the exact value depends on the cross-section and the velocity distribution function. Due to rates involved in the dielectronic recombination process, the last relation may be given the following form (corona model):

$$P^{diel} \cong \sum_z \sum_k \sum_i \mathcal{C}^{z+1}_{k,il} n^{z+1}_{k,1} n_e \frac{\mathcal{D}_{k,hi}}{(\mathcal{D}^z_{k,hi} + \mathcal{A}^z_{k,1i})} (E^z_{k,i} - E^z_{k,h}) \quad (48)$$

Owing to the relations (36),(36a,b)and (43) the rate of change of the energy density of the whole plasma as given by Eq. (35) can thus be put into the following simple form :

$$\Omega_{ext} = \frac{\partial \bar{E}^{tr}_e}{\partial t} + \frac{\partial \bar{E}^{tr}_h}{\partial t} + \frac{\partial \bar{E}^{int}_h}{\partial t} + \underset{\sim}{\nabla} \cdot \underset{\sim}{q} + \Psi^{rad} \quad (49)$$

It clearly shows where the input power goes : It is used to increase the translational energy of the electrons and the translational and internal energies of the heavy particles, and it compensates the energy losses due to heatconduction and radiation. Should once more be pointed out that the form of Eq. (49) is based on an energy model which gives all internal energy to the heavy particles.

Remark :When one adopts an energy model in which the excitation energy of every atom or ion is used without taking into account the ionization energy, one has to add to the thermal energy of the electrons the internal energy associated with the different ionization stages. In this case the rate of

change of the energy density in given by the following formula

$$\Omega_{ext} = \frac{\partial \bar{E}_e^{tr}}{\partial t} + \frac{\partial \bar{E}_h^{tr}}{\partial t} + \frac{\partial \bar{E}_h^{exc}}{\partial t} + \hat{I}\,\frac{dn_e}{dt} + \underset{\sim}{\nabla}\cdot\underset{\sim}{q} + \Psi^{rad} \qquad (50)$$

where $\bar{E}_e^{tr}$, $\bar{E}_h^{tr}$, and Ψ^{rad} have the same meaning as in Eq. (45) $\bar{E}_h^{exc}$ is the internal energy density contained in the excited states only. $\underset{\sim}{\nabla}\cdot\underset{\sim}{q}$ accounts for diffusion of $\bar{E}_e^{tr} + \bar{E}_h^{tr} + \bar{E}_h^{exc}$. The term $\hat{I}\,dn_e/dt$ takes into account temporal variation *and* diffusion of ionization energy, since the total derivative dn_e/dt is composed of two terms and has for the present case the form (see also Eq. (10)) $dn_e/dt = \partial n_e/\partial t + \underset{\sim}{\nabla}\cdot(n_e\langle\underset{\sim}{V}_e\rangle)$. $\hat{I}$ is the "effective ionization energy" defined by the weighted mean

$$\hat{I} = \frac{\sum_z \sum_k \sum_i E^z_{k,1} n^z_{k,i}}{\sum_z \sum_k \sum_i z\, n^z_{ki}} = \frac{\sum_z \sum_k \sum_i E^z_{k,1} n^z_{k,i}}{n_e} \qquad (51)$$

and which depends on the instantaneous charge state of the heavy particles. $E^z_{k,1}$ is the usual ionization energy necessary to produce a z-times ionized atom in the ground state.

The terms which account for diffusion of excitation and expecially of ionization energy can play an important role in regions where the charge states of the particles show large changes, e.g. in a region where OII disappears and OIII is formed, etc...

4. THE CORONA MODEL.

The Eqs. (44) to (47) give the radiative power losses as functions of the particle densities $n^z_{k,i}$. In the most general case, the $n^z_{k,i}$ must be calculated from a system of coupled rate equations of type (1) coupled with the rate equations for the transfer of momentum, energy and photons and taking into account initial and boundary conditions. This is a very difficult task and can in practice never lead to exact solutions, since one is necessarily forced to introduce simplying assumptions due to the physical and mathematical complexity of the problem.

At high temperatures and not too high electron and impurity densities one can assume that the "corona model" applies. In this case one can neglect in the ionization-recombination processes all collisional interactions of electrons (and other particles) with the excited states. This yields the particle distribution over the different ionization stages as a function of temperature T_e ; the electron density does not intervene. In a separate procedure one then calculates the population densities of particles in the excited states with the (coronal) assumption that the latter are only populated by electron collisions from the ion ground state and only depopulated by spontaneous emission. The procedure is obviously only justified as long as dielectric recombination is neglected, since inclusion of di-electronic recombination leads to extremely large populations of the highly excited levels with principal quantum numbers ranging from 20 to 500. The absolute populations and the distribution over the quantum levels is a strong function of n_e, as may be seen from Fig. 2 which refers to Fe^{7+}. The quantity b_i is the SAHA decrement defined by

$$n_i^{actual} = b_i \, n_i^{(saha)} \tag{52}$$

These populations are directly connected to the recombination coefficient $Fe^{8+} + e \rightarrow Fe^{7+}$ shown in Fig. 3. Due to the fact that the Einstein coefficients $A^z_{k,ij}$ for transitions between highly excited states are much smaller than for the lower lying resonance transitions one can to a first approximation neglect radiation losses originating from highly excited levels. However, one should not neglect in the model calculations the collisions of electrons with the doubly excited states. The problem is discussed in detail by BURGESS and SUMMERS [46] and SUMMERS [47], see also SUMMERS [48]. The electron density-dependent effect of dielectronic recombination is due to the perturbation of the highly excited levels by the electric microfield and due to the collisional ionization according to reaction (37). Until now there does not exist a detailed study of the n_e-dependence of the dielectric recombination coefficient of "highly" ionized atoms of Fe, Mo, and W. The density effect is generally assumed to be not very important under solar corona conditions ($n_e \simeq 10^8 cm^{-3}$). How the density affects the dielectronic recombination rates is exactly only seen by solving the ensemble of coupled rate equations. As these calculations are very time consuming one generally applies a method suggested by BURGESS [49] who intro-

duced a correction factor

$$D = \sum_{n=n_\ell}^{n_t} \alpha_{diel}(n) / \sum_{n=n_\ell}^{\infty} \alpha_{diel}(n) \tag{53}$$

where n_ℓ is the smallest principal quantum number allowed, n_t is the "thermal continuum limit". Excited states having principal quantum numbers $n > n_t$ are assumed to lie in the continuum. The effective dielectronic recombination coefficient is then given by

$$\alpha_{diel} = D \sum_{n_\ell}^{\infty} \alpha_{diel}(n) \tag{54}$$

This expression has been applied by JORDAN [50] and MERTS et al. [51] . It is to be noted that α_{diel} has been calculated by several authors. The proposed values differ considerably from each other (see later).

When one assumes an implicite n_e-dependence of the dielectronic recombination coefficient, the total recombination of ions of charge state z can be expressed by

$$\alpha_k^z = \alpha_{k,rad}^z(T_e) + \alpha_{k,diel}^z(T_e, n_e) \tag{55}$$

where the radiative recombination coefficient is given by

$$\alpha_{k,rad}^z = \sum_i R_{k,i}^z \tag{56}$$

where summation is only over non-autoionizing levels. In the frame of the corona model, the number density of particles in the ground state (1) is then given by

$$\frac{\partial n_{k,1}^z}{\partial t} = S_{k,1}^{z-1} n_{k,1}^{z-1} n_e - S_{k,1}^z n_{k,1}^z n_e + \alpha_k^{z+1} n_{k,1}^{z+1} n_e - \alpha_k^z n_{k,1}^z n_e - \frac{1}{r} \frac{\partial}{\partial \underset{\sim}{r}} (r \underset{\sim}{\psi}_{k,1}^z) \tag{57}$$

where $S_{k,1}^z$ is the ionization coefficient and $\underset{\sim}{\psi}_{k,1}^z$ the flux vector. In all calculations for TOKAMAK systems and Θ-pinches, equations of type (57) are applied. The Fig. 4 shows the ionization balance of carbon calculated by NUSSBAUM and STOREY [52] . One clearly sees that already the inclusion of the metastable states yields a considerable modification of the ionization balance compared to the true corona model which neglects such states.

When the ground state densities are known, the populations of the excited states are calculated from the balance relation

$$C^z_{k,j1} n^z_{k,1} n_e = \sum_{i<j} A^z_{k,ij} n^z_{k,j} \tag{58}$$

This yields for the population density of level j

$$n^z_{k,j} = \frac{C^z_{k,j1}\, n^z_{k,1}}{\sum_{i<j} A_{k,ij}} n_e \tag{59}$$

Introducing this relation into Eq. (46) yields the power loss due to bound-bound transitions as a function of the excitation coefficients $C^z_{k,j1}$; for the optically thin case :

$$P^{b-b} = \sum_z \sum_k \sum_{i,j} C^z_{k,j1} n^z_{k,1} n_e \frac{A^z_{k,ij}}{\sum_{i<j} A^z_{k,ij}} (E^z_{k,j} - E^z_{k,i}) \tag{60}$$

$$= \sum_z \sum_k \sum_j C^z_{k,j1} n_{k,1} n_e (E^z_{k,j} - E^z_{k,1})$$

When the ratio $n^z_{k,j}/n^z_{k,1}$ is divided by the Boltzmann ratio $(n^z_{k,j}/n^z_{k,1})^{\text{Boltzmann}}$, one obtains the so-called Boltzmann decrement a_j which is a measure for deviations from L.T.E. population. Fig. 5 gives an example for optically thin NV and OVI according to SUCKEWER [53] who calculated the populations from a complete collisional-radiative model.

In the corona regime and in L.T.E., the ratio of two line intensities of the same ionization stage is independent of n_e. Fig. 6 shows that this may not be true for ions of light elements at electron densities presently reached in TOKAMAKS.

Two-photon decay and proton (deuteron)-induced transitions are generally neglected as well as self-absorption. HUTCHEON and McWHIRTER [54] have discussed all three effects.

In a fully stripped ion-electron plasma the radiation loss is due to bremsstrahlung. Species of ion charge z contribute to the power with

$$P^{z}_{brems} = 4.8 \cdot 10^{-31} n_e n^z z^2 (kT_e)^{1/2} \text{ W cm}^{-3} \quad (61)$$

(kT_e in KeV)

For a pure hydrogen plasma, z = 1 holds ; see also Fig. 7.

5. IMPURITIES OBSERVED IN PRESENT FUSION RESEARCH MACHINES.

In present machines only a limited number of impurity elements are found, namely, hydrogen, carbon, oxygen, iron, chromium, nickel, molybdenum and tungsten. They are liberated from the walls and the limiter due to plasma-wall interaction. Their charge state depends on the plasma conditions. In all experiments, oxygen is already found during the initial phase of the discharge, indicating that it is already present as impurity in the filling gas. When quartz tubes are used as wall material one also observes silicium. Carbon, iron, chromium and nickel are constituents of stainless stell used for the liner. Molybdenum and tungsten are currently used as limiter materials. As these high-Z elements lead to high radiation losses one discusses to employ boron- and titanium carbids for the limiter which will consequently lead to boron, titanium and carbon impurities.

Fig. 8 shows measured power losses of a θ-pinch as a function of time compared with model calculations assuming that the radiation losses are essentially due to resonance radiation of oxygen (DÜCHS et al. [55]). The populations of OI and OII were assumed to correspond Saha equilibrium, the remaining charge states were calculated from the corona equations. No dielectronic recombination was taken into account.

Fig. 9 shows the temporal evolution of the O^{5+} particle density in the TFR TOKAMAK as a function of time and radial distance. The absolute number density was calculated from ABEL-inverted line intensity measurements of the O VI line λ = 1032 Å (TFR-group [56]). Initially the impurities are nearly uniformly distributed across the dicharge (see example for t = 6 ms). After the initial ionization phase, O^{5+} is concentrated in a relatively thin shell the radial position of which changes with time. The location of the shell corresponds to the region where the electron temperature is of the order of or slightly lower than the ionization potential of O^{5+}. The variation of the shell position with time corresponds to the electron temperature evolution. Later on, when the plasma current has reached its plateau value, the different ionization stages of oxygen follow each other in small distances (see e.g. Fig. 3 in [56]). The peak density of O^{5+} ions is 10^{12} cm^{-3}. This value is obtained from absolute line intensity measurements together

with independent measurements of $T_e(r)$ and $n_e(r)$ and assuming that coronal excitation applies. The measurements indicate that the electron density in the plasma periphery (r = 10 ... 20 cm) is entirely determined by oxygen impurities liberated on the walls and diffusing into the plasma.

For a plasma current of 300 KA and a magnetic field of 50 KG, Mo^{30+} ions were observed in the central part of the TFR machine. From absolute line intensity measurements, a Mo^{30+} ion density of approx. $3 \cdot 10^{10}$ cm^{-3} was deduced [56]. As nothing is known about the atomic datae, this value must be considered as preliminary. It may be correct within a factor of two or of ten. As the electron density in the center is $3 \cdot 10^{13}$ cm^{-3}, an impurity level of $3 \cdot 10^{10}$ cm^{-3} for Mo^{30+} would correspond to 1 °/₀₀ contamination by molybdenum. The Fig. 10 shows the temporal evolution of the measured photon fluxes of three different Mo^{z+} lines and two different current plateau .

Fig. 11 shows the X-ray spectrum of the ST-TOKAMAK Princeton (Von GOELER et al. [57]) measured by pulse height analysis. Two distinct slopes of the continuous background radiation correspond to a thermal contribution and a runaway tail due to fast electrons. Superposed are lines originating from wall and limiter materials. In this soft X-ray region, recombination radiation due to high-z-impurities constitutes the dominant fraction of the total continuum radiation. The dominant impurities are oxygen and iron. Spectroscopic analysis led to the result that the limiter material does not dominate over iron used for the liner. For z_{eff}, values ranging from 2.4 to approximately 10 were deduced from spectroscopic measurements.

6. IONIZATION BALANCE OF IMPURITIES.

In the energy balance of impurities intervene the relative abundances $n_k^z / \sum_z n_k^z$ of charge states z of a chemical element k considered. To a first approximation one can assume that the divergency of the particle flux is negligibly small and that ionization and recombination rates are locally balanced. This is the so-called homogeneous stationary state model. For high-temperature low density plasmas the corona model applies. In Fig. 4, and in the Figs. 12 to 21 the relative abundances are shown for the prominent plasma impurities, calculated by different authors for corona conditions. In all cases a Maxwell distribution has been assumed.

CARBON : Figs. 4 and 12.

In Fig. 4, z = 1 and z = 2 have equal abundances at $T_e = 3 \cdot 10^4$ K, in Fig. 12 the temperature is $1.4 \cdot 10^4$ K. In Fig. 4, the maxima for z = 1,2 and 3 occur at $T_e = 2 \cdot 10^4$, $5 \cdot 10^4$, and $8.6 \cdot 10^4$ K respectively. In Fig. 12, the corresponding values are $T_e = 2 \cdot 10^4$, $8 \cdot 10^4$, $1.2 \cdot 10^5$ K. For a given temperature, the abundances can differ by orders of magnitude, e.g. in Fig. 4, $n^2/n^3 \simeq 10^{-1}$ at $T_e = 1 \cdot 10^5$ K, whereas in Fig. 12 the value is $n^2/n^3 \approx 1$ at the same temperature.

OXYGEN : Figs. 13, 14 and 15.

The Fig. 13 shows the influence of the electron density on the ionization equilibrium due to the density dependence of the dielectronic recombination coefficient, in Fig. 14 one can see how the inclusion of dielectronic recombination modifies the ionization balance. The curves in Fig. 15 refer to calculations in which no density corrections of the dielectronic recombination coefficient were made. The results of the TFR group [60] and of JORDAN [50] agree rather well, their results deviate from those of BURGESS and SUMMERS [46] especially in the temperature values for which maximum abundances are obtained. (See also the comment on page 520 of [50]).

SILICIUM : Fig. 16

This figure shows the influence of dielectronic recombination on the ionization equilibrium of silicium. The ionization equilibrium has also been calculated by TUCKER and GOULD [76] and ANSARI et al. [77]. In ANSARI et al. one also finds ionization equilibria for C,N,O,Ne,Mg,Si,S, and Fe and a general disucssion of formulas for α_{diel}.

IRON : Figs. 17, 18 and 19.

The Fig. 17 shows the results of JORDAN's calculations [50] with and without dielectronic recombination, in the Figs. 18 and 19 we show those of the TFR group [60] and of BRETON et al. [61]. These figures are of special interest, since they reveal how sensitive the results depend on the assumptions made. Comparison of the Figs. 17b and 18b (balance without dielectronic recombination) shows that there is broad agreement of the results. But when one considers the abundances

at a given temperature one discovers discrepancies. The following table 1 gives the temperatures T_e for maximum relative abundance of particles in charge state z. The discrepancies between Figs. 17b and 18b are only due to discrepancies in the rate coefficients for electronic ionization and radiative recombination.

TABLE 1

Temperatures T_e [K] at which maximum relative abundances of Fe^{z+} occur.

Charge state z	Fig. 17b Ref.[50]	Fig. 18b Ref.[60]	Fig. 17a Ref.[50]	Fig. 18a Ref.[60]	Fig. 19 Refs.[61][62]
14	$1.2\cdot10^6$	$1.2\cdot10^6$	$1.9\cdot10^6$	$2.3\cdot10^6$	$2.6\cdot10^6$
15	$1.6\cdot10^6$	$1.6\cdot10^6$	$2.5\cdot10^6$	$3.0\cdot10^6$	$3.7\cdot10^6$
16	$2.3\cdot10^6$	$2.5\cdot10^6$	$(3-6)\cdot10^6$	$3.5\cdot10^6$	$5.1\cdot10^6$
17	$4.1\cdot10^6$	$3.6\cdot10^6$	$8.0\cdot10^6$	$4.5\cdot10^6$	$7.8\ 10^6$
18	$4.6\cdot10^6$	$4.2\cdot10^6$	$9.5\cdot10^6$	$5.3\cdot10^6$	$9.3\cdot10^6$
19	$9.5\cdot10^6$	$5.1\cdot10^6$	$1.1\cdot10^7$	$6.2\cdot10^6$	$1.1\cdot10^7$
20		$6.1\cdot10^6$	$1.2\cdot10^7$	$7.2\cdot10^6$	$1.2\cdot10^7$
21		$7.0\cdot10^6$	$1.5\cdot10^7$	$8.0\cdot10^6$	$1.4\cdot10^7$
22		$8.6\cdot10^6$	$2.5\cdot10^7$	$9.5\cdot10^6$	$1.6\cdot10^7$
23		$1.2\cdot10^7$		$1.3\cdot10^7$	$1.8\cdot10^7$
24		$3.3\cdot10^7$		$3.3\cdot10^7$	$3.5\cdot10^7$
25		$1.0\cdot10^8$		$1.2\cdot10^8$	$1.1\cdot10^8$
26		$>3\cdot10^8$			$>3\cdot10^8$

Substantial discrepancies exist between the abundances of Fig. 17a and Fig. 18a including dielectronic recombination(see table 1 and consider especially the abundances for z=15 and z=16). In the calculations which lead to Fig. 18a only those autoionizing states have been considered which belong in the Li- to F- isoelectronic sequence to one excited state due to a transition of type (x=1 for B, x=5 for F ,see Table 2)

$$1s^2\ 2s^2\ 2p^x \longrightarrow 1s^2\ 2s\ 2p^{x+1} \qquad (62)$$

of the inner electron. In the calculations which yield the results of

Table 2

Electron configuration in the isoelectronic sequence.

sequence	K 1s	L 2s	L 2p	M 3s	M 3p	M 3d	N 4s	N 4p	N 4d
H	1								
He	2								
Li	2	1							
Be	2	2							
B	2	2	1						
C	2	2	2						
N	2	2	3						
O	2	2	4						
F	2	2	5						
Ne	2	2	6						
Na	2	2	6	1					
Mg	2	2	6	2					
Al	2	2	6	2	1				
Si	2	2	6	2	2				
P	2	2	6	2	3				
S	2	2	6	2	4				
Cl	2	2	6	2	5				
A	2	2	6	2	6				
K	2	2	6	2	6		1		
Ca	2	2	6	2	6		2		
Sc	2	2	6	2	6	1	2		
Ti	2	2	6	2	6	2	2		
V	2	2	6	2	6	3	2		
Cr	2	2	6	2	6	5	1		
Mn	2	2	6	2	6	5	2		
Fe	2	2	6	2	6	6	2		
Co	2	2	6	2	6	7	2		
Ni	2	2	6	2	6	8	2		
Cu	2	2	6	2	6	10	1		
Zn	2	2	6	2	6	10	2		
Ga	2	2	6	2	6	10	2	1	
Ge	2	2	6	2	6	10	2	2	

sequence	shell	N 4s	N 4p	N 4d	N 4f	O 5s	O 5p	P 6s
As	KLM	2	3					
Se	KLM	2	4					
Br	KLM	2	5					
Kr	KLM	2	6					
Rb	KLM	2	6			1		
Sr	KLM	2	6			2		
Y	KLM	2	6	1		2		
Zr	KLM	2	6	2		2		
Nb	KLM	2	6	4		1		
Mo	KLM	2	6	5		1		
⋮								

sequence	shell	O 5s	O 5p	O 5d	P 6s	P 6p	P 6d	Q 7s
Hf	KLMN	2	6	2	2			
Ta	KLMN	2	6	3	2			
W	KLMN	2	6	4	2			
⋮								

Fig. 17a obviously additional transitions have been accounted for. (In the publication [50] the levels of the inner excited electron have not been mentioned). When one takes for the inner electron the two following excitation transitions into account (see Table 2)

$$1s^2\ 2s^2\ 2p^x \rightarrow 1s^2\ 2s\ 2p^{x+1}$$
$$1s^2\ 2s^2\ 2p^x \rightarrow 1s^2\ 2s\ 2p^x\ 3d \qquad (63)$$

the abundances of Fig. 18a change into those displayed in Fig. 19. They are now much similar to those of Fig. 17a and also agree relatively well with the results obtained by MERTS et al. [51]. These latter authors also accounted for the two transitions (6 3). Abundances of Fe^{8+} to Fe^{16+} have also been calculated by BELY [78].

In principle, the inner electron has the possibility to make many other transitions (and also simultaneous excitation of two inner electrons is virtually possible). This leads to further doubly (and triply) excited states which will affect the dielectronic recombination coefficient too. Corresponding numerical studies do not yet exist.

MOLYBDENUM : Figs. 20 and 21.

The only existing calculations are those of the TFR group [60][63]. The ionization balance without dielectronic recombination is displayed in Fig. 20. When dieletric recombination is included one obtains the results of Fig. 21. For all charge states from z = 24 to z = 40 two resonance transitions of the inner electron have been taken into account.

HYDROGENIC IONS (z = 2 through z = 25)

Dieletronic recombination coefficients α_{diel} for hydrogenic ions are given in graphical form in a special Culham report (DONALDSON [64]) including the electron density effects, see also DONALDSON and PEACOCK [65]. In this context, the tables given by DRAWIN and EMARD [69] and by BURGESS and SUMMERS [79] may also be useful.

Further useful references are Van RENSBERGEN [80] and SHORE [81]. The dielectronic recombination coefficients have not yet been measured directly, however, there are sufficient experimental indications that dielectronic recombination is the dominant recombination process in high-temperature low-density plasmas, see e.g. GABRIEL et al. [82] - [85] and POSPIESZCZYK [86].

7. RADIATION POWER LOSSES.

When the ion ground state densities are known one can calculate the total power loss P_{total}. For a given temperature, the results depend not only on the dielectronic recombination coefficients (which determine P^{diel}) but also on the excitation coefficients $C^{z}_{k,1j}$. As the latter are not well known and because of the fact that bound-bound transitions dominate all other loss mechanisms, all power loss calculations must therefore be considered as

estimates.

For a given element and within the validity of the corona model one obtains "reduced" power loss curves when the actual power loss P is divided by n_e and the impurity density n_{IMP}. Corresponding curves for oxygen, iron and molybdenum are given in Figs. 22 to 24.

Both the impurity radiation losses and the hydrogenic bremsstrahlung rates are volume losses both of which vary in the same way with n_e. One therefore obtains a direct information about the influence of impurities on the radiation losses compared to a pure hydrogen plasma when one calculates the ratio

$$R = \frac{P^{IMP}_{total}/n_e n_{IMP}}{P^{H^+}_{brems}/n_e n_{H^+}} \qquad (64)$$

Using the results of Figs. 22, 23 and 24 for oxygen, iron, molybdenum and of the Fig. 7 for hydrogen one obtains the solid curves of Fig. 25. The horizontal lines at high temperatures indicate how much the bremsstrahlung rate of a "hydrogenic impurity plasma" exceeds the one of a pure hydrogen plasma, on an atom-for-atom basis. (This is just the coefficient Z^2). When one extrapolates to impurities of higher Z-number one obtains for tungsten the broken curve. Also indicated are the contributions originating from selected ions (curves·-·-·-) according to POST [16]. Finally we have indicated the temperature region of a future D-T reactor. One sees that an impurity concentration of 1 °/₀₀ of the *heavy elements* cannot be admitted when one wants to realize an economically working fusion reactor. One also sees *how important it is to know in this region all relevant atomic datae with a precision substantially better than a factor of two.*

8. INFLUENCE OF DIFFUSION

So far it has been assumed that the ion distribution is independent of the velocity with which the impurities penetrate into the plasma (so-called static local ionization - recombination equilibrium). However, as may be seen from Eq. (57) the impurity flux $\underset{\sim}{\psi}^z_{k,l}$ enters into the rate equations which determine the ion densities of the different charge states. Thus, all above given ion abundances refer to a static local corona equilibrium and are only valid in the limit where $\partial n/\partial t \to 0$ and $\underset{\sim}{\psi} \to 0$.

The Figs. 26 and 28 show how the radial abundances are modified by a constant inward diffusion velocity of $v^{\circ} = 1 \cdot 10^{3}$ cm/sec. The curves refer to the radial electron density and electron temperature profiles of the Tokamak TFR during the current plateau (plasma current 140 KA, magnetic field 26 KG, the profiles are given in Ref. [61]). The broken curves indicate how the ion distribution would look in the case of static local corona equilibrium. The solid curves are obtained when a stationary state ($\partial n/\partial t = 0$) is reached with a superposed diffusion flux. The ions penetrate now much deeper into the plasma than in case of vanishing velocity, since they have not sufficient time to reach the "static" ionization-recombination equilibrium locally. A consequence is that the radiation losses increase, since the ions of low charge state "see" electron densities and temperatures at which they would already have disappeared in the case of static corona equilibrium. Fig. 27 represents the photon flux which corresponds to the dynamic dictribution given in Fig. 26 and supposing $\psi_{imp} = 1$ particle/cm^{2}sec. The following lines have been considered in the calculations : OII λ = 833 Å, OIII λ = 703 Å, OIV λ = 790 Å, OV λ = 630 Å, OVI λ = 1033 Å ($2^2P^{\circ} \rightarrow 2^2S$), OVII λ = 21.8 Å (singlet-triplet transition $1s\,2p\ ^3P \rightarrow 1s^2\ ^1S$), OVIII Ly$\alpha$.

The diffusion process in TOKAMAK discharges is still very obscur. The recycling mechanism of the impurities is not yet clear. From measurements deduced inward impurity fluxes appear to high to explain the slow increase of the electron density during the current plateau for which a stationary state can be assumed. It has therefore been proposed that the inward diffusion fluxes of particles in the lower charge states are compensated by outward fluxes of highly ionized atoms. These highly ionized atoms have not yet been detected in the plasma periphery. As highly ionized particles are better trapped than atoms of low ion charge the diffusion velocity should decrease when the ion charge increases. It is therefore difficult so see why the highly ionized particles should cross the whole plasma radius with an outward flux equal to the inward flux. Also the energy equation contradicts this effect, since it requires that the ions take with them their internal energy (for O^{8+} ions 1953.26 eV/particle) and the center kinetic energy ((3/2)kT/particle), leading to a loss rate too high compared to radiation losses. It might be that a solution to this problem is the inclusion of charge exchange processes with highly excited impurity ions formed during dielectronic recombination (see Section 9.d.).

The solid curves in Figs.26 and 28 have been calculated in the following

manner: In the steady state and for a cylindrical plasma geometry the system of equations (57) reduces to

$$\begin{aligned}
&\frac{1}{r}\frac{d}{dr}(r\psi^0) = \frac{v^0}{r}\frac{d(rn^0)}{dr} = S^0 n^0 n_e - \alpha^1 n^1 n_e \\
&\vdots \\
&\frac{1}{r}\frac{d}{dr}(r\psi^z) = \frac{v^0}{r}\frac{d(rn^z)}{dr} = S^{z-1} n^{z-1} n_e - S^z n^z n_e + \alpha^{z+1} n^{z+1} n_e - \alpha^z n^z n_e \\
&\vdots \\
&\frac{1}{r}\frac{d}{dr}(r\psi^Z) = \frac{v^0}{r}\frac{d(rn^Z)}{dr} = -S^{Z-1} n^{Z-1} n_e + \alpha^Z n^Z n_e
\end{aligned} \tag{65}$$

where Z is the charge number of the bar nuclei. In the radial fluxes $\psi^z = v^0 n^z(r)$ the diffusion velocity v^0 is assumed to be the same for all particles. ψ^z is positive if the flux is directed inward .Since the impurities enter into the plasma at r = a in charge state z = 0, the boundary conditions are

$$\left.\begin{aligned}
&\psi_{imp}\, 2\pi a = 2\pi a\, n^0(a)\, v^0 \\
&n^z(a) = 0 \quad \text{of} \quad z > 0
\end{aligned}\right\} \tag{66}$$

with ψ_{imp} in (atoms/cm^{2}sec). Summing up the Z+1 equations of system (65) one gets the continuity condition

$$2\pi r\, v^0 \sum_z n^z(r) = 2\pi a \psi_{imp} \tag{67}$$

It has further been assumed that everywhere in the plasma the condition $\sum z n^z(r) \ll n_e$ is fulfilled. With the boundary conditions $n^0(a) = 1$, and $n^z(a) = 0$ if $z > 0$, the system (65) can easily be solved for given distributions $T_e(r)$ and $n_e(r)$. In the corona regime and under the assumption that only one level j is excited for each ion stage, the photon production rate due to the presence of ions of charge state z thus becomes (see also Eq. (66)) :

$$\mathcal{P}^z = C^z_{j1} n^z_1 n_e \tag{68}$$

Multiplying by $h\nu^z_{ij}$ yields the radiation power with which these ions contribute to the total power loss. The ions of charge state Z finally leave the plasma center, travers the column and become neutralized on the wall.

9. SOME CRITICAL REMARKS

So far we have only considered the ionization balance and radiation losses in the frame of the corona regime. All energy balance considerations as well as spectroscopic determinations of impurity levels are based on the assumption that the electrons have a Maxell distribution. This has never been checked experimentally. It is assumed that cascade processes can be neglected. It is assumed that it suffices to account only for one or two excited states of the inner electron in the calculation of the dielectronic recombination coefficient. The density dependence of the dielectronic recombination coefficient is generally neglected.

a. Electron energy distribution

The electrons of the high-energy tail are responsable for excitation and ionization. This especially holds for the excitation process during the formation of doubly excited states which lead to dielectronic recombination. When up to 50% of the ohmic power input are lost in form of radiation one must seriously doubt the validity of a Maxwell distribution for the electrons. One generally justifies the Maxwell distribution by applying the usual relation for equi-partionning around an energy of kT_e.

However, one does not only need a Maxwell distribution at $E \approx kT_e$, but up to much higher energies, i.e. beyond energies which correspond to the most prominent bound-bound and bound-free transitions. It seems useful to solve the Boltzmann equation for the electrons under TOKAMAK conditions including all elastic and inelastic (super-elastic) collision processes in order to see whether deviations from a Maxwell distribution exist or not. Also experimental work should be undertaken in this direction.

b. Corona model.

In the corona model one neglects in the calculation of the ionization balance all intermediate transitions between the ground state and the continuum. In 1963, ATHAY and HYDER [66] have shown that already a two-step ionization process especially in the presence of a metastable state modifies the ionization equilibrium under corona conditions. Calculations have been made for the ions Fe^{9+} to Fe^{14+}. The ionization balance then becomes n_e-dependent. Also the calculations of NUSSBAUM and STOREY (see Fig. 4) go in this direction.

Emission from highly excited levels strongly populated due to the dielectronic recombination process is generally neglected. It seems useful to check whether this simplification is justified or not. MIHALAS, HUMMERS and CONTI [67] have for instance found that the radiation of the NIII lines λλ 4640 and 4097 Å in Of stars is primarily due to dielectronic recombination and not due to excitation from the ground state as was initially assumed.

c. Averageing over velocity distribution function

The excitation and ionization coefficients have a complicated form as a function of energy. The rate coefficients for excitation ($C^z_{k,ji}$) and ionization ($S^z_{k,i}$) are obtained by averageing the cross-sections over the electron velocity distribution. When this averageing is not done correctly one can commit non-negligible errors. Discrepancies between the results of Mc WHIRTER and HEARN [68] and DRAWIN and EMARD [69] for instance must to a large part be imputed to simplifications of the averageing procedure in ref. [68], see also KOHSIEK [70].

d. Dielectronic recombination

The very highly excited levels play an important role in the dielectronic recombination process.As fusion plasmas are submitted to high magnetic fields the latter could have a nonnegligible influence on the dielectronic recombination rates via different effects.The following effects will probably lead to an increase of α_d due to redistribution of l-states:1. Enhanced mutual overlapping of wavefunctions due to ordinary Zeeman-effect,2.due to Lorentz-electric fields created by the particles moving in the confining magnetic field, 3.due to the quasi-static and turbulent electric fields,and due to 4.collisional processes. - On the other hand,lowering of the dielectronic recombination coefficient will take place due to enhanced merging of the high l-states into the continuum as a consequence of the same processes as above.All effects will strongly depend on the stage of ionization. - To the author's knowledge these problems have not yet been treated in the litterature.

e. Charge exchange

It is generally assumed that charge exchange processes can be neglected in the formation of excited states of ions. Recent measurements of the LOUVAIN-group [71] seem to indicate that the excited states of He^+ are strongly populated in the following charge exchange process :

$$H^o(n) + He^{2+} \rightarrow H^+ + He^+ \left\{ \begin{matrix} 2p \\ 3p \\ 4p, \text{ etc.} \end{matrix} \right\} \qquad (69)$$

Due to measurements of the same group the cross-sections for charge exchange processes of type

$$H^o(n) + He^{2+} \rightarrow H^+ + He^+(n') \qquad (70)$$

seem to reach values of the order of 10^{-10} cm^2 for principal quantum numbers

n=11 to n=29.

The question arises whether highly excited states formed during dielectronic recombination can modify the ionization balance and the radiation losses due to reactions of type

$$A^{z+}(n) + B^{(z+2)+}(m) \longrightarrow A^{(z+1)+}(n') + B^{(z+1)+}(m') \qquad (71)$$

This reaction is a generalization of reactions (69) and (70).

Studies of this type of reaction have not yet been undertaken (to the knowledge of the author of the present article).

f. Penning-type ionization

Reactions of type

$$A(1) + B^{o}(n) \rightarrow A^{+} + B^{o}(1) + e^{-} \qquad (72)$$

play an important role in low-pressure discharges. In this case $B^{o}(n)$ represents in general a metastable atom the excitation energy of which is larger than the ionization energy of the ground state atom $A^{o}(1)$.

Due to the strong population of highly excited states during the dielectronic recombination process reactions of type

$$A^{z+}(1) + B^{z'+}(n) \rightarrow A^{(z+1)+} + B^{z'+}(1) + e^{-} \qquad (73)$$

between highly excited impurity atoms might eventually contribute to the ionization balance. Reaction (73) is a generalization of reaction (72).

g. Further problems

Impurities have still other influences on the properties of high-temperature plasma. Some of them have been discussed in a special report (EQUIPE TFR [72]):

- influence on the energy balance of ions ;
- influence on ion temperature measurement by means of neutrals leaving the plasma ;
- influence on heating by neutral beam injection ;
- influence on heating by high-frequency waves ;
- influence on the ion confinement time ;
- influence on electrical resistivity and, thus, on the peak current ;

To these we add the energy transport by impurity driven modes (very recently studied in a theoretical paper by COPPI et al. [73]) and the modification of the spatial distribution of protons (deuterons) in the presence of relatively small amounts of light impurities (DNESTROVSKIJ et al. [74]).

At higher densities (for instance in machines working with cold gas blankets) radiation transport may play an important role in the general energy loss mechanism.

1. CONCLUSION

Impurities in present high-temperature plasmas and especially in TOKAMAK machines have a great influence on the power balance, since they convey out energy by radiation which is not reabsorbed in the plasma. When the impurity level is not reduced to very low concentrations it will be difficult to realize economically working D-T fusion reactors. Using presently known cross-sections it is possible to estimate the radiation limits to TOKAMAK operation. The essential results are summarized in Fig. 25 from which can be concluded that in a future fusion reactor the impurity concentration of the heavy elements iron and molybdenum must be as low as 10^{-3} to 10^{-4}. This is in agreement with recent calculations of GIBSON [75]. When tungsten is used as wall or limiter material the impurity concentration must be less than 10^{-5}.

In present machines one finds only a limited number of impurity elements, namely

C(Z=6) ; O(Z=8) ; Al(Z=13) ; Si(Z=14);
Cr(Z=24) ; Fe(Z=26) ; Co(Z=27) ; Ni(Z=28) ;
Mo(Z=42) ; W(Z=74) ,

to which we have in the near future probably to add

B(Z=5) and Ti(Z=22).

All originate from the wall and limiter materials used. Spectral lines belonging to the different ionization stages of these elements have been detected spectroscopically. Absolute intensity measurements have led to "order of magnitude estimates" of the impurity concentrations using for the excitation coefficients scaling laws and assuming a Maxwellian velocity distribution.

Bolometric measurements have led in some cases to power losses due to impurity radiation which corresponds to approximately 10% to 50% of the ohmic input power.

Ionization balance calculations of different authors lead for the same parameters to different results because of a different choice for the cross-sections and of different assumptions about the essential physical processes intervening in the ionization-recombination mechanism.

For the mentioned elements one needs for all ionization stages the following atomic datae :

a. the exact ionization energies for all possible ground state configurations ;

b. the exact ionization energies of the lower lying excited states, especially of metastable levels ;

c. the wavelengths of the most prominent lines in the vacuum ultraviolet and in the soft X-ray regions ;

d. the wavelengths of transitions originating from autoionizing levels ;

e. the excitation and ionization cross-sections for electron collisions. It suffices to have the values for the states mentioned under a., b. and d. ;

f. the radiative recombination coefficients ;

g. the n_e-dependent dielectronic recombination coefficients ;

h. the Einstein coefficients for the most prominent transitions and the Einstein coefficients of lines originating from auto-ionizing levels.

i. the knowledge of charge exchange cross-sections for highly excited levels populated due to the dielectronic recombination process should be profitable for future ionization and power balance calculations.

j. the transport properties for all ionization stages and for well-defined plasma conditions.

It is the author's opinion that a precision of a factor of two (i.e. of $^{+\ 100\%}_{-\ 50\%}$*) is by far not sufficient for future work. Due to the large number of different ionization stages there can occur accumulation of errors in the same direction when one calculates for instance the penetration of the impurities into the plasma. - Furthermore, the precision of excitation cross-sections and Einstein coefficients enters linearly into the accuracy to which the impurities are deduced from spectral line intensity measurements.*

When one requires for the calculation of the degree of ionization a precision of $\pm$ *20%, the ionization coefficients and the radiative plus dielectronic recombination coefficients must each be known to an accuracy of* $\pm$ *10%.*

Since possible deviations from Maxwell distribution also enter into the error calculation, the relevant cross-sections must be known to an accuracy of better than ± 10%. When one is contented with a precision of ± 10% for the spectroscopically determined impurity level one has to require at least an accuracy of ± 5% for the excitation cross-section and for the Einstein coefficients, since also experimental errors must be accounted for.

It follows from these considerations that a quantitative knowledge of impurity effects and the impurity levels depends directly on the precision to which the atomic datae are known.

REFERENCES

[1] - POST, R.F., "Controlled Fusion Research - an Application of the Physics of High Temperature Plasmas, Rev. Mod. Phys. 28 (1956) 338-362.

[2] - LAWSON, J.D., Some Criteria for a Power Producing Thermonuclear Reactor, Proc. Phys. Soc. (London) 70 B (1957) 6-10.

[3] - TELLER, E., "Peaceful Uses of Fusion", Proceedings Second United Nations International Conf. on the Peaceful Use of Atomic Energy, Geneva, Sept. 1958, Vol.31, pp.27 to 33, United Nations, Geneva 1958.

[4] - BUTT, E.P., CARRUTHERS, R., MITCHELL, J.T.D., PEASE, R.S., THONEMANN, P.C., BIRD, M.A., BLEARS, J., HARTILL, E.R., "The Design and Performance of"ZETA" ", Proc. of the Second United Nations International Conference on the Peaceful Use of Atomic Energy, Geneva, September 1958, Vol. 32, pp. 42 to 64, United Nations, Geneva 1958.

[5] - THOMPSON, W.B., EDWARDS, S.F., HUBBARD, J. , ROBERTS, S.J., " Theoretical Problems Suggested by ZETA", Proceedings of the Second United Nations International Conference on the Peaceful Use of Atomic Energy Geneva, September 1958, Vol. 32, pp. 65 to 71, United Nations, Geneva 1958.

[6] - TUCK, J.L., "Review of Controlled Thermonuclear Reserach at Los Alamos for mid 1958", Proceedings of the Second United Nations International Conference on the Peaceful Use of Atomic Energy, Geneva, September 1958, Vol. 32, pp. 3 to 25, United Nations, Geneva 1958.

[7] - GOLOVIN, I.N., IVANOV, D.P., KIRILLOV, V.D., PETROV, D.P., RAZUMOVA, K.A., YAVLINSKY, N.A., "Stable Plasma Column in a longitudinal magnetic field", Proceedings Second United Nations International Conference on the Peaceful Use of Atomic Energy, Geneva, September 1958, Vol. 32, pp. 72 to 81, United Nations, Geneva 1958.

[8] - DOLGOV-SAVELIEV, G.G., IVANOV, D.P., MUKHOVATOV, V.S., RAZUMOVA, K.A., STRELKOV, V.S., SHEPELYEV, M.N., YAVLINSKY, N.A., "Investigations of the stability and heating of plasmas in toroidal chambers". Proceedings Second United Nations International Conference on the Peaceful Use of Atomic Energy, Geneva, September 1958, Vol. 32, pp. 82 to 91, United Nations, Geneva 1958.

[9] - AYMAR, R., ETIEVANT, C., HUBERT, P., SAMAIN, A., TAQUET, B., TOROSSIAN, A., "Experimental Studies of the Pinch Phenomenon", Proc. Second United Nations International Conference on the Peaceful Use of Atomic Energy, Geneva, September 1958, Vol. 32, pp. 92 to 99, United Nations, Geneva 1958.

[10] - ANDREOLETTI, J., BRETON, C., CHARON, J., HUBERT, P., JOURDAN, P., VENDRYES, G., "High intensity discharges in deuterium in a metal wall torus", Proc. Second United Nations Intern. Conf. on the Peaceful Use of Atomic Energy, Geneva, September 1958, Vol. 32, pp. 100 to 105, United Nations, Geneva 1958.

[11] - HARDING, G.N., DELLIS, A.N., GIBSON, A., JONES, B., LEES, D.J., Mc WHIRTER, R.W.P., RAMSDEN, S.A., WARD, S., "Diagnostic Techniques Used In Controlled Thermonuclear Research at HARWELL", Proc. Second United Nations International Conference on the Peaceful Use of Atomic Energy, Geneva, September 1958, Vol. 32, pp. 365 to 378, United Nations, Geneva 1958.

[12] - LUKYANOV, S. Yu., SINITSIN, V.I., "Spectroscopic Study of High-Temperature Plasma", Proc. Second United Nations International Conference on the Peaceful Use of Atomic Energy, Geneva, September 1958, Vol. 32 pp. 358 to 364, United Nations, Geneva 1958.

[13] - SPITZER Jr., L., "The Stellarator Concept", Proc. Second United Nations International Conference on the Peaceful Use of Atomic Energy, Geneva September 1958, Vol. 32, pp. 181 to 196, United Nations, Geneva 1958.

[14] - BURNETT, C.R., GROVE, D.J., PALLADINO, R.W., STIX, T.H., WAKEFIELD, K.E., "The Divertor, a Device for Reducing the Impurity Level in a Stellarator", Proc. Second United Nations International Conference on the Peaceful Use of Atomic Energy, Geneva, September 1958, Vol. 32, pp. 225 to 232, United Nations, Geneva 1958.

[15] - KNORR, G., Über den Ionisationszustand und die Ausstrahlung von Fremdgasen in einem Wasserstoffplasma ", Z. Naturforschg. 13a (1958) 941-950.

[16] - POST, R.F., "Impurity Radiation Losses From A High Temperature Plasma", pp. 313 to 346, International Summer Course in Plasma Physics

1960, Risö Report n°18, Danish Atomic Energy Commission, Research Establishment Risö, November 1960, see also : Plasma Physics (J. Nucl. Energy Part C) 3 (1961) 273-286.

[17] - JONES, B.B., WILSON, R., "Spectroscopic Studies of Ion Energies in ZETA", Nucl. Fusion, 1962 Supplement, Part 3 pp. 889 to 893, I.A.E.A. Vienna 1962.

[18] - HOBBS, G.D., Mc WHIRTER, R.W.P., GRIFFIN, W.G., JONES, T.J.L., "The temporal variation of line radiation from impurities in ZETA", Proc. 5th Intern. Conf. Ionization Phenomena in Gases, Munich 1961, H. Maecker (Ed.) Vol. 2, pp. 1965 to 1976, North-Holland, Amsterdam 1962.

[19] - HEARN, A.G., JONES, B.B., RAMSDEN, S.A., "The variation with time of the profiles of spectral lines emitted from a high-current toroidal discharge", Plasma Physics (Nucl. Energy Part C) 4 (1962) 23-30.

[20] - BURTON, W.M., WILSON, R., "Spectroscopic Investigations of Plasma Containement in ZETA", Proc. Physical Soc. London 78 (1971) 1416-1438.

[21] - HOBBS, G.D., ROSE, M.A., "The life history of impurity atoms in a plasma possessing a time varying electron temperature and density", Report CLM-R3, Culham Laboratory, Abingdon (1963).

[22] - HUGHES, T.P., WILLIAMS, R.V., "The spectroscopic measurements of very high temperatures in SCEPTRE", Hilger Journal 1, n°2 (1958) 19-25.

[23] - WILLIAMS R.V., KAUFMAN, S., "The measurement of electron temperature in high temperature plasmas", Proc. Phys. Soc. (London) 75 (1960) 329-336.

[24] - CURZON, F.L., CHURCHILL, R.J., HOWARD, R., "Pressure dependent characteristics of the z-pinch in argon and nitrogen", Proc. Phys. Soc. (London) 81 (1963) 349-355.

[25] - LUK'IANOV, S. Yu., SINITSYN, V.I., "Spectroscopic investigations of intense pulsed discharges in hydrogen", Part I : J. Atomic Energy 1 (1956) 88-96 ; part II : Soviet Physics J.E.T.P. 34 (1958) 587-591.

[26] - GRIEM, H.R., ELTON, R.C., KOLB, A.C., LUPTON, W.H., HINTZ, E., "The PHAROS Experiment for producing high-temperature plasmas".

[27] - KOLB, A.C., "Radiation losses from high-temperature gas discharges", J. Quant. Spectros. Radiat. Tansf. 3 (1963) 365-375.

[28] - HINNOV, E., "Interpretation of observed impurity radiation in a discharge of the C-Stellarator", Phys. Fluids 7 (1964) 130-137.

[29] - HIRSCHBERG, J.G., "Doppler temperatures in the C-Stellarator", Phys. Fluids 7 (1964) 543-547.

[30] - HINNOV, E., "Excitation and ionization rates of neon ions in a Stellarator discharge", J. Opt. Soc. Am. 56 (1966) 1179-1188.

[31] - BRETON, C., PLATZ, P., SCHWOB, J.L., "Etudes de spectroscopie dans T.A. 2000", B.I.S.T. du C.E.A., n°101, Février 1966, pp.1-27. This paper is a summary of all measurements made on T.A. 2000.

[32] - DÜCHS, D., GRIEM, H.R., Computer study of the dynamic phase of a small θ-pinch, Phys. Fluids 9 (1966) 1099-1109.

[33] - LOTZ, W., "Electron impact ionization cross-sections and ionization rate coefficients for atoms and ions", Astrophys. J. Suppl. 14, n°128 (1967) 207-238, see also Z. Phys. 216 (1968) 241-247.

[34] - HINNOV, E., "On multiple ionization in high-temperature plasmas", Report MATT-777, Princeton University, September 1970.

[35] - DECROISETTE, M., PIAR, G., "Influence des impuretés et de l'inhomogénéité d'un plasma sur la mesure de sa température électronique", J. Quant. Spectrosc. Radiative Transfer 12 (1972) 587-601.

[36] - BRETON, C., YA'AKOBI, B., "Plasma confinement in a high density toroidal hard-core device", Plasma Phys. 15 (1973) 1067-1082.

[37] - BURTON, W.M., BUTT, E.P., COLE, H.C., GIBSON, A., MASOW, D.W., PEASE, R.S., WHITEMAN, K., WILSON, R., "Plasma loss in ZETA", Nuclear Fusion, 1962, Suppl, Part 3, pp. 903-919, I.A.E.A. Vienna, 1962.

[38] - ARTSIMOVICH, L.A., "Controlled nuclear fusion research, September 1961 ; Review of Experimental Results", Nuclear Fusion, 1962, Suppl. Part 1, pp.15-20 ; I.A.E.A. Vienna, 1962.

[39] - ECKHARTT, D., KEILHACKER, M., "Neue experimentelle Ergebnisse bei der Erforschung der physikalischen Grundlagen der steuerbaren thermonuklearen Fusion", Die Naturwissenschaften 53 (1966) 571-581.

[40] - DRAWIN, H.W., "Elementary reactions and the interpretation of measurements of chemically reacting non L.T.E. plasmas", J. Pure and Appl. Chem. ___ (1976) ----- (in the press)

[41] - FINKELNBURG, W., MAECKER, H., "Elektrische Bögen und thermisches Plasma", Handbuch der Physik, Vol.22 (S. Flügge, Ed.) Springer Verlag, Berlin-Heidelberg 1956.

[42] - DRAWIN, H.W., "Transport properties of plasmas", Ch.4 in Reactions under Plasma Conditions, Vol.1. (M. Venugopalan, Ed.) ; Wiley-Interscience New York 1971.

[43] - DRAWIN, H.W., "Thermodynamic properties of the equilibrium and non-equilibrium states of plasmas", Ch.3 in Reactions under Plasma Conditions, Vol.1 (M. Venugopalan, Ed.) ; Wiley-Interscience, New York 1971.

[44] - HOLSTEIN, T., "Imprisonment of resonance radiation in gases", Phys. Rev. 83 (1951) 1159-1168, see also Phys. Rev. 72 (1947) 1212.

[45] - DRAWIN, H.W., EMARD, F., "Optical escape factors for bound-bound and free-bound radiation from plasmas", Beiträge aus der Plasmaphysik 13 (1973) 143-168.

[46] - BURGESS, A., SUMMERS, H.P., "The effects of electron and radiation density on dielectric recombination", Astrophys. J. 157 (1969) 1007.

[47] - SUMMERS, H.P., Dielectronic recombination of the solar corona", Monthly Notices Roy. Astron. Soc. 169 (1974) 633-640.

[48] - SUMMERS, H.P., "Tables and graphs of collisional dielectronic recombination and ionization coefficients and ionization equilibria of H-like to Ar-like ions of elements", Special Report, Internal Memo I.M. 367, Astrophysics Research Division, Appleton Laboratory, CULHAM Laboratory, Abingdon/Oxon.

[49] - BURGESS, A., "Dielectronic recombination", in Special Report n°174, Smithsonian Institution, Astrophysical Observatory. Cambridge, Mass. (USA), pp.47-58, May 1965.

[50] - JORDAN, C., "The ionization equilibrium of elements between carbon and nickel", Monthly Not. Roy. Astron. Soc. 142 (1969) 501-521.

[51] - MERTS, A.L., COWAN, R.D., MAGEE, N.H., "The calculated power output from a thin iron-seeded plasma", Special Report LA-6220 MS, Los Alamos Scientific Laboratory, Los Alamos, New Mexico 87545, March 1976.

[52] - NUSSBAUM, H., STOREY, P.J., "The ionization balance of C^{o} to C^{4+} ", Astron. & Astroph. 44 (1975) 321-327.

[53] - SUCKEWER, S., "Population of excited levels of atoms and ions : electron temperature and density from relative line intensities of the C IV , N V , and O VI lines", Phys. Rev. 170 (1968) 239-244.

[54] - HUTCHEON, R.J., McWHIRTER, R.W.P., "The intensities of the resonance lines of highly ionized hydrogen-like ions", J. Phys.(B) 6 (1973) 2668-2683.

[55] - DÜCHS, D., ENGELHARDT, W., KÖPPENDÖRFER, W., "Radiation losses from non-stationary plasmas due to oxygen impurities", Nuclear Fusion 14 (1974) 73-78.

[56] - TFR Group, "Space- and time-resolved study of impurities in TFR TOKAMAK plasmas", Phys. Rev. Lett. 36 (1976) 1306-1309.

[57] - VON GOELER, S., STODIEK, W., EUBANK, H., FISHMAN, H., GREBENSHCHIKOV, S., HINNOV, E., "Thermal X-ray spectra and impurities in the ST-TOKOMAK", Nuclear Fusion 15 (1975) 301-311.

[58] - COX, D.P., TUCKER, W.H., "Ionization equilibrium and radiative cooling of a low-density plasma", Astrophys. J. 157 (1969) 1157-1167.

[59] - HOUSE, L.L., "Ionization equilibrium of the element from H to Fe", Astrophys. J., Suppl. Series 8 (1964) 307-328.

[60] - TFR Group, "Line radiation in the visible and in the ultraviolet in TFR TOKOMAK plasmas", Nuclear Fusion 15 (1975) 1053-1066.

[61] - BRETON, C., DE MICHELIS, C., MATTIOLI, M., "Radiation losses from oxygen and iron impurities in a high temperature plasma", Report EUR-CEA-FC-822, Fontenay-aux-Roses 1976,and Nuclear Fusion 16N°6(1976).

[62] - BRETON,C.,DEMICHELIS,C.,MATTIOLI,M.,"Ionization equilibrium and radiative cooling of a high-temperature plasma",Report EUR-CEA-FC-853 (1976)

[63] - TFR Group, "Ionization equilibrium and radiation losses of molybdenum in a high temperature plasma",Report EUR-CEA-FC 861 (1976),submitted to Plasma Physics.

[64] - DONALDSON, T.P., "Dielectric recombination in laser generated plasmas", Report CLM-R-153, Culham Laboratory, Abingdon/Oxon, March 1976.

[65] - DONALDSON, T.P., PEACOCK, N.J., "Tables for the computation of dielectronic recombination coefficients". J. Quant. Spectr. Radiat. Transfer 16 (1976) 599-604. Two sets of tables are presented which facilitate rapid calculation of hydrogenic ion dielectronic recombination coefficients for ion charge states $z \leq 17$ and $z > 17$. Examples are given for He II, F IX, Ar XVIII, Fe XXVI .

[66] - ATHAY, R.G., HYDER, C.L., "Coronal ionization by two-step collision processes", Astrophys. J. 137 (1963) 21-25.

[67] - MIHALAS, D., HUMMER, D.G., CONTI, P.S., "On the N III λλ 4640,4097 lines in Of stars", Astrophys. J. 175 (1972) L 99-104.

[68] - McWHIRTER, R.W.P., HEARN, A.G., "A calculation of the instantaneous population densities of the excited levels of hydrogen-like ions in a plasma", Proc. Phys. Soc. 82 (1963) 641-654.

[69] - DRAWIN, H.W., EMARD, F., "Instantaneous population densities of the excited levels of hydrogen atoms and hydrogen-like ions in a plasma", Physica (in the press). See also the report EUR-CEA-FC-534, Fontenay-aux-Roses 1970.

[70] - KOHSIEK, W., "Excitations of He^+ in a hollow cathode are discharge", J. Quant. Spectr. Radiat. Transfer 16 (1976) in the press.

[71] - LOUVAIN-la-NEUVE Group, "Formation of highly excited states in charge exchange collisions", presented at the "Colloque sur les états de Rydberg en Physique et Astrophysique", Ecole Normale Supérieure, Paris, June 3, 1976.

[72] - TFR Group, "Rôle des impuretés sur certaines caractéristiques d'un plasma confiné dans un TOKAMAK", Report EUR-CEA-FC-779, Fontenay-aux-Roses, Février 1976.

[73] - COPPI, B., REWOLDT, G., SCHEP, T., "Plasma decontamination and energy transport by impurity driven modes", Phys. Fluids 19 (1976) 1144-1162.

[74] - DNESTROVSKIJ, Yu.N., INOVENKOV, I.N., KOSTOMAROV, D.P., "Calculation of the diffusion of light impurities in TOKAMAKS", Nuclear Fusion 16 (1976) 513-519.

[75] - GIBSON, A., "Radiation limits to TOKAMAK operation", Nuclear Fusion 16 (1976) 546-550.

[76] - TUCKER, W.H., GOULD, R.J., "Radiation from a low-density plasma at $10^6 - 10^8$ °K ", Astrophys. J. 144 (1966) 244-258. In this paper a simple formula for α_{diel} is given and applied to He,C,N,O,Ne,Mg,Si,S .

[77] - ANSARI, S.M.R., ELWERT, G., MÜCKLICH, P., "On dielectronic recombination", Z. Naturforschg. 25a (1970) 1781-1797.

[78] - BELY,O.,"The influence of the autoionization effect on the ionization equilibrium",Ann.d'Astrophysique 30(1967)953-956

[79] - BURGESS,A.,SUMMERS,H.P.,"The recombination and level populations of ions- I:Hydrogen and hydrogenic ions",Mon.Not.Roy.Astron.Soc.174(1976) 345-391

[80] - Van RENSBERGEN,W."The influence of doubly excited levels on the ionization formula for the solar corona",Solar Physics 1(1967)354-360

[81] - SHORE,B.W.,"Dielectronic recombination",Astrophys.J. 158(1969)1205-1218

[82] - GABRIEL,A.H.,PAGET,T.M.,"Measurement and interpretation of dielectronic recombination satellite line intensities",J.Phys. B 5(1972)673-685

[83] - GABRIEL,A.H.,"Dielectronic satellite spectra in the soft X-ray region", Space Science Rev. 13(1972)655-664

[84] -GABRIEL,A.H.,"Dielectronic satellite spectra for highly charged helium-like ion lines,I",Mon.Not.Roy.Astron.Soc. 160 (1972)99-119

[85] - BHALLA,C.P.,GABRIEL,A.H.,PRESNYAKOV,L.P.,"Dielectronic satellite spectra for highly charged helium-like ions-II: Improved calculations",Mon.Not. Roy.Astron.Soc. 172(1975)359-375

[86] - POSPIESZCZYK,A.,"Dielectronic recombination of Ne IX-,F VIII-, and O VII-ions", Astron.&Astrophys. 39(1975)357-370

FIGURES

Fig.1 - Schematic representation of level system and energies adopted in the present paper.

Fig.2 - Saha decrement of the populations of Fe^{7+}, after Burgess and Summers [46]

Fig.3 - Recombination coefficient for the process $Fe^{8+} + e \rightarrow Fe^{7+}$ including dielectronic recombination, after Burgess and Summers [46].

Fig.4 - Ionization balance of carbon in the corona regime, after Nussbaum and Storey [52].

Fig.5 - Boltzmann decrement of the populations of N^{4+} and O^{5+} (spectroscopic notation N V and O VI respectively), after Suckewer [53].

Fig.6 - Intensity ratio of the lines $\lambda = 173$ Å ($3^2d \rightarrow 2^2p$) and $\lambda = 150$ Å ($3^2p \rightarrow 2^2s$) of O VI (Li-like system), after Suckewer [53].

Fig.7 - Radiation loss rate of a pure hydrogen plasma due to bremsstrahlung.

Fig.8 - Radiation loss rate due to oxygen impurities in a fast θ-pinch, after Düchs et al. [55].

Fig.9 - Evolution of O^{5+} ions in the Fontenay-aux-Roses TOKAMAK TFR, after TFR group [56].

Fig.10 - Measured photon flux originating from line emission of Mo-ions in the Fontenay-aux-Roses TOKAMAK TFR, after TFR group [56].

Fig.11 - Measured X-ray spectrum of the Princeton ST - TOKAMAK, after Von Goeler et al. [57].

Fig.12 - Ionization balance (corona regime) of carbon, after Cox and Tucker [58].

Fig.13 - Ionization balance (corona regime) of oxygen, after Burgess and Summers [46] including dielectronic recombination.

Fig.14 - Ionization balance (corona regime) of oxygen, after House [59] without and after Jordan [50] with dielectronic recombination.

Fig.15 - Ionization balance (corona regime) of oxygen including dielectronic recombination, after TFR group [60].

Fig.16 - Ionization balance (corona regime) of silicium after House [59] without and after Jordan [50] with dielectronic recombination.

Fig.17 - Ionization balance (corona regime) of iron, after Jordan [50].
a - including dielectronic recombination,
b - excluding dielectronic recombination.

Fig.18 - Ionization balance (corona regime) of iron, after TFR group [60],
a - including dielectronic recombination;
b - excluding dielectronic recombination;
Only one resonance transition of the inner excited electron has been taken into account. No n_e-dependent corrections made.

Fig.19 - Ionization balance (corona regime) of iron after Breton, Demichelis, and Mattioli [62], including dielectronic recombination. Two resonance transitions of the inner excited electron have been taken into account ; no n_e-dependent corrections made.

Fig.20 - Ionization balance (corona regime) of molybdenum, without dielectronic recombination, after TFR group [60].

Fig.21 - Ionization balance (corona regime) of molybdenum, with dielectronic recombination, after TFR group [63].

Fig.22 - Radiation power due to oxygen impurities, after Breton et al. [61],

Fig.23 - Radiation power due to iron impurities, after Breton et al. [61].

Fig.24 - Radiation power due to molybdenum impurities, after TFR group [63].

Fig.25 - Ratio of power radiated by impurities to power due to bremsstrahlung of a pure hydrogen plasma. For details see text.

Fig.26 - Abundances of oxygen ions in the Fontenay-aux-Roses TOKOMAK TFR. Solid lines are for a constant diffusion velocity of $v^o = 1 \cdot 10^3$ cm/sec, after Breton et al. [61]. Broken curves would be obtained for static ionization-recombination equilibrium using the distribution of Fig.15.

Fig.27 - Photon production rate for the dynamic distribution given by the solid lines of Fig.26 and with an impurity flux of $\psi_{imp} = 1$ particle/cm^2 sec , after Breton et al. [61].

Fig.28 - Abundances of iron ions in the Fontenay-aux-Roses TOKAMAK TFR. Solid lines are for a constant diffusion velocity of $v^o = 1 \cdot 10^3$ cm/sec, after Breton et al. [61]. Broken curves would be obtained for static ionization-recombination equilibrium using the distribution of Fig.19.

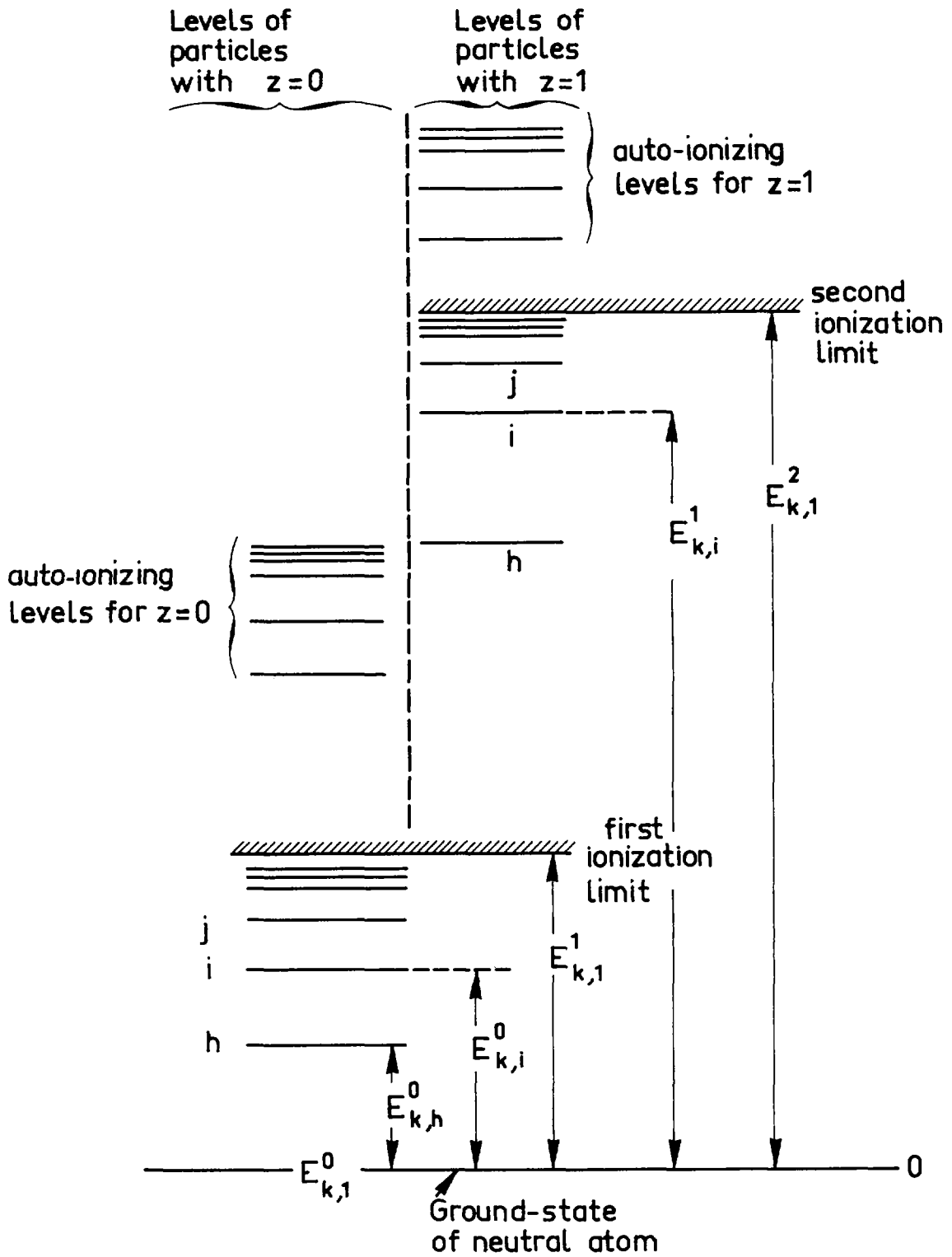
Levels of particles with z=0
Levels of particles with z=1
auto-ionizing levels for z=1
second ionization limit
j
i
h
$E^2_{k,1}$
$E^1_{k,i}$
auto-ionizing levels for z=0
first ionization limit
j
i
h
$E^1_{k,1}$
$E^0_{k,i}$
$E^0_{k,h}$
$E^0_{k,1}$
0
Ground-state of neutral atom

Fig.1

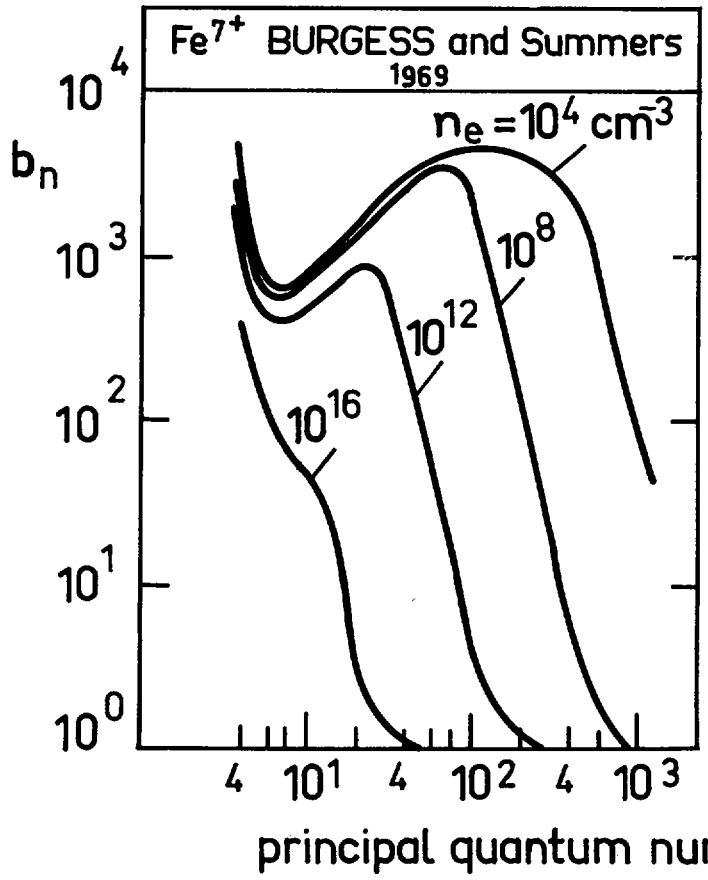
Fe7+ BURGESS and Summers
1969
ne = 10^4 cm^-3
10^8
10^12
10^16
bn
10^4
10^3
10^2
10^1
10^0
4 10^1 4 10^2 4 10^3
principal quantum number n

Fig. 2

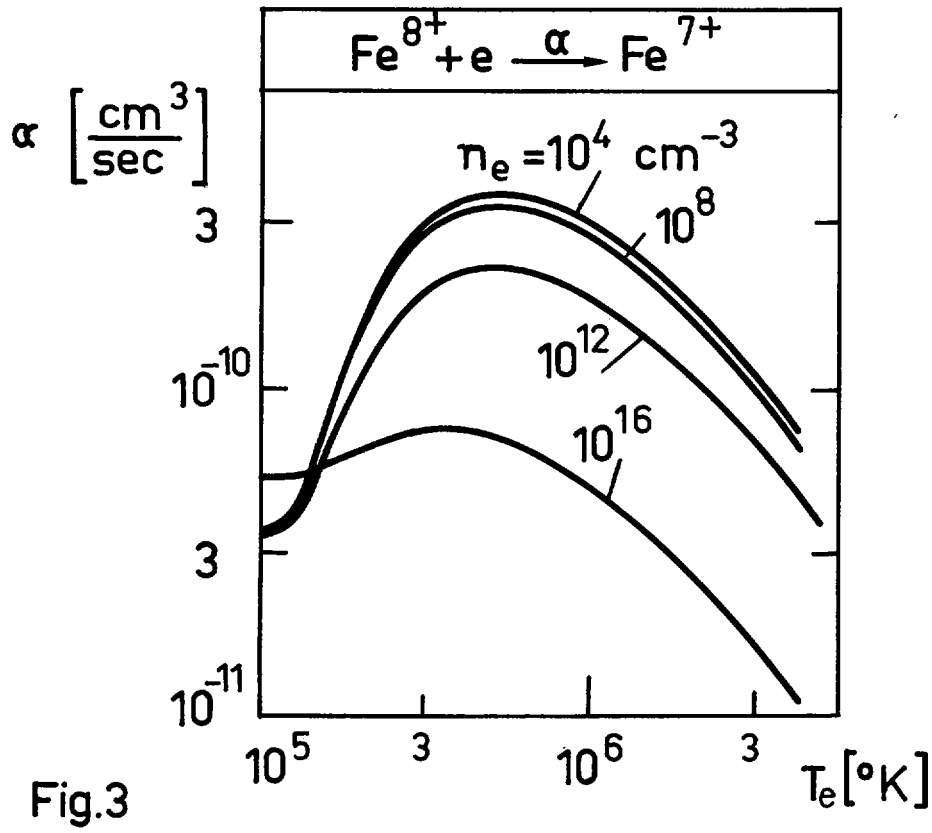
$Fe^{8+} + e \xrightarrow{\alpha} Fe^{7+}$
$\alpha \left[\frac{cm^3}{sec}\right]$
$n_e = 10^4\ cm^{-3}$
10^8
10^{12}
10^{16}
10^{-10}
3
10^{-11}
3
10^5
3
10^6
3
$T_e[°K]$

Fig.3

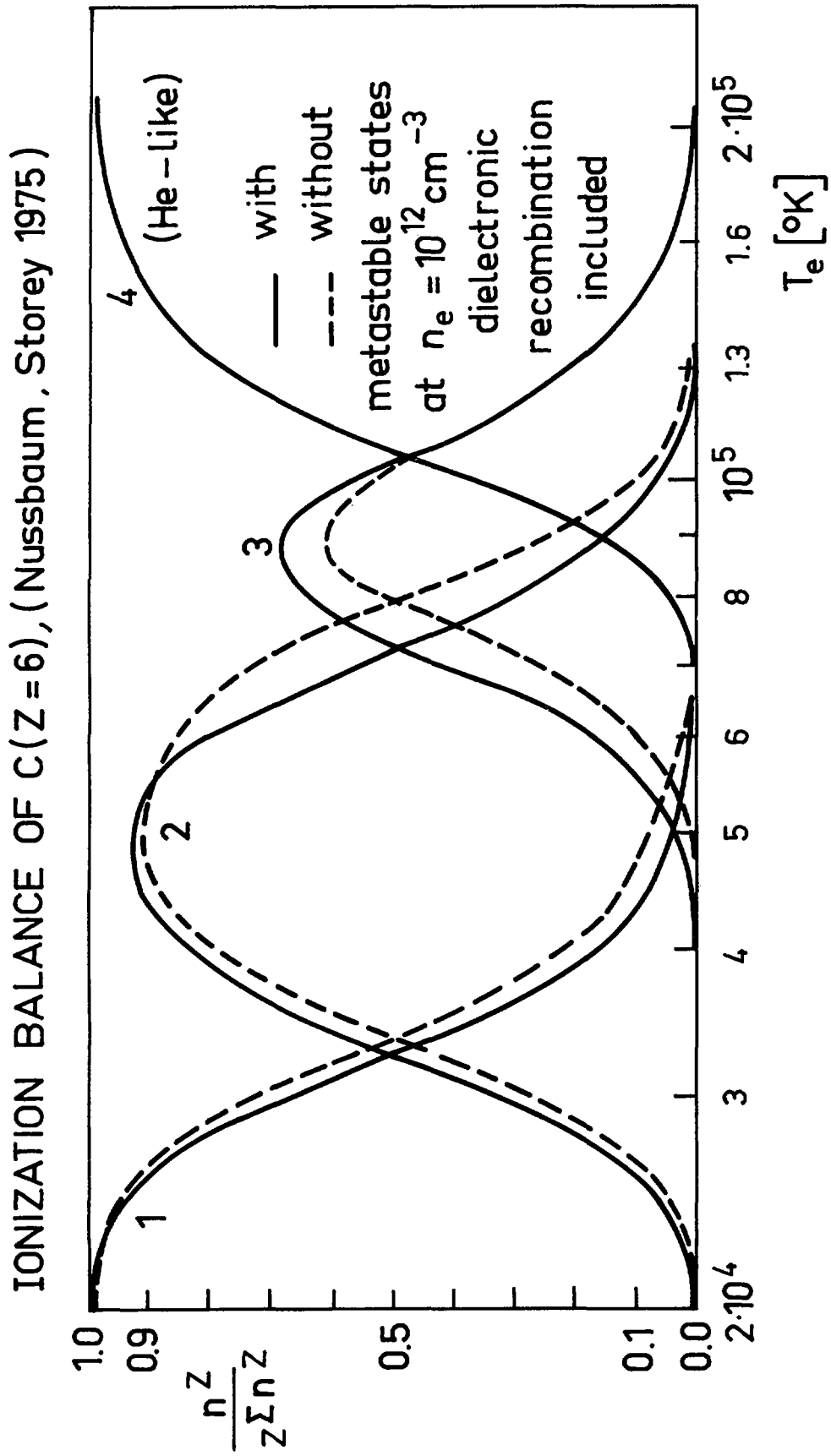
IONIZATION BALANCE OF C(Z=6), (Nussbaum, Storey 1975)
4 (He-like)
with
without
metastable states
at $n_e = 10^{12} cm^{-3}$
dielectronic
recombination
included
1
2
3
4
$\frac{n^Z}{\sum n^Z}$
1.0
0.9
0.5
0.1
0.0
$2 \cdot 10^4$
3
4
5
6
8
10^5
1.3
1.6
$2 \cdot 10^5$
T_e [°K]

Fig. 4

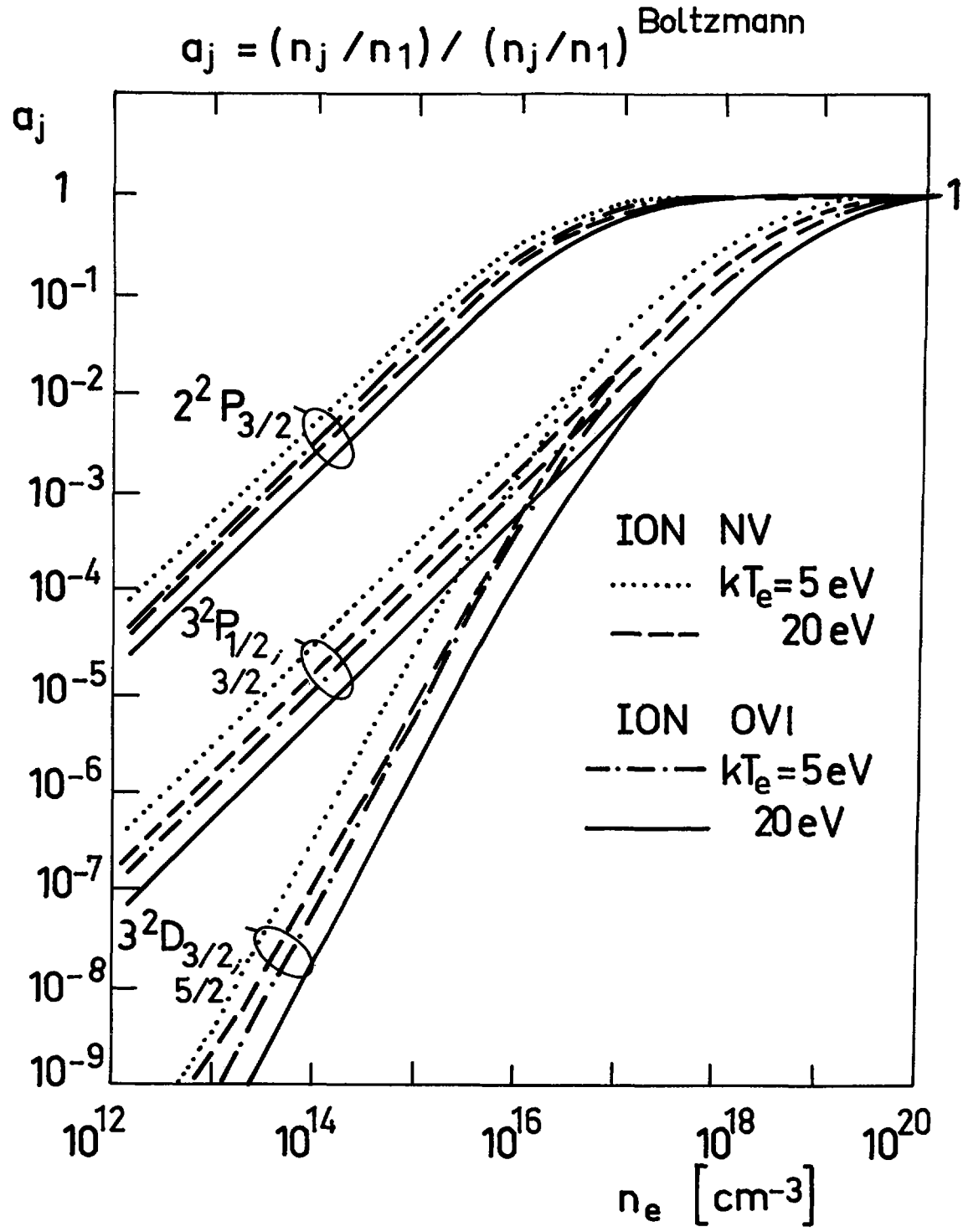
$a_j = (n_j / n_1) / (n_j / n_1)^{Boltzmann}$
a_j
1
10^{-1}
10^{-2}
10^{-3}
10^{-4}
10^{-5}
10^{-6}
10^{-7}
10^{-8}
10^{-9}
$2^2P_{3/2}$
$3^2P_{1/2,}$
3/2
$3^2D_{3/2,}$
5/2
ION NV
kT_e=5 eV
20 eV
ION OVI
kT_e=5eV
20eV
10^{12}
10^{14}
10^{16}
10^{18}
10^{20}
n_e [cm^{-3}]

Fig.5

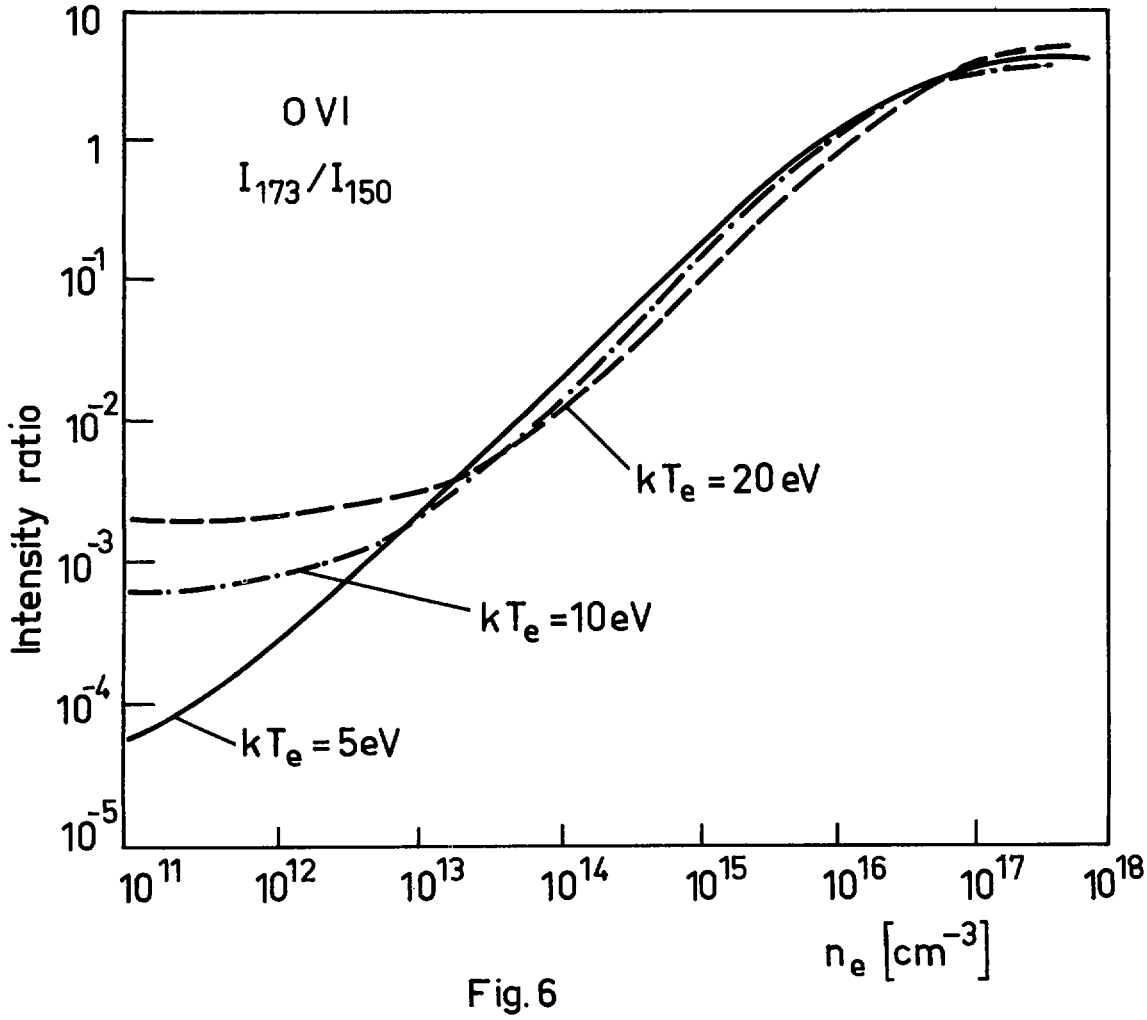
10
1
10^{-1}
10^{-2}
10^{-3}
10^{-4}
10^{-5}
O VI
I_{173}/I_{150}
Intensity ratio
$kT_e = 20\,eV$
$kT_e = 10\,eV$
$kT_e = 5eV$
10^{11}
10^{12}
10^{13}
10^{14}
10^{15}
10^{16}
10^{17}
10^{18}
$n_e\ [cm^{-3}]$

Fig. 6

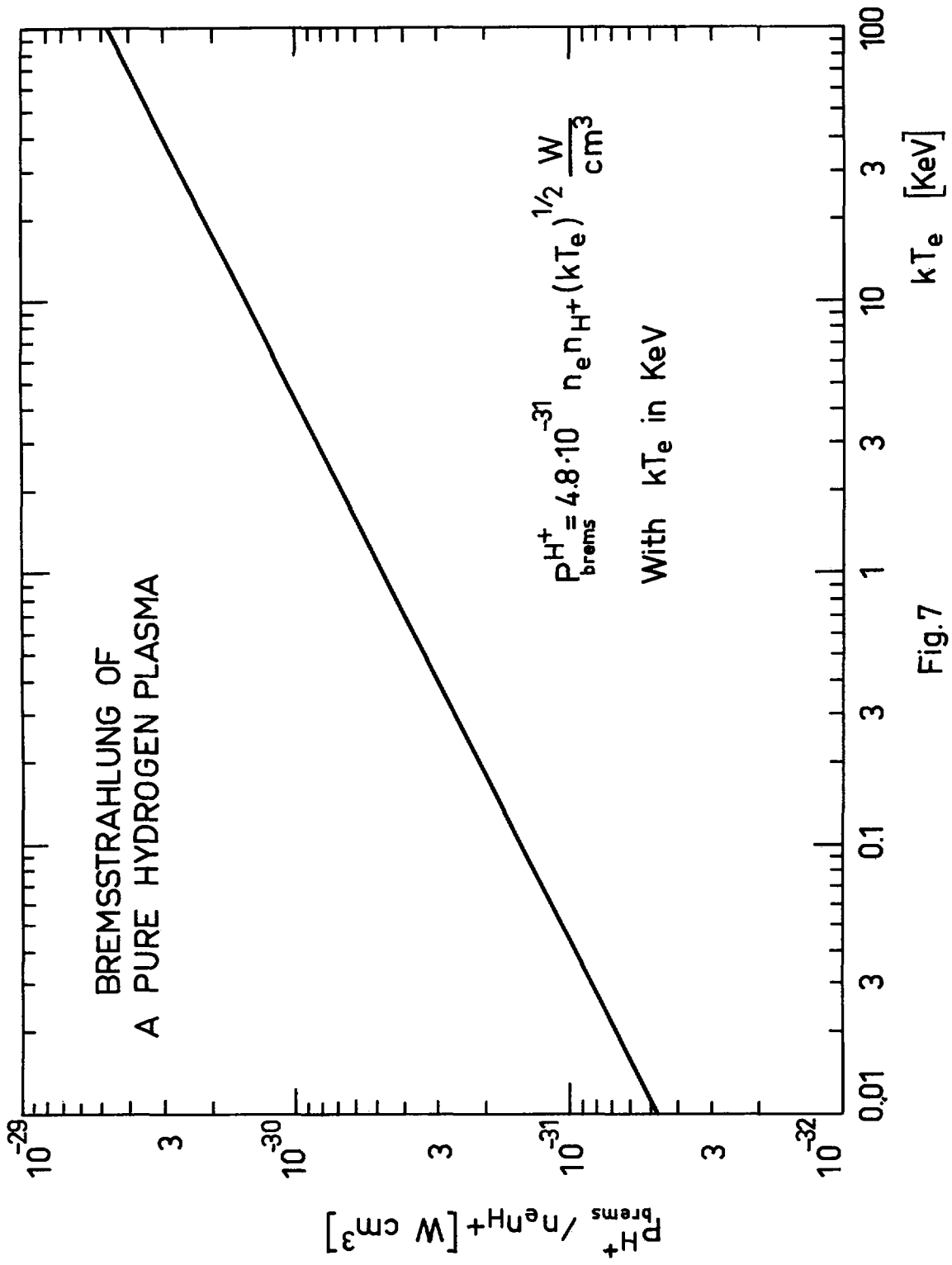
BREMSSTRAHLUNG OF
A PURE HYDROGEN PLASMA
$P^{H^+}_{brems} = 4.8 \cdot 10^{-31} n_e n_{H^+} (kT_e)^{1/2} \frac{W}{cm^3}$
With kT_e in KeV
$P^{H^+}_{brems} / n_e n_{H^+}$ [W cm³]
kT_e [KeV]
10^{-29}
10^{-30}
10^{-31}
10^{-32}
3
0,01
0.1
1
10
100

Fig.7

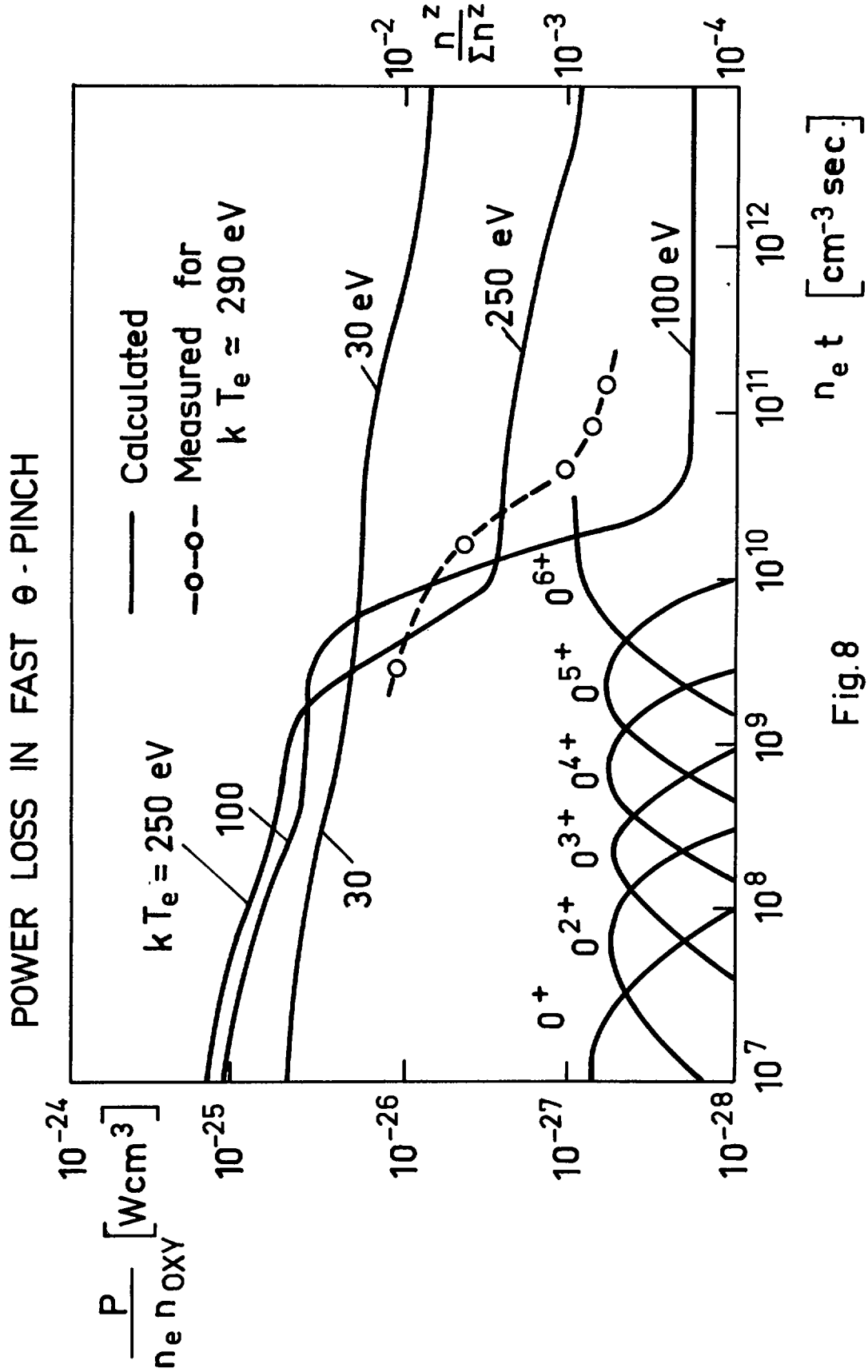
POWER LOSS IN FAST θ - PINCH
Calculated
Measured for
k Te ≈ 290 eV
k Te = 250 eV
100
30
30 eV
250 eV
100 eV
O+
O2+
O3+
O4+
O5+
O6+
P / ne nOXY [Wcm3]
n z / Σn z
ne t [cm-3 sec]

Fig. 8

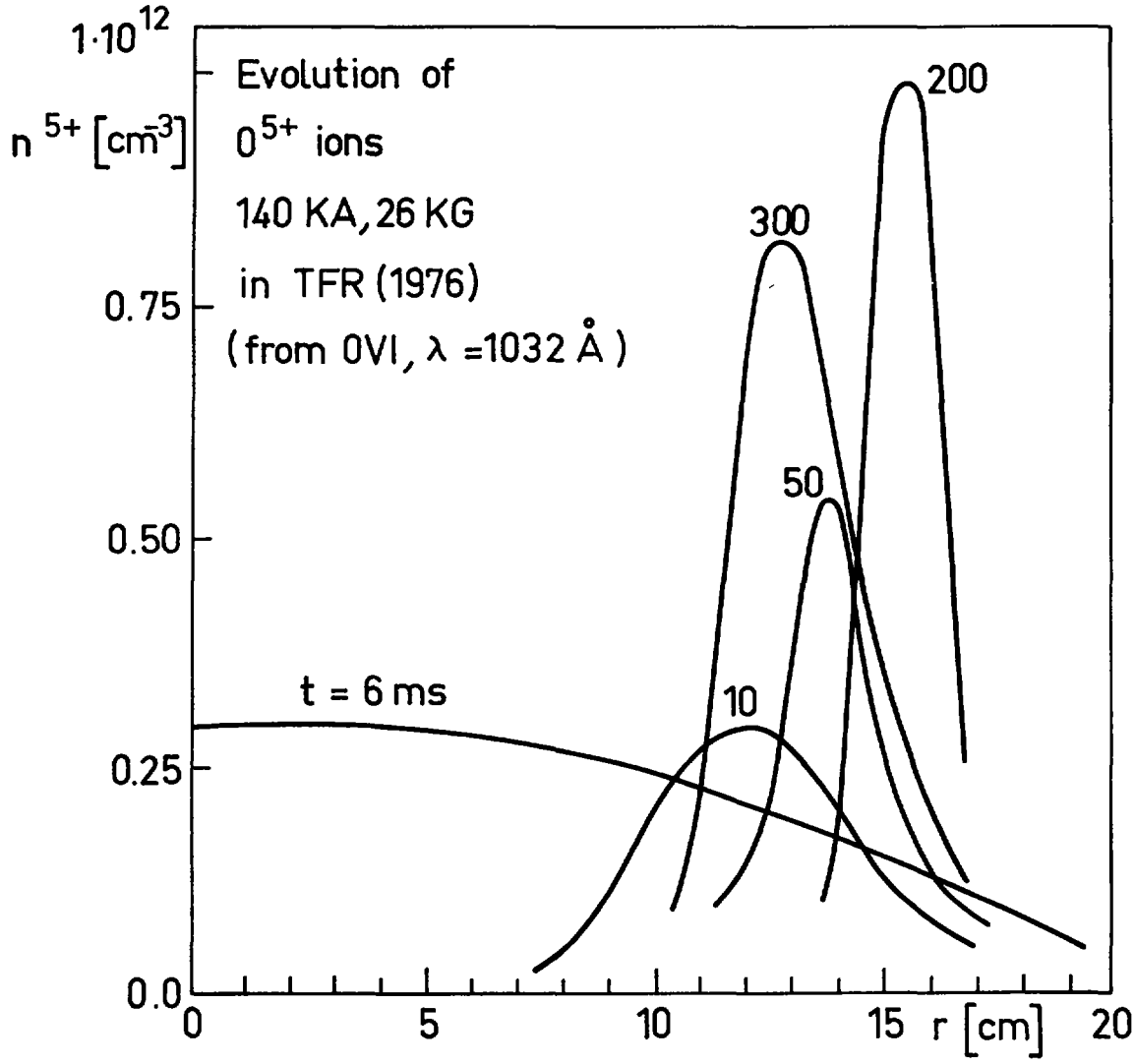
1·10^12
n 5+ [cm^-3]
Evolution of
O5+ ions
140 KA, 26 KG
in TFR (1976)
(from OVI, λ =1032 Å)
0.75
0.50
0.25
0.0
0
5
10
15
r [cm]
20
200
300
50
10
t = 6 ms

Fig. 9

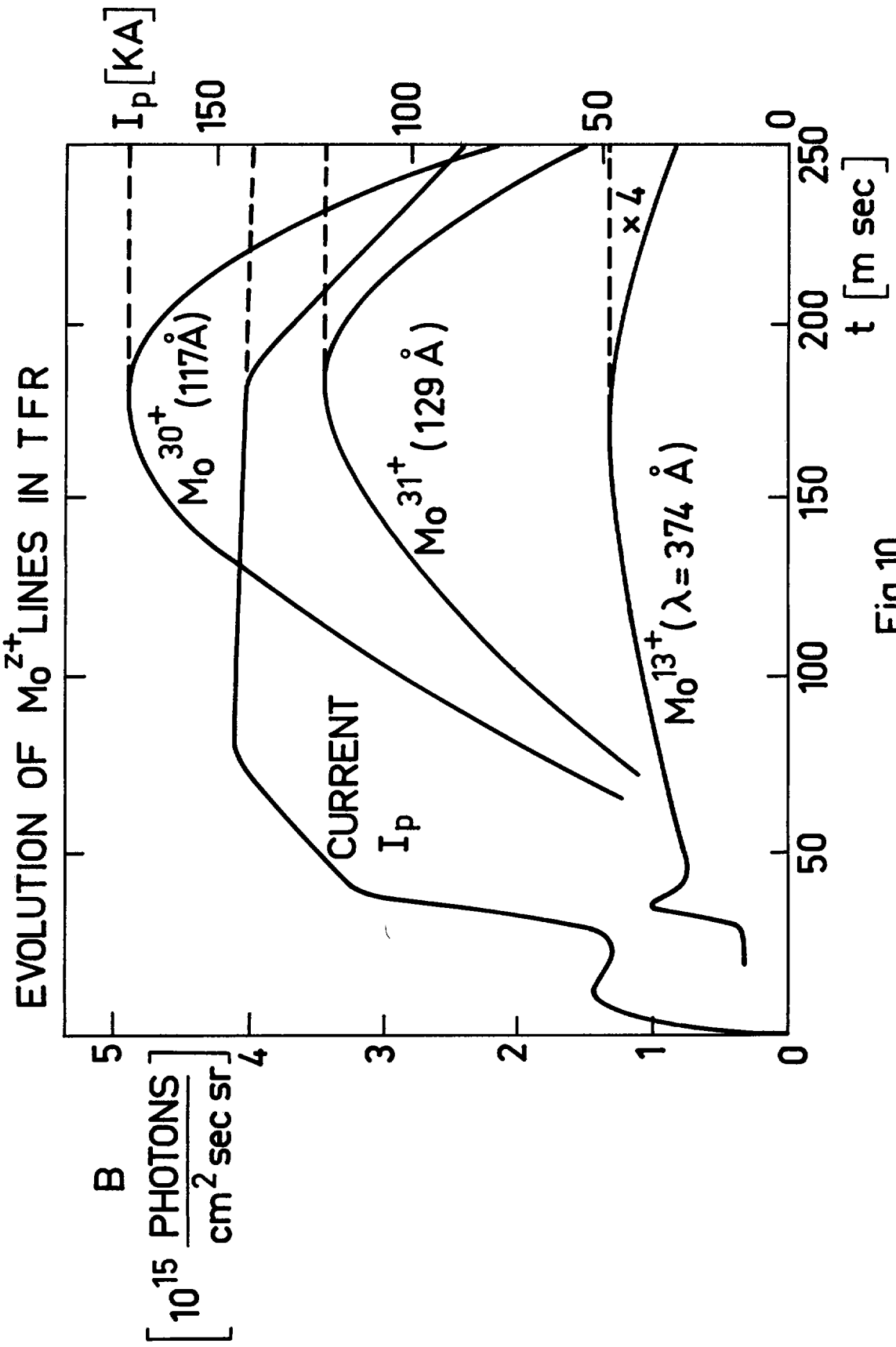
EVOLUTION OF Mo^{z+} LINES IN TFR
I_p [KA]
150
100
50
0
B
$[10^{15} \frac{\text{PHOTONS}}{\text{cm}^2 \text{ sec sr}}]$
5
4
3
2
1
0
CURRENT
I_p
Mo^{30+} (117Å)
Mo^{31+} (129 Å)
Mo^{13+} (λ= 374 Å)
x 4
50
100
150
200
250
t [m sec]

Fig.10

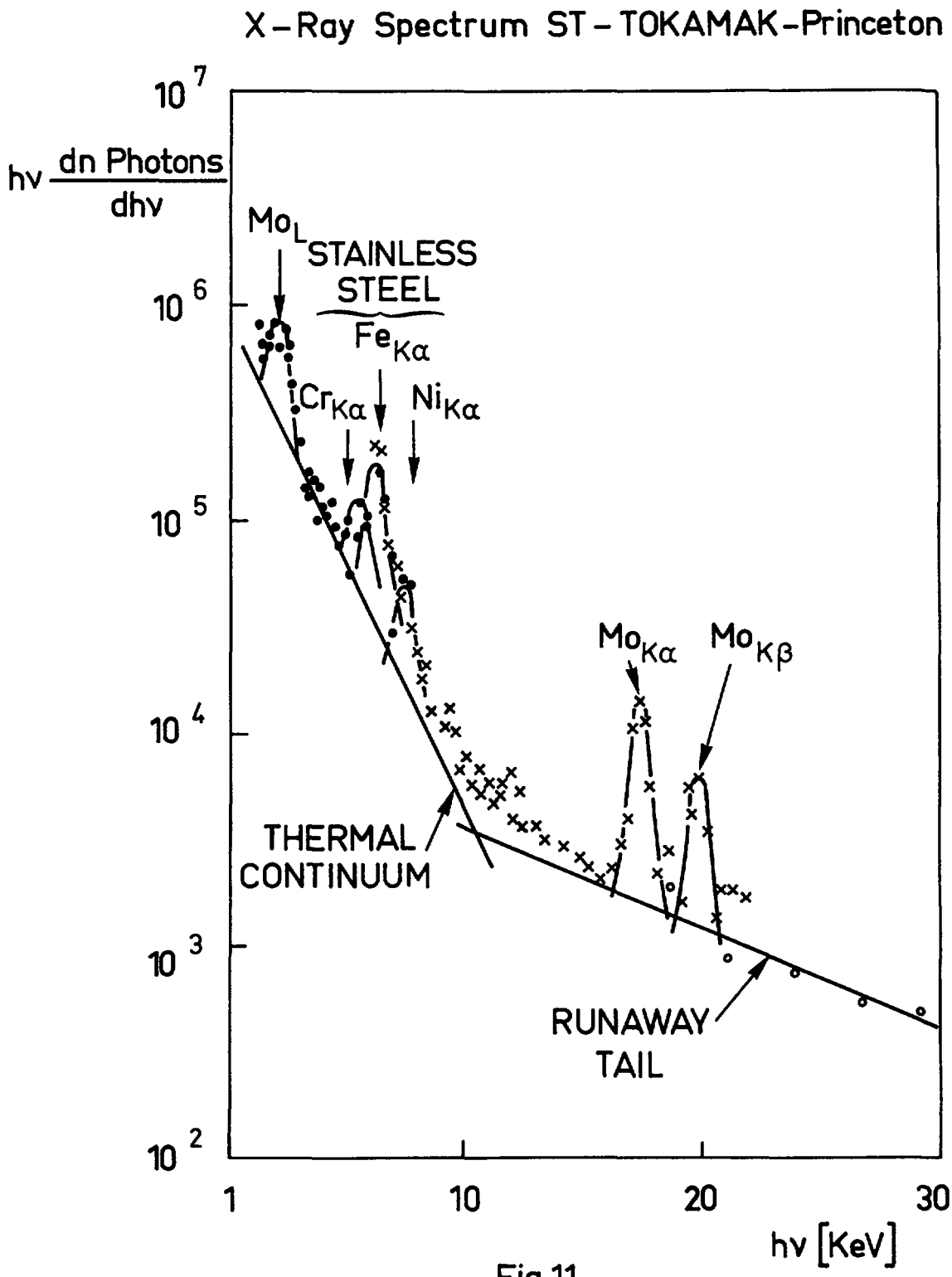
X-Ray Spectrum ST-TOKAMAK-Princeton
hν dn Photons / dhν
10 7
10 6
10 5
10 4
10 3
10 2
Mo L
STAINLESS STEEL
Fe Kα
Cr Kα
Ni Kα
Mo Kα
Mo Kβ
THERMAL CONTINUUM
RUNAWAY TAIL
1
10
20
30
hν [KeV]

Fig.11

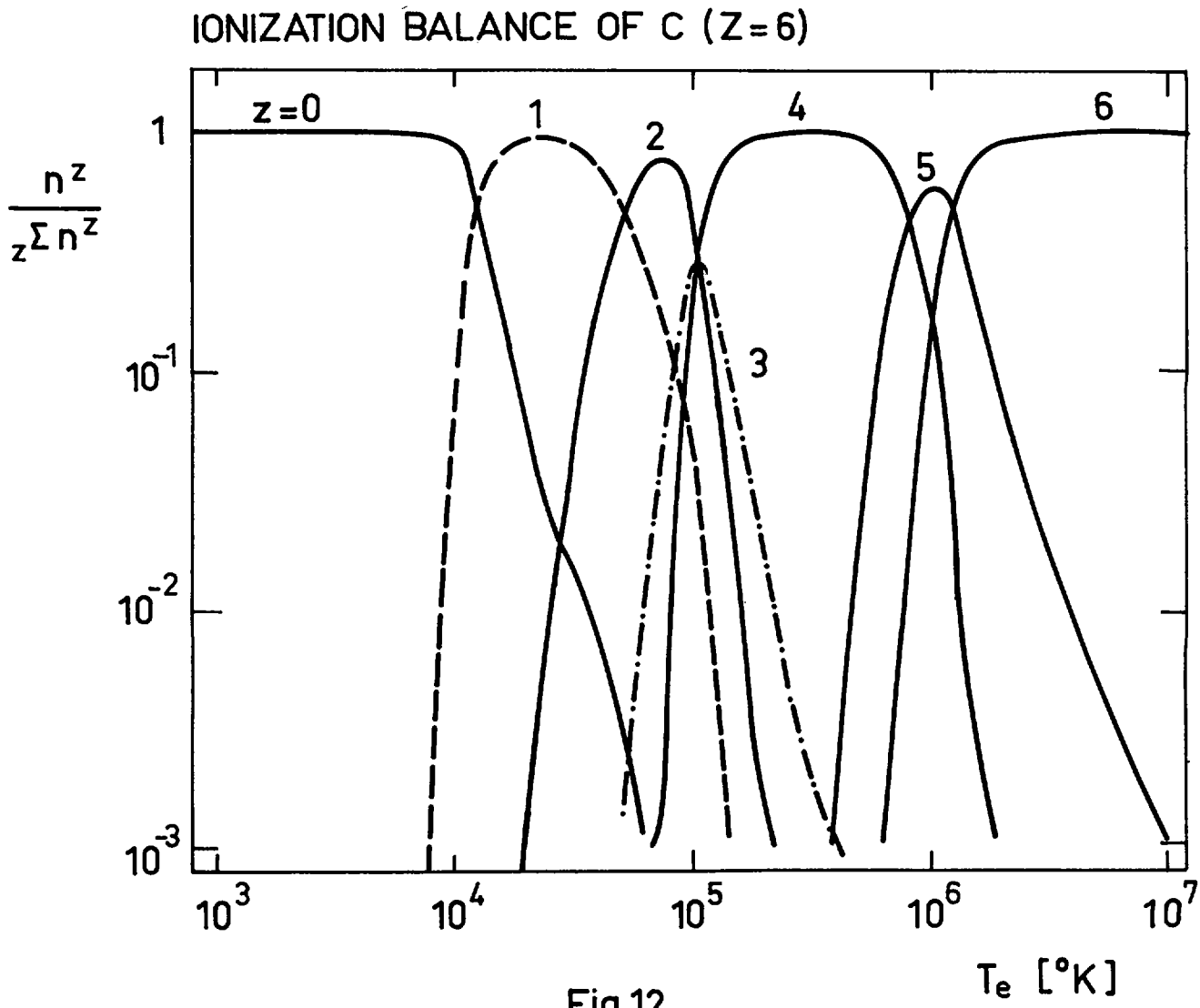
IONIZATION BALANCE OF C (Z=6)
$\frac{n^z}{\sum_z n^z}$
z=0
1
2
3
4
5
6
1
10^{-1}
10^{-2}
10^{-3}
10^3
10^4
10^5
10^6
10^7
T_e [°K]

Fig.12

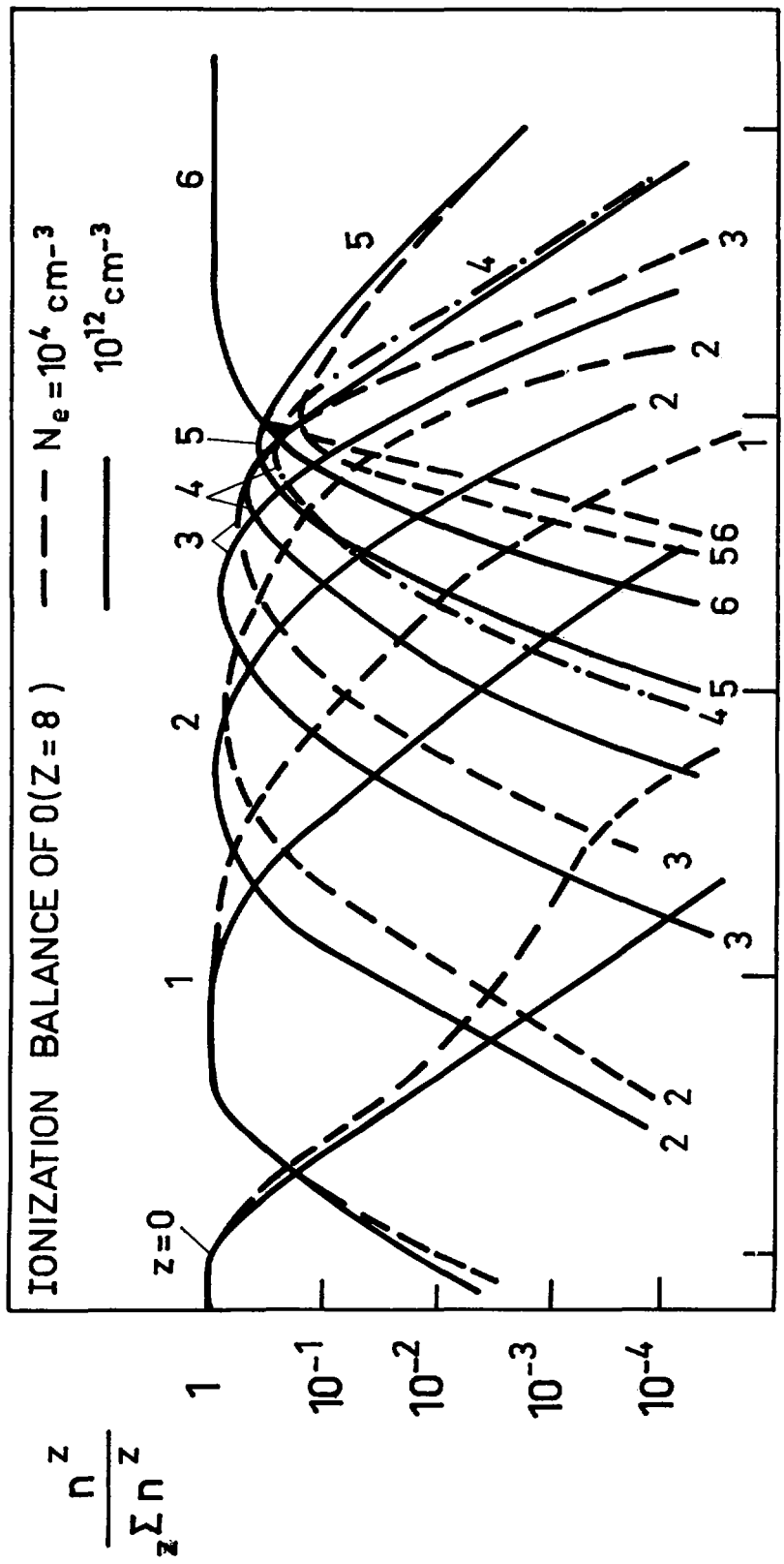
IONIZATION BALANCE OF O(Z=8)
$N_e = 10^4$ cm^{-3}
10^{12} cm^{-3}
z=0
1
2
3
4
5
6
$\frac{n_z}{\sum_z n_z}$
1
10^{-1}
10^{-2}
10^{-3}
10^{-4}
10^4
3
10^5
3
10^6
T_e [°K]

Fig.13

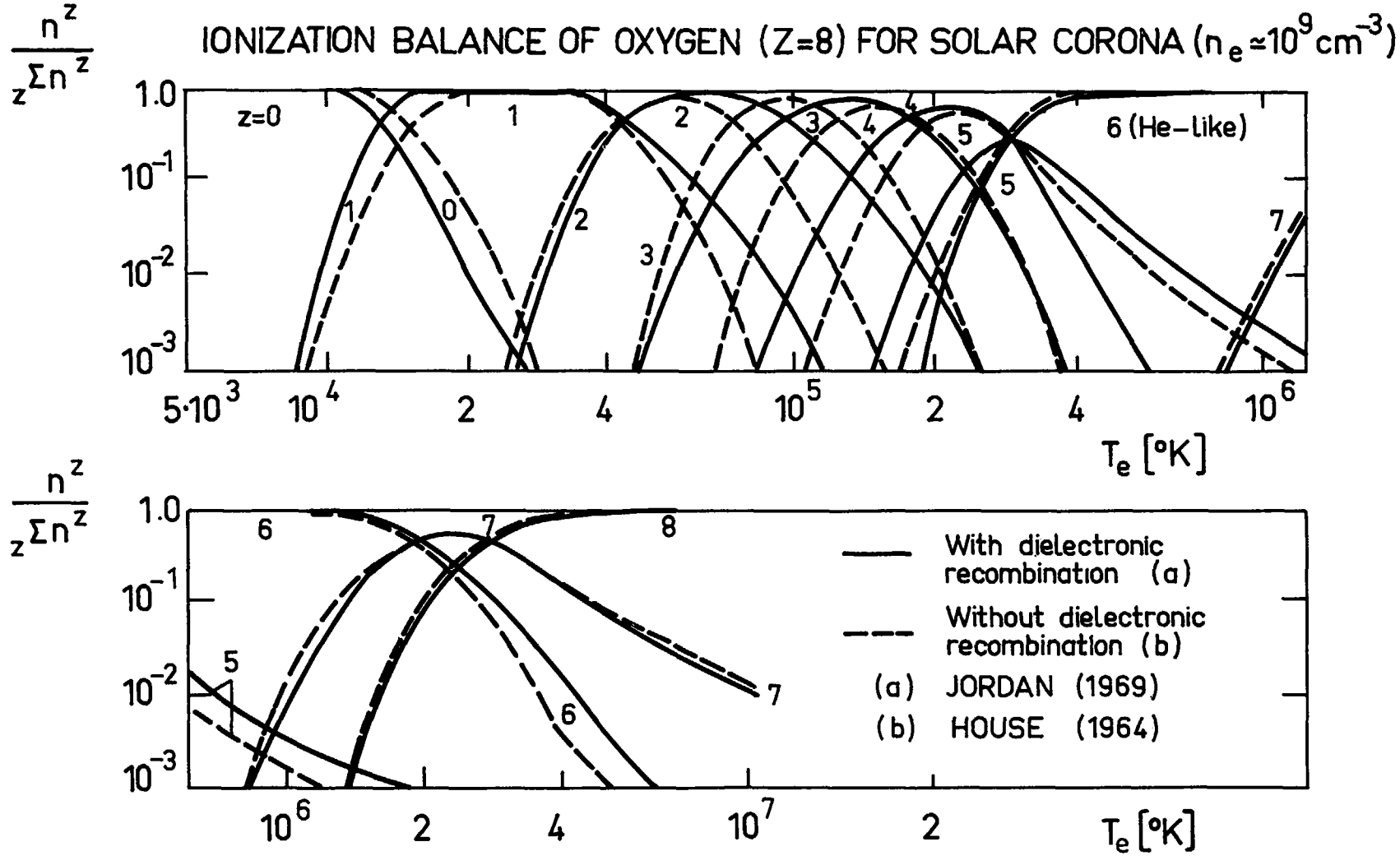
IONIZATION BALANCE OF OXYGEN (Z=8) FOR SOLAR CORONA ($n_e \simeq 10^9 cm^{-3}$)
$\frac{n^z}{\sum_z n^z}$
1.0
10^{-1}
10^{-2}
10^{-3}
z=0
1
2
3
4
5
6 (He-like)
7
0
$5 \cdot 10^3$
10^4
2
4
10^5
2
4
10^6
T_e [°K]
$\frac{n^z}{\sum_z n^z}$
1.0
10^{-1}
10^{-2}
10^{-3}
6
7
8
5
With dielectronic recombination (a)
Without dielectronic recombination (b)
(a) JORDAN (1969)
(b) HOUSE (1964)
10^6
2
4
10^7
2
T_e [°K]

Fig.14

IONIZATION OF OXYGEN (Z=8) including dielectronic recombination

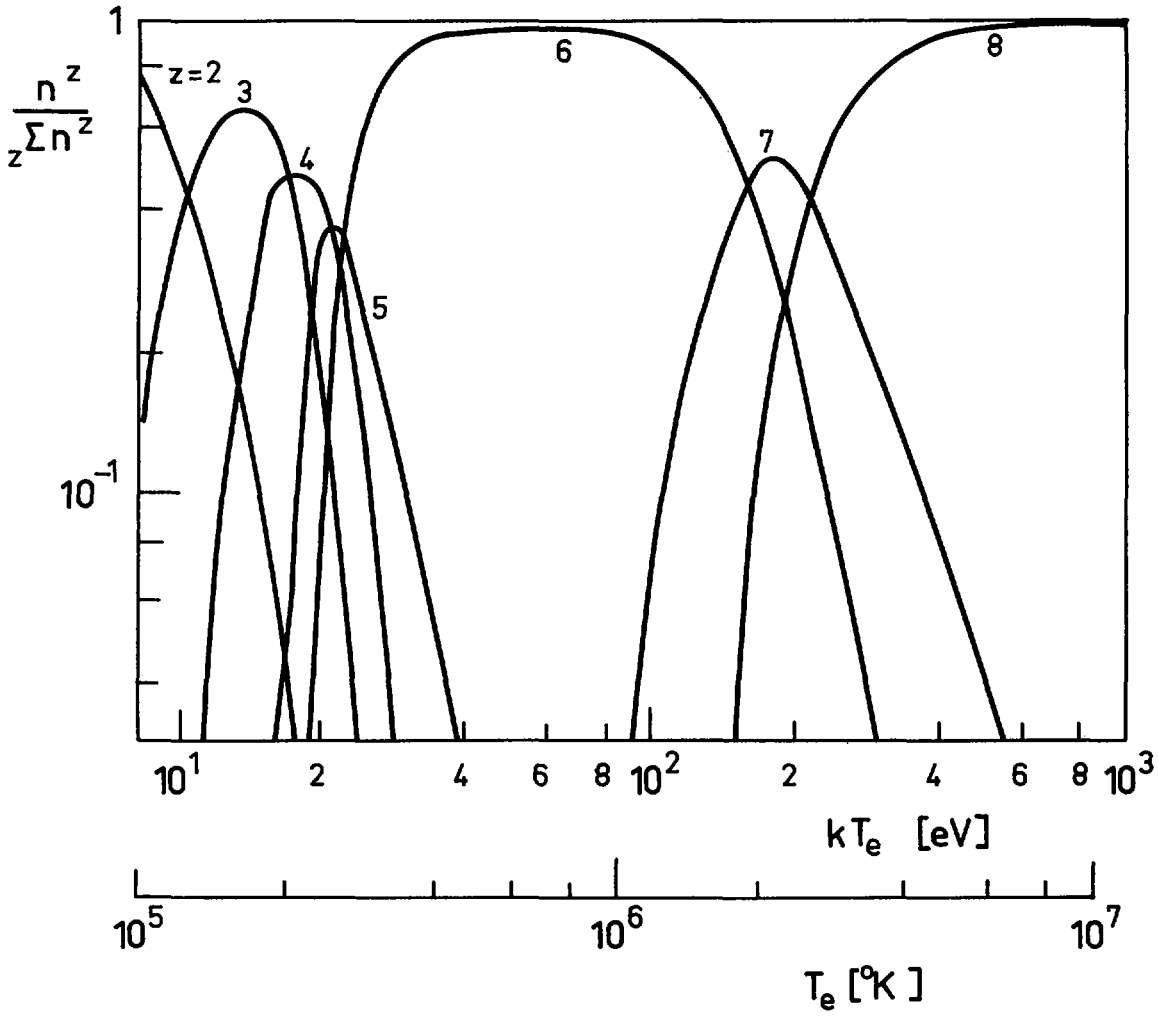

Fig.15

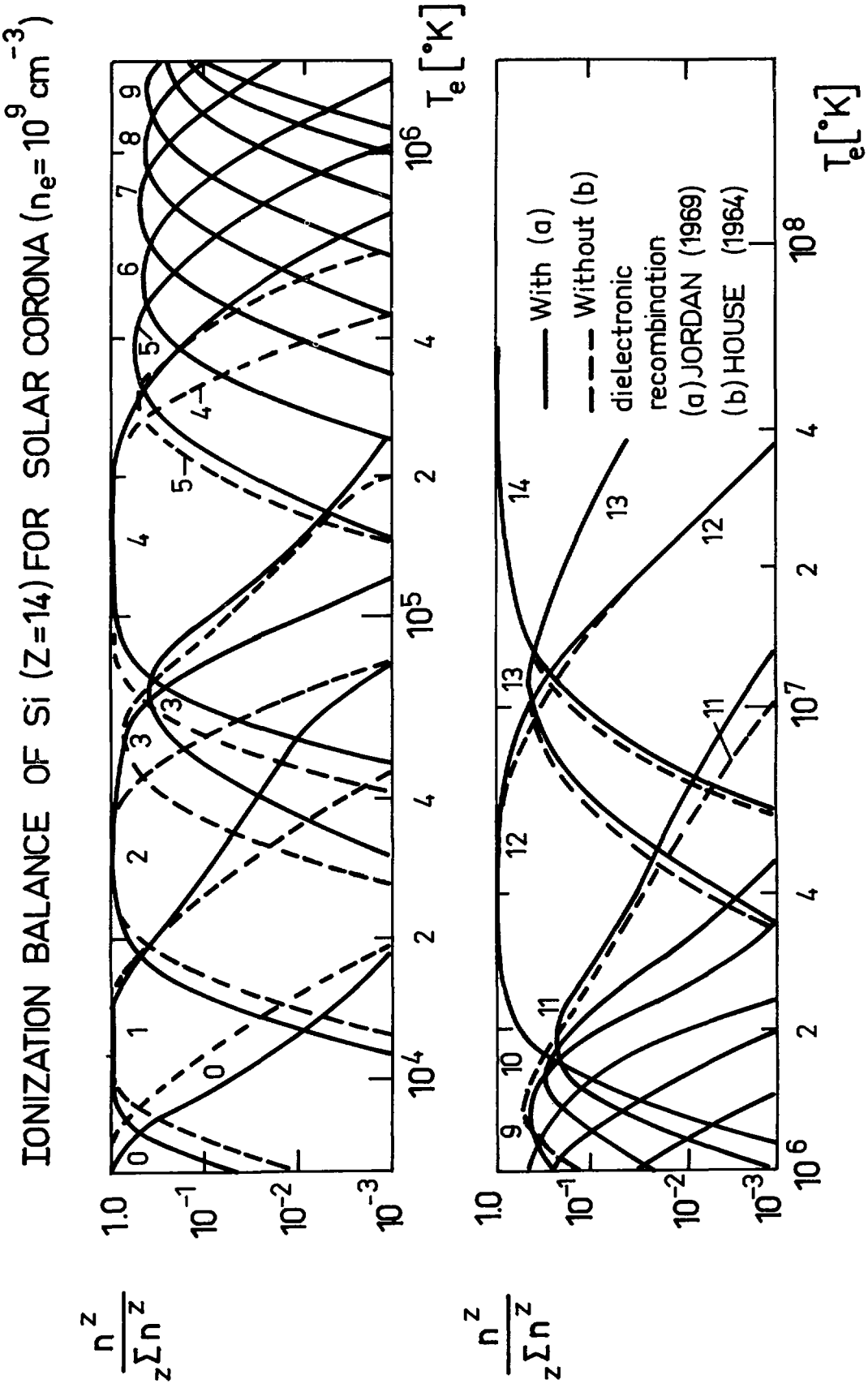
IONIZATION BALANCE OF Si (Z=14) FOR SOLAR CORONA ($n_e = 10^9 cm^{-3}$)
$\frac{n^z}{\sum_z n^z}$
T_e [°K]
With (a)
Without (b)
dielectronic recombination
(a) JORDAN (1969)
(b) HOUSE (1964)

Fig.16

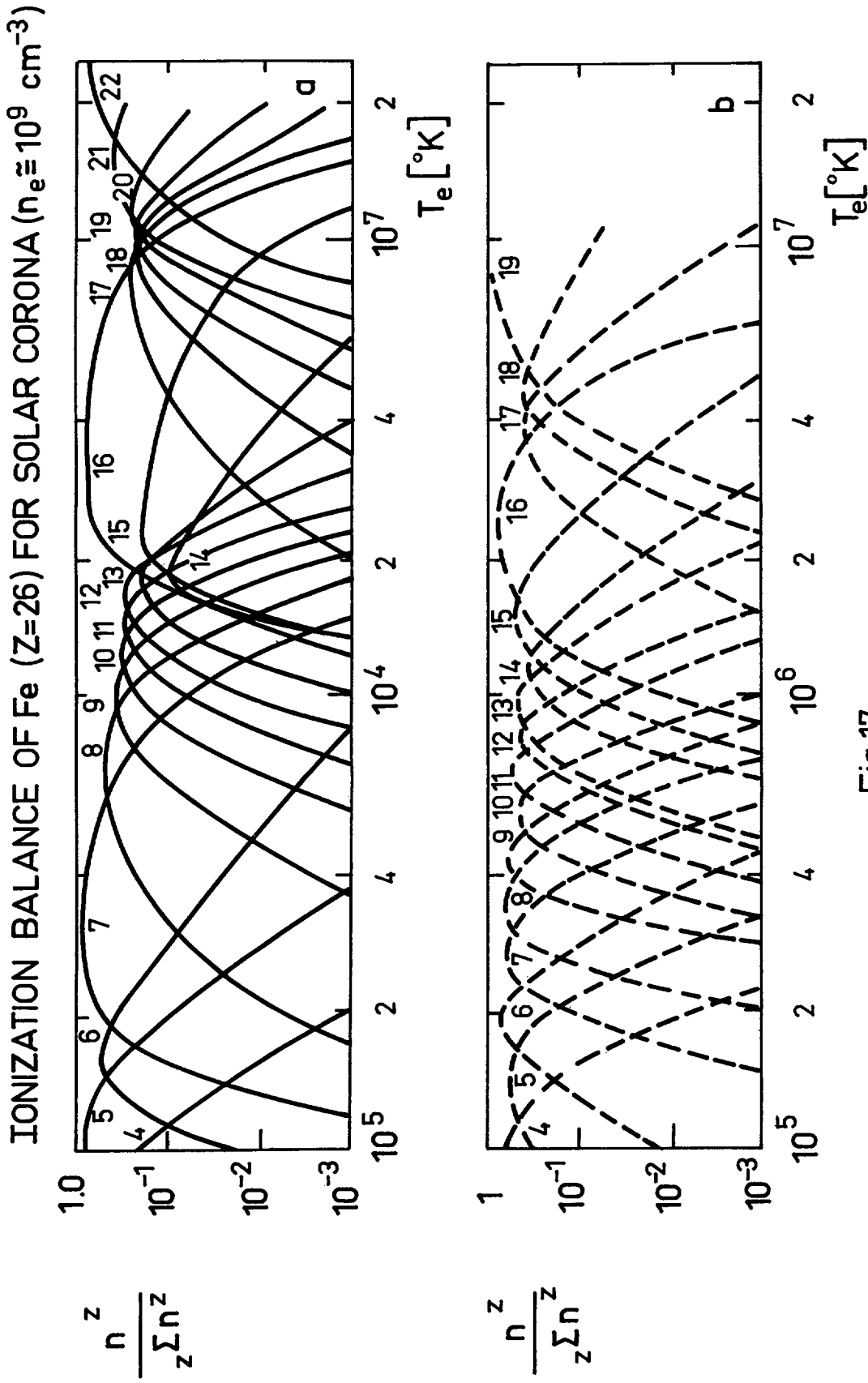
IONIZATION BALANCE OF Fe (Z=26) FOR SOLAR CORONA ($n_e \cong 10^9$ cm^{-3})
$\frac{n^z}{\sum_z n^z}$
T_e [°K]
a
b

Fig.17

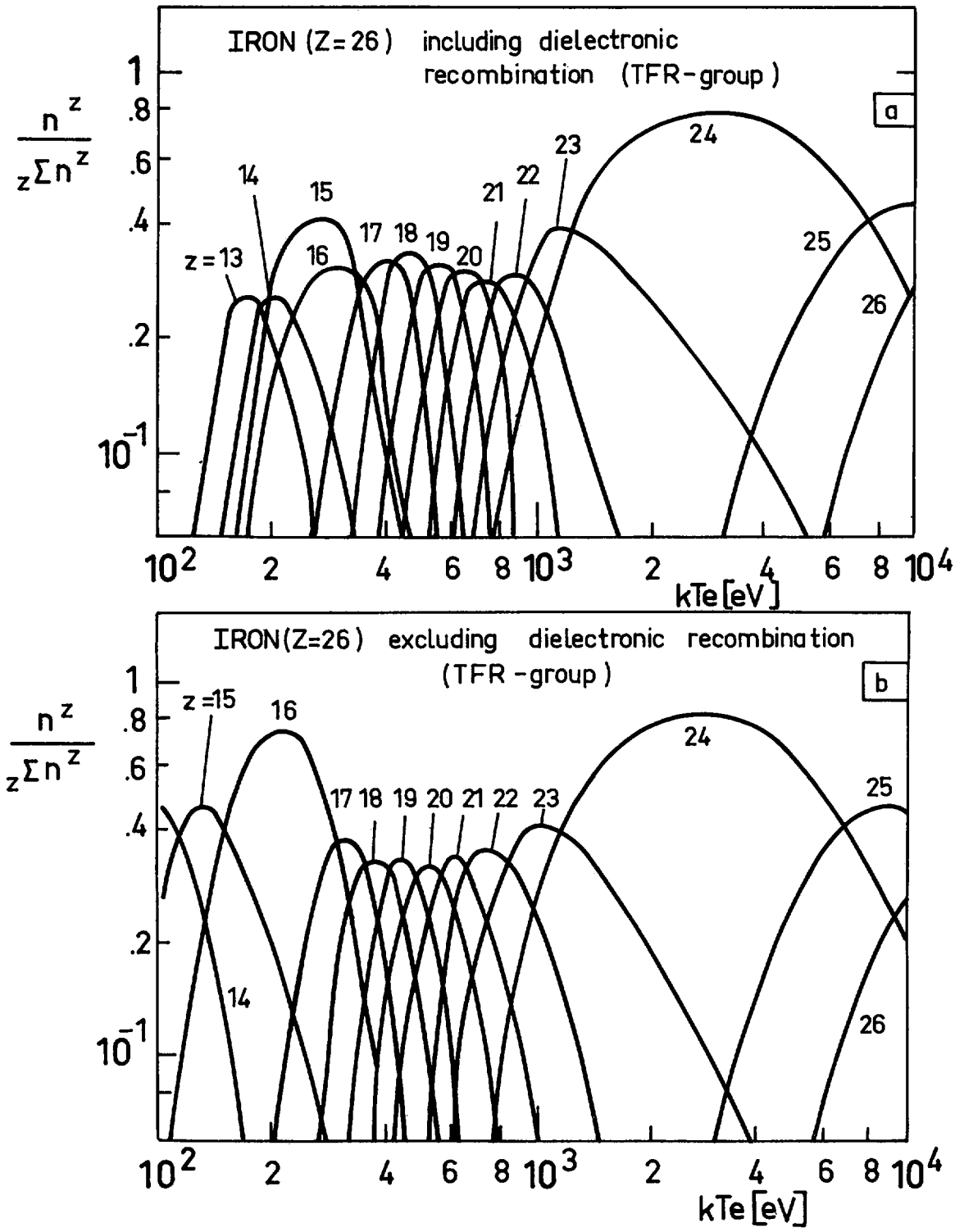
IRON (Z=26) including dielectronic recombination (TFR-group)
a
$\frac{n^z}{{}_z\Sigma n^z}$
1
.8
.6
.4
.2
10^{-1}
z=13
14
15
16
17
18
19
20
21
22
23
24
25
26
10^2
2
4
6
8
10^3
2
4
6
8
10^4
kTe [eV]
IRON(Z=26) excluding dielectronic recombination (TFR-group)
b
$\frac{n^z}{{}_z\Sigma n^z}$
z=15
16
17
18
19
20
21
22
23
24
25
14
26
kTe [eV]

Fig.18

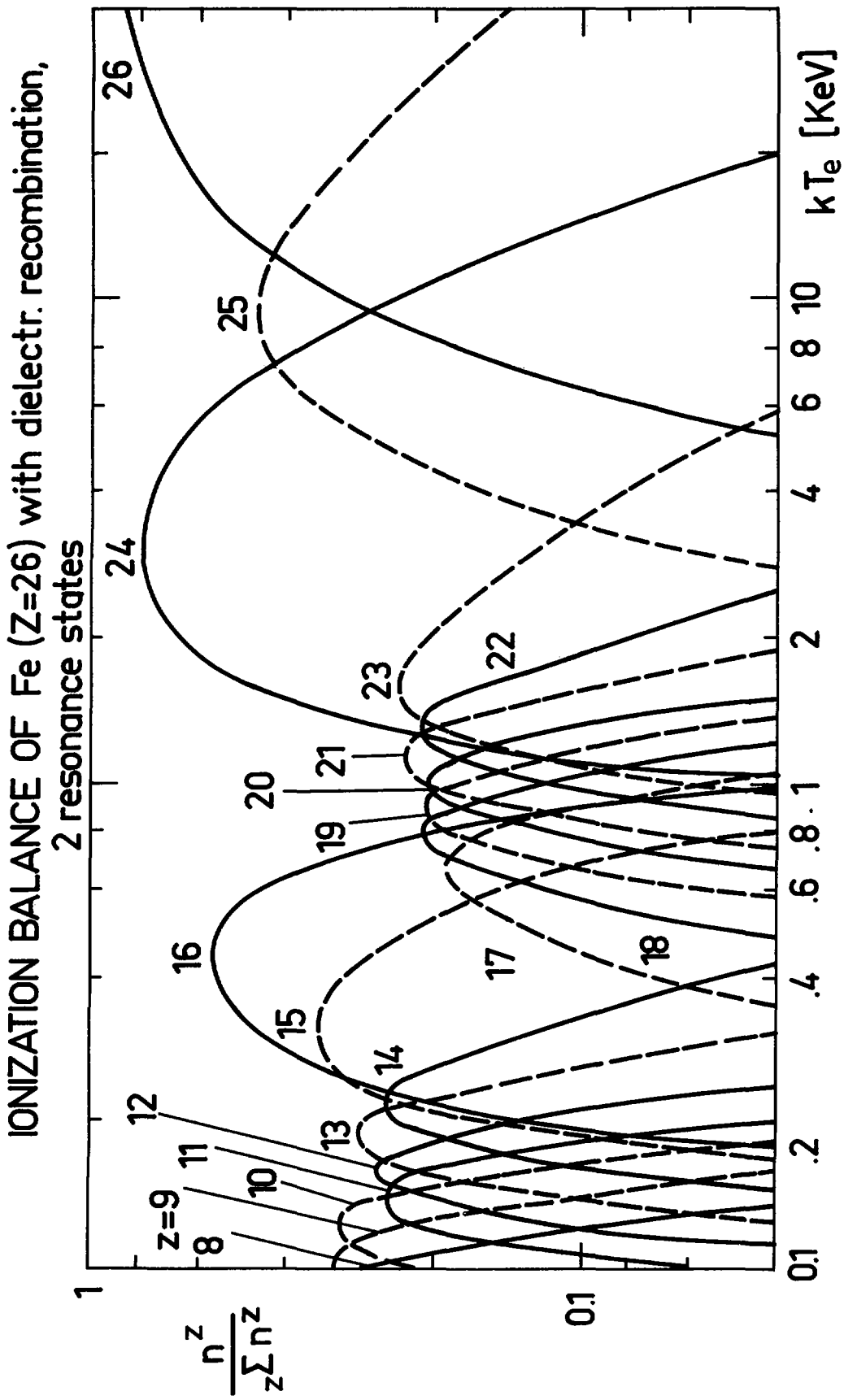
IONIZATION BALANCE OF Fe (Z=26) with dielectr. recombination,
2 resonance states
$\frac{n^z}{\sum_z n^z}$
1
0.1
z=9
8
10
11
12
13
14
15
16
17
18
19
20
21
22
23
24
25
26
0.1
.2
.4
.6
.8
1
2
4
6
8
10
kT_e [KeV]

Fig. 19

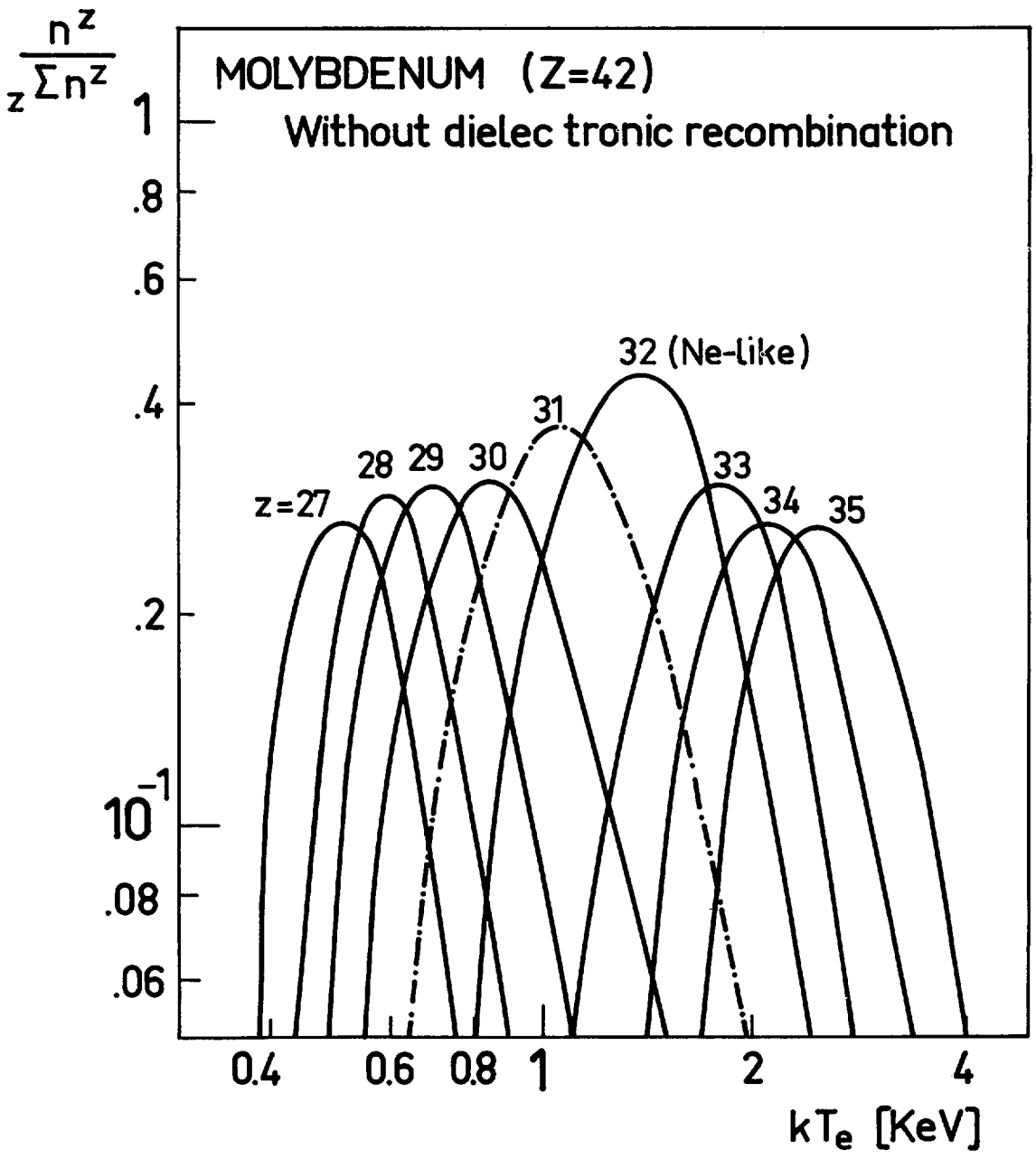
$\frac{n^z}{\sum_z n^z}$
MOLYBDENUM (Z=42)
Without dielec tronic recombination
1
.8
.6
.4
.2
10^{-1}
.08
.06
z=27
28
29
30
31
32 (Ne-like)
33
34
35
0.4
0.6
0.8
1
2
4
kT_e [KeV]

Fig. 20

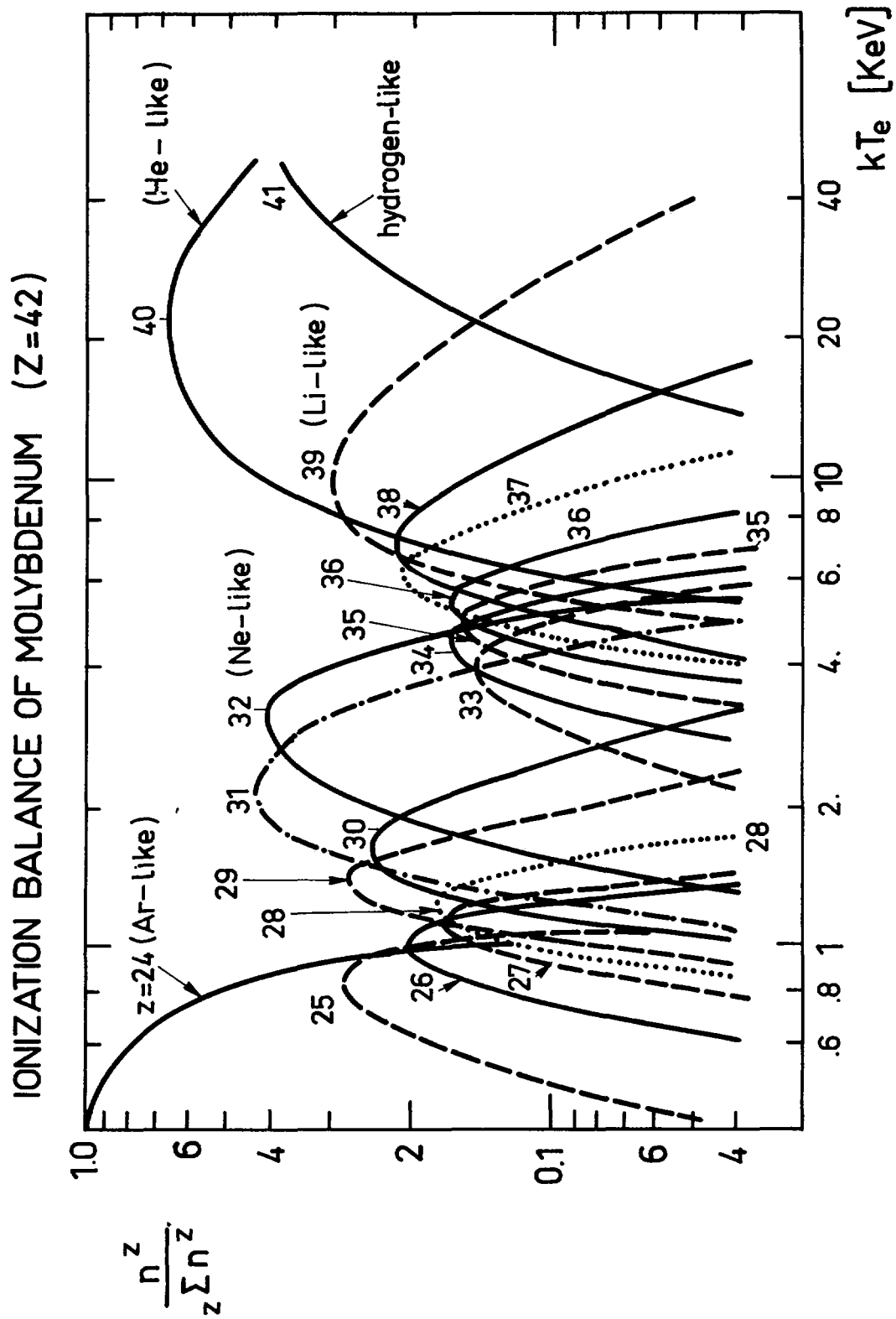
IONIZATION BALANCE OF MOLYBDENUM (Z=42)
$\frac{n^z}{\sum_z n^z}$
1.0
6
4
2
0.1
6
4
.6
.8
1
2.
4.
6.
8
10
20
40
kTe [KeV]
z=24 (Ar-like)
(He- like)
hydrogen-like
(Li-like)
32 (Ne-like)
25
26
27
28
29
30
31
33
34
35
36
37
38
39
40
41

Fig.21

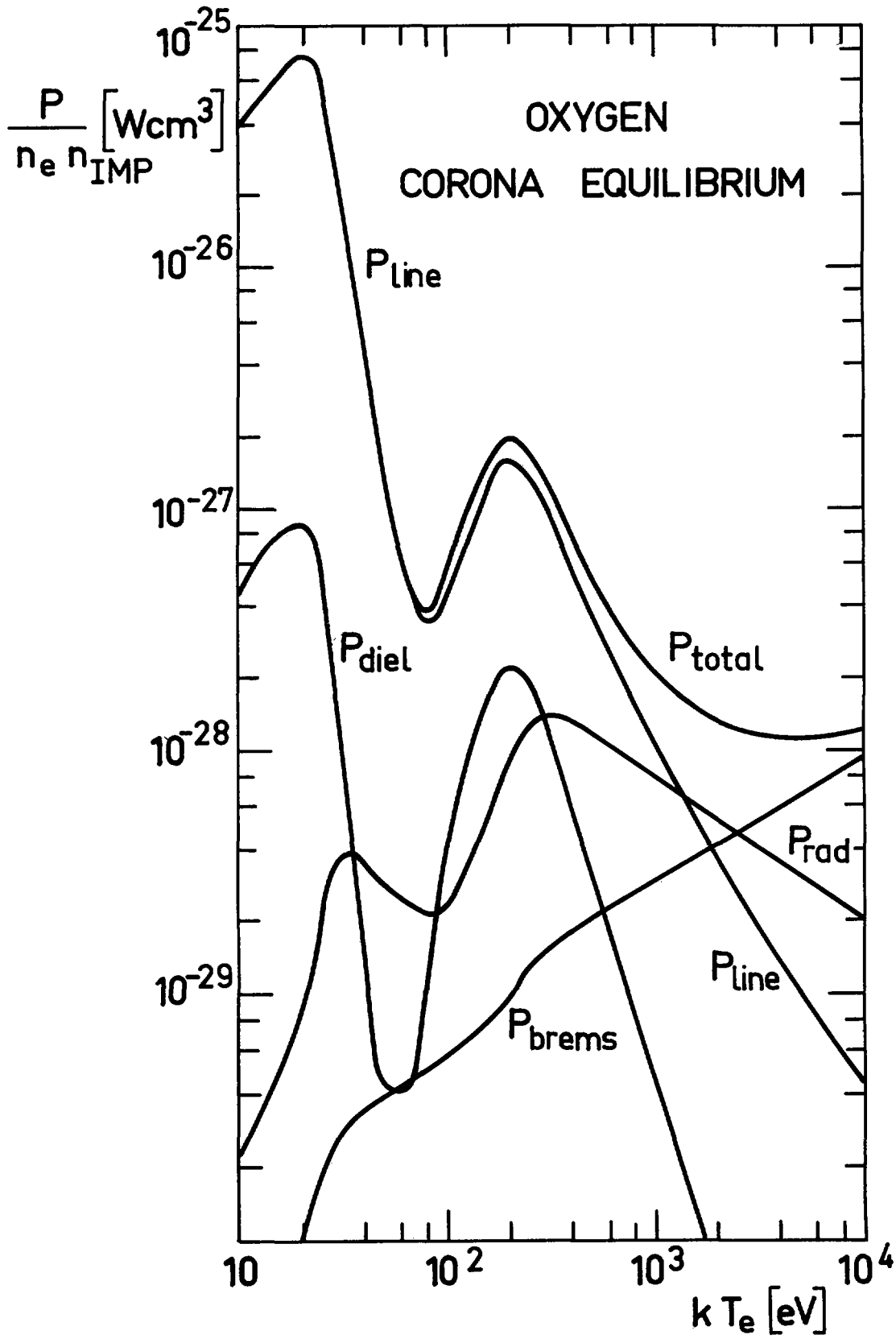
10^{-25}
$\frac{P}{n_e n_{IMP}}$ [Wcm^3]
OXYGEN
CORONA EQUILIBRIUM
10^{-26}
P_{line}
10^{-27}
P_{diel}
P_{total}
10^{-28}
P_{rad}
10^{-29}
P_{line}
P_{brems}
10
10^2
10^3
10^4
k T_e [eV]

Fig.22

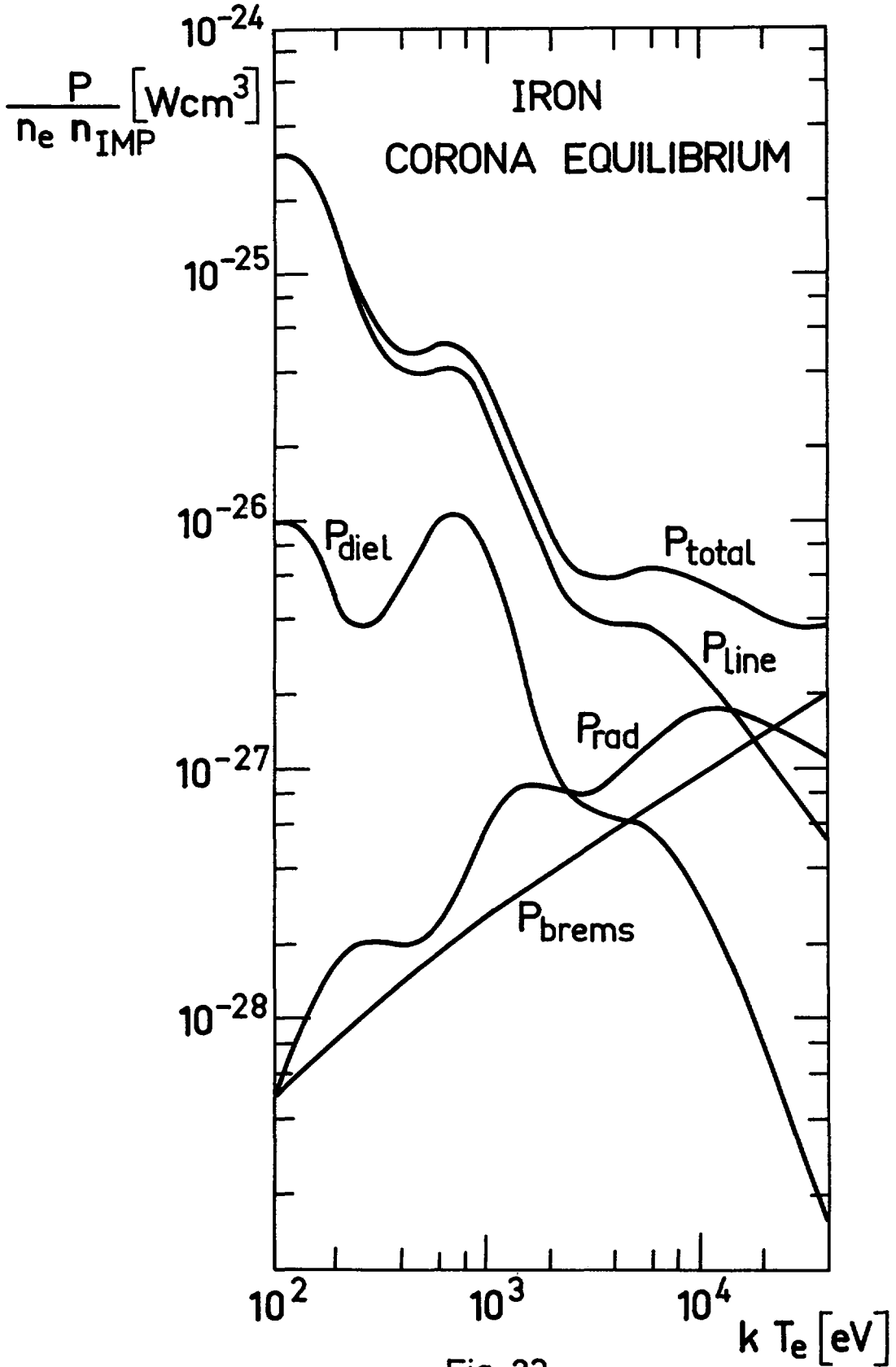
10^{-24}
$\frac{P}{n_e\, n_{IMP}}$ [Wcm^3]
IRON
CORONA EQUILIBRIUM
10^{-25}
10^{-26}
P_{diel}
P_{total}
P_{line}
P_{rad}
10^{-27}
P_{brems}
10^{-28}
10^2
10^3
10^4
k T_e [eV]

Fig. 23

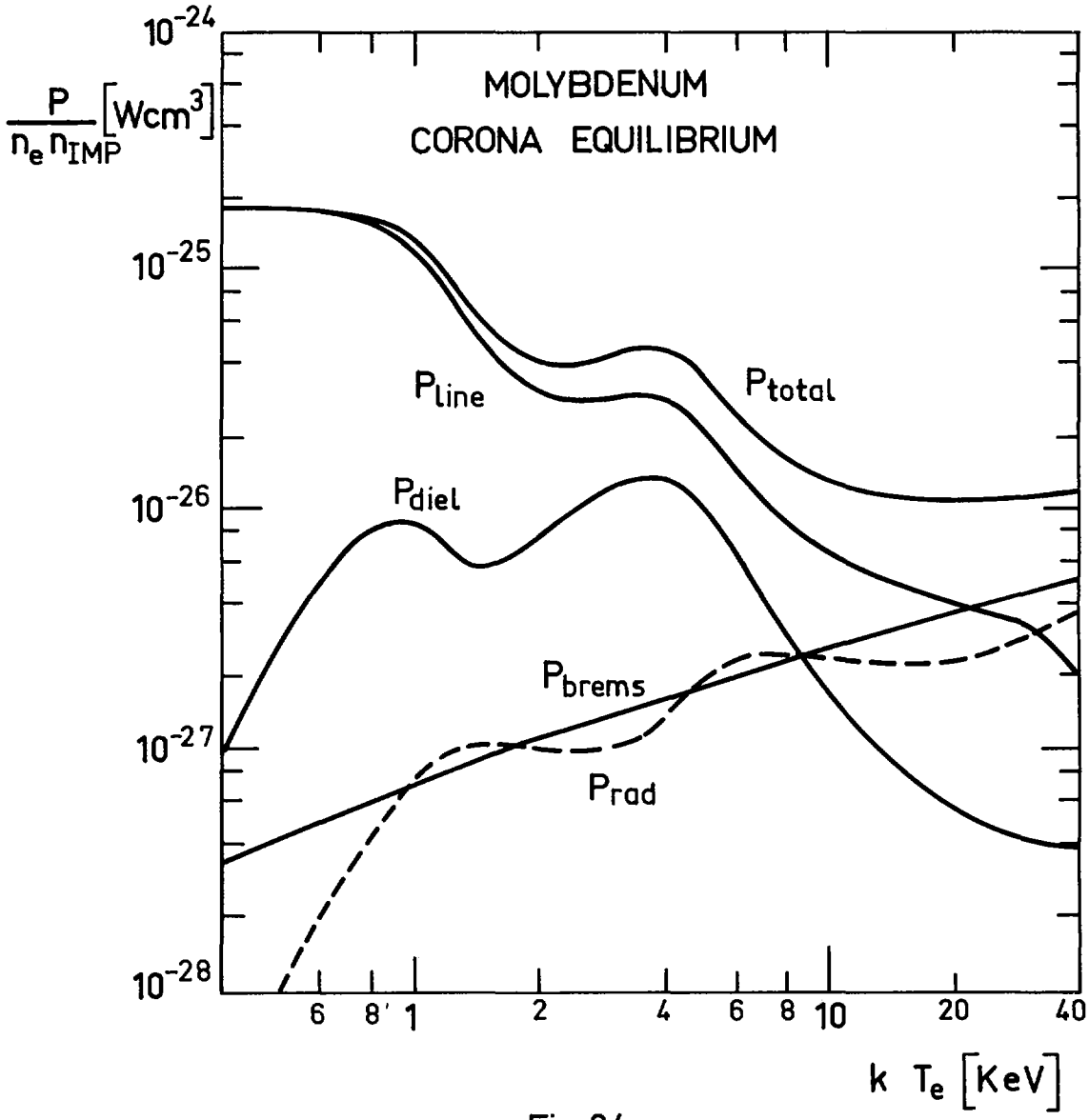
MOLYBDENUM
CORONA EQUILIBRIUM
$\frac{P}{n_e n_{IMP}}$ [Wcm^3]
10^{-24}
10^{-25}
10^{-26}
10^{-27}
10^{-28}
P_{line}
P_{total}
P_{diel}
P_{brems}
P_{rad}
6 8 1 2 4 6 8 10 20 40
k T_e [KeV]

Fig. 24

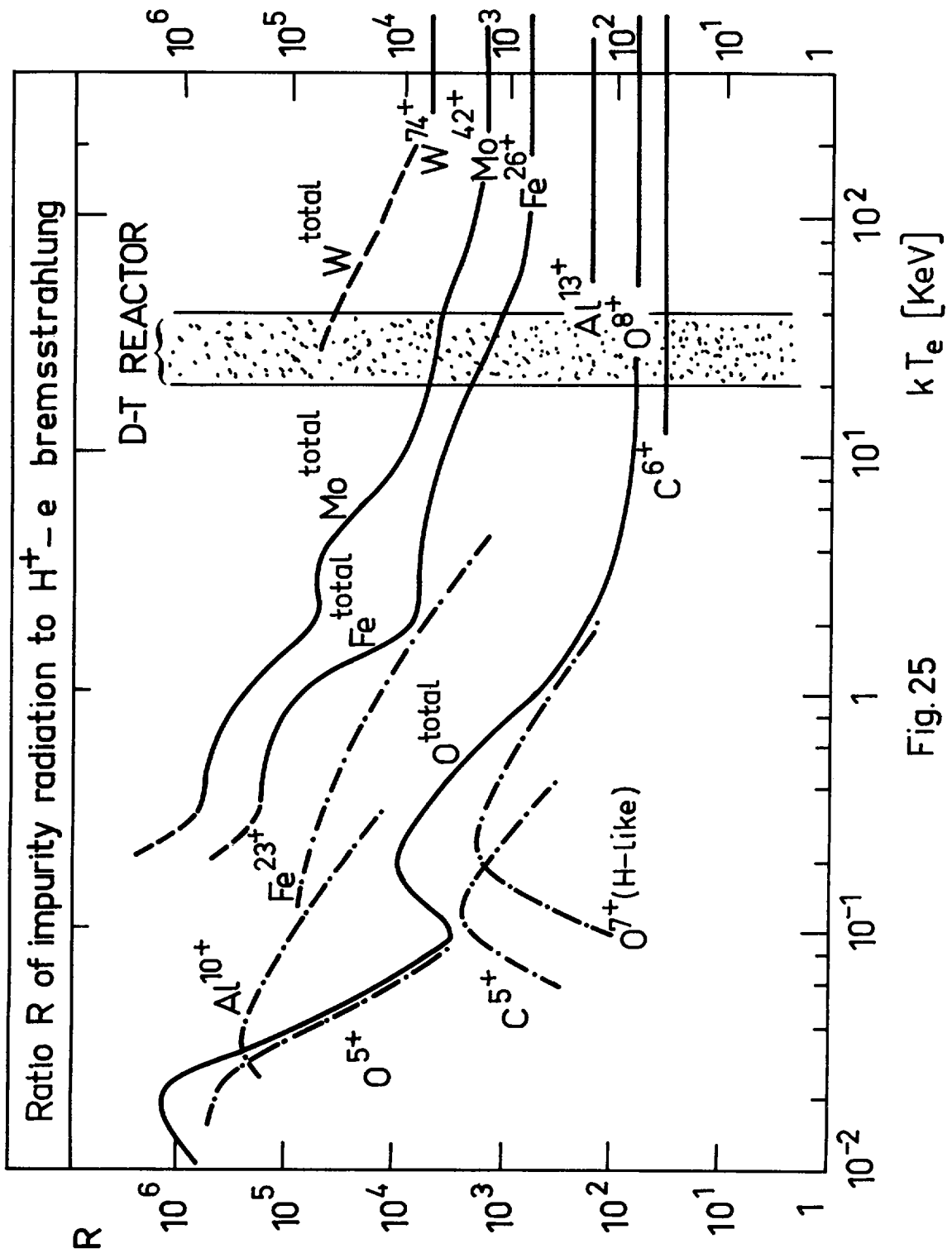
Ratio R of impurity radiation to H+ - e bremsstrahlung
D-T REACTOR
R
kTe [KeV]
W total
Mo total
Fe total
O total
W74+
Mo42+
Fe26+
Al13+
O8+
C6+
Al10+
Fe23+
O5+
C5+
O7+(H-like)

Fig. 25

DYNAMIC DISTRIBUTION OF O^{z+} IONS IN TFR

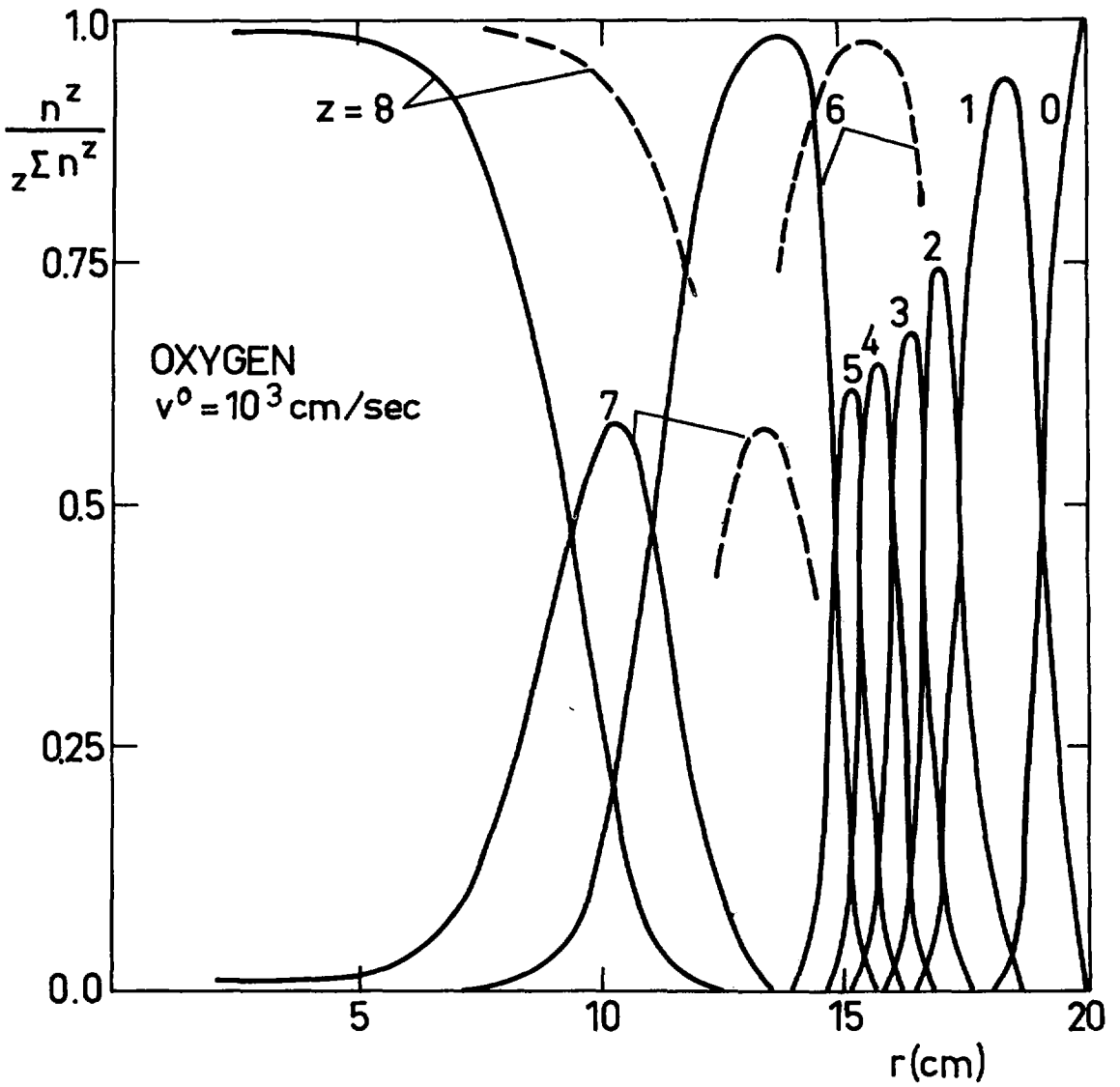

Fig. 26

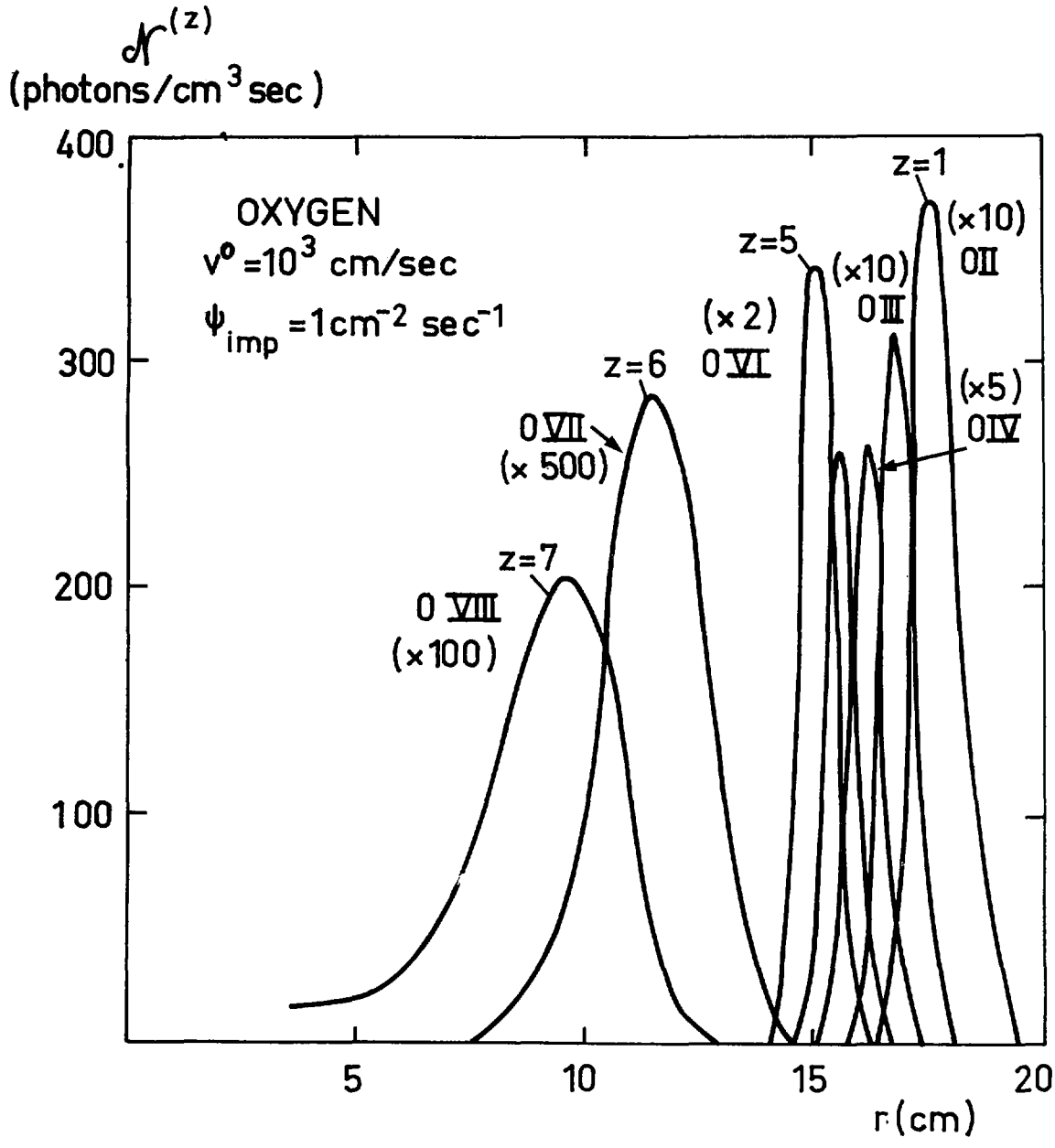
$\mathcal{N}^{(z)}$
(photons/cm^{3}sec)
400
300
200
100
OXYGEN
$v^o = 10^3$ cm/sec
$\psi_{imp} = 1 cm^{-2} sec^{-1}$
z=1
(×10)
OII
z=5
(×10)
OIII
(×2)
OVI
z=6
OVII
(× 500)
(×5)
OIV
z=7
O VIII
(×100)
5
10
15
20
r (cm)

Fig. 27

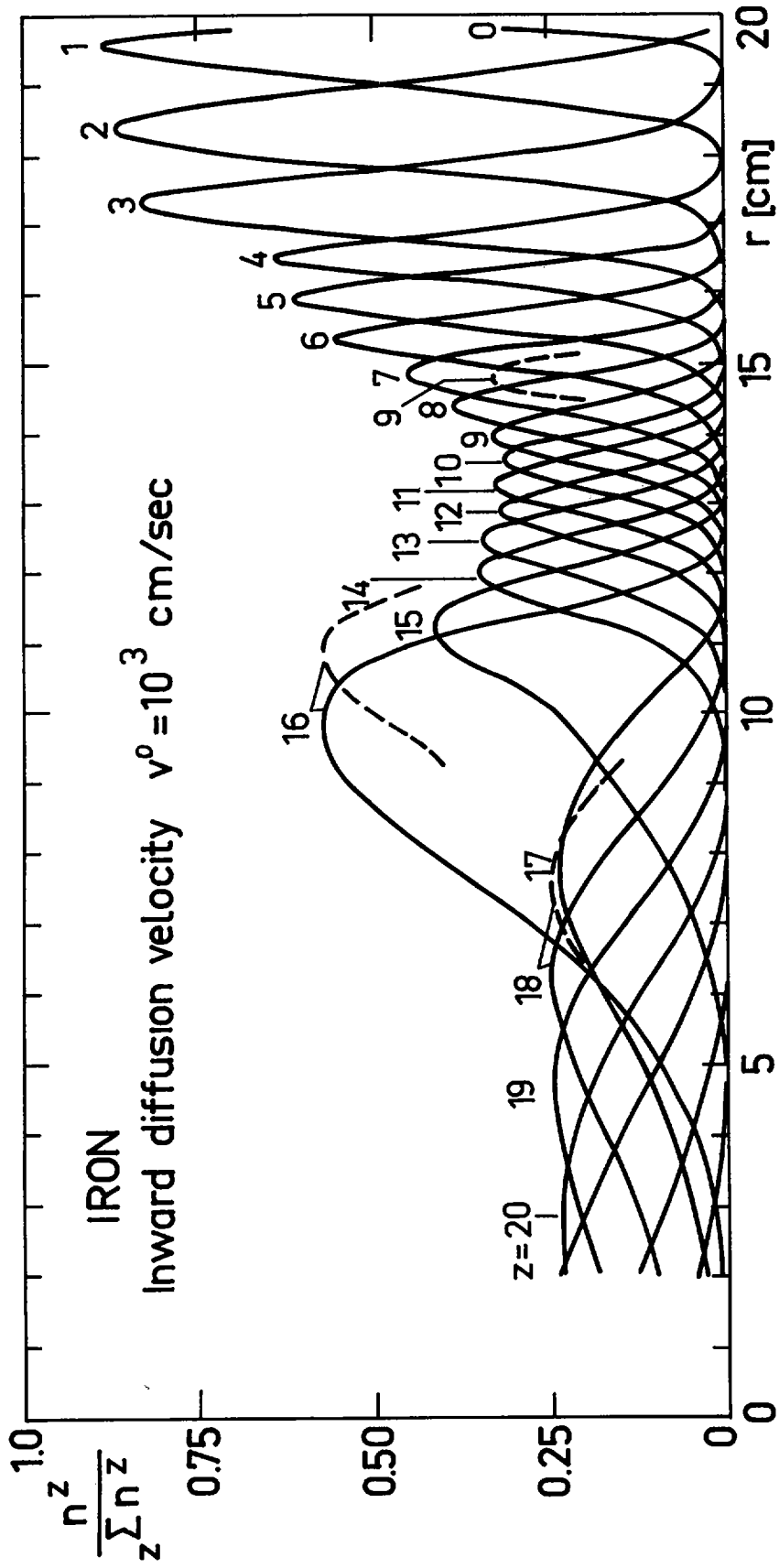
DYNAMIC DISTRIBUTION OF Fe^{z+} IONS IN TFR
IRON
Inward diffusion velocity $v^o = 10^3$ cm/sec
$\frac{n^z}{\sum_z n^z}$
1.0
0.75
0.50
0.25
0
0
5
10
15
20
r [cm]
z=20
19
18
17
16
15
14
13
12
11
10
9
8
7
6
5
4
3
2
1
0

Fig.28

Cross Section Data Including Atoms and Ions in the Highly Excited Rydberg States

Shunsuke OHTANI

Institute of Plasma Physics, Nagoya University, Nagoya, Japan

A spectroscopic study of the contact phenomenon of a plasma with a neutral gas is one of the major courses of investigations using the device named TPD-I[1] at the Institute of Plasma Physics (IPP), Nagoya, Japan. The TPD (Test Plasma by Direct-current discharge) is a stationary, quiescent high-density plasma source normally operated with helium.

Under the normal operating condition, the plasma column looks dominantly yellow (HeI 5876Å). When another gas (helium in this case) is introduced into the plasma region, the downstream side of the plasma column begins to glow locally with remarkable brightness. This phenomenon has been firstly investigated in detail by Otsuka and coworkers.[2] They measured absolute spectral intensities in visible region, and obtained the population density n_i of the highly excited level i of He^+ (i = 4, 5, 6, 7, 8, 9, 10). They found that the population densities of these levels of ions in the bright region are much higher than the values expected for the equilibrium state with the measured electron temperature T_e and electron density n_e. In Fig.1(a) are shown the population densities divided by the statistical weights of each level.

Recently, Sato and coworkers[3] extended these studies of the population anomaly of He^+ to the lower excited states (i = 2, 3, 4, 5) by measuring the intensities of HeII Lyman series in extreme ultra violet region.

Fig.1(b) shows the population densities of these levels. As is shown, the population densities are not only still high, but are inverted between these levels. In order to explain these population anomaly, one must, at first, think of what processes happen to occur when a plasma is in contact with a neutral gas.

Under the normal operation, the helium plasma of TPD-I is composed predominantly of He^{++}, and has a high electron temperature, ca. 30 eV and a high electron density, ca. 10^{15} cm^{-3}. As soon as the neutral helium gas is introduced into the plasma, electrons in plasma lose their energy due to excitations of neutral atoms through collisions and consequently electron temperature is lowered. Then, the three-body collisional recombination

may become dominant process at first, because the initial electron density is so high that the mean distance between an electron and He^{++} ion is well within the orbits of high Rydberg states of the He^{+} ion and the slow electrons in the plasma begin to fall into such an orbit. The ions in highly excited states are by no means stable because they are perturbed by frequent collisions due to its large orbit radius and a high electron density of the plasma. In this stage, various kinds of atomic processes happen to occur in addition to three-body recombination, such as excitation, de-excitation and ionization by electron impact, radiative recombination, spontaneous transition, photoionization, charge transfer collision, and so on.

One can not explain the population anomaly until the rate equations are solved for the population densities of relevant energy levels including the possible processes mentioned above. A fundamental difficulty in any modeling of the recombining plasma which is caused by the contact with a neutral gas comes from the lack of reliable collisional rate coefficient data. While most excitation, de-excitation and radiative transition rates are known or may be estimated, there are few data in concern with the rates of collisional ionization from the highly excited state and collisional processes between atoms and ions such as charge transfer into the excited states. Since the three-body recombination which is important in this case is the inverse process of collisional ionization, it is usually deduced by detailed balance method.

It should be emphasized that the obtainment of such fundamental data of collisional processes including excited atoms and ions is very important in order to have a right understanding of the contact phenomenon, because it is strongly related to gas blancket between plasma and wall and heavy desorption of gases from the wall.

Meanwhile, the spectroscopic study of impurity ions in a plasma, which is one of common techniques of plasma diagnostics, is of importance to understand the impurity transport and their effect on the overall energy balance of the plasma. However, the plasma temperature being high, most of the ions exist in a fully stripped state, such as O^{8+} or C^{6+}, and can no longer be observed spectroscopically. One of the possible methods of investigating the fully ionized ions to be considered is the active method by projecting an energetic beam across a plasma region. The following reaction could occur;

$$X_{beam} + \left(\begin{matrix} O^{8+} \\ C^{6+} \end{matrix}\right) \rightarrow X^{+} + \left(\begin{matrix} O^{7+*} \\ C^{5+*} \end{matrix}\right) .$$

The electron transfer from X atom to impurity ion must take place into a highly excited state. The spectral line from the highly excited state of the ion would truly reflect the characteristics of fully ionized ions, since it is regarded that electron excitation of ground state ion into this higher lying state occurs scarcely and there exists few neutral atom in the plasma. Space-and time resolved distributions of density and temperature of the fully ionized ion could be obtained from the measurements of absolute intensity and Doppler profile.

Analogously, using the following electron capture collision with H^{+} in the plasma;

$$X_{beam} + H^{+} \rightarrow X^{+} + H^{*},$$

temperature and density distribution of H^+ is measurable.

These new methods of active plasma diagnostics by the use of neutral particles are being planned and the possibility is being explored by Fujita and his group of IPP, Japan.

In order to succeed in these diagnosis, also needed are the broad and accurate knowledge of charge transfer collision including atoms and ions in highly excited state, that is, the absolute cross section data for each final state as a function of relative energy. Existence of wide variety of data would make it possible to choose a suitable element for X_{beam}.

At the IPP, Nagoya, only recently extensive studies have been started on the collisional processes including atoms and ions in high Rydberg states. Several works[4] are also being carried out besides those in Nagoya to solve these problems and should add valuable contributions to the investigation of collisional processes among highly excited ions and atoms in plasma.

References

1) see, for example Ann. Rev. of Inst. Plasma Phys. Nagoya Univ.

2) M. Otsuka, R. Ikee and K. Ishii, J. Quant. Spectrosc. Radiat. Transfer 15, 995 (1975)

3) K. Sato, M. Shiho, M. Hosokawa, H. Sugawara, T. Oda and T. Sasaki, Phys. Rev. Letters to be published.

4) M. Matsuzawa, J. Chem. Phys. 55, 2685 (1971); J. Chem. Phys. 58, 2674 (1973); J. Phys. Soc. Japan. 32, 1088 (1972); ibid 33, 1108 (1972); J. Electron Spectrosc. Relat. Phenom. 4, 1 (1974)
T. Shibata, T. Fukuyama and K. Kuchitsu, Chem. Lett. (1974), p.75

Figure Caption

Fig.1 Population density n_i divided by the statistical weight g_i of level i.
a): obtained from the measurements in visible region by Otsuka et al.,[2]
b): obtained from the measurements in extreme ultra violet region by Sato et al[3]

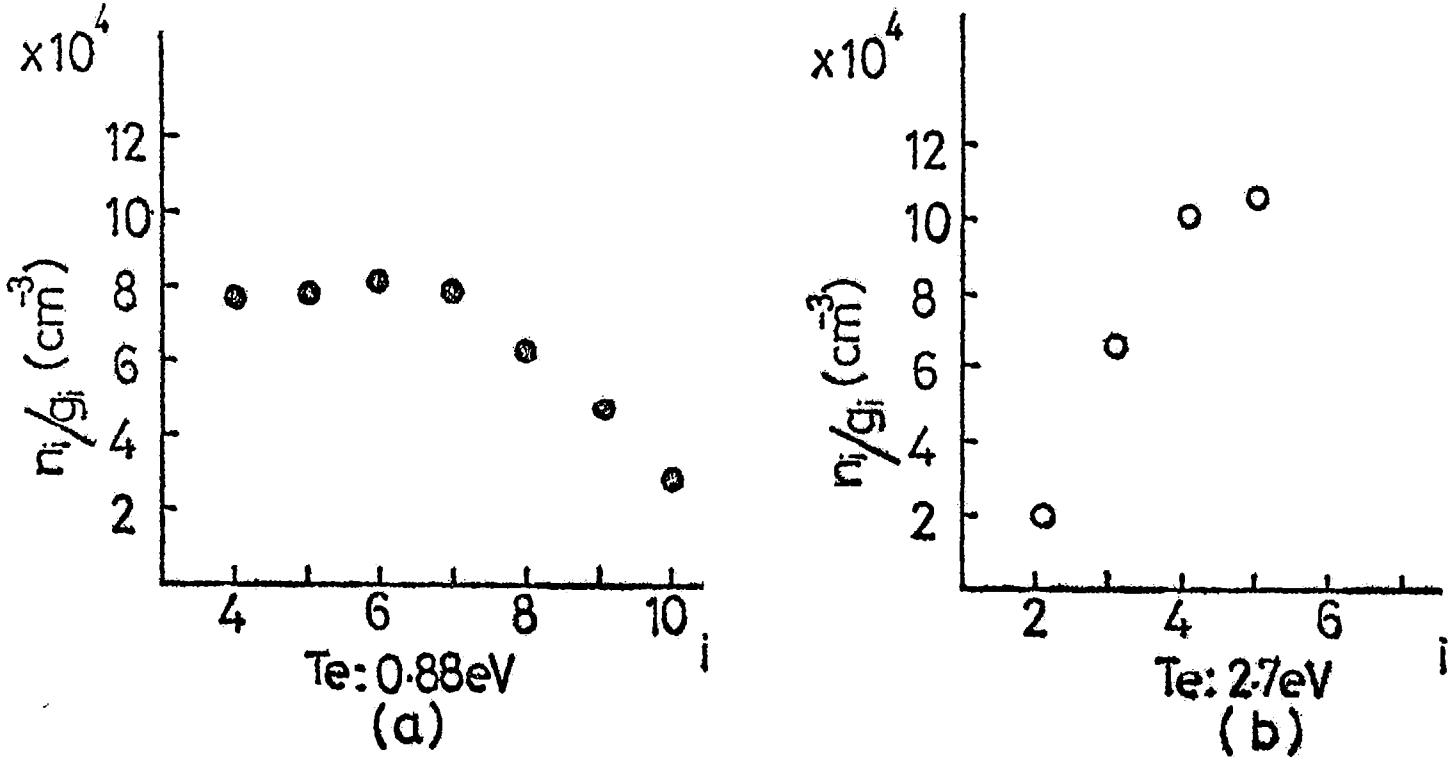

Fig.1

Population density n_i divided by the statistical weight g_i of level i.
a): obtained from the measurements in visible region by Otsuka et al.,[2)]
b): obtained from the measurements in extreme ultra violet region by Sato et al.[3)]

Data Needs, Priorities and Accuracies for Plasma Spectroscopy

by

R.W.P. McWhirter,

Appleton Laboratory, Abingdon, OX14 3DB, UK.

1. Introduction

This paper presents the theory underlying plasma spectroscopy as it applies to both laboratory and astronomical sources. Particular attention is paid to the development of diagnostic methods by which it is possible to derive the plasma properties. Many of these methods have been developed for the interpretation of astronomical spectra and some of these can with care be applied to laboratory plasmas.

The main difference between laboratory and astronomical plasmas is physical size. Lifetime is also important and time dependent effects are now recognised as sometimes significant in astronomical cases. Time-dependence has always been recognised as central to the understanding of laboratory plasma spectroscopy.

In the theory developed below it is shown that the intensity of a spectral line from the type of plasma with which we are concerned is given by the sum of two terms each consisting of the product of the electron and ion density with an excitation rate coefficient. The terms refer respectively to the ground and metastable levels of the ion. If the line in question is one of a number arising from the same upper level then the whole must also be multiplied by the ratio of transition probabilities. Thus the atomic data required for the calculation of spectral intensities are primarily the excitation rate coefficients from the ground and metastable levels of the ion. Sometimes radiative transition probabilities are also needed. The accuracy of the calculated intensity is directly proportional to the accuracy of this data. The time-dependence of such excitation processes and subsequent decay is generally sufficiently rapid that there is no need to take account of the time-constant of the atomic processes.

To calculate the population density of ions in ground and metastable levels it is necessary to solve the time-dependent ionisation equation. In this case the atomic time-constants are generally important and it is this aspect of the problem that gives the time-dependence to the results. In discussing the ionisation equation it is shown that the following processes are important.

a. Ionisation by electron impact with both ground level and metastable ions.
b. Auto-ionisation from the same levels.
c. Radiative recombination.
d. Dielectronic recombination.
e. Collisional-radiative recombination.

Values for each of these rate coefficients is required for the solution of the equation. However, while the plasma is ionising before the steady-state is reached the recombination coefficients have much less influence and only the first two, a and b, need be known with any accuracy. Once the plasma has had time to reach the steady-state of ionisation equilibrium then all five coefficients are needed. It should be pointed out that a proper physical solution should include plasma transport such as diffusion and that these terms require to be included in a simultaneous solution.

It is shown that the time-constant to reach the steady-state for ionisation balance is given very roughly as $10^{12}/n_e$ and is therefore about $^1/_{10}$ seconds for a typical tokamak plasma. This may be comparable with particle containment times and emphasises the need to take account of time-dependence.

The calculation of the population density of metastable ions requires in addition to the coefficients already listed coefficients of collisional excitation and of radiative decay from the metastable levels - so-called forbidden transitions. Since frequently the metastable levels are more highly populated than the ground level it is important to have reliable values for these important coefficients.

Through the application of the theory that is developed in this paper it is possible to make estimates of the following quantities.

a. The concentration of impurities.
b. The effective Z of the plasma.
c. The radiated power loss.
d. The electron temperature.
e. The electron density.
f. The extent to which the plasma departs from ionisation balance.

However, the successful application of these methods requires a range of reliable atomic data. The availability of this is indicated now.

The electron impact excitation of positive ions is the subject of a recent review by Seaton. He discusses theoretical methods that require large computers and which have as their objective the calculation of rate coefficients having accuracies better than ± 20% - sometimes considerably better. A list giving access to some of the most recent calculations is given as an appendix to this paper.

Some attempts have been made to measure excitation rates experimentally. Accuracies of measurement are about ± 50% absolute and ± 20% relative. For Li-like ions good agreement is found. Thus temperature measurements are possible and these ions can be used to estimate impurity concentrations with good reliability. Recent crossed-beams measurements of cross-sections for 2s-2p excitation of Li-like ions are in good agreement with close-coupling calculations (Taylor et al. 1977). For other types of ions the situation is much less satisfactory. In the case of Be-like ions discrepancies between theory and experiment of up to a factor 4 have been found - considerably in excess of the measurement accuracy. Thus methods of measuring electron density by the Be-like lines ratio method are, to say the least, suspect at this time. Currently there is a very intensive programme that is world-wide to study Be-like lines - quantum-mechanically, astrophysically and in the laboratory. Thus maybe in a year a more satisfactory picture will emerge but at the moment it looks like discrepancies of up to a factor 4.

Ionisation rate coefficients are probably the next most important class of atomic data. These rates are essential for predicting the radiated power loss from a plasma. For the purposes we are concerned with here the values of the cross-sections near threshold are those that matter and we have recently completed a set of comparisons between theory and experiment in this region. (Burgess et al. 1977.) There are various methods of calculation of these coefficients of which the Coulomb Born is the most respectable. Since only a limited range of ions have been treated this way it is common to use one of the two simpler methods known as Seaton's empirical formula (SEF) and the Exchange Classical Impact Parameter (ECIP) method. The comparison we have done favours the ECIP method. Present methods apparently can in some circumstances give errors up to a factor 2. It should also be pointed out that our comparison is based on a rather small sample (17 different ions) and that further crossed-beam measurements especially for multiple charged ions would be of great value.

The theoretical calculation of radiative transition probabilities is by its nature a simpler process - the difference between a two body and a three body collision - and consequently better agreement is found with experiment. Such calculations and corresponding measurements are nonetheless important, not only for the values provided but also because they allow an intermediate check on the theoretical wave-functions being used for the much more difficult electron impact problem. Attention should be drawn particularly here to the need for values of the spontaneous transition probabilities for the radiation decay of metastable levels - through intermediate coupling, electric quadrupole, magnetic dipole, etc. Beam foil spectroscopy offers the possibility of valuable contributions here.

Recent progress in the theoretical calculation of these various rate coefficients is impressive and promises well for the future. Then it will be possible to apply the theory developed in the remainder of this paper to various studies that should lead through spectroscopy to a better understanding of plasma physics.

Figure 1.1 illustrates some of the concepts and magnitudes associated with spectroscopy. It is useful to be familiar with both wavelength and energy units for photons. The units Angstroms ($\equiv 10^{-8}$ cms $\equiv {}^{1}/_{10}$ nm) and electron volts are used. It is convenient to remember that a 100 Å photon has an energy of about 100 eV. The whole range of photon wavelengths from the visible to the x-ray include the main spectral lines of all elements and their ions. The available techniques for the study of spectra serve to divide the region into spectral ranges by which they are known. Thus reference is made to the visible, the quartz ultraviolet, the grazing incidence, etc. The scale at the bottom of the diagram gives the temperature corresponding to the mean energies of the photon scale. In a very crude way it serves to indicate the magnitude of plasma temperature required to excite the corresponding spectral wavelengths.

The concept of temperature is bound up with the idea of thermodynamic equilibrium and although all the plasmas to be discussed are very far from thermodynamic equilibrium many of the concepts are important in what follows.

2.1 Maxwellian distribution of particle velocities

Consider a system of particles contained in some way such that there is no loss or gain of particles or energy. The particles exchange energy with each other by making collisions in which the total kinetic energy will take up an equilibrium distribution where the movement of particles out of one region of velocity space is balanced by an equal movement into the same space. The details of the argument leading to the specific derivation of the velocity distribution are to be found in various texts on statistical mechanics such as Ter Haar's "Elements of Statistical Mechanics" (1955). The outline of the argument is as follows.

Particles are identified by their position and velocity co-ordinates (x,y,z) and (u,v,w) respectively. A velocity distribution function $f(u,v,w)\,du\,dv\,dw$ is introduced and is the number of particles per unit volume having velocities in the interval u to $u + du$, v to $v + dv$ and w to $w + dw$. The equilibrium distribution function has the property that $df/dt = 0$. The method is to identify two regions of velocity space (u_1,v_1,w_1) and (u_2,v_2,w_2) and consider collisions that transfer particles between them assuming conservation of momentum and kinetic energy and any

reasonable law of force between them. In this way it may be shown that

$$\frac{df_1}{dt} = - \int (f_1 f_2 - f_1' f_2') \, a \, du_2 \, dv_2 \, dw_2 \, d\omega$$

where the primes relate to the instant after the collision, a is determined by the law of force between the colliding particles and ω is the angle of scatter. Thus the equilibrium condition is met if $f_1 2_2 = f_1' f_2'$ no matter what the value of a and ω. In other words the details of the individual collisions do not influence the nature of the equilibrium distribution function. On the other hand the assumptions of the conservation of kinetic energy and momentum are important. The requirement that $f_1 f_2 = f_1' f_2'$ is met by the Maxwellian velocity distribution thus: (see figure 2.1)

$$f(u,v,w) = n \left(\frac{m}{2\pi kT}\right)^{3/2} \exp \left(- \frac{m(u^2+v^2+w^2)}{2kT}\right)$$

where n is the total number of particles per unit volume and $\frac{3kT}{m} = \overline{c^2} =$ mean value of $u^2+v^2+w^2$. If m is the mass of an individual particle (all of which are assumed to be the same) then T is defined as their kinetic temperature (k is Boltzmann's constant). If there is more than one kind of particle then in equilibrium they will take up the same temperature and their mean velocities will be related inversely as the square roots of their masses. In the case of a hydrogen plasma composed of free electrons and protons the ratio of the mean (RMS) velocities is $\frac{m_p}{m_e} = 43$

ie in an equilibrium mixture of electrons and protons the electrons on average have velocities 43 times greater than the protons. This will be seen to have a number of important consequences in what follows and is dramatically illustrated in figure 2.2.

For the concept of temperature to be applicable requires that there be Maxwellian distributions of particle velocities. The extent to which this is realised in practice is one of the important matters discussed later.

2.2 Saha-Boltzmann population distribution

If account is taken of the atomic structure of the particles in the previous example so that some of the energy of the system goes to exciting and ionising the atoms then a quantum statistical argument may be used to derive the equilibrium population distribution among the excited levels. This is expressed in the Saha-Boltzmann

$$\frac{n_e n(z+1,g)}{n(z,p)} = \frac{\omega(z+1,g)}{\omega(z,p)} \, 2 \, \frac{(2\pi m_e kT)^{3/2}}{h^3} \exp \frac{-\chi(z,p)}{kT}$$

where $n(z+1,g)$ is the population number density in the ground level g of ions having charge $z+1$.
$n(z,p)$ is the same thing for level p of ions z.
$\omega(z+1,g)$ and $\omega(z,p)$ are the corresponding statistical weights.
$\chi(z,p)$ is the ionisation potential of level p of ion z.

By expressing the distribution in the above manner it is possible to avoid some difficulties that arise in the more usual formulation (the Saha equation) which is in terms of partition functions. The partition function is the statistical weight summed over all levels of the ion and

depends on particle density and temperature.

When attention is confined to one species of ion then the Boltzmann equation is useful

$$\frac{n(z,p)}{n(z,q)} = \frac{\omega(z,p)}{\omega(z,q)} \exp - \frac{\chi(z,p-q)}{kT}$$

$\chi(z,p-q)$ is the difference in excitation potential between levels p and q of ion of charge z.

2.3 Black-body radiation and the Planck function

So far in discussing equilibrium distributions account has been taken of elastic and inelastic collision processes in redistributing the available energy between the available energy states. Since charged particles and atoms are involved there is the additional possibility that energy appears in the form of radiation. To meet the basic equilibrium requirement means that radiation energy must also be contained within the system - say by having hypothetical fully reflecting walls. Under these conditions the radiation builds up to a distribution given by the Planck function and is called black-body radiation

$$B(\nu) = \frac{2h\nu^3}{c^2} \frac{1}{\exp(h\nu/kT)-1}$$

$h\nu$ is the energy of a photon of frequency ν.

2.4 Complete thermodynamic equilibrium and local thermal equilibrium

A system that meets all these statistical relations is in the complete thermodynamic equilibrium. It is a hypothetical situation although it comes close to being met in practice in the laboratory where black-body furnaces are used for the calibration of absolute radiation detectors.

In the case of plasmas discussed in this paper the radiation escapes relatively easily but the particles are at least partially retained by such forces as magnetic or gravitational fields. Under these conditions the Planck function does not describe the radiation but it sometimes happens that the particle collision rate is sufficient to ensure that the Saha-Boltzmann and Maxwellian distributions are good descriptions. Such a plasma is said to be in Local Thermal Equilibrium - LTE. The conditions necessary for LTE to apply are discussed later.

2.5 The principle of detailed balance

It follows from these considerations of a system in complete thermodynamic equilibrium that the rate at which particles move from one state to another is exactly balanced by the rate in the inverse direction. It may be shown that transitions from the initial to the final state through a third state must be treated separately and that only the direct processes must balance. This principle results in a number of useful relationships between the coefficients used to describe individual processes (such as collision rate coefficients) in forward and inverse directions in systems that are very far from thermodynamic equilibrium. It is frequently easier to calculate the rate of an inverse process and use the principle of detailed balance to evaluate the required direct process.

3.1 Low density plasmas

Most of the plasmas discussed depart significantly from any of the equilibrium configurations discussed above and since, of these LTE is the most common, they are often called non-LTE plasmas. However, it is usually better to refer to them as low density plasmas. There are two main physical reasons for departures from equilibrium viz:

a. At densities lower than that required for LTE it generally happens that when an electron moves from a level of higher energy to one of lower it does so by giving energy to radiation. In contrast movement from lower to higher levels requires a collision process involving particles only. Such processes are not inverse in the detailed balance sense and cannot therefore give rise to LTE population distributions. The best known example is the ionisation balance in the solar corona where for hydrogen-like ions (to take the simplest case) ionisation by electron collision is balanced by radiative recombination. In general the balance is between a multitude of collisional and radiative processes to be discussed later.

b. The second reason for departure from LTE (which may be additional to the first) is that the plasma conditions (particularly temperature and density) are changing on a time scale shorter than the relaxation times for the atomic processes establishing the population distributions.

In discussing non-LTE population distributions it is convenient to separate to some extent the establishment of the distribution among the ions (designated by their charge) from that among the bound levels of individual ions. When considering the stage of ionisation it is generally adequate to take account only of the population in the ground level and sometimes a metastable level. This point will be returned to later when the distribution among the excited levels is considered but is assumed in the meantime.

3.2 Collisional ionisation and excitation

When an electron of sufficient kinetic energy strikes an atom or ion one of the things that can happen is that a bound electron is knocked out and becomes free - ionisation. A measure of this process is the ionisation cross-section Q that the target ion offers the electron in units of cm^2 (sometimes πa_o^2 - a_o: radius of first Bohr orbit in Hydrogen = $0.529.10^{-8}$cm). Clearly such a cross-section has a threshold below which the electron energy is not sufficient to cause ionisation (= ionisation potential). Above threshold ionisation cross-sections rise to a maximum at an energy about two or three times threshold and then, for electric dipole transitions, fall off to an asymptotic value proportional to $^{\log E}/E$. Each of the bound electrons of the atom or ion contributes to the total cross-section.

For plasmas it is generally more convenient to use ionisation rate coefficients S rather than cross-sections Q. These are related by $S = \langle Q.v \rangle$ where the average is taken over the velocity (v) distribution of the electrons assumed to be Maxwellian. Rate coefficients are generally expressed in $cm^3\ s^{-1}$.

Theoretical calculations and experimental measurements of these cross-sections have been reviewed by Bely and Van Regemorter (1970), by Dolder

(1969), by Kunze (1972) and by Burgess et al. (1977). A recent review by Seaton (1975) also touches on this work. On the basis of a comprehensive survey of all available experimental measurements of cross-sections (up to 1967) Lotz (1967) has devised an expression to represent electron-impact ionisation cross-sections. The expression has three free parameters which have been tabulated to give cross-section values that the author claims to represent the measured values to + 40-30%. The method has been extended to atoms and ions for which there are no measurements by interpolation and extrapolation of the parameters and by using theory as a guide. An extensive tabulation of values is given in a report IPPL/62 by the same author.

Figures 3.1 and 3.2 illustrate comparative values according to three authors whose work will be discussed later. The values ascribed to Jordan are based on an expression for near threshold ionisation due to Seaton (1964) (referred to as SEF - semi-empirical formula) based on some theoretical and some experimental measurements for positive ions and using classical theory as a guide for extrapolation. Summers' values are based exclusively on theoretical calculations using the exchange classical impact parameter approximation (Burgess 1964). Lotz values are based on his 3 parameter empirical fit formula that is very useful because so little ambiguity arises in its use. Jordan and Summers but not Lotz include auto-ionisation contributions to the total coefficients.

The comparison (figures 3.1 and 3.2) shows the good agreement between Lotz and Jordan at low temperatures. The SEF expression used by Jordan is intended to be used only in the threshold region. Summers' values are about a factor $\frac{1}{2}$ of those by Lotz but Kunze (1972) points out that more recent experimental values for ions are in good agreement with Summers' values. (See also Burgess et al. 1977.)

It is often adequate and certainly simpler to use an empirical formula developed by Wilson and White (unpublished) thus:

$$S = \zeta \frac{0.90\times10^{-5}}{\chi^{3/2}} \frac{(kT_e/\chi)^{\frac{1}{2}}}{(4.88+kT_e/\chi)} \exp \quad -\chi/kT_e \qquad cm^3\ s^{-1}$$

where χ is the ionisation potential in eV
T_e is the electron temperature in K and
ζ is the total number of outer electrons having the same principal quantum number.

When compared with values calculated by Lotz this simple formula gives results that agree within a factor 3.

It is convenient to consider also at this stage the related process of collisional excitation where the impinging electron causes a bound-bound transition from a level of lower energy to one of higher. In this paper the term de-excitation will be used for the inverse process.

A useful review of electron impact excitation of positive ions has been completed recently by Seaton (1975). It updates and extends earlier related reviews by Gabriel and Jordan (1972), Bely and van Regemorter (1970), Kunze (1972).

A remarkable feature of excitation cross-sections for positive ions is their finite value at threshold. Typical of these are the two sets of curves shown in figure 3.3. Notice that for atomic hydrogen these calculations predict zero cross-section at threshold and that there is a greater difference between the atom case (Z = 1) and hydrogen-like helium (Z = 2) than between hydrogen-like helium and hydrogen-like ion of infinite charge.

Again for plasmas it is more convenient to use rate coefficients than cross-sections. The following simple expression (Seaton 1964) allows values to be calculated for dipole transitions and for $kT_e \lesssim \chi$

$$X(p,q) = \frac{1.71\times10^{-3}\,\bar{g}f(p,q)}{T_e^{\frac{1}{2}}\,\chi(p,q)} \exp - \frac{1.16\times10^{4}\chi(p,q)}{T_e} \quad cm^3\ s^{-1}$$

$\bar{g}$ is the effective mean Gaunt factor which Seaton suggests should be put equal to 0.2 to get results that agree with more sophisticated calculations to within a factor 3. Seaton's value applies to threshold excitation, ie $kT_e < \sim \chi$. For excitation at higher values of (kT_e/χ) reference should be made to a paper by van Regemorter (1962).
$f(p,q)$ is the absorption oscillator strength for the transition
$\chi(p,q)$ is the excitation potential in eV and
T_e is the electron temperature in K.

Specific calculations and some measurements of greater accuracy have been done for a number of transitions and for these reference should be made to the review papers mentioned above.

3.3 Radiative recombination and spontaneous radiative decay

Radiative recombination takes place when a free electron in the field of a positive ion makes a radiative transition to a bound level thus forming an ion or atom of charge one less than initially.

$$N(z) + e \rightarrow N(z-1) + h\nu$$

The photon carries away the excess energy of the interaction, ie the kinetic energy of the electron, before recombination plus the ionisation potential of the final bound level. Thus the recombination spectrum is characterised by discontinuities corresponding to the energies of the ionisation potentials of the relevant bound levels. These lie to the long wavelength end of the recombination continuum spectrum.

Radiative recombination, unlike collisional recombination, is a two body process so that the rate at which it takes place is proportional to the product of the electron and ion densities. The remaining factor in the product is the radiative recombination coefficient and is usually given the symbol α. Its value depends on the level to which recombination takes place, ie on the atomic structure of the ion and the temperature of the free electrons. Since it is essentially a two body process it can be evaluated with better precision than collisional ionisation for example. The difficulty of the calculation is the determination of the atomic structure. The problem of calculating radiative recombination coefficients for the formation of hydrogen-like ions has been treated by Menzel and Pekeris (1935) and corrected by Burgess (1958). On the basis of their treatment Seaton (1959) has derived a three term expression for the Gaunt factor giving for the radiative recombination coefficient into all levels of a hydrogen-like ion of nuclear charge Z:

$$\alpha = 5.20\times10^{-14}\ Z\ \lambda^{\frac{1}{2}}\ \{\ 0.43 + \tfrac{1}{2}\ln\lambda + 0.47\ \lambda^{-1/3}\ \}\ cm^3\ s^{-1}$$

where $\lambda = 1.58 \times 10^5\ Z^2/T$.

This formula has been used to calculate the values plotted in figure 3.4 which compares them with collisional ionisation coefficients from the ground levels of hydrogen-like ions.

Recombination coefficients into the individual levels of H-like ions are also given in the paper by Seaton.

For radiative recombination to form ions other than H-like ions (or hydrogen) the calculation of rate coefficients requires account to be taken of the more complex structure of the ions involved. However, by assuming a simple Coulomb field and using non-integral effective quantum numbers results of good accuracy are obtained. This method is discussed by Burgess and Seaton (1960).

The inverse of radiative recombination is photo-ionisation and the rate at which it takes place is proportional to the radiation flux, and in order that it balances radiative recombination to give a Saha-Boltzmann population distribution (principle of detailed balance) the flux density and spectrum must be that of a black-body at the temperature of the electrons. For the plasmas discussed here this is never the case.

The spectral lines whose study is the subject of the present paper arise from the spontaneous radiative decay from an upper to a lower bound level. The coefficient used to describe the rate of this process is the spontaneous transition probability. It is given the symbol A(p,q) and measured in s^{-1}. Its calculation and measurement for many atoms and ions is an important branch of atomic physics. This work is continually kept under review by a group at the Bureau of Standards in Washington. The latest addition to their bibliography is by Fuhr and Wiese (1973) and their main compilations are by Wiese, Smith and Glennon (1966) and Wiese, Smith and Miles (1969). From a study of systematic trends among known values, Wiese and Weiss (1968) have suggested methods of extrapolation from existing data to estimate values that are not otherwise available. A useful generally applicable method of estimating transition probabilities for electron dipole transitions is due to Bates and Damgaard (1949). The basis of the method is similar to that of Burgess and Seaton for radiative recombination. The latter was developed from the former.

Oscillator strengths, f-values and radiative lifetimes are directly related to spontaneous transition probabilities. Also related through the principle of detailed balance are the two coefficients for induced transitions: photo-excitation B(q,p) and stimulated emission B(p,q) defined here in terms of radiation density. These are all inter-related as follows:

$$\begin{aligned}\omega(p)\,A(p,q) &= \omega(p)\,\frac{8\pi h\nu(p,q)^3}{c^3}\,B(p,q)\\ &= \omega(q)\,\frac{8\pi h\nu(p,q)^3}{c^3}\,B(q,p)\\ &= \frac{8\pi^2 e^2 \nu(p,q)^2}{mc^3}\,\omega(q)\,f(q,p)\end{aligned}$$

where $\omega(p)$ is the statistical weight of level p.
$\nu(p,q)$ is the frequency of the radiation.
$f(q,p)$ is the absorption of f-value or oscillator strength.

$$\omega(q)\,f(q,p) = \omega(p)\,f(p,q)$$

where $f(q,p)$ is the emission f-value or oscillator strength.

The radiative lifetime τ is the reciprocal of the sum of all the radiation coefficients affecting the level in question. Usually

$$\tau(p) = \frac{1}{\sum_q A(p,q)}\ \text{s}$$

3.4 Collisional-radiative recombination and ionisation

In calculating the radiative recombination coefficient it was tacitly assumed that the total coefficient for an ion was the sum of the coefficients into each of the quantum levels separately. On the other hand only ground level ionisation was considered. The basis of these assumptions will now be considered and this will lead to a discussion of the collisional-radiative model first described in the following series of papers: Bates, Kingston and McWhirter (1962a and b), Bates and Kingston (1963) and McWhirter and Hearn (1963).

These authors considered the atomic interactions between the particles of a system composed of hydrogen-like ions of charge (Z-1), electrons and fully stripped nuclei of charge Z. The processes taken account of, and which contribute to the interaction, are as follows:

a. Collisional excitation (and de-excitation) from (or into) any bound level q to (or from) an upper level p

$N(Z-1,q) + e \rightleftharpoons N(Z-1,p) + e$ Rate coefficients $X(q,p), X(p,q)$

b. Collisional ionisation from, and three body recombination into, any level p

$N(Z-1,p) + e \rightleftharpoons N(Z) + 2e$ $S(p)$, $\beta(p)$

c. Spontaneous radiative decay from any level p into a lower level q

$N(Z-1,p) \rightarrow N(Z-1,q)\ h\nu$ $A(p,q)$

d. Radiative recombination into level p

$N(Z) + e \rightarrow N(Z-1,p) + h\nu$ $\alpha(p)$

These processes are illustrated in figure 3.5.

It is assumed that the density of radiation is small (including that arising from processes (c) and (d) so that photo-ionisation and photo-excitation may be neglected. Note, however, that the second paper by Bates, Kingston and McWhirter, mentioned above (1962b), takes account of the plasma being optically thick. In order to limit the problem to a manageable size the possible presence of He-like and other ions has been ignored.

The time rate of change of the population density $n(p)$ of level p may be expressed thus:

$$\frac{dn(p)}{dt} = -n(p)\left\{ n_e \left[S(p) + \sum_{q\neq p} X(p,q) \right] + \sum_{q<p} A(p,q) \right\}$$
$$+ n_e \sum_{q\neq p} n(q)\, X(q,p) + \sum_{q>p} n(q)\, A(q,p)$$
$$+ n_e n(Z)\, \alpha(p) + n_e^2\, n(Z)\, \beta(p)$$

The level p or q is identified by its principal quantum number where the relative populations of the sub-levels, identified by their inner quantum numbers, are assumed to be statistical. In principle p and q take all values between 1 and infinity leading to an infinite set of equations and containing sums to infinity. Nevertheless it has been possible to obtain a solution because of the following two properties of the physical

system.

a. The reciprocal lifetime of a level p is the sum of radiative and collisional components. For all levels but the ground level the lifetime is therefore shorter than or equal to the radiative lifetime. For hydrogen the latter are about 10^{-7} secs and for hydrogen-like ions are shorter (τ proportional to Z^{-4}). The lifetime of the ground level which cannot decay radiatively, is determined by collisions and depends particularly, therefore, on the electron density. In the solar atmosphere ground level lifetimes are between 10^2 and 10^4 secs and even in most laboratory plasmas it is a good approximation to say that excited levels lifetimes are very much shorter than for the ground level. This leads to the quasi-steady-state approximation where $\frac{dn(p)}{dt}$ is equated to zero except for p = 1. It may be shown that this leads to valid solutions for times greater than about $10^{-7}/Z^4$ secs.

b. Inspection of the numerical values of the various coefficients shows the following trends: the radiative coefficients (A and α) decrease with increasing p whereas the collisional coefficients (X, S and β) increase. Thus to any desired accuracy there is always some level p above which it is a good approximation to neglect radiative processes. Since each collision process is accompanied by its inverse the principle of detailed balance may be applied and leads to the populations of these levels being adequately given by the Saha-Boltzmann equation. This connects the population densities of these levels to the continuum of free electrons and population density of stripped ions n(Z).

With these two approximations the infinite set of differential equations reduces to a finite set of simultaneous equations and one differential equation. Thus a solution is possible by numerical methods and the results may be expressed in the following simplified form:

$$n(p) = n_o(p) + n_1(p)\, n(1)$$

$$\frac{dn(1)}{dt} = - n_e\, n(1)\, S_{CR} + n_e\, n(Z)\, \alpha_{CR}$$

The coefficients $n_o(p)$ and $n_o(p)$ have been tabulated and allow the calculation of the population density level p under circumstances where the plasma is undergoing dynamic ionisation or recombination. S_{CR} and α_{CR} are the collisional-radiative ionisation and recombination coefficients respectively. At very low densities they reduce to the collisional ionisation coefficient for the ground level and the radiation recombination coefficient summed over all levels.

The results of these calculations can be presented in a more general way by adopting reduced temperatures Θ and densities η_e. These are related to their actual equivalents by the following Z scaling laws:

$$\Theta = \frac{T}{Z^2}$$

$$\eta_e = \frac{n_e}{Z^7}$$

Table 3.1

Relaxation Time Constants $Z^4 \tau(p)$ secs.

Θ	$\eta(c)$	p = 1	p = 2	p = 3	p = 15
4000	10^{8}	3.1^{+11}	2.1^{-9}	1.0^{-8}	1.1^{-6}
4000	10^{18}	3.1^{+1}	1.4^{-11}	2.8^{-13}	1.2^{-16}
16000	10^{8}	1.2^{+2}	2.1^{-9}	1.0^{-8}	2.1^{-6}
16000	10^{18}	1.2^{-8}	1.8^{-12}	1.7^{-13}	2.5^{-16}
64000	10^{8}	5.4^{-1}	2.1^{-9}	1.0^{-8}	3.5^{-6}
64000	10^{15}	5.4^{-8}	7.4^{-10}	2.3^{-10}	4.9^{-13}
64000	10^{18}	5.4^{-11}	1.1^{-12}	2.3^{-13}	4.9^{-16}
256000	10^{8}	1.3^{-1}	2.1^{-9}	1.0^{-8}	5.5^{-6}
256000	10^{12}	1.3^{-5}	2.1^{-9}	9.8^{-9}	9.8^{-10}
256000	10^{15}	1.3^{-8}	9.3^{-10}	4.1^{-10}	9.8^{-13}
256000	10^{18}	1.3^{-11}	1.7^{-12}	4.3^{-13}	9.8^{-16}

The population density of an excited level p may also be presented in reduced form thus

$$\eta(p) = \frac{Xn(p)}{Z}$$

where $X = n_e/n(Z)$ and for plasma neutrality is less than or equal to Z.

In table 3.1 are given values of the excited state lifetimes, showing that only in very extreme conditions of high density and temperature does the lifetime of the ground level approach 10% of that of the excited levels. However, the table does illustrate the limits of validity of the quasi-steady-state approximation.

The validity of second approximation is shown in figure 3.6 which illustrates the way in which radiative processes give way to collisions as p increases. The Collision Limit marked in this figure is defined as the lowest level from which an electron has a greater probability of making a transition upwards as compared with downwards (excluding p = 1). Above the collision limit collisions dominate. As the electron density increases collisions become more dominant at lower and lower levels as shown in figure 3.7 where at a density of $\eta_e = 10^{16}$ cm^{-3} collisions exceed radiative processes in populating the ground level. This value is relative independent of temperature. The approach of the excited level population densities to their Saha-Boltzmann values is shown in figure 3.8.

Figure 3.9 gives values for the collisional radiative recombination coefficient and shows how at higher electron density the density independent radiative coefficient increases as the collisional processes take over. At high density the coefficient is proportional to density in the same way as a three-body recombination coefficient.

The dependence of collisional-radiative ionisation coefficients on density is much less dramatic and resembles a step function. The step corresponds to the onset of stepwise excitation as the collision limit comes down to p = 2. Values are plotted in figure 3.10.

3.5 Dielectronic recombination

If an electron collides with an ion at an energy just below the threshold for excitation it is possible for this excitation to take place but because the impinging electron does not then have the energy to escape from the Coulomb field it becomes captured in an outer orbital. This is the first step of dielectronic recombination. It has already been noted that excitation cross-sections for positive ions at threshold are finite so their extrapolation below threshold means that there is a relatively high probability of capture. The inverse process to capture is autoionisation where the ion makes a radiationless transition to its ground level and an electron is ejected. Competing with autoionisation is the so-called stabilisation process that makes dielectronic recombination effective. Stabilisation takes place when the excited electron (the lower of the two) makes a spontaneous radiative decay thus reducing the total internal energy of the recombined ion to below its ionisation potential. In some circumstances radiative decay does not take the ion below its ionisation potential and gives rise to the possibility of Secondary autoionisation (Blaha, 1972). Finally the captured electron cascades down to a lower level.

The dielectronic recombination process has been reviewed recently by Seaton and Storey (1977) and has been worked out in detail by Burgess (1965 and 1964). The quantitative calculation of the rate of dielectronic

recombination is presented as follows. Dielectronic capture and autoionisation may be represented thus:

$$N(z,i) + e \rightleftharpoons N(z-1, n\ell)$$

The symbols C_d and A_a are used to represent the coefficients for these two processes such that their rates are respectively $n_e.n(z,i).C_d$ and $n(a-1,j,n\ell).A_a$. Since these are inverse processes their rate coefficients are related by detailed balance thus:

$$\frac{A_a}{C_d} = S(T) = \frac{2(2\pi mkT)^{3/2}}{h^3} \frac{\omega(z,i)}{\omega(z-1,j,n\ell)} e^{E_o/kT}$$

where S(T) is calculated using the Saha-Boltzmann equation.

The stabilisation process may be represented thus:

$$N(z-1,j,n\ell) \rightarrow N(z-1,i,n\ell) + h\nu(i,j)$$

and its rate coefficient is given the symbol A_r.

Thus the recombination rate is the rate of dielectronic capture multiplied by the ratio of stabilisation on the total of autoionisation plus stabilisation thus:

$$n_e\, n(z,i)\, \alpha_d = \Sigma\, n_e\, n(z,i)\, C_d \frac{A_r}{A_a + A_r}$$

The summation sign indicates the need to sum over all the possible alternative routes for the recombination process to take. Thus there may be a number of different levels j available for excitation by the impinging electron. Also there are many alternative levels $n\ell$ into which it may be captured. Introducing the Saha-Boltzmann ratio S(T) and cancelling the particle densities gives

$$\alpha_d = \Sigma \frac{1}{S(T)} \frac{A_a A_r}{A_a + A_r}$$

$$\simeq \frac{h^3}{2(2\pi mkT)^{3/2}} \frac{1}{\omega(z,i)} \sum_j A_r\, e^{-E_o/kT} \sum_{n\ell} \frac{A_a}{A_a + A_r} \omega(z-1,j,n)$$

The problem now resolves itself into the determination of the terms where $A_a > A_r$ when $\frac{A_a}{A_a + A_r} \sim 1$ and those where $A_a < A_r$ when $\frac{A_a}{A_a + A_r} \sim 0$ and the process may be neglected. Thus paradoxically it is the levels that autoionise most strongly that contribute most to dielectronic recombination.

An approximate calculation of the dielectronic recombination coefficient gives the following expression

$$\alpha_d = \frac{8.2 \times 10^{-4}}{T_e^{3/2}} \frac{z^{\frac{1}{2}}(z+1)^2}{(z^2 + 13.4)^{\frac{1}{2}}} \exp(-E_o/kT_e)$$

$$\sum_j \frac{f(i,j)\, E_o^{\frac{1}{2}}}{(1 + 0.105x + 0.015x^2)} \text{ cm}^3\, \text{s}^{-1}$$

where $x = 0.0735\, (E_o/(z+1)$
E_o is the excitation potential i-j in eV
f is the absorption oscillator strength for i→j
z is the charge on the recombining ion.

Detailed calculations have been carried out by H P Summers (1974) for all ions of elements from hydrogen to argon. Further data is available in an Appleton Laboratory Report Number IM 367.

When dielectronic recombination and collisional-radiative recombination are coupled together, as was done by Summers in the work mentioned above, quite complicated effects result as shown in figure 3.11; coefficients are not additive but the full set of equations describing the processes affecting the populations of each individual level must be treated in detail. The effect of density on the collisional-dielectronic recombination coefficients may be seen from the curves in figure 3.11. Dielectronic recombination does not take place for H-like ions. The curves show only a slight influence of density due to collisional-radiative recombination where the $n_e = 10^{16}$ cm^{-3} curve lies slightly above the others at the low temperature end. The same effect is seen for He-like ions but now dielectronic recombination has enhanced the total between 10^6 and 10^7K. However, an increase of density reduces the dielectronic contribution as can be seen in the figure. The physical reason for this is that the captured electron in the outer orbital ($n\ell$) suffers collisional ionisation before it can cascade down. The Be-like curves show the same effects more dramatically.

3.6 Autoionisation

When an atom or ion suffers a collision it is possible for an inner electron to be raised to an excited level which may lie above the ionisation potential of the unperturbed atom or ion. An atom or ion excited in this way will interact with the adjacent continuum and autoionisation may take place whereby the electron becomes free leaving the ion in its ground level. As in the case of dielectronic recombination the excited ion may decay radiatively when no change in stage of ionisation takes place. Thus the rate at which autoionisation takes place may be expressed thus:

$$S_a = \sum_p \frac{A_a(p)}{A_a(p) + A_r(p)} \; X(g,p)$$

where p is a level from which autoionisation can take place. $A_a(p)$ and $A_r(p)$ are the probabilities of autoionisation and radiative decay from level p, and $X(g,p)$ is the rate of collisional excitation of level p from the ground level of the atom or ion. For the lower levels

$$A_a(p) >> A_r(p)$$

and the ratio of the probabilities becomes unity. The autoionisation rates should be added to the direct ionisation rates to give the total rates.

Autoionisation has been studied by Goldberg, Dupree and Allen (1965) and Bely (1968). Summers (1974) has used the same methods to obtain numerical values for some of the most important cases. These are illustrated in table 3.2 which shows total ionisation rates over the direct rate only. In some circumstances it may be seen that autoionisation increases the direct rate by almost ten times.

4.1 The steady-state ionisation balance

In order to calculate the state of ionisation of a plasma that does not meet the requirements of LTE it is necessary to take account of individual ionisation and recombination mechanisms. In this chapter

Table 3.2

Autoionisation Corrections

Tabulations of S_{cd} (including autoionisation)/S_{cd}

(z-I is the ion charge)

Te/z^2	$2s^2 2p$ Ionisation				$2p^6 3s$ Ionisation				
z	2	4	6	8	2	4	6	10	16
2.0^3	1.01	3.49	2.33	1.92	1.00	1.00	1.00	1.01	1.00
5.0^3	1.12	2.10	1.57	1.40	1.00	1.00	1.11	2.38	1.80
1.0^4	1.31	1.52	1.36	1.25	1.00	1.26	2.57	6.89	4.74
2.0^4	1.19	1.32	1.18	1.12	1.02	2.80	5.81	9.85	6.95
5.0^4	1.12	1.16	1.08	1.06	1.32	4.95	6.80	7.67	5.90
1.0^5	1.09	1.10	1.05	1.03	1.79	4.81	5.29	5.33	4.38
2.0^5	1.06	1.07	1.04	1.03	2.06	3.97	4.15	4.07	3.49
5.0^5	1.05	1.06	1.03	1.02	1.97	3.15	3.15	3.02	2.70

consideration is given to steady-state plasmas which have been sufficiently constant with time that their state of ionisation has settled to a steady value. Such conditions are seldom found in the laboratory for low density plasmas but the theory is widely assumed for astronomical plasmas such as the solar corona. Its specific application to the solar corona is discussed later.

In treating this problem all possible ionising and recombination processes have to be included but in practice only the processes discussed in the previous chapter are included. The dominant processes are collisional ionisation and radiative recombination but dielectronic recombination and autoionisation are also very important. At larger density collisional radiative processes take over.

In its formal treatment the problems required the solution of a set of equations as follows.

$$\frac{dn(z)}{dt} = n_e \left\{ - n(z)\, S(z) + n(z-1)\, S(s-1) - n(z)\, \alpha(z) + n(z+1)\, \alpha(z+1) \right\}$$

$z = 0$ to Z where Z is the nuclear charge.

In the steady-state $\frac{dn(z)}{dt} = 0$ for all values of z and the equations reduce to

$$\frac{n(z)}{n(z+1)} = \frac{\alpha(z+1)}{S(z)}$$

$S(z)$ and $\alpha(z+1)$ are the ionisation and recombination coefficients for ions of initial charge z and $z+1$. They include all the appropriate components such as collisional and autoionisation and radiative and dielectronic recombination.

It is generally assumed that the abundances of the element in question remains constant for all temperatures and densities, ie

$$\frac{n(E\ell)}{n(H)} = \sum_z \frac{n(z)}{n(H)}$$

where $n(H)$ is the Hydrogen (atom and ion) number density. (In both astronomical and laboratory fusion plasmas the main constituent is hydrogen with small additions of heavier elements.)

Calculations have been done for the most abundant elements by a number of authors. The most widely used is that by Jordan (1969) and includes all the significant processes mentioned above. A more recent calculation by Summers treats the recombination process in a more sophisticated manner and uses ionisation rate coefficients calculated by the ECIP method. It should be noted that the experimental evidence such as it is favours these values (see Burgess et al. 1977). For ions of low charge the discrepancy between Jordan's and Summers' results is small but it increases with charge and for iron there are large differences. At this time such differences should be treated as the approximate range of uncertainty in the calculations. The results of these two sets of calculations are illustrated in figure 4.1 for neon. These illustrate the relatively large differences between the results for Li-like ions (Ne VIII) but good agreement for H-like (Ne X). Figure 4.1 also illustrates a number of other features common to both calculations. Thus the discontinuity at Ne VIII of the otherwise regular progression of the curves is due to the extra difficulty in ionising a He-like ion which starts a new shell. The shoulder on the Li-like ion population to the high

temperature side of the peak arises because of the relatively high population of He-like ions at these temperatures and available therefore for recombination to form Li-like ions. This shoulder has important consequences for the sun's spectrum.

When these calculations are applied specifically to the solar atmosphere account has to be taken of a number of additional effects. The main dependence of the ionisation and recombination coefficients is on temperature. However, there is a smaller dependence in density but Summers' calculations are for constant values of density (figure 4.1 is for $n_e = 10^8$ cm^{-3}). Jordan's on the other hand includes the density variations in the solar atmosphere. For atoms and singly charged ions the photospheric radiation has a significant effect in causing photoionisation and photoexcitation. Summers' calculations do not include this but Jordan's do.

A remarkable feature of the solar atmosphere is the steep temperature gradient in the transition zone between the top of the chromosphere at a temperature less than 10^4K and the corona at a temperature of more than 10^6K. The presence of this gradient means that the atmosphere is stratified into layers each having a characteristic ion species. The resulting steep concentration gradients mean that diffusion is important including thermal diffusion.

At this stage the discussion leaves the solar atmosphere and returns to a consideration of the theoretical problem of ionisation balance in a homogeneous plasma of higher density. The theory of collisional-radiative recombination and ionisation shows how as the density increases the state of ionisation and population density of excited levels approaches the description given by the Saha-Boltzmann equation. It has already been shown that this happens when the density rises to a value where collisions completely dominate over radiative decay processes. The plasma conditions required for this to happen have been calculated and give rise to criteria for LTE to be a valid description of the plasma. This problem has been discussed by Griem (1963), Wilson (1962) and McWhirter (1968). The latter defines the criterion as the density at which the rate of transitions between all pairs of levels caused by collisions is ten times the corresponding radiative rates, ie

$$n_e \, X(p,q) > 10 \, A(p,q)$$

Using the expression given earlier for the excitation rate coefficient and the standard relation between f-values and transition probabilities this reduces to

$$n_e > 1.6 \times 10^{12} \, T_e^{\frac{1}{2}} \, \chi(p,q)^3 \; cm^{-3}$$

T_e : electron temperature in K,
$\chi(p,q)$ excitation potential in eV.

For a given ion to be in LTE this inequality must be met by all pairs of levels of the ion. Since it is least easily met by the pair having the greatest excitation potential it is sufficient if the criterion is satisfied by this largest value of $\chi(p,q)$ for the ion.

When this criterion is compared with the results of more detailed collision-radiative calculation for 10% departure from LTE good agreement is found. The criteria developed by Griem and Wilson (references above) give densities that agree within a factor 2 with the above despite differences in their derivation.

McWhirter (loc. cit.) also discusses the rate of approach of the population densities of the ions of a plasma to LTE following a change in the plasma conditions. This question is more conveniently considered later.

5.1 Equipartition times for electrons and positive ions

Before considering the problem of the time dependence of ionisation and recombination it is convenient to consider the times for equipartition of kinetic energy between the constituent particles of a plasma. In this case it is the rate of elastic collisions that matter. The problem is discussed by Spitzer (1956). He expresses the time required for the distribution of kinetic energies of identical particles to approach a Maxwellian distribution as the self-collision time 't_c' thus

$$t_c = \frac{m^{\frac{1}{2}} (3kT)^{3/2}}{5.71 \pi n e^4 Z^4 \ell n \Lambda} \quad s$$

where m is the mass of the particles
T is their temperature
n is their number density
e the electronic charge
Z the ionic charge,

and $\ell n \Lambda$ is defined by Spitzer and depends on the Debye shielding distance ($\ell n \Lambda \sim 20$).

Values based on this expression are plotted in figure 5.1 for electrons and protons. This shows that electrons come into equipartition with themselves more quickly than do protons in the ratio of the square root of their mass ratio ($\sim$ 50 times faster). This is another consequence of the much higher velocities of electrons compared with ions.

Spitzer also gives an expression for the equipartition time for test particles in a field of particles of another kind, viz

$$t_{eq} = \frac{3mm_1 k^{3/2}}{8(2\pi)^{\frac{1}{2}} n_1 Z^2 Z_1^2 e^4 \ell n \Lambda} \left(\frac{T}{m} + \frac{T_1}{m_1}\right)^{3/2} \quad s.$$

The symbols have the same meaning as before with the subscript $_1$ referring to the field particles. This expression was used to calculate the values of the equipartition time between electrons and protons plotted in figure 5.1.

6.1 Time-dependent ionisation and recombination

Most laboratory plasmas are produced by pulsed electrical discharges and are therefore of short time duration. In these circumstances it turns out to be necessary in predicting the stage of ionisation of the plasma to solve the full set of differential equations describing the rates of ionisation and recombination

$$\frac{dn(z)}{dt} = n_e \left\{ -n(z)\, S(z) + n(z-1)\, S(z-1) - n(z)\, \alpha(z) + n(z+1)\, \alpha(z+1) \right\}$$

z is the charge of the ion and runs from z = 0 to z = Z (the nuclear charge). S(z) and $\alpha(z)$ are the appropriate ionisation and recombination coefficients that have already been discussed. For laboratory plasmas of the type discussed here it turns out that the rates of the atomic processes are not fast enough for the plasma to approach a steady-state balance within its lifetime. Recent satellite observations of the sun show that there are time variations

of intensity in periods short compared with ionisation or recombination times leading to the need to use the full time rate equations here too. This possibility is only rarely considered in the astronomical literature but is fundamental to most treatments of pulsed laboratory plasmas.

Satisfactory analytical solutions of the set of differential equations are not available but the problem can be solved by numerical methods using computers. Since in general density n_e and temperature T are varying with time the ionisation and recombination coefficients also vary with time. Thus a numerical solution is the only satisfactory approach.

To illustrate the nature of the solution and indicate the magnitude of the atomic times consider the solution for a hypothetical plasma of constant temperature and density into which is introduced, at time zero, a small sample of some element (say nitrogen). Figure 6.1 shows how the ionisation takes place as successive electrons are stripped off. It is clear that recombination plays a negligible role until the system approaches the steady-state. From this type of calculation it is possible to predict the time required by such a plasma to reach the steady-state of ionisation balance. An approximate estimate of this may be made as follows. It may be seen from figure 3.4 that the values of the coefficients α and S at which corresponding values are equal lie along a band of values in the neighbourhood of $S = \alpha = 10^{-12}$ cm^3 s^{-1}. At these temperatures neighbouring ions have equal populations and are the dominant ions in the plasma. Thus the time for the last ion to be produced is given by

$$t_{ion} = \frac{1}{n_e \, 10^{-12}} \text{ s.}$$

and this is about equal to the time required for the plasma to reach its steady-state of ionisation.

Time resolved observations of spectral intensities from pulsed laboratory plasmas can provide reassuring evidence of the essential applicability of the type of analysis of ionisation given above. Thus figure 6.2 shows traces of the intensities of lines showing first the development of ionisation and then recombination during the discharge cycle. The full understanding of these observations requires also some consideration of the mechanism of excitation which will be discussed more fully below. Processes of plasma loss or in-flow may also modify the data. These are discussed later. Usually the spectrum of a pulsed plasma is dominated by ionisation only (such as a theta-pinch) or recombination only (such as a laser-produced plasma).

7.1 Excitation and spectral line intensities

The practical measurement of a spectral line intensity either in the laboratory or from an astronomical object requires the setting up of a spectrometer with possibly a light collector (telescope) and a detector. The signal measured by this system depends not only on the sensitivity of this system but also the volume of the source viewed by, and the acceptance cone of, the system. It also depends on the extent to which the radiation is attenuated by the intervening space including re-absorption by the source itself. This last point of radiation trapping is discussed later in a brief treatment of optically thick plasmas but the other more practical questions are outside the scope of this paper.

The remaining question of the atomic excitation mechanisms is discussed

here and, taking account of these aspects only, the intensity of a spectral line is given by

$$I = \frac{1}{4\pi} n(p)\, A(p,q)\, h\nu \text{ erg cm}^{-3} \text{ s}^{-1} \text{ sterad}^{-1}$$

Thus the atomic physics problem reduces to the calculation of the population density of the upper excited level p. For plasmas in LTE this is relatively simple and requires the application of the Saha-Boltzmann equation. Such plasmas are liable also to be optically thick and it is in taking account of this that the major problems of interpretation of spectral intensities lie for LTE plasmas. The case of low density optically thin plasmas is treated in this chapter.

Before discussing specific kinds of ions some mention should be made of continuum radiation. This arises from free-bound and free-free transitions of electrons in the fields of ions and gives rise to recombination radiation and bremsstrahlung respectively. For low density plasmas it is relatively weak compared with spectral lines. It will not be discussed further in this chapter but is mentioned later in connection with other aspects.

7.2 Hydrogen and Hydrogen-like ions

The excitation of hydrogen and hydrogen-like ions has already been discussed under the heading of collisional-radiative recombination and ionisation. However, it is useful to isolate some of the principal features of that somewhat complex treatment in order to build up a physical picture of the excitation mechanism. In the treatment of collisional-radiative processes the concept of the quasi-steady-state was introduced to obtain a solution for times longer than the radiative plus collisional relaxation times of the excited levels. Some modification of this approach may be necessary for ions having metastable levels but this will be left out of account at the moment and returned to later.

The population density of an excited level p is given by the expression quoted earlier

$$n(p) = n(1)\, n_1(p) + n_o(p).$$

The coefficients $n_1(p)$ and $n_o(p)$ are tabulated in the papers quoted previously for a number of values of p and for ranges of electron density and temperature. For low levels p and small values of density the first term is very much greater than the other. Physically this corresponds to the situation where p is excited from the ground level and decays again radiatively with negligible interference by other processes. Thus

$$\frac{dn(p)}{dt} = n_e\, n(1)\, X(1,p) - n(p) \sum_{r<p} A(p,r)$$

Applying the quasi-steady-state approximation gives

$$n(p) = n_e\, n(1)\, \frac{X(1,p)}{\sum_{r<p} A(p,r)}$$

and for the intensity

$$I = \frac{1}{4\pi}\, n_e\, n(1)\, X(1,p)\, \frac{A(p,q)}{\sum_{r<p} A(p,r)}\, h\nu$$

If (p,q) is the dominant transition the ratio of the As is very near to unity. Thus the intensity is determined by the excitation rate coefficient from the ground level.

For higher levels p (but below the collision limit) the contribution from $n_o(p)$ increases until above the collision limit it dominates. However, these higher transitions are much weaker and it is seldom that the spectral lines are sufficiently intense to be studied for the low density plasmas with which we are concerned.

Hutcheon and McWhirter (1973) have extended the collisional-radiative theory to plasmas of lower density where the metastable 2s level modifies the trend of the earlier results. They identify three regions of electron density between which there is a change in the intensity ratio of Ly α/Ly β. Figure 7.1 identifies the regions and figure 7.2 gives the calculated values of the ratio. It may be noted that the mid-density region gives the maximum intensity ratios. The physical reason for the change at low density is due to the possibility of 2 photon decay of the 2s level. This provides an alternative escape path to the emission of Ly α by the 2p level to which electrons in the 2s level are transferred by collisions with both positive ions and electrons.

7.3 Lithium-like ions

Of all ions in a low density plasma lithium-like are the simplest because they have no metastable levels. Nitrogen V has been studied extensively and its term scheme is shown in figure 7.3. All the spectral lines with which we are concerned arise from transitions by the single electron lying outside the $1s^2$ inner shell.

As before the intensities of the spectral lines are given under the quasi-steady-state approximation by their rates of collisional excitation from the ground (2s) level. Accurate quantum mechanical excitation rate coefficients for many of these levels have been published so the prediction of intensities is possible with good reliability. Some excitation rates for N V are shown in figure 7.4. From this it may be seen that the temperature dependence of the 2s 2p excitation is quite different from excitations to higher levels. This leads to the important possibility of using a measurement of the intensity ratio to determine the temperature of the plasma. The ratio of the intensity 2s 2p to any other line of the ion may be used, say the 2s 3p transition. The intensities are

$$I(2s\ 2p) = \frac{1}{4\pi} n_e\ n(2s)\ X(2s\ 2p) \text{ photons cm}^{-3}\ s^{-1}\ \text{sterad}^{-1}$$

and

$$I(2s\ 3p) = \frac{1}{4\pi} n_e\ n(2s)\ X(2s\ 3p) \text{ photons cm}^{-3}\ s^{-1}\ \text{sterad}^{-1}.$$

Thus the ratio is

$$\frac{I(2s\ 2p)}{I(2s\ 3p)} = \frac{X(2s\ 2p)}{X(2s\ 3p)} \quad \text{(Intensities in photons)}.$$

The dependence of this ratio on the plasma temperature is illustrated in figure 7.5 for a number of different Li-like ions. The steep dependence makes this a particularly sensitive method of determining temperature.

For plasmas that are in steady-state ionisation balance such as is generally assumed for the solar atmosphere above the chromosphere the particular population distribution of the Li-like ions means that special care

has to be taken in interpreting measurements. It was noted when discussing the ionisation balance that there was a shoulder on the density/temperature distribution of these ions to the high temperature side of the maximum. This gives rise to a weighting of the intensities to high temperatures when these are averaged over the full depth of the plasma.

In the solar plasma electron densities are sufficiently low that there is no need to take account of any of the additional mechanisms that complicate the simple excitation of these ions. This is not always the case for laboratory plasmas where the high collisional excitation rate of the 2p level and its relatively low radiative decay rate (coupled possibly with radiation trapping) can lead to the 2p level having a population comparable to the ground level. Thus excitation to the higher levels includes a contribution from the 2p level while the intensity of the 2s-2p line is reduced. However, sufficient atomic data is available to take account of these complications and successful interpretation is possible (figure 7.6). Spectra arising from the decay of doubly excited Li-like ions produced in the dielectronic recombination of He-like ions are considered with the spectral lines of the latter ions.

7.4 Beryllium-like ions

Beryllium-like ions have two electrons in the second shell making four in total. The excitation of the spectral lines is complicated over the relatively simpler lithium-like ions by the presence of the low-lying metastable $2s2p\,^3P$ level. Because the metastable level is relatively low-lying (unlike the 2s level of hydrogen-like ions) it can be populated to an extent comparable with the ground level. (This can be seen by calculating the Boltzmann factor between the metastable and ground levels and is confirmed by the detailed consideration of the populating processes that follow.) The relatively large population density of the metastable level means that excitation from this level also influences the populations of all the other levels. Figure 7.7 illustrates the process. Thus the first step in calculating the spectral intensities from such an ion (and the same considerations apply to other ions such as boron-like) following the determination of its stage of ionisation, is to determine the relative populations of the metastable and ground levels. The processes that need to be considered for this purpose may be discussed with reference to the partial term diagram of a beryllium-like ion illustrated in figure 7.8.

Radiative transition probabilities for the $2s^2\,{}^1S_o$-$2s2p\,{}^3P_1$ lines have been calculated by Garstang and Shamey (1967) on the intermediate coupling approximation. Values for the magnetic quadrupole transition $2s^3\,{}^1S_o$-$2s2p\,{}^3P_2$ have also been calculated by Garstang (1967). The values are compared with the allowed $2s^2\,{}^1S$-$2s2p\,{}^1P$ probabilities below.

	$2s^2\,{}^1S$-$2s2p\,{}^1P$	$2s^2\,{}^1S_o$-$2s2p\,{}^3P_1$	$2s^2\,{}^1S_o$-$2s2p\,{}^3P_2$
Be I	$5.5 \times 10^8\ s^{-1}$	$0.71\ s^{-1}$	$1.6 \times 10^{-4}\ s^{-1}$
Si XI	$6.4 \times 10^9\ s^{-1}$	$6.5 \times 10^5\ s^{-1}$	$0.21\ s^{-1}$

These three sets of values serve to define the boundaries between four density region. At high density where the rates of collisional transitions exceed the fastest radiative rates the ion meets the LTE criterion and the

Saha-Boltzmann equation gives the population densities. A more interesting situation arises at somewhat lower densities when all the lower levels but the metastable and ground levels decay radiatively and their collisional decay may be neglected. In this density regime the metastable level has a relatively small probability of radiative decay. Its population density is determined by the balance between its collisional excitation from the ground level and its collisional de-excitation into singlet levels $2s2p\ ^1D$ and $2s2p\ ^1P$. Thus although collisions dominate in these processes the population ratio departs from its Boltzmann value.

The next lower density regime starts when the radiative decay of the metastable level via the intercombination line $2s^2\ ^1S_0$-$2s2p\ ^3P_1$ is equal to or greater than its rate of collisional mixing between the sub-levels of $2s2p\ ^3P_{0,1,2}$. There are three important mechanisms by which this takes place.

a. Electron collisions causing transitions directly
b. Proton collisions causing transitions directly
c. Electron collisions exciting $2p^2\ ^3P$ from which radiative decay back to $2s2p\ ^3P$ redistributes the populations among the J levels.

Finally the next lower density regime starts when collisional de-excitation of the J = 2 sub-level gives way to its radiative decay by the magnetic quadrupole transition.

Results of a preliminary calculation for OV are presented in figure 7.9. In this the upper LTE density regime is excluded (it starts about $n_e = 5.10^{17}\ cm^{-3}$). The values for the various excitation rate coefficients upon which this graph is based were calculated by Eissner and are unpublished. More recent calculations by Malinovsky (1975) show that Eissner under-estimated the $2s2p\ ^3P$-$2p^2\ ^3P$ collision rate thus giving rise to an under-estimate of the metastable radiative decay rate. Thus the curve labelled n(m)/n(g) should be lowered by about $\frac{1}{2}$ in the range 10^7-$10^{11}\ cm^{-3}$. At the same time this correction extends the region where λ760/λ629 intensity ratio is sensitive to electron density to lower values of density ($\sim 10^{10}\ cm^{-3}$). Such differences in the values of basic data lead to uncertainty in the interpretation of astronomical spectra.

The spectra of beryllium-like ions have been studied in the laboratory but it has only been possible to do this in the density regime of about 10^{14}-10^{15} electrons cm^{-3} whereas astronomical spectra are produced in lower density regimes. Nevertheless useful measurements can be made but at this stage the accuracy is not adequate to help in choosing between alternative theoretical rate coefficients. The laboratory experiments are discussed later.

Since the metastable $2s2p\ ^3P$ level can develop population densities comparable with the ground level the basis of the quasi-steady-state approximation has to be examined again. In a recent calculation (unpublished) I estimated the population ratio n(m)/n(g) as a function of time for an ionising plasma consisting initially of boron-like ions and being ionised through beryllium-like to lithium-like. It turned out that the population ratio quickly reaches a value within 25% of the steady-state value calculated by the simpler method. Thus the error introduced by assuming the quasi-steady-state is less than the uncertainty in the values of the rate coefficients.

In the boundary regions between the density regimes discussed above some of the line ratios of these beryllium-like ions are sensitive to the

value of the electron density. At the same time intensity ratios including one of the transitions from an upper level are sensitive to the electron temperature. These ions are therefore particularly useful diagnostic probes of plasma conditions and the determination of reliable rate coefficients are particularly important.

7.5 Helium-like ions

The excitation processes considered in this section fall into two categories. In the first the collisional excitation of helium-like ions in much the same way as for other ions is considered while in the second the excitation of the dielectronic satellites is discussed. In both cases the initial target ions are helium-like although the satellite lines are strictly from lithium-like ions since a recombination process is involved. All the lines lie close in wavelength to the main $1s^2\ {}^1S\text{-}1s2p\ {}^1P$ resonance line and this is an additional reason for considering them together under the helium-like heading.

The features which distinguish helium-like ions from others are as follows:

a. Compared with ions having more bound electrons, helium-like ions have exceptionally large ionisation potentials corresponding to the relatively greater difficulty of removing the first electron from the innermost shell.

b. Compared with the ionisation potential the excitation potential of the lowest excited levels is relatively large (excitation potentials are about 0.8 of the corresponding ionisation potentials). In this respect they resemble hydrogen-like ions.

c. There are two metastable levels of which one ($1s\ 2s\ {}^3S$) is the lowest level of the triplet series.

Figure 7.10 illustrates the term scheme of O VII (not to scale) and the collisional and radiative processes taken into account in discussing its excitation. Because of the relatively small differences between the excitation potentials of the excited levels the line ratios of this ion are not used as indicators of electron temperature (however, see the later discussion of satellite lines) and attention is concentrated on calculating intensities of lines arising from levels having principal quantum number 2. For these in a similar way to beryllium-like ions the small radiative transition probabilities associated with the metastable levels make the line ratios sensitive to the electron density in specific density ranges. The relevant transition probabilities are as follows:

a. $1s^2\ {}^1S\text{-}1s2p\ {}^1P$ is an allowed electric dipole transition scaling as Z^4.
b. $1s^2\ {}^1S\text{-}1s2p\ {}^3P_1$ is allowed through a breakdown of L-S coupling at a rate that scales as Z^9.
c. $1s^2\ {}^1S\text{-}1s2p\ {}^3P_2$ is a magnetic quadrupole transition and scales as Z^8.
d. $1s^2\ {}^1S\text{-}1s2s\ {}^1S$ decays by 2 photon emission scaling as Z^6.
e. $1s^2\ {}^1S\text{-}1s2s\ {}^3S$ can take place by a relativistic magnetic dipole transition and scales like Z^{10}.

Because of the large scaling powers with Z the last four become relatively more important than the main resonance line at high Z. The following table

gives some sample value for their radiative transition probabilities (Gabriel and Jordan, 1972).

Values in s^{-1}

Ion	1^1S-2^1P	$1^1S-2^3P_1$	$1^1S-2^3P_2$	1^1S-2^1S	1^1S-2^3S
Scaling:	Z^4	Z^9	Z^8	Z^6	Z^{10}
C V	8.87×10^{11}	2.84×10^{7}	2.58×10^{4}	3.31×10^{5}	4.86×10^{1}
O VII	3.30×10^{12}	5.53×10^{8}	3.26×10^{3}	2.31×10^{6}	1.04×10^{3}
Ne IX	8.87×10^{12}	5.43×10^{9}	2.23×10^{6}	1.00×10^{7}	1.09×10^{4}
A XVII			3.18×10^{8}		4.71×10^{6}
Fe XXV					2.00×10^{8}

Where the electron collision rate exceeds the fastest of these radiative rates the ion meets the requirements for LTE and the Saha-Boltzmann equation may be used. For somewhat lower densities the singlet levels (except 2^1S) decay radiatively and the metastable levels suffer collisional transfer to the levels that can radiate or are ionised. Thus in this regime the metastable level population densities are determined by collisions which, however, are not in detailed balance because of the part played by levels that have a high probability of radiative decay.

In the next lower density regime the intercombination transition ($1^1S-2^3P_1$) takes over as the most probable decay route for the triplet metastable level (2^3S). The 2^3P level is rapidly populated from the metastable level by collisions which also ensure through this process (2^3S-2^3P) that the sub-levels ($J = 0,1,2$) are statistically populated. At lower densities the $1^1S-2^3P_2$ magnetic quadrupole transition adds its contribution to this decay mechanism - the levels being so close that this cannot be distinguished as a separate spectral line. The on-set of the magnetic quadrupole does not modify the intensity of 2^1S-2^3P since all the triplets decay by this route anyway.

The next lower density regime is entered when the singlet metastable level 2^1S has a greater probability of decay by two-photon emission than by collisions to the 2^1S level. When this happens the resonance line becomes relatively weaker and the 2 photon continuum appears. There has been one report of the latter having been detected in the laboratory but none from an astronomical source.

Finally at even lower densities the relativistic magnetic dipole decay of the 2^3S level takes over from 1^1S-2^3P as the most probable decay route for the triplets. This gives rise to the forbidden lines of ions such as O VII first identified correctly in the solar spectrum.

Together these three lines and the two photon continuum give rise to a varying pattern of spectral intensities from which it is possible to deduce the plasma electron density over a wide range. This is illustrated in figure 7.11 for the case of O VII. The calculations for this figure required values for many collision rate coefficients. For these theoretical calculations based on the Coulomb-Born-Oppenheimer approximation have been used (Bely, 1968 and Burgess et al., 1970). Such calculations suffer from relatively large uncertainties and further theoretical work on these ions is required.

These calculations do not include contributions to the rate of populating the levels having principal quantum number 2 by cascade from upper

levels nor that due to recombination particularly into the triplet levels. Bely (in the paper quoted in the previous paragraph) has estimated the effect of the former to be an increase of up to 40% in the population density of the triplet levels. It appears that no account has been taken of the latter. This is the population coefficient corresponding to the $n_o(p)$ term in the hydrogen-like case where it is generally negligible in the plasmas we are considering. However, it may make a significant contribution to the triplets in the helium-like ions.

The second part of this section on helium-like ions concerns the theory of the satellite lines found to the long wavelength side of the $1^1S\text{-}2^1P$ resonance line. These arise primarily from the dielectronic recombination process but also from inner-shell excitation of the corresponding lithium-like ions. The theory of these lines has been developed by Gabriel (1972) and by Bhalla, Gabriel and Presnyakov (1975). They show that the relative intensities of these lines with respect to the $1^1S\text{-}2^1P$ resonance line depend on the electron temperature of the plasma and that the extent to which the ion is in a state of transient ionisation may also be deduced. Thus when taken together with the intercombination line ($1^1S\text{-}2^3P$) and the forbidden line ($1^1S\text{-}2^3S$) these together provide a very powerful diagnostic probe for the plasma from which they are emitted.

Inspection of the expression given earlier for the dielectronic recombination coefficient leads to the intensity of one of the satellite lines arising from this process having an intensity given by

$$I_s = \frac{1}{4\pi} n_e \, n(He) \, \frac{h^3}{2(2\pi mkT)^{3/2}} \, \frac{\omega(Li,j,n\ell)}{\omega(He,g)} \, \frac{A_r \, A_a}{A_r + A_a} \exp - \frac{E_s}{kT} \text{ ph cm}^{-3} \text{ s}^{-1} \text{ ster}^{-1}.$$

where E_s is the energy difference between the upper level of the satellite line and the helium-like ground level designated by the symbols (quantum numbers) $(Li,j,n\ell)$ and (He,g) respectively. When the ratio of the intensity of the satellite line is taken to the resonance line in the electron and ion densities cancel and there remains only a term dependent on the electron temperature and the particular satellite line.

For high Z ions, such as iron, inner shell excitation of lithium-like ions also contributes to the excitation of the satellite lines. This contribution is proportional to the population density of the lithium-like ions as well as electron temperature and is therefore a measure of the extent to which the ion departs from steady-state ionisation balance. Since different satellite components depend differently on the two basic excitation mechanisms it is possible to distinguish between them by measuring selected components.

8.1 Radiation trapping and the equation of radiative transfer

In the formal treatment of the theory of the intensities of spectral lines and continuum the equation of radiative transfer is sometimes taken as the starting point. It represents a mathematically simpler statement of the intensity of a spectral feature in the most general case but since it does not help to elucidate the most important physics of the problem considered here, this approach has been avoided. However, when it comes to a discussion the re-absorption of radiation in an optically thick plasma it can be helpful.

So far there has been very little discussion of the effects of opacity and this chapter will deal with it only very briefly. Radiation which is emitted within the volume of a plasma has a finite probability of being

reabsorbed or scattered as it escapes from the plasma and passes through the intervening medium on its way to the spectrometer and detection system. Although absorption by the intervening medium can be very important, as for example the absorption of the ultraviolet component of star light by interstellar hydrogen at wavelengths less than λ915Å, it is a matter outside the general range of this paper and will not therefore be discussed further.

The reabsorption of radiation within the plasma can also be very important. Of the possible processes the reabsorption of resonance radiation is the most important here. By this process a photon, which is produced by the radiative decay of an excited level to the ground level of the ion, has a high probability of finding a similar ion in its ground level and can be absorbed by it with a relatively high probability - hence the name of resonance radiation. Reabsorption of this nature has a number of effects on the emitted spectral line radiation, viz:

a. It can become an important mechanism of populating the upper level of the resonance transition. Thus the statistical calculation of the population densities of the excited levels may have to be modified to take account of it.

b. Since the extent of the reabsorption depends on the depth of plasma though which the radiation has to pass, it is possible that for plasmas that are far from spherical the angular distribution of radiation is modified by the plasma shape. Trapped radiation has the greatest probability of escape along the shortest dimension.

c. Where the upper level has an alternative means of de-excitation (either by collision or by the emission of an alternative photon) the resonance line intensity is reduced by the effect of opacity. Note, however, that the intensity of a line from a level that has no other means of decaying is not reduced by the effect of opacity (but see (b) above).

d. Where there is an alternative radiative transition for the upper level of an optically thick line (for example the Hα-Lyβ combination in hydrogen) the effect of trapping the resonance line is to enhance the intensity of the alternative transition.

e. Finally it should be mentioned that opacity modified the spectral shape of a line. For most of the lines from the plasmas considered there thermal Doppler effect is the dominant broadening mechanism. The full calculation of the diffusion of a Doppler broadened line through a plasma is complex but it is possible to see qualitatively that there is a greater probability of absorption of a photon near the line centre and less in the wings where the probability of finding another ion with the same component of velocity is much less. Thus radiation trapping has the effect of broadening the lines. It may also be noted in this connection that usually a plasma is surrounded by a layer of cooler material. Optically thick lines emitted by such a plasma will have the narrower cores of their profiles depleted in intensity by reabsorption in this boundary layer. Such profiles are said to be self-reversed and it may be shown that the effect is even possible although the temperature of the outer layers is not less than the interior.

8.2 The equation of radiative transfer

It is necessary to start with a number of new definitions that will be related to some of the earlier concepts as the argument develops.

$J(\nu)$ is the coefficient of emissivity which is defined as the power radiated by unit mass of the plasma per unit frequency (ν) interval per unit solid angle.

$\chi(\nu)$ is the absorption coefficient such that if intensity $I(\nu)$ falls on a layer of thickness ds, mass density ρ, the change of intensity in the layer is

$$dI(\nu) = - I(\nu)\ \chi(\nu)\ \rho ds + J(\nu)\ \rho ds$$

$\tau(\nu)$ is the optical depth at frequency ν and is given by

$$\tau(\nu) = \chi(\nu)\ \rho ds$$

Thus the first equation may be re-written in terms of the optical depth

$$\frac{dI(\nu)}{d\tau(\nu)} = - I(\nu) + \frac{J(\nu)}{\chi(\nu)}$$

This is the equation of radiative transfer and $J(\nu)/\chi(\nu)$ is called the source function.

In its simpler application consider a uniform plasma where the particle collision rate is sufficiently great as to maintain the population distribution in LTE. Thus the emission and absorption coefficients are related such that the ratio $J(\nu)/\chi(\nu)$ is the Planck function. Because the plasma is uniform the integration of the equation of radiative transfer is simple and gives

$$I(\nu) = \frac{J(\nu)}{\chi(\nu)} \{1 - \exp\ [-\chi(\nu)\ \rho D\ ]\}$$

where D is the physical depth of the plasma. This rather trivial result shows that for large optical depths ($\tau(\nu) \equiv \chi(\nu)\rho D \gg 1$) the plasma radiates like a black body whereas for $\tau(\nu) \ll 1$ it reduces to

$$I(\nu) = J(\nu)\ \rho D$$

which is the result used hitherto for optically thin plasmas. By substituting the expression for the absorption coefficient for hydrogen continuum radiation given by Cillié (1932) viz

$$\chi(\nu) = \frac{n_e\ n_p}{\pi\rho}\ \frac{2^6\pi^3}{(6\pi)^{3/2}}\ \left(\frac{m}{kT_e}\right)^{\frac{1}{2}}\ \frac{e^6}{hcm^2}\ \frac{1}{\nu^3}\ \left(1 - \exp\ [-\ h\nu/kT_e\ ]\right)$$

it is possible to see how the continuum spectrum of a plasma moves from being black body at long wavelengths to optically thin bremsstrahlung at short wavelengths. A more general treatment would include recombination radiation.

8.3 Population densities in an optically thick plasma

In this section of the modification to the expression obtained earlier for the population density of an excited level due to one of the lines arising from the decay of that level having an opacity greater than unity. Stimulated emission is neglected in this treatment. The previous expression for the rate of change of the population density of an excited level p is

modified for absorption at the frequency of the transition (p,q) where q is the lower level thus

$$\frac{dn(p)}{dt} = - n(p)\, A(p,q) + n(q)\, B(q,p)\, \frac{4\pi}{c} \int_o^\infty \bar{I}(\nu)\, f(\nu)\, d\nu + \begin{matrix}\text{(collisional and}\\ \text{(other radiative}\\ \text{(terms}\end{matrix}$$

where $I(\nu)$ is the intensity of radiation averaged over direction and $f(\nu)$ is the form factor of the absorption profile of the transition (p,q)

$$\int_o^\infty f(\nu)\, d\nu = 1$$

The first two terms of the right-hand side of this equation may be expressed thus

$$\frac{dn(p)}{dt} = - n(p)\, A(p,q)\, g(\bar{\tau}_o) + \ldots$$

where

$$g(\bar{\tau}_o) = 1 - \frac{n(q)}{n(p)} \frac{\omega(p)}{\omega(q)} \frac{c^2}{2h\nu_o^3} \int_o^\infty \bar{I}(\nu)\, f(\nu)\, d\nu$$

In deriving this the relationship between the Einstein coefficients has been used. $g(\bar{\tau}_o)$ is known as the escape factor.

Use is now made of the expression derived for a uniform plasma

$$I(\nu) = \frac{J(\nu)}{\chi(\nu)} \{1 - \exp\, [\, -\chi(\nu)\, \rho\bar{D}\,]\}$$

where this time the source function may not be equated to the Planck function since the plasma is not in LTE. $\bar{D}$ is of the order of the smallest linear dimension of the plasma (for a sphere it is the radius).

It is now assumed that the source function is independent of frequency and that the line is Doppler broadened such that

$$\chi(\nu) = \frac{n(q)}{\sqrt{\pi}\, \Delta\nu_D} \frac{h\nu_o}{\rho c} B(q,p) \exp\{ -(\nu-\nu_o)^2/\Delta\nu_D^2\}$$

where

$$\Delta\nu_D = \sqrt{\frac{2RT}{M}}\, \frac{\nu_o}{c}$$

ν_o is the central frequency of the line where the average opacity

$$\tau_o = \frac{n(q)}{\sqrt{\pi}\, \Delta\nu_D}\, \bar{D}\, \frac{h\nu_o}{c} B(q,p)$$

Substitution gives finally

$$g(\bar{\tau}_o) = 1 - \frac{1}{\sqrt{\pi}} \int_{-\infty}^{+\infty} \exp\,(-x^2)\ \{1 - \exp\, [\, - \bar{\tau}_o \exp\,(-x^2)\,]\}\, dx$$

Holstein has derived the following approximate value for

$$1/g(\bar{\tau}_o) = \bar{\tau}_o\, (\pi\, \ell n\, \bar{\tau}_o)^{\frac{1}{2}}$$

For $\bar{\tau}_o$ greater than 2 it gives values within a few per cent of values obtained by numerical integration of the full integral. Thus by using the escape factor it is possible to take approximate account of the effect of opacity on the populations of excited levels. The escape factor is a function of the average optical depth $\bar{\tau}_o$ at the frequency of the line centre given by the expression above.

A full treatment of the problem requires the simultaneous solution of the equations of radiative transfer of all the optically thick lines together with the equations describing the collisional processes affecting the population densities.

9.1 Radiation cooling

In the development of the subject so far the requirements of plasma spectroscopy as a diagnostic technique for the measurement of electron temperature, density, abundance, etc, have been foremost. In this section consideration is given to radiation cooling as an energy loss mechanism. As will be seen, much of the same basic physics enters this problem.

Radiation cooling is important in laboratory plasmas, particularly in the field of fusion research where the influx of impurities and subsequent power loss is a problem currently receiving a lot of attention. In astronomy radiation cooling where the spectrum resembles a black body is clearly fundamental to the energy balance of many objects. In the present context consideration is given to the radiated power from more tenuous atmospheres which emit spectral lines. As an example the solar corona and transition region down to the top of the chromosphere is taken. Figure 9.1 summarised current ideas about the overall energy balance in this part of the solar atmosphere. The primary heating mechanism for the corona is some form of mechanical waves - probably m.h.d. or acoustic. The energy thus deposited in the upper layers is conducted back down again except for a small part which provides the energy for the solar wind. As the conducted energy passes down towards the surface it establishes the steep temperature gradient and provides on its way the energy for the radiation loss from this increasingly more dense region of the atmosphere. The mechanical waves in passing through this region cause additional broadening of the spectral lines so that the spectroscopist has a chance of seeing the effects of the energy twice - once on its way up as mechanical energy and then as the power in spectral lines after it has been conducted back down towards the surface.

In the case of the solar atmosphere the radiated power loss has been calculated with the approximation of the steady-state ionisation balance. In the fusion plasma case the steady-state approximation may be adequate for a rough initial estimate of radiation loss but detailed time dependent calculations will be needed at some stage in designing these experiments.

9.2 Radiated power loss in the steady-state approximation

Three sets of calculations have been done for astronomical plasmas and these will serve to illustrate the method of the calculation which may then be adapted for any comparable low density plasma. Two of the calculations have been done for general cosmological plasmas and use cosmic abundances of the elements (Pottasch, 1965 and Cox and Tucker, 1969). The third was done with the sun in mind and will be discussed in more detail (McWhirter, Thonemann and Wilson, 1975). The calculation is an attempt to add together the intensities of all the spectral lines and continuum emitted by a steady-state low density plasma containing elements in the abundances found in the

sun. It is further assumed that the plasma is optically thin in all this radiation although the criterion for it being optically thin is not as severe as it often is. The radiation may be absorbed and re-emitted many times as it diffuses out of the plasma provided the probability that an excited level so produced suffers de-excitation by collision is negligibly small, ie it does not matter how long it takes the radiation to diffuse out of the plasma so long as it all escapes.

The power radiated by a spectral line from unit volume is given by

$$P(p,q) = n_e\ n(g)\ X(g,p)\ \frac{A(p,q)}{\sum_r A(p,r)}\ h\nu\ (p,q)\ \text{erg s}^{-1}\ \text{cm}^{-3}$$

From an analysis of the solar spectrum the five or six strongest lines for each ion present were identified and these were added together in the calculation to give the power for each ion thus

$$P(z,El) = \sum_p n_e\ n(g)\ X(g,p)\ \frac{A(p,q)}{\sum_r A(p,r)}\ h\nu\ (p,q)$$

$$= n_e\ n(H)\ \frac{n(El)}{n(H)}\ \frac{n(z)}{n(El)} \sum_p X(g,p)\ h\nu\ (g,p)$$

For ions with important metastable levels care was taken to include excitation from metastable levels in the calculation

n(H) is the number density of hydrogen atoms and ions
n(El) is the number density of the ions of the element in question.

In evaluation the sum excitation rate coefficients were calculated using the $\bar{g}$ approximation as a means of scaling the rates where the value of $\bar{g}$ was taken from the best available source especially for lines that were strong in the spectrum and therefore accounting for an important fraction of the radiation of that ion.

The next stage was the sum over all the ions of the element. The ratio $\frac{n(Z)}{n(El)}$ was assumed constant over temperature and was taken from the steady state ionisation balance calculations of Summers (1974) or of Jordan (1969). It may be noted that the factors following $n_e\ n(H)\ \frac{n(El)}{n(H)}$ is a function of electron temperature and of the ions of the element only. Thus for each element there is a power loss curve such as those illustrated in figures 9.2, 9.3 and 9.4 for hydrogen, carbon and neon respectively. The total power curves are designated the radiated power functions for the elements in question. They apply to all steady plasmas of low enough density for the excitation model to apply.

The radiated power functions have a number of common features that mainly reflect the shell structure of atoms. This can be helpful in interpolating between elements. The hydrogen curve is the simplest and is made up of two components. The greater at lower temperature is due to the excitation of atomic hydrogen while the other is due to bremsstrahlung and recombination continuum resulting from the interaction of electrons and positive ions of hydrogen. At temperatures lower than 10^4K radiation from negative ions of hydrogen becomes important but this has not been included in these calculations. The carbon curve illustrates the importance of excitation of the electrons in the second shell from particularly boron-like, beryllium-like and lithium-like ions. The lines which contribute most are the transitions between levels having principal quantum number 2. This pattern is

repeated for neon but with everything shifted to higher temperatures. Elements with electrons in three shells show a third peak at lower temperature but this is less dramatic than the difference between shells one and two.

To calculate the total radiated power loss function for the sun it is now necessary to multiply the individual radiated power functions by the appropriate elements abundances $\frac{dn(El)}{dn(H)}$ and add them all together giving finally

$$P(Sun) = n_e\, n(H) \sum_{El} \frac{n(El)}{n(H)} \sum_{z} \frac{n(z)}{n(El)} \sum_{p} X(g,p)\, h\nu\,(g,p) \text{ erg } s^{-1} \text{ cm}^{-3}$$

The final result is shown in figure 9.5 and also for comparison the results of the other two calculations. The differences between them are consistent with the different abundances used and different rate coefficients.

9.3 Radiation cooling in a time dependent situation

The useful question to answer for a laboratory plasma (such as is used in fusion research) is how much energy is required to bring a neutral atom introduced into the plasma to its steady-state ionisation balance? Energy is required for three reasons, viz (a) radiation loss; (b) ionisation; and (c) to heat the electrons released in the ionisation process to the ambient temperature. For simplicity the temperature and density of the plasma will be assumed to be constant. Consider the power required per unit volume when the atom has reached a stage of ionisation of charge z.

$$P = n_e \sum_{p} X(g,p)\, h\nu(g,p) + n_e\, S(z)\, \{\chi(z) + {}^3/_2\, kT\}$$

It will spend a time of order $\frac{1}{n_e S(z)}$ in this stage of ionisation so the energy required to get it to the next stage is

$$\frac{1}{n_e S(z)} \{n_e \sum_{p} X(g,p)\, h\nu(g,p) + n_e\, S(z) \left[\chi(z) + {}^3/_2\, 2kT\right]\}$$

Thus the energy required to take an ion from its neutral state to its maximum charge for the plasma z(MAX) (determined possibly in the steady-state ionisation balance) is

$$\sum_{z=0}^{z(MAX)} \left\{ \frac{\sum_{p} X(g,p)\, h\nu(g,p)}{S(z)} \right\} + \chi(z) + {}^3/_2 kT \text{ erg}$$

Difficulties arise with numerical calculations due to the problem of defining z(MAX) in a realistic manner. However, calculations for hydrogen-like ions have been done by McWhirter and Hearn (1963). (Note that their calculation does not include the ${}^3/_2 kT$ term.) These calculations show that for ${}^T/_{Z^2} = 3.10^4 K$ the energy required for each ionisation is about ten times the ionisation potential of the ion. At higher temperatures less energy is required. See figure 9.6.

ACKNOWLEDGMENT

This paper is published with the permission of the Director of Appleton Laboratory.

REFERENCES

BATES, D.R. and DAMGAARD, A., Phil. Trans. Roy. Soc. A242 (1949) 101.
BATES, D.R., KINGSTON, A.E. and MCWHIRTER, R.W.P., Proc. Roy. Soc. A267 (1962a) 297.
BATES, D.R., KINGSTON, A.E. and MCWHIRTER, R.W.P., Proc. Roy. Soc. A270 (1962b) 155.
BATES, D.R. and KINGSTON, A.E., Planetary and Sp. Sci. 11 (1963) 1.
BELY, O., J. Phys. B. 1 (1968) 23.
BELY, O., Phys. Lett. 26A (1968) 408.
BELY, O. and Van Regemorter, H., Ann. Rev. Astron. and Astrophys. 8 (1970) 329.
BHALLA, C.P., GABRIEL, A.H. and PRESNYAKOV, L.P., Mon. Not. Roy. astr. Soc. 172 (1975) 359.
BLAHA, M., Astrophys. Lett. 10 (1972) 179.
BURGESS, A., Mon. Not. Roy. astr. Soc. 118 (1958) 477.
BURGESS, A. and SEATON M.J., Mon. Not. Roy. astr. Soc. 120 (1960) 121.
BURGESS, A., AERE Report 4818 (1964).
BURGESS, A., Astrophys. J. 139 (1964) 776.
BURGESS, A., Ann. Astrophys. 28 (1965) 774.
BURGESS, A., HUMMER, D.G. and TULLY, J.A., Phil. Trans. Roy. Soc. 266 (1970) 225.
BURGESS, D.D. and SKINNER, C.H., J. Phys. B. 7 (1974) L297.
BURGESS, A., SUMMERS, H.P., COCHRANE, D.M. and MCWHIRTER, R.W.P., Mon. Not. Roy. astr. Soc. (1977) (in press).
CHAPMAN, S. and COWLING, T.G., "The Mathematical Theory of Non-Uniform Gases" Cambridge University Press (1939 and 1952).
CHAPMAN, S., Proc. Phys. Soc. 72 (1958) 353.
CILLIE, G., Mon. Not. Roy. astr. Soc. 92 (1932) 820.
COX, D.P. and TUCKER, W.H., Astrophys. J. 157 (1969) 1157.
DANCE, D.F., HARRISON, M.F.A. and SMITH, A.C.H., Proc. Roy. Soc. A264 (1961) 361.
DELACHE, P., Ann. d'Astrophys. 30 No. 5 (1967).
DOLDER, K.,"Case Studies in Atomic Collision Physics"1 (1969).
FOSTER, E.W., Reports on Progress in Physics 27 (1964).
FUHR, J.R. and WIESE, W.L., NBS Special Publication 320 Supp. 2 (1973).
GABRIEL, A.H. and JORDAN, C., "Case Studies in Atomic Collision Physics" 2 (1972) 211, N-H Amsterdam.
GABRIEL, A.H., Mon. Not. Roy. astr. Soc. 160 (1972) 99.
GARSTANG, R.H. and SHAMEY, L.J., Astrophys. J. 148 (1967) 665.
GARSTANG, R.H., Astrophys. J. 148 (1967) 579.
GOLDBERG, L., DUPREE, A.K. and ALLEN, J.W., Ann. d'Astrophys. 28 (1965) 589.
GRIEM, H.R., Phys. Rev. 131 (1963) 1170.
HUTCHEON, R.J. and MCWHIRTER, R.W.P., J. Phys. B. 6 (1973) 2668.
JORDAN, C., Mon. Not. Roy. astr. Soc. 142 (1969) 501.
KUNZE, H.J., Space Science Rev. 13 (1972) 565.
LOTZ, W., Z fur Phys. 206 (1967) 205.
LOTZ, W., Z fur Phys. 216 (1968) 241.
MALINOVSKY, M., Astron. Astrophys. 43 (1975) 101.
MENZEL, D.H. and PEKERIS, C.L., Mon. Not. Roy. astr. Soc. 96 (1935) 77.
MCWHIRTER, R.W.P. and HEARN, A.G., Proc. Phys. Soc. 82 (1963) 641.
MCWHIRTER, R.W.P., in "A Survey of Phenomena in Ionised Gases" International Atomic Energy Agency (1968).
MCWHIRTER, R.W.P., THONEMANN, P.C. and WILSON, R., Astron. and Astrophys. 40 (1975) 63.
POTTASCH, S.R., Bul. Astron. Inst. Netherlands 18 (1965) 7.

SEATON, M.J., Mon. Not. Roy. astr. Soc. 119 (1959) 81.
SEATON, M.J., Planetary and Space Science 12 (1964) 55.
SEATON, M.J., Adv. in Atom. & Molec. Phys. (ed. D.R. Bates & B. Bederson) Academic Press 111 (1975) 83.
SPITZER, L., "Physics of Fully Ionised Gases" (1956).
SUMMERS, H.P., Mon. Not. Roy. astr. Soc. 169 (1974) 663.
SUMMERS, H.P., Appleton Laboratory Report No. IM 367 (1975).
TAYLOR, P.O., GREGORY, D., DUNN, G.H. and GRANDALL, D.H., abstract APS meeting, Knoxville (February 1977).
TER HAAR, D., Elements of Statistical Mechanics (Constable) (1955).
TWORKOWSKI, A. (1975) (unpublished).
VAN REGEMORTER, H., Astrophys. J. 136 (1962) 906.
WIESE, W.L., SMITH, M.W. and GLENNON, B.M., NSRDS-NBS4 1 (1966).
WIESE, W.L. and WEISS, A.W., Phys. Rev. 175 (1968) 50.
WIESE, W.L., SMITH, M.W. and MILES, B.M., NSRDS-NBS22 22 (1969).
WIESE, W.L., Nucl. Inst. and Methods 90 (1970) 25.
WILSON, R., J.Q.S.R.T. 2 (1962).

CAPTIONS TO THE DIAGRAMS

Fig.1.1 Some properties of radiation in the wavelength range 0.1-100,000 Angstroms.

Fig.2.1 Plot of the number of particles against speed for a Maxwellian distribution.

Fig.2.2 Maxwellian distributions for electrons and protons at the same temperature and total number density.

Fig.3.1 Comparison of the ionisation rate coefficients for O I to O VIII proposed and used by various authors
1. - - - - - Jordan MNRAS 142 (1969) 501
2. ——·—— Summers MNRAS in press
3. ———— Lotz Z fur Phys 216 (1968) 241

Fig.3.2 Comparison of ionisation rate coefficients for some ions of Sulphur according to various authors
1. - - - - - Jordan MNRAS 142 (1969) 501
2. ——·—— Summers MNRAS in press
3. ———— Lotz Z fur Phys 216 (1968) 241

Fig.3.3 Cross-sections for transitions in hydrogenic ions calculated in the Coulomb-Born approximation (Born Z = 1). Z^4Q is plotted against $(W/\Delta E)$, W being the incident electron energy and ΔE the transition energy difference.
a. 1s → 2s calculations by Tully (1960)
b. 1s → 2s calculations by Burgess (1961)

Fig.3.4 Ionisation and recombination coefficients for hydrogen-like ions in the limit of low electron density. (Bates et al. Proc. Roy. Soc. A267 (1962) 297).

Fig.3.5 Processes included in collisional-radiative calculation.

Fig.3.6 The relative rates of the five processes populating the first thirteen principal quantum levels for a plasma with reduced temperature T_{e/Z^2} = 64000 K and reduced electron density $n_{e/Z^7} = 10^{10}$ cm^{-3}.

Fig.3.7 The relative rates of the four processes which populate the ground level at reduced temperature T_{e/Z^2} = 32000 K.

Fig.3.8 Population density ratios as functions of principal quantum number. Reduced electron temperature $\Theta = 10^4$K and ground level population density n(1) = 0.

Fig.3.9 Collisional-radiative recombination rate coefficients.

Fig.3.10 The ratio of the collisional-radiative ionisation coefficient to its value at the limit of low density at various values of the reduced temperature T_{e/Z^2}.

Fig.3.11 The temperature and density dependence of the recombination coefficients of some ions of oxygen. (Summers, 1974).
The numbers on the curves are electron densities in cm^{-3}
—— Recombination to form Be-like ions
---- Recombination to form He-like ions
····· Recombination to form H -like ions

Fig.4.1 The fractional abundances of the ions of neon $n(z)/n(El)$ as functions of temperature.
——— J: Jordan MNRAS 142 (1969) 501
—·—· S: Summers MNRAS 169 (1974) 663

Fig.5.1 Times for equipartition of energy among electrons and protons (Spitzer, 1956)

Fig.6.1 The time dependent ionisation of neon at $T = 5 \times 10^5$K and $n_e = 10^{14}$ cm^{-3}.

Fig.6.2 Observed waveforms of the output of a photomultiplier when set to detect the line indicated (each the average of 5 shots).

Fig.7.1 Boundaries of density régimes

Fig.7.2 Variation of the theoretical steady-state Lyman α/Lyman β ratio with temperature. Curve A is calculated from the original CR model but with improved cross-sections. Curve B is calculated from the two-photon CR model with the same cross-sections as Curve A. Curve C is calculated from the Saha equation.

Fig.7.3 Nitrogen V term scheme.

Fig.7.4 The curves are theoretical excitation coefficients based on cross-sections calculated by Burke et al. (Proc. Phys. Soc. 87 (1966) 209). The points are our measured values.

Fig.7.5 Lithium-like ion line intensity ratios for electron temperature measurement.

Fig.7.6 The effect of electron density on the $\frac{2s-2p}{2s-3p}$ line ratio of N V. The quantity plotted is $\frac{X(2s2p)}{X(2s3p)+\frac{n(2p)}{n(2s)}\,X(2p3p)}$ thus no correction has been made for collisional transitions between the 3s3p and 3d levels. The latter may be as much as 30% at 10^{16} and a factor 2 at 10^{17} in either direction. The cross-section theory of Burke, Tait, Taylor and Lewis has been used for the basic data.

Fig.7.7 Excitation processes in the presence of a metastable level.

Fig.7.8 Partial term scheme of a beryllium-like ion.

Fig.7.9 Intensity ratios of oxygen V against electron density.

Fig.7.10 Partial term scheme of oxygen VII.

Fig.7.11 Oxygen VII intensities v. electron density.

Fig.9.1 Solar Corona Heating.

Fig.9.2 The radiated power function for Hydrogen.

Fig.9.3 The radiated power function for Carbon.

Fig.9.4 The radiated power function for Neon.

Fig.9.5 The Total radiated power loss function for the solar corona.

—.— S.R.Pottasch, Bul. Ast. Inst. Neth. 18 (1965) 7

— — — D.P.Cox and W.H.Tucker, Ap.J. 157 (1969) 1157

——— R.W.P.McWhirter (to be published)

Fig.9.6 The energy required to ionise a hydrogen-like ion.

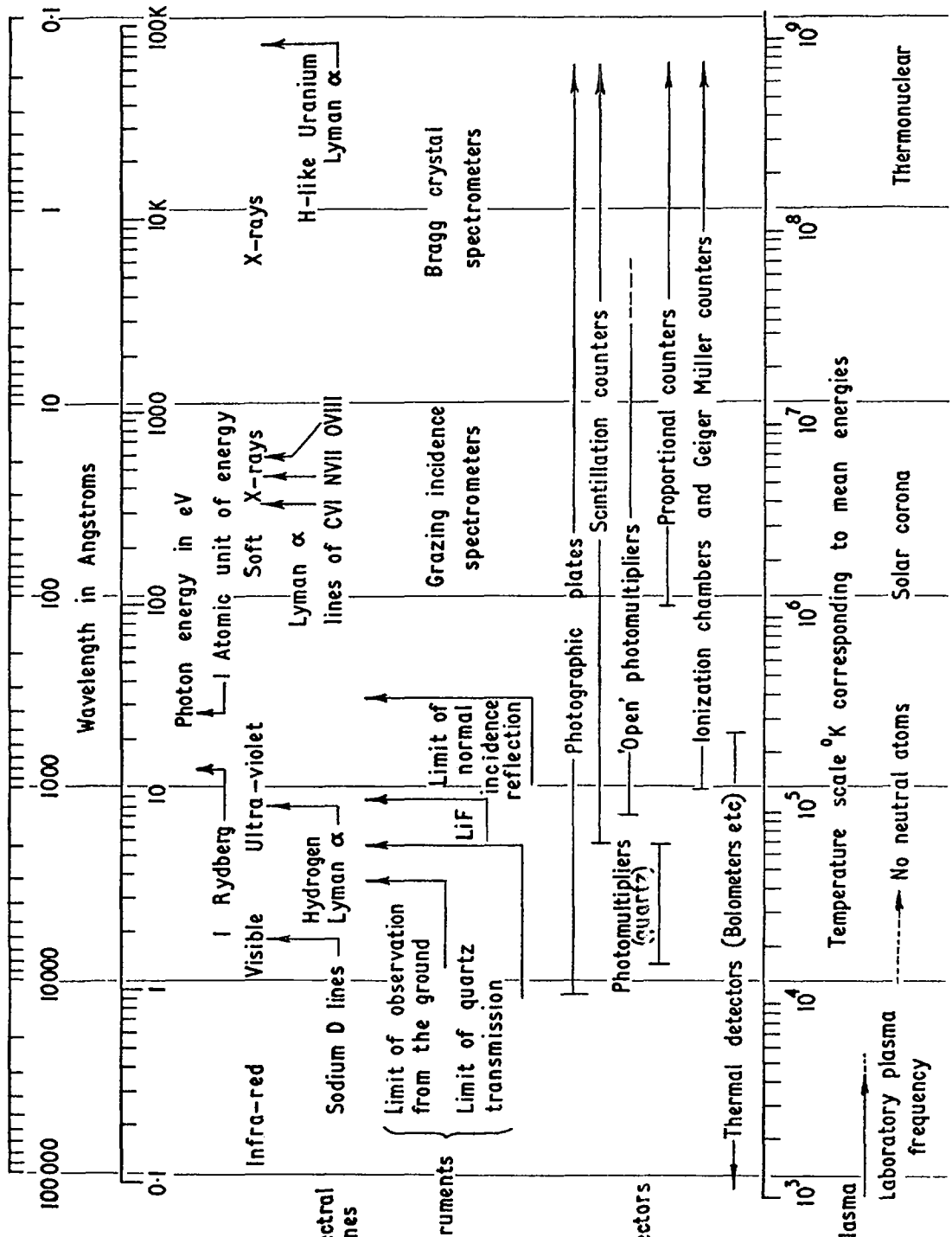

Fig.1.1 **Some properties of radiation in the wavelength range 0·1 to 100,000 Angstroms**

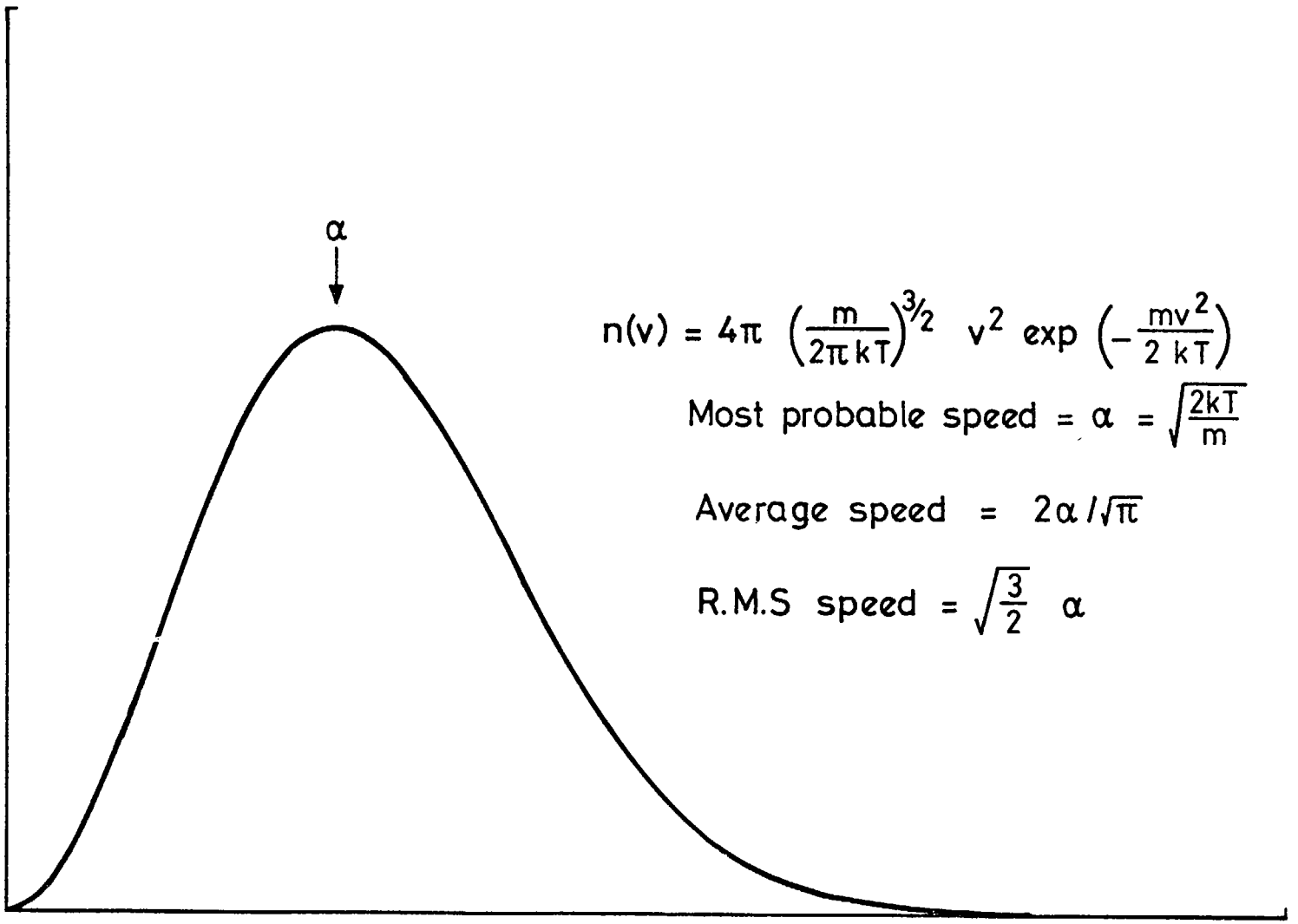
α
$n(v) = 4\pi \left(\frac{m}{2\pi kT}\right)^{3/2} v^2 \exp\left(-\frac{mv^2}{2kT}\right)$
Most probable speed = $\alpha = \sqrt{\frac{2kT}{m}}$
Average speed = $2\alpha/\sqrt{\pi}$
R.M.S speed = $\sqrt{\frac{3}{2}}\ \alpha$
Speed

Fig.2.1

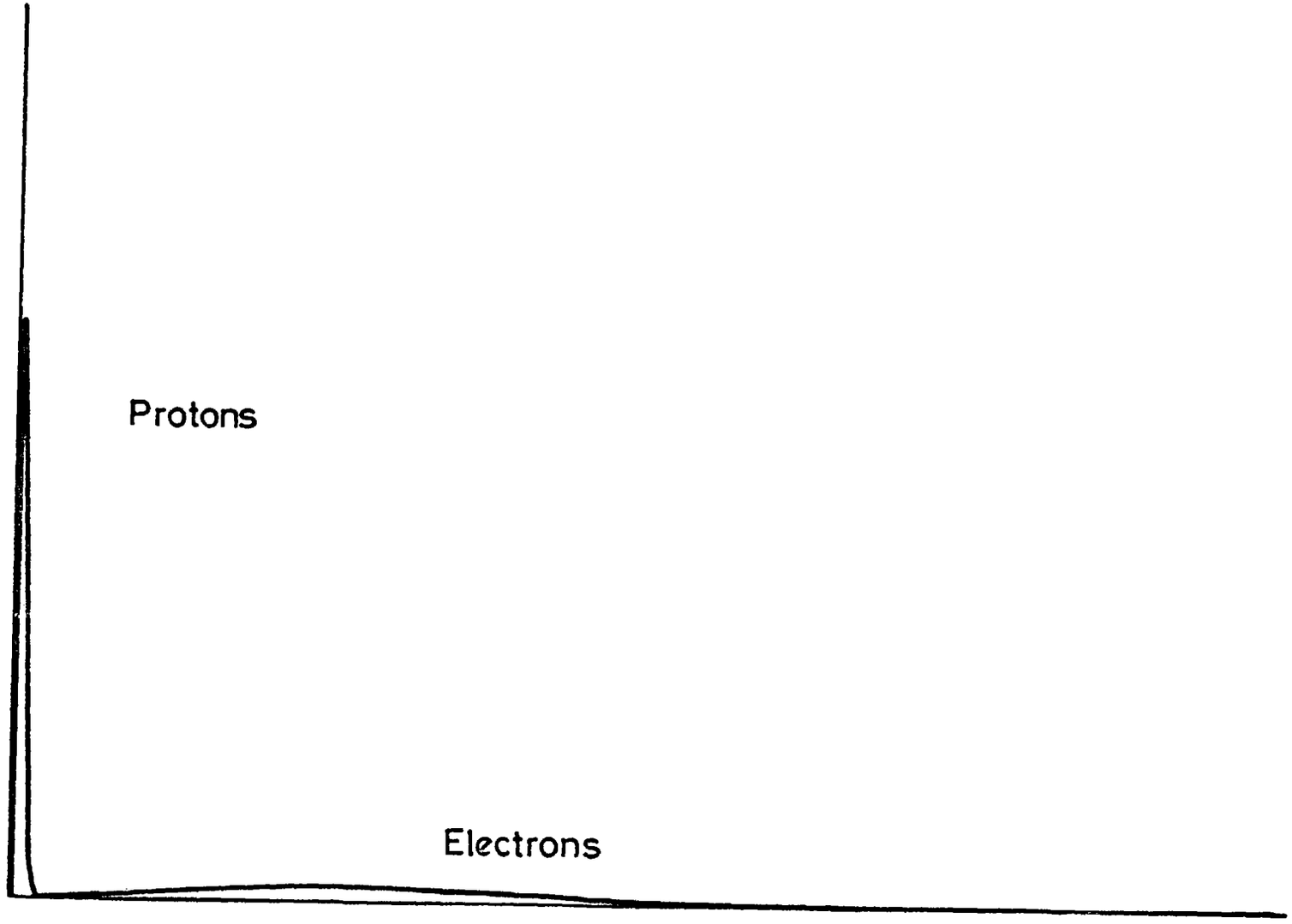

Fig.2.2

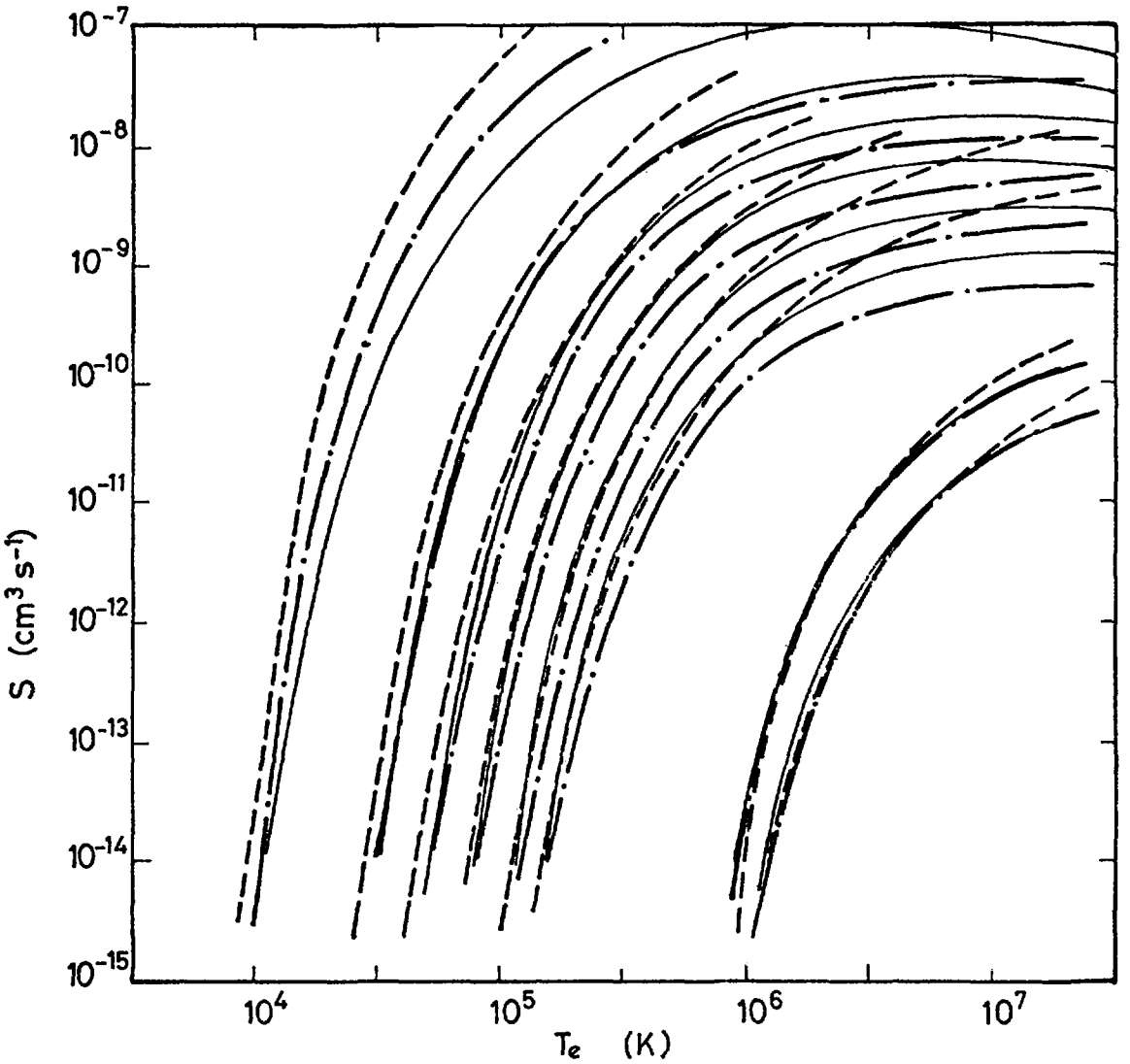

Fig.3.1 Comparison of ionization rate coefficients for OI to OVIII proposed and used by various authors

1 ———— Jordan MNRAS 142 p 501 (1969)

2 ——·—— Summers MNRAS in press

3 ———— Lotz fur Phys 216 p 241 (1968)

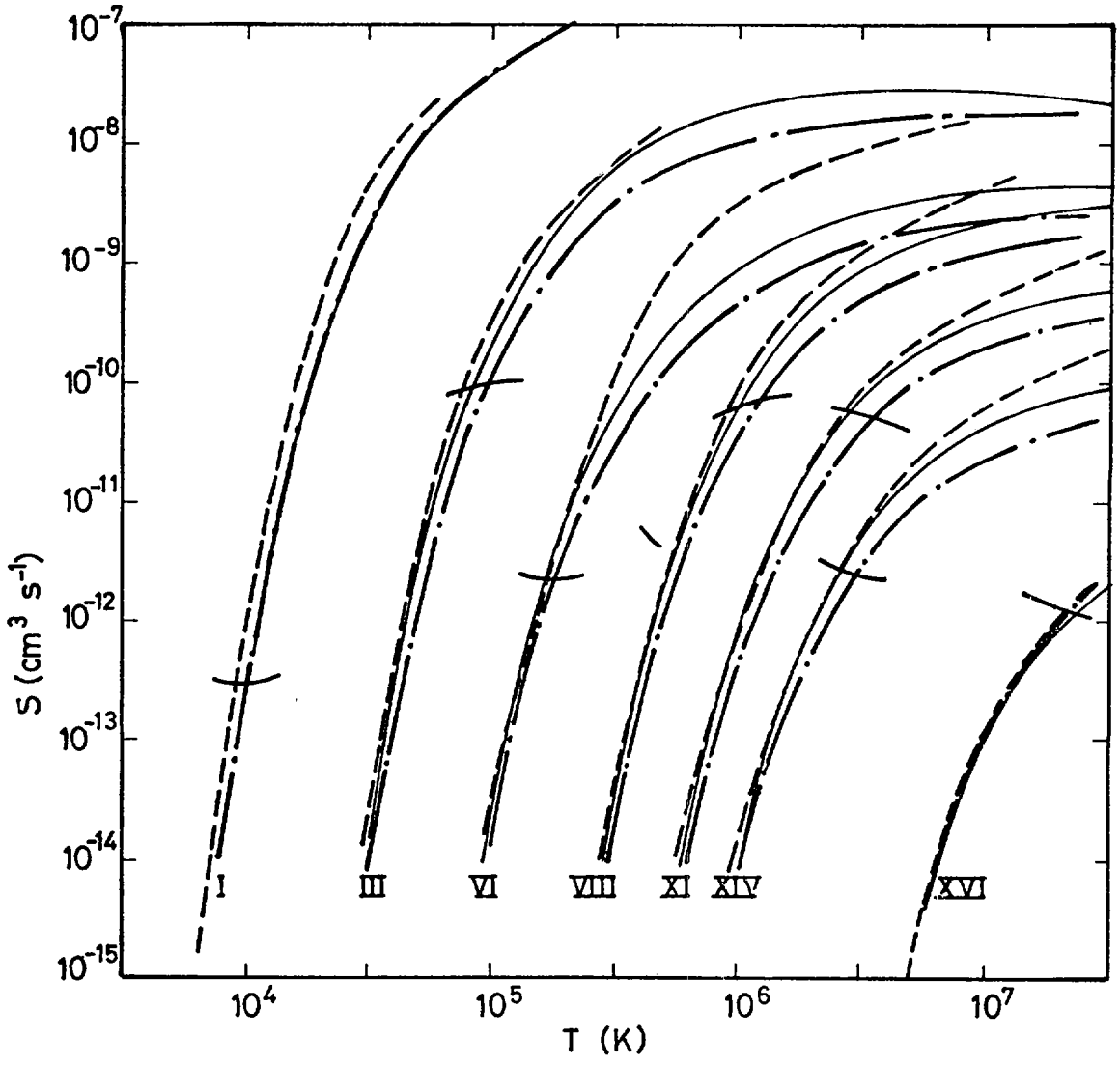

Fig.3.2 Comparison of ionization rate coefficients for some ions of sulphur according to various authors

1 ———— Jordan MNRAS 142 p 501 (1969)

2 ——·—— Summers MNRAS in press

3 ———— Lotz Z fur Phys 216 p 241 (1968)

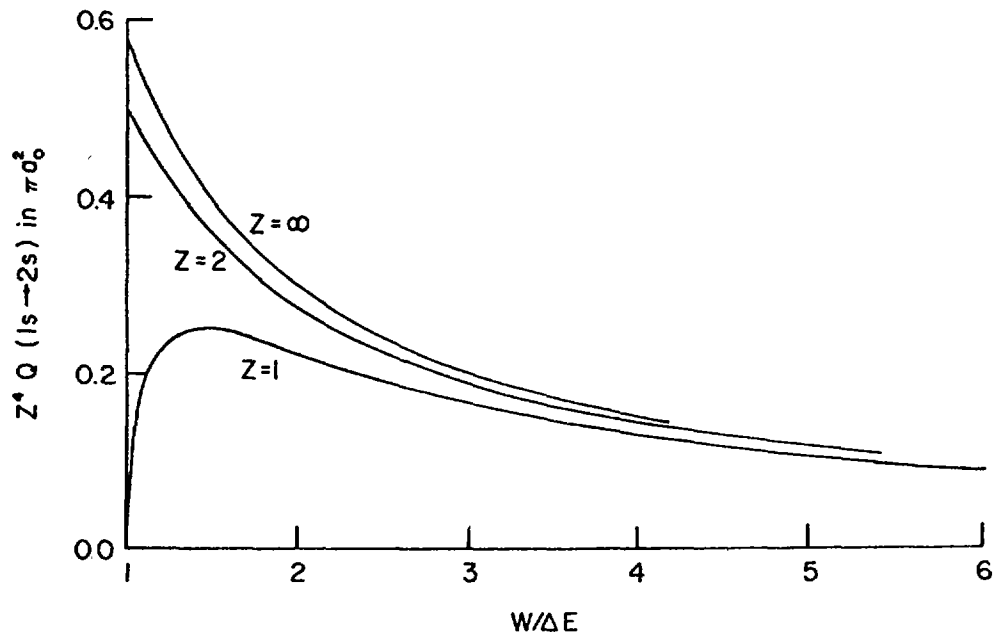

Fig.3.3 Cross sections for transitions in hydrogenic ions calculated in the Coulomb-Born approximation (Born for $Z = 1$). Z^4Q is plotted against $(W/\Delta E)$, W being the incident electron energy and ΔE the transition energy difference. (a) $1s \rightarrow 2s$ calculations by Tully (1960); (b) $1s \rightarrow 2p$ calculations by Burgess (1961).

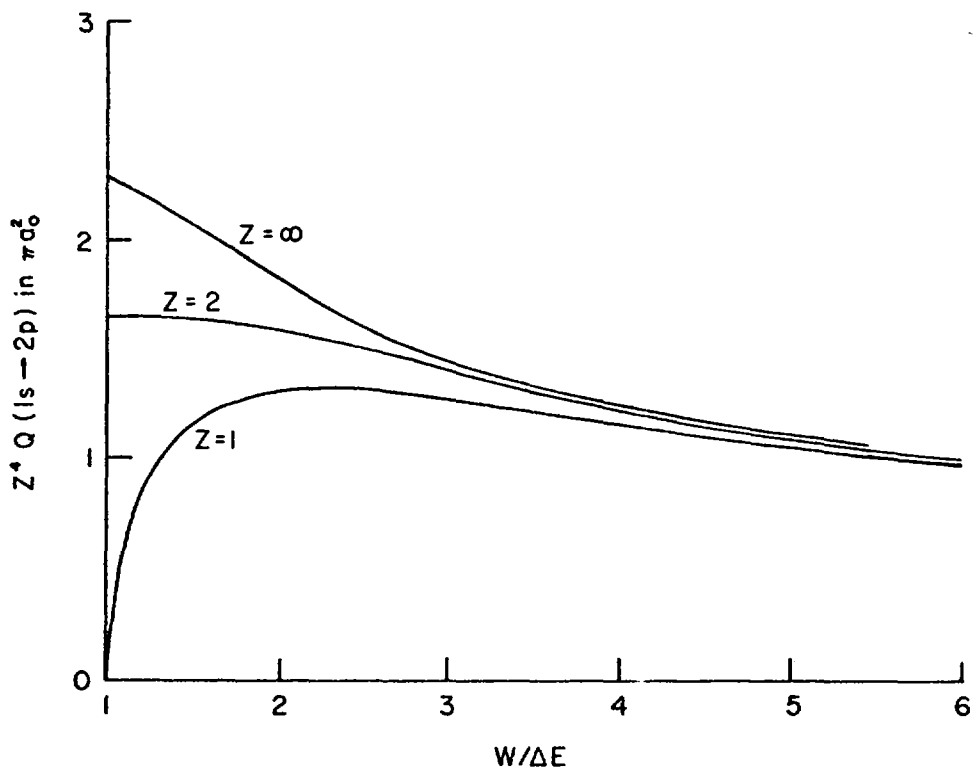

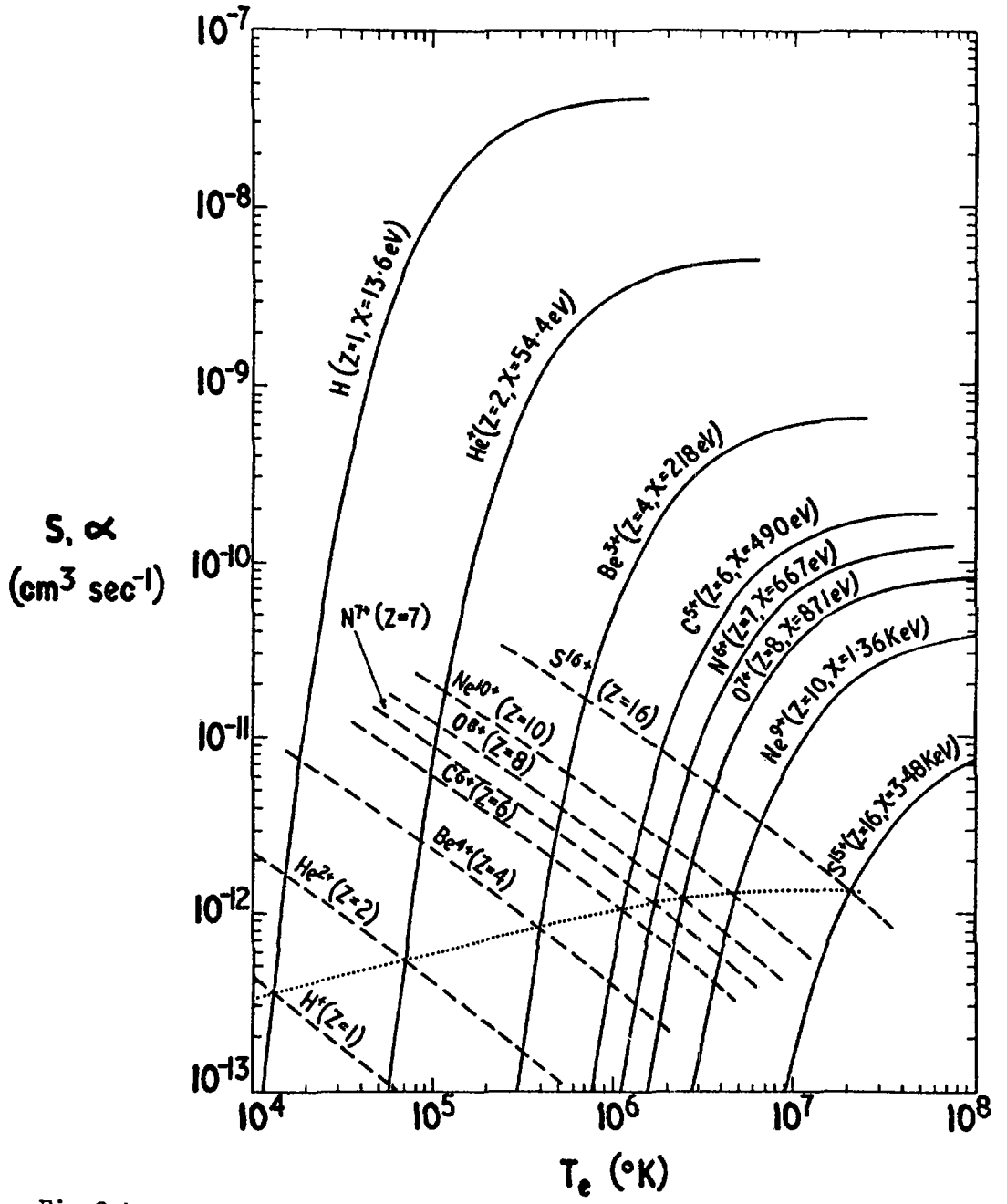

Fig.3.4

Ionization and recombination coefficients for hydrogen-like ions in the limit of low electron density. (Bates et al. Proc. Roy. Soc. A267, p.297, (62)).

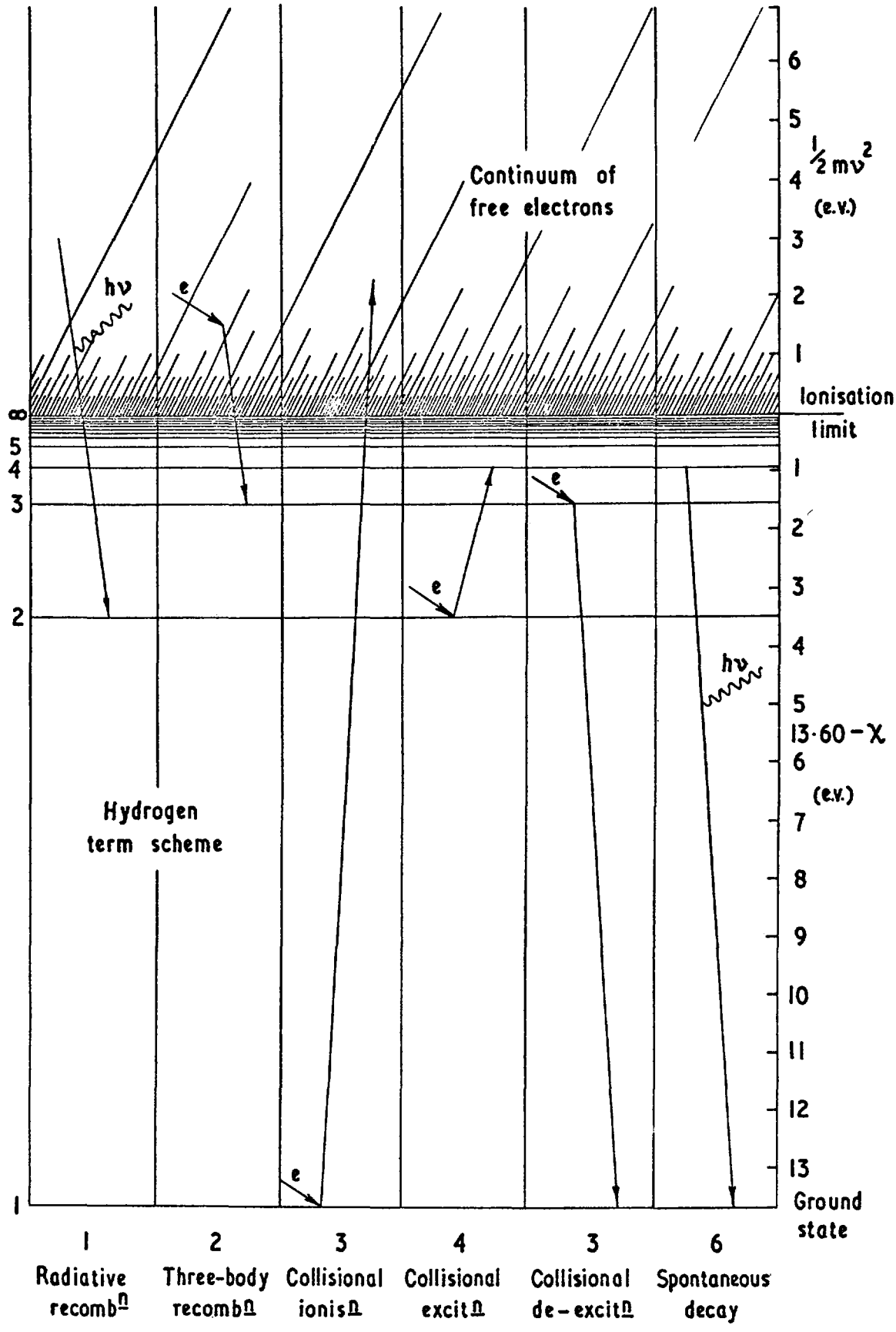
Continuum of free electrons
½ mv² (e.v.)
Ionisation limit
hν
e
Hydrogen term scheme
13·60 − χ (e.v.)
Ground state
1 Radiative recombⁿ
2 Three-body recombⁿ
3 Collisional ionisⁿ
4 Collisional excitⁿ
3 Collisional de-excitⁿ
6 Spontaneous decay

Fig.3.5

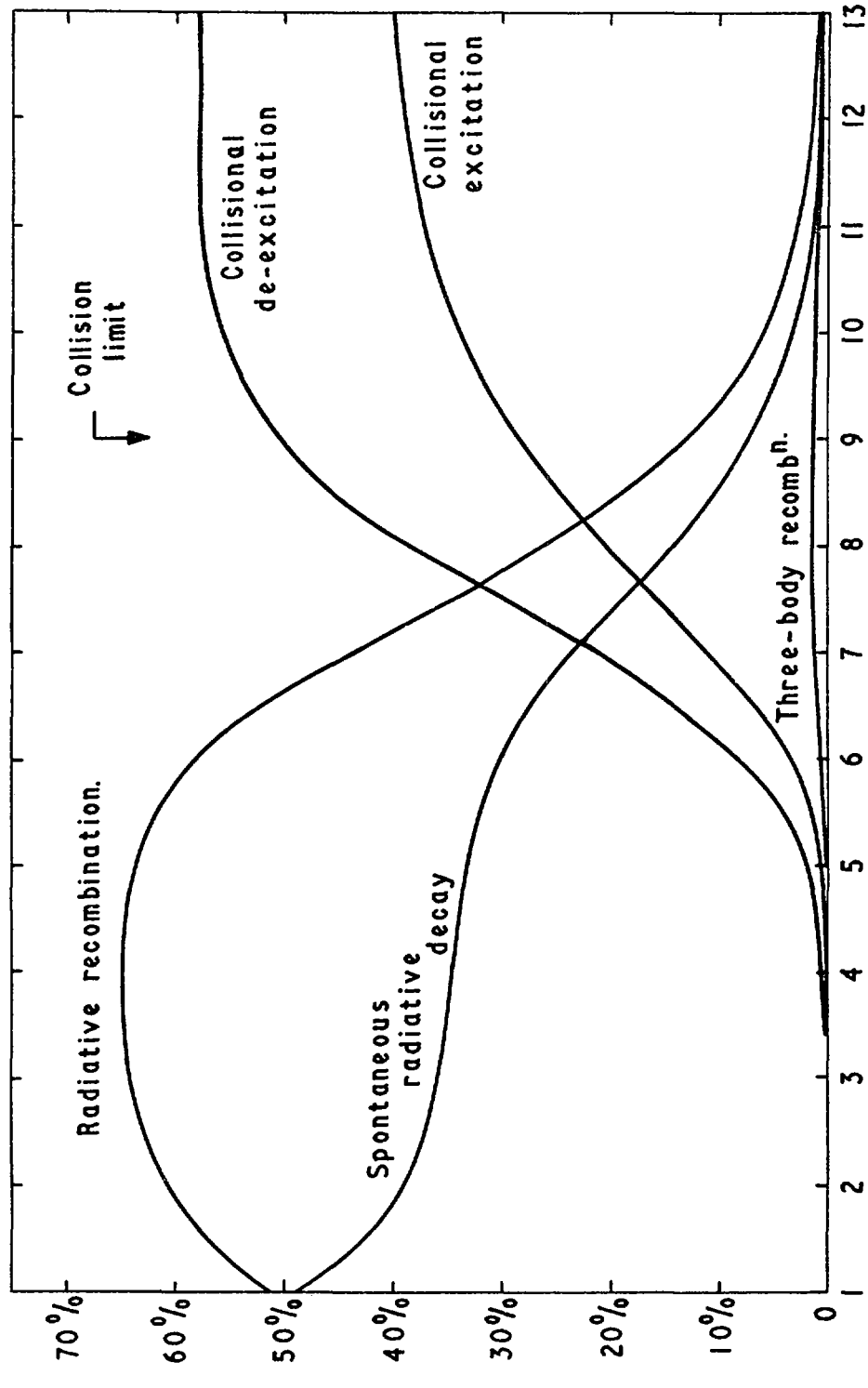

Fig.3.6 **The relative magnitudes of the five processes populating the first thirteen principal quantum levels for a plasma with Θ=64000°K and η(c)=10^{10} cm^{-3}.**

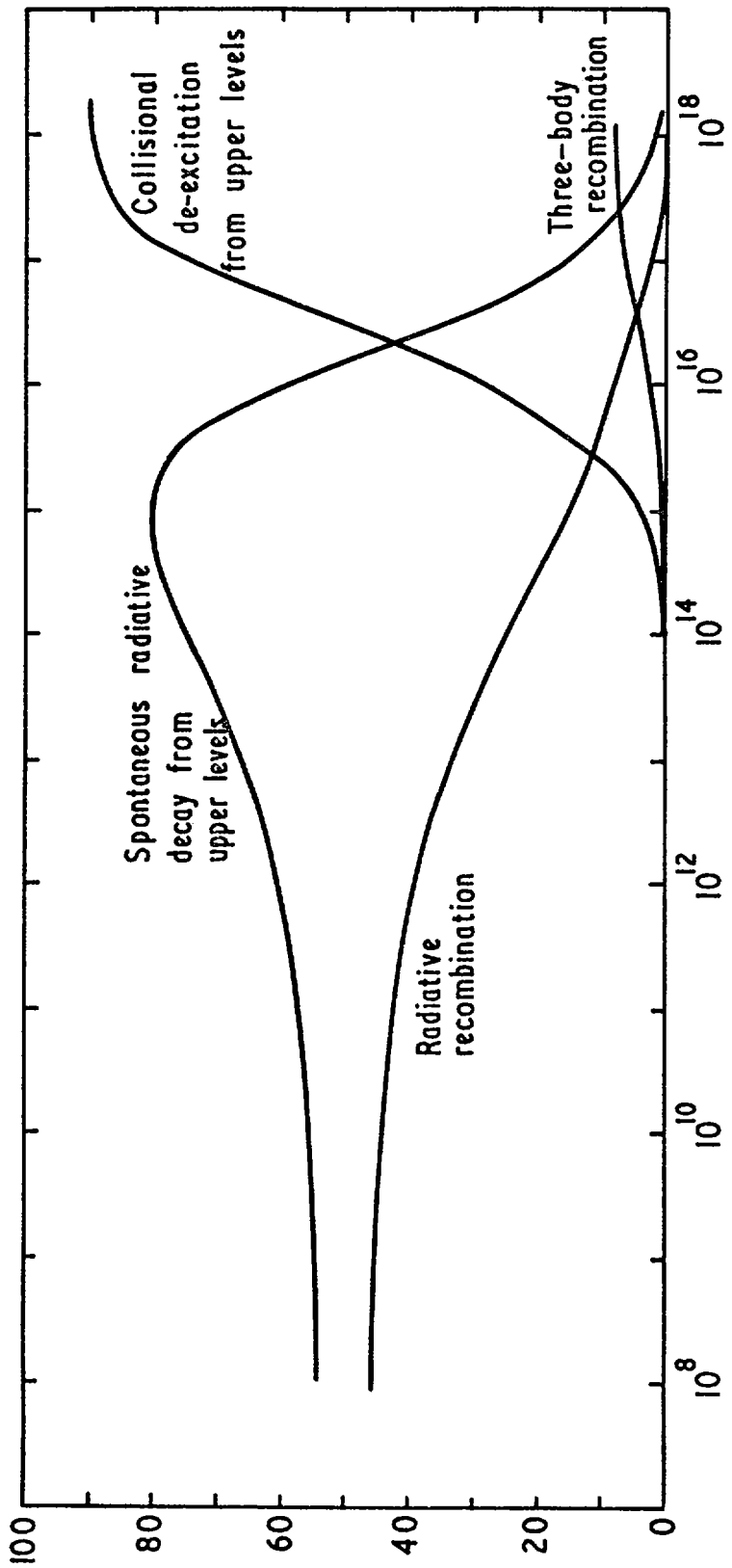

Fig.3.7

The relative magnitudes of the four processes which populate the ground level at (H) = 32000°K

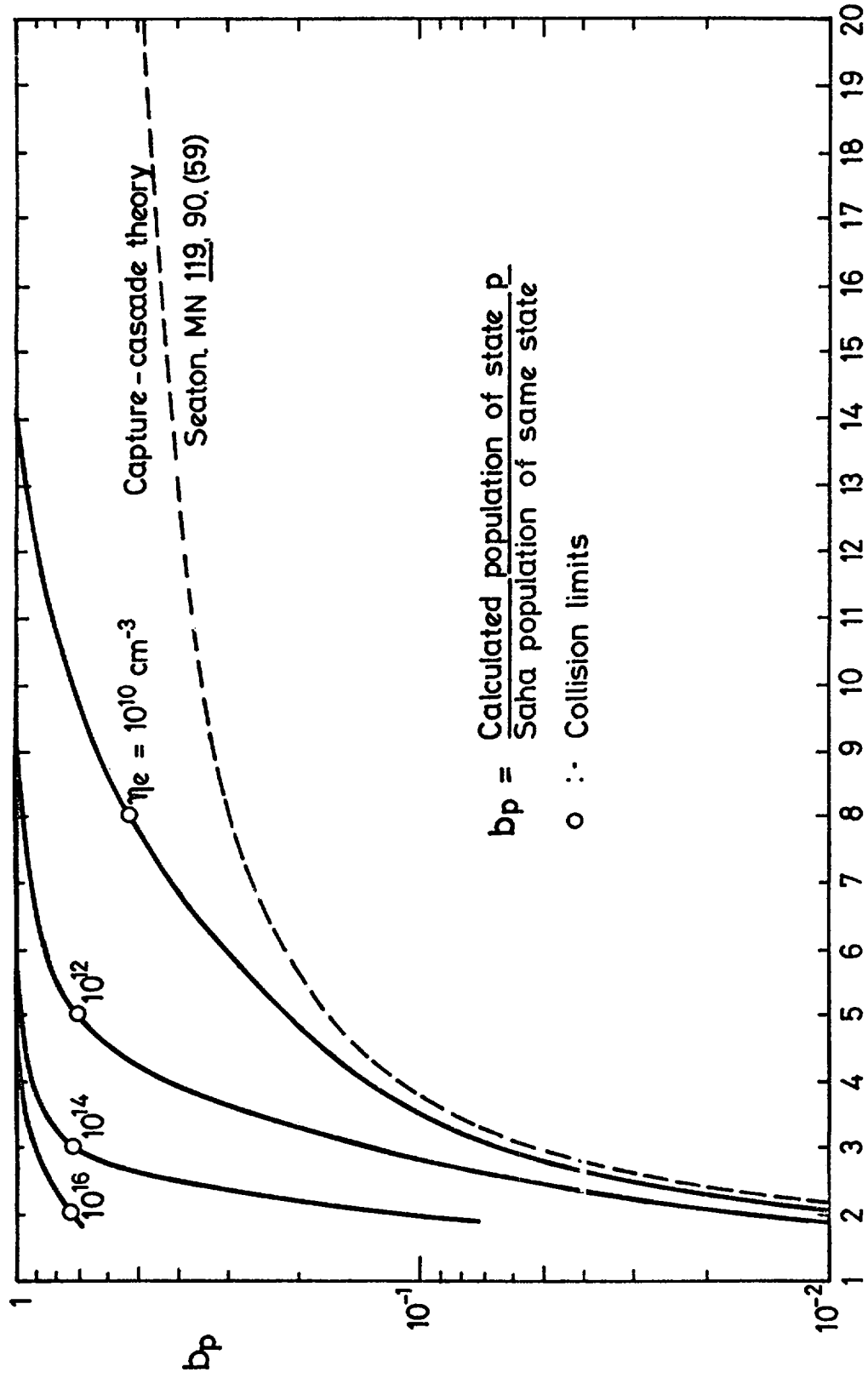
Capture-cascade theory
Seaton, MN 119, 90, (59)
$\eta_e = 10^{10}$ cm^{-3}
10^{12}
10^{14}
10^{16}
$b_p = \frac{\text{Calculated population of state p}}{\text{Saha population of same state}}$
o :· Collision limits
b_p
1
10^{-1}
10^{-2}
1 2 3 4 5 6 7 8 9 10 11 12 13 14 15 16 17 18 19 20
Principal quantum number (p) of state

Fig.3.8

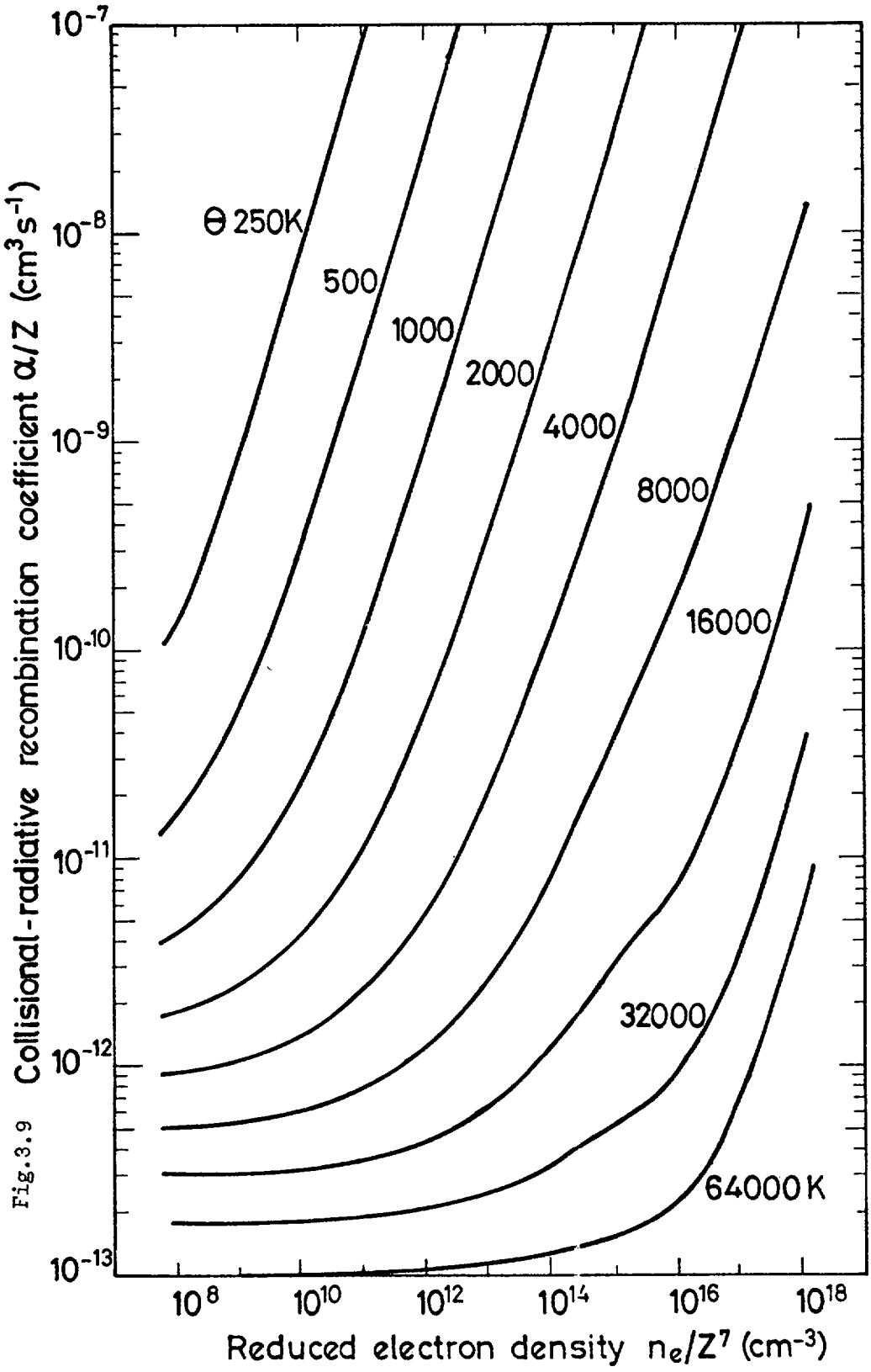
Collisional-radiative recombination coefficient α/Z (cm³s⁻¹)
10⁻⁷
10⁻⁸
10⁻⁹
10⁻¹⁰
10⁻¹¹
10⁻¹²
10⁻¹³
Θ 250K
500
1000
2000
4000
8000
16000
32000
64000 K
10⁸
10¹⁰
10¹²
10¹⁴
10¹⁶
10¹⁸
Reduced electron density nₑ/Z⁷ (cm⁻³)

Fig.3.9

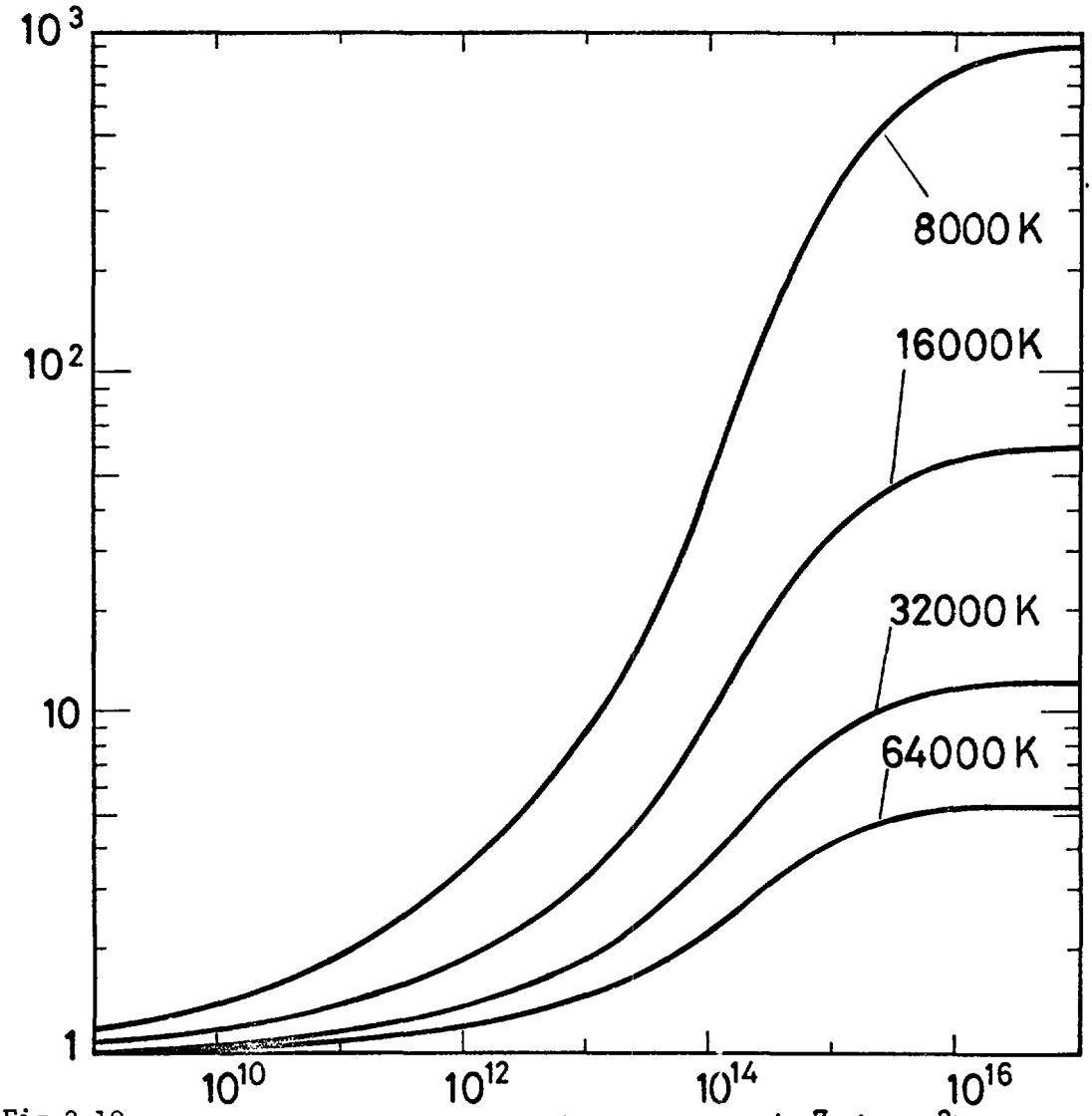

Fig.3.10 The ratio of the collisional-radiative ionisation coefficient to its value at the limit of low density at various values of the reduced temperature T_e/Z^2

Fig.3.11 The temperature and density dependence of the recombination coefficients of some ions of oxygen.
(Summers, H.P., Mon. Not. R.A.S., 169 pp 667-680(1974))

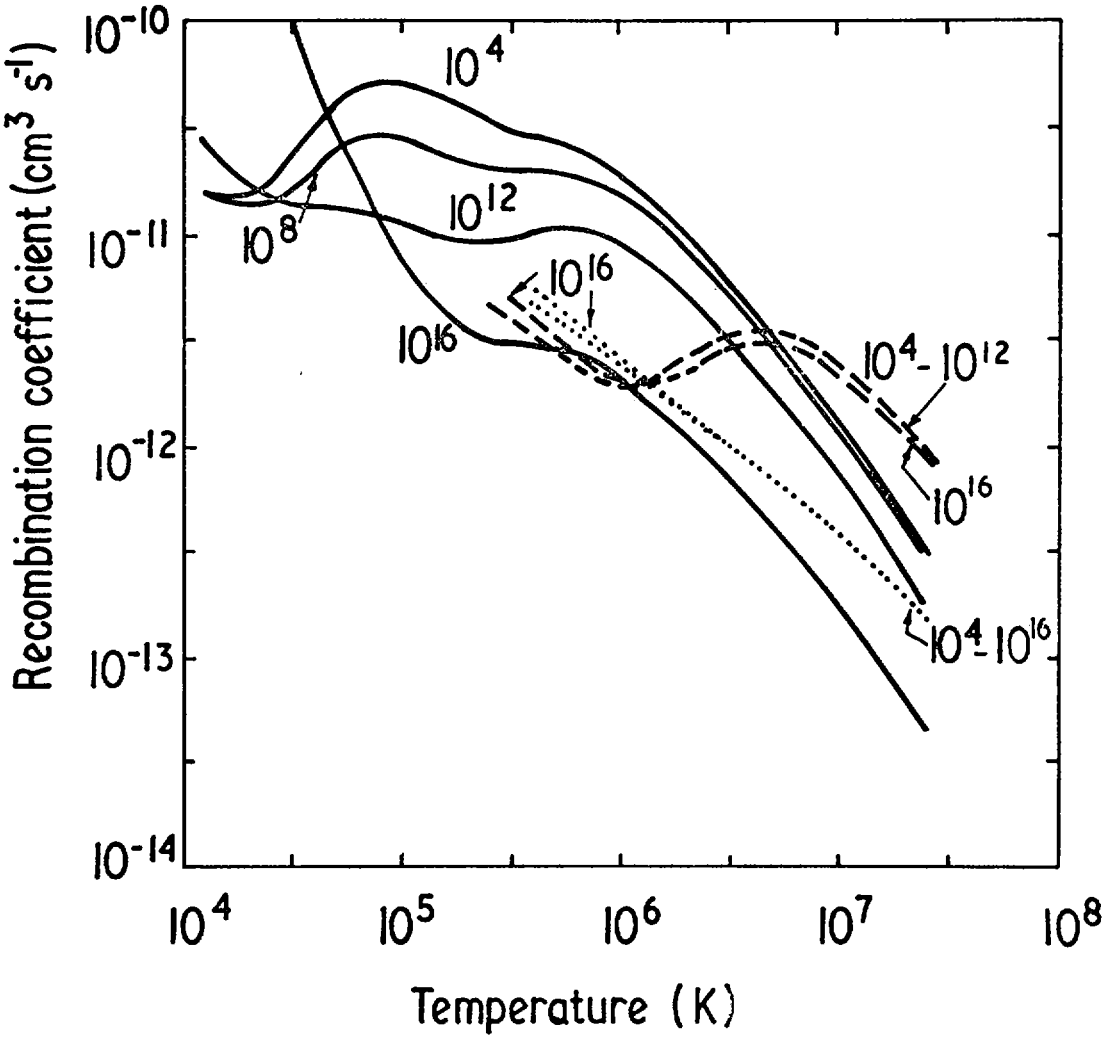

The numbers on the curves are electron densities in cm^{-3}

—— Recombination to form Be-like ions

---- Recombination to form He-like ions

..... Recombination to form H - like ions

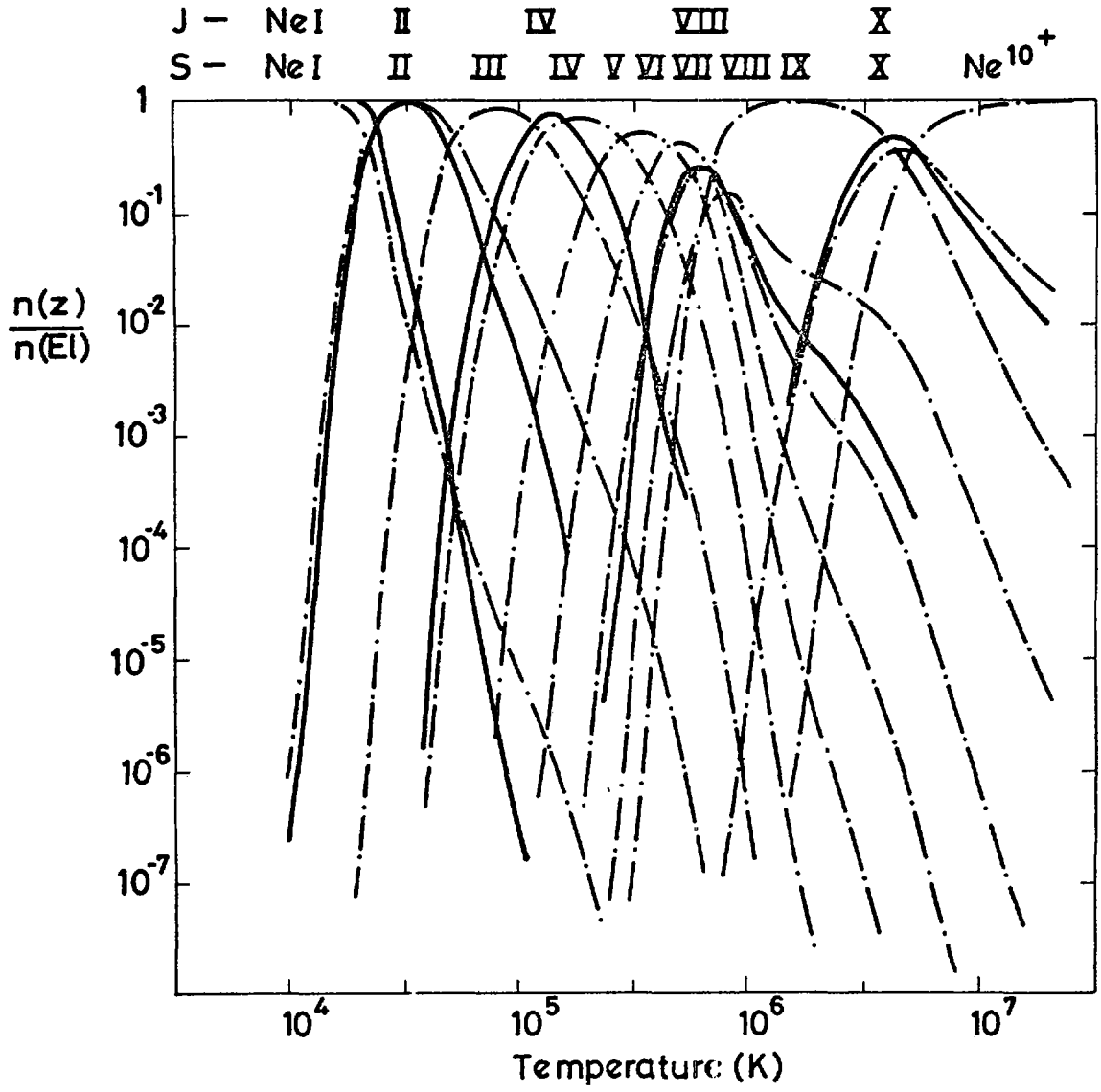

Fig.4.1

The fractional abundances of the ions of neon $n(z)/n(El)$ as functions of temperature.

——— J: Jordon Mon. Not. R.A.S. 142, 501, (1969)

—·—·— S: Summers Mon. Not. R.A.S. 169, 663, (1974)

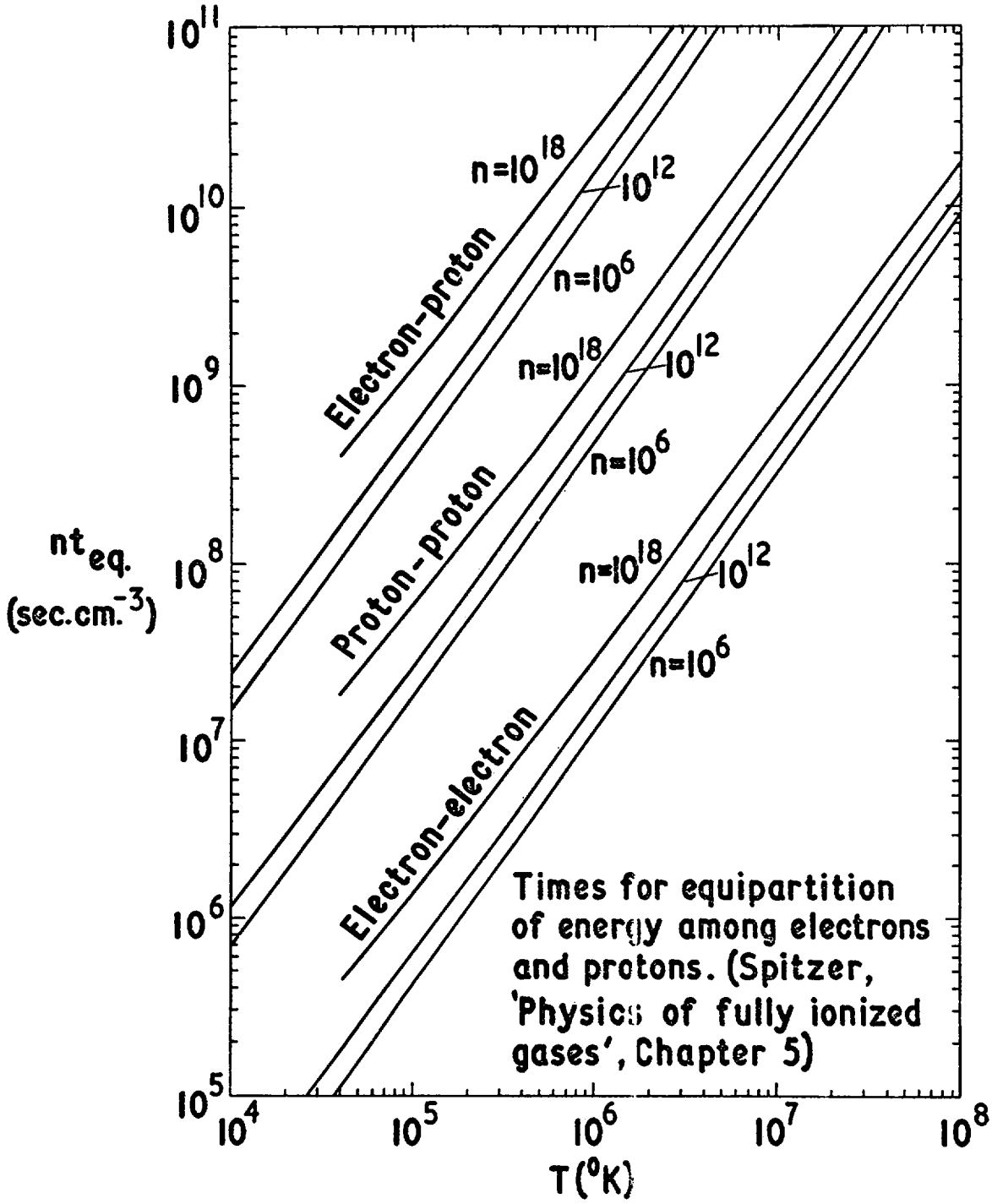
10^{11}
10^{10}
10^{9}
10^{8}
10^{7}
10^{6}
10^{5}
$nt_{eq.}$
(sec.cm.$^{-3}$)
10^{4}
10^{5}
10^{6}
10^{7}
10^{8}
T(^{0}K)
Electron-proton
n=10^{18}
10^{12}
n=10^{6}
Proton-proton
n=10^{18}
10^{12}
n=10^{6}
Electron-electron
n=10^{18}
10^{12}
n=10^{6}
Times for equipartition of energy among electrons and protons. (Spitzer, 'Physics of fully ionized gases', Chapter 5)

Fig.5.1

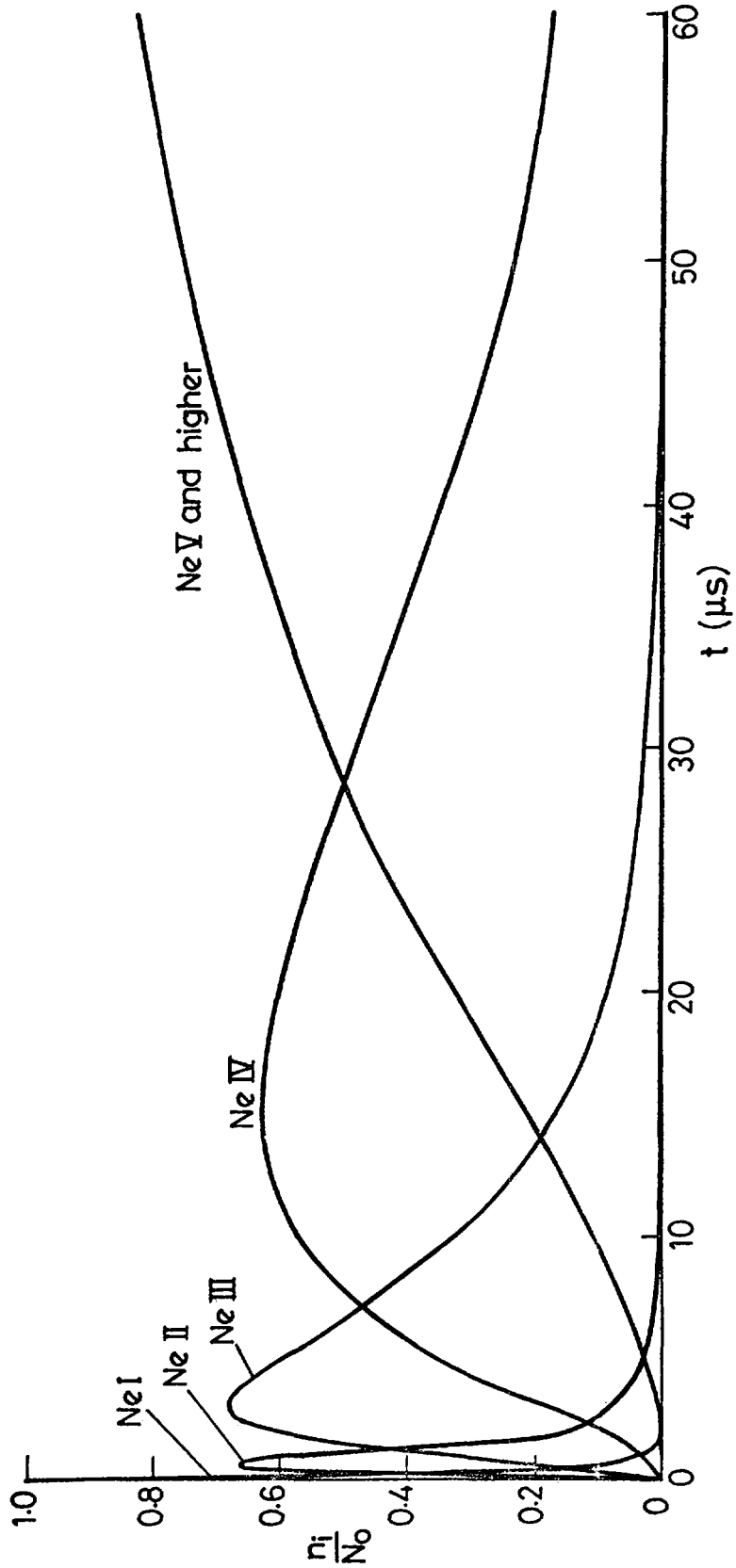
Ne V and higher
Ne IV
Ne III
Ne II
Ne I
1.0
0.8
0.6
0.4
0.2
0
$\frac{n_i}{N_o}$
0
10
20
30
40
50
60
t (μs)

Fig.6.1

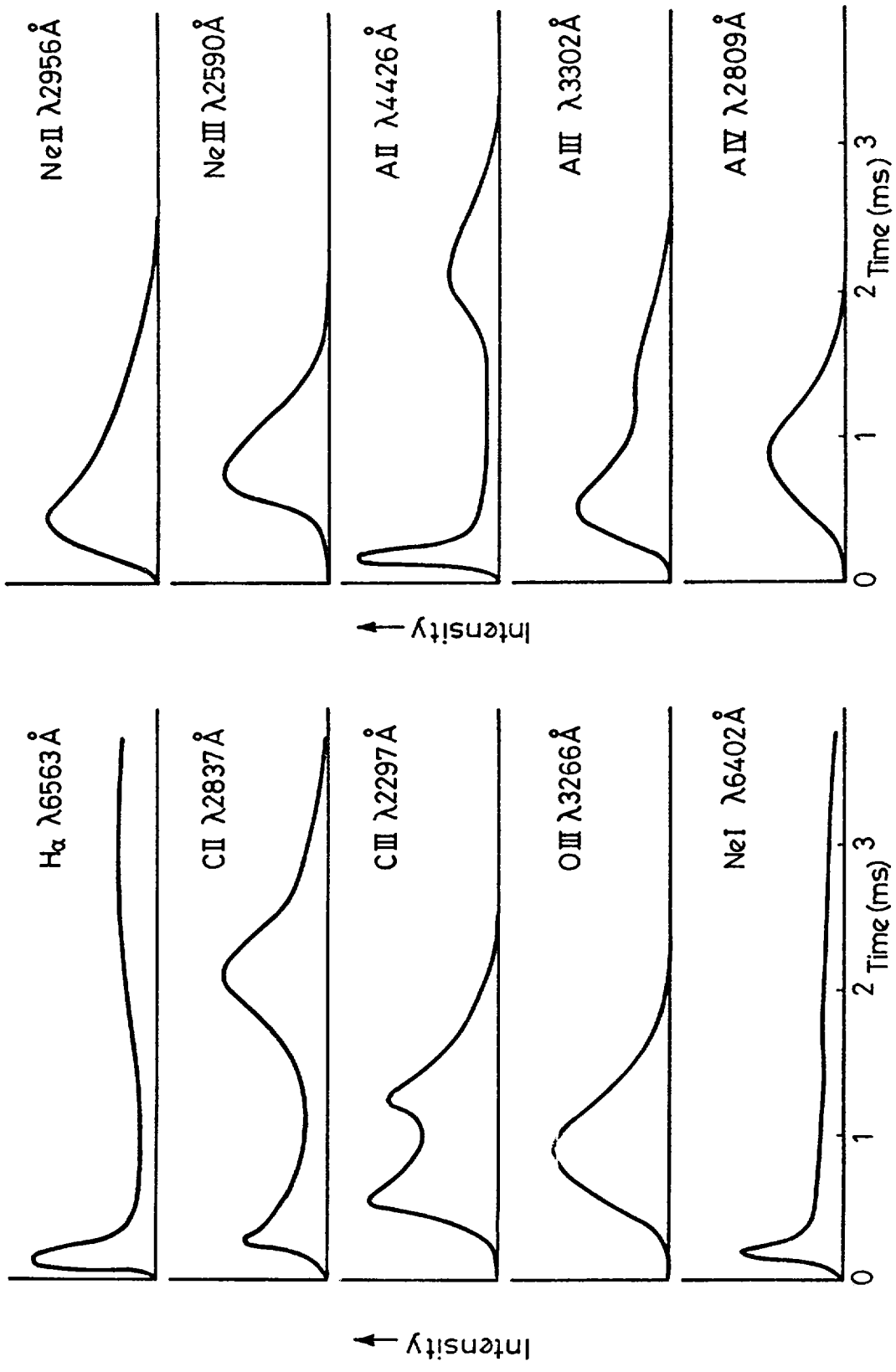
Hα λ6563Å
CII λ2837Å
CIII λ2297Å
OIII λ3266Å
NeI λ6402Å
Intensity
0
1
2
3
Time (ms)
NeII λ2956Å
NeIII λ2590Å
AII λ4426Å
AIII λ3302Å
AIV λ2809Å
Intensity
0
1
2
3
Time (ms)

Fig.6.2

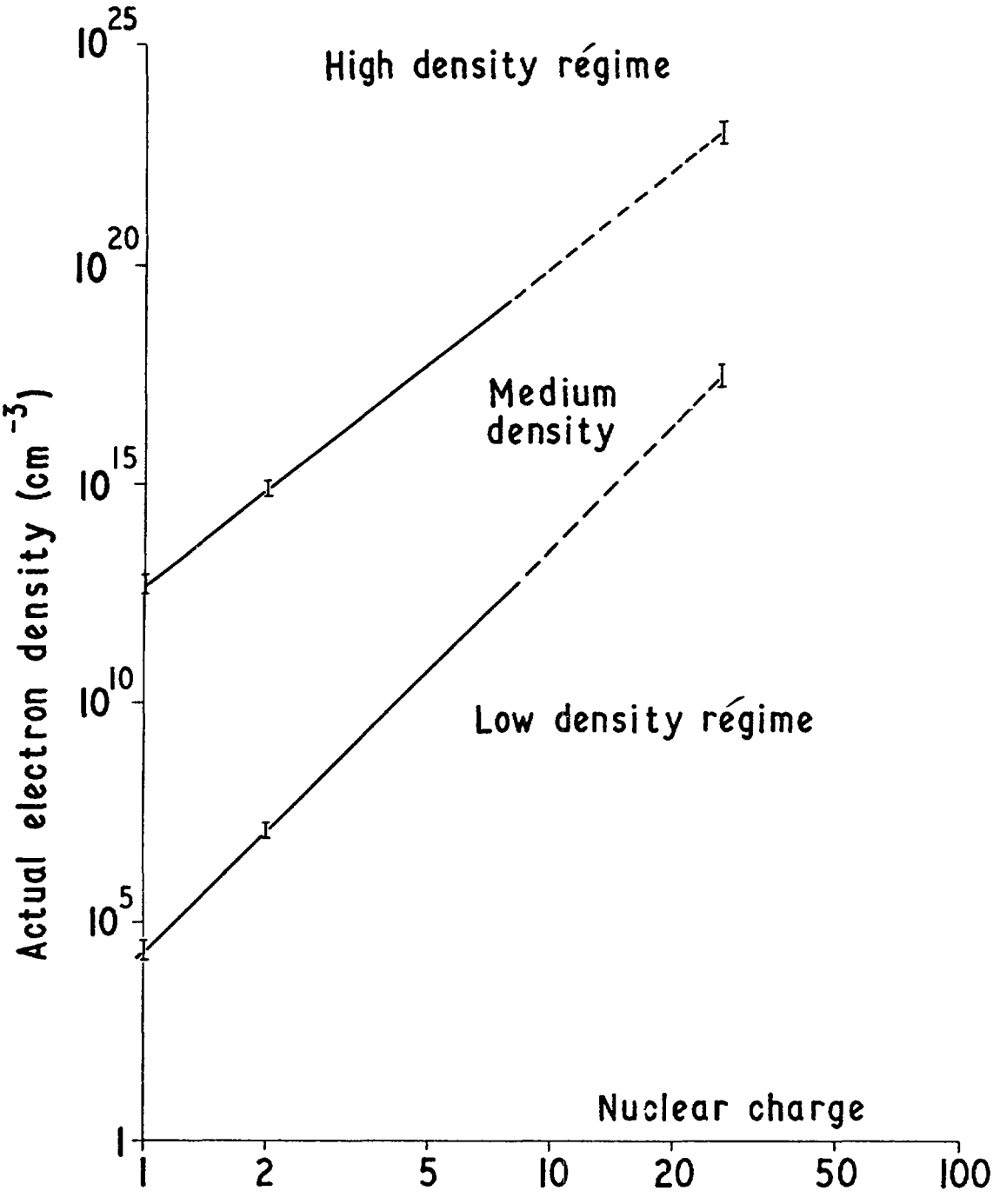
High density régime
Medium density
Low density régime
Actual electron density (cm^{-3})
10^{25}
10^{20}
10^{15}
10^{10}
10^{5}
1
Nuclear charge
1
2
5
10
20
50
100
Boundaries of density régimes

Fig.7.1

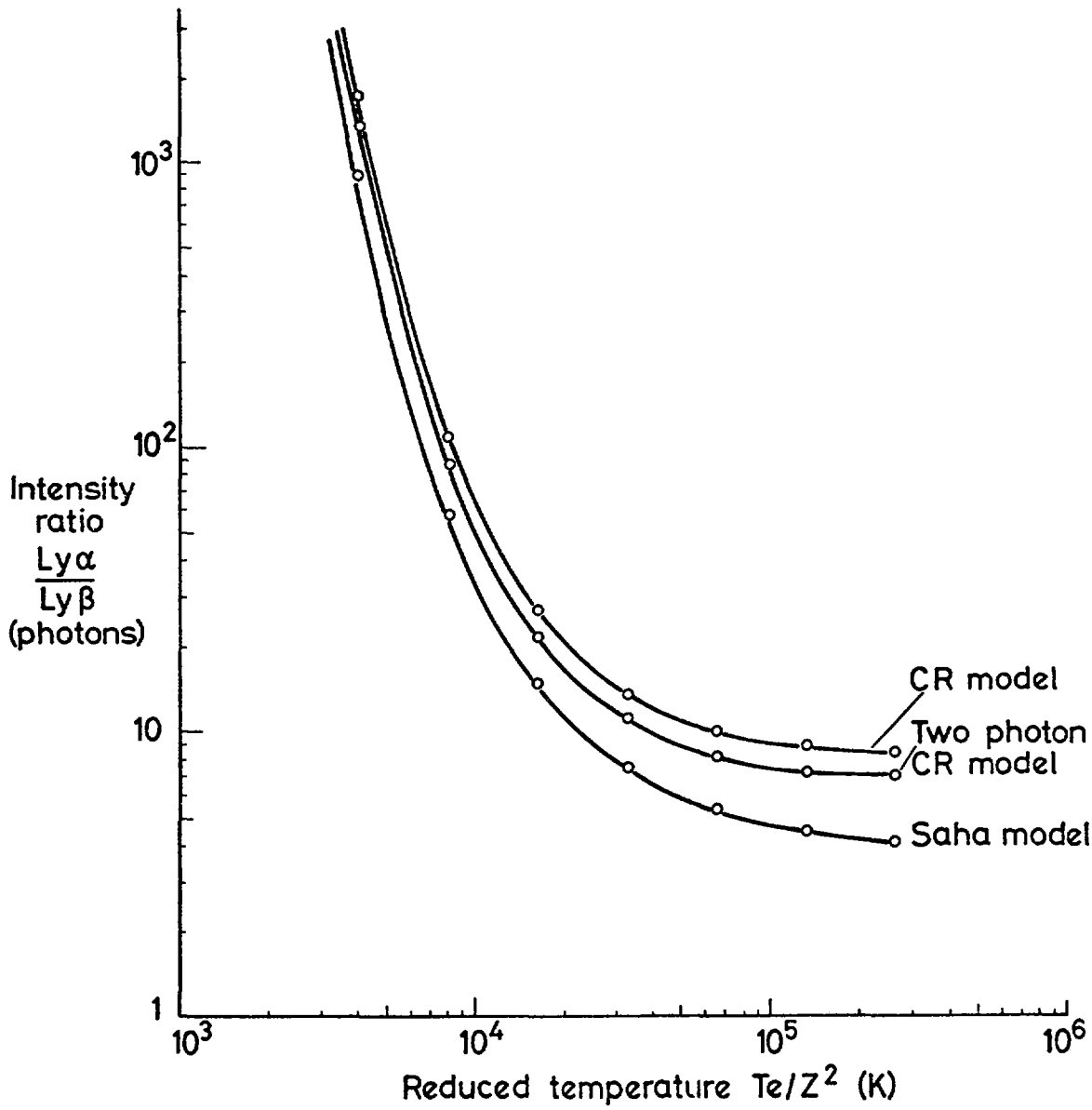
10^3
10^2
10
1
Intensity ratio $\frac{Ly\alpha}{Ly\beta}$ (photons)
CR model
Two photon CR model
Saha model
10^3
10^4
10^5
10^6
Reduced temperature Te/Z^2 (K)

Fig.7.2

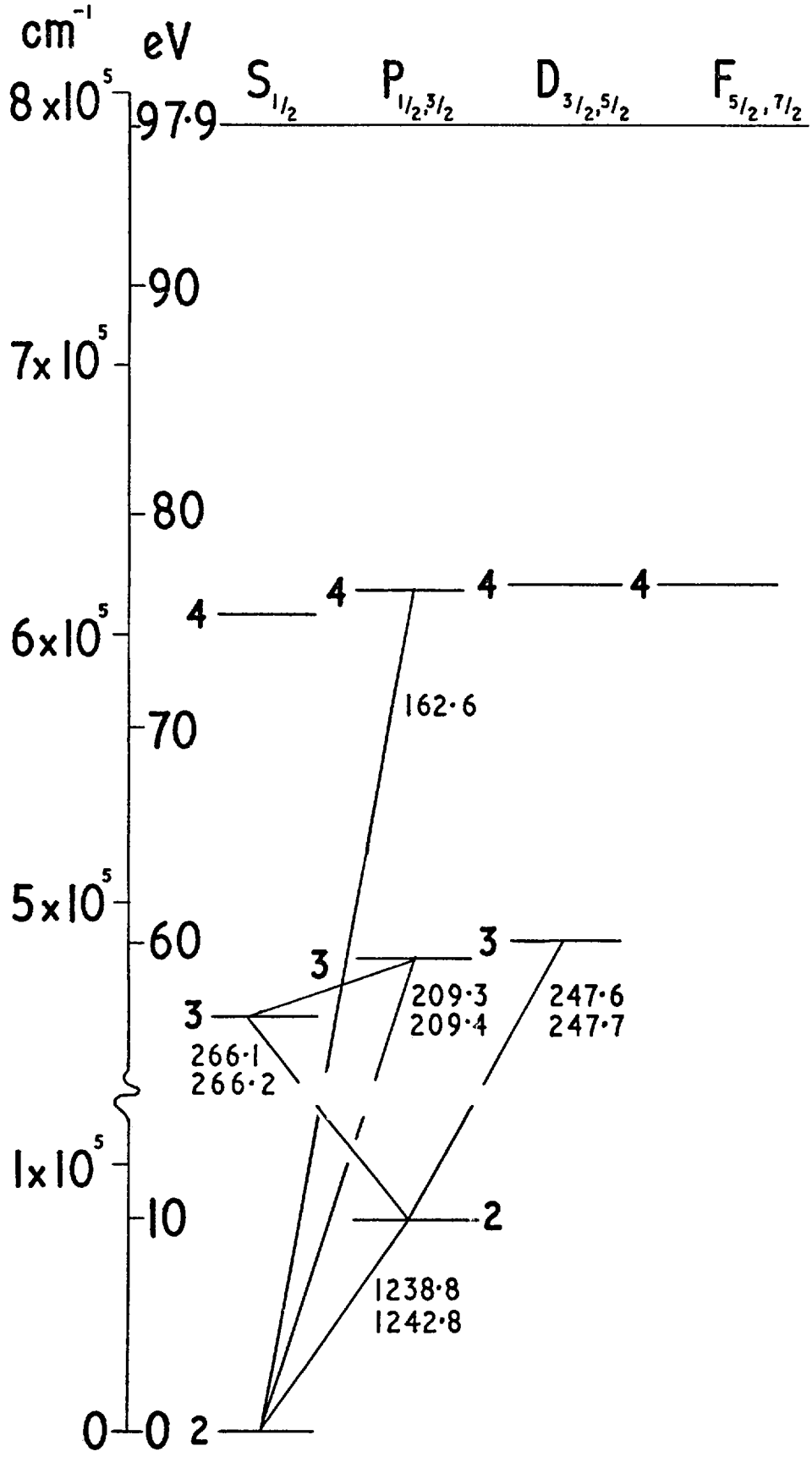

Fig.7.3 Nitrogen V term scheme

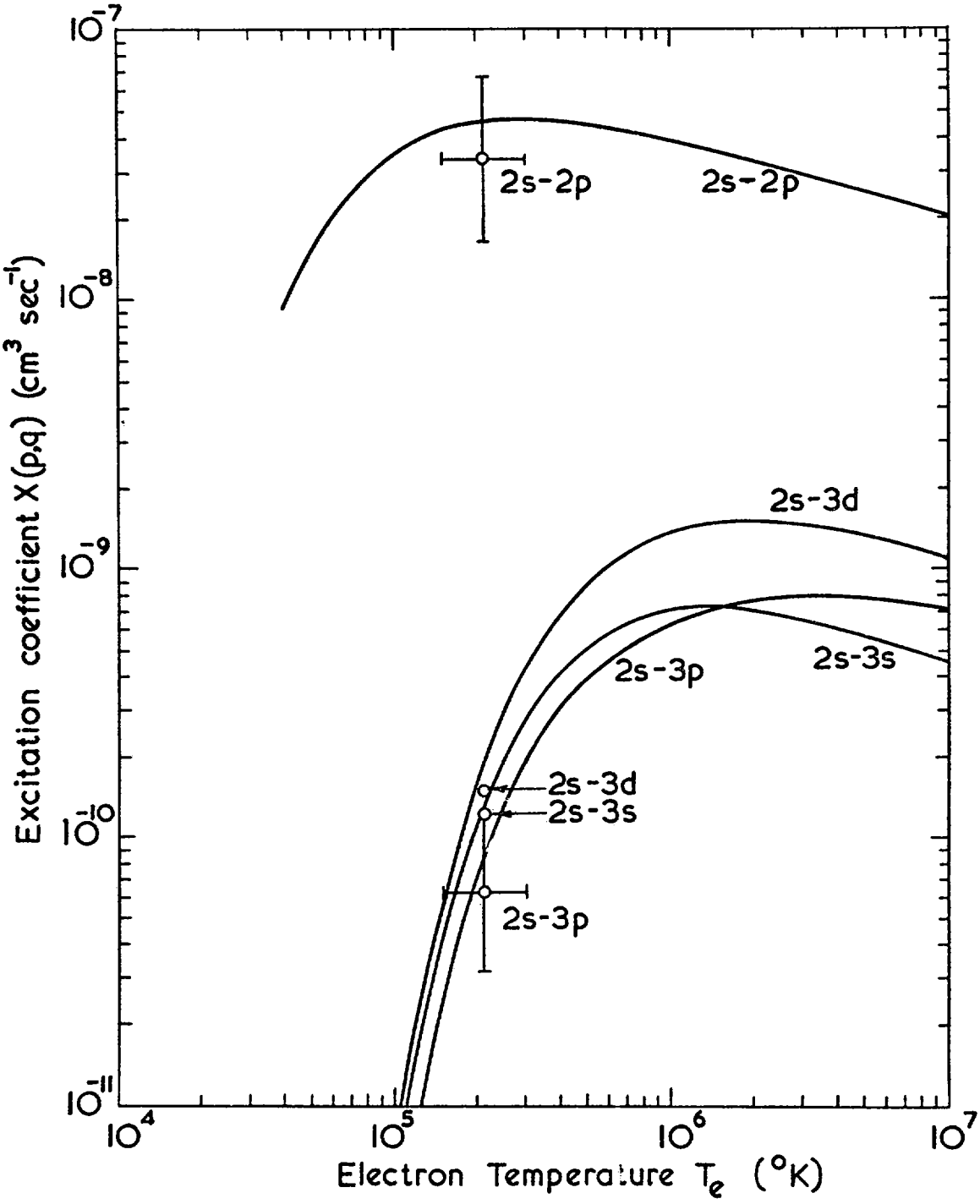

Fig.7.4 The curves are theoretical excitation coefficients based on cross-sections calculated by Burke et al. (Proc. Phys. Soc., 87, 209, [1966]). The points are our measured values.

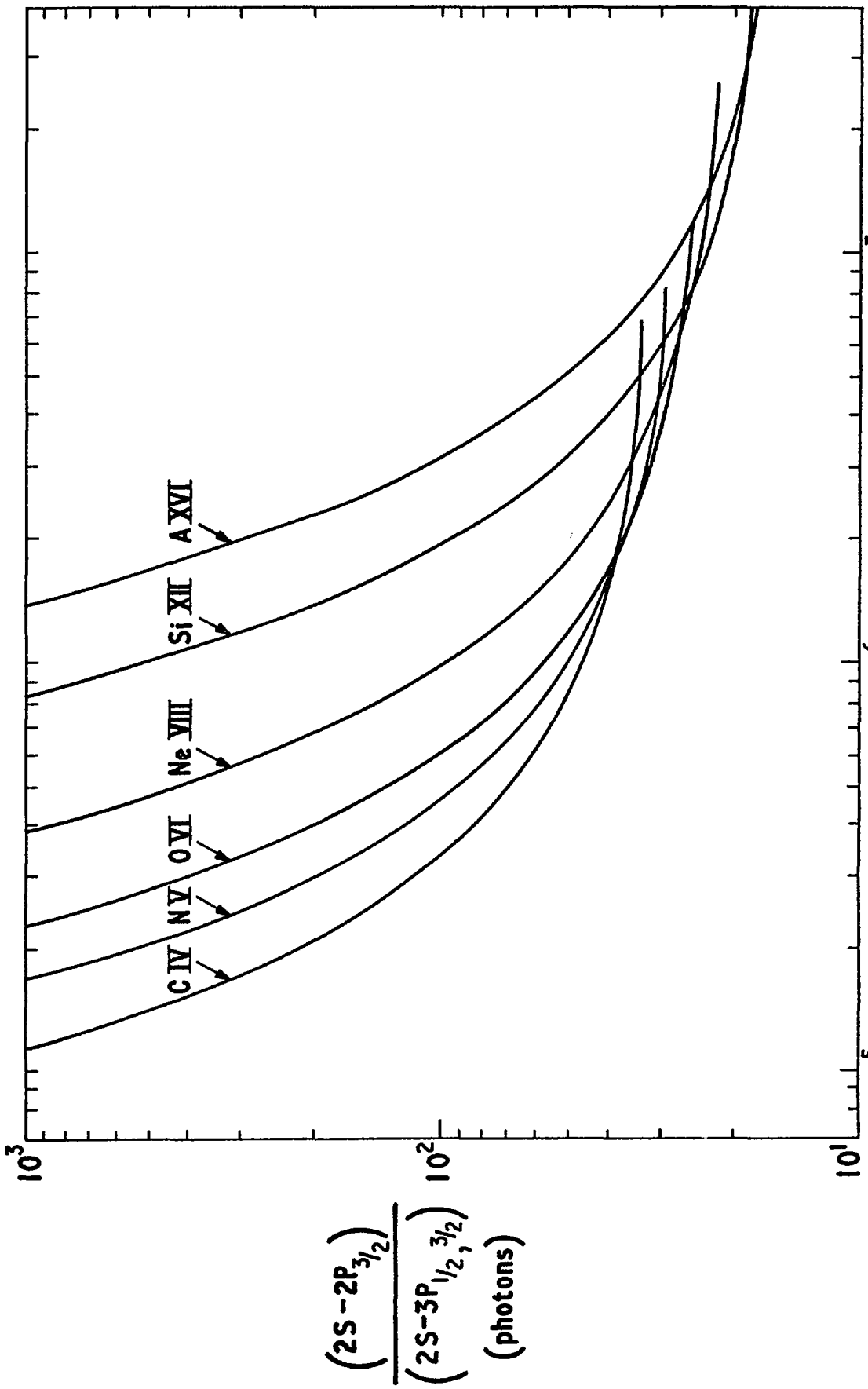

Fig.7.5 Lithium like ion line intensity ratios for electron temperature measurement.

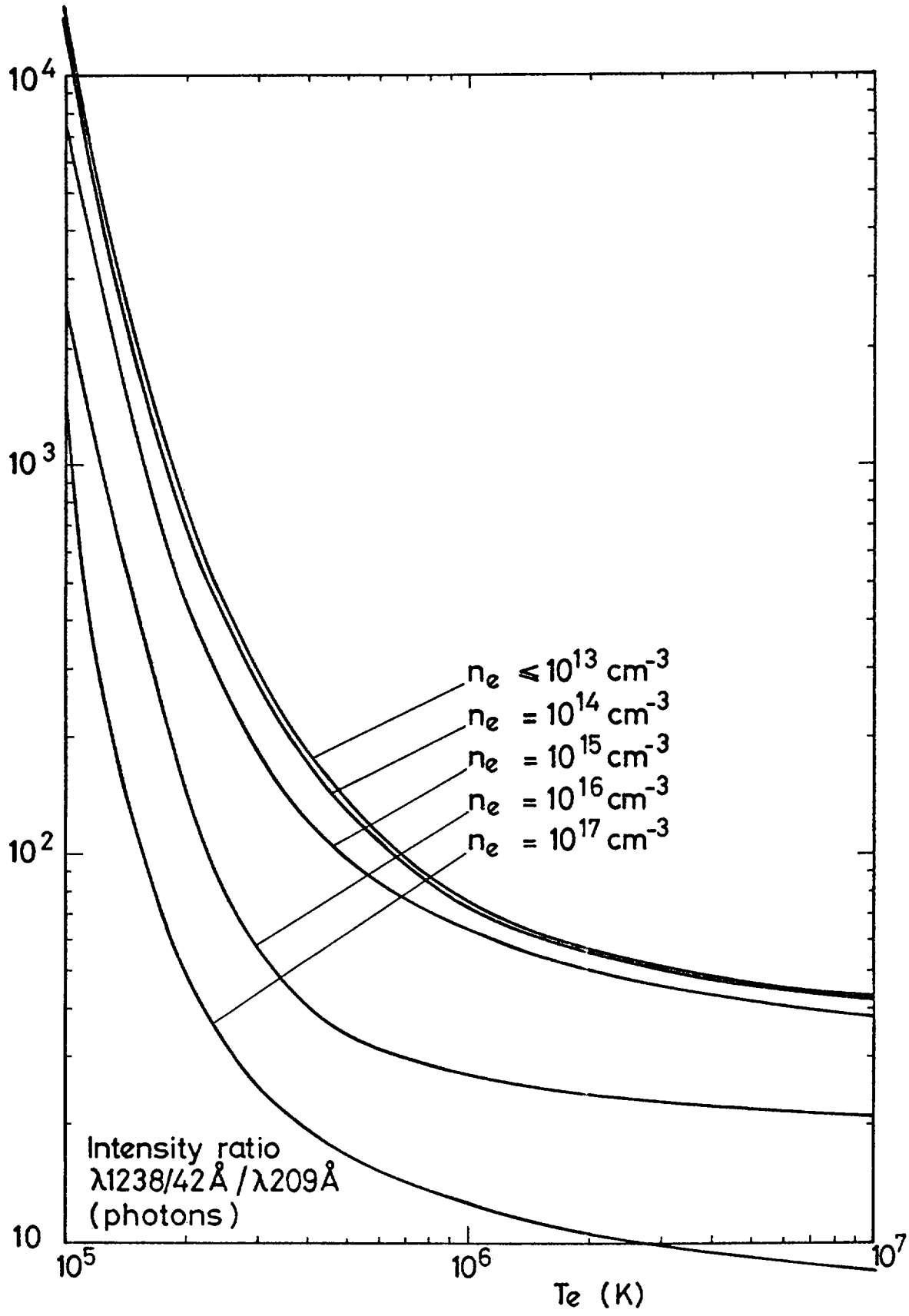
10^4
10^3
10^2
10
10^5
10^6
10^7
Te (K)
$n_e \leq 10^{13}$ cm^{-3}
$n_e = 10^{14}$ cm^{-3}
$n_e = 10^{15}$ cm^{-3}
$n_e = 10^{16}$ cm^{-3}
$n_e = 10^{17}$ cm^{-3}
Intensity ratio
λ1238/42Å / λ209Å
(photons)

Fig.7.6

$$I(p,q) = n_e \left[n(g) X(g,p) + n(m) X(m,p) \right] \frac{A(p,q)}{\sum_r A(p,r)}$$

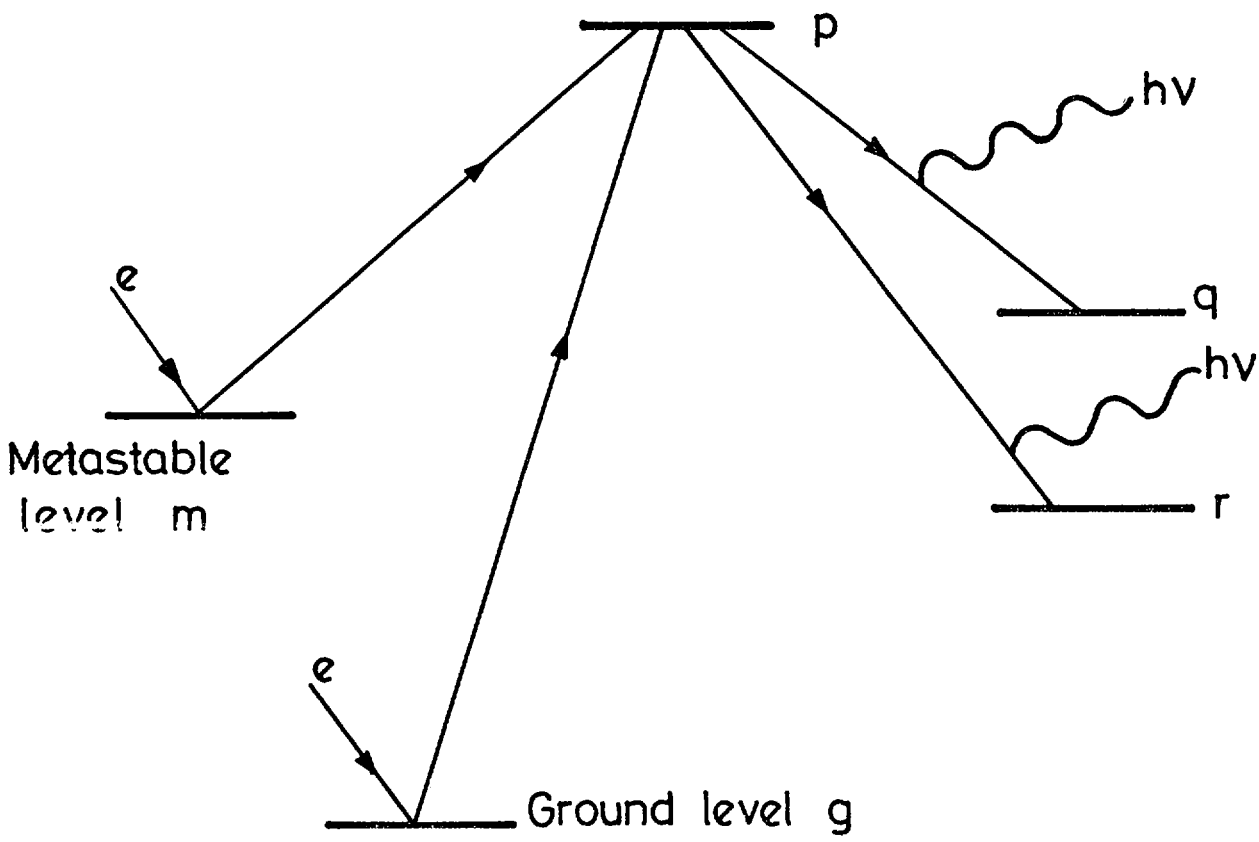

Fig.7.7

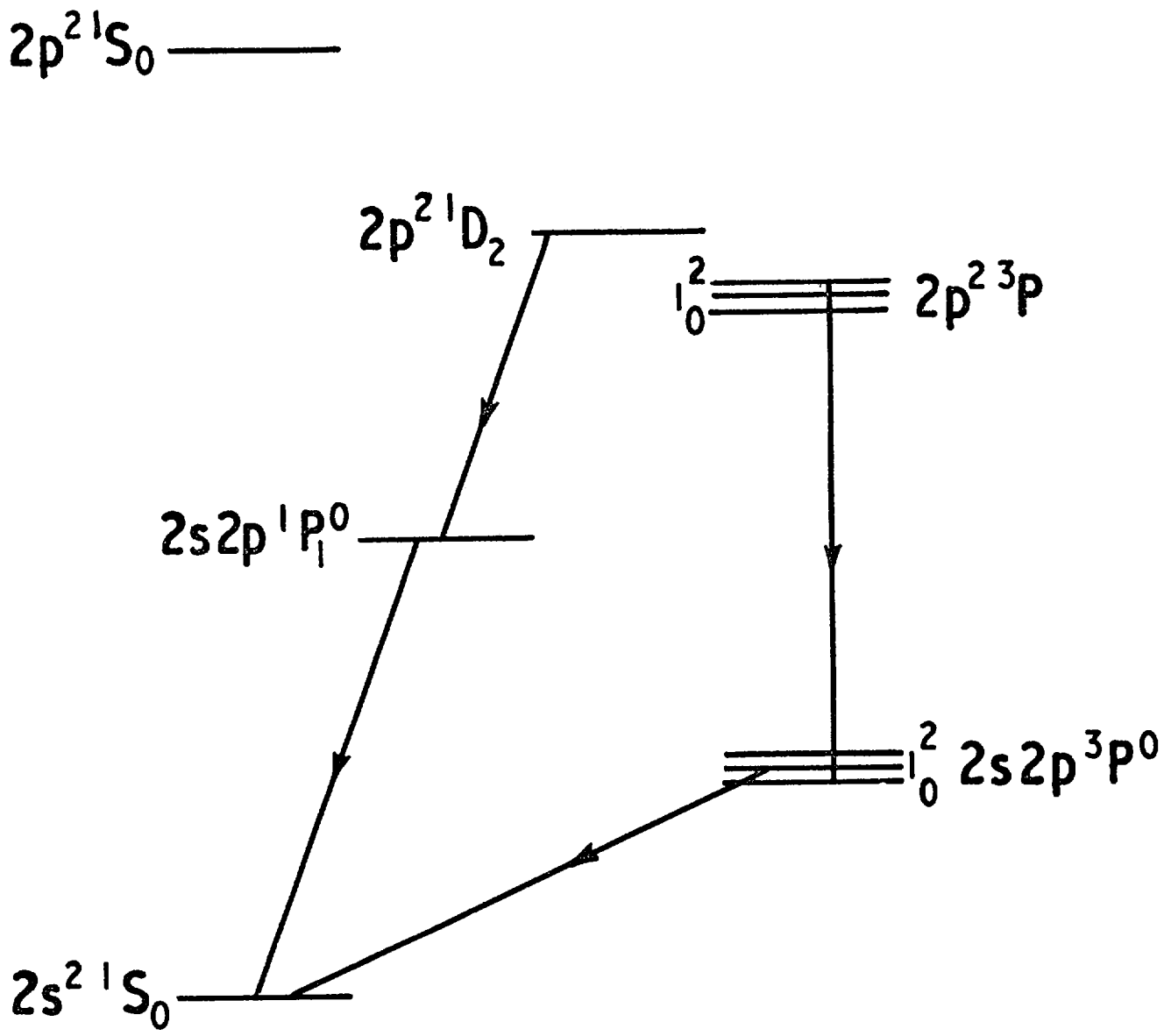

Fig.7.8

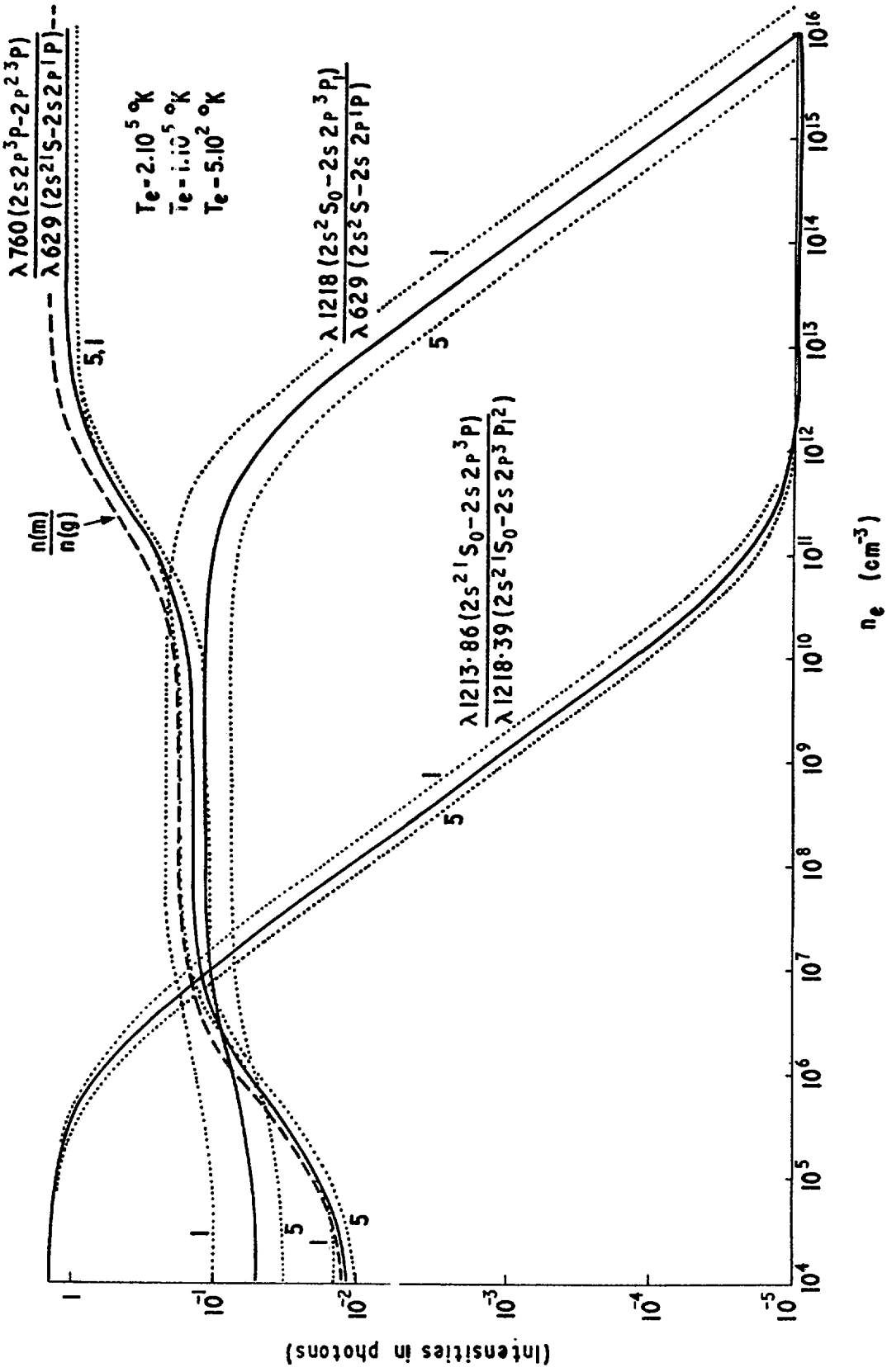
λ760(2s2p³P-2p²³P) / λ629(2s²¹S-2s2p¹P)
n(m)/n(g)
Te-2.10⁵ °K
Te-1.10⁵ °K
Te-5.10² °K
λ1218(2s²S₀-2s2p³P₁) / λ629(2s²S-2s2p¹P)
λ1213·86(2s²¹S₀-2s2p³P) / λ1218·39(2s²¹S₀-2s2p³P₁²)
(Intensities in photons)
ne (cm⁻³)

Fig.7.9

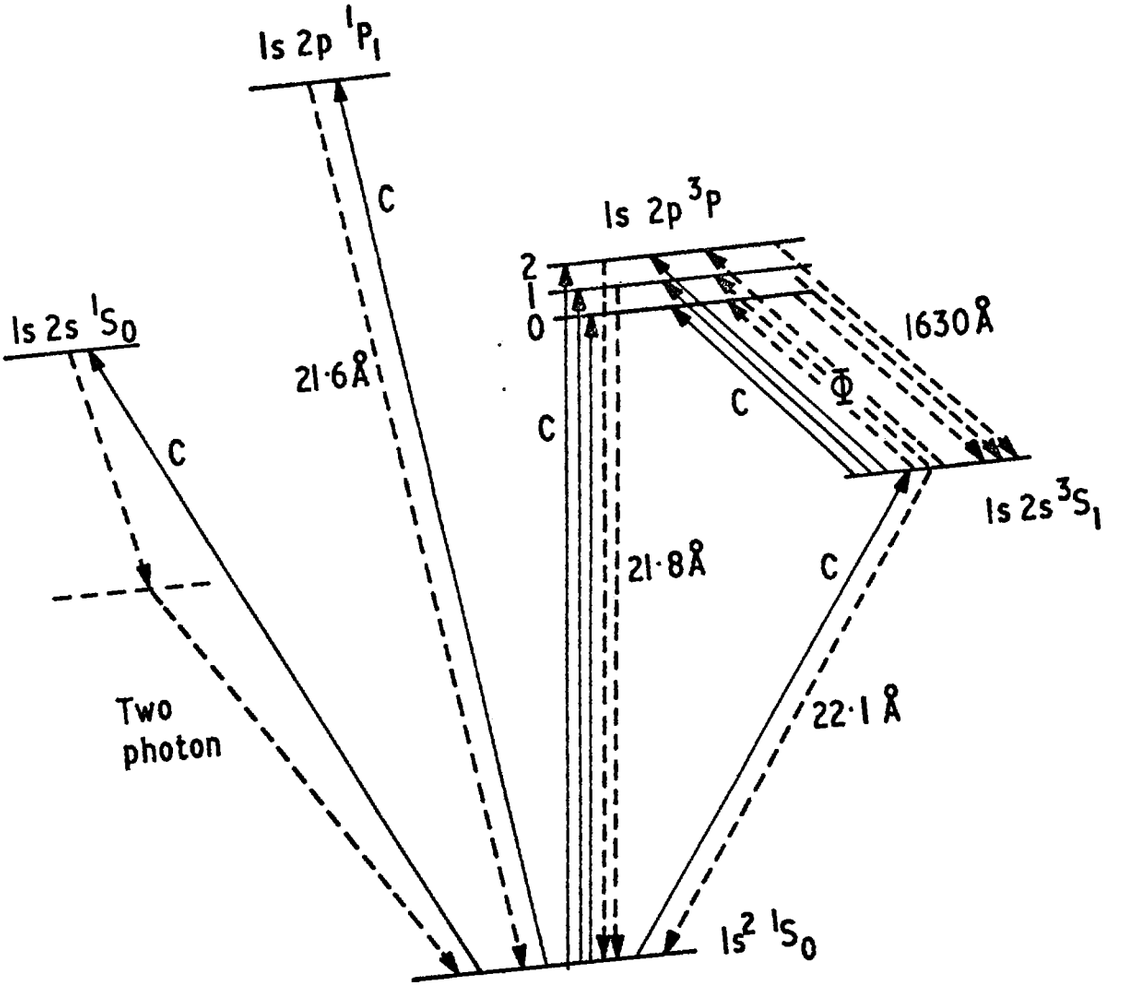
1s 2p $^1P_1$
C
1s 2p ^3P
2
1
0
1s 2s $^1S_0$
21·6Å
C
C
Φ
1630Å
1s 2s $^3S_1$
C
21·8Å
C
22·1 Å
Two
photon
1s^2 $^1S_0$

Fig.7.10

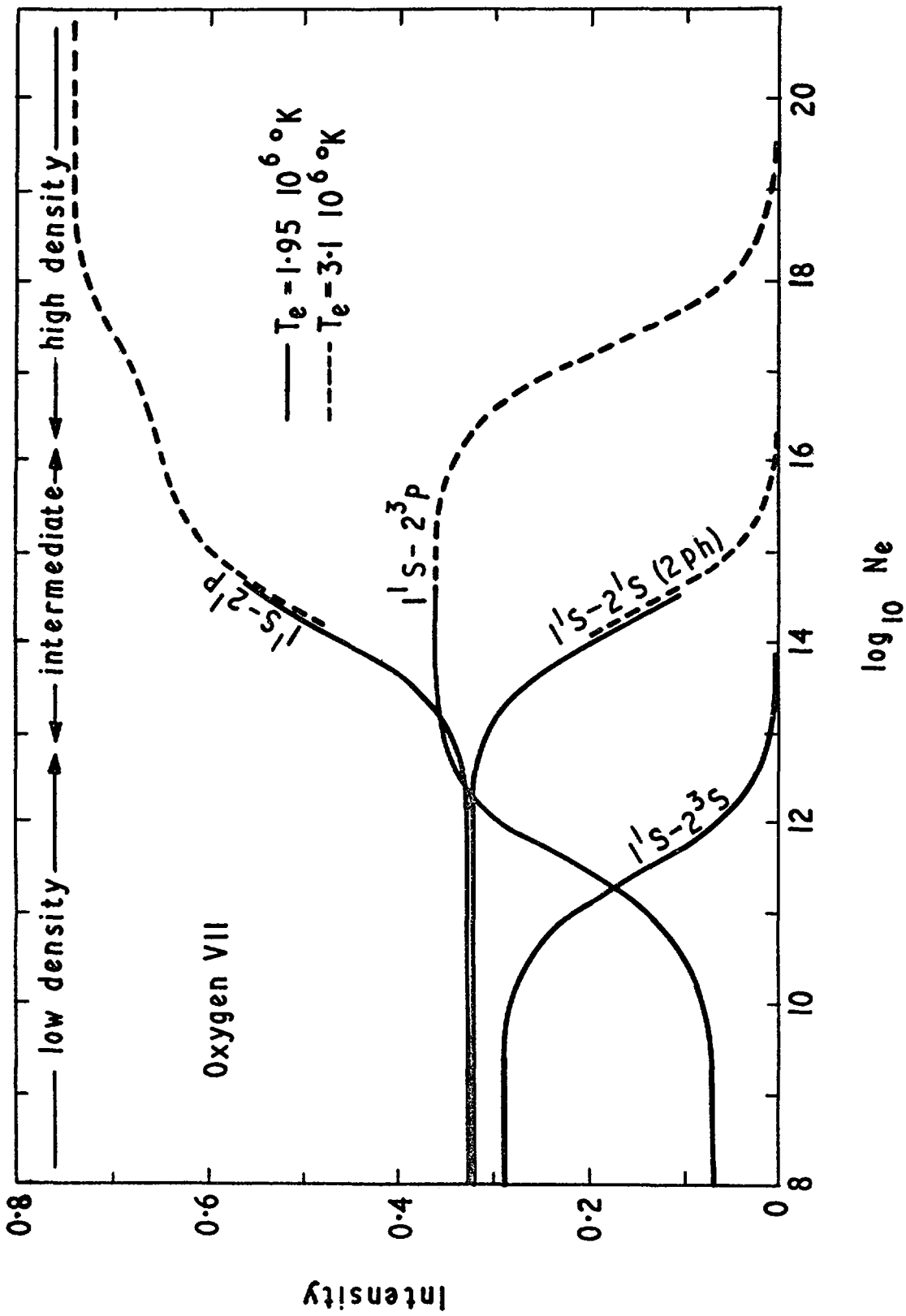
low density
intermediate
high density
T_e = 1·95 10^6 °K
T_e = 3·1 10^6 °K
Oxygen VII
1^1S-2^3P
1^1S-2^1S (2ph)
1^1S-2^3S
2^3S-2^1S
Intensity
0·8
0·6
0·4
0·2
0
8
10
12
14
16
18
20
$\log_{10}$ Ne

Fig.7.11

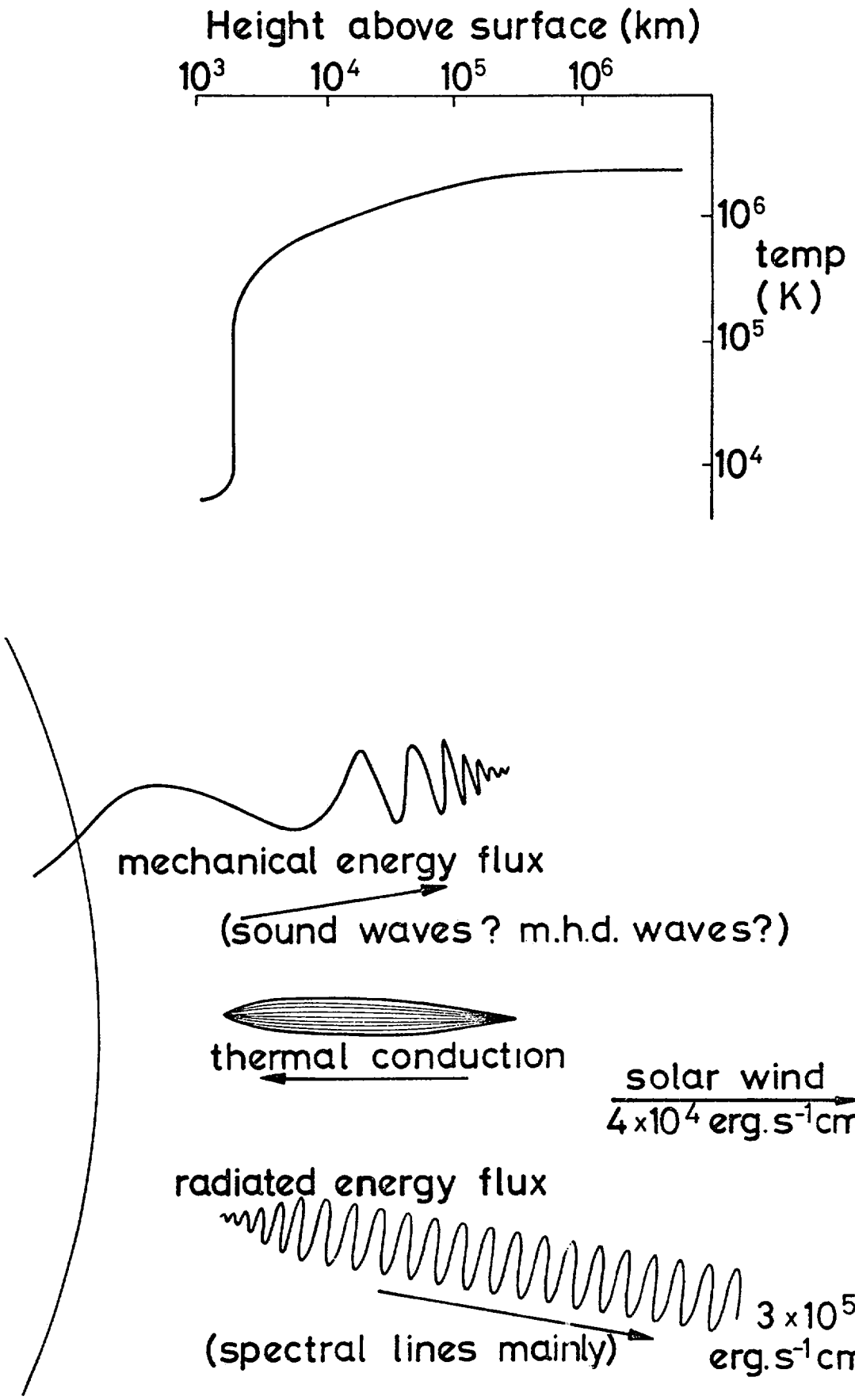
Height above surface (km)
10³
10⁴
10⁵
10⁶
10⁶
temp
(K)
10⁵
10⁴
mechanical energy flux
(sound waves? m.h.d. waves?)
thermal conduction
solar wind
4x10⁴ erg.s⁻¹cm⁻²
radiated energy flux
3x10⁵
erg.s⁻¹cm⁻²
(spectral lines mainly)
Solar Corona Heating

Fig.9.1

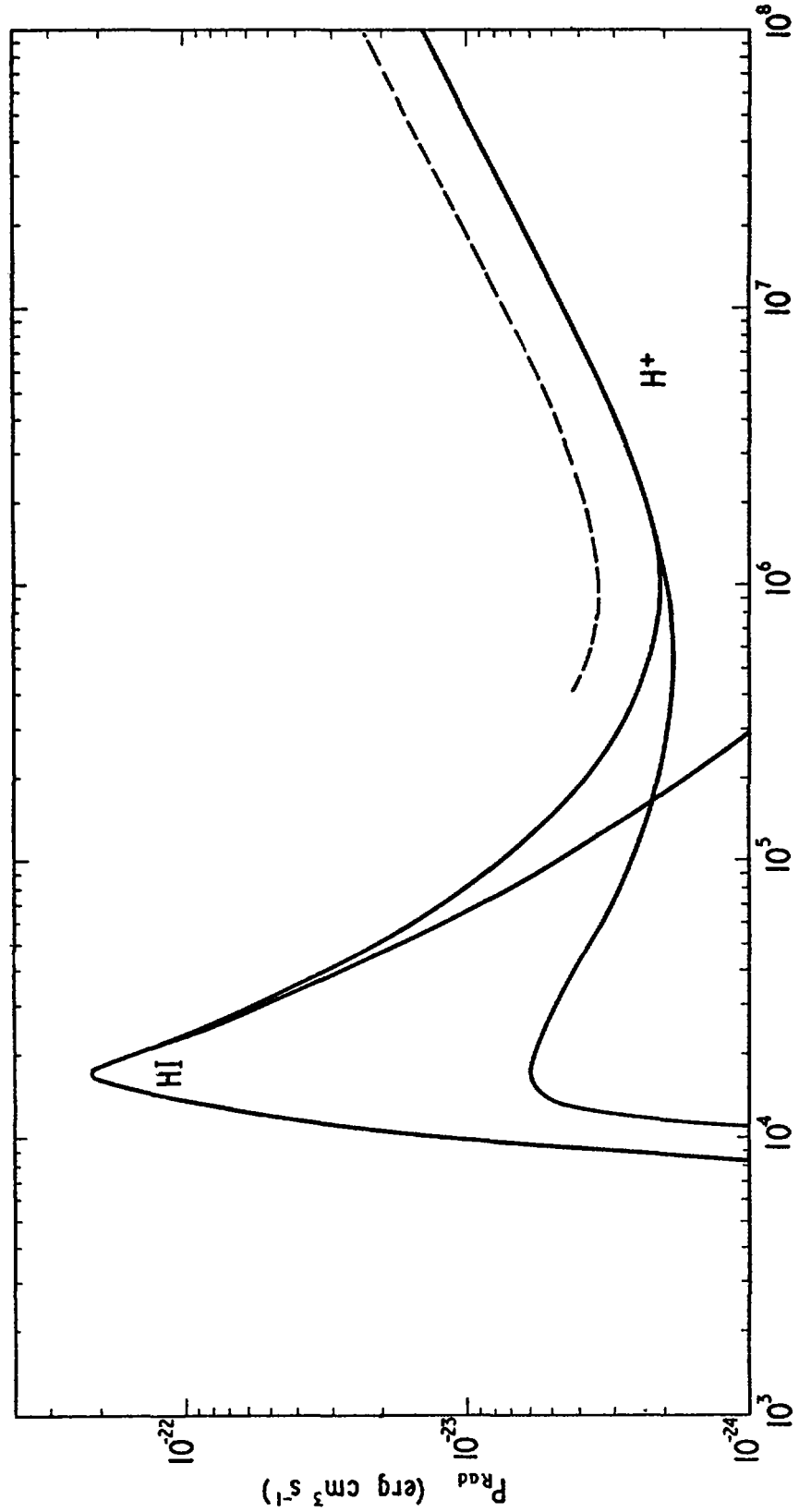

The radiated power function for Hydrogen

Fig. 9.2

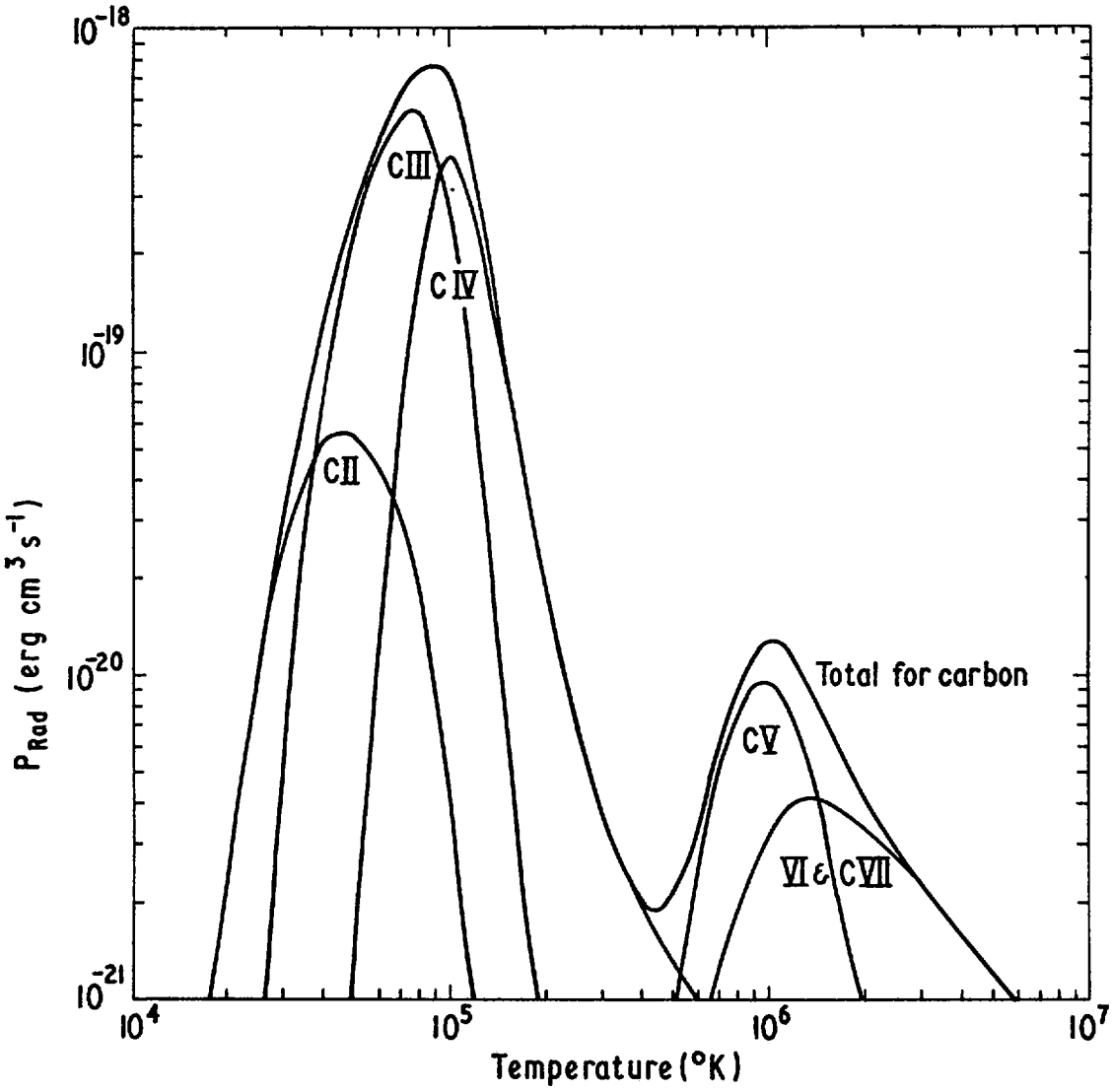

The radiated power function for carbon

Fig.9.3

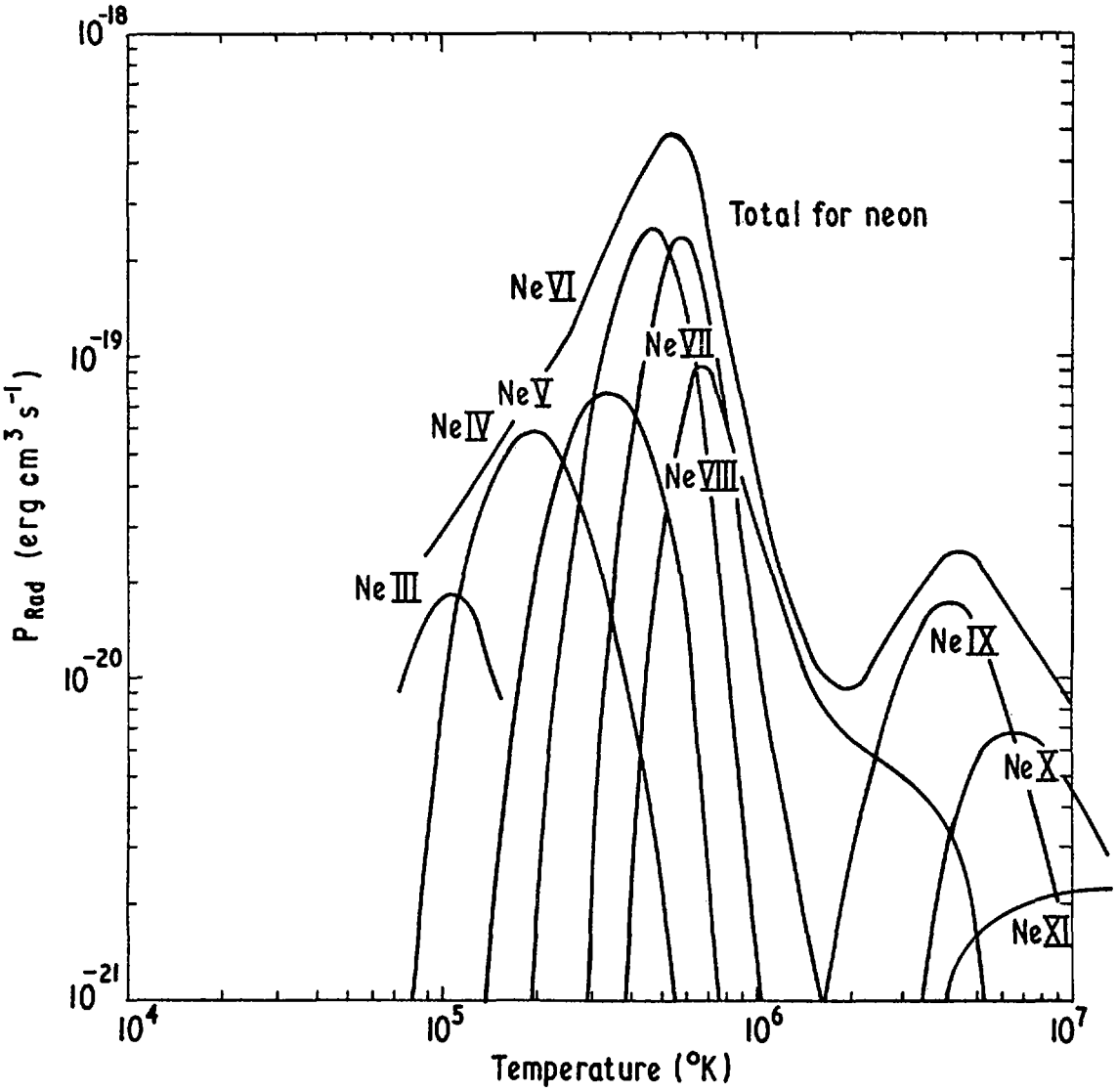

The radiated power function for neon

Fig.9.4

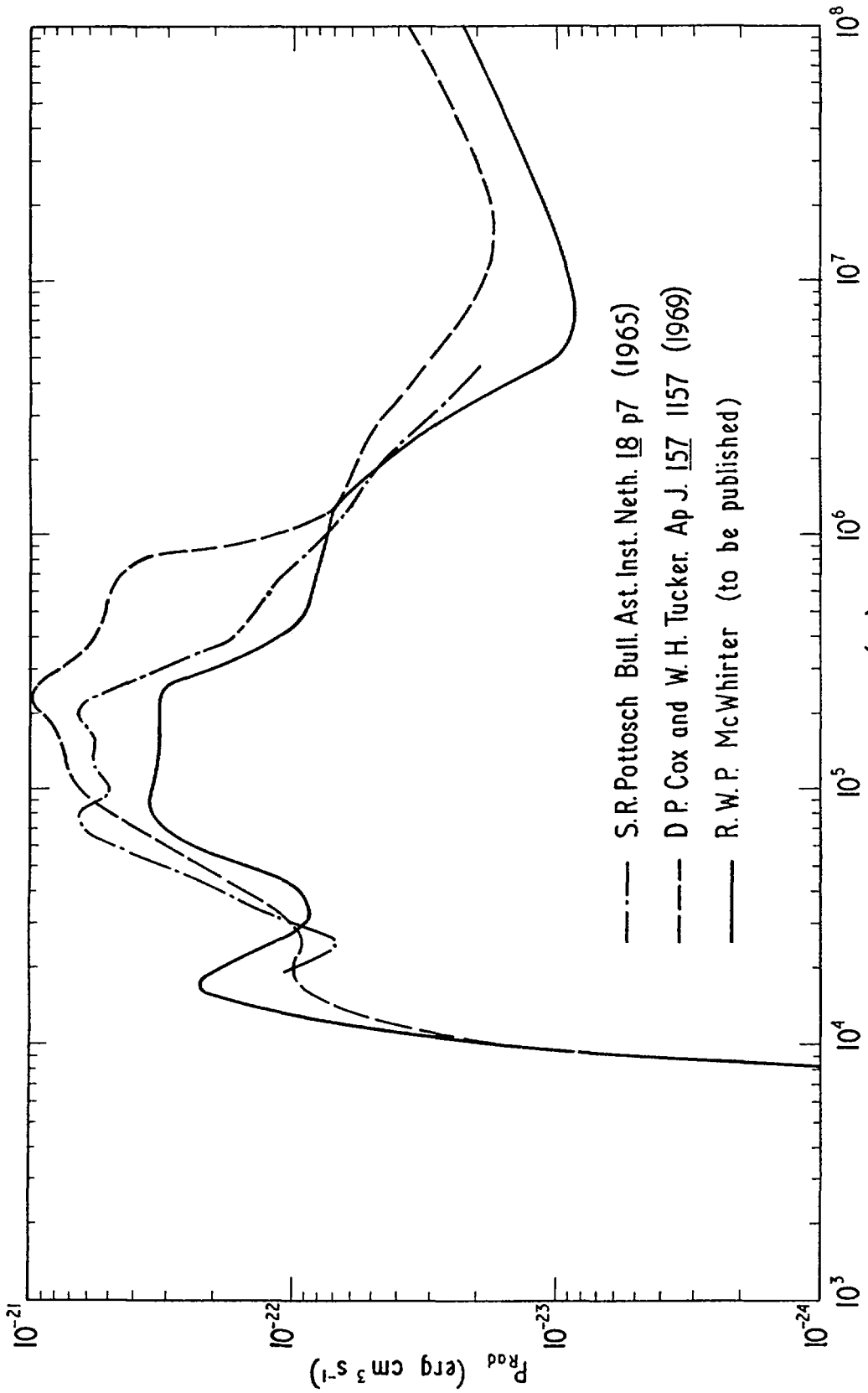

Fig.9.5 The Total radiated power loss function for the solar corona

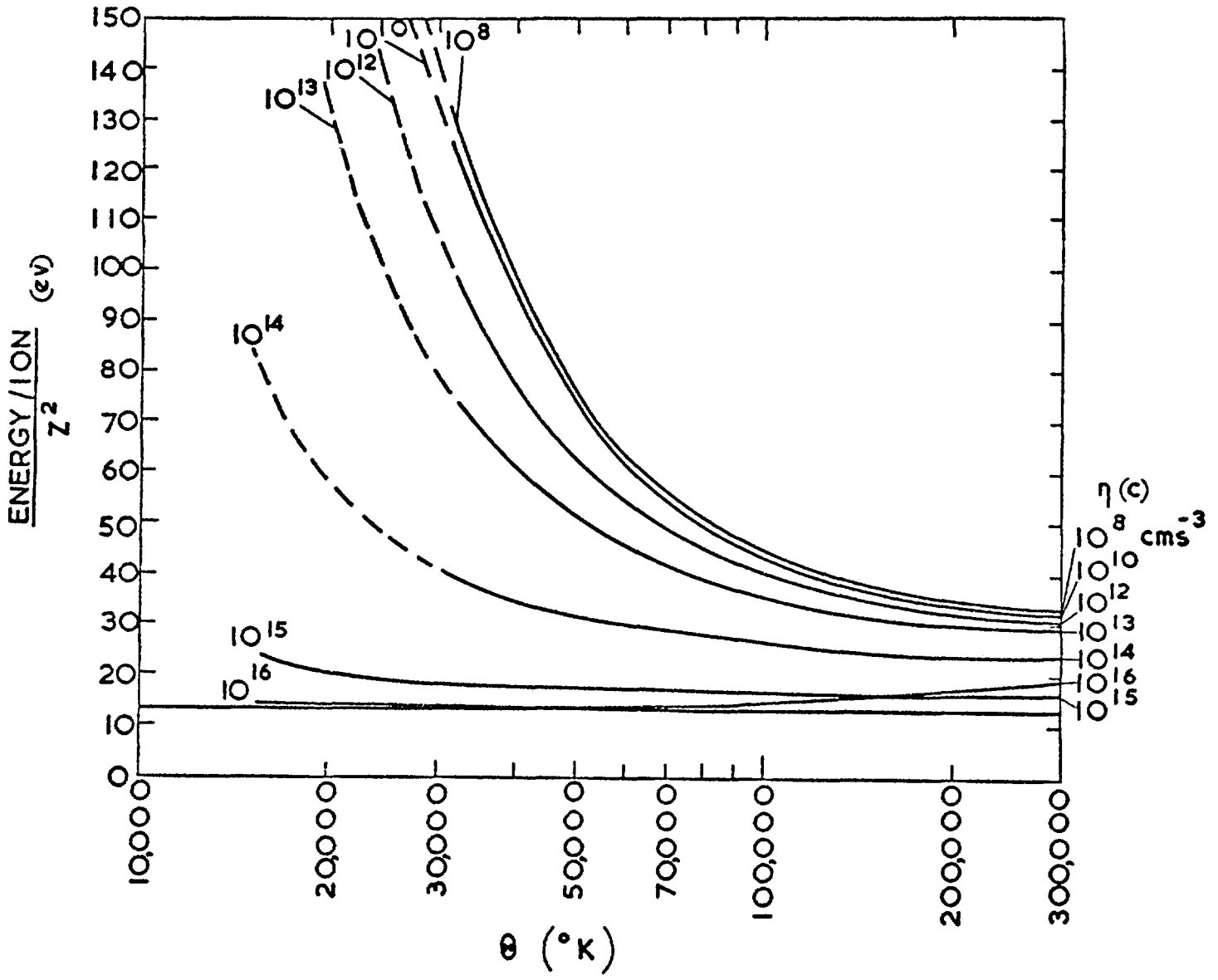
ENERGY / ION / Z² (eV)
150
140
130
120
110
100
90
80
70
60
50
40
30
20
10
0
10,000
20,000
30,000
50,000
70,000
100,000
200,000
300,000
θ (°K)
10⁸
10¹⁰
10¹²
10¹³
10¹⁴
10¹⁵
10¹⁶
η (c)
10⁸ cms⁻³
10¹⁰
10¹²
10¹³
10¹⁴
10¹⁶
10¹⁵

Fig.9.6

TECHNIQUES FOR THE CALCULATION OF ATOMIC DATA REQUIRED FOR PLASMA DIAGNOSTICS

H. E. SARAPH

Department of Physics and Astronomy
University College London
Gower Street, London WC1E 6BT

1. DATA REQUIREMENTS

The temperature, density and chemical composition of a plasma can be obtained from a study of its spectrum. For this analysis, atomic data are required to determine the populations of all energetically accessible stages of excitation and ionization of all the elements that are present in the plasma. This huge problem is being attacked by experimentalists and theoreticans all over the world. The atomic data obtained may be in error by as little as 5% up to as much as a factor of 10. The computing requirements for transition rates in any one ion, using existing program packages, range from 50-100 hours on a high powered machine plus six months work by the researcher, down to a few hours work using a hand calculator. The order of magnitude estimates for atomic processes are essential to fill the many gaps where elaborate calculations or experiments have not yet been carried out, and to indicate where extensive calculations are necessary. This report deals with computational techniques aiming for results with errors less than 25%. The ranges of validity of the various techniques are discussed.

2.1. CALCULATION OF ATOMIC STRUCTURE AND RADIATIVE TRANSITION PROBABILITIES

The ab initio calculation of atomic structure was pioneered by Hartree [1]. For ions with nuclear charge $Z \leq 30$ it suffices to solve the non-relativistic Schrödinger equation

$$(H - E)\Psi^E = 0 \quad , \tag{1}$$

where H is the Hamiltonian given by

$$H = \sum_{i=1}^{N} \left[-\frac{\hbar^2}{2m} \nabla_i^2 - \frac{Ze^2}{r_i} + \sum_{j>i} \frac{e^2}{r_{ij}} \right] \quad . \tag{2}$$

In equations (1) and (2), N is the total number of electrons, e and m are the charge and mass of the electron, r_i is the distance of the ith electron from the nucleus and r_{ij} the distance between the ith and jth electrons. The wave function Ψ^E of the atom at energy E is represented by a sum over products of single electron orbitals with given angular properties. The radial parts of the orbitals are determined such that the energy is minimised. In principle, see Hartree [1], the atomic structure problem can be solved exactly, if the wave function is expanded over all configurations of the same parity. In practice, only the most important configurations are included, namely those of

a) the same complex as the ground configuration (Layser [2]),
b) single electron substitution, and
c) single electron excitation (mainly for neutral elements).

Calculations that include only the ground configuration can achieve sufficient accuracy only in those special cases where perturbation from other states can be neglected, strong optically allowed transitions for example. To compensate for the truncation of the configuration expansion, polarization potentials or polarised orbitals are sometimes used. To economise in a structure calculation, some or all of the complicated inter-electron potential e^2/r_{ij} may be replaced by a model potential. This method is particularly applicable to the representation of the closed shells in a many electron system.

Oscillator strengths $f_{\alpha\beta}$ for radiative transitions between two states with energies E_α and E_β are computed using first order perturbation theory, where

$$f_{\alpha\beta} \propto (E_\beta - E_\alpha) |\langle \psi_\beta \mid \mathbf{P} \mid \psi_\alpha \rangle|^2 \quad , \tag{3}$$

and $\mathbf{P}$ is the transition operator. In the case of photoionization, the final state wave function includes free electron orbitals, and this is discussed in the next paragraph.

2.2. ELECTRON IMPACT EXCITATION

In the asymptotic region, that is where the incident electron is sufficiently far from the atom, the wave function for the compound system of atom plus electron (Ψ) is given by

$$\Psi_\alpha^{\mathcal{L}}(r_1, r_2) \underset{r_2 \to \infty}{\sim} \psi_\alpha(r_1)\chi_\alpha(\theta_2\phi_2)k_\alpha^{-\frac{1}{2}} \exp(-ik_\alpha r_2)/r_2 - \sum_\beta \psi_\beta(r_1)\chi_\beta(\theta_2\phi_2)k_\beta^{-\frac{1}{2}} \exp(ik_\beta r_2)/r_2 \, S_{\beta\alpha}^{\mathcal{L}} \tag{4}$$

where α and β refer to states of the target atom represented by wave functions of the type $\psi_\gamma(r_1)$. $\chi(\theta_2\phi_2)$ is the angular part of the free electron wave function, k_γ^2 is the energy of the free electron relative to the atomic energy level γ and **S** is the scattering matrix. The cross section Q is obtained from **S**:

$$Q(\alpha,\beta) \propto \sum_{\mathcal{L}} |\delta_{\alpha\beta} - S_{\alpha\beta}^{\mathcal{L}}|^2 \tag{5}$$

where the sum is over all angular momenta $\mathcal{L}$ which contribute. The equations satisfied by the wave function $\Psi_\alpha^{\mathcal{L}}(r_1,r_2)$ are derived using the variational principle and keeping the target wave functions frozen. Inelastic collisions are produced by the electron-electron potential $V_{\alpha\beta}$. The validity of methods used for the calculation of $S_{\alpha\beta}^{\mathcal{L}}$ depends on the relative importance of the potentials present. For a discussion of the general theory of electron-ion collisions, see Seaton [3].

2.2.1. COULOMB BETHE APPROXIMATION

For strong optically allowed transitions, the contributions from the high angular momenta ($\mathcal{L}>12$), can be estimated by expressing the cross section in terms of the radiative transition probability between states α and β, and known functions of the energy and $\mathcal{L}$ (see Burgess et al. [4]).

2.2.2. COULOMB BORN APPROXIMATION

For large values of the net charge on the ion, z, Coulomb waves (Θ) can be used to represent the free electron for angular momenta high enough that coupling with the core electrons can be neglected. The **S** matrix is obtained using perturbation theory:

$$S_{\alpha\beta}^{\mathcal{L}} = \langle \Theta_\alpha | V_{\alpha\beta} | \Theta_\beta \rangle \quad . \tag{6}$$

2.2.3. DISTORTED WAVE APPROXIMATION

The equations for the wave functions of the scattered electron are reduced to simple second order differential equations by the omission of all exchange and coupling potentials. The solutions are used in place of the Coulomb functions (Θ) in the expression (6) above. The approximation is applicable for all angular momenta when $z>5$, and for large angular momenta ($\mathcal{L}>6$) with all values of z.

2.2.4. CLOSE COUPLING METHOD

The coupled second order integro-differential equations describing the scattered electron are solved. The **S** matrix is obtained by fitting

the solution to the correct expression (4) in the asymptotic region. The close coupling method should be used whenever there is strong competition between the various potentials acting on the electron. It is the method that makes the most demand on resources, and much research effort has been spent on making the computer codes used as economical as possible. The method is used mainly for the description of low energy electron impact excitation of metastable levels in neutrals, and systems with $z \geq 5$. It is also used for the calculation of elastic scattering cross sections and in accurate structure calculations for excited bound systems and negative ions. The wave functions can also be used for the determination of oscillator strengths and photoionization cross sections.

The most important atoms of the first row of the periodic table and their isoelectronic ions have been treated by this method; work is in progress on the second row. Near neutral elements with Z>20 prove to be too complex for a consistent application of the close coupling method to be carried out on existing computers.

3.1. RELATIVISTIC EFFECTS

We write the complete Hamiltonian as

$$H = H_{NR} + H_R \qquad (7)$$

where H_{NR} is the non-relativistic Hamiltonian discussed in §2, and H_R is the relativistic part. The leading terms in H_R are of order of magnitude $\alpha^2 Z_{eff}^3$, where $\alpha = (1/137)$ is the fine structure constant, and Z_{eff} is the effective charge seen by an atomic electron, which is in general, a function of radial distance. It follows that for $\alpha^2 Z_{eff}^3 \ll 1$, the radial part of the wave function is only slightly changed by the introduction of H_R. For such ions the Breit-Pauli approximation discussed below is used. As Z increases the innermost core electrons will be affected first, and if these are not directly involved in the transition of interest, relativistic effects can be simulated by additional parameters in the potential for the core electron cloud. For still higher Z the full Dirac equations have to be solved. Much work is in progress to develop methods for a solution of the large Z problem that can be accomodated on present computers.

3.2. BREIT-PAULI APPROXIMATION

Relativistic correction potentials are obtained from the Dirac equations and evaluated using non-relativistic wave functions [5]. The most obvious effect is the coupling of states with different orbital and spin angular momenta (L and S) by off-diagonal spin-orbit interaction. Intersystem combination lines in atomic spectra can be described by this mixing. It has been shown by Ermolaev and Jones [6] that the Breit-Pauli approximation gives energies correct to order $\alpha^2 Z^3$ if exact solutions of the non-relativistic Hamiltonian are employed. It is important to bear in mind that for complex ions generally, only approximate solutions are available.

Electron impact excitation between fine structure levels can also be obtained using LS coupling results and subsequent transformations to intermediate coupling, see [7] and [8].

4. COORDINATION OF EFFORT

Apart from publications and communications at conferences it has been

found necessary to circulate newsletters to prevent unnecessary duplication of effort. Inclusion on the mailing list is usually by personal application only. Below, we list those concerned with atomic data.

Atomic data for Fusion: Editors C.F.Barnett and W.L.Wiese, obtainable from Oak Ridge National Laboratory, P.O. Box X, Building 6000, Oak Ridge, Tennessee 37830, U.S.A.

Circular of the European Group for Atomic Spectroscopy: Editor E.Meinders, Zeeman Laboratorium Plantage Muidergracht 4, Amsterdam-C, Netherlands.

Information Quarterly on the calculation of Atomic data: Editor D.W.Norcross, J.I.L.A., University of Colorado, Boulder, Colorado 80309, U.S.A.

REFERENCES

[1] HARTREE, D.R., The calculation of atomic structures, Wiley, New York (1957).
[2] LAYZER, D.L., Ann. Phys. **8** (1959) 271.
[3] SEATON, M.J., Adv. Atom. Molec. Phys. **11** (1975) 83.
[4] BURGESS, A., HUMMER, D.G. and TULLY, J., Phil. Trans. Roy. Soc. Lond. A**266** (1970) 225.
[5] EISSNER, W., JONES, M. and NUSSBAUMER, H., Comp. Phys. Commun. **8** (1974) 270.
[6] ERMOLAEV, A.M. and JONES, M., J. Phys. B **6** (1973) 1.
[7] SARAPH, H.E., Comp. Phys. Commun. **3** (1972) 256.
[8] Jones, M., Phil. Trans. Roy. Soc. Lond. A**277** (1975) 587.

Measurements of Atomic Transition Probabilities in Highly Ionized Atoms by Fast Ion Beams.

I. Martinson and L.J. Curtis

Department of Physics, University of Lund, S-223 62 Lund, Sweden

A. Lindgård

Chemistry Laboratory III, H.C. Ørsted Institute, University of Copenhagen, DK-2100 Copenhagen Ø, Denmark

Abstract

A summary is given of the beam-foil method by which level lifetimes and transition probabilities can be determined in atoms and ions. Results are presented for systems of particular interest for fusion research, such as the Li, Be, Na, Mg, Cu and Zn isoelectronic sequences. The available experimental material is compared to theoretical transition probabilities.

1. Introduction

In connection with spectroscopic studies of impurities in high temperature plasmas it is of vital interest to know the oscillator strengths for the observed transitions (1, 2, 3). It is by no means an easy task to measure oscillator strengths in highly ionized atoms. Recent developments in experimental atomic physics using fast ion beams from accelerators (beam-foil spectroscopy) (4, 5) have given very promising results, however. With the beam-foil method one measures the lifetime τ_i of an excited level which is related to the atomic transition probability A_{if} and oscillator strength f_{fi} as follows

$$\tau_i^{-1} = A_{if} = \frac{6.67 \cdot 10^{15} \cdot k \cdot f_{fi}}{\lambda^2} \qquad (1)$$

where λ is the transition wavelength in Å and $K = g_f/g_i$ the ratio of the statistical weights of the lower and upper levels. The transition probability in Eq (1) is expressed in s^{-1}; typical values for electric dipole transitions are 10^7 - 10^9 s^{-1}.

A variety of methods have been developed for experimental determination of lifetimes and transition probabilities. The methods include emission and absorption measurements, the Hanle effect technique, electron excitation using pulsed or modulated beams as well as the beam-foil method. We will here only consider the last mentioned method which is the only one that has been applied to +3 and higher ionization states. All other methods so far known are only useful for f-value studies in neutral or a few times ionized systems. For a review of the field see Ref. (6).

2. Survey of the beam-foil technique.

The beam-foil method has been in use for more than ten years (7, 8) and a large number of atoms and ions have already been studied in this way. The principle is schematically shown in Fig. 1. A beam of fast ions is obtained from a particle accelerator, e.g. a Van de Graaff generator. After magnetic analysis the isotopically pure beam is directed through a thin exciter foil, 500 - 1 000 Å in thickness. As a result of collisions with the foil atoms the fast ions can undergo stripping and excitation. The excited atoms decay in flight and the light emitted can be analyzed spectroscopically as shown in Fig. 1. The foil-excited ion beam is thus a spectroscopic light source with several interesting properties.

1) Practically any element can be ionized and accelerated in present-day machines. Beam-foil spectra of more than 60 chemical elements have already been observed. A large interval of ionization degrees are available, ranging from neutrals to some thirty times ionized species. Using a 714 MeV Kr beam from the Berkeley Super-HILAC, Gould and Marrus (9) have thus been able to measure lifetimes in helium-like krypton, Kr XXXV.

2) The beam-foil light source is a time-resolved one. The foil-excited ions travel with a uniform velocity which can be determined to a few per cent accuracy (or better), e.g. using an electrostatic analyzer as shown in Fig. 1. By measuring spectral line intensities, usually by photon-counting techniques, at various distances from the foil one obtains decay curves from which radiative lifetimes can be conveniently extracted. Lifetimes ranging from a few ps to several hundred ns have been measured in this way. The excited ions decay in vacuum and the beam-foil method thus avoids problems such as collisional de-excitation and trapping of resonance radiation.

In the following we shall concentrate on lifetime measurements and results. We have selected transitions in relatively simple systems (1-2 valence electrons) which have appreciable oscillator strengths, i.e. the $\Delta n=0$ resonance lines in the

Li, Be, Na, Mg, Cu and Zn isoelectronic sequences. As shown in Refs (1-3) these are particularly important in the studies of plasma impurities.

3. Lifetime measurements.

In the simplest case the level lifetime τ_i can be obtained from the relation

$$I(x) = I(0) \exp(-x/v\tau_i) \qquad (2)$$

where I(x) is the intensity at a distance x from the foil and v the velocity of the ions. However, the beam-foil excitation is not a selective one, instead many levels are usually populated. This leads to cascading processes, by which the levels under study are repopulated from higher-lying states. Experimentally one obtains decay curves that do not follow the simple equation (2) but must be approximated by a sum of several exponentials. Examples of such decay curves are shown in Fig. 2. The cascading introduces experimental uncertainties and demands very good counting statistics for unambiguous extraction of lifetimes. Fortunately such problems have been studied for quite some time and a number of remedies are available which reduce the uncertainties even in the case of heavy cascading (10). In most cases modern beam-foil experiments now give f-values with 5-10% uncertainties. This fact can be checked by comparing beam-foil data for neutral atoms to f-values obtained from Hanle-effect measurements. The latter method here gives uncertainties of only a few percent.

The lower limit for lifetime measurements is given by the spatial resolution along the foil-excited beam, which is approximately 0.1 mm. Using high-energy beams from powerful accelerators (e.g. Tandem Van de Graaffs, cyclotrons or heavy-ion linear accelerators) as well as good optical imaging methods it is now possible to measure lifetimes as short as a few ps (11, 12). Such lifetimes are not unusual in very highly ionized systems.

Parallel to this development on the experimental side there are important refinements in theoretical calculations of oscillator strengths. Many such results are found in the tables issued by Wiese et al. (13). The Coulomb-approximation method

of Bates and Damgaard (14) gives reliable f-values in simple systems. Lindgård and Nielsen (15) have recently applied a numerical Coulomb-approximation by which a large number of f-values (even for transitions between low levels) have been calculated. The problems of electron correlation have been successfully tackled by several authors, e.g. Weiss (16), Sinanoglu (17), Nicolaides and Beck (18), and Hibbert (19).

Configuration-interaction studies, applicable to heavier elements, have also been reported by Froese Fischer (20) and Biémont (21). A Z-expansion method, developed by Dalgarno and coworkers (22) permits f-value calculations for whole isoelectronic sequences. It is also worth emphasizing that it is now possible to calculate rigorous error bounds for theoretical f-values (23).

Relativistic effects on f-values have recently received much attention. Kim and Desclaux (24) have thus studied highly ionized members of the Li and Be isoelectronic sequences. Weiss (25) reports a similar study for Be-like ions while Sinanoglu and Luken (26) investigate the B sequence. Some of these results will be commented below.

When comparing experimental and theoretical f-values it is often enlightening to search for systematic trends and regularities in the available material. Wiese and Weiss (13) have investigated such regularities, e.g. with respect to isoelectronic and homologous systems as well as spectral series. The regularities within isoelectronic sequences are of special interest in the present context.

According to perturbation theory the oscillator strength for a given transition, e.g. $2s\ ^2S - 2p\ ^2P$ in the Li isoelectronic sequence (Li I, Be II, B III etc.) can be written as a power series in $1/Z$, i.e.

$$f = f_0 + f_1(1/Z) + f_2(1/Z^2) + \qquad (3)$$

where f_0 is the hydrogenic value, being equal to zero for $\Delta n=0$ transitions. It is instructive to graphically display f-values vs $1/Z$. As shown by Smith and Wiese (13) it is possible to estimate unknown f-values by this technique. In the present case we shall study such curves for the resonance lines in the Li I, Be I, Na I, Mg I, Cu I and

Zn I isoelectronic sequences. Here beam-foil measurements have provided a wealth of experimental data which can be compared to theoretical values. Another reason for selecting these cases is that transitions with appreciable f-values (in the 0.1-1 range), such as the above-mentioned resonance lines in high Z systems, are very important in quantitative studies of impurity concentrations in Tokamak plasmas (1, 2).

The following discussion shows that beam-foil experiments have not yet reached these very highly ionized species which are observed in plasmas, e.g. Fe XXIV. Here only theoretical f-values are available at present. However, as already pointed out by Wiese and Younger (3) beam-foil studies of low Z ends of isoelectronic sequences are of great value in checking various theoretical approaches. In view of present developments in accelerator technology we can safely expect extensions of beam-foil work to very high ionization states.

Li I sequence.

The 2p ^{2}P level lifetime in Li-like systems has been measured for Li I to Na IX by beam-foil methods. The results are generally in good agreement with various theoretical calculations. Recently Martin and Wiese (27) have made a thorough analysis of the oscillator strengths in the Li I sequence and much information about theoretical and experimental f-values for various transitions in Li-like ions can be obtained from their paper. In the present context lithium-like metal ions are of special significance. In Fig. 3 we show the theoretical lifetimes for levels in Fe XXIV, calculated by the Coulomb approximation (28). We note a very typical trend, the n=3 and n=4 terms have very short lifetimes while the first excited level, 2p ^{2}P has an order of magnitude longer lifetime. Since the Coulomb approximation calculations take advantage of experimental excitation energies and quantum defects relativistic effects on f-values are partly accounted for. However, a more specific study of such effects on the 2s-2p transitions in the Li I sequence can be found in Refs. (24) and (27). These calculations show that the relativistic and non-relativistic multiplet f-values are rather close to each other for Z<30. However, the 2s $^2S_{1/2}$-2p $^2P_{3/2}$ f-value starts to show an increase from

4. Summary and conclusion

We have given a short survey of the beam-foil method by which transition probabilities in highly ionized atoms can be determined. A wealth of such data, even for transitions in the far UV and soft X-ray regions, has been accumulated, of which we here have discussed f-values for $\Delta n=0$ resonance lines in the Li I, Be I, Na I, Mg I, Cu I and Zn I isoelectronic sequences.

As emphasized e.g. in Ref. (5) modern beam-foil work has in many cases yielded f-values that are much smaller than the results of conventional HF calculations, sometimes order-of-magnitude differences exist. More extensive calculations in which electron correlations are included have usually led to very good agreement with the experimental f-values. This is also illustrated in Figs. 4, 5, 7 and 8. However, also in such cases we note that the theoretical and experimental f-values tend to depart from each other when Z increases in an isoelectronic sequence, indeed this occurs before relativistic effects on f-values start to play a role. This is a serious problem which has to be solved before safe conclusions can be drawn about f-values in very highly ionized systems, e.g. Li-like Mo.

One possible explanation for shortcomings on the experimental side is cascading into the level under study. However, our simulated decay curves for the first excited level in the Na I and Cu I sequences (Figs. 6 and 8, respectively) show that the cascading problems become less serious when Z increases. After an initial rise the constructed curves follow rather closely the expected $np\ ^2P$ (n=3, 4) decay time. The reason for this is also shown in Fig. 3 where the $2p\ ^2P$ level survives all n=3 and n=4 levels. The fact that such resonance lines with $\Delta n=0$ have much lower transition rates than $\Delta n=1$ lines in highly ionized systems should also permit lifetime measurements with the beam-foil method of cases such as the 2p level in Fig. 3.

With new powerful heavy-ion accelerators (43) we can therefore expect important breakthroughs in lifetime measurements in highly ionized species within the near future. As an illustration of this, Fig. 11 shows a beautiful beam-foil spectrum of iron, obtained at the Oak Ridge tandem accelerator by Bashkin and coworkers (44). The $3s\ ^2S$-$3p\ ^2P$ doublet in Fe XVI, at 335.4 and 360.8 Å and the $3s^2\ ^1S$-$3s3p\ ^1P$

resonance line in Fe XV, at 284.1 Å are clearly observable, together with many other important transitions in highly ionized iron. Lifetime measurements, which already are in progress (44) might well resolve some of the present difficulties, discussed above.

In this review we have mainly discussed f-value studies of importance for determining impurity concentrations in high temperature plasmas. It is equally important to have good knowledge of the atomic energy levels and wavelengths (1, 2, 46). Several groups are actively engaged in this work and much important material of relevance to plasma diagnostics has been obtained in recent years.

We have already mentioned that our new lifetime program has initiated a study of ionized Ga. Additional investigations of the Cu I and Zn I sequences are also being undertaken at the University of Lund because the data available at present are often very unsatisfactory. In addition to the inherent interest in obtaining accurate level energies and ionization limits, such material is also of importance in beam-foil investigations of lifetimes and theoretical calculations of oscillator strengths.

Acknowledgements:

We are grateful to Professor S. Bashkin and Dr. R.J.S. Crossley for clarifying discussions.

REFERENCES

(1) HINNOV, E., Princeton University Report No. MATT-1022 (1974).

(2) "Report of the Research Panel on Atomic, Molecular and Nuclear Physics in CTR" (U.S. Atomic Energy Commission, Washington, D.C., 1974).

(3) WIESE, W.L. and YOUNGER, S.M., in "Beam-Foil Spectroscopy" (edited by I.A. Sellin and D.J. Pegg, Plenum, New York, 1976) p. 951

(4) BASHKIN' S., in "Progress in Optics" (edited by E. Wolf, North-Holland, Amsterdam, 1974) p. 287.

(5) MARTINSON, I., and GAUPP, A., Phys. Reports 15C (1974) 113.

(6) CORNEY, A., Advan. Electronics Electron. Phys. 29 (1970) 116.

(7) KAY, L., Phys. Letters 5 (1963) 36.

(8) BASHKIN, S., Nucl. Instr. Methods 28 (1964) 88.

(9) GOULD, H., and MARRUS, R., in "Beam-Foil Spectroscopy" (edited by I.A. Sellin and D.J. Pegg, Plenum, New York, 1976) p. 317.

(10) CURTIS, L.J., BERRY, H.G., and BROMANDER, J., Physica Scripta 2 (1970) 216.

(11) IRWIN, D.J.G. and DROUIN, R. in "Beam-Foil Spectroscopy" (edited by I.A. Sellin and D.J. Pegg, Plenum, New York, 1976) p. 347.

(12) KNYSTAUTAS, E.J., and DROUIN, R. in "Beam-Foil Spectroscopy" (edited by I.A. Sellin and D.J. Pegg, Plenum, New York, 1976) p. 377.

(13) WIESE, W.L., SMITH, M.W., and GLENNON, B.M., "Atomic Transition Probabilities, Vol. I NSRDS-NBS 4 (U.S. Govt. Printing Office, Washington, D.C., 1966).

WIESE, W.L., and WEISS, A.W., Phys. Rev. 175 (1968) 50.

WIESE, W.L., SMITH, M.W., and MILES, B.M., "Atomic Transition Probabilities, Vol. II NSRDS-NBS 22 (U.S. Govt. Printing Office, Washington, D.C., 1969).

SMITH, M.W. and WIESE, W.L., Astrophys. J. Suppl. Ser. 23 (1971) 103.

(14) BATES, D.R., and DAMGAARD, A., Phil. Trans. Roy. Soc. A242 (1949) 101.

(15) LINDGÅRD, A., and NIELSEN, S.E., J. Phys. B. 8 (1975) 1183.

(16) WEISS, A.W. in "Advances in Atomic and Molecular Physics" (edited by D.R. Bates and B. Bederson, Academic Press, New York, 1973) Vol. 11, p. 1.

(17) SINANOGLU, O., Nucl. Instr. Methods 110 (1973) 193.

(18) NICOLAIDES, C.A., and BECK, D.R., Chem. Phys. Letters 36 (1975) 79.

(19) HIBBERT, A., Rep. Progr. Phys. 38 (1975) 1217.

(20) FROESE FISCHER, C., Can. J. Phys. 54 (1976) 1465.

(21) BIEMONT, E., J. Quant. Spectrosc. Radiat. Transfer 15 (1975) 531.

(22) DALGARNO, A., Nucl. Instr. Methods 110 (1973) 183 and refs. quoted therein.

(23) SIMS, J.S., and WHITTEN, R.C., Phys. Rev. A8 (1973) 2220.

(24) KIM, Y.-K., Phys. Rev. Letters 36 (1976) 139.

(25) WEISS, A.W., in "Beam-Foil Spectroscopy" (edited by I.A. Sellin and D.J. Pegg, Plenum, New York, 1976) p. 51.

(26) SINANOGLU, O. and LUKEN, W., Chem. Phys. Letters 20 (1973) 407.

(27) MARTIN, G.A. and WIESE, W.L., Phys. Rev. A13 (1976) 699.

(28) LINDGÅRD, A. and NIELSEN, S.E., to be published.

(29) NUSSBAUMER, H., Astron. Astrophys. 16 (1972) 77.

(30) CROSSLEY, R.J.S., CURTIS, L.J., and FROESE FISCHER, C., Phys. Letters 57A (1976) 220.

(31) VICTOR, G.A., STEWART, R.F., and LAUGHLIN, C., to be published

(32) CROSSLEY, R.J.S., and DALGARNO, A., Proc. Roy. Soc. A286 (1965) 510.

(33) CURTIS, L.J., LINDGÅRD, A., and MARTINSON, I., to be published.

(34) BERRY, H.G., DESESQUELLES, J., TRYON, P., SCHNUR, P., and GABRIELSE, to be published in Phys. Rev.

(35) SØRENSEN, G., Phys. Rev. A7 (1973) 85.

(36) LIVINGSTON, A.E., Thesis, University of Alberta (1973).

(37) FROESE FISCHER, C., to be published.

(38) CURTIS, L.J., HULDT, S., and MARTINSON, I., to be published.

(39) LITZÉN, U., and CURTIS, L.J., to be published.

(40) LITZÉN, U., work in progress.

(41) HINNOV, E., private communication.

(42) WARNER, B., Mon. Not. Roy. Astron. Soc. 140 (1968) 53.

(43) STELSON, P.H., in "Beam-Foil Spectroscopy" (edited by I.A. Sellin and D.J. Pegg, Plenum, New York, 1976) p. 401.

(44) GRIFFIN, P.M., PEGG, D.J., SELLIN, I.A., JONES, K.W., PISANO, D.J., KRUSE, T.H., BASHKIN, S., and LEAVITT, J.A., to be published.

(45) IRWIN, D.J.G., and LIVINGSTON, A.E., Can. J. Phys. 54 (1976) 729.

(46) BARNETT, C.F., in "The Physics of Electronic and Atomic Collisions" (J.S. Risley and R. Geballe, eds., Univ. Wash. Press, Seattle, 1976) p. 846.

Figure captions

Fig. 1. Experimental arrangement for beam-foil studies of lifetimes.

Fig. 2. Three examples of decay curves, encountered in lifetime measurements using the beam-foil technique. In (a) cascading is virtually absent while (b) and (c) show the effects of repopulation from a shorter-lived (b) or a longer-lived (c) higher level.

Fig. 3. Theoretical lifetimes (in ps) for n=2, 3 and 4 terms in Fe XXIV (Li I sequence), calculated in the Coulomb approximation (28). The lifetimes for n=3 and n=4 terms are too short to be measurable by beam-foil. However, the 2p lifetime could probably be studied experimentally. Thus if Fe-ions are accelerated to, say, 300 MeV and sent through a foil, the excitation of the 2p ^{2}P level in Fe XXIV is quite probable. A lifetime of 20 ps would then correspond to a 1/e decay length of 0.7 mm, about 10 times longer than the spatial resolution in modern beam-foil work (11, 12).

Fig. 4. Comparison between theoretical and experimental oscillator strengths for the $2s^2\ ^1S$-$2s2p\ ^1P$ transition in the Be I sequence. The experimental points were critically selected from various beam-foil papers, see e.g. Refs. (23) and (29).

Fig. 5. Comparison between theoretical and experimental oscillator strengths for the 3s ^{2}S-3p ^{2}P transition in the Na I sequence. The data sources are found in Refs. (3), (20) and (30).

Fig. 6. Simulated decay curves for the 3p ^{2}P level in the Na I sequence. More than 20 cascading levels were included in the analysis and initial populations according to $(2\ell+1)(n^*)^{-3}$ were assumed, ℓ and n^* being the azimuthal quantum number and effective quantum number respectively. Theoretical lifetimes (28) were also used. Note the initial intensity

rise in e.g. Ar VIII, explainable by cascading from higher levels with lifetimes shorter than that for $3p\ ^2P$.

Fig. 7. Comparison between theoretical and experimental oscillator strengths for the $3s^2\ ^1S$-$3s3p\ ^1P$ transition in the Mg I sequence. The data sources are discussed in the text and Ref. (45).

Fig. 8. Comparison between theoretical and experimental oscillatorstrengths for the $4s\ ^2S$-$4p\ ^2P$ transition in the Cu I sequence. The data sources are Refs. (3), (35), (36) and (37).

Fig. 9. Simulated decay curves for the $4p\ ^2P$ level in the Cu I sequence, obtained in the same way as the curves in Fig. 6.

Fig. 10. Comparison between experimental and theoretical oscillator strengths for the $4s^2\ ^1S$-$4s4p\ ^1P$ transition in the Zn I sequence. The data are from Refs. (28), (35), (36) and (42).

Fig. 11. Beam-foil spectrum of iron in the grazing-incidence region. Ions of Fe were accelerated to 35 MeV in the Oak Ridge tandem accelerator and the wavelength spectrum was analyzed with a 2.2 m grazing-incidence monochromator (44).

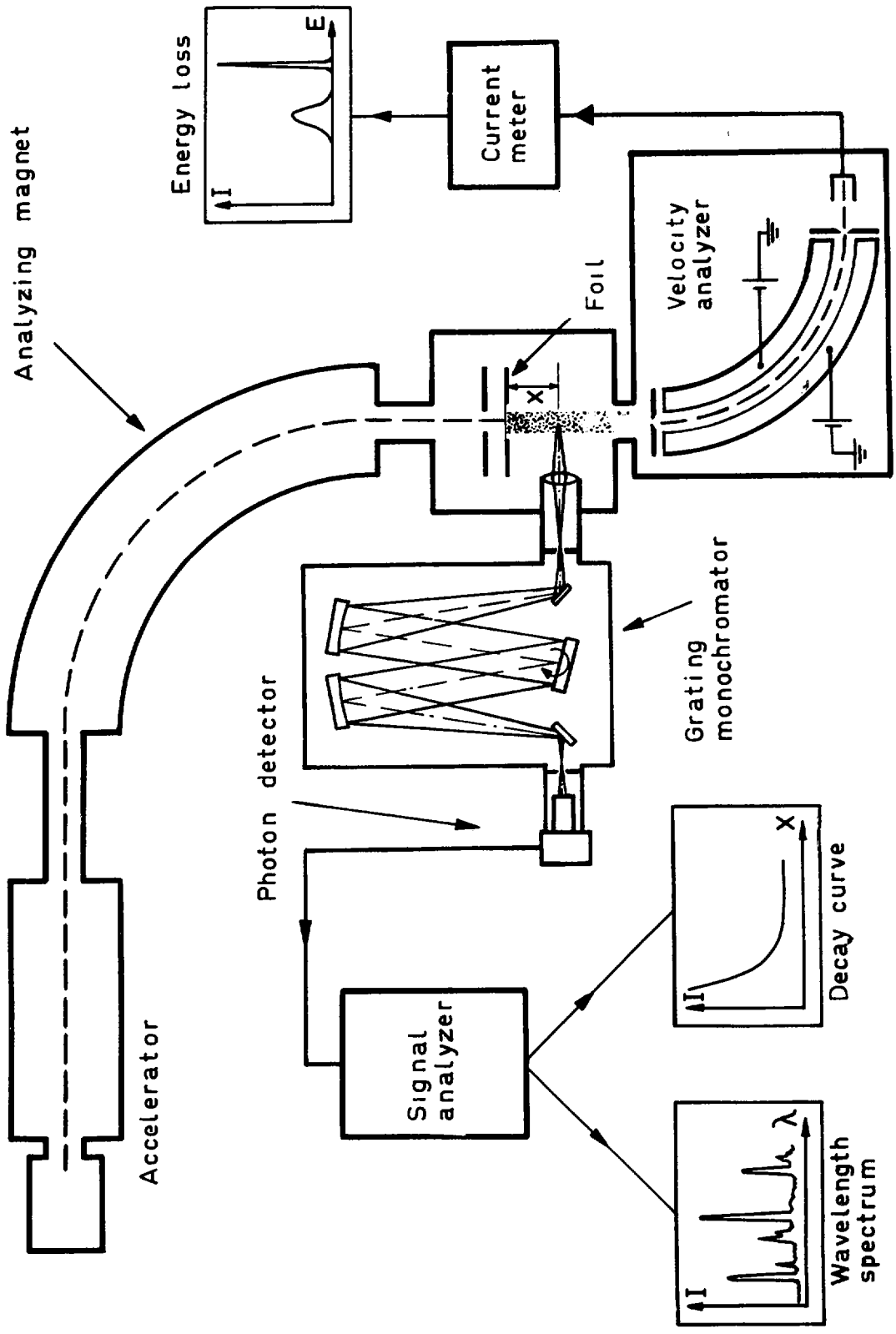
Energy loss
E
I
Current meter
Analyzing magnet
Foil
Velocity analyzer
x
Grating monochromator
Photon detector
Accelerator
Signal analyzer
x
I
Decay curve
λ
I
Wavelength spectrum

Figure 1

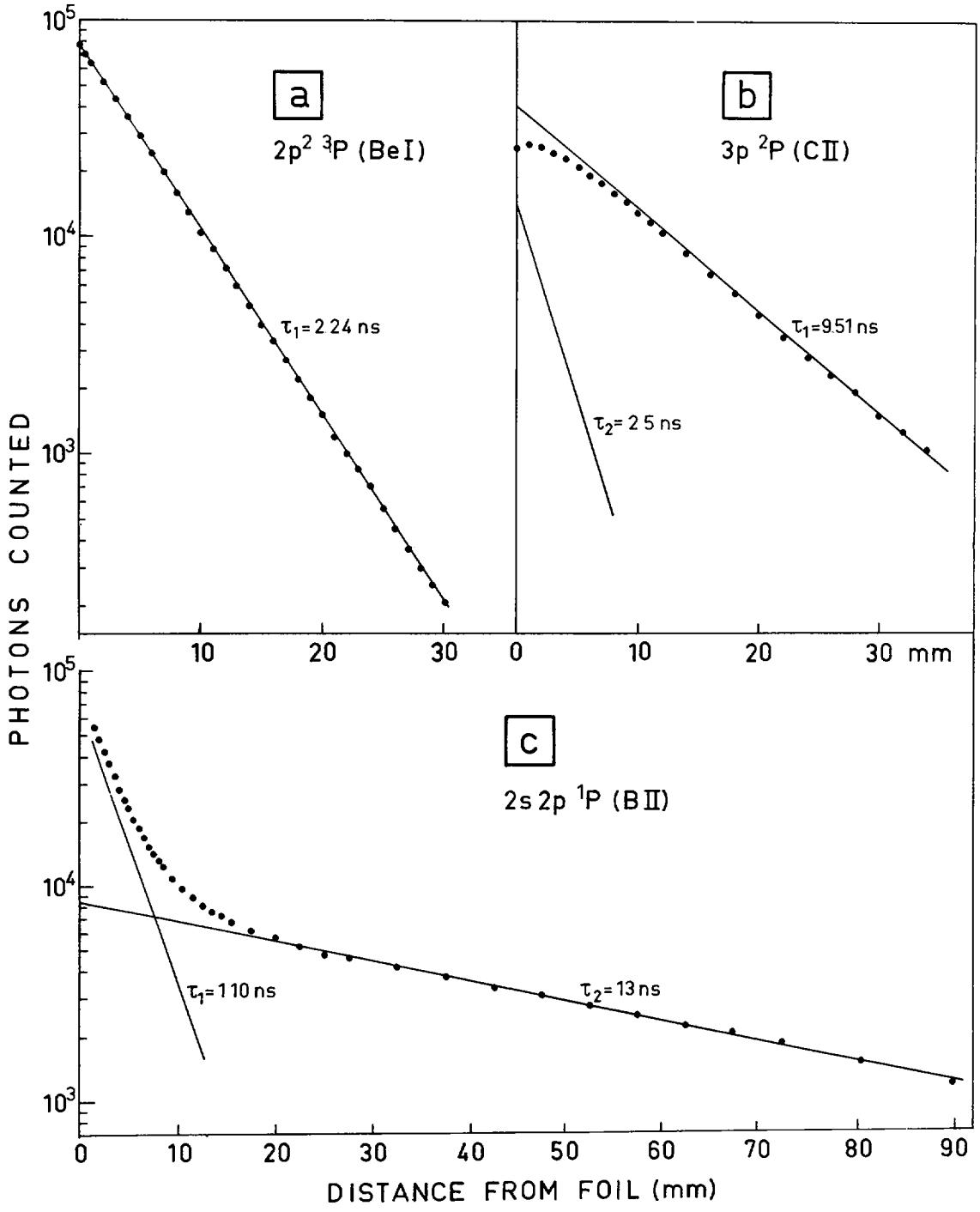
a
2p² ³P (BeI)
τ₁= 2.24 ns
b
3p ²P (CII)
τ₁=9.51 ns
τ₂= 2.5 ns
c
2s 2p ¹P (BII)
τ₁= 1.10 ns
τ₂= 13 ns
PHOTONS COUNTED
DISTANCE FROM FOIL (mm)
mm

Figure 2

Fe XXIV, theoretical lifetimes (ps)

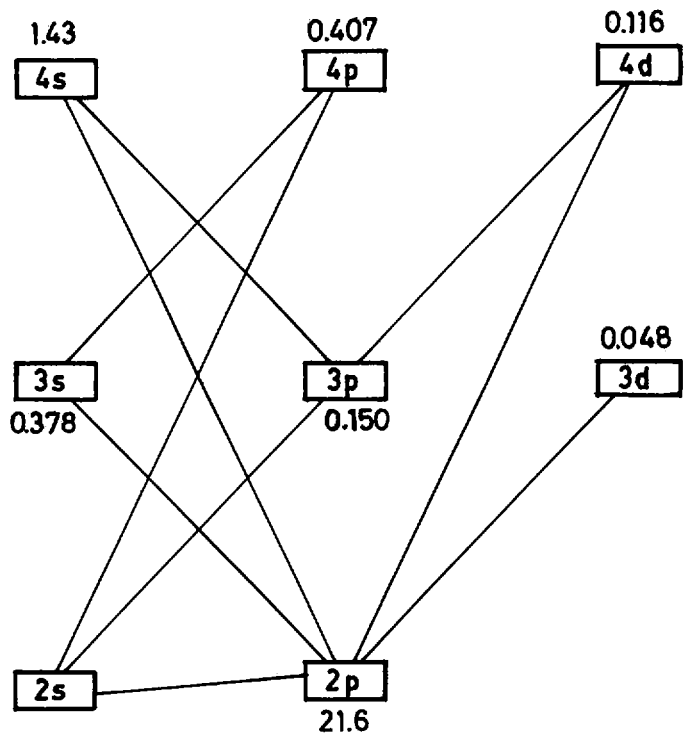

Figure 3

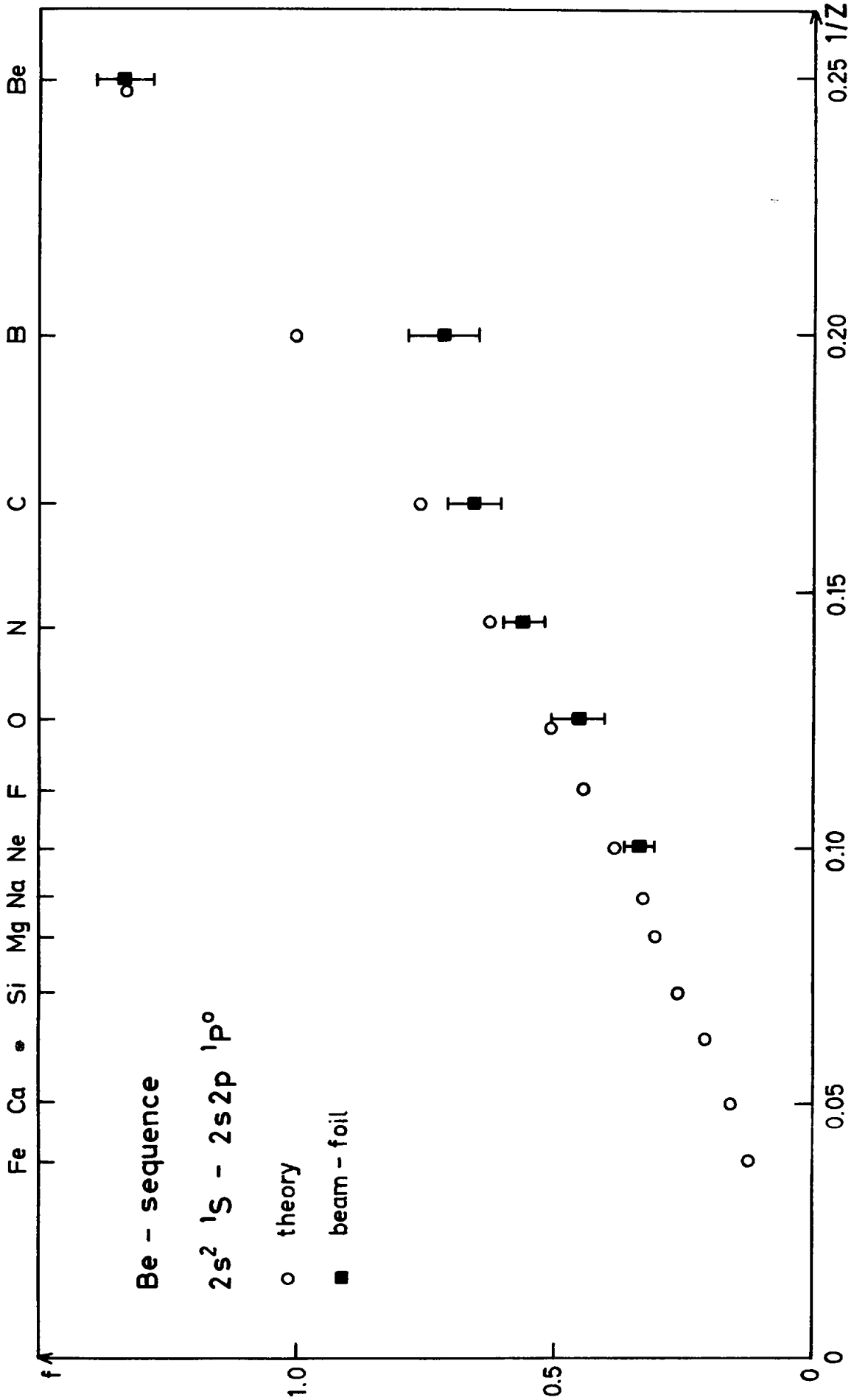
Be
B
C
N
O
F
Ne
Na
Mg
Si
Ca
Fe
1/Z
0.25
0.20
0.15
0.10
0.05
0
f
1.0
0.5
0
Be - sequence
$2s^2\ ^1S - 2s2p\ ^1P^o$
theory
beam - foil

Figure 4

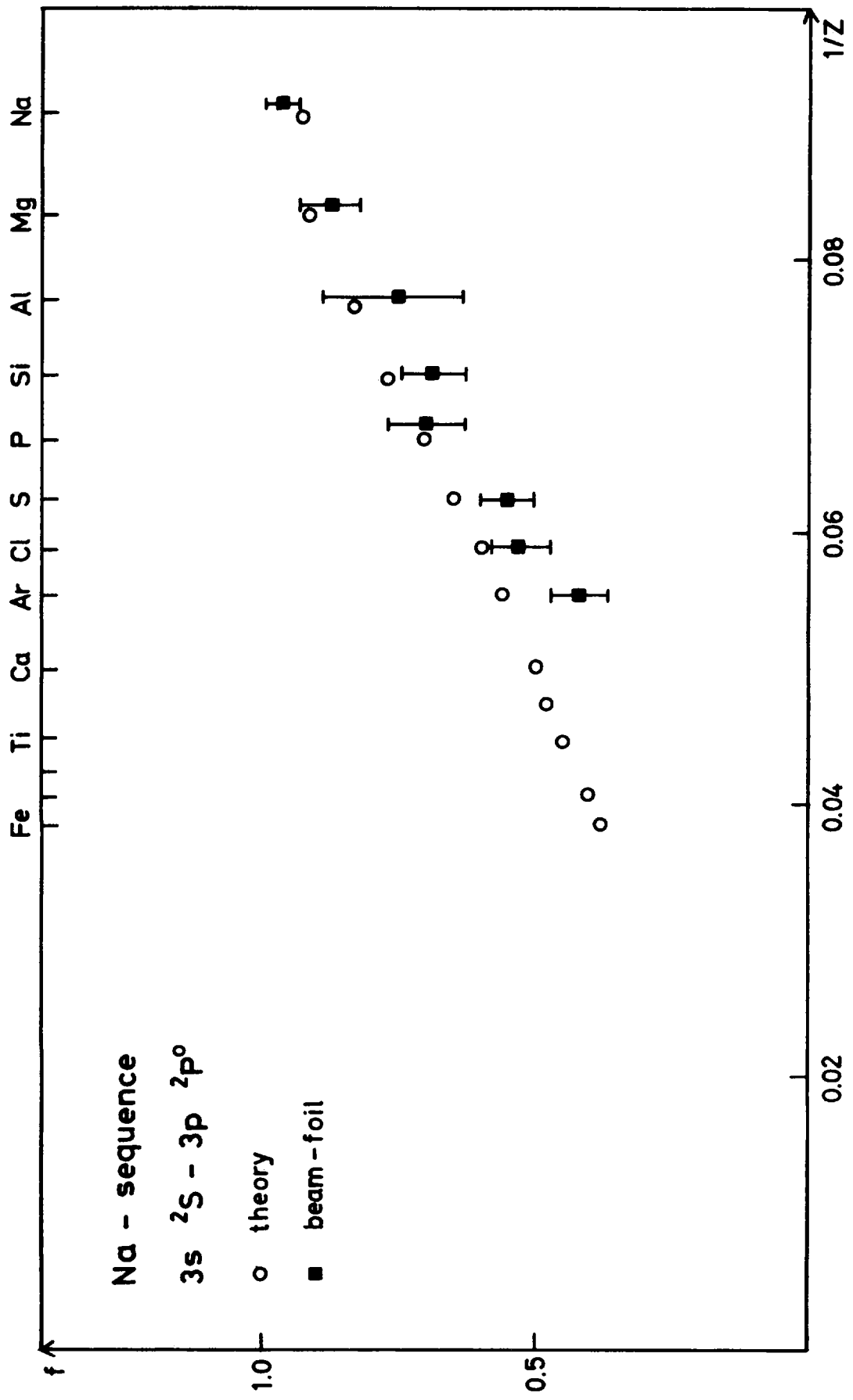
Na - sequence
3s ²S - 3p ²P°
o theory
■ beam-foil
f
1.0
0.5
1/Z
0.08
0.06
0.04
0.02
Fe Ti Ca Ar Cl S P Si Al Mg Na

Figure 5

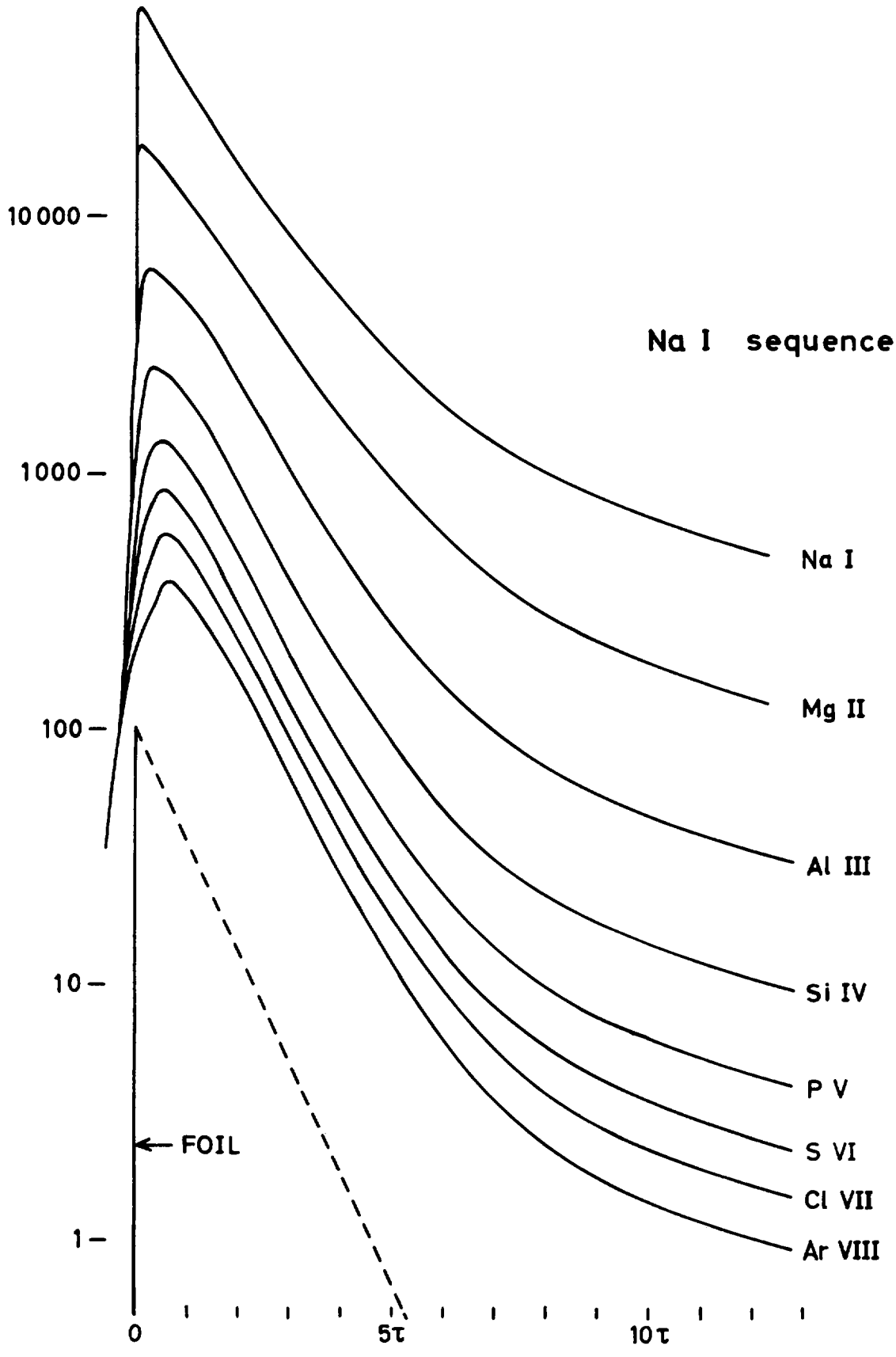
10 000
1000
100
10
1
Na I sequence
Na I
Mg II
Al III
Si IV
P V
S VI
Cl VII
Ar VIII
FOIL
0
5τ
10τ

Figure 6

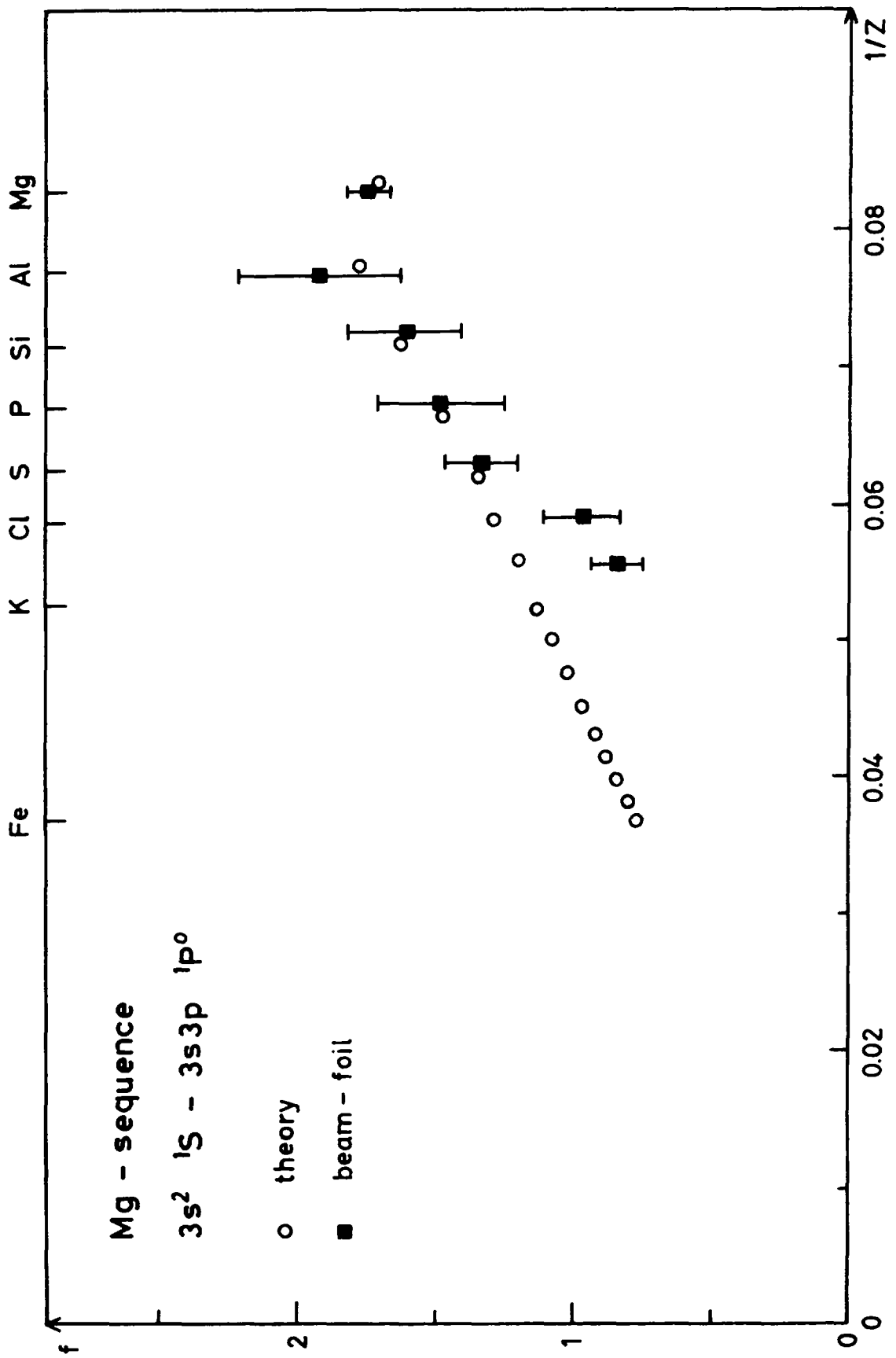
Mg - sequence
3s² ¹S - 3s3p ¹P°
o theory
■ beam - foil
Fe
K
Cl
S
P
Si
Al
Mg
f
2
1
0
0
0.02
0.04
0.06
0.08
1/Z

Figure 7

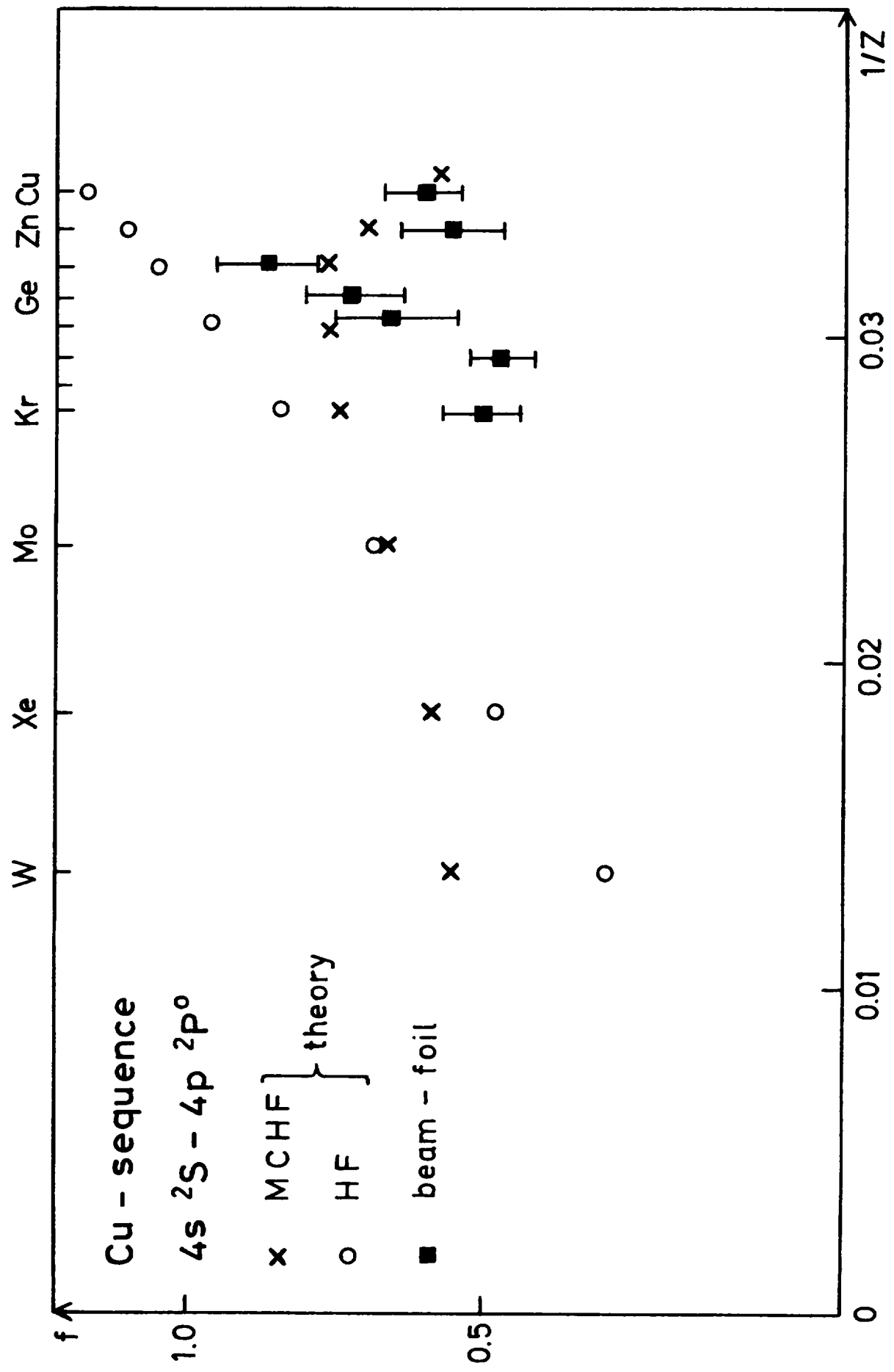
Cu - sequence
4s ²S - 4p ²P°
× MCHF
theory
o HF
■ beam - foil
f
1.0
0.5
0
0.01
0.02
0.03
1/Z
W
Xe
Mo
Kr
Ge
Zn
Cu

Fig. 8

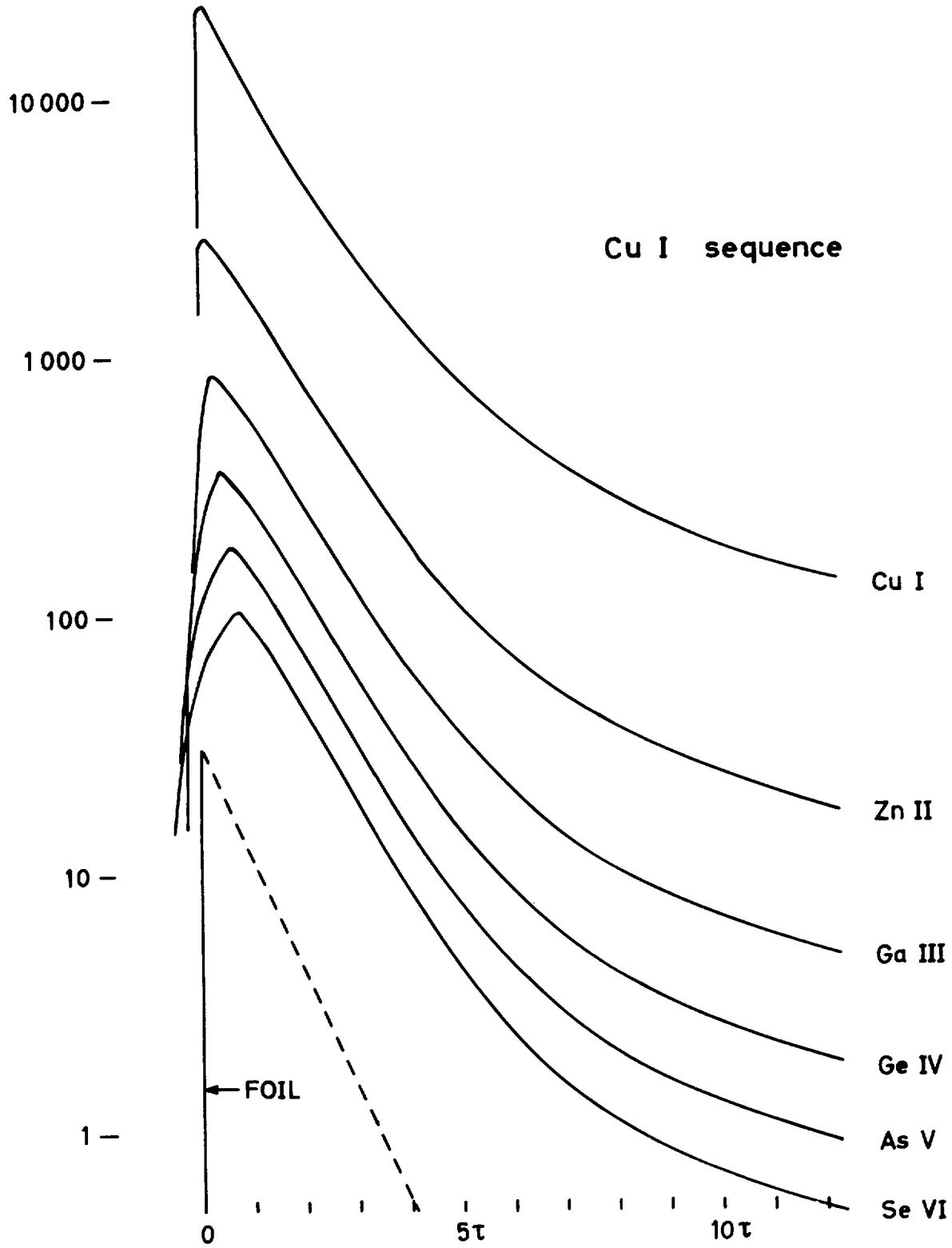
10 000
1 000
100
10
1
Cu I sequence
Cu I
Zn II
Ga III
Ge IV
As V
Se VI
FOIL
0
5τ
10τ

Figure 9

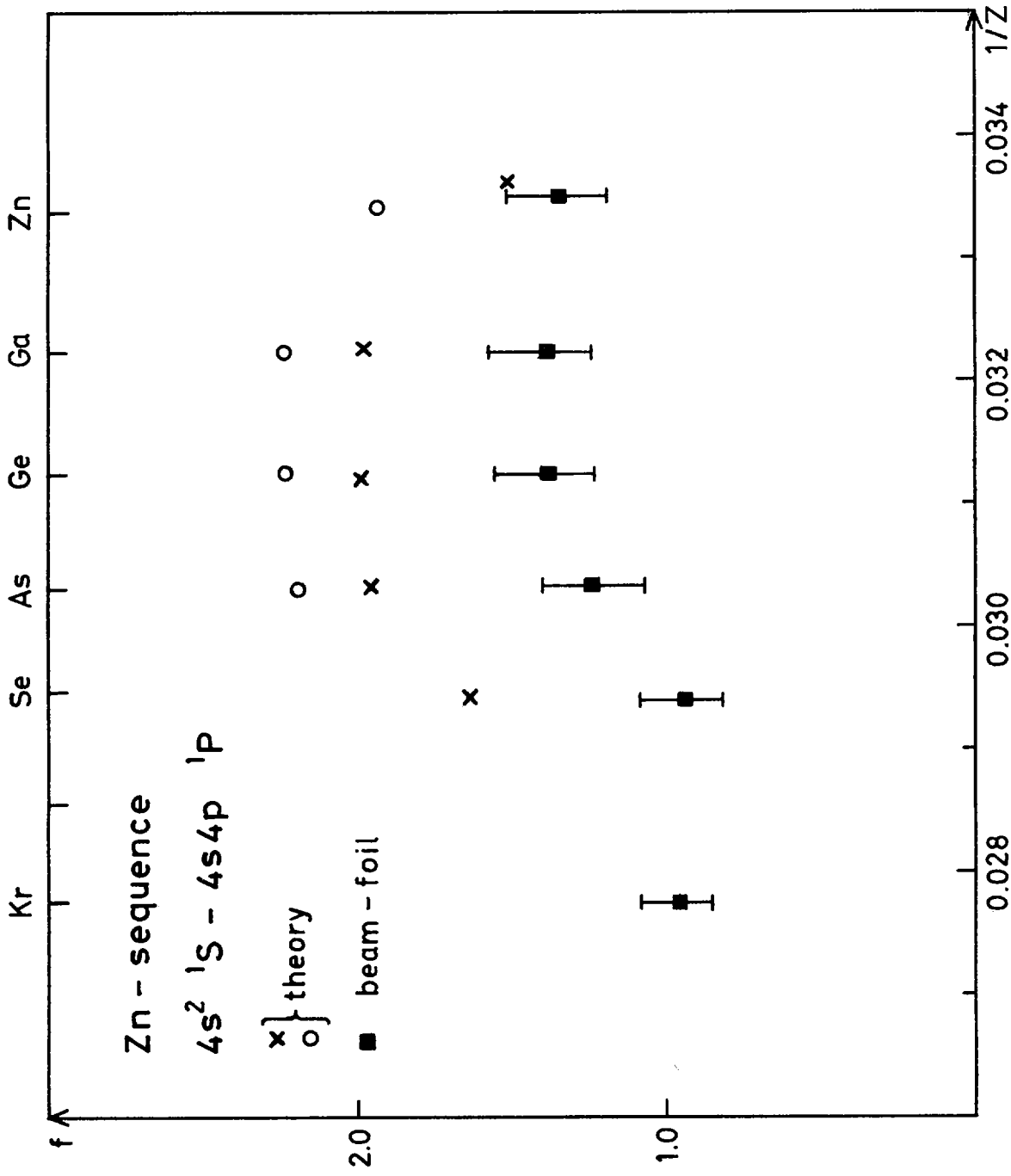
Zn - sequence
$4s^2\ ^1S - 4s4p\ ^1P$
theory
beam - foil
f
2.0
1.0
Kr
Se
As
Ge
Ga
Zn
0.028
0.030
0.032
0.034
1/Z

Figure 10

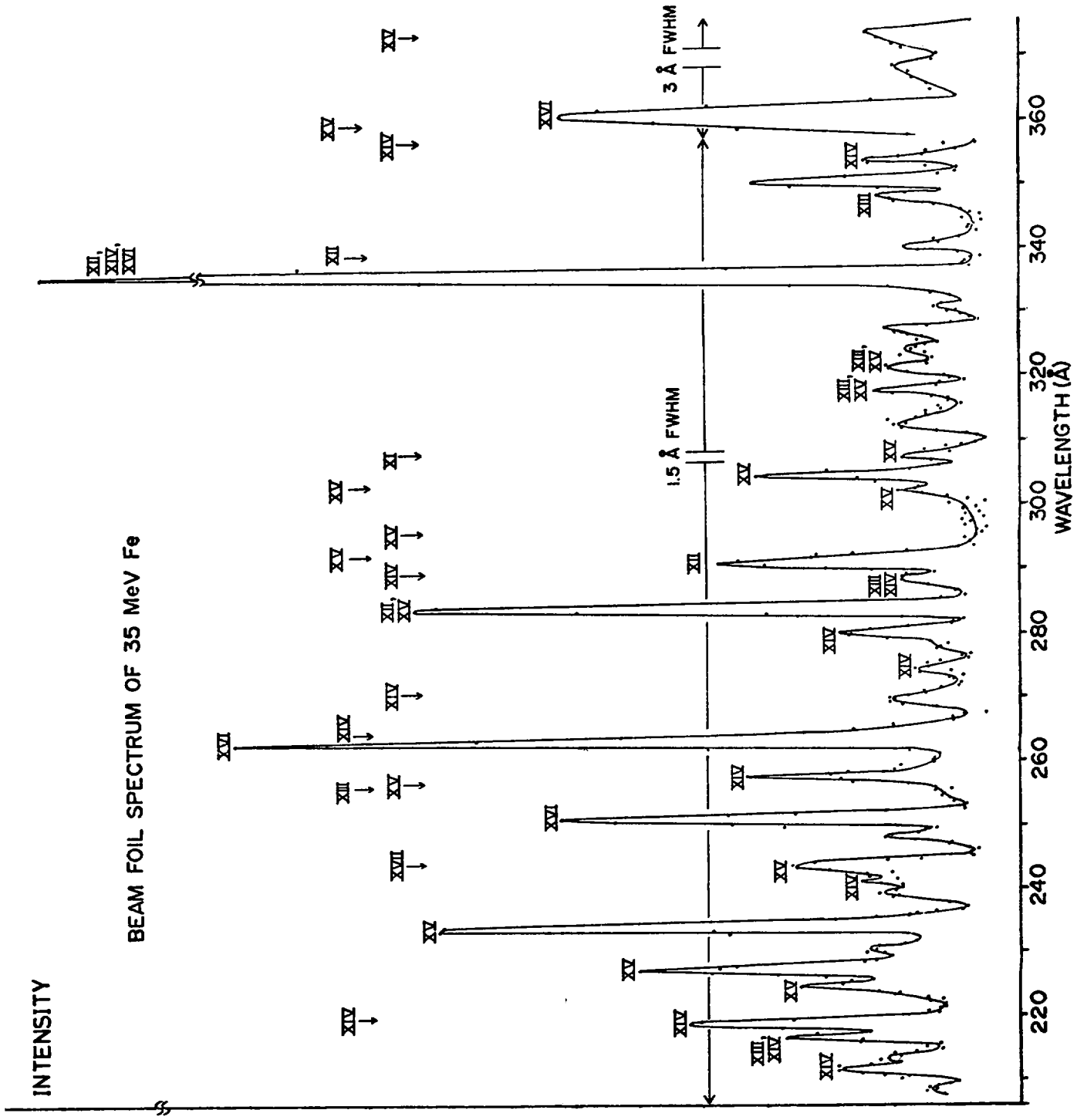
BEAM FOIL SPECTRUM OF 35 MeV Fe
INTENSITY
WAVELENGTH (Å)
220
240
260
280
300
320
340
360
3 Å FWHM
1.5 Å FWHM

Figure 11

B. NATIONAL PROGRAMMES AND EMPHASIS

Translated from French

Review Paper B1

NATIONAL PROGRAMMES ON ATOMIC AND MOLECULAR DATA FOR FUSION IN FRANCE

J.L. Delcroix

Culham, 1-5 November 1976

THE "GAPHYOR" SYSTEM: A COMPUTERIZED RETRIEVAL SYSTEM OF THE PROPERTIES OF ATOMS, MOLECULES AND GASES

State of the system on 1 March 1976

J.L. Delcroix
Plasma Physics Laboratory, Université Paris-Sud,
91405 - ORSAY

SUMMARY - GAPHYOR (GAz PHYsique ORsay) is a retrieval system of the simple properties of atoms and molecules (energy levels, lifetimes, dipole moments, polarizability etc.), of the interaction properties between these particles (cross-sections, reaction rates etc.) and of the macroscopic properties of the corresponding gases (viscosity, electronic and ion mobility, thermodynamic functions etc.). The chemical systems described must be based on a small number of elements (1 to 4 in the most recent version) and composed of molecules having 8 atoms at the most. In the present article the fundamental principles of GAPHYOR are described and by means of a few simple statistics the present state of the bank after five years of operation is analysed. On 1.11.76 the file contained more than 33,000 lines, and these increase by about 10,000 per year. The information comes from about 300 periodicals, although 45% of the results are taken from 4 principal journals. Geographical analysis of the file provides useful information about the scientific work of the various research centres and the scientific publishing policies of the different countries. Finally, the qualities, difficulties and possible improvements of GAPHYOR are analysed.

1. INTRODUCTION

The basic properties of single atoms or molecules (energy levels, lifetimes of excited states, etc.), the properties of interaction between such particles (cross-sections for various collision processes etc.) and certain basic macroscopic properties (transport coefficients, etc.) are the fundamental data of the physics of gases. This set of data is complex and constantly undergoing change. In the present report the work done at the Orsay Plasma Physics Laboratory is described for purposes of classification and analysis of the data in question, and a classification method which permits the handling of bibliographical information by computer is proposed.

The system which has evolved is called "GAPHYOR" (GAz - PHYsique - ORsay). It is in effect a computer-based data bank for documentation. Conceived in broad outline at the beginning of 1972, GAPHYOR was initially tried out at the laboratory level. Early in 1973, it was offered as a specialized documentation service for users in France. In 1975, the service was extended to users in other countries.

2. DEMARCATION OF THE FIELD

The approach has been to select and classify data from the standpoint of a specific group of users - physicists, physical chemists and engineers concerned with atomic and molecular physics and the physics of neutral or ionized gases under conditions of temperature and pressure attainable on Earth. Therefore no attempt has been made to meet the needs of nuclear physicists interested in very high energies or of chemists studying complex molecules. More precisely, the approach has been to limit the field studied according to the following guidelines:

- Only systems based on a small number of chemical elements are studied. In its 1972 version, GAPHYOR only included systems based on a chemical element X or two elements X and Y. For example, it covered the properties of N_2 (1 element), or of the mixtures $N_2 - O_2$, $NO - N_2 - O_2$ (2 elements), but not those of CH_3OH or of the mixture $N_2 - CO_2$ (3 elements). The elimination of systems with more than two elements seemed essential for the compilation of data lists of reasonable size. However, in practice this limitation proved too restrictive and, more recently, the extenstion of GAPHYOR to 3-element (GAPHYOR 3) and 4-element (GAPHYOR 4) systems has been studied. Moreover, an a posteriori statistical analysis influenced the decision: Figure 1 shows that GAPHYOR 3 contains a large proportion of useful information, that GAPHYOR 4 contains very little and that GAPHYOR 5 hardly exists at all. In view of these conditions it was decided to set up GAPHYOR 3, which has been in operation since early 1976, and GAPHYOR 4, which will come into operation in 1977.

- In the systems defined above only the properties of "small" molecules (or ions) containing at the most 8 atoms are studied. Therefore the properties of NH_3, CH_4 and SF_6 are described, but not those of benzene. However, in order to help certain users, an element in the code has been provided which makes it possible to show which publications deal with larger molecules.

- As far as the energies involved are concerned, a maximum of 10 keV (in the centre-of-mass system) has been taken as a limit. In other words, references which only contain information relating to energies above 10 keV have been eliminated. This does not mean that our lists contain no information in this energy range since numerous publications contain information straddling this limit (these are shown by a special code letter).

- With regard to low energies, no lower limit has, of course, been fixed. As this is the field which most interests physicists and physical chemists working on gases, a special code letter for references below 10 eV has been provided.

3. SCANNING OF JOURNALS AND BOOKS

With due regard to the field as defined above and the facilities available, the scientific press is scanned in two stages: about 30 journals which seem to us to be the most important[1/] are analysed as soon as they come out. A list of them is shown below in Table 3.

Also the following documents are scanned systematically:

Conference proceedings;

Reference books;

and in a less systematic fashion the following documents:

Internal laboratory reports;

French theses.

Finally, we obtain a wider overall view by using section 165 of the Abstracts Bulletin of the National Scientific Research Centre (C.N.R.S.).

1/ The choice of these journals is in fact influenced by an a posteriori statistical analysis of the contents of the file as presented in Table 3.

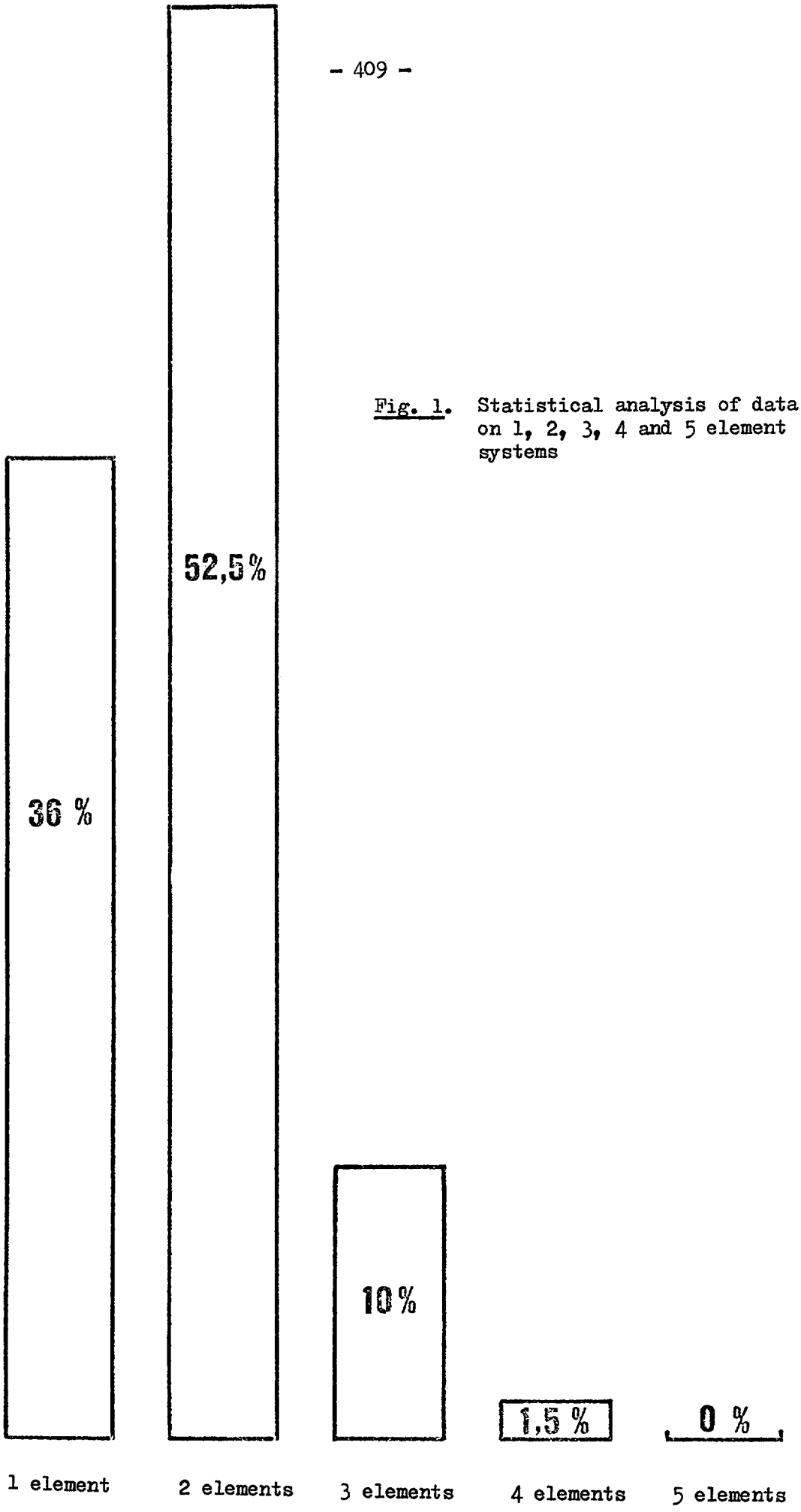

Fig. 1. Statistical analysis of data on 1, 2, 3, 4 and 5 element systems

From each reference we make up one or more "computer lines". Each of these lines is composed of a set of "descriptors" and recorded in the computer memory. All these "computer lines" together make up the "GAPHYOR" file.

4. DESCRIPTION OF A COMPUTER LINE

4.1. Descriptors carried by a computer line

Each computer line carries the following descriptors:

(a) Archive descriptor:

Entry number

(b) Classification descriptors:

Families A, B, C and D		(D_1)
Category K		(D_2)
Molecule P indices (subscripts/superscripts)	ℓ m n p, i x	(D_3)
Molecule Q indices (subscripts/superscripts)	ℓ' m' n' p', i' x'	(D_4)
Molecule R indices (subscripts/superscripts)	ℓ'' m'' n'' p'', i'' x''	(D_5)
Simplified description		(D_6)
Molecule S indices (subscripts/superscripts)	r s t u, j y	(D_7)
Molecule T indices (subscripts/superscripts)	r' s' t' u', j' y'	(D_8)
Molecule U indices (subscripts/superscripts)	r'' s'' t'' u'', j'' y''	(D_9)
Year of publication		(D_{10})

(c) Information and filtering descriptors

Experimental order V

Experimental order W

Elements concerned X, Y, Z and Z'

Marginal and qualitative descriptors

(d) Localization descriptors

- Journal ("Revue")
- Volume ("Tome")
- Page ("Page")
- Author ("Auteur")
- Country ("Nation")
- Province ("Province")
- City ("Cité")

The set of these descriptors can be represented by the following formula:

$$F = \underline{A}, \underline{B}, \underline{C}, \underline{D}/X, Y, Z, Z'/\underline{K}/\underline{P}, \underline{Q}, \underline{R}/V/\underline{DS}/\underline{S}, \underline{T}, \underline{U}/W/$$
$$/REV, TOM, PAG, AUT/\underline{ANN}/NA, PR, CI/QUAL/\underline{NUM}/$$

in which classification descriptors are underlined. A more detailed analysis of each of these descriptors is given below.

4.2. Mendeleev families (A, B)

All the processes concerned relate to a chemical system with one element X, two elements X and Y, three elements X, Y, Z or four elements X, Y, Z and Z'. Initial classification of the data is based not on the particular elements concerned but on the Mendeleev families to which they belong. These families are designated by A, B, C, D. This approach simplifies classification because very often a given author is studying in a given publication the properties of all the elements X of one family A with respect to a certain process. In other words, the whole set of 92 x 91 x 90 x 89 combinations X, Y, Z, Z' can be brought together using the Mendeleev families into a more manageable set of combinations A, B, C and D, which is well adapted to actual needs. After a few experiments we therefore decided to classify the elements into families according to the following list:

R	He Ne Ar Kr Xe Rn
H	H
1A	Li Na K Rb Cs Fr
1B	Cu Ag Au
2A	Be Mg Ca Sr Ba Ra
2B	Zn Cd Hg
3A	B Al Ga In Tl
3B	Sc Y La Ac
4A	C Si Ge Sn Pb
4B	Ti Zr Hf
5A	N P As Sb Bi
5B	V Nb Ta
6A	O S Se Te Po
6B	Cr Mo W
7A	F Cl Br I At
7B	Mn Te Re
8A	Fe Co Ni
8B	Ru Rh Pd
8C	Os Ir Pt
9A	Ce Pr Nd Pm Sm
9B	Eu Gd Tb Dy Ho
9C	Er Tm Yb Lu
9D	Th Pa U Np Pu
10	general articles (see below)

It can be seen that the elements are in this way classified more or less in order of electro-positive valence (from 0 to 7), and within a single family in order of their atomic masses. For convenience the "triads", rare-earth elements and actinides have been placed in positions 8 and 9.

The order thus defined can be considered as a ranking order and the expressions

$A<B$

$X<Y$

mean that family A comes before family B in this order, and similarly for X and Y (for example: $H<1A$, $4B<5A$, $Li<Na$, etc.).

In general terms, a group of 4 families will always be written

A B C D

on the assumption that

$A \leq B \leq C \leq D$

Groups of less than 4 families are written by inserting zeroes on the right as follows:

A, B, C, 0

A, B, 0, 0

A, 0, 0, 0

Using these writing rules, the two groups A B C D and A', B', C', D' will be classified in the order

A B C D < A' B' C' D'

if one of the following conditions is fulfilled:

$A < A'$

$A = A', B < B'$

$A = A', B = B', C < C'$

$A = A', B = B', C = C' = D < D'$

Where the 0 is the first of the families, so that one has for example:

A, B, C, 0 < A B C D

Finally, in the bibliography, we sometimes find publications treating a specific process but without being limited to a specific chemical system (synthetic articles, theoretical studies, etc.). These are to be classified by introducing the "family" 10 which can be combined with all the others to form groups such as 10-0-0-0, 10-10-0-0, 10-10-10-0, R-10-0-0 etc.

4.3. Process categories (K)

In the same way that the elements are grouped in families, the process involved is rapidly identified by the "process category" descriptor K. The categories considered are:

1. Properties of atoms and molecules;

2. Photon collisions;

3. Electron collisions;

4. Atom-atom, atom-molecule and molecule-molecule collisions (including the corresponding ions);

5. Macroscopic processes.

4.4. Description of the process

4.4.1. Initial state (P,Q,R)

The process under consideration is normally identified by the following code letters:

P,Q, R/S, T,U

In the case of collisions between particles (process categories 2-4) the above is the classical method in collision physics of writing down the reaction:

$$P + Q + R \rightarrow S + T + U$$

P,Q,R signify the initial state and S,T,U the final state. By convention this notation will be extended to two other process categories, according to rules that will be described later. Therefore, in general, the "initial" state will be described as follows:

P,Q,R/ - for a problem involving 3 bodies;

P,Q/ - for a problem involving 2 bodies;

P/ - for a problem involving 1 body.

The symbols P, Q and R may represent a photon, an electron or, more generally, an atom or molecule of the A - B - C - D system which may be ionized and/or excited:

$$A_\ell \, B_m \, C_n \, D_p^{\,ix}$$

The subscripts ℓ, m, n and p thus define the empirical formula of the molecule while the superscripts i and x show (using the following conventions), the ionization and excitation states of the molecule as appropriate:

i = superscript denoting ionization

i = 0 neutral atom or molecule
i = 1 positive ion with 1 charge
i = 2 positive ion with 2 charges
- - - - - - - - - - - - - - - - - -
i = 5 positive ion with more than 4 charges[2/]
- - - - - - - - - - - - - - - - - -
i = 6 negative ion with 1 charge
i = 7 negative ion with 2 charges
- - - - - - - - - - - - - - - - - -
i = 9 inner shell ionized atom or molecule

x = superscript denoting excitation

x = 0 ground state
x = 1 rotational excitation (r)
x = 2 vibrational excitation (v)
x = 3 electron excitation (*)
x = 4 oriented atom or molecule (s)
x = 5 excitation (* r)
x = 6 excitation (* v)
x = 7 excitation (* s)
x = 8 excitation (r v)
x = 9 excitation (* r v)

In conjunction with this system the following rules are used for purposes of ranking the various bodies that make up the initial state:

Generally, in the case of a collision between three heavy particles the inital state P, Q, R will be written as follows:

$$A_\ell\ B_m\ C_n\ D_p^{ix}\ ,\ A_{\ell'}\ B_{m'}\ C_{n'}\ D_{p'}^{i'x'}\ ,\ A_{\ell''}\ B_{m''}\ C_{n''}\ D_{p''}^{i''x''}$$

two molecules being written in the following order:

$$A_\ell\ B_m\ C_n\ D_p^{ix} < A_{\ell'}\ B_{m'}\ C_{n'}\ D_{p'}^{i'x'} \qquad (1)$$

if one of the following conditions is met:

2/ With respect to positive ions with more than 4 charges, the exact state of charge is shown by the use, as an exception, of the superscripts i" and x".

$$p < p' \qquad (2)$$

$$p = p',\ n < n' \qquad (3)$$

$$p = p',\ n = n',\ m < m' \qquad (4)$$

$$p = p',\ n = n',\ m = m',\ \ell > \ell' \text{ (N.B.!)} \qquad (5)$$

$$p = p',\ n = n',\ m = m',\ \ell = \ell',\ i > i' \qquad (6)$$

$$p = p',\ n = n',\ m = m',\ \ell = \ell',\ i = i',\ x > x' \qquad (7)$$

- Where one or two of the particles involved are light particles (photons or electrons) they are considered to correspond to $\ell = m = n = p = 0$, and are written in first place in the P,Q positions beginning with the photon;
- In problems involving two bodies it is assumed that R = 0 and the particles are ranked in the order P,Q according to the same rules as for problems involving three bodies (formulae (2) to (7));
- In problems involving one body, Q = R = 0 is assumed;
- These rules make it possible in general to write the initial state P,Q,R in an unequivocal way. However, there are possible cases of ambiguity: where two of the families A,B,C,D considered are identical. The special rules concerning these cases are discussed in Appendix A.

It may happen in certain cases that ranking order P,Q,R defined by the preceding rules is ill suited to the experimental conditions involved. For example, in charge exchange collisions most experiments are made with a beam of fast particles which play a special role and which it is therefore logical to write in the initial position, even though according to rules (2) to (7) these particles should possibly occupy position Q or R. In these circumstances the bodies will nevertheless be written in the order P,Q,R as defined by formulae (2) to (7), but the different order (e.g. Q,P,R) that is best suited to the experimental situation will be indicated by the code sign V using the following conventions:

V = 0 (PQR) , 1 (QPR) , 2 (PRQ) , 3 (RPQ) , 4 (QRP) , 5 (RQP)

4.4.2. Final state: detailed description (S,T,U)

In process categories 2-6 (collisions) the final state, if it is known completely, is indicated according to the same rules as the initial state, as follows:

$$A_r\ B_s\ C_t\ D_u^{jy} < A_{r'}\ B_{s'}\ C_{t'}\ D_{u'}^{j'y'} < A_{r''}\ B_{s''}\ C_{t''}\ D_{u''}^{j''y''}$$

S T U

The rules for ranking S,T,U are the same as for P,Q,R; if an "experimental" order is preferred, this is indicated by the descriptor W. With: W = 0 (STU), 1 (TSU), 2 (SUT), 3 (UST), 4 (TUS), 5 (UTS).

If the final state involves more than three particles they are ranked according to the same rules and only the last three are written.

If the final state is only partially known, only the bodies actually known are to be written, beginning with S and leaving blank the unknown bodies.

4.4.3. Final state: simplified description (D S)

In the case of some collision processes, such as elastic collision or symmetric charge transfer, there is no need to describe the final state in detail. In other cases, the process in question is a superposition of several elementary processes resulting in different final states. Lastly, in process categories 1 and 5 the very concept of a final state loses all meaning.

For dealing with these cases a simplified description of the process is introduced - an abbreviation consisting of two code letters. (Appendix B contains a list of the abbreviations used in each process category).

Since the concept of the final state lacks all meaning in categories 1 and 5, the code is used in the following way:

DS is a substantive

S, T, U are complements

Example: DS = MI S = H_2O^+ → mobility of H_2O^+ ions.

5. ELEMENTS CONCERNED (X, Y, Z, Z')

The Mendeleev families (A, B, C, D) relating to a given publication having been indicated, it should be stated which elements of these families are concerned; this is done by means of the descriptors X, Y, Z, Z'.

These can have the values 1, 2, 3, 4, 5, 6, where the figures 1, 2, 3, 4, 5, 6 denote the rank of an element in the family under discussion.

6. MARGINAL AND QUALITATIVE DESCRIPTORS (QUAL)

Marginal and qualitative descriptors are as follows:

- M (molecules) means publications dealing with systems containing molecules with more than eight atoms.
- H (high energies) means publications describing collision processes in the energy range above 10 keV (in the centre-of-mass system).
- L (low energy) means publications describing collision processes in the energy range below 10 eV (in the centre-of-mass system).
- N (nucleus) means publications involving isotopic effects.
- E,T mean publications containing work with an experimental or a theoretical bias, while S means review articles.
- Finally, it should be said that certain special conventions have proved useful during experiments with the system. These conventions, which are sometimes exceptions to the overall code, are described in Ref. [3].

7. BIBLIOGRAPHICAL REFERENCES (REV, TOM, PAG, AUT)

The title of the journal, the volume, the page, the first author and the year of publication are written in code language according to the following scheme:

REV	TOM	PAG	AUT	AN
70	22	1341	DUPONT J L	74

For this the main journals have been classified according to a code [1] of which an abridged version is given in Appendix C (e.g. "70" means "Physical Review").

The sign 00 placed in position REV means Conference Proceedings and 97 reviews in book form. The list of these works constitutes an annexed file [1]; the corresponding references are indicated where necessary in position TOM in the place of the volume number.

Similarly, the signs 98 and 99 placed in position REV mean laboratory reports and theses.

8. GEOGRAPHY OF LABORATORIES

The above bibliographical references do not always give exact information on where a given "GAPHYOR" result has been obtained. It often happens in fact that a researcher working in a given country A publishes his results in a journal appearing in another country B.

For this reason we have specified the geographical location of the laboratory where work mentioned in a publication has been carried out, by means of a three-stage code:

NAtion	U S
PRovince	M A
CIté	C A

where the above example means United States, Massachusetts, Cambridge. A geographical code of countries, provinces and cities [2] has been drawn up. This code is unequivocal in the sense that, for example, two different towns in the same province are shown by two different abbreviations. When the publication concerned mentions several places where the work has been carried out, the one shown in GAPHYOR corresponds to the address of the first author.

9. STORAGE IN THE FILE

Storage in the file is effected by using the classification descriptors according to a hierarchy corresponding to the order in which we have written them. In other words, two lines F and F' characterized by the descriptors D_1, D_2 ..., D_{10} and D'_1, D'_2, ..., D'_{10} will be classified in the order

F before F'

if one of the following conditions is fulfilled:

$D_1 < D'_1$

$D_1 = D'_1$ and $D_2 < D'_2$

$D_1 = D'_1$ $D_2 = D'_2$ and $D_3 < D'_3$

.....

As a last resort, if their 10 classification descriptors are the same, the lines F and F' are ranked according to entry number. For these classification rules to be applied, an ordering of the values for each of the descriptors D_1 to D_{10} must therefore be established. For the descriptors D_2, D_3, D_4, D_5, D_7, D_8, D_9, D_{10} which have been coded in a numerical form, this is simple: their values are ranked according to the natural order of whole numbers[3/] (for this ranking it is to be understood that a blank space comes before a zero).

For the descriptor D_1 a ranking order has been worked out from the list of Mendeleev families as we have seen in section 4.2.

Finally, the ranking of the values of descriptor D_6 must be established for each process category: the order chosen is that which appears in Appendix A. Apart from this it is accepted that when this descriptor is not specified (D S spaces left blank), this corresponds to an infinite value of D_6. In other words, the lines where this descriptor is not shown are classified after all those on which it is.

3/ When a photon (P) or electron (E) is involved it has been agreed that P<E<0.

10. RETRIEVAL FROM THE FILE

Retrieval is effected by specifying the classification descriptors D_1 to D_{10} with, if required, selection based on the filtering descriptors. For this it is necessary only to fill in an order form. On the form, the "client" fills in the non-coded part and we translate the information into code language. The computer responds by printing a list of references relating to the phenomena thus specified. If the client wants fairly extensive information, he writes only the first descriptors (e.g. D_1 and D_2). The computer then provides a set of references ranked on the basis of the established GAPHYOR ordering, i.e. according to the values of the descriptors left free (D_3, D_4 ..., D_{10} in the example chosen). The list obtained is sent to the client with a simple explanation of the code used. As an example we show here the result of a question on nitrogen - zinc, cadmium, mercury systems (publication years 1970-75).

11. STATISTICAL ANALYSIS OF THE GAPHYOR FILE

11.1. Theoretical volume of the GAPHYOR file

It is useful to calculate the theoretical volume of the GAPHYOR file, i.e. the number of spaces it contains, a space being defined by a series of values taken by the descriptors D_1 to D_{10}. A simple calculation shows an enormous number, of the order of:

10^{35} spaces per year of publication for GAPHYOR 4.

The number of lines actually contained in GAPHYOR on 1.11.1976 was about 33,000 and is increasing by about 10,000 lines per year. It can be seen how few of the spaces in the file are filled.

11.2. Years of publication

Statistical analysis by years of publication is shown in Table 1 which calls for the following remarks:

The sharp increase between 1969 and 1970 reflects the launching of GAPHYOR in 1970; the lines previous to 1970 only represented a partial scanning of the literature;

FAMILIES			C	INITIAL STATE			DE	FINAL STATE			YR	RCD NUM	ELEMENTS MENTIONED			JOUR-	VOL.	PAGE	AUTHOR	MARGIN		GEOGRAPHY		
AA	BB	CC	P	P	Q	R	SI	S	T	U	19	INSCR	X	Y	Z	NAL				DESCRI	V	COU	PR	CI
28	5A		1	12 C6			EN				73	9619	3	1		48	95	732	STRAUSZ	E				
28	5A		4	1C CC	C1 OC		SN				72	5233	3	1		16	50	1938	V WIJNGAAR	H E				
28	5A		4	1C CC	C1 OC		LN				72	5234	3	1		16	50	1938	V WIJNGAAR	H E				
28	5A		4	1C CC	C1 1C						73	7662	3	1		70	7	937	V WIJNGAAR	H NE				
28	5A		4	1C C3	C2 C		DX				74	15504	3	1		CC	6C	1C6	BURNHAM R	T L E				
28	5A		4	1C 03	02 0		DX				74	17243	3	1		28	35	953	LANIEPCE B	L E				
28	5A		4	1C C3	02 0		DX				74	17562	3	1		28	35	941	LAHAYE B	LNE				
28	5A		4	1C 03	C2 0		DX				74	17954	2	1		16	52	2228	CZAJKOWSKI	L E				
28	5A		4	1C 03	02 0		DX				74	18153	3	1		3C	61	5158	BURNHAM R	T L E				
28	5A		4	10 03	C2 0		DX				75	32361	2	1		20	29	421	BRECKENRID	T LNE		US	UT	SL
28	5A		4	1C 03	C2 0		ER	10 C3			75	30016	3	2		20	31	577	KRAUSE H F	L E		US	TN	CR
28	5A		4	1C C3	C2 0			10 C3	02 0		74	15505	3	1		CC	6C	1C6	BURNHAM R	T L E				
28	5A		4	1C C3	02 C			10 C3	C2 0		74	17242	3	1		28	35	953	LANIEPCE B	L E				
28	5A		4	1C 03	C2 0			10 C3	02 0		74	18154	3	1		3C	61	5158	BURNHAM R	T L E				
28	5A		4	1C 03	C2 C3			E	12 1		72	21242	3	1		57	7C	6C1	LAMPE F W	T NS				
28	5A		4	1C CC	02 C3			10 C3	02 0		70	3709	3	1		20	5	128	CALLEAR A	L E				
28	5A		4	1C OC	C2 C3			10 C3	02 0		73	11170	3	1		44	77	875	MADHAVAN V	TM LNE				
28	5A		4	1C 03	C2 C		DX				71	4387	3	1		123	44	1213	HORIGUCHI	T L E				
28	5A		4	1C 02	02 C		DX				72	6755	3	1		70	6	2101	PITRE J	L E				
28	5A		4	1C C3	C2 0		DX				72	6757	2	1		28	33	853	LANIEPCE B	L E				
28	5A		4	1C 03	02 0		DX				72	7270	1	1		22	275	187	CREMER G	E				
28	5A		4	1C 02	02 0		DX				73	9988	3	1		88	69	97	CALLEAR A	T L E				
28	5A		4	1C 03	02 0		DX				73	11173	3	1		44	77	875	MADHAVAN V	TM LNE				
28	5A		4	1C C3	C2 C			10 CC			70	266	3	1		20	6	417	CALLEAR A	E				
28	5A		4	1C 03	C2 C			10 CC	C2 03		73	11168	3	1		44	77	875	MADHAVAN V	TM LNE				
28	5A		4	1C C3	02 0			10 C3	C2 0		71	4388	3	1		123	44	1213	HORIGUCHI	T L E				
28	5A		4	1C 02	02 0			10 C3	C2 0		72	6754	3	1		7C	6	2101	PITRE J	L E				
28	5A		4	1C C3	02 0			10 C3	C2 0		72	6756	2	1		28	33	853	LANIEPCE B	L E				
28	5A		4	1C 02	02 0			10 C3	C2 0		72	8045	3	1		7C	7	1442	PITRE J	L E				
28	5A		4	1C 03	C2 C			10 C3	02 0		73	11167	3	1		44	77	875	MADHAVAN V	TM LNE				
28	5A		4	10 02	10 CC	C2 C		2C C3	C2 0		73	10613	3	1		7C	8	2982	PHANEUF R	L E				
28	5A		4	1C 04	C2 C			1C C3	C2 0		70	342	2	1		28	31	545	LANIEPCE B	E				
28	5A		4	1C C7	02 0			1C C3	C2 0		72	7271	1	1		22	275	187	CREMER G	E				
28	5A		4	1C C7	C2 C			1C C3	C2 0		73	7665	3	1		16	51	724	PHANEUF R	L E				
28	5A		4	1C C7	C2 C			1C C3	C2 0		74	19859	3	1		90	29	661	BAUMANN M	T L E		DB		TU
28	5A		4	2C CC	C1 C7			2C C	01 03		70	2346	2	1		28	31	545	LANIEPCE B	L E				
28	5A		4	2C 03	C2 C			2C C3	C2 0		73	10614	3	1		7C	8	2982	PHANEUF R	L E				
28	5A		5	C2			DN	10			71	4767	3	1		684	4	91	STRUMIA F	E				
28	5A		5	1C	02		PD				73	9991	3	1		30	59	983	GOLDSTEIN	E				
28	5A		15	10	02		PD				73	10612	3	1		70	8	2982	PHANEUF R	L E				

GAPHYOR DATA BANK PAGE 1. END OF CARD INDEX 40 ENTRIES.

RETRIEVAL SPECIMEN: Nitrogen - zinc, cadmium, mercury systems.

TABLE 1

Statistics by year of publication (on 1.3.1976)

YEAR	NUMBER OF CARDS	%
< 1968	1462	6
1968	290	1
1969	603	2
1970	1675	7
1971	2350	9
1972	3712	14
1973	5333	19
1974	7240	26
1975	4624	16

TABLE 2

Statistics by process categories (on 1.3.1976)

K	NUMBER OF CARDS	%
Properties of atoms and molecules	11.863	43
Photon collisions	2.138	8
Electron collisions	3.352	11
Collisions between atoms and/or molecules	7.559	29
Macroscopic properties of gases	2.343	9

The progressive increase between 1970 and 1974 is due to the refinement of our scanning methods rather than to an increase in scientific work. A more detailed analysis should be undertaken with the aim of better understanding the influence of these two factors.

On 1.3.1976 the scanning of the first six months of 1975 was complete. An effort must be made to accelerate scanning and acquisition by the file. This seems possible by making scanning techniques more systematic. Since 1975 we have been updating the file quarterly so that articles that appear in months n to n + 3 should shortly be included in the file by month n + 6 or n + 7. Conversely, it should be pointed out that the launching of GAPHYOR 3 and 4, on which we are at present engaged, is tending to retard the scanning process.

11.3. Process categories

Statistical analysis by process category is shown in Table 2. It can be seen that GAPHYOR, originally conceived as a retrieval system for the physics of gases, is becoming more and more a retrieval system for atomic and molecular physics.

11.4. Mendeleev families

Statistical analysis by Mendeleev family is shown in Fig. 2. It can be seen that the most studied systems are, as is to be expected:

In GAPHYOR 1 (1 element system):

Rare gases

Hydrogen

Oxygen

Nitrogen

In GAPHYOR 2 (2 element systems):

Carbon - oxygen (CO, CO_2, etc.)

Nitrogen - oxygen ($N_2 + O_2$, NO, N_2O, etc.)

Hydrogen - oxygen ($H_2 + O_2$, H_2O, etc.)

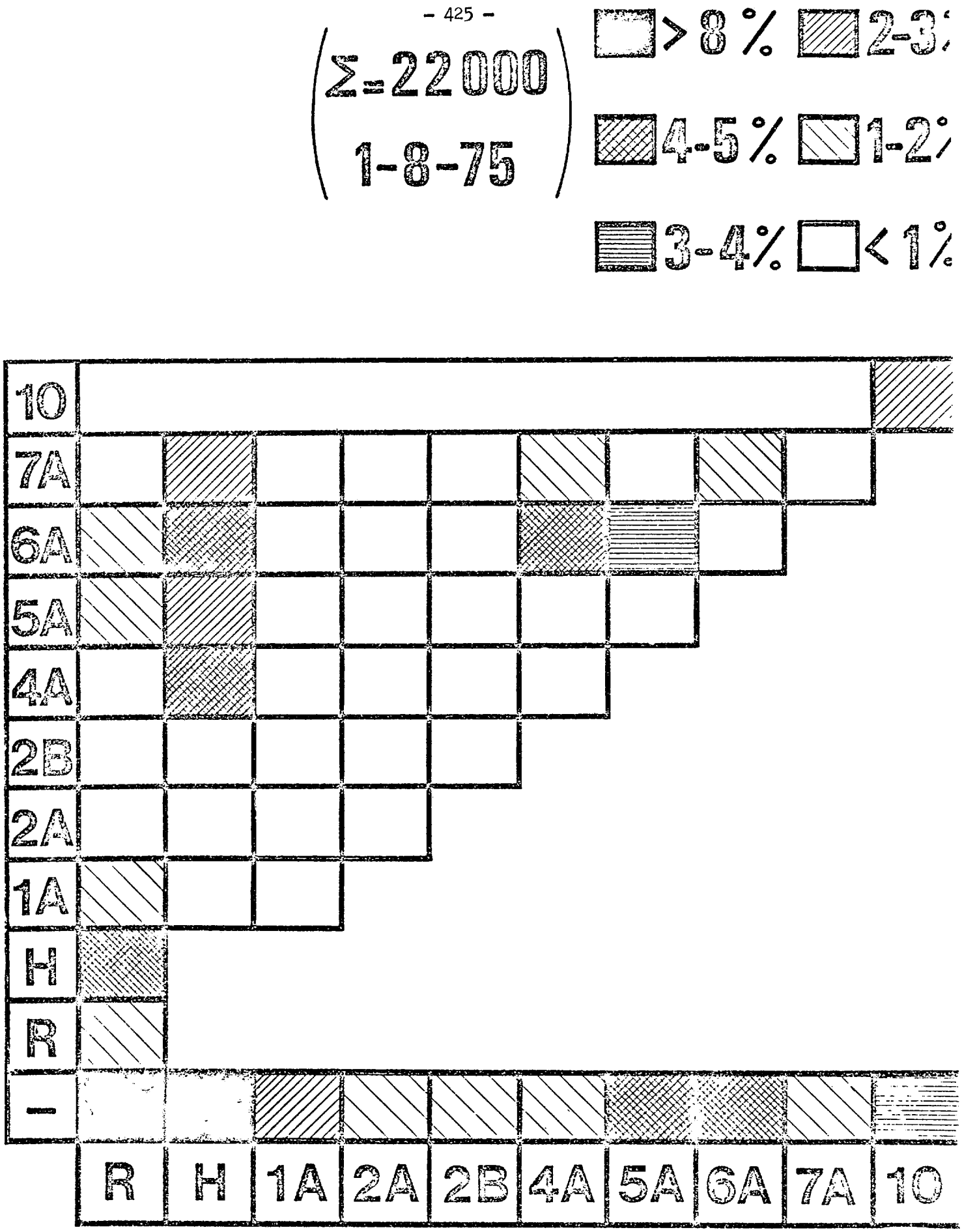

Fig. 2. Statistics by families

Hydrogen - carbon (hydrocarbons, etc.)

Rare gases - hydrogen

There are as yet no statistics for GAPHYOR 3 and 4.

11.5. Scientific journals

Statistical analysis by journal is shown in Table 3.

In the column entitled "Scanning method" the following symbols are used:

+ Direct scanning

(+) Direct but not systematic scanning

- Indirect scanning from the Abstracts Bulletin of the National Scientific Research Centre (C.N.R.S.)

- + Indirect scanning until 1974, direct from 1975.

Analysis of this table shows that:

- 54% of the information is obtained by scanning only the four most important journals and conference proceedings;
- To obtain 83% of the information, books, theses and 8 other journals must be included;
- The 23 journals which follow provide only 16% of information;
- The last portion of information (12%) is scattered over all the other journals (about 300 in the present state of the file).

Figure 3 shows these same results in a graphic form; this statistical information is very useful for studying possible ways of perfecting the GAPHYOR system.

11.6. Geography of laboratories

11.6.1. Statistics by countries

The statistics by journals that we have just described do not give any exact information on the countries from which material contained in GAPHYOR was obtained. It frequently happens that a researcher working in a given country A publishes his results in a journal appearing in another country B. In order to analyse in detail the

TABLE 3

Statistics by journal (on 1.8.1975)

	JOURNAL	Scanning method	Number of cards	%
1	Journal of chemical physics	+	4.403	20,7
2	Physical Review A	+	2.445	11,5
3	Lectures	+	1.697	8,0
4	Journal of physics B	+	1.601	7,5
5	Chemical physics letters	+	1.282	6,0
	Σ =		11.428	53,7
6	Books	(+)	602	2,8
7	French theses	(+)	463	2,2
8	Internat. J. mass spec. ion phys.	+	405	1,9
9	Physica	+	378	1,8
10	J. of molecular spectroscopy	+	365	1,7
11	Phys. rev. lett.	+	338	1,6
12	Z. naturforschung A	+	321	1,5
13	Phys. lett. A	+	306	1,4
14	Optics and spectroscopy	+	305	1,4
15	J. of quant. spect. rad. transf.	+	289	1,4
	Σ =		15.200	71,4
16	Canad. J. of physics	+	258	1,2
17	J. of the opt. soc. of Amer.	+	221	1,0
18	J.E.T.P.	+	215	1,0
19	Reports	(+)	212	1,0
20	Molecular physics	- +	198	0,9
21	Atom. and nuclear data	+	190	0,9
22	J. chem. soc. Faraday I	- +	184	0,9
23	Theor. chem. acta	- +	176	0,8
24	J. chem. soc. Faraday II	- +	155	0,7
25	Proceedings B	+	153	0,7
26	J. de physique	+	149	0,7

TABLE 3 (Continued)

Statistics by journal (on 1.8.1975)

	JOURNAL	Scanning method	Number of cards	%
27	Physica scripta	-	147	0,7
28	Z. für phys.	+	146	0,7
29	Proc. Roy. Soc. A	-	142	0,7
	Σ =		17.746	83,4
30	Int. J. quant. chem.	-	119	0,6
31	J. of phys. chem.	-	116	0,6
32	J. of the amer. chem. soc.	-	104	0,5
33	Chem. phys.	- +	93	0,4
34	Sov. phys. techn. phys.	-	88	0,4
35	J. of electron spec. relat. phen.	-	87	0,4
36	Faraday Discussions. Chem. soc.	-	86	0,4
37	J. of the phys. soc. Jap.	+	82	0,4
38	Ber. Bunsengesellsch. phys.	-	82	0,4
- -	----------			
44	J. of phys. chem. ref. data	+	66	0,3
	Σ =		18.669	87,7
	Various		2.613	12,3
	Σ Σ =		21.282	

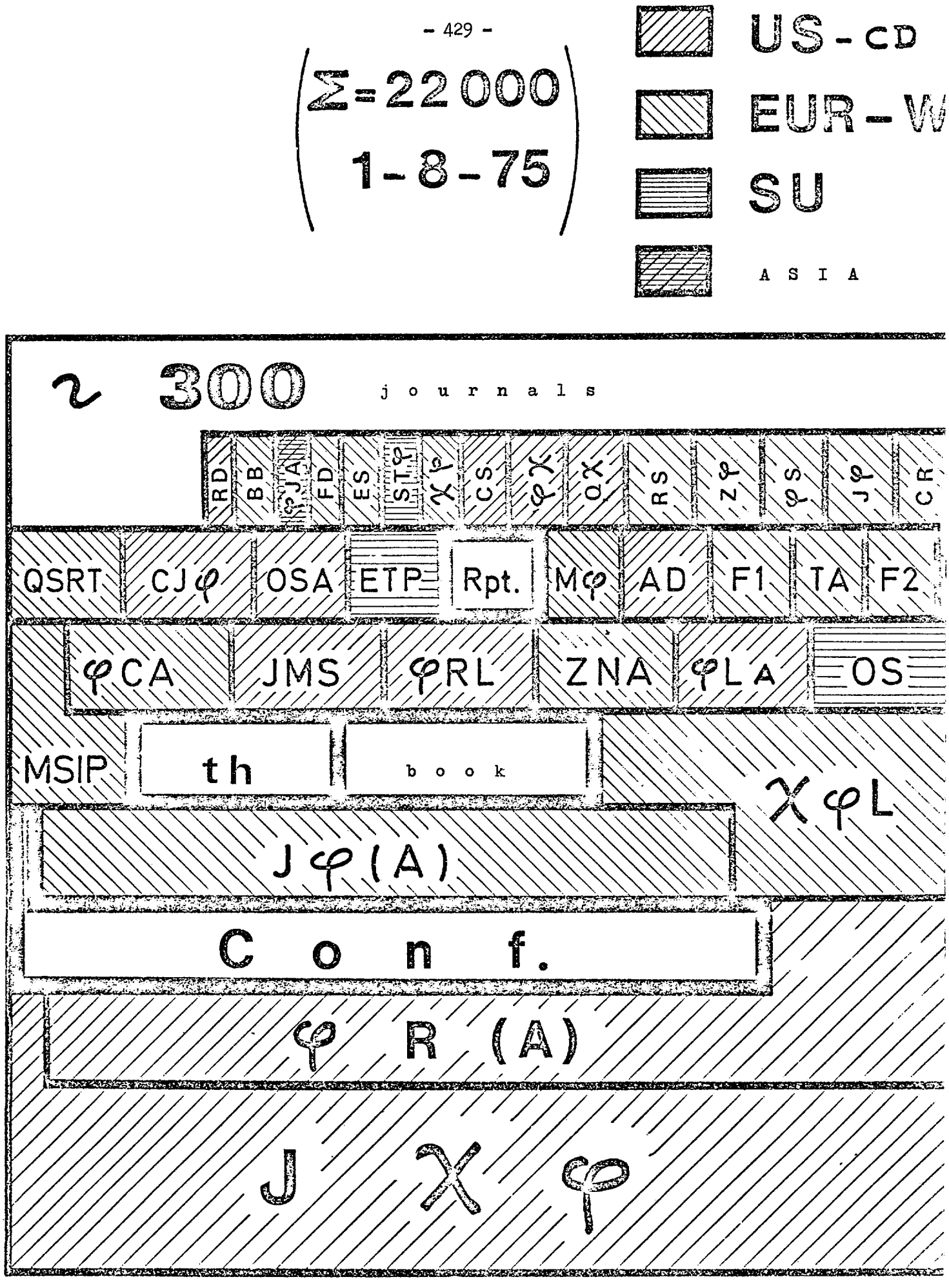

Fig. 3. Statistics by journals

scientific work of the various countries and their scientific publishing policies, geographical descriptors must be used, i.e. Country, Province or Town. Unfortunately, we have but recently introduced these descriptors into GAPHYOR and we only have statistics on a little more than 2000 lines (quarterly editions 1975 - 1 and 2). With the necessary reservations about the imprecise nature of these statistics, we do, however, believe it useful to indicate the most striking findings.

Figures 4 and 5 show the relative importance of various countries as regards production (Fig. 4) or publication (Fig. 5) of GAPHYOR material. Table 4 shows the positions of the top nine countries from these two points of view.

It will be seen in particular that France's position as far as production is concerned (5.3% of total production) is commendable, but is rather disastrous with regard to publications (1% of the total). It might be thought that this is due to the language problem; however, more detailed analysis will show that it is due more to a certain social and cultural behaviour of research people in France. In this connection we have characterized each of the nine most important countries with two indices:

The export index X_e of scientific work as defined by the formula:

$$X_e = \frac{\text{amount of GAPHYOR material published abroad}}{\text{total amount of GAPHYOR material produced in the country}}$$

and the import index X_i of scientific publications as defined by the formula:

$$X_i = \frac{\text{amount of foreign GAPHYOR material published in the country}}{\text{total amount of GAPHYOR material published in the country}}$$

The diagram of co-ordinates X_e and X_i in Fig. 6 shows how the different countries compare. The four sides of this diagram represent extreme behaviour:

- Nationalists $X_e = 0$ (no exports)
- Generous $X_e = 1$ (many exports)

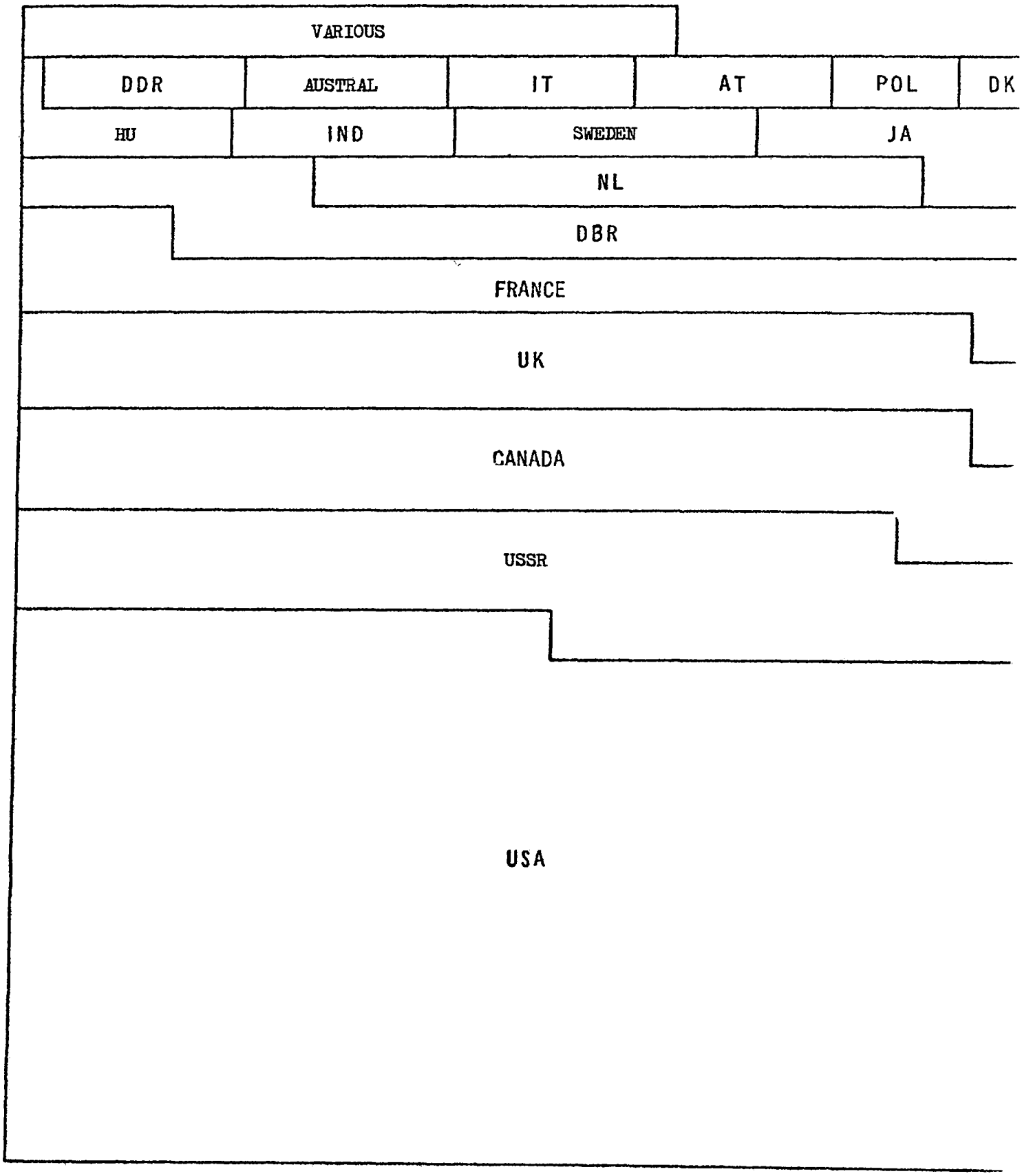

Fig. 4. Production of GAPHYOR material classified by country (1st quarter of 1975)

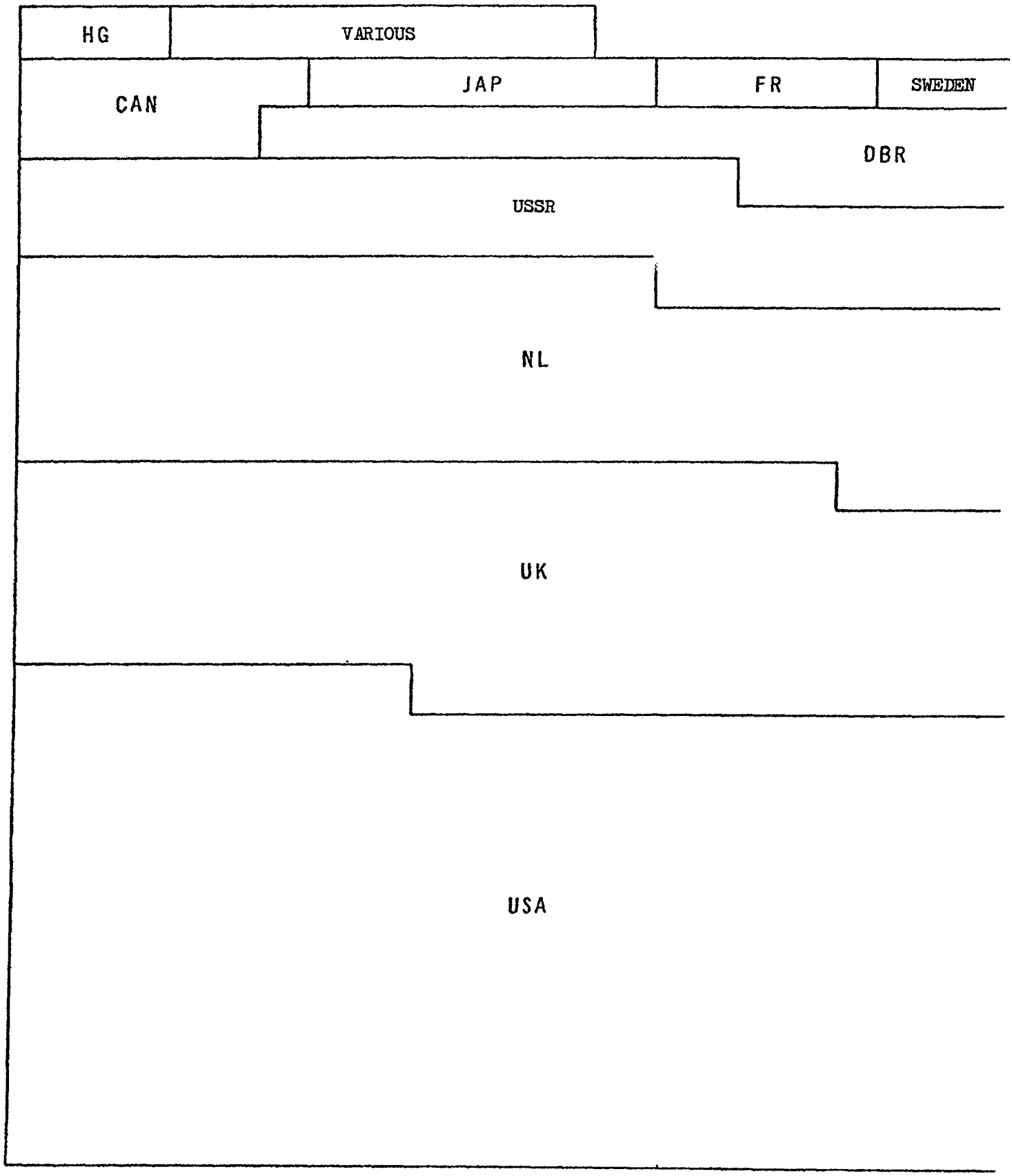

Fig. 5. Publication of GAPHYOR material classified by country (1st quarter of 1975)

TABLE 4

Classification of countries according to production or publication of GAPHYOR material (the last column shows the difference between these two classifications)

	PRODUCTION		PUBLICATION	
1	U S A	1	U S A	(0)
2	U S S R	2	U K	(+ 2)
3	C A N A D A	3	N L	(+ 4)
4	U K	4	U S S R	(- 2)
5	F R A N C E	5	D B R	(+ 1)
6	D B R	6	C A N A D A	(- 3)
7	N L	7	J A P	(+ 1)
8	J A P	8	F R A N C E	(- 3)
9	S W E D E N	9	S W E D E N	(0)

TABLE 5

Production of GAPHYOR material in France (Σ = number of GAPHYOR cards over a period of about 9 months from October 1974 to June 1975)

TOWN	Σ	TOWN	Σ
ORSAY	112	BREST	4
PARIS	84	DIJON	4
STRASBOURG	26	FONTENAY	4
SACLAY	22	RENNES	4
REIMS	14	ST. CLOUD	4
GRENOBLE	12	CACHAN	3
LILLE	11	CHATENAY	2
MARSEILLE	10	MONTROUGE	2
BELLEVUE	9	NANCY	2
MEUDON	9	PAU	2
CAEN	8	TOULOUSE	2
BORDEAUX	7	ANGERS	1
LYON	7	NICE	1
POITIERS	6	TOURS	1

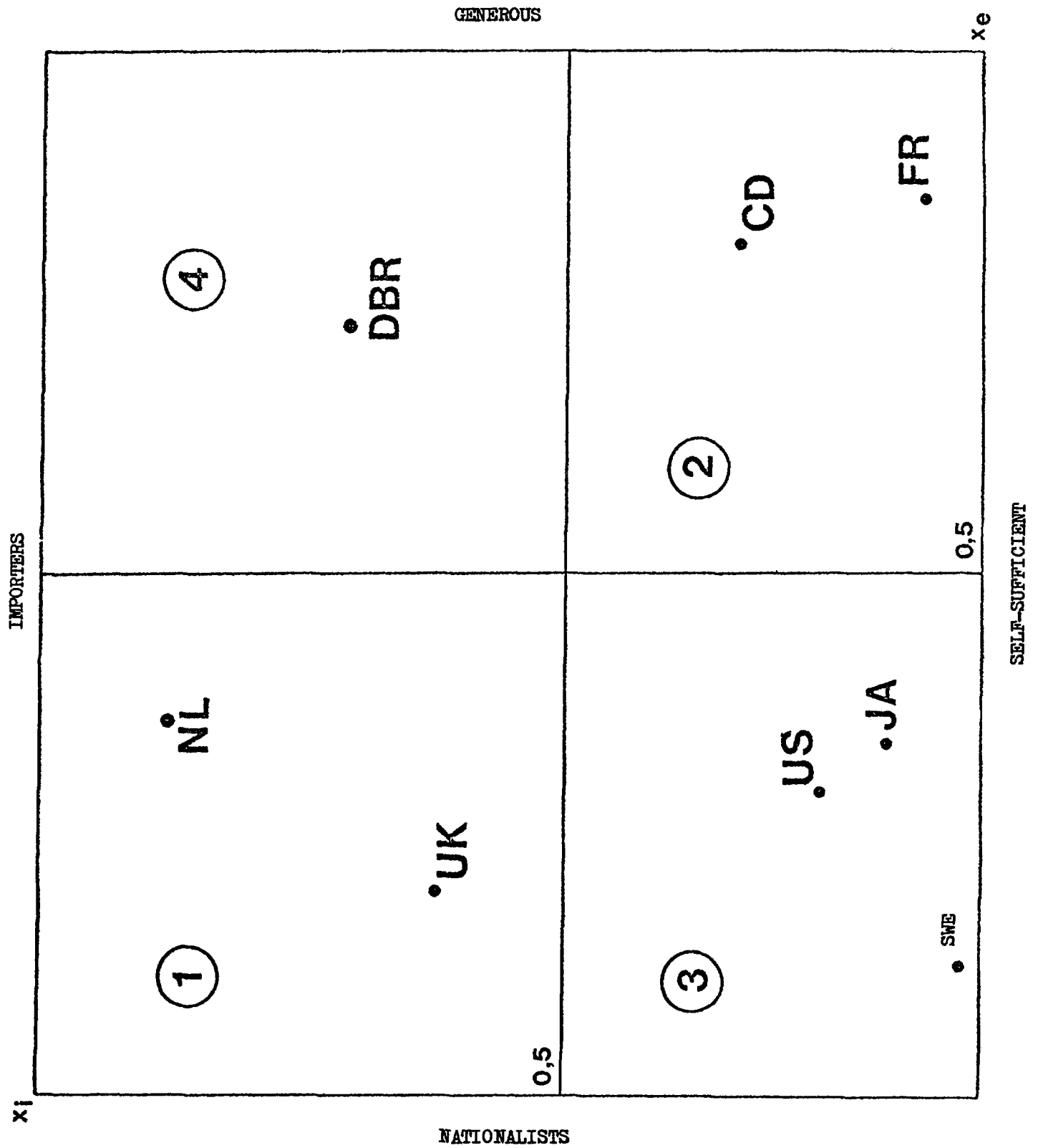

Fig. 6. Scientific publishing policies of various countries (see text for definition of X_e and X_i

- Self-sufficient $X_i = 0$ (no imports)
- Importers $X_i = 1$ (many imports).

It will be seen then that the first eight countries can be classified with regard to their scientific publishing policy in four groups:

Group 1 - nationalist and importer: United Kingdom, Netherlands;

Group 2 - generous and self-sufficient: France, Canada;

Group 3 - nationalist and self-sufficient: USA, USSR, Japan;

Group 4 - generous and importer: West Germany.

The countries in Group 1 publish the majority of their scientific results in their own country and succeed in attracting a large number of publications from other countries. These are the overall winners of Table 4.

The other countries in Group 2 only publish in their own journals a small proportion of their scientific results. Moreover, they succeed in attracting only very few publications from other countries. They are the overall losers of Table 4. France is the best example of this.

The countries in Groups 3 and 4 have an attidude which produces a certain equilibrium, as two opposing effects cancel each other out. They are either open in both directions (e.g. West Germany) or closed in both directions (e.g. USSR). The case of the USA is rather unusual in view of its dominant position in terms of production. Although it exports only a moderate amount in relative terms (X_e = 0.27), in absolute terms it is the leading exporter and its exports represent 32% of all material exported by all countries. It is also a significant importer in absolute terms (30% of all results exported go to the USA).

11.6.2. Statistics by towns in France

A more detailed analysis of the amounts of scientific material that various research centres produce can be made using the descriptor "CIté". The results of this statistical study are given for France in Table 5 and Fig. 7.

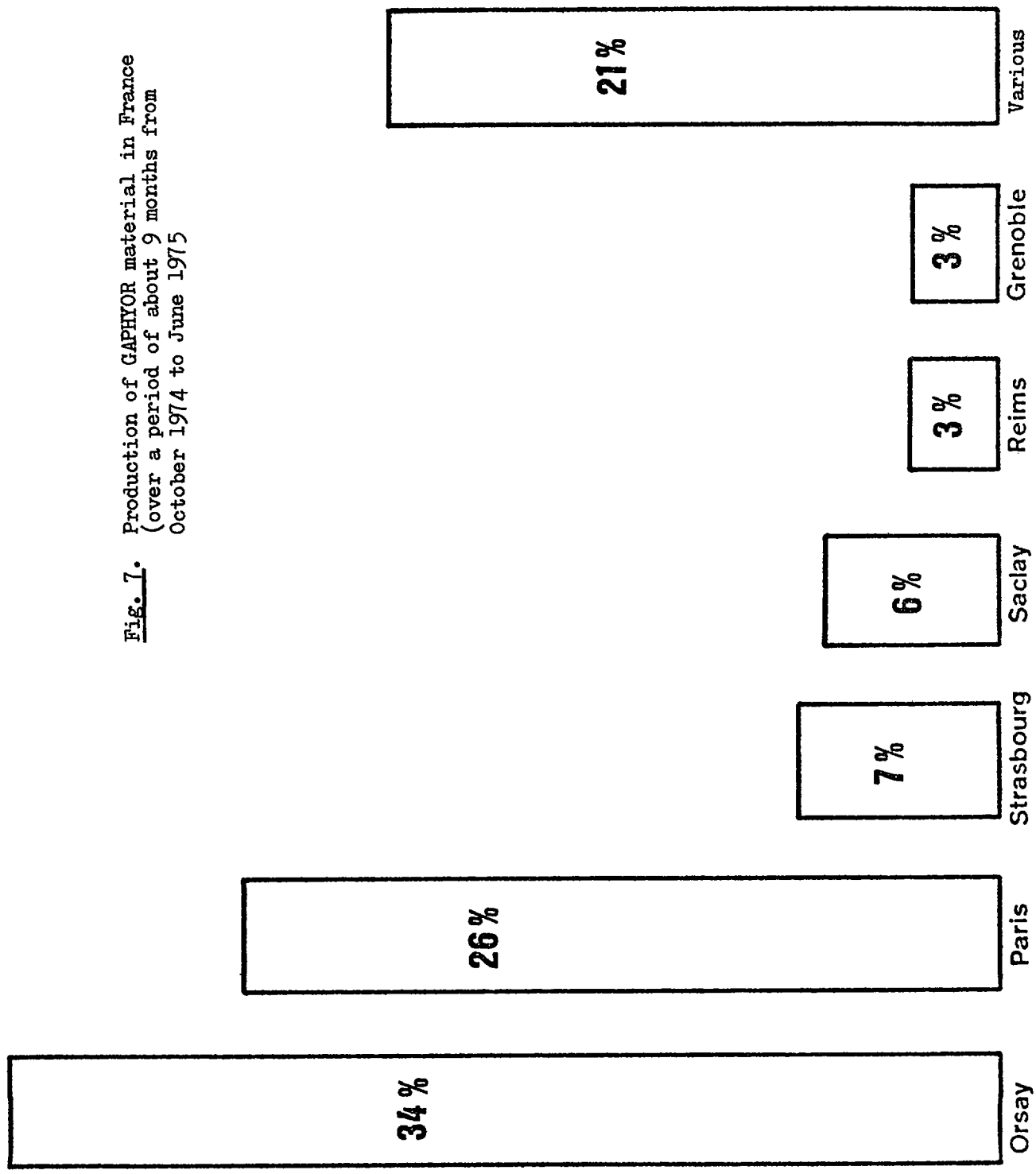

Fig. 7. Production of GAPHYOR material in France (over a period of about 9 months from October 1974 to June 1975

12. CONCLUSION AND FORECASTS

12.1. Advantages of the GAPHYOR system

We believe that the GAPHYOR system offers a large number of advantages:

(a) It possesses internal logic and is not based solely on the use of keywords co-ordinated to a greater or lesser degree. It is therefore quite a powerful documentation tool. Here, for instance, are two rather difficult problems which it is able to deal with immediately:

- Classify literature on negative ions in gases;
- Find and classify literature on the reactions which produce carbon monoxide.

(b) It appears to meet a real need which has not so far been satisfied by any other system.

12.2. Disadvantages of the GAPHYOR system and ways of improving it in the future

The advantages of the GAPHYOR system arise from the fact that its scope is strictly limited and that the relevant information lends itself quite well to a quantified logical description based essentially on conventional chemical notation, the Mendeleev periodic table and simple concepts of atomic and molecular physics. Nevertheless, there are two disadvantages in the present system which should be noted:

(a) GAPHYOR clients consult our file by making a specific request each time they need it. This method of examination on request is the most flexible. Its main disadvantage is a certain slowness (3-5 days' wait, taking postal delays into account). Nor does it favour rapid expansion of our system. Consultation on request produces a sort of snowball effect, but it is a method that is slow in the beginning. For this reason we have for some time been proposing three consultation methods:

- Consultation on request
- Subscription to the whole file (4 instalments per year)
- Subscription to a specified part of the file (4 instalments per year).

It might be thought that in the long run the ideal method of consultation would be a conversational system allowing clients to consult our file directly by means of a visual display. In the present state of our experience this would seem dangerous to us, as it very often happens that we are asked to interpret questions put by clients so that the computer can provide them with the optimum response.

(b) Also, it should be said that the operation of ambitious information systems like GAPHYOR raises certain manpower problems, since it presupposes the active participation of experienced research workers specializing in the field of interest. At present, GAPHYOR depends entirely on a small team led by J.L. Delcroix.

Transition to the stage where serving the client is more important than research aimed at developing the system is presenting a few problems. In fact, our aim is to provide a self-financing service which will permit research workers making scanning work for GAPHYOR to get some extra-money and thereby help to solve the manpower problem. It must be realized, however, that self-financing will probably be possible only if the system is successful internationally, and that may well take several years.

In any case it seems to us that the active part-time participation of research workers in such a service provides most interesting experience which in the future should be extended to many other spheres, for the greater good of scientific documentation and of the research workers themselves.

BIBLIOGRAPHICAL REFERENCES

Internal reports

[1] GAPHYOR code of journals. Plasma Physics Laboratory, Université de Paris-Sud, Centre d'Orsay.

[2] GAPHYOR geographical code. Plasma Physics Laboratory, Université de Paris-Sud, Centre d'Orsay.

[3] Special conventions associated with the GAPHYOR code. Plasma Physics Laboratory, Université de Paris-Sud, Centre d'Orsay.

A P P E N D I X A

RULES FOR WRITING TWO IDENTICAL FAMILIES

It may happen that the chemical system under consideration appears to involve two different elements from the same Mendeleev family. A group of families to be considered could, for example, be written:

A A C D (1)

A B B D etc. (2)

In this case the way one molecule is written is ambiguous. For example, if case (1) is considered, the indices ℓ and m seem to be interchangeable. In fact two different things may happen:

(1) Although family A occurs twice in the system it may be that this is via different elements. For example, in the writing of molecule O_2S the family 6A appears twice, once via oxygen and once via sulphur; it is therefore easy to differentiate the two meanings of A by saying, for example:

A' = 6A in relation with O (the lightest element)

A" = 6A in relation with S (the heaviest element)

When this reasonable distinction has been made the group of families (1) will be written:

A' A" C D

We now have four different families, and the ambiguity is removed;

(2) In other cases it is impossible a priori to distinguish the two occurrences of the same family A. The most frequent case is where the indeterminate family 10 is involved. This can appear twice as in the groups A B 10 10 and 10 10 0 0, three times as in A 10 10 10 and 10 10 10 0, and even four times as in 10 10 10 10.

We will consider the most complex occurrence of the group 10 10 10 10, as the other cases can be easily deduced from it. We have then to write and rank three molecules

$$X_\ell\ Y_m\ Z_n\ Z'_p\ ,\quad X_{\ell'}\ Y_{m'}\ Z_{n'}\ Z'_{p'}\ ,\quad X_{\ell''}\ Y_{m''}\ Z_{n''}\ Z'_{p''} \qquad (3)$$

Here the four elements X, Y, Z, Z' are a priori different but indeterminate. As order X, Y, Z, Z' is not a priori definite, in order to find the ranking order of (3) a scheme who is invariant with respect to a permutation of the elements X, Y, Z, Z' must be used. This will be done by introducing symmetrical functions:

$$\Sigma_1 = \ell + m + n + p \tag{4}$$

$$\Sigma_2 = \ell m + \ell n + \ell p + mn + mp + np \tag{5}$$

$$\Sigma_3 = \ell mn + mnp + np\ell + p\ell m \tag{6}$$

$$\Sigma_4 = \ell mnp \tag{7}$$

and the analagous functions $\Sigma'_1, \Sigma'_2, \Sigma'_3, \Sigma'_4$ and $\Sigma''_1, \Sigma''_2, \Sigma''_3, \Sigma''_4$ relative to the indices ℓ', m', p' and ℓ'', m'', n'', p'' and by defining the ranking order:

$$X_\ell\, Y_m\, Z_n\, Z'_p < X_{\ell'}\, Y_{m'}\, Z_{n'}\, Z_{p'} \tag{8}$$

by one of the conditions:

$$\Sigma_1 > \Sigma'_1 \tag{9}$$

$$\Sigma_1 = \Sigma'_1 \qquad \Sigma_2 > \Sigma'_2 \tag{10}$$

$$\Sigma_1 = \Sigma'_1 \qquad \Sigma_2 = \Sigma'_2 \qquad \Sigma_3 > \Sigma'_3 \tag{11}$$

$$\Sigma_1 = \Sigma'_1 \qquad \Sigma_2 = \Sigma'_2 \qquad \Sigma_3 = \Sigma'_3 \qquad \Sigma_4 > \Sigma'_4 \tag{12}$$

When the four sums Σ and Σ' are equal to each other (which means that $\ell = \ell'$, m = m', n = n' and p = p') the ranking is done with the indices i and x according to one of the following conditions:

$$i > i' \tag{13}$$

$$i = i' \qquad x > x' \tag{14}$$

As the molecules P, Q and R have been ranked according to invariant criteria by permutation of the elements X, Y, Z, Z' it is now useful to choose a way of writing them that is as unequivocal as possible. It should be recalled that the elements X, Y, Z and Z' are different but undetermined; the only criteria that differentiate them are the indices ℓ, m, n, p; ℓ', m', n', p'; ℓ'', m'', n'', p'' which are shown in the writing of the process under discussion.

Now the rules for writing these indices must be chosen: it is agreed that two indices m and n are written in the order

$m \prec n$ (m before n)

if one of the following conditions is fulfilled:

$$m > n \tag{15}$$

$$m = n \qquad m' > n' \tag{16}$$

$$m = n \qquad m' = n' \qquad m'' > n'' \tag{17}$$

These rules make it possible to rank the indices ℓ, m, n, p in a determined order (except in the exceptional case where, for example, we have $m = n$, $m' = n'$, $m'' = n''$; but in this case the two ways of writing obtained by the interchangeability of m and n are identical).

For the molecules S, T, and U of the final state the ranking is done according to rules analagous with those of formulae (9) to (14). However the problem of interchangeability of the indices ℓ, m, n, p does not in general arise, as formulae (15) to (17) have already made it possible to establish the way they are written.

A P P E N D I X B

SIMPLIFIED DESCRIPTION OF PROCESSES

Category 1

EN Energy levels, wave function

CP Compton profiles

DP Dipole moments

NP Multipole moments

PE Electric polarization

VR Curves of potential, structure of molecules

TR Transition probabilities, lifetimes

Category 2

AN Absorption

EL Elastic collision

P2 2-photon interaction

P3 3-photon interaction

PN Multiphoton interaction

EE Production of electrons

Category 3

SN Total and transport cross-sections

EL Elastic collision

ER Line emission

EE Production of electrons

PP Production of positive charge

Category 4

SN Total and transport cross-sections

EL Elastic collisions

TE Excitation transfer

DX Quenching

10 Charge transfer 10 (fast particles)

20 Charge transfer 20 (fast particles)

LN LN charge transfer (fast particles)

MP MP charge transfer (target particles)

LP LM/NP charge transfer

ER Line emission

EE Production of electrons

PP Production of positive charge

Category 5

ZT Partition functions

CO Correlations

PV Compressibility, equation of state, vapour pressure

FT Thermodynamic functions

DN Scattering

VI Viscosity

CT Thermal conductivity

DT Thermal diffusion

DM Diffusion of metastables

RN Relaxation in neutral gases

ME Electronic mobility

DE Electron diffusion

PI First Townsend coefficient

AT Attachment

DT Detachment

PC Power exchanges by electron - neutral collision

MI Ionic mobility

DI Ion diffusion

DA Ambipolar diffusion

RC Recombination

PD After-glows

A P P E N D I X C

CODE OF PRINCIPAL JOURNALS

02 Adv. atom. molec. phys.
03 Adv. chem. phys.
04 Adv. electronics electron. phys.
06 Adv. mass. spectrometry.
07 Appl. phys. lett.
08 Ann. der phys.
09 Astrophys. J.
10 Atomic data.
12 Austral J. Phys.
14 Canad. J. chem.
16 Canad. J. Phys.
20 Chem. Phys. lett.
22 Proceedings of Ac. Sc. B.
24 High temperatures (1024 in Russian).
26 Internat. J. mass. spec. ion phys.
27 Int. J. quant. chem.
28 J. de phys.
30 J. of chem. phys.
32 J. of electron. sp. relat. ph.
34 J. of geophys. res.
36 J. of molecul. spectroscopy.
38 J. of molecul. struct.
40 J. of phys. B (Proc. phys. soc.).
42 J. of phys. D
44 J. of phys. chem.
46 J. of quant. spect. rad. transf.
47 J. of the amer. chem. soc.
48 J. of the chem. soc. Faraday trans. I.
49 J. of the chem. soc. Faraday trans. II.
50 J. of the opt. soc. Amer.
52 J. of the phys. soc. Jap.

54 Khim. vys. energ.
56 Molecular phys.
58 Opt. and spectroscopy (1058 in Russian).
60 Physica A.
61 Physica B + C.
62 Phys. lett. A.
64 Phys. of fluids.
66 Phys. scripta.
68 Phys. rev. lett.
70 Phys. rev. A.
72 Proc. roy. soc. A.
74 Rev. mod. phys.
76 Rev. roum. phys.
78 Sov. phys. doklady (1078 in Russian).
80 Sov. phys. J.E.T.P. (1080 in Russian).
82 Sov. phys. J.E.T.P. lett. (1082 in Russian).
84 Sov. phys. tech. phys. (1084 in Russian).
86 Sov. phys. uspekhy (1086 in Russian).
88 Theor. chem. acta.
90 Z. naturforschung.
92 Z. phys.
94 Z. phys. chem.

NATIONAL PROGRAMMES AND EMPHASIS ON A + M DATA FOR FUSION IN THE FEDERAL REPUBLIC OF GERMANY

F. Waelbroeck
Institut für Plasmaphysik der Kernforschungsanlage Jülich Gmbh
Association EURATOM-KFA

ABSTRACT

Fusion research in the Federal Republic of Germany is centered on plasma confinement in toroidal devices. The effort is part of the Fusion Programme of the European Community. The A + M data acquisition activities are consequently strongly concentrated within but a few areas of this very broad field, with a strong emphasis on plasma-wall-interaction (Garching, Jülich, to some extent HMI, Berlin). Further activities on cluster acceleration (Karlsruhe), Lithium, Tritium equilibrium and kinetics (Jülich) and data compilation (Karlsruhe, Garching and Düsseldorf) also take place. Data on electron impact ionisation and excitation are the main programme of some university laboratories, and are also gathered, when the need arises, in the course of the confinement programme.

I. INTRODUCTION

It is difficult to decide today which A + M data are of greatest significance for the development of the fusion programme. Areas can be well defined, as was done in the report /1/ prepared by the International Nuclear Data Committee of the IAEA, but in each area, an extremely large, quasi-infinite, number of data could be collected, some of which may in end effect prove to be unconnected to the problem of fusion. In addition, new areas appear from time to time: this was recently the case for "cold gas refueling" (II.C.4 here) and for the "surface chemistry of hydrogen in statu nascendi" (III.B.4 here) which leads to the release of low Z atoms from metallic walls. The setting of priorities for the data requirement within each area can only be made from an analysis of the needs of the evolving fusion programme. Depending on whether a laboratory or group of laboratories centers its activities on heating using neutral injection of fast atoms, mirror machines, pellet implosion, or others, the A + M data need and data acquisition rate in the different areas will be completely different.

Within the collaborative programme of the European Community, the central emphasis in the field of plasma-wall interaction lies within the Federal Republic of Germany.Two of the largest devices being built or prepared (ASDEX at Garching, TEXTOR at Jülich) aim at improving our understanding of impurity generation in toroidal devices, and at developing methods to control and depress this noxious phenomenon.

In ASDEX, an axisymmetric divertor will be used to examine the possibility of screening a confined tokamak plasma from impurities coming from the walls. In TEXTOR, the role of wall materials, of their temperature (up to 600^{o}C), and geometrical configuration will be studied, as are the efficiences of other possible plasma purification methods.

It is expected that the results of these devices and of the accompanying programmes will clarify the problem of impurity generation in toroidal systems, not exclusively of the tokamak type, and be of great importance for the planning and design of oncoming larger facilities.

In what follows, we shall attempt to indicate the A + M activities in the FRG. The subdivision into areas and also the ordering of topics suggested in the IAEA report /1/ will be used. It will not be tried to enumerate the

experimental results already obtained which are to be found in the literature, but rather to indicate briefly what is being done or being planned in the A + M field within the FRG, i.e. where scientific and apparative potential exists. Since, in some areas, very little coordination exists, forgivenness is asked for eventual omissions.

II. INJECTION SYSTEMS

A. Plasma Heating by Injection of Beams of Fast Neutral Particle

The main development along this line is centered at Fontenay-aux-Roses (France) and Culham laboratories (U.K.). Garching and Jülich limit their effort to the adaptation of source types developped elsewhere to the local confinement devices (Wendelstein VII, ASDEX, TEXTOR). Whence no intense A + M data activity takes place in this sector.

B. Plasma Heating by Injection of Particle Cluster

A significant programe is underways at Karlsruhe since several years /2/. The main problems solved to date are: formation of H_2 clusters in interesting mass spectral ranges, cluster ionisation, acceleration to the MeV range, and cluster neutralisation. The possible use of this technique for the obtention of negative ion source is also being examined.

C. Plasma Fueling

1) Injection of fast neutral particle (see II.A. above)

2) Particle clusters (see II.B. above)

3) Solid fuel injection. Experiments to study the behaviour and influence of solid H_2 pellets in a Tokamak plasma have just started on Pulsator (Garching).

4) "Cold Gas" injection. In tokamak discharges, when the initial degree of wall contamination is low, the electron density n_e, decreases with time after the start-up phase. It is possible then to maintain n_e constant or even to let it increase in time by injection cold gas into the hot plasma torus. This was demonstrated and studied in particular in Alcator (MIT) /3/ and Pulsator (Garching) /4/. The phenomenon seems closely related to the plasma purity. The rate of permissible n_e increase is limited most probably by the radiation of

impurities still present within the plasma, and also of the parent H_2 molecules injected and of the resulting generation of atoms, in addition to the additional power lost via charge exchange and through the ionisation of the injected gas. This new operation mode of tokamak systems is expected both to provide and to require for its interpretation, a number of A + M data.

III. INTERACTION OF PLASMA WITH SURFACES

A.1. Sputtering

The Garching laboratory is equiped with a wide range of apparatus allowing /5/ to measure sputtering coefficients on various metals by different gases in an energy range starting at tens of keV down to a few hundreds eV.Besides metals, carbon, and carbides have recently also been studied.

In Jülich, the problem of the different occupation of the excited energy levels of sputtered particles has been studied experimentally for iron /6/. In addition, sputtering of low Z materials in the energy range 50 eV to 1 keV is being investigated in the Institute for Chemistry I in collaboration with the Institute for Plasma Physics of the KFA. Here, emphasis is laid on the role of chemical effects on the abrasion rate, and also on the retention rate of H isotopes. The latter might affect the tritium inventory and the breeding ratio in the initial phase of operation of a reactor.

A.2. Blistering

Here again, the work carried out at Garching has played a major role in our understanding of blistering processes /5/, of its relevance, but also on the possibility to limit its nefarious consequences /7/. Also, the work at the Hahn-Meitner-Institute Berlin /2/ on the helium implantation profiles in metals must be mentioned.

B.1.-4. Surface absorption, adsorption, reflexion, evaporation

At Garching, the problem of back-scattering of H atoms in metal has been examined both numerically, using the MARLOWE code originally developed at Oak Ridge, and experimentally as a function of the energy of incident particles and of the lattice properties. The angular dependency, energy spectrum, as well as the charge state of the back scattered particles have been studied in details. In the framework of the ASDEX development, the absorption properties of special metals and alloys are being examined

as well with regard to hydrogen as also other light impurities.

The adsorption of gases in inconel and for various low Z materials envisaged for JET is being studied in Jülich /9/. The absorption of H in low Z materials and metals is studied, not only in the energy range 50eV - 1 keV (as mentioned above) but also using quasi-thermal hydrogen atom beams /10/.

B.5. Surface Chemistry under influence of Hydrogen atoms and atomic ions

The early appearance of oxygen, carbon, in toroidally confined plasma is probably explained by the release of water and methane produced in the surface - near domain by the action of atomic hydrogen species (H^0, H^+) with some oxydes and with lattice carbon. The H_2O and hydrocarbon released are cracked and ionised in the hot plasma. The rate of such reaction of atomic hydrogen particles with metallic wall impurities is studied in Jülich /11/ where the high efficiency of wall cleaning techniques based on the results of this investigation has been demonstrated /11/. See also ref, /10/ part 1.

IV. PLASMA CHARACTERISTICS - IMPURITIES AND COOLING

As mentioned, in the introduction, no coordinated activity exists in Germany in this sector. Many data are acquired in the research centers as need arises in the course of the developing programme /12/. In addition the following activities are pursued in different University laboratories:

Ruhr-Universität Bochum

P. Heckmann: Transition probabilities, doubly excited states of highly ionised atoms, by beam foil spectroscopy.

H.J. Kunze: Spectra of highly ionised atoms in the X-ray region, using a vacuum spark.
Excitation and ionisation rate coefficients of highly ionised atoms, using a thetapinch plasma.
Transition probabilities of neutrals, using selective laser excitation.

Universität Kiel

J. Richter: Transition probabilities of highly ionised metallic ions, using an "iron" arc.

Universität München

H. Walther: Transition probabilities by selective laser excitation.

V. PLASMA DIAGNOSTICS

The list of diagnostic techniques relying on the utilisation of A + M data or/and capable of furnishing new relevant data, as installed on fusion devices would go beyond the scope of this document. We should however here mention among new developments:
In Garching: the development of QWAASS, a surface analysis apparatus allowing to examine wall samples quasi in-situ by Auger Electron Spectroscopy, and secondary Ion Mass Spectroscopy, this after they have been exposed to a number of plasma discharges /13/.
In Jülich: the use of Scanning Auger Electron Spectroscopy combined with an argon sputter gun to study the depth profiles of the impurity species in technical materials after various pretreatments (welds, sand blasting, etching, etc.) /14/.

Also in Jülich, the development of techniques based on resonant laser scattering to detect the very small amounts ($\leqslant 10^{-8}$) of impurities which are expected to be present between the wall and the plasma edge as a consequence of sputtering; also methods to measure atomic hydrogen by resonant scattering are developed /15/.

VI. ADDITIONAL PROBLEMS

The work of Jülich on the liquid-vapom equilibrium Li-T and the corresponding reaction kinetics should be mentioned here. It could be shown in particular that the existence of hydrides such as Li_1H, Li_2H, LiH_2, Li_2H_2 in the gas phase strongly influences the separation constant in a distillation system, and this in a favourable way.

VII. DATA COMPILATION

The effort in this direction in the F.R.G. is indicated in a detailed manner in the IAEA report on A + M needs for fusion /1/. To this list should be at least added the activity of J. Hackmann and J. Uhlenbusch (Physikal. Institut II der Universität Düsseldorf) on the compilation of relevant cross-sections for the description of atomic and ionic phenomena in the cooler wall-near plasma regions.

REFERENCES

/1/ A. Lorenz et al. Survey of Atomic and Molecular Data Needs for Fusion, IAEA report INDC (NDS)-72. LNA. Jan. 1976.

/2/ See amongothers: K. Buchheit, W. Henkes, Z. für Angew. Physik 24, 191, 1968.
W. Henkes, F. Mikosch, Int. Journ. of Mass Spectr. and Ion Physics, 13, 151 (1974)
O.F. Hagena, W. Henkes, U. Pfeiffer, Symposium on Fusion Technology, Garmisch-Partenkirchen, June 1976

/3/ Alcator Group. 6th Int. Conf. on Plasma Physics and Contr. Nucl. Fusion Research, Berchtesgaden, Oct. 1976. Paper A.5.

/4/ S. Sesnic et al. Ibid. Paper A.6.

/5/ For a recent review, see B.M.V. Scherzer et al. Intern. Symposium on Plasma-Wall Interaction Jülich, Oct. 1976, Invited Paper.

/6/ A. Elbern. Ibid. paper D.6

/7/ R. Behrisch. Symposium on Fusion Technology, Garmisch-Partenkirchen, June 1976.

/8/ J.P. Biersack, et al. International Symposium on Plasma-Wall Interaction, Jülich, Oct. 1976, paper C.18.

/9/ K.G. Tschersich, KFA IGV, Ibid. paper C.13.

/10/ C.H. Wu et al. KFA ICH I, Ibid., paper C.5.
K.J. Dietz et al. J. Nucl. Mat. 63 (1976) in Publication.

/11/ K.J. Dietz, F. Waelbroeck, Intern. Symposium on Plasma-Wall Interaction, Jülich, Oct. 1976, paper C.21.

/12/ To the authors knowledge, the latest extensive compilation from a center in this field is the Report IPP 1/50 Garching, by W. Lotz, 1966.

/13/ P. Staib, G. Staudenmayer and TFR Group. Int. Symp. on Plasma-Wall Interaction, Jülich, Oct. 1976, paper A.2.

/14/ J. Kirchner et al., Symposium on Fusion Technol., Garmisch-Partenkirchen June 1976.

/15/ A. Elbern et al. and P. Bogen et al., Intern. Symp. on Plasma-Wall Interaction, Jülich, Oct. 1976, papers D.4. - D.7.

PRESENT STATUS OF ACTIVITIES IN COMPILATION AND ACQUISITION OF ATOMIC AND MOLECULAR DATA FOR FUSION IN JAPAN

Hirosi SUZUKI
Sophia University, Kioicho, Chiyoda-ku, Tokyo, Japan

This is to report on the status of current and projected activities in compilation and dissemination of atomic and molecular data in Japan, and to survey their domestic research activities in the related fields which will enable us to acquire the necessary data for fusion research. In addition to the above, short remarks will be given on the possible users of atomic and molecular data. A few examples of data needs will be mentioned in connection with some large scale plasma devices operated or projected in several central CTR institutes.

1. CURRENT AND PROJECTED COMPILATION ACTIVITIES OF ATOMIC AND MOLECULAR DATA IN JAPAN

Bibliographic Compilations

The most lasting effort to compile bibliographic references is being continued by K. Takayanagi (Institute of Space and Aeronautical Science, University of Tokyo) covering the whole field of atomic collisions. Bibliographies of 11 volumes[1,2] have been published from 1965 to 1975, including about 7000 references with short annotations in English. Some volumes contain the index to some selected processes. Among his bibliographies those on the electron-atom (molecule) collisions are supposed to be near perfect up to the period 1970 (theoretical) or 1967 (experimental). Succession of publication of his bibliography, however, is interrupted now and then, because of limitation of available time for him, although the effort of accumulation of references are continued up to date.

Among large amount of individual compilations of bibliographical references, a reference library of W. Shearer-Izumi and T. Watanabe (Faculty of Engineering, University of Tokyo) is the most eminent. This compilation contains about 18,000 references with abstracts on the structure, radiative and collisional processes involving excited atoms, from 1967 to the date.

Numerical Data Compilations

A series of efforts to compile and evaluate numerical data of electron-molecule collisions has been made by K. Takayanagi and his collaborators

from about ten years ago[3-8]. Cross section data for various types of electron collisions with N_2, O_2, O, H_2 and CO_2 have been compiled in interest of the atomic and molecular processes in the space science. In some cases when required cross section data were not available, they tried to estimate those data with help of known values of the optical oscillator strength.

In addition to the above, individual reviews and collections of collision cross section data have been published by atomic collision physicists [9,10]. Numerical tables of some atomic data useful for radiative transitions in plasmas have been reported in a view of plasma diagnostics by K. Fukuda and his collaborators (Faculty of Engineering, Kyoto University)[11, 12].

There was no systematic activity in compilation of numerical data in relation to atomic processes for fusion research and plasma physics before the Study Group (SG) for Data Compilation of Atomic Processes, Institute of Plasma Physics (IPP), Nagoya University started its work.

The Study Group, IPP

This group started under the leadership of K. Takayanagi as a small workshop in autumn of 1973. At first the group made a extensive survey on request of cross section data by sending questionaires to 597 researchers who constitute the Nuclear Fusion Group in Japan. Filled up 58 questionaires could be collected. On the basis of this information a report was published, which includes a comprehensive list of cross section data under the urgent need[13]. This report also contains a list of bibliographical references relevant to data and informations for atomic processes, in order to meet the convenience of researchers in a wide variety of specialities.

The current SG was organized in Spring of 1974 under the leadership of H. Suzuki (Sophia University, Tokyo and IPP). As the first action of the SG, the following two considerations had to be made simultaneously.

(1) In order to understand correctly the data requirements in the elementary processes in fusion research and plasma physics, the SG members, who were primarily atomic and molecular physicists, had to learn basic knowledge of CTR by experts in the field of fusion research. A document recording an instruction meeting was published[14].

(2) It was necessary to establish what kind of atomic data are to be actually compiled and what is the most useful format for compilation and dissemination of data.

The working team consists of specialists in the fields of atomic collision physics and atomic and molecular spectroscopy, who participate in this joint-research project from different universities and institutes all over Japan. The working team of the present SG consists of 10 experimental, 7 theoretical atomic and molecular physicists and 3 plasma physicists.

After the above preparations, the SG started their compilation in summer 1974, and have issued their first compilation "Cross Sections for Atomic Processes" Vol.1, 1st edition[15] in May 1975. This volume contains the cross section data for processes involving hydrogen isotopes (H, D and T) and their ions which are the main constituents of fusion plasmas, and electrons and photons. This volume includes Radiative Processes, Electron Collisions, Ion Collisions, the Recombination and Electron Attachment, Collisions between Neutral Atoms, the Formation and Dissociation of Molecules, the Related Problems including for instance the passage of beams through gases or the lifetime of the metastable atoms and so on. Some useful tables of universal constants and conversion constants are given in the Appendix. Both theoretical and experimental values of cross sections

are plotted mainly in figures. Some corrections were made in the published values if it was thought definitely necessary. A binder form system is adopted to make it easy adding or replacing with the updated data sheets. The first issue consists of about 300 pages. The figure captions and annotations of tables are all written in English. The explanations are, however, mostly in Japanese, because the publication was intended to the utilization within Japanese researchers at that time. Preparation for publication of the English Edition of the "Cross Sections for Atomic Processes" Vol.1 is in advance. The first issue of the English edition is expected to appear in January, 1977.

Revision and enlargement of the Vol.1 are almost all completed at present. Enlarged part, which consists of mainly Fast Collisions between Neutral Atoms, the Dissociation of Molecules by Ion Impact, and the Broadening and Shift of Spectral Lines in Hydrogen Plasmas and others, will be issued in November, 1976. This addition is about 150 pages, far exceeding the first estimate.

In succession to the Vol.1, and following some discussions with the fusion experts, the compilation works are continued for the publication of the second and the third volumes simultaneously. The second volume will contain the systematic and comprehensive compilation of cross section data, similar to in the Vol.1, on all types atomic processes involving helium, hydrogen, their ions, electrons and photons.

A part (about one half) of the second volume which consists of the Radiative Processes, Electron Collisions and Ion Collisions is nearly completed. Its issue is expected in January, 1977.

In the third volume the SG is intending collection of data on the processes involving impurity atoms and their ions in fusion plasmas. The processes relating to the plasma diagnostics, the neutral injection heating and other fusion technological problems are also included. Information on these processes is one of those areas with the highest demand at the present stage of fusion research. Since so many kinds of atoms are involved in these processes, systematic compilations as in the first and the second volumes were not practical. Related to the impurity elements, rather systematic survey is being done concerning the availability of data on energy levels of their highly ionized ions, cross sections for excitation and ionization by electron collisions, cross sections for charge exchange by collision with hydrogen atoms or ions, and other processes. The task of compilation for some parts of the volume three has been nearly completed. These parts will be issued as preprints as follows:

1. TAWARA, H., "Cross Sections for Charge Transfer of Hydrogen Beams in Gases and Vapors in the Energy Range 10 eV - 10 keV." IPPJ-AM-1, to be published in December, 1976.
2. KATO, T., "Excitation and Ionization of Ions by Electron Impact - a Review of the Calculation by Means of Semi-Empirical Formulae" IPPJ-AM-2, to be published in December, 1976.
3. MORI, K. et al., "Energy Levels and Grotrian Charts of Highly Ionized Ions of Iron (F_e^{n+}) n = 8 ~ 26" to be published in February, 1977.

Finally the SG set up as its sub-group a group for data compilation on the plasma-wall interactions in the beginning of the 1976 fiscal year. Current leader of the group is J. Okano (Osaka University). Members of the group consists of about 10 specialists who are following the research in surface physics and vacuum technology.

Official Plans Announced by the Institutes in Fusion Research

1) The IPP has a plan to establish the Research Information Center on

a three years program, starting at the next fiscal year. The activities of the SG described in the preceding section are expected to be succeeded officially in one of divisions of this center as its own activities and be extended further. For the long range plan to computarize the bibliographic and numerical data, the IPP has installed a large scale computer system FACOM-M190, and planned to purchase a filing system, a class of IBM115981-D01.

2) A committee was organized for atomic and molecular data in Japan Atomic Energy Research Institute (JAERI) in July, 1976. The Committee consists of about 20 scientists, belonging respectively to different divisions of JAERI. Chairman of the Committee is K. Tsukada (Division of Physics, JAERI). The Nuclear Data Center (Chief, T. Fuketa) of JAERI, to which the Nuclear Data Laboratory (JAERI) was officially promoted on June 1976, announces its plan to enlarge its organization in a three years schedule beginning at the fiscal year of 1977, and to start a compilation and dissemination of atomic and molecular data as its additional activities.

2. BRIEF SURVEY OF RESEARCH ACTIVITIES ON ATOMIC AND MOLECULAR DATA FOR FUSION IN JAPAN

Almost all physicists in Japan join the Physical Society of Japan and/or the Japan Society of Applied Physics, membership of which is about 15,000 and 8,000, respectively. Physicists less than a few percent of them are possibly interested in the production of atomic and molecular data directly. Larger part of original works is published in monthly journals: Journal of Physical Society of Japan, Japanese Journal of Applied Physics and the Progress of Theoretical Physics. Informations acquired by preliminary measurements or calculations are given frequently in bulletins or reports which are issued by respective institutes or faculties. A monthly circular "Kakuyugo-Kenkyu" (Fusion Research) for the Nuclear Fusion Group in Japan includes results of preliminary studies in the field of CTR and plasma physics. Proceedings of symposia or workshops are often issued as the Supplements of this circular.

A) Researchs on Atomic Structure

We have a long history since the achievements by Nagaoka and Takamine in the atomic and molecular spectroscopy in Japan. The Spectroscopical Society of Japan has a membership of about 950. At present, however, only a minor part of the members is engaging in the atomic and molecular spectroscopy, which is useful to produce data on atomic structures such as energy levels, their lives, oscillator strengths and so on.

Besides to the above society, the Mass Spectroscopy Society of Japan has also a membership of about 1000. Monthly journal "Mass Spectroscopy", which is published by this society, contain original papers (mostly written in Japanese or English), dealing with data on structures and formation of various species of atomic or molecular ions.

On the other hand, there is an enduring group of theoretical physicists, who are mainly engaging in the theoretical calculation of atomic and molecular structures. Progress Report, Contributions from the Research Group on Atoms and Molecules, which is published annually, contains the annual reports by the members of the group and a list of publications of all the members. This Progress Report is prepared and offered by E. Ishiguro (Faculty of Science, Ochanomizu University). The latest number of this publication, No.12, was issued in May, 1976. A membership of the group is about 80.

Some members of the above group consists of a group for developing a Library of Computer Program for the large scale quantum mechanical calculations of atomic and molecular structures. This is one of the Application Program Libraries of the Computer Centre, University of Tokyo, and the leadership of this is taken by K. Hijikata (The University of Electro-Communications).

A list of investigators who are involved in the studies which are expected to produce atomic structure data is given in Appendix 1. Only those who are supposed to have large possibility to supply data directly related to fusion research are included in this list. Although this one leaves much to be filled up, this kind of list is desirable to be completed because of its convenience of referring to possible sources of new data.

B) Researchs on Atomic Collisions

We have about 200 researchers, including graduate students, in the field of electronic and atomic collisions. They consist a rather definite group. A circular for the group is issued bimonthly, the latest issue, of which No.48, was distributed in September, 1976. Progress Reports, Studies of Atomic Collisions and Related Topics in Japan, was published in March, 1971 and March, 1974. These reports, edited by K. Takayanagi, which contain not only the reports of respective activities of the researchers in this field but a comprehensive list of publications by the group members.

A review which describe research activities in this field in Japan until 1974 has been published [16]. On the basis of these courses, establishment of the Society for Atomic Collision Research (Japan) is being anticipated in October, 1976. The progress report is planned to be published annually from the 1976 academic year by the Society.

A list of researchers, who are following the atomic collision studies, is given in Appendix 2.

C) Researchs on Surface Interactions

Several programs of experiments have started to acquire quantitative informations on the plasma-wall interactions. Data on sputtering and blistering of first wall materials by plasma-particle impingements are considered to be the most important. Names of investigators and their subjects, which aim directly at these data for developing the CTR devices, are listed in Appendix 3.

On the other hand, we have many researchers in a variety of fields relating to the interactions between atoms (molecules) and solid surfaces. In the joint conference of the International Vacuum Congress and the Conference on Solid Surfaces, held in Kyoto at 1974, 600 Japanese scientists participated.

Many of the studies has for their object respective application areas. We can expect, however, useful data especially to fusion technology from the studies as follows: (1) Studies of adsorption and desorption of gaseous atoms (molecules), which were started initially for applications to catalytic actions. (2) Studies of ion impingement, with applications to ion implantation technology. (3) Studies of ion scattering, electron diffraction, electron scattering, Auger emission, photoelectric emission etc., which were made for applications to surface structures. (4) Studies of atom-surface interactions, accompanied by the vacuum technology.

3. SHORT REMARKS ON POSSIBLE USERS OF ATOMIC AND MOLECULAR DATA IN JAPAN

We have about 700 persons who are engaging in the field of CTR in Japan. When we make a plan of national scope for compilation and dessemination of atomic and molecular data, we will ought to prepare it based on the idea that the greater part of the above persons will be the possible users of the data.

A few examples will be mentioned about the data needs which are essential to resolve the problems in the intermediate or large scale toroidal plasma devices operated or planned in the central institutes for CTR in Japan.

Two intermediate scale tokamak devices, JFT-2 and JFT-2a (DIVA), are under operation in JAERI [17]. Spacial distributions of densities of oxygen impurity ions, from OIV to OVIII , was recently measured in JFT-2, by means of the extreme ultraviolet and soft X-ray spectrometry [18]. Similar measurements on carbon, iron and molybdenum are in progress. In the diagnostics using spectroscopic measurements in JFT-2a, data of line spectra of Au ions are particularly needed, because this device has limiters covered by gold films. Energy analyses of neutral particles for determination of ion temperatures of plasmas in the both tokamak are also under way. A neutral beam injector, 30 keV and about 7 A, was recently installed to JFT-2 tokamak.

A large tokamak JT-60 is now under design at JAERI [19]. A series of calculations has been performed about the transport, density distributions and radiation losses of impurity ions in a tokamak devices [20-21]. According to a tentative conclusion by the designers group for JT-60, its first walls will be made of all molybdenum. Design of a large neutral beam injector is also in advance [22]. JAERI also has a plan for JT-4, a tokamak device with axisymmetric divertors [23].

A intermediate scale device JIPP T-II, which has a hybrid configuration of tokamak and stellarator, started its run recently at IPP [24]. Diagnostics of plasmas using the vacuum ultraviolet and soft X-ray spectroscopy and the passive and active type fast neutral analyses are in preparation. A neutral injector for additional heating of JIPP T-II is also under construction. A designing of RFC-XX, which is a large scale device for radio-frequency plugging of multi-ion plasmas in a cusped field, is in advance at IPP. The designers of this device require particularly a set of data of charge transfer cross sections of H, He, Li and their ions with possible residual gases in a vacuum. Their requests are also on the ionization and charge changing cross sections of Nb ions by electron and neutral molecule collisions.

Finally one of special requests is found in a plan for high β experiment. Data on plasma-wall interactions in the fused quartz material are in the special needs by the designers of a new toroidal screw pinch device, ETL TPE-2, which is planned at the Electrotechnical Laboratory.

REFERENCES

[1] Bibliography of Atomic and Molecular Collisions
I. Heavy Particle collisions with electronic transition (theory)
II. Rotational and vibrational transitions in collisions (theory)
III. Theory of intermolecular forces
Science Reports of the Saitama University, Series A, V 1 (1965) 14.
[2] Bibliography of Atomic Collisions, prepared by TAKAYANAGI, K.,

Institute of Space and Aeronautical Science, University of Tokyo
No.1 Rotational and vibrational transitions in molecular collisions (experimental, 1927-1964) (1966)
No.2 Ionic impact (experimental, 1923-1965) (1967)
No.3 Ionic impact (experimental, 1966,1967) (1968)
No.4 Heavy particle collisions with electronic transitions (theoretical, 1964-1967) (1969)
No.5 Electron collisions with atoms and molecules (experimental, 1921-1960) (1969)
No.6 Electron collisions with atoms and molecules (theoretical, 1924-1963) (1971)
No.7 Electron collisions with atoms and molecules (experimental, 1961-1967) (1973)
No.8 Electron collisions with atoms and molecules (theoretical, 1964-1967) (1974)
No.9 Electron collisions with atoms and molecules (theoretical, 1968-1970) (1975)
No.10 Theory of rotational and vibrational transitions in molecular collisions (1965-1975) (1976)

[3] TAKAYANAGI, K., TAKAHASHI, T., Effective Cross Sections for Collision Processes between Molecular Nitrogen and Slow Electrons, Bulletin of Institute of Space and Aeronautical Science, University of Tokyo 2 (1966) 1309-1355 (in Japanese, with Abstract in English).

[4] TAKAYANAGI, K., TAKAHASHI, T., Effective Cross Sections for Collision Processes between Molecular Oxygen and Slow Electrons, ibid. 3 (1967) 521-547.

[5] TAKAYANAGI, K., Atomic and Molecular Processes in Ionosphere, ibid. 4 (1968) 26-48.

[6] TAKAYANAGI, K., ONDA, K., Effective Cross Section for Collision Processes between Atomic Oxygen and Slow Electrons, ibid. 4 (1968) 49-64.

[7] TAKAYANAGI, K., NAKATA, K., Effective Cross Sections for Collision Processes between Molecular Hydrogen and Slow Electrons - with Application to the Upper Atmosphere of Jupiter, ibid. 6 (1970) 849-888.

[8] ITIKAWA, Y., SHIMIZU, M., Effective Cross Sections for Collision Processes between Carbon Dioxide and Slow Electrons - with Application to the Martian Upper Atmosphere, ibid. 7 (1971) 64-92.

[9] TAWARA, H., RUSSEK, A., Charge Changing Processes in Hydrogen Beams, Rev. Mod. Phys. 45, 2 (1973) 178-229.

[10] ITIKAWA, Y., Momentum Transfer Cross Sections for Electron Collisions with Atoms and Molecules, Atomic Data and Nuclear Data Tables 14 (1974) 1-10.

[11] FUJIMOTO, T., SUGIYAMA, I., FUKUDA, K., Collisional-Radiative Coefficients and Population Coefficients of Hydrogen Plasma, Memoirs of the Faculty of Engineering, Kyoto University, 34, 2 (1972) 249-277.

[12] OGATA, Y., FUKUDA, K., Collisional-Radiative Model of Quasi-Stationary Helium Plasma and Its Application to the Plasma in Positive Column, Memoirs of the Faculty of Engineering, Kyoto University, 35 (1973) 177-199.

[13] TAKAYANAGI, K., editor, "Report of Research Group in IPP on a Planning of Atomic and Molecular Data Compilation" IPPJ-DT-44 (1974) (with bibliography on atomic processes) (in Japanese).

[14] FUJITA, J., YANO, S., INOUE, N., KONDO, T., Informal Talks on the Role of Atomic and Molecular Collision Processes in Plasma Diagnostics, IPPJ-DT-46 (1975) (in Japanese).

[15] TAKAYANAGI, K., SUZUKI, H., ed., "Cross Sections for Atomic Processes" Vol.1, Processes Involving Hydrogen Isotopes, Their Ions, Electrons

and Photons, IPPJ-DT-48 (1975).
[16] TAKAYANAGI, K., "Atomic Collision Research in Japan" Comments Atom. Mol. Phys. 5 (1975) 13-18.
[17] Japanese Organizing Committee, Fifth Conference on Plasma and Controlled Nulcear Fusion Research, Tokyo (1974), ed., "Nuclear Fusion and Plasma Physics Research in Japan" 7 ~ 10.
[18] FUNAHASHI, A., et al., private communication (August, 1976).
[19] YOSHIKAWA, M., "Conference Report, Large Tokamak Experiments" Nuclear Fusion 15 (1975) 928-931.
[20] TAZIMA, T., INOUE, K., TANAKA, M., AZUMI, M., YOSHIKAWA, M., "Theoretical Studies of Impurity Problems" IAEA-CN-33/A 1-2 Part 2, (1974) 23-29.
[21] TAZIMA, T., et al., "Density Distributions of Impurities and Related Energy Losses in Tokamak Plasmas" JAERI-M 6606 (1976).
[22] SHIRAKATA, H., "Additional Heating in the Japanese Tokamak JT-60" Third Intl. Meeting on Theoretical and Experimental Aspects of Heating of Toroidal Plasma, Grenoble, France (1976).
[23] KITSUNEZAKI, A., SEKI, S., SAITO, R., "JT-4 Program" Intl. Symposium on Plasma Wall Interaction, Jülich (1976) to be published.
[24] "Project JIPP T-II" Res. Rep. IPP-Japan, IPPJ-205, Activities of IPP personnel are reviewed in "Annual Review" Institute of Plasma Physics, Nagoya University.

Appendix 1.

A list of research groups on Atomic Structure Data with key personnel

K. Mori, K. Ando
[The Institute of Physical and Chemical Research]
Plasma Spectroscopy, particularly in extreme ultra-violet and soft x-ray regions.

K. Fukuda, K. Ishii, H. Suemitsu, R. Okasaka, T. Fujimoto
[Faculty of Engineering, Kyoto University]
Plasma spectroscopy in extreme ultraviolet region.
Beam-foil spectroscopy.
Determination of population dencity of atoms and ions in plasmas, using Hook method.
Other studies on elementary processes including excited atoms.

M. Nakamura
[Faculty of Science, Tokyo University of Education]
Atomic and molecular spectroscopy, and photoelectron spectrometry of rare gases and small molecules in vacuum ultraviolet region.

H. Takeyama, T. Oda, R. Ikee, M. Yamagishi*
[Faculty of Science, Hiroshima University]
*[Faculty of Education, Tottri University]
Plasma spectroscopy.

M. Otsuka, K. Sato
[Institute of Plasma Physics, Nagoya University]
Plasma spectroscopy, spectroscopic studies of plasma in contact with some neutral gases.

A. Funahashi
[Division of Thermonuclear Fusion Research, Japan Atomic Energy Research Institute]
Plasma spectroscopy, particularly in extreme ultraviolet region, JAERI JFT-2 and JFT-2a.

I. Hirota, Y. Maejima
[Tanashi Branch, Electrotechnical Laboratory]
Plasma spectroscopy.

T. Sasaki, S. Yamaguchi*, M. Nakamura**, T. Sagawa***
[College of General Education, University of Tokyo]
[* Faculty of Science, Tokyo Metropolitan University]
[** Faculty of Science, Tokyo University of Education]
[*** Faculty of Science, Tohoku University]
Atomic and molecular and solid state spectroscopy, using a 300 MeV storage ring of synchrotorn orbital radiation (SOR-RING).

M. Seya, T. Namioka
[Institute for Optical Research, Tokyo University of Education]
Instrumentations of vacuum ultraviolet spectroscopy.
High resolution spectroscopy of simple molecules.

T. Ishimura
[Faculty of Engineering, Osaka University]
Plasma spectroscopy in extreme ultraviolet region.

T. Kagawa, T. Murai
[Department of Physics, Nara Women's University]
Relativistic Hartree-Fock-Roothaan calculation.
Relativistic multi-configuration self-consistent field calculation of atomic energy levels.
Exact-electronic energies and wave functions of simple molecules by B-O approximation.

K. Ohno, F. Sasaki, K. Tanaka
[Faculty of Science, Hokkaido University]
Quantum mechanical calculations of atomic and molecular structures.
Atomic level and oscillator strength by C. I. and SCF calculation.
ab initio LCAO SCF MO calculation of polyatomic molecules.

H. Tatewaki
[Research Institute for Catalysis, Hokkaido University]
Atomic SCF calculations using Slater-type bases.

S. Iwata
[The Institute of Physical and Chemical Research]
C. I. Calculation with perturbation of molecular states.

O. Matsuoka, H. Taketa*
[The University of Electro-Communications]
[*General Education Department, Kyushu University]
SCF calculation of diatomic molecules, using Gaussian type orbitals.

E. Ishiguro, H. Sato
[Department of Physics, Ochanomizu University]
SCF calculation of molecules, using Slater-type orbitals.

K. Oohata, R. Akamatsu
[Faculty of Science, Kyushu Univeristy]
Calculation of electronic states and reaction process in molecules using BO approximation.

Appendix 2

A list of research groups on Atomic Collision Data with key personnel

S. Ohtani, T. Iwai, K. Okuno
[Institute of Plasma Physics, Nagoya University]
Measurements of excitation, ionization and charge transfer cross sections of highly ionized ions in collision with electrons or neutral atoms are being prepared.

J. Fujita, K. Kadota
[Institute of Plasma Physics, Nagoya University]
Diagnostics of JIPP-T2 by means of fast neutral analysis. Excitation cross section measurement for neutral-neutral collision, on purpose to utilize it for the active plasma diagnostics with the use of neutral beam.

S. Ohtani, H. Suzuki, H. Nishimura
[Institute of Plasma Physics, Nagoya University]
Differential cross sections for ionization and excitation of hydrogen atom by low energy electron impact are being measured. Auger electrons ejected from an atom by electron impact near threshold are also being observed.

H. Suzuki, Y. Wakiya, T. Takayanagi
[Faculty of Science and Technology, Sophia University]
Differential cross sections for excitations of some atoms and molecules by electron impact are being measured with electron spectrometry. Auto-ionizations and Auger effects are being investigated in detail.

T. Iwai, S. Tsurubuchi, M. Kimura
[Faculty of Science, Osaka University]
Inelastic collision processes of water molecule by electron and ion impact are being investigated. Spectroscopical method are used in a variety of collision experiments.

M. Sakisaka, F. Fukuzawa
[Faculty of Engineering, Kyoto University]
Innershell ionization of atoms by ion impact, beam-gas spectroscopy, using 4 MeV van de Graaf accelerator.

Y. Kaneko, K. Okuno, N. Kobayashi
[Faculty of Science, Tokyo Metropolitan University]
Ion-neutral reactions are being studied using an ion-drift tube and double mass spectrometer. Some vibrational excitation cross sections for ion-molecule collisions by means of ion energy-loss spectra are in progress.

N. Oda, F. Nishimura
[Research Laboratory of Nuclear Reactor, Tokyo Institute of Technology]
Atomic process as the fundamental processes of radiation effects on the materials are being studied. Differential cross sections for ionizing collisions of electrons with atoms and molecules have been measured. Experiments on ion-e, ion-$h\nu$ collisions are in preparation.

H. Inoue, Y. Sato
[Research Institute for Scientific Measurements, Tohoku University]
Integrated and differential cross sections for elastic and inelastic collisions of alkali ions with rare gas atoms and some diatomic molecules are being measured.

M. Inoue
[The University of Electro-communications]
Ion-Neutral reactions are being studied using an ion cyclotron resonance mass spectrometer.

T. Arikawa
[Faculty of Technology, Tokyo University of Agriculture and Technology]
Low energy ion-neutral collision processes are being studied by crossed-beam method.

S. Morita, K. Ishii, H. Tawara*
[Faculty of Science, Tohoku University]
[* Faculty of Engineering, Kyushu University]
Measurements of inner shell ionization cross section of various elements by heavy charged particle impact, using a 4 MeV van de Graaff accelerator. The similar measurements in electron impacts, using 300 MeV Lineac.

T. Hamada, Y. Awaya, T. Takahashi
[The Institute of Physical and Chemical Research]
Measurements of inner shell ionization and excitation cross sections for the X-ray production, by high energy and highly ionized ion impacts, using 160-cm cyclotron.

K. Ozawa
[Division of Physics, Japan Atomic Energy Research Institute]
Measurements of the K X-ray emission cross section from various solid targets in collision with high energy ions, using 2 MeV van de Graaf accelerator.

Y. Nakai
[Division of Physics, Japan Atomic Energy Research Institute]
Planning of measurement of cross sections for charge-changing processes of highly ionized ions, by the use of van de Graaff accelerator.

K. Takayanagi, Y. Itikawa, I. Shimamura
[Institute of Space and Aeronautical Science, University of Tokyo]
Electronic, atomic and molecular collision processes are being studied theoretically. Among others, electron transfer processes from highly-ionized atoms to protons and inelastic collisions between highly-excited hydrogen atoms and charged particles have been studied recently, and collision processes in magnetic field are being investigated.

S. Nakazaki
[Faculty of Engineering, Miyazaki University]
Excitation cross sections are being calculated in the Coulomb-Born approximation for some electron-positive ion collisions.

H. Narumi, A. Tsuji
[Faculty of Science, Hiroshima University]
Calculations of ionization and excitation cross sections by Glauber

approximation. Atomic structure of exotic atoms are also investigated.

M. Matsuzawa
[The University of Electro-communications]
Reactions of highly excited Rydberg atoms with other atoms and molecules are investigated theoretically.

T. Watanabe, H. Nakamura
[Faculty of Engineering, University of Tokyo]
Theoretical studies of electronic and atomic collisions in a variety of collisional systems. Structure studies on atoms in excited atates, including super-excited states. Various kinds of resonances are also interested in.

J. Hata

[Faculty of Science, Osaka City University]
Close coupling calculation of resonance scattering of electrons with atoms.

Appendix 3.

A list of research groups on Data of Surface Interactions for Fusion Technology

J. Okano
[College of General Education, Osaka University]
Secondary ion mass spectrometry by various ion impact from the solid target.

H. Akimune
[Faculty of Engineering, Osaka University]
Observations of blistering on the solid surface by proton impact.

Y. Ishibe
[Laboratory of Nuclear Fusion Research, The Institute of Physical and Chemical Research]
Measurement of outgassing rate from solid surface by electron impact.

K. Akaishi
[Institute of Plasma Physics, Nagoya University]
Studies of plasma-wall interaction by means of the ion back-scattering technique and measurements of the sputtering yields using a microbalance.

K. Sone
[Division of Thermonuclear Fusion Research, Japan Atomic Energy Research Institute]
Measurement of sputtering yields of molybdenum and graphite by low energy (0.1-6 keV) proton impact.
Sputtering and blistering experiment by high energy (30-400 keV) ion impact are in preparing.

K. Kamada
[Division of Physics, Japan Atomic Energy Research Institute]
Observations of blistering on the solid surface.

Activities on Atomic and Molecular Data for Fusion in Japan Atomic Energy Research Institute

Yohta NAKAI
Division of Physics
Japan Atomic Energy Research Institute

1. Committee of atomic and molecular data for fusion

A clear aim at tokamak type fusion reactor features the nuclear fusion research in Japan Atomic Energy Research Institute (JAERI). The main devices in operation are JFT-2, a tokamak with major radius of 90 cm and aspect ratio of about 3.6, and JFT-2a, a tokamak with non-circular cross section and divertor. In 1976, the construction of JT-60, a large tokamak with plasma volume of 60 m^3, was started and a planning of a non-circular cross-section tokamak JT-4 is also in progress. Through the activities of this research project, needs of atomic and molecular data have ever been growing.

On the other hand, atomic and molecular data are also naturally important to various fields of researches for the development of atomic energy, for example radiation measurement, radiochemistry, solid state physics, health physics, and so on. Therefore, researchers rather colsely related to the atomic and molecular data are scattered in various laboratories or divisions in JAERI. And the potential research activities and needs for fusion research in JAERI were triggered by the movement of the IAEA meetings to organize an internal committee of atomic and

molecular data for fusion on the 1st of July 1976.

The members of this committee consist of twenty-one scientists within JAERI who are involved in A & M data and/or fusion researches. The committee deals with survey of the present status of A & M data, collection and evaluation of A & M data, recommendation on the measurements of A & M data activities. Three working groups are presently formed within the committee, namely the working groups on (i) atomic structure and computation, (ii) atomic collision and reaction, and on (iii) surface interaction.

2. Present Research Activities on Atomic and Molecular Processes related to Fusion

2.1. A & M research related to tokamak devices

In JAERI according as recent rapid progress of fusion research, especially increasing in confinement time, plasma density, and temperature for tokamak-type devices, many specific atomic and molecular physics problems which are of major importance to the fusion research are realized.

These problems should be solved immediately for the design of proposed scale-up plasma machines such as JT-60, as well as for the progress of current fusion programs.

Because of above reason, research groups involved in fusion are studying these atomic and molecular processes from sheer necessities by their own efforts.

ERRATUM

Page 2. between line 6 and 7

Insert: needed urgently, and planning of long range scopes of A & M data

(1) Studies on plasma-wall interaction

An experimental apparatus to study basic processes of plasma-wall interaction had been constructed. This apparatus as shown in Fig.1 consists of a duoplasmatron ion source, a beam transport system, and target chamber with ultrahigh vacuum system.

The target chamber provides several measuring instruments for various experiments; a cylindrical mirror Auger electron spectrometer, an ion energy analyzer with a quadrupole mass spectrometer and a vacuum electro-micro-balance.

The first experiment by using this apparatus is to measure sputtering yields by low energy proton impact of Mo(polycrystalline) and C(pyrolytic graphite). The former has been done by an in-situ measurement of Auger signals from Mo atoms deposited on a W substrate. The vacuum electromicro-balance is used to calibrate the Auger signals. The measured proton sputtering yields are shown in Fig.2. To the best of our knowledge, these are the first results with regard to proton sputtering yield of molybdenum in the energy range less than 1 KeV. For the latter, a quantitative measurement of hydro-carbon production by the quadrupole mass spectrometer has been done for chemical sputtering yields as well as physical sputtering yields, which are shown in Fig.3.

Subsequent studies which will be done are the measurements of sputtering yields of various materials, for example, Mo of honeycomb structure, SiC, etc. and reflection/re-emission rate of incident light ions from these materials.

(2) Spectroscopic studies on multi-charged heavy impurity atoms

Vacuum ultraviolet emissions of impurity atoms in the plasma of JFT-2 are measured in the wavelengths between 10 and 1300 Å with a grazing incidence monochrometer, which is calibrated by the branching ratio method. The Abel-inverted profiles of emissions from oxygen 1st resonance line (O IV, O V, O VI, O VII, and O VIII) are obtained at the current plateau (80 ms) in the case of B_t = 18 KG, I_p = 160 KA, ne(o) = 2.3 x $10^{13}cm^{-3}$, and T_e = 1.2 KeV. Using the coronal model, oxygen densities in peak emissions are approximately $10^{10}cm^{-3}$ for O V, O VI and $10^{11}\sim10^{12}cm^{-3}$ for O VII - O VIII. Iron and molybdenum densities are found to be about $10^{9}cm^{-3}$. These density profiles are shown in Fig.4.

In JFT-2a, the studies, such as observation of new resonance emission from gold, impurity transport, radiation losses, particle recycling processes, and particle releases from the wall are under way.

2.2. Other activities

By the 2MV Van de Graaff accelerators of JAERI, ion beams such as H^+, D^+, He^+, N^+, Ar^+, and some of more highly charged are now available, with which following studies are being in progress in Division of Physics.

(1) Surface damage studies by ion bombardments

Fig.5 shows the SEM image of (110) surface of Mo bombarded

with 300 KeV Ar^+ ion. With the increase of fluences from $6x10^{17}$ to $2.8x10^{18}$ ions/cm^2, blisters are found to disappear.

Fig.6 is the SEM images of (110) surface of Ge. The image at upper-right shows the surface bombarded with 450 KeV Ar^+ ions at their smallest fluences, where the blisters are seen appearing. At the larger fluences (upper-left) blisters seem not to increase but gas edjection seems to occur as seen from the pores appearing on the surface. At this stage the surface structure proves to be amorphous. Lower two images are enlargements of upper ones.

(2) Inner shell excitation of low atomic number materials by ion bombardments

X-rays from targets such as Be, BeO, B, BN, B_2O_3, Li_2O, MgO and Al_2O_3 bombarded with H^+, He^+, N^+ and Ar are analized by means of crystal x-ray spectrometer. Cross sections for K-α excitations agree well qualitatively with the binary encounter approximation, while those for K-α^2 excitations do not. Spectra with heavy ion excitations are interpreted by the electron promotion mechanism. Chemical shift are observed for B K-α ray and its satellites for the target BN and B_2O_3.

(3) Measurement of atomic collision cross section

In Division of Physics, it has been just started to do experiments for the measurements of ionization and charge transfer cross sections of multi-charged heavy ions in gases. An apparatus to measure the both cross sections simultaneously has been designed and now is being made. As a first experiment,

cross sections for the reactions

$$A^{n+} + G \longrightarrow A^{n+} + G^{+} + e$$
$$\longrightarrow A^{(n-1)+} + G^{+} \quad ,$$

where A's are Ne and Ar; ns, from 2 to 5; and G's H_2 and He should be measured in the energy range from 0.5 to 2 MeV for proton by the end of this fiscal year.

3. Future Prospects

3.1. Research committee of A & M data of JAERI

It may be expected that the present internal committee in Tokai Research Establishment shall be expanded and reinforced as the Research committee of A & M data of JAERI next fiscal year. We also have a plan to make Atomic and Molecular Data Center.

The efforts for data compilation and evaluation should be done by this center in co-operation with other organizations.

3.2. Experimental facilities

(1) A 20MV tandem heavy ion accelerator will be operational and used for researches including atomic physics by the beginning of 1979.

(2) A facility for the in situ observation of surface damages by heavy and light ions are-being constructed and installed at the JAERI 2MV Van de Graaff accelerator. It will be in operation by March 1977.

Figure Captions

Fig. 1 Schematic representation of the experimental apparatus. EMB: electro-micro-balance, QMS: quadrupole mass spectrometer, and AES: Auger electron spectrometer.

Fig. 2 Experimental data of proton sputtering yield for molybdenum target as a function of proton energy. Finfgeld's data are also shown.

Fig. 3 Experimental data of proton physical sputtering yield of pyrolytic graphite as a function of proton energy. Target temperature: 500 °C

Fig. 4 Impurity density profile in the plasma of JFT-2.

Fig. 5 SEM images of (110) surface of Mo bombarded with 300 KeV Ar^+.

Fig. 6 SEM images of (110) surface of Ge bombarded with 450 KeV Ar^+.

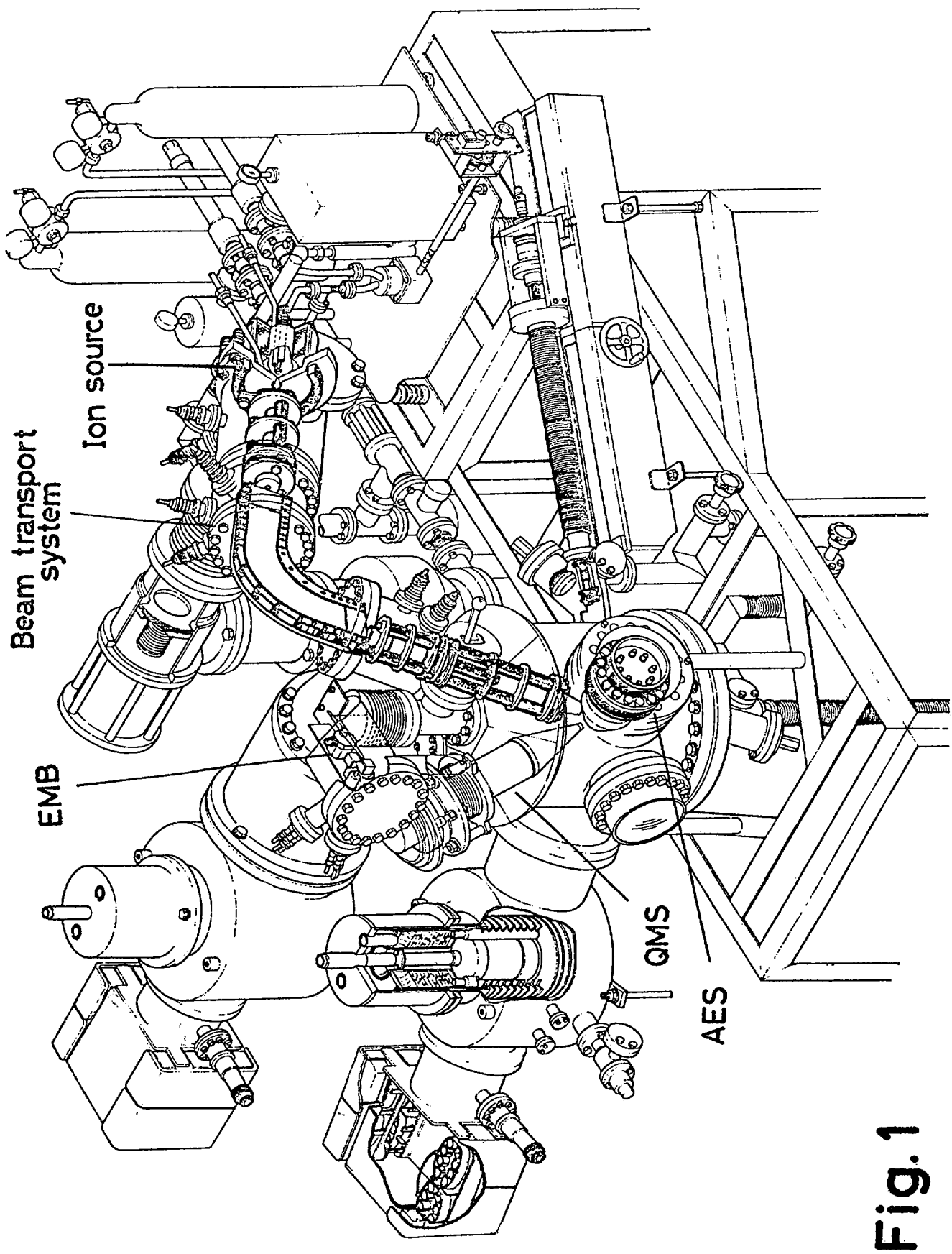

Fig.1

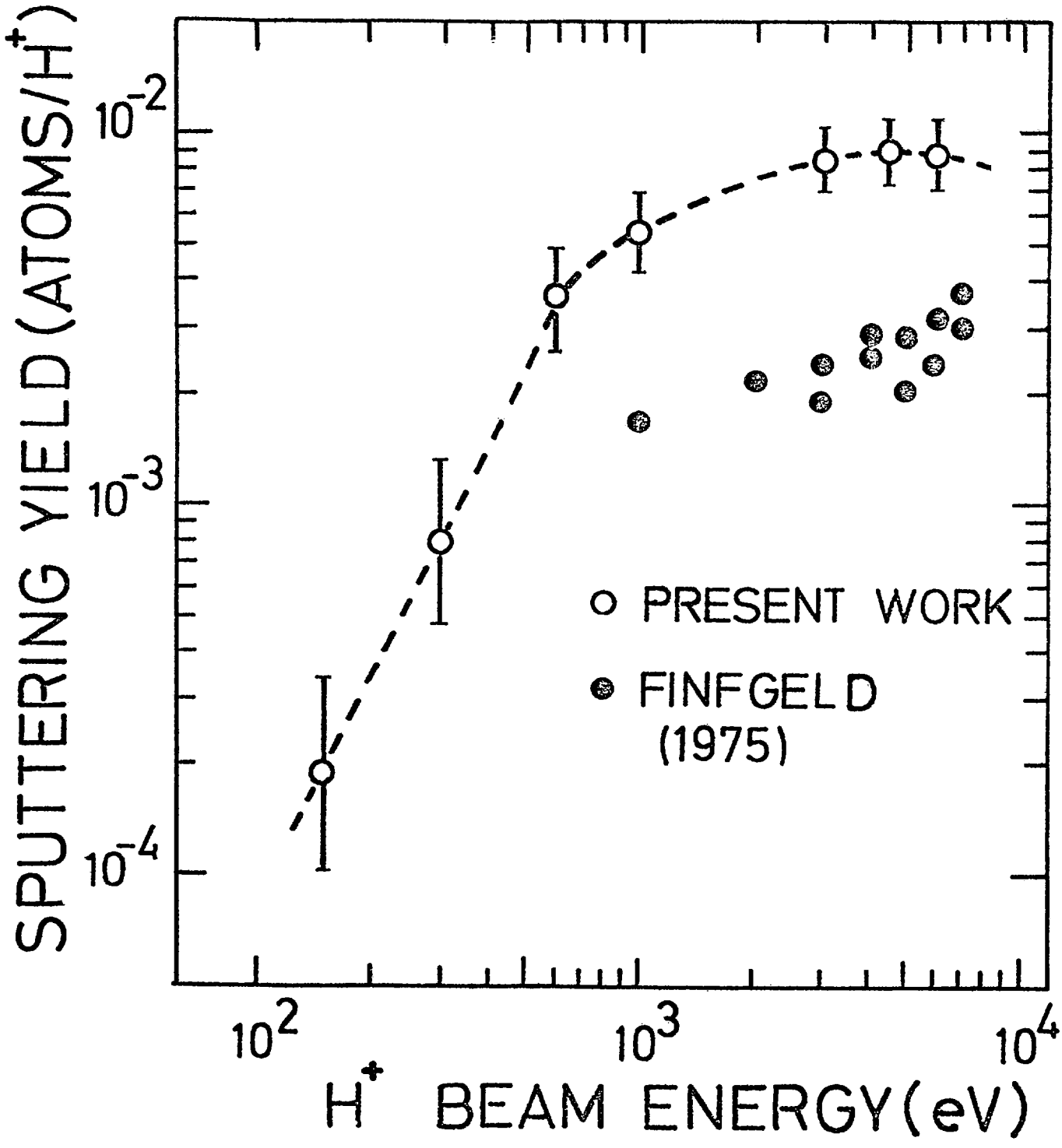
SPUTTERING YIELD (ATOMS/H+)
10-2
10-3
10-4
PRESENT WORK
FINFGELD
(1975)
10²
10³
10⁴
H+ BEAM ENERGY (eV)

Fig.2

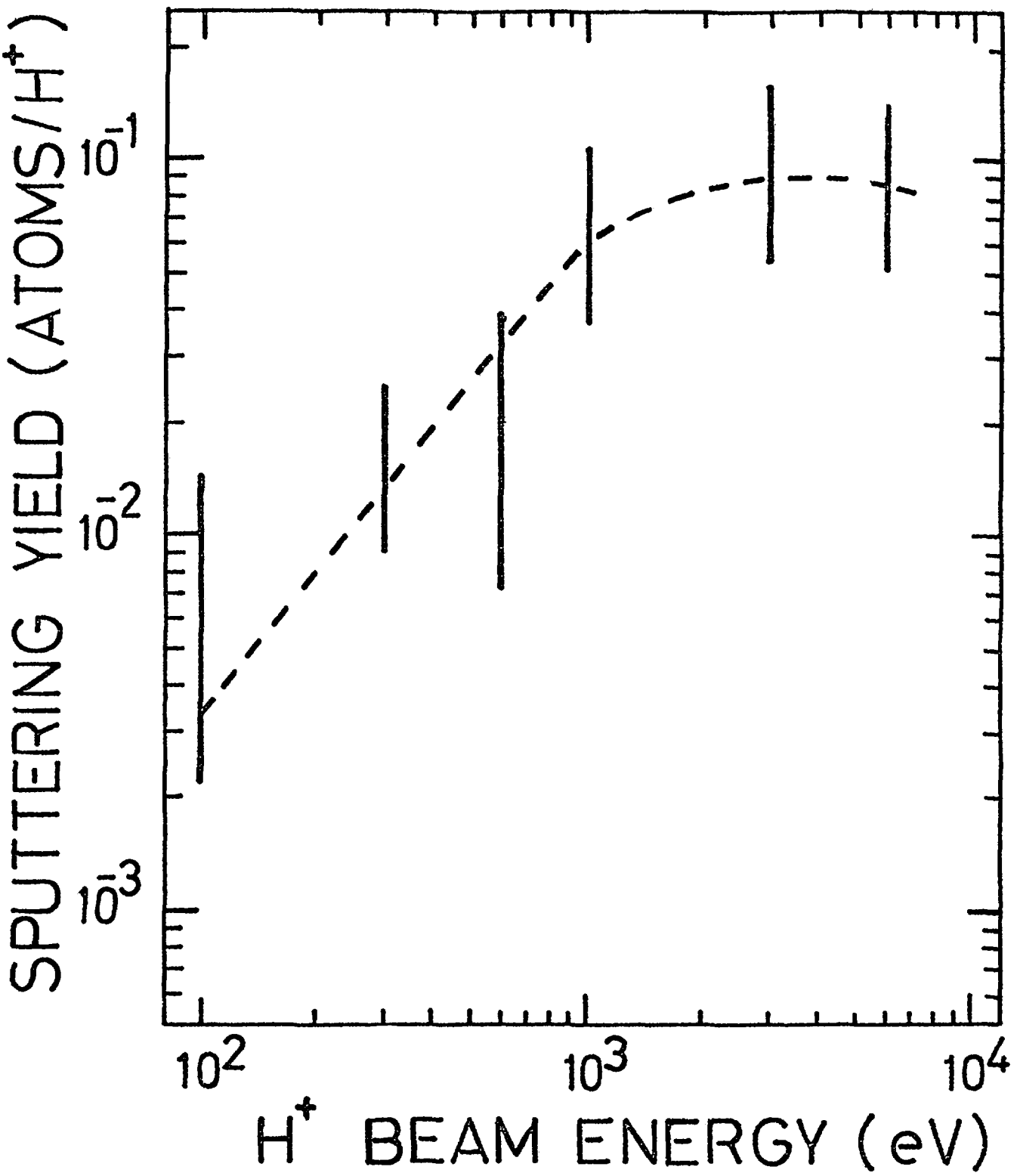
SPUTTERING YIELD (ATOMS/H+)
10-1
10-2
10-3
10²
10³
10⁴
H+ BEAM ENERGY (eV)

Fig.3

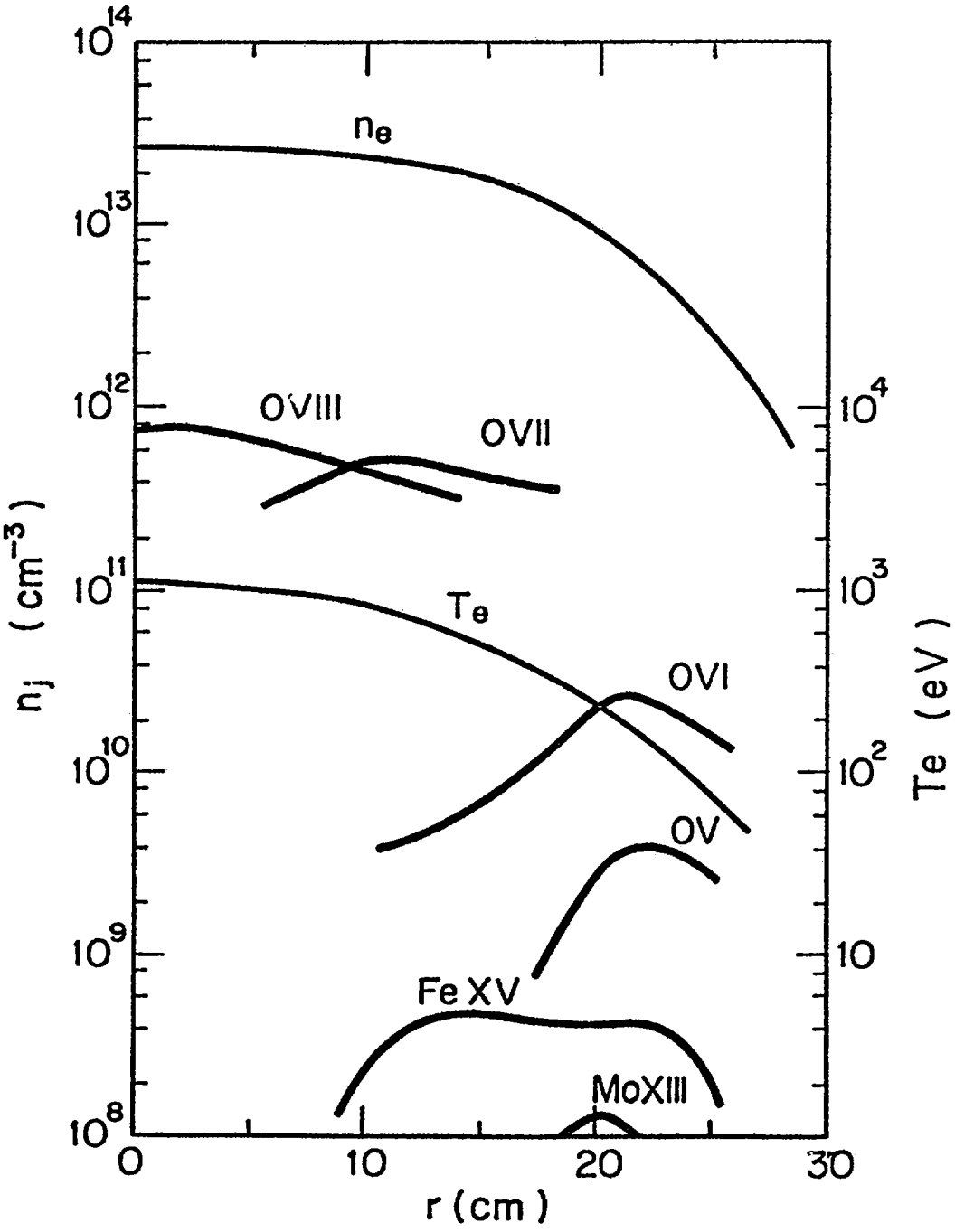
10^{14}
10^{13}
10^{12}
10^{11}
10^{10}
10^{9}
10^{8}
n_j (cm^{-3})
n_e
OVIII
OVII
T_e
OVI
OV
Fe XV
MoXIII
10^4
10^3
10^2
10
Te (eV)
0
10
20
30
r (cm)

Fig. 4

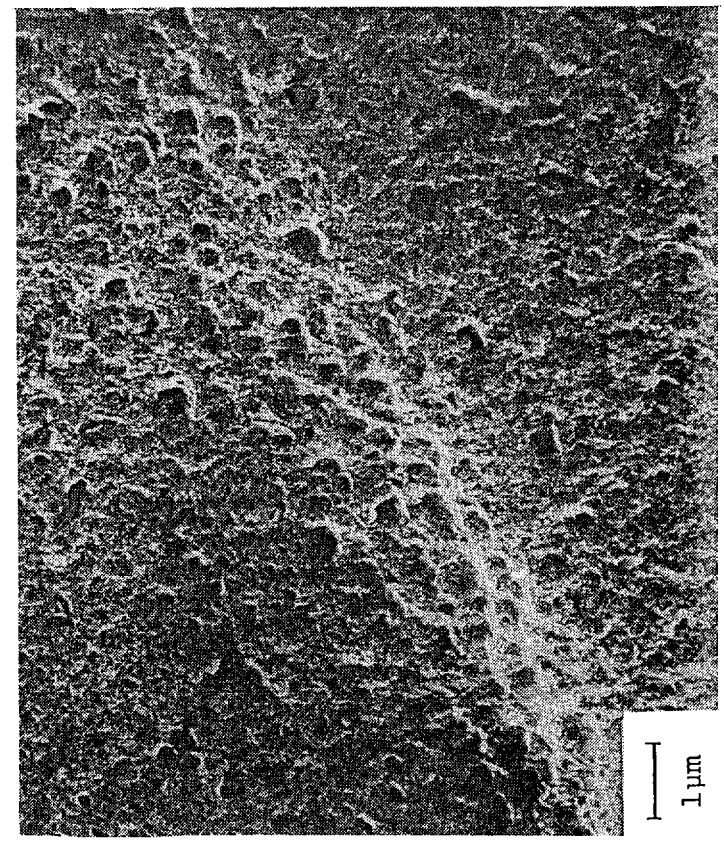

300KeV Ar^+ ; 2.8×10^{18} IONS/CM^2

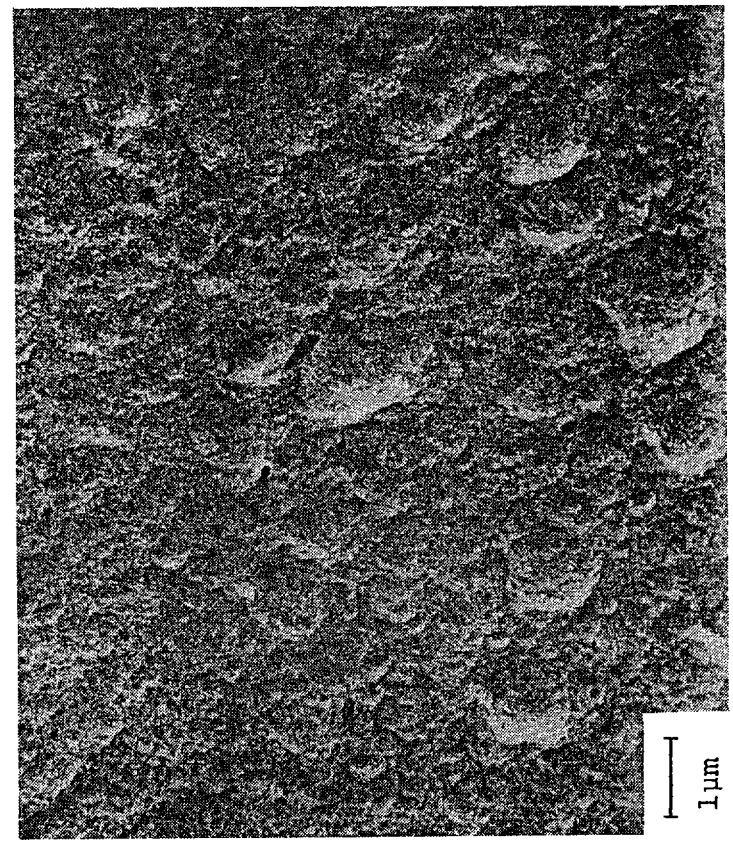

300KeV Ar^+ ; 6.2×10^{17} IONS/CM^2

Fig.5

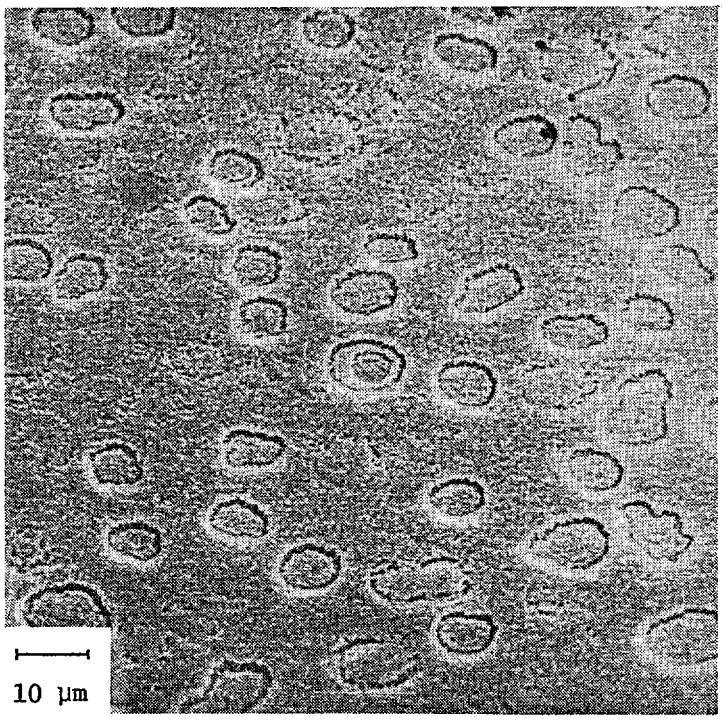

450KeV Ar^+ ; $\sim 10^{17}$ IONS/CM^2

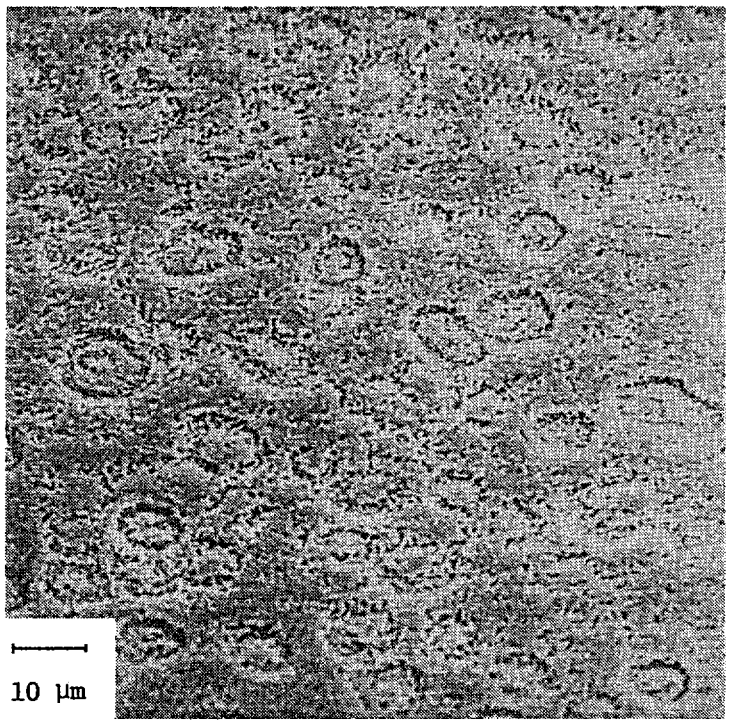

450KeV Ar^+ ; $\sim 10^{18}$ IONS/CM^2

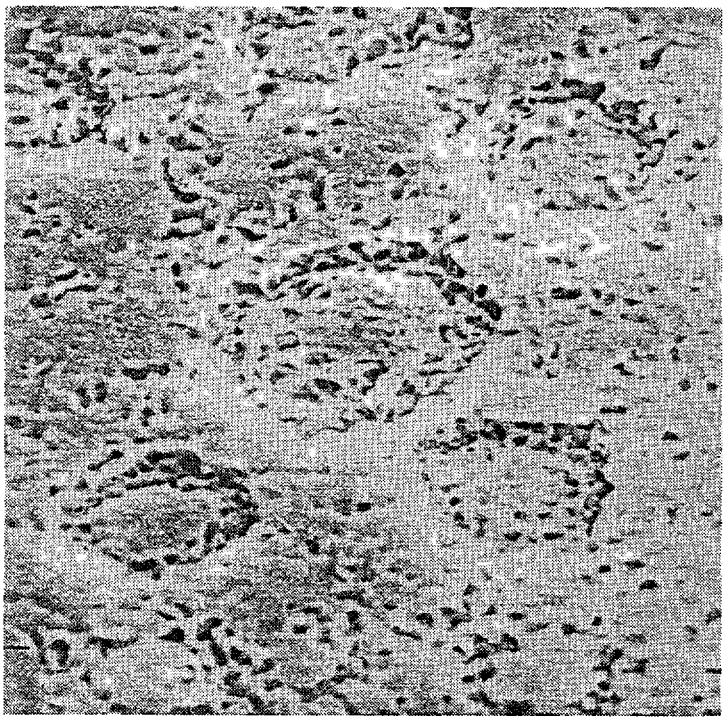

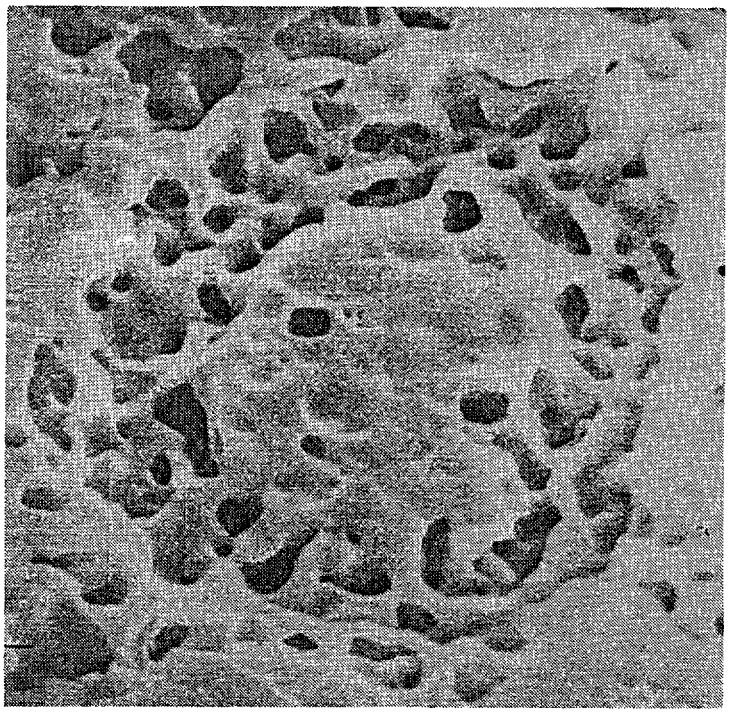

Fig.6

Translated from Russian

Review Paper B4

ATOMIC AND MOLECULAR DATA FOR NUCLEAR FUSION IN THE USSR

V.A. Abramov and Yu. V. Martynenko
I.V. Kurchatov Institute of Atomic Energy, Moscow, USSR

At present controlled nuclear fusion research is being intensified throughout the world. Every year the number of laboratories and personnel engaged in this field is increasing, and new experimental facilities are being built and designed. The development of fusion research at the present stage is associated with the construction of large and costly research facilities requiring the efforts not of one institute but of many organizations.

The USSR has a nuclear fusion programme embracing both pure plasma physics and applied problems, a programme designed to combine the efforts of many organizations. Studies of different reactor systems are being planned, but the main effort will be concentrated on the development of Tokamaks, which are now regarded as the most probable prototypes of future fusion reactors. The main problems in this direction are:

1. The initial stage of discharge;
2. Equilibrium of the plasma column, and various instabilities;
3. Methods of additional plasma heating;
4. Plasma-wall interaction;
5. Fuel injection;
6. Plasma diagnostics;
7. Technical aspects.

Almost all the above problems require a knowledge of atomic and molecular (A + M) data for their solution. In this connection, a number of laboratories engaged in the study of atomic and molecular processes are now taking up work under the controlled fusion programme. For example, Afrosimov's laboratory (Leningrad Physico-Technical Institute) is working on corpuscular plasma diagnostics. There is, however, no unified programme aimed at obtaining specific A + M data as yet. Relevant studies are being

carried out in individual laboratories, but not as part of a coherent programme subordinated to the general aims. Nevertheless, abundant data have been accumulated to date, and there are possibilities of obtaining a large amount of the A + M data needed for controlled nuclear fusion.

At present, the following data of interest for fusion are available in the USSR:

1. The cross-section for ionization and excitation of molecular and atomic hydrogen by electrons [1];
2. The cross-section for dissociation of molecules by electrons [2];
3. The cross-section for the formation of negative hydrogen ions [3];
4. The cross-section for charge-exchange of hydrogen ions on hydrogen atoms and molecules [4];
5. The cross-section for stripping of positive and negative hydrogen ions on atoms and breakdown of negative ions by electrons and the electric field [1, 3];
6. The cross-section for excitation and ionization of atoms and ions with different degrees of ionization [1, 5];
7. Cross-sections for excitation and ionization in collisions between ions, including collisions between multiply charged ions [6];
8. Ionization potentials and electron energy levels of multiply charged ions [7];
9. Oscillator strengths for transitions in multiply charged ions [1, 8];
10. Cross-sections for bremsstrahlung on multiply charged ions [9];
11. Recombination cross-sections [4, 10], including di-electron recombination [10];
12. The characteristics of X-ray spectra [7];
13. Ionization cross-sections for the internal shells of atoms and ions in collisions with electrons and ions [6];

14. Coefficients of ion-induced sputtering for different materials [11, 12].

A large amount of information on A + M data is contained also in individual articles which are not cited in the list of references.

A + M data are compiled in the USSR in the form of monographs such as:

"Tables of spectrum lines", A.R. Striganov and N.S. Svetitskij;

"Cross-sections for excitation and ionization of atoms and ions by electron impact", L.A. Weinstein, I.I. Sobelman and E.A. Yukov;

"Atomic collisions and elementary processes in plasma", B.M. Smirnov;

and also in review papers, for example:

"X-ray spectroscopy of high-temperature plasma", L.P. Presnyakov, Usp. Fiz. Nauk 119 1 (1976).

Bibliographic data are collected in the periodic publications of the Institute of Scientific Information of the Committee on Science and Technology and the Academy of Sciences of the USSR, viz. the monthly Referativnyj Zhurnal "Fizika", a composite volume containing, in particular, sections on "The Physics of Atoms and Molecules", "Spectroscopy" and "Interactions between Radiations and Solids".

Referativnyj Zhurnal prints abstracts of articles and monographs 4-12 months after their publication.

"Signal'naya informatsiya" contains bibliographic indexes on individual branches of physics and is published twice monthly - 24 bulletins a year. The description of an article appears in a bulletin 2-3 months after its publication. From the standpoint of A + M data for nuclear fusion, the issues of "Atomy i Molekuly" and "Plazma" are of the greatest interest.

In the USSR, there are several centres for the collection of A + M data:

1. "Centre for Atomic Spectra of Highly-Excited Atoms" (vacuum ultraviolet), Institute of Spectroscopy of the USSR Academy of Sciences, Eh. Ya. Kononov;

2. "Spectrum Lines Centre for Plasma and Laser Specialists", I.V. Kurchatov Institute of Atomic Energy, A.R. Striganov;

3. "Centre for Molecular Spectroscopy" of the Siberian Branch of the USSR Academy of Sciences (Novosibirsk);

4. "Centre for Atomic and Molecular Constants" under the State Service for Standard and Reference Data. This Centre was established in 1975; its data bank is still small and mainly contains data on the structural constants of complex molecules.

At present a centre of A + M data for fusion is being established at the I.V. Kurchatov Institute of Atomic Energy, whose purpose will be to collect bibliographic material and compile and evaluate A + M data for fusion. International co-operation on A + M data for nuclear fusion within the framework of the IAEA will also enlist the services of this Centre. We regard such co-operation as absolutely essential.

For the purpose of facilitating international exchange of information it is advisable to devise a single international format for recording bibliographic and reference material and also a code for computer storage and retrieval of the information.

The format and code should obviously be prepared at the IAEA on the basis and after the analogy of those already in existence at the IAEA and at national centres. It will obviously be desirable to adopt codes already in use at nuclear data centres, wherever possible, in order to achieve saving on computer processing.

REFERENCES

[1] WEINSTEIN, L.A., SOBELMAN, I.I., YUKOV, E.A., Secheniya vozbuzhdeniya atomov i ionov (Excitation cross-sections of atoms and ions), Izd. "Nauka" (1973).

[2] Khimiya plazmy (Plasma chemistry) (SMIRNOV, B.M., Ed.), Atomizdat, 1 (1974); 2 (1976).

[3] Iony i vozbuzhdennye atomy v plazme (Ions and excited atoms in a plasma) (SMIRNOV, B.M.), Atomizdat (1974).

[4] Atomnye Stolknoveniya i Ehlementarnye Protsessy v Plasme (Atomic collisions and elementary processes in plasma) (SMIRNOV, B.M.), Atomizdat (1968).

[5] Cycle of studies of the Uzhgorod State University, laboratory of I.P. Zapesochnyj, see Optika i Spektroskopiya 1965-1976.

[6] Cycle of studies of the Leningrad Physico-Technical Institute, laboratory of V.V. Afrosimov, see Zh. Ehksp. Teor. Fiz. and Zh. Tekh. Fiz. 1962-1976.

[7] WEINSTEIN, L.A., SAFRONOVA, U.I., Preprint, Inst. of Spectroscopy, USSR Academy of Sciences, No. 6, Moscow (1975).

[8] PENKIN, N.P., */ 4 1 (1964) 41-94.

[9] GERVIDS, V.I., KOGAN, V.I., Pis'ma Zh. Ehksp. Teor. Fiz., 22 6, 308-312.

ZHDANOV, V.P., CHIBASOV, M.I., Pis'ma Zh. Ehksp. Teor. Fiz. 23 4 (1976) 199.

KIRILLOV, V.D., TRUBNIKOV, B.A., TRUSHIN, S.A., Fiz. Plazmy 1 2 (1975) 218.

[10] BEIGMAN, I.L., WEINSTEIN, L.A., SYUNYAEV, R.A., Usp. Fiz. Nauk. 95 (1968) 267.

[11] PLESHIVTSEV, N.V., Katodnoe raspylenie (Cathode sputtering), Atomizdat (1968).

[12] GUSEV et al., Preprint, I.V. Kurchatov Institute of Atomic Energy No. 2545, Moscow (1975).

*/ Title missing in the original.

COMPILATION AND DISSEMINATION WITHIN THE UK OF ATOMIC AND MOLECULAR DATA RELEVANT TO FUSION RESEARCH

M F A Harrison

Euratom-UKAEA Association for Fusion Research, Culham Laboratory
Abingdon, Oxfordshire OX14 3DB, UK.

Theoretical and experimental research into a wide range of atomic and molecular processes is strongly based within the United Kingdom. The major sponsor is the Science Research Council who support work in both the universities and their own establishments such as the Appleton Laboratory at Culham. Some studies have direct applications to fusion research but the bulk of data has stemmed from initial interests in fundamental atomic properties and in astrophysics. The United Kingdom Atomic Energy Authority also sponsors fusion related studies within the universities and it carries out modest programmes within its Culham and Harwell establishments.

Numerous reviews of relevant data have been produced within the UK and have been published in the international scientific press. In addition the Institution of Electrical Engineers provides both abstracts and subject classifications in their publication "Physics Abstracts". A substantial amount of data is published monthly by the Institute of Physics in its "Journal of Physics B: Atomic and Molecular Physics". Occasional reviews appear in the Institute's series "Reports on Progress in Physics" and details of experimental techniques appear in "Journal of Physics D: Applied Physics". Important papers also appear in the "Proceedings of the Royal Society (Series A)" and in both the "Transactions" and the "Discussions of the Faraday Society".

Within the Institute of Physics there is the Atomic and Molecular Sub Committee (Chairman Professor G W Series) who take responsibility for organising conferences in the field; the main event being the annual National Conference on Atomic and Molecular Physics (ATMOL).

The Oxford University Press in particular has been responsible for the publication of some of the leading reference books in the field, for example "Electronic and Ionic Impact Phenomena" (five volumes) by H S W Massey, E H S Burhop and H B Gilbody and "The Theory of Atomic Collisions" by N F Mott and H S W Massey. Most reference books are reviewed by the Institute of

Physics in its monthly publication "The Physics Bulletin".

There is no national body dedicated to the dissemination of data for fusion research although the Culham Laboratory occasionally publishes reports containing particular compilations; examples are:-

Neutral Injection Heating of Toroidal Reactors, editor D R Sweetman, CLM-R112 (1971).

Reaction Cross Sections of Relevance to Hydrogen Plasmas in Ion Sources, A R Martin, CLM-R157 (1976).

Atomic Processes in Plasma Physics Experiments; Analytic expressions for selected cross sections and Maxwellion rate coefficients.
I - R L Freeman and E M Jones, CLM-R137 (1974)
II - E M Jones (1976).

The Appleton Laboratory also produces compilations of data specifically directed towards astrophysics but which are relevant to fusion research. Two such publications are:-

Tables and graphs of collisional dielectronic recombination and ionization coefficients and ionization equilibria of H-like to A-like ions of elements, H P Summers, I.M.367 (1974).

Bibliographic notes on calculations of excitation of positive ions by electron impact, R W P McWhirter (reproduced for this meeting).

Queen's University Belfast has pioneered the setting up of computerised databanks within the UK; the on line databank at the Computer Centre is described by Professor F J Smith at this meeting. In addition the Department of Computer Science has an international library of programmes particularly relevant to atomic, molecular and astrophysics.

Contributed Paper to Topic B5

THE QUEEN'S UNIVERSITY OF BELFAST

COMPUTER STORAGE, RETRIEVAL AND GENERATION OF ATOMIC DATA

Francis J. Smith
Department of Computer Science
The Queen's University of Belfast
Northern Ireland

Talk given to a meeting of the International Atomic Energy Agency at Culham.

2 November 1976

COMPUTER STORAGE, RETRIEVAL AND GENERATION OF ATOMIC DATA

Francis J. Smith
Department of Computer Science
The Queen's University of Belfast
Northern Ireland

A B S T R A C T

A system has been built at Belfast for the storage, manipulation and retrieval of critical data related to atomic interactions. Included in the data bank are over 2000 interaction potentials which can be retrieved with their reference data in whatever form or units are required by the user. A least square curve fit to the stored data can also be obtained with the correct asymptotic limits in the form of a table, a graph plot sent in the post next morning, as a pseudo-plot on a terminal or as a FORTRAN subroutine which can generate the data. If the data required is not available the system may be able to compute approximate values from other data in the system since relations between sets of data as well as the data itself are stored. For example, from the interaction potentials one can obtain deflection angles, phase shifts, differential and total cross sections and shortly also exchange cross sections, transport properties, virial coefficients, etc., at any energy or temperature for which some data is available.

1. INTRODUCTION

In Belfast we have been building and studying a data bank for Atomic and Molecular Physics. We soon discovered that to cover the whole field of Atomic and Molecular Physics and to do this well was a much greater problem than we had at first envisaged and was beyond the means available to us. We therefore decided to concentrate and specialise first on one specific area of data, that concerned with Atomic Interactions. It is now our view that it is better that we should continue to concentrate on collecting data on one or two areas only and do this well, rather than try to cover the whole field and perhaps do this inadequately. This strategy of specialisation, if it was adopted by all research centres interested in collecting data, would be of benefit to all; some international body such as the International Atomic Energy Agency should assist with the decision on which areas of data should be collected by each centre.

At first in Belfast we set out with the straightforward aim of collecting the data, storing it in computer form, writing software both to manage the data and to help with its critical evaluation. The first phase of this work is almost complete and it is worth noting before going on to the main theme of this paper that the problems associated with data management and security were found to be the most difficult computer problems in this exercise. Nevertheless they were straightforward. What was not so straightforward was the way the retrieval system evolved into something more powerful than was at first envisaged. To understand this it is necessary first to digress into a discussion on how a computer can be used for scientific data handling.

2. SCIENTIFIC DATA HANDLING BY COMPUTER

Basic Facilities

The basic facilities of any computer system for storing and retrieving numerical data are fairly clear: it must be able to provide the user not only with the data itself but also with the reference information from which that data was obtained. It must also be able to keep the data up-to-date; provided the system is designed for immediate updating it should be possible to insert or amend data in the data bank as soon as it is published, or as soon as an addition or amendment is received, and any user should then be able to retrieve this data immediately by means of a terminal.

The ability to obtain up-to-date data as soon as it is needed by any user is only one of the reasons why we believe that a computer numerical data system to-day should be designed for on-line retrieval (and indeed for on-line storage and management). The system should still be able to print out up-to-date copies of tables of the data as most computerised data systems do at present.[1] However, although a scientist can always extract the information he needs from these tables, it is often after much effort. As we shall see it is faster, more convenient and more effective if he can obtain the information directly using a terminal.

The data bank needs to be interrogated by the scientist himself and not by an intermediary, such as a librarian, not only because the cost of such an intermediary is prohibitive to-day, but also because the most powerful part of a well designed on-line data system lies in the interactions of the scientist with the system. Since the basis of this is that the scientist adapts his searches and his commands to the responses he gets from the system no intermediary, unless he is actively involved

in the research or work of the scientist, can be expected to know or to anticipate the reactions of the scientist to the information and questions coming from the system.

Because the on-line data system has to be interrogated by scientists who only occasionally use it and who cannot therefore be expected to remember details of how to use it or to have available a manual for its use, the system has to be simple and self-instructive. This can be done most simply by the scientist answering a series of multiple-choice questions with the option always open to him to seek further information on what to do next.[2] This can be both effective and fast - particularly if the scientist has to type the minimum in reply to each question (he is usually not a good typist). Because numerical data is so much more complicated than reference data it is not easy to produce more direct command languages for a numerical data system as have been produced for on-line reference systems.[3] It may be that the answering of multiple-choice questions is the only way of interrogating numerical data systems in practice.

Units

An on-line data bank such as the one we have described is still difficult to justify when we compare it with the convenience and relative low cost of a book or report. In many cases its expense can only be justified when it begins to do things which the book cannot do. The simplest of these is the changing of the units to suit the user. The user would first answer

a question on the units he requires and the system would give him any subsequent data in those units. This gets rid of one minor inconvenience.

Interpolation

More useful is the ability to interpolate when the data is represented as a table of values such as the table of cross sections in Figure 1. This is a typical example, relevant for much data in Fusion research. The cross sections are known in units 10^{-16} cm^2 at a discreet set of values in units of energy, cal/mole. The user may wish to work in energy units, eV, and to know the values of the cross sections in atomic units. The energies at which he specifically wishes to know the cross sections are unlikely to correspond exactly to the known values. If one of these lies at an energy between two points on the graph, e.g., at point A, then it is a simple matter by using polynomial or spline or some other appropriate form of interpolation to find the corresponding value.[4] Although relatively simple, it takes time and is a source of error and inconvenience to the user. The computer can give him the value he needs at a negligible cost in computer time in the units he wants.

Extrapolation

If the scientist wants data at a point outside the range of the stored data then it is possible to obtain estimates by extrapolation. For example, in Figure 1, the scientist may wish to know the cross sections at point B on the graph. In this case the computer should be able to advise the scientist that it is out of range and, if he wishes, to give him an approximate value by extrapolation. However, to do this effectively, the system would need to have built into it the asymptotic form of the data particularly if the point B is distant from the stored data points. Making such a facility easy to use by any scientist is dangerous as it is likely to provide results with possible very large and unknown errors[5]; therefore, the system should always estimate the possible error and give it along with the data.

Accuracy

The need to give accuracies or possible errors in the data is clearly necessary in the above example where it is well known that extrapolation can cause large errors. However, it is more generally necessary: in our view it is extremely important that the accuracy of data should always be stored with the data. This is particularly important for a system which is going to manipulate the data as it needs to be known if calculations on the data (such as extrapolation) have any meaning for data of the accuracy stored. The storing of accuracy means some separate critical evaluation of the data as it is well known that authors either give no estimates of possible errors in their data or seriously underestimate it.

Curve-fitting

The need for stored error estimates is also apparent when we look at a familiar situation with respect to stored data illustrated in Figure 2: in this there is more than one set of data on a particular cross section represented by the lines on the graph. These sets may overlap, there may be gaps between the data and often we know the asymptotic forms at low or high energies. The scientist may want information on some or all of these sets of data with their reference material. However, he is also very likely to want a "best" value at one or more energies, obtained by drawing a smooth "best" curve through the data. With the conventional data bank he has to retrieve the sets of data, change their units to a common base, use some curve-fitting procedure and calculate the values he needs. However, it is possible to design the data system to incorporate this facility automatically within the system so that a curve fit, the dotted line in the figure, can be obtained if the user wants it - but only if the accuracy of the data is stored with the data.[6]

This automatic procedure must be followed with care. In Figure 3 we have an example of the result obtained when an automatic curve fitting program is used to fit two sets of data representing an interaction potential which has one minimum. Because the two sets of data have found the position of the minimum at two different values of the inter-nuclear distance the curve-fitting procedure has found a curve-fitted potential with a non-existent undulation (or even a double minimum). By interacting with the system the scientist should be able to detect this and select from the data stored only those sets which he wants to have curve-fitted to produce a smooth curve. It is worth noting that such decisions cannot be taken by an intermediary.

Graphs

One of the most convenient methods of comparing different sets of data is by drawing all of the data on the one graph; the same method is effective for examining the curve fit or for displaying any data generated by the system. Doing this with a computer is straightforward but tedious. The data system at Belfast gets rid of these problems by producing graph plots automatically as required. In answer to simple questions the user gives information on the units, the range of data required, his name and address. The system then enters a job in the batch stream to produce a graph-plot of the data required overnight. The graph-plot also prints out his name and address so that the graph can be posted to him first thing in the morning. Such a facility can save a great deal of time and allows comparisons not otherwise possible.

It is also possible to produce pseudo-graphs on a terminal, i.e. approximate graphs produced by characters on each line of print as close as possible to the curve. Because of their inaccuracy these have limited use.

Subroutines

The scientist often wants to extract data from a data bank to use in some calculation of his own. If the data he wants is a single number this presents no difficulty; if he needs a set of numbers at equally spaced points, for example, it is a straightforward matter for the data system to produce the data for the user in computer form at the points and in the units he requires for reading into a program of his own. This can be either on cards or paper tape, or more likely in the future, on a cassette tape or disc.

Another method, more convenient in many cases, is the production of a subroutine which can generate the data he requires when that data can be represented as a function of one (or more) variables. Below we give an example of such a function or subroutine in FORTRAN IV:

```
      FUNCTION XSECT(E)
C  THIS ROUTINE WAS PRODUCED BY THE BELFAST
C  QUISDATA SYSTEM ON 2 NOV 1976.  XSECT IS THE
C  TOTAL ELASTIC CROSS SECTION IN A.U., ENERGY
C  E IN KEV.
C  IT IS VALID IN THE RANGE    1    KEV TO    10   KEV
C  IT WAS CALCULATED BY CURVE FITTING DATA
C  OBTAINED FROM THE FOLLOWING REFERENCES
C     A.B. JONES, J. Chem. Phys. V123, 456-78 (1969)
C     C.D. SMITH, Phys. Rev. V9876, 543-4 (1970)
C
      DIMENSION C(12)
      C(1)=2.4376549
      C(2)=3.5498436
       .
       .
       .
      RETURN
      END
```

This can be printed out on a terminal or produced in computer form like the data above. One advantage of this approach is that within the comments of the function routine it is possible to give clearly the date on which the data was produced and all the source material.

3. GENERATION OF DATA

When we first started building a data bank at Belfast we intended to try to produce a system such as the one described in the previous chapter, a system which contained a number of useful and convenient tools to help the scientist obtain the data he needs, but nothing (apart from extrapolation) to help him when the data was absent.[7] An appropriate use of one of our subroutines which generates data from the data bank is its use in a program which computes such absent data. Thus a scientist can generate the data he really needs from the data made available to him by the system. In its simplest form this type of additional step has already been taken by the system when it changes units or interpolates or extrapolates. However this idea can be taken much further. A scientist may need the total elastic collision cross section at a range of energies at which no data is available, and for which it is impossible to obtain approximate values by extrapolation. Yet within the data bank other data may exist, such as differential cross sections, which give enough information to determine the data he needs quite accurately—if he knows how and if he knows the other data is there. Even if he does know the relationship between the stored data and his own data it may not be straightforward and it may require a major effort for him to perform the calculations. However, if the relations and connections between the different types of data were stored within the system, as well as the data itself, the scientist should then be able to obtain approximate values of the data he needs if related data exists within the data bank. For example, when he asks for his total cross sections, the system should respond that no data is available and ask him if he would like approximate values generated from other data in the system. He could then obtain

these values provided such other data existed and provided that the relations between different types of data were built into the system along with the data. As before, he would be able to obtain all source material, including the source of the methods used for the calculation of his approximate cross sections.

When we examined this concept in relation to atomic collision or interaction data it was clear that the basic or source data for a wide range of properties of atoms was the interaction potentials between atoms. Once these are known it is possible to compute from them a wide range of properties of atoms quickly and accurately if the appropriate numerical methods are used.[8,9,10] This is illustrated diagramatically in Figure 4. We therefore built our data system round a data bank of interatomic potentials. Thus if we obtain some data on the differential cross sections for the scattering of two atoms, if it is possible, instead of storing the cross sections, we store the equivalent interaction potential for the atoms. The system can then regenerate the original data when needed by computation; however, in addition, it is able to generate a whole range of other data from the potential, or rather from a curve fit to this potential obtained from all data for the atom pair. By this means we are able to build a data system of very much greater power and usefulness than would be possible by storing alone the results of the respective experiments (although, of course, the results of these experiments should also be stored). It also gives us a powerful tool with which to compare different data for consistency.

The most important aspect of the system for Fusion research is that it allows us to generate data with some confidence in cases where experimentation would be difficult or still not possible. For example, differential scattering cross sections can probe the short range interaction potentials which can then be used to generate high temperature thermal conductivities or viscosities.

Of course, the physics in the above paragraphs is not new: there is no new physics in our data system. What is new is that the relations between the data (and thus the physics) are built into the system with the data and the scientist is able in 5 or 10 minutes on a terminal to do what might take him weeks to do otherwise. For the untrained scientist, an expert in another discipline, only wanting some data and an estimate of its accuracy, the difference is fundamental. With the computer system he might obtain approximate data in 15 minutes; without it he obtains nothing.

An outline of the computer system we are aiming to build at Belfast is shown in Figure 4. Much of this is already in operation, more than enough to show that the basic principles on which the system was designed appear to be sound.

Undoubtedly, these sets of data provide an appropriate, almost closed, system of data suitable for the concept of building an intelligent data system storing relations between data as well as the data itself. However, we believe that it is far from unique and that the same principles could be applied gainfully to other data systems.

REFERENCES

1. Wigington, R.L., "Information Organisation and Storage... A Review", CODATA Bulletin (March, 1975) 4-13.

2. Kent, G., "Blackboard to the Computer", Ward Lock Educational, London (1969) 106-17.

3. Hall, J.L., "On-line Information Retrieval: A Guide to Systems, Databases and to the Literature", in preparation (U.K.A.E.A., Culham Laboratory, Abingdon, Oxfordshire).

4. Wendroff, B., "Theoretical Numerical Analysis", Academic Press, London (1966) Ch.1.

5. Richards, J.W., "Interpretation of Technical Data", Iliffe Books Ltd., London (1967) 23.

6. Hayes, J.G., "Curve Fitting by Polynomials in One Variable", Numerical Approximation to Functions and Data, Ed. J.G. Hayes, Athlone Press (1970) 48-9.

7. Smith, F.J., "On-line Data Bank in Atomic and Molecular Physics", Physics of Electronic and Atomic Collisions, 7th International Conference, North Holland, London (1972) 492-6.

8. Hirschfelder, J.O., Curtis, C.F. and Bird, R.B., "Molecular Theory of Gases and Liquids", John Wiley, New York (1954).

9. Hirschfelder, J.O. (Editor), "Intermolecular Forces". Advances in Chemical Physics, Vol.12, John Wiley, New York (1967).

10. O'Hara, H. and Smith, F.J., "Transport Collision Integrals for a Dilute Gas", Comp. Phys. Comm., 2 (1971) 47-54.

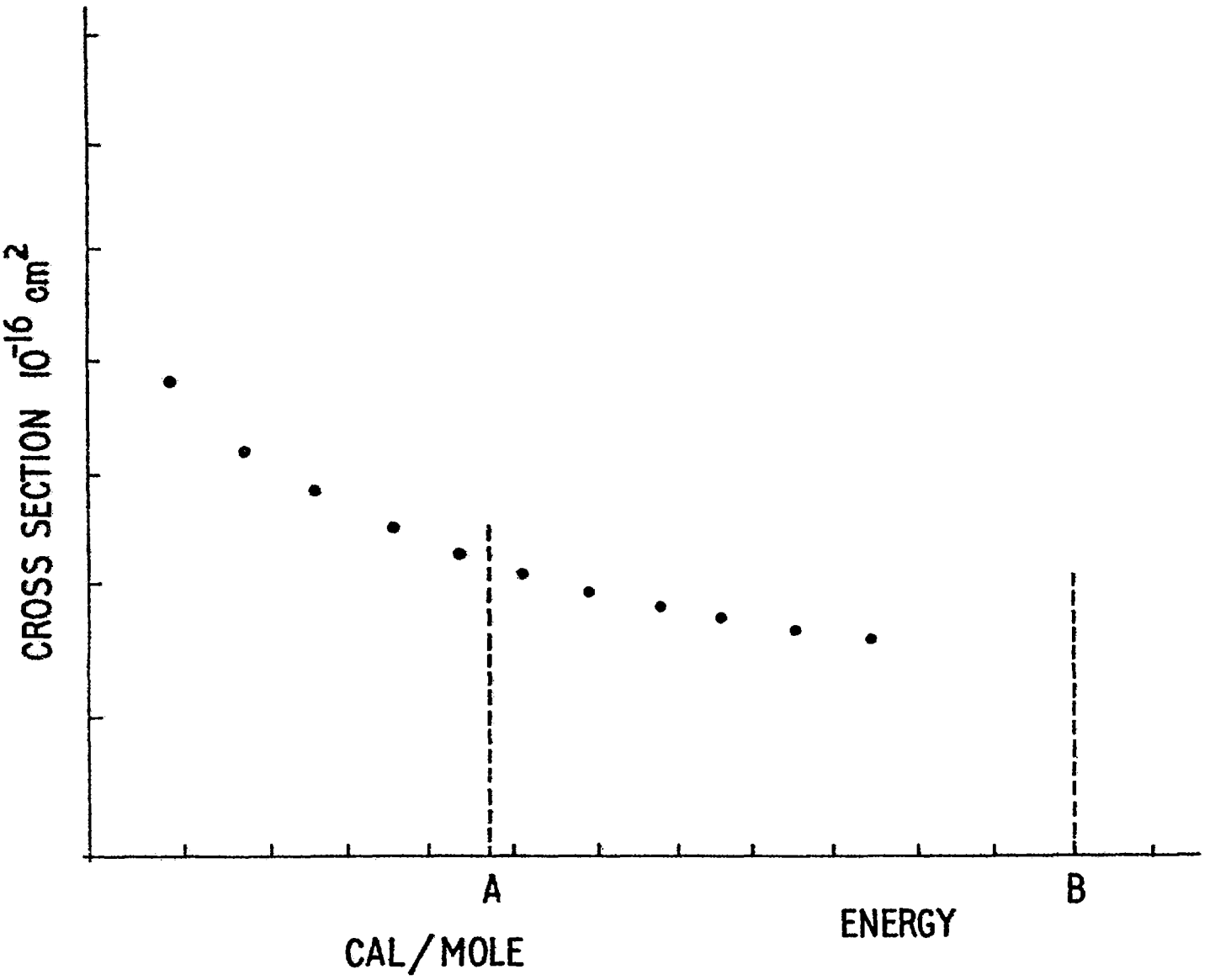

FIG. 1 Cross Section data in units $10^{-16}cm^2$ at a specific set of energies in units cal/mole. The scientist may require cross sections at other energies such as at A and B. The system should be able to obtain these cross sections by interpolation or extrapolation in the units required by the scientist.

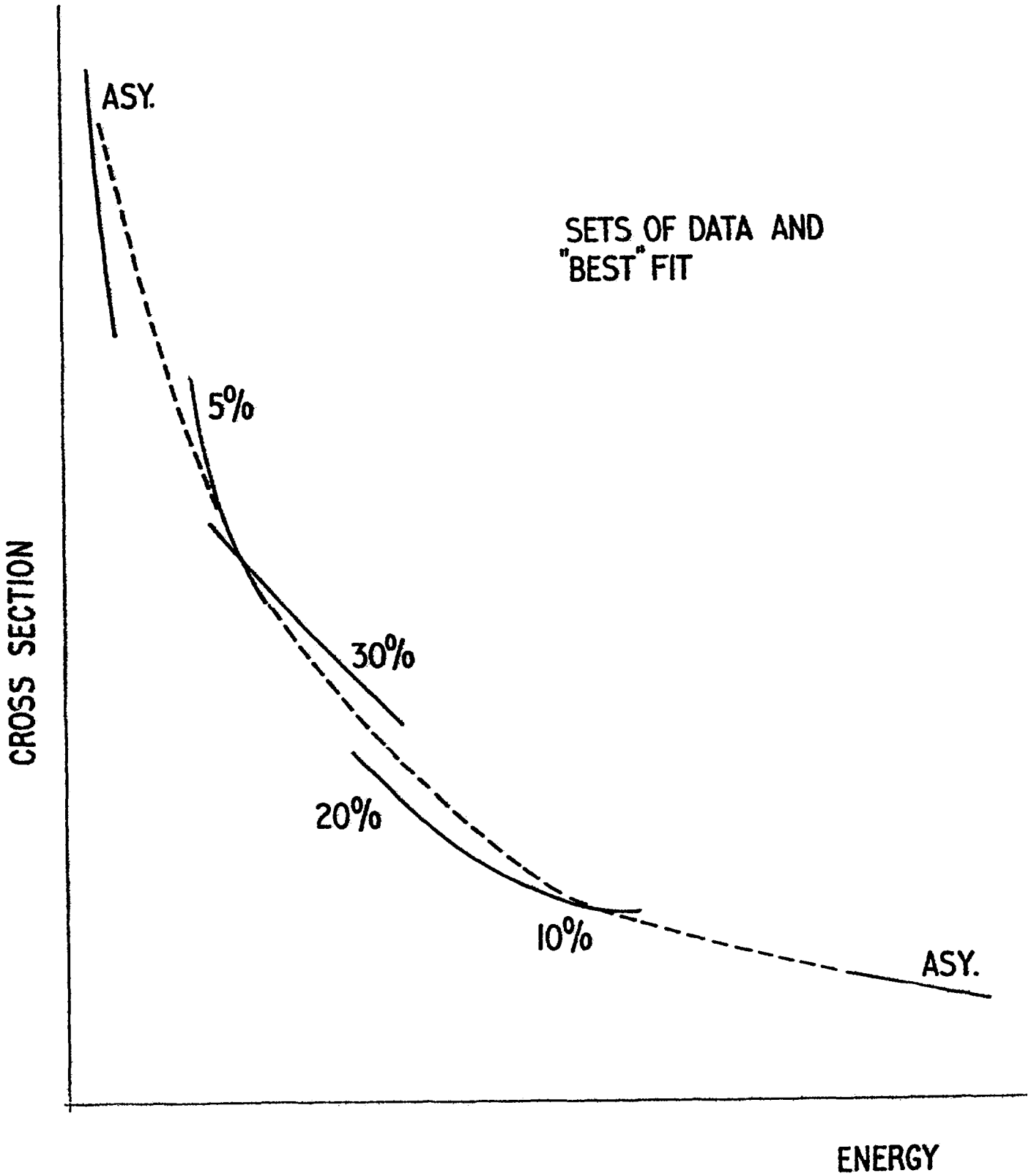

FIG. 2 Typical sets of data (full lines) and asymptotic values (ASY) with recorded accuracies given as percentages. The dashed line is a weighted least square curve fit or "best" fit which is most often what is required by the user of a data system.

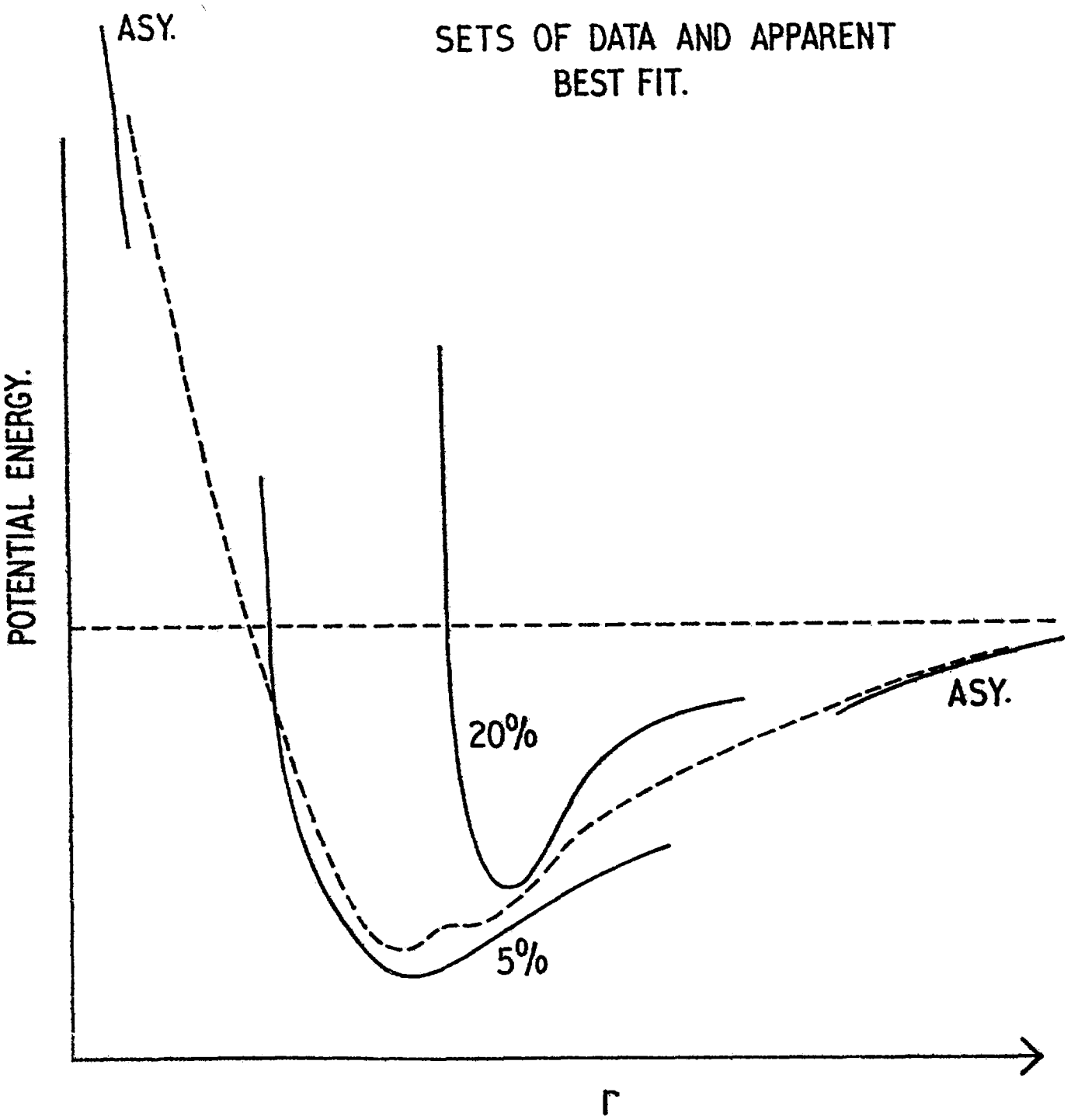

FIG. 3 A least square curve fit which has produced a spurious undulation in the fitted potential. Clearly one of the sets of data showing a minimum is in error by a larger amount than indicated (5% and 20%). This shows the need for interaction and control by the scientist.

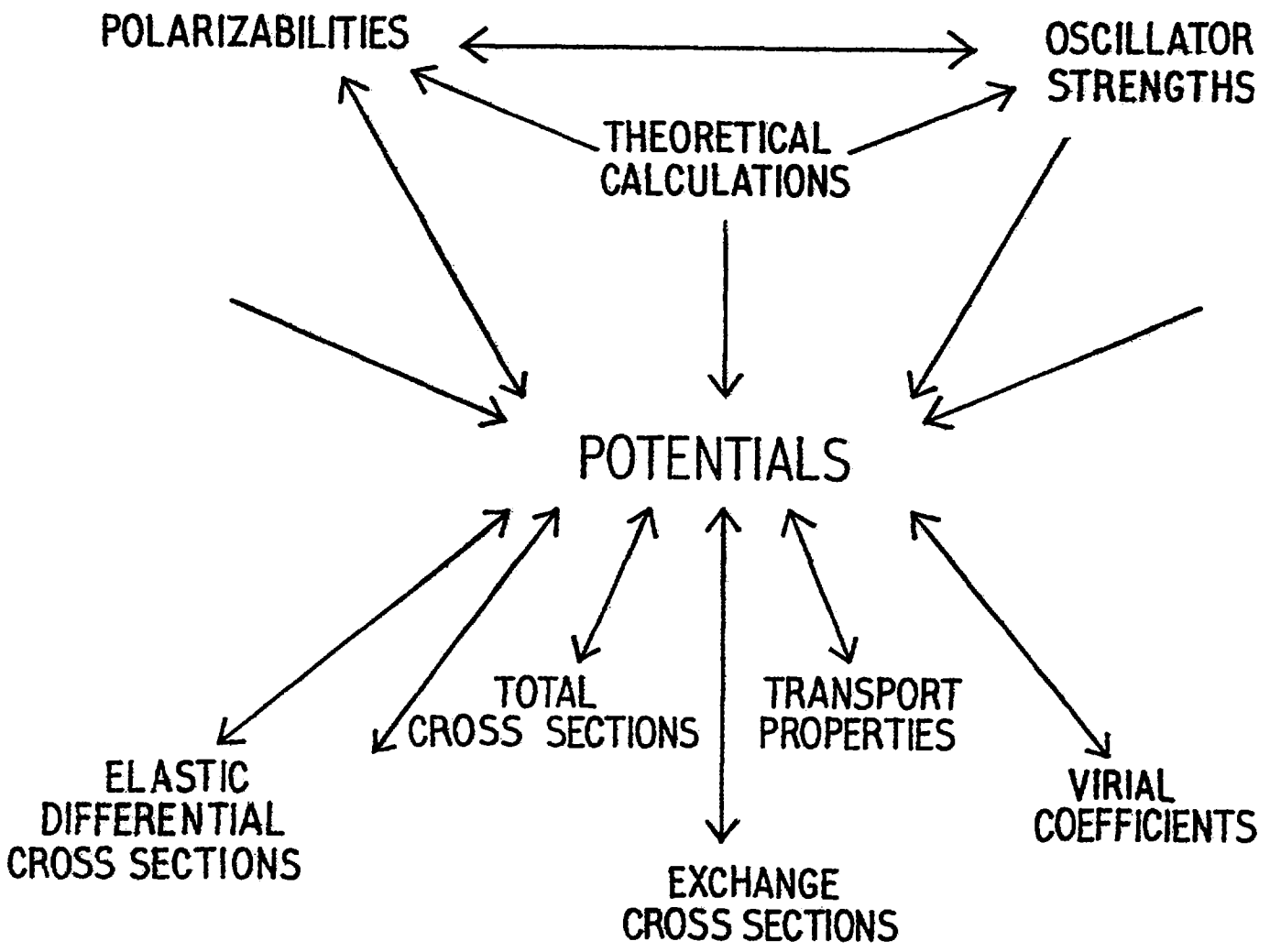

FIG. 4 This illustrates the relationship between different data associated with atomic interactions. By storing interaction potentials and the relations between these and other data it is possible to generate the other data when required.

COMPILATION AND EVALUATION OF ATOMIC AND MOLECULAR DATA RELEVANT TO CONTROLLED THERMONUCLEAR RESEARCH NEEDS: USA Programs

C. F. Barnett
Oak Ridge National Laboratory*
Oak Ridge, Tennessee 37830

A. Introduction

During the early 1960's several agencies in the United States government recognized the need for the compilation and evaluation of numerical data in the physical sciences. Funds were allocated to formally establish data centers or information analysis centers whose main objectives were to search the literature, extract numerical data, and to compile the data after evaluation. Some misunderstanding has been encountered in the use of the terms, "compile and evaluate". Usually, the term compile refers to the process of composing data tables out of material from other documents. In the field of atomic data, one finds an assortment of values obtained by different authors for a given quantity. After data have been compiled, the data are evaluated which involved the evaluator in examining and judging the data. Thus, the evaluator is forced to compare the results through adopted standards to determine best values which he recommends to his colleagues. These best "values" appear in the form of a table or graph in which a number of experimental or theoretical results from different laboratories appear as a single data set or graph. These evaluated data are particularly relevant

---

*Operated by Union Carbide Corporation for U.S. ERDA.

to controlled thermonuclear research in that plasma physicist are not well versed in atomic physics and require only one set of data plotted on a single curve.

The widely proliferation of data analysis centers demanded a means of publication of the evaluated data. This need has been fulfilled with the establishment of two journals: "Atomic and Nuclear Data Tables" and "Journal of Physics and Chemistry Standard Reference Data".

"Atomic Data Tables" was established in 1965 with K. Way as editor and published commercially by Academic Press. "Atomic Data" presents tables and compilations of evaluated experimental and theoretical data on various areas of atomic physics including data on energy levels, wavefunctions, line-broadening parameters, collision processes, various interaction cross sections of atoms and simple molecules, transition probabilities, and particle penetration through matter.

The "Journal of Physics and Chemistry of Standard Reference Data" is a joint publishing venture of the American Physical Society and the American Chemical Society. This publication was started in 1972 with David Lide, Jr. as editor and is an outgrowth of the Office of Standard Reference Data of the National Bureau of Standards. This office was created by a legislative act to coordinate the compilation and evaluation of physical science data in the U.S. The scope of this journal is much broader than that of Atomic Data.

In discussing the U.S. role in the compilation and evaluation of atomic data for the CTR I have divided the presentation in three parts: (1) atomic structure data; (2) atomic collision data; and (3) surface data. A brief description is given of each center along with past and future publications and the present activities. Dr. Joe Martinez of the U.S. Energy Research and Development Administration will present in the next paper the U.S. overall

program on the measurements and calculations of atomic and molecular data to meet the needs of the fusion program. In the U.S. a few data centers exist whose scope is of marginal interest to the CTR program. These will be omitted in the present discussion.

B. Atomic Structure Data Centers

a. Atomic Energy Levels

The Atomic Energy Level was probably the first data center in the U.S. to compile in a systematic manner atomic data. The work was begun in 1946 under Dr. Charlotte Moore and her publications of atomic energy levels have been invaluable to atomic scientists. The center is now under the direction of W. C. Martin at the National Bureau of Standards and is supported by the Office of National Standard Reference Data and the Optical Physics Division of the National Bureau of Standards. Since its inception the center's mission has been the critical appraisal of data on atomic spectra, classification of spectral lines, and determination of atomic energy levels. In addition to the regular publications, the center maintains a complete reference source for both energy levels and wavelength data.

Past publications include (1) C. E. Moore, "Atomic Energy Levels", NSRDS-NBS 35 (1971); (2) L. Hagan and W. C. Martin, "Bibliography on Atomic Energy Levels and Spectra, July 1968-June 1971", NBS Spec. Publ. 363 (1972); (3) B. Kaufman and B. Edlen, "Reference Wavelengths from Atomic Spectra in the Range 15 Å to 25,000 Å", J. Phys. Chem. Ref. Data 3, 825 (1974); (4) J. Reader and J. Sugar, "Energy Levels of Iron, Fe IV through Fe XXVI", J. Phys. Chem. Ref. Data 4, 353 (1975); C. E. Moore, "Selected Tables of Atomic Spectra", NSRDS-NBS 3, Sec. 1 (Si II, III, IV) 1965, Sec. 2 (Si I) 1967, Sec. 3 (C I-VI) 1970; Sec 4 (N IV VII) 1971, Sec. 6 (H, I, D, T) 1972; C. E. Moore, "Atomic Ionization Potentials Z = 1 → 95 and Bibliography", NSRDS-NBS 34 (1970).

Current emphasis are a series of compilations on the energy levels of all spectra of the iron-group elements including "Energy Levels of Chromium, Cr I through Cr XXIV" which has been submitted to the Journal of Phys. Chem. Ref. Data. The next publication, which is in preparation, will cover the Mn spectra.

b. Atomic Energy Levels Information Center

This center, started approximately 8 years ago under the direction of S. Bashkin, is located at the University of Arizona. Its principle objective is the compilation of atomic energy levels and transitions from one spectroscopic term to another. The transitions are presented in the form of Grotrian diagrams. Recently, North Holland Publishing Co. published the centers first compilation - "Atomic Energy Levels and Grotrian Diagrams I - Hydrogen I to Phosphorus XV". The second volume in the series will be a compilation for the element sulfur through calcium. Tentative plans have been made to publish Grotrian diagrams and energy levels for uranium.

c. Atomic and Ionic Emission Lines

This effort is directed by R. L. Kelley at the Naval Post-Graduate School and has as its primary mission the critical tabulation of energy levels or spectral lines below 2000 Å. In 1968 a compilation was published as NRL Report 6648 - "Atomic Emission Lines Below 2000 Å, H_2 through Ar". Recently, Prof. Kelley in collaboration with L. J. Palumbo published "Atomic and Ionic Emission Lines Below 2000 Å, H through Kr", NRL Report 7599 (1973). The data include wavelengths, intensities, term assignments, as well as the ionization potentials for all states of ionization. Work is now being performed to extend the spectra to the 2000-3000 Å region for the same elements.

d. Atomic Transition Probability Data Center

This information analysis center was established by Dr. W. L. Wiese in 1960 at the National Bureau of Standards. The center's mission is to collect all relevant literature, compile and analyze numerical data, and publish bibliographies and tables of best atomic transition probabilities. Some of the well known and widely used publications in the past few years include: (1) B. M. Miles and W. L. Wiese, "Bibliography on Atomic Transition Probabilities (Jan. 1916 through June 1969)", NBS Spec. Publ. 320 (1970); (2) J. R. Fuhr and W. L. Wiese, "Bibliography on Atomic Transition Probabilities (July 1969-June 1971", NBS Spec. Publ. 320 Suppl. 1 (1971); (3) "Bibliography on Atomic Transition Probabilities (July 1971-June 1973)", NBS Spec. Publ. 320 Suppl. 2 (1973); (4) W. L. Wiese, M. W. Smith and B. M. Glennon, "Atomic Transition Probabilities - Hydrogen through Neon", NSRDS-NBS 4 (1966). A study of the relativistic corrections to computed transition probabilities for highly ionized atoms in the hydrogen isoelectronic sequence resulted in a publication by S. M. Younger and A. W. Weiss, "Relativistic Effects on Line Strengths for Transitions in the Hydrogenic Isoelectronic Sequence", J. Research Nat. Bur. Stand. Sec. A 79, 629 (1975). Current emphasis is on the critical evaluation and compilation of transition probabilities for all ionic states of vanadium through maganese, which follows the publication of W. L. Wiese and J. R. Fuhr, "Atomic Transition Probabilities for Scandium and Titanium", J. Phys. Chem. Ref. Data 4, 263 (1975). Systematic trends along isoelectronic sequences of light elements are being used to predict data for highly ionized heavy elements. Future plans include a critical evaluation of transition probabilities for iron, cobalt and nickel. A complete bibliography on transition probabilities is being prepared and will be published in 1977. Particular attention has been paid to oscillator strengths for the isoelectronic

sequence. These studies have resulted in two recent publications: (1) G. A. Martin and W. L. Wiese," Atomic Oscillator Strengths Distribution in Spectral Series of the Lithium Isoelectronic Sequence", Phys. Rev. A 13, 699 (1976); and (2) G. A. Martin and W. L. Wiese, "Tables of Critically Evaluated Oscillator Strengths for the Lithium Isoelectronic Sequence", J. Phys. Chem. Ref. Data 5, 1976.

C. Atomic and Molecular Collision Data Centers

a. JILA Information Analysis Center

The JILA information analysis center was established in 1960 by L. J. Kieffer and is now directed by E. C. Beatty. The center was established to compile and critically evaluate low energy atomic collision data for use in modeling gas discharges lasers, MHD plasmas, planetary atmospheres, and astrophysical plasmas. Analysis is made of low energy electron collision cross sections, photo-absorption and ionization cross sections, and electron transport and rate data. In the past several evaluated compilations have been published. These include: (1) L. J. Kieffer, "Low Energy Electron Collision Cross Section Data - Part I. Ionization, Dissociation, Vibrational Excitation", Atomic Data 1, 19 (1969); Part 2 "Electronic Excitation Cross Sections", Atomic Data 1, 120 (1969); (2) B. Bederson and L. J. Kieffer, "Total Electron-Atom Collision Cross Sections at Low Energy - A Critical Review", Rev. Mod. Phys. 43, 601 (1971); (3) L. J. Kieffer, "A Compilation of Electron Collision Cross Section Data for Modeling Gas Discharge Lasers", JULA Report #13 (1973); (4) L. J. Kieffer, "Low Energy Electron Collision Cross Section Data. Part III. Total Scattering-Differentical Elastic Scattering", Atomic Data 2, 293 (1971); (5) B. L. Moiseivitsch and S. J. Smith, "Electron Impact Excitation of Atoms", Rev. Mod. Phys. 40, 238 (1968). More recent publications are L. J. Kieffer, "Bibliography of Low-Energy Electron and Photon Cross Section Data Through 1974",

NBS Spec. Publ. 426 (1976) and E. C. Beatty and J. W. Gallagher, "Bibliography of Low Energy Electron and Photon Cross Section Data Through 1975", Supplement to NBS Spec. Publ. 426 (1975). Major projects now underway are a critical re-evaluation of electron impact excitation being performed by E. C. Beatty and J. Rumbel; complete evaluation compilation of electron affinities; and a compilation of atomic data for modeling of MHD plasmas being done by Jim Land and Art Phelps.

b. Controlled Fusion Atomic Data Center

In response to the needs of the controlled fusion research program for atomic data an informal data center was started in 1959 at the Oak Ridge National Laboratory under the direction of C. F. Barnett. The mission of the undertaking was to collect, review, evaluate, and compile numerical atomic collision data of interest to CTR. Since the CTR requirements were and are changing with time, the decision was made to include heavy particle collisions, charged particles penetrating into macroscopic matter, electron collisions, photon collisions, and particle and photon transport.

In 1960 the first compilation of direct interest to the fusion community was published as "σ CTR" ORNL Report #3113. This publication was followed by a revised version in 1964. In 1974 an additional revision was started and is now in the process of publication and will be titled "Atomic Data for Controlled Fusion Research", ORNL Report #5206, Vol I and ORNL Report #5207, Vol. II. Data are presented in both tabular and graphical form. Work is now underway to update this publication on an annual basis.

An extensive annotated bibliographical file with approximately 10^5 references is stored on a computer for off-line retrieval and printouts. At the present time the period 1950-1975 is covered. Up until 1970 an annual bibliography was published as ORNL-AMPIC Reports 1-12. Budgetary cut-backs

resulted in the termination of the publication of these bibliographies. We expect to publish a comprehensive bibliography for the years 1950-1975 during the coming year. The bibliographies are indexed by author, reaction process and reactants.

A decision was made during the data center's formative years that the evaluated compilations would be a series of monographs published by a commercial publisher. Four monographs were published by Wiley-Interscience Publishers. They were (1) "Ion-Molecule Reactions", by E. W. McDaniel, V. Čermák, A. Dalgarno, E. E. Ferguson, and L. Friedman; (2) "Theory of Charge Exchange", by R. A. Mapleton; (3) "Dissociation by Heavy Particle Collisions", by G. W. McClure and J. M. Peek; (4) "Excitation by Heavy Particle Collisions", by E. W. Thomas. The series was discontinued in 1973 due to the low sales volume and the problem encountered in updating the compilations.

In Jan. 1975 a joint effort with W. L. Wiese of National Bureau of Standards was initiated to publish bimonthly a newsletter, "Atomic Data for Fusion". The objective was to provide interested fusion researchers with the most recent data applicable to fusion work. Included in the contents are references on atomic energy levels, wavelengths, line identification, and atomic physics in plasma diagnostics. An attempt has been made to summarize the work in progress throughout the world. Also, a section is devoted to tabulating recent theoretical and experimental data. These tabulations are a means to provide needed atomic data to fusion researchers several months before the refereed publication appears.

Computer programs have been written to convert our evaluated cross section data to rates and analytical expressions as a function of energy or

temperature. Plans are to store this on the US-CTR computer at the Livermore Laboratory for on-line retrieval.

D. Surface Interactions

Particle interactions with solids are included within the scope of the Controlled Fusion Atomic Data Center. The literature is scanned for the following topics:

1. Sputtering (electron and heavy particle)
2. Secondary electron emission by electron and heavy particle impact
3. Photoelectric emission of electrons
4. Reflection of electrons from surfaces
5. Reflection of heavy particles from surfaces
6. Production of electromagnetic radiation by electron and heavy particle impact
7. Surface ionization
8. De-excitation and neutralization at surfaces
9. Gas desorption by electrons, ions and photons
10. Blistering and voids in metals
11. Radiation damage in metals
12. Ion implantation in metals.

Difficulties have been encountered in attempting to evaluate surface data. Most experiments performed in the past paid little or no attention to the surface characteristics or the surrounding vacuum conditions. Additional problems are also encountered in that no systematic attempts have been made to obtain reliable and repeatable data. At the present time one can only compile surface interaction data.

E. Acknowledgement

The author is grateful to W. C. Martin, W. L. Wiese, S. Bashkin and E. C. Beatty for providing descriptions and the present status of their data center.

ERDA Support for Magnetic Fusion-Related Atomic Physics

J.V. Martinez, Division of Physical Research
Phil Stone, Division of Magnetic Fusion Energy
USERDA, Washington, D.C. 20545

Research in magnetic fusion-related atomic and molecular (A+M) physics is supported by the US Energy Research and Development Administration (ERDA) in two divisions reporting to the assistant administrator for solar, geothermal and advanced energy systems (ASGA). These two divisions are the Division of Physical Research (DPR) and the Division of Magnetic Fusion Energy (DMFE). Whereas the mandate to sponsor this type of research in the latter division is explicit, similar research is sponsored by DPR under the provision that it support research that assists all energy technologies particularly these identifiable within ERDA's context. The nature of research supported in each division is generally quite different. DMFE's support is oriented toward very specific needs while DPR's support is not as specific but frequently involves obtaining specific results as a matter of course that are usable to DMFE.

As an illustration, DMFE will support research specifically aimed to obtain cross-section values for particular interactions, e.g. charge exchange between highly ionized iron and neutral hydrogen atoms obtained either through experiment or by machine computation using best available parameter values and computer codes. On the other hand, DPR characteristically will support development of better methods to obtain similar values but the emphasis is on the development of new and improved methods not the values themselves. Obviously the same cross-section may be obtained as a spin-off of using test cases in this method development research. Another distinction in the nature of research supported by both divisions can be seen to exist in the long and short range objectives.

Close communication takes place between both divisions in this area in order to insure that maximum benefits are derived from the support available to both programmes. Thus far, the combined support available for such research is approximately two million dollars annually and it appears that this amount will not change significantly in the near future. Neither division has a say on how funds are to be deployed in each other's programme. However, DMFE needs are used to map out the physics of interest to DPR.

DMFE support of fusion-related A+M physics is viewed in terms of (1) an immediate need to provide a fundamental data base for the prediction, evaluation and diagnosis of existing and planned experiments; (2) a near-term

need to provide accurate data relating to heavy ion impurities and their effect on the confinement of plasmas; (3) a longer term need to establish comprehensive, critically evaluated standardized data sets for reactor systems. It is this basis which DMFE uses for deployment of its support and it is this basis which DPR uses to map an even larger field for research. Present directions of this research - as near as they can be now defined - are (1) to scale-up the present level of support as much as possible to concentrate on the impurity problem using both theory and experiment; (2) to support the immediate establishment and use of the fusion plasma research facility; (3) to have organized the required data sets to assure they will be ready at the time they will be needed; and (4) to support acquisition of knowledge in a balanced manner dictated by formulae used in modelling a burning plasma.

The research support available in A+M physics from both divisions is deployed at ERDA laboratories, universities and non-profit institutions at the present time. While DMFE places a large share of its support in non-university laboratories, relatively speaking, the opposite is true of DPR's support. Another vivid comparison is that a larger portion of DPR's support is for theoretical research. Surface related work is not supported by the same offices that support the non-surface A+M physics and this is especially true of DMFE where no surface work is supported by the office that supports the A+M physics. Some, but little, surface work is supported by DPR's atomic physics programme.

The lists of principal investigators and their affiliation are shown separately for DMFE and DPR. These lists do not include all the scientists working on magnetic fusion-related problems and that is because only the principals are listed. Many more scientists of junior administrative status with respect to these contracts work on these contracts and these may include visiting scientists and research associates (post-doctorates).

The principal projects supported by DMFE and DPR are placed in different categories. These are listed as (1) line identification, (2) transition probabilities and lifetimes, (3) excitation and ionization cross-sections, (4) molecules and negative ions, (5) charge exchange, (6) standards and nuclear data, (7) data center, and (8) general theory for atomic physics in fusion plasmas. For each category, the problems, the areas of application of the knowledge acquired and the principal investigators supported by ERDA are shown. As a result of the activities that take place under several contracts, certain investigators can be listed in more than one category. Whenever this occurs, the project is identified with an asterisk. This multiplicity is not so much a sign of priority of the contract, but rather the result of not having an irreducible representation of categories to communicate this information.

ENERGY RESEARCH AND DEVELOPMENT ADMINISTRATION

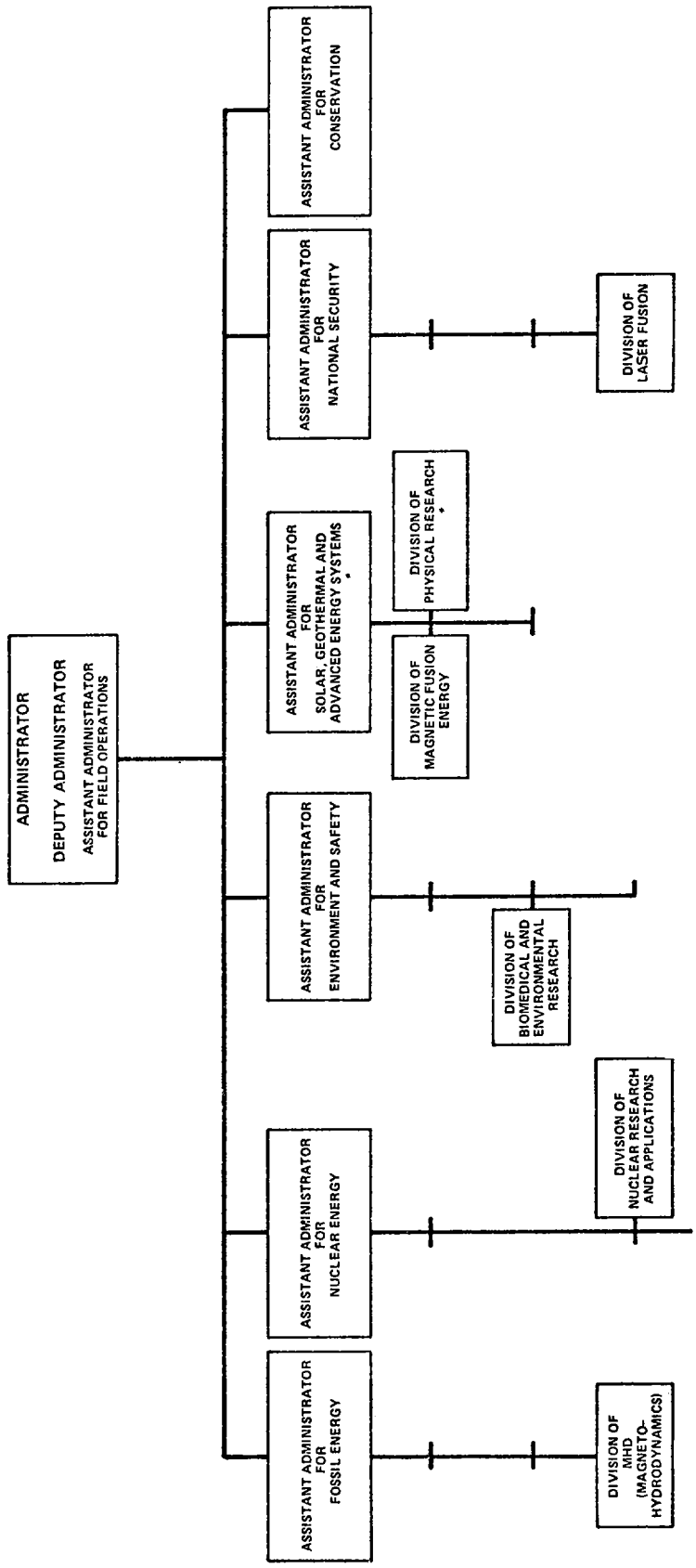

Principal Investigators Supported by ERDA's Division of Physical Research to Conduct Research in Atomic Physics Related to Magnetic Fusion Energy

YEHUDA BAND
ARGONNE NATIONAL LABORATORY

GORDON H. BERRY
ARGONNE NATIONAL LABORATORY

CHANDER BHALLA
KANSAS STATE UNIVERSITY

JOSEPH CALLAWAY
LOUISIANA STATE UNIVERSITY

DAVE CRANDALL
OAK RIDGE NATIONAL LABORATORY

ALEXANDER DALGARNO
HARVARD COLLEGE OBSERVATORY

SHELDON DATZ
OAK RIDGE NATIONAL LABORATORY

UGO FANO
UNIVERSITY OF CHICAGO

WILLIAM FELDMAN
LOS ALAMOS SCIENTIFIC LABORATORY

PETER GARY
THE COLLEGE OF WILLIAM AND MARY

DONALD GEMMELL
ARGONNE NATIONAL LABORATORY

RONALD HENRY
LOUISIANA STATE UNIVERSITY

KEITH JONES
BROOKHAVEN NATIONAL LABORATORY

MANFRED KAMINSKY
ARGONNE NATIONAL LABORATORY

KARL KESSLER
NATIONAL BUREAU OF STANDARDS

NEAL LANE
RICE UNIVERSITY

JAMES MACDONALD
KANSAS STATE UNIVERSITY

RICHARD MARRUS
LAWRENCE BERKELEY LABORATORY

JAMES MCGUIRE
KANSAS STATE UNIVERSITY

HENRY MOTZ
LOS ALAMOS SCIENTIFIC LABORATORY

DAVID NORCROSS
JOINT INSTITUTE FOR LABORATORY ASTROPHYSICS

PATRICK RICHARD
KANSAS STATE UNIVERSITY

DAVID THOMSON
LOS ALAMOS SCIENTIFIC LABORATORY

GEORGE VICTOR
HARVARD COLLEGE OBSERVATORY

Principal Investigators Supported by ERDA's Division of Magnetic Fusion Energy to Conduct Research in Atomic Physics

CLARENCE BARNETT
OAK RIDGE NATIONAL LABORATORY

GORDON DUNN
JOINT INSTITUTE FOR LABORATORY ASTROPHYSICS

RAY ELTON
NAVAL RESEARCH LABORATORY

ROBERT FEENEY
GEORGIA TECH

YUKAB HAHN
CONNECTICUT

WALTER HUEBNER
LOS ALAMOS SCIENTIFIC LABORATORY

JIM LEISS
NATIONAL BUREAU OF STANDARDS

TOM MORGAN
WESLEYAN

WARREN MOOS
JOHNS HOPKINS

DAVE NAGEL
NAVAL RESEARCH LABORATORY

RON OLSON
STANFORD RESEARCH INSTITUTE

JIM PEEK
SANDIA LABORATORIES-ALBUQUERQUE

ROBERT PYLE
LAWRENCE BERKELEY LABORATORY

DOUGLAS SAMSON
PENNSYLVANIA STATE

MAJOR COMPONENTS

MFE NEEDS → / TECHNICAL ACTIVITY ↓	DIAGNOSTICS	NEUTRAL BEAM HEATING	PLASMA COOLING
LINE IDENTIFICATION	HEAVY IONS		HEAVY IONS
TRANSITION PROBABILITIES	HEAVY & LIGHT IONS		HEAVY IONS
EXCITATION & IONIZATION CROSS SECTIONS	• ALL IONS FOR CONCENTRATION MEASUREMENT • HE-LIKE IONS FOR ION TEMPERATURE • ION BEAM EXCITATION		HEAVY & LIGHT IONS
MOLECULES & NEGATIVE IONS		• H AND D MOLECULE STRUCTURE • D^- FORMATION AND STRIPPING	
CHARGE EXCHANGE		LIGHT AND HEAVY IONS ON N_2, H_2, H	D^0 ON ALL IONS
STANDARDS & NUCLEAR DATA	FAR UV, X-RAY AND NEUTRONS		
DATA CENTER	COMPILE AND DISSEMINATE ATOMIC DATA		

HEAVY IONS ⇒ Fe, Mo, W, Au
LIGHT IONS ⇒ C, O, N, Rare Gases

SUMMARY BY TECHNICAL ACTIVITY

ACTIVITY	RELATIONSHIP TO MFE NEEDS
1. LINE IDENTIFICATION	IMPURITY DIAGNOSTICS AND COOLING
2. TRANSITION PROBABILITIES	IMPURITY DIAGNOSTICS AND COOLING
3. EXCITATION AND IONIZATION CROSS SECTIONS	IMPURITY COOLING ION BEAM DIAGNOSTICS
4. MOLECULES AND NEGATIVE IONS	NEUTRAL BEAM HEATING
5. CHARGE EXCHANGE	IMPURITY COOLING, BEAM SOURCE DEVELOPMENT
6. STANDARDS AND NUCLEAR DATA	DIAGNOSTICS OF IMPURITIES, NEUTRONS
7. DATA CENTER	ALL MFE AREAS
8. ATOMIC PHYSICS THEORY	ALL MFE AREAS

1. LINE IDENTIFICATION

PROBLEM

- DETERMINE WAVELENGTHS
- HEAVY IONS, HIGHLY IONIZED
- RESONANCE AND OTHER STRONG LINES

APPLICATION

- SIGNIFICANT LOSS OF ENERGY IN TOKAMAKS
- IDENTIFICATION DIFFICULT
  - BACKGROUND RADIATION
  - FOREST OF LINES
- USE TO ESTIMATE AND MEASURE LOSS
- USE TO MEASURE IMPURITY CONCENTRATION
- DETERMINE ISOELECTRONIC SEQUENCE BEHAVIOR

LABORATORY	INVESTIGATOR	TOPIC
NBS	WIESE /READER	SPARK AND LASER DISCHARGES
*NRL	NAGEL	LASER DISCHARGE
*JOHNS HOPKINS	MOOS	TOKAMAK MEASUREMENTS
*LASL	HUEBNER/MERTS	CALCULATIONS OF RADIATIVE LOSS
*KANSAS STATE	RICHARD/ MACDONALD	INNER SHELL X-RAY SPECTRA MEASUREMENTS
BNL	JONES	BEAM FOIL SPECTROSCOPY $M^{+n}(\langle n \rangle \leq 30$, Ni & Fe)

2. TRANSITION PROBABILITIES & LIFETIMES

PROBLEM

- HEAVY, LIGHT IONIZED IONS
- LIGHT, MULTIPLY IONIZED IONS
- LINE EMISSION, INCLUDING DIELECTRONIC RECOMBINATION
- CONTINUUM EMISSION: BREMSSTRAHLUNG AND RADIATIVE RECOMBINATION

APPLICATION

- RECOMBINATION RATES - FOR IONIZATION STAGES
- RECOMBINATION AND BREMSSTRAHLUNG - FOR RADIATIVE ENERGY LOSS
- LINE RATES - FOR IMPURITY CONCENTRATIONS
- LINE RATES - FOR EXCITATION AND IONIZATION CROSS SECTION ESTIMATES
- DETERMINE ISOELECTRONIC SEQUENCE BEHAVIOR

LABORATORY	INVESTIGATOR	TOPIC
NBS	WIESE/ROBERTS	THEORY AND THETA-PINCH
*NRL	NAGEL	LASER DISCHARGE
*JOHNS HOPKINS	MOOS	TOKAMAK MEASUREMENTS
*LASL	MERTS	CALCULATION OF RATES
CONN.	RUSSEK	DIELECTRONIC RECOMBINATION THEORY
*NBS	KESSLER/WIESE	OSC STRENGTHS - Be, Mg & Zn ISOELECTRONIC SEQUENCES
LBL	MARRUS	SUPER HILAC - IONS THROUGH Kr^{+34}
*ANL	BERRY	BEAM FOIL SPECTROSCOPY, V^{+n} AND Ni^{+n} $(n= 3-8)$

3. EXCITATION & IONIZATION CROSS SECTIONS

PROBLEM

- IONIZATION FOR HEAVY IONS
- EXCITATION FOR C, N, O IONS
- EXCITATION FOR ION PROBE SPECIES (Tl^+, Cs^+, ETC.)
- ACCURATE EXPERIMENTS AND THEORY - FEW CASES
- EMPIRICAL THEORY - HUNDREDS OF CASES

APPLICATION

- IONIZATION STAGES OF HEAVY IONS
- ENERGY LOSS CALCULATIONS BY LINE RADIATION
- SPECTROSCOPIC MEASUREMENTS OF IMPURITY CONCENTRATIONS
- INTERPRETATION OF ION BEAM PROBE MEASUREMENTS FOR POTENTIAL AND ELECTRON TEMPERATURE
- HE-LIKE IONS FOR DOPPLER MEASUREMENT OF ION TEMPERATURE
- DETERMINE ISOELECTRONIC SEQUENCE BEHAVIOR

LABORATORY	INVESTIGATOR	TOPIC
NBS	DUNN/PHANEUF	CROSSED BEAMS, AT HNL
GA. TECH.	FEENEY	CROSSED BEAMS - FOR ION BEAMS
LASL	ROBB	THEORY - CLOSE COUPLING
SLA	PEEK	THEORY - DISTORTED WAVE
PA. STATE	SAMSON	THEORY - IONIZATION
LOUISIANA STATE	CALLAWAY/HENRY	THEORY - CARBON, HELIUM CLOSE COUPLING
RICE	LANE	THEORY - RARE GAS STRUCTURE
JILA	NORCROSS	THEORY - Cu-LIKE AND Na-LIKE SEQUENCES
LASL	THOMSON/JONES	THETA PINCH - HIGH Z IMPURITY SPECTRA - Ne, Kr, O
ORNL	DATZ	CORE EXCITATION AND IONIZATION BY CHANNELING - Si, Al, Ag, O
*ANL	BERRY	BEAM FOIL SPECTROSCOPY - H, B, C,

4. MOLECULES & NEGATIVE IONS

PROBLEM

- ELECTRONIC AND VIBRATIONAL STRUCTURE
- H_2, H_3, $H_2^{\pm}$, $H_3^{\pm}$, D_2, D_3, ETC.
- ELECTRON COLLISIONS ON DEUTERIUM MOLECULES TO FORM D^-
- REACTION KINETICS OF D^+, D° ON SURFACES
- D^+, D_2^+, D_3^+ ON ALKALIES TO FORM D^-
- D^- COLLISIONS WITH H_2, He, N_2, O_2, Ne, ETC., TO FORM D°
- PROPERTIES OF $H_x^{\pm n}$, $D_x^{\pm n}$, $\overline{HeD}^+$, $\overline{CH}^+$, $\overline{OH}^+$, $\overline{OH_2}^+$, ETC.

APPLICATION

- UNDERSTANDING OF BASIC PROCESSES OF ION SOURCES
- FORMATION OF D^- IN GASES
- FORMATION OF D^- ON SURFACES OF Cs, Mg, Na, ETC.
- STRIPPING IN GAS CELLS TO OBTAIN NEUTRAL BEAM

LABORATORY	INVESTIGATOR	TOPIC
LBL	PYLE	CROSS SECTION, SURFACES, STRIPPING
HNL	BARNETT	D^- EQUILIBRIUM FRACTIONS
WESLEYAN	MORGAN	D^- FORMATION RATES
ANL	GEMMELL	CHANNELING AND MOLECULAR ION POTENTIAL ENERGY

5. CHARGE EXCHANGE

PROBLEM

- MEASUREMENTS AND THEORY FOR CROSS SECTIONS
- DEUTERIUM ON LIGHT AND HEAVY IONS TO FORM D^+
- SINGLY IONIZED IMPURITIES ON GASES IN ION SOURCES (N_2, H_2, He)

APPLICATION

- DETERMINE ENERGY STAGES OF IMPURITY IONS
- CALCULATIONS OF RADIATIVE ENERGY LOSS
- EVALUATE NEUTRAL BEAM INJECTION OF IMPURITIES

LABORATORY	INVESTIGATOR	TOPIC
HNL	BARNETT	IMPURITY - D° CROSS SECTIONS AT INJECTION ENERGIES ($\geq 2 \times 10^8$ CM SEC^{-1})
SRI	OLSON	CALCULATIONS OF RATES AT INJECTION ENERGIES
NRL	ELTON	CARBON - D° MEASUREMENTS
+YALE	BAYFIELD	LOW Z-ION (H, B, C) ON H°
ORNL	CRANDALL	LOW Z-ION (C, N, O) ON H°
*RICE	NEAL	THEORY - He^{++} ON H° AND D°

6. STANDARDS & NUCLEAR DATA

PROBLEM

- PROVIDE STANDARD SOURCES AND DETECTORS FOR FAR UV AND SOFT X-RAY (<200 Å) SPECTRA
- PROVIDE CALIBRATION SERVICES FOR MEASUREMENT EQUIPMENT
- DEVELOP NEUTRON DETECTORS AND STANDARDS FOR 14 MEV NEUTRONS
- MEASURE D-T FUSION CROSS SECTIONS AT 50 KEV

APPLICATION

- IMPURITY CONCENTRATION MEASUREMENTS
- ION TEMPERATURE DIAGNOSTICS
- NEUTRON PRODUCTION EVALUATION
- PROVIDE AN ALTERNATE MEASUREMENT OF D-T CROSS SECTIONS

LABORATORY	INVESTIGATOR	TOPIC
NBS	SPARROW	X-RAY STANDARDS
NBS	SALOMON	FAR UV RADIOMETRY
NBS	BOWMAN	NEUTRON STANDARDS

7. DATA CENTER

PROBLEM

- COMPILE DATA ON ENERGY LEVELS, WAVELENGTHS, CROSS SECTIONS AND TRANSITION RATES
- DISSEMINATE DATA IN CONVENIENT AND RAPID MANNER
- EVALUATE DATA ON CRITICAL PROCESSES

APPLICATION

- ALL AREAS OF CTR INTEREST: DIAGNOSTICS, BEAM DEVELOPMENT, IMPURITY CONTROL
- IDENTIFY MISSING AND POOR DATA
- STIMULATE EXPERIMENTS AND THEORY
- INPUT DATA FOR COMPUTER MODELING

LABORATORY	INVESTIGATOR	TOPIC
HNL	BARNETT	NEWSLETTER, COMPILATIONS, OVERVIEW
NBS	WIESE	ENERGY LEVELS

8. GENERAL THEORY IN FUSION-RELATED ATOMIC PHYSICS

PROBLEM

- PLASMA TRANSPORT PROPERTIES
- MOMENTUM AND ENERGY EXCHANGE RATES
- SHOCK WAVE PROPAGATION
- ENERGY LEVELS, TRANSITION PROBABILITIES, DIELECTRONIC RECOMBINATION
- GAS PHOTOABSORPTION AND ELECTRON COLLISION EXCITATION
- CHARGE EXCHANGE
- AUTOIONIZATION AND RADIATIVE RATES

APPLICATION

- GENERALLY TO ALL ASPECTS OF FUSION PLASMAS
- EMPHASIS ON METHOD DEVELOPMENT

LABORATORY	INVESTIGATOR	TOPIC
LASL	FELDMAN	ENERGY INTERCONVERSION & TRANSPORT
WILLIAM & MARY	GARY	PLASMA & SHOCK WAVE
HARVARD	DALGARNO/VICTOR	ENERGY LEVELS & CHARGE EXCHANGE
CHICAGO	FANO	ELECTRON EXCITATION & PHOTO PROCESSES
ANL	BAND	PROTON-ATOM CHARGE EXCHANGE

Atomic Data Compilation and Evaluation Programs at NBS Pertinent of Fusion Research

W. L. Wiese
National Bureau of Standards, Washington, D. C. 20234

The U.S. National Bureau of Standards operates, under the National Standard Reference Data System (NSRDS), a number of data centers in various fields of the physical sciences. Among them, the following three centers compile atomic data of interest to Thermonuclear Fusion Research:

(1) The Atomic Energy Levels Data Center, at NBS, Washington, D. C. (Director: Dr. W. C. Martin)

(2) The Data Center on Atomic Transition Probabilities and Line Shapes, at Washington, D. C. (Director: Dr. W. L. Wiese)

(3) The Joint Institute for Laboratory Astrophysics (JILA) Atomic Collision Information Center, at Boulder, Col. (Director: Dr. E. C. Beaty).

The first two data centers are partially supported by the U.S. Energy Research and Development Administration and have concentrated their data compilation activities on atomic ion species of primary interest in magnetic fusion research.

The principal output of the NBS data centers has been listed by C. F. Barnett in his review paper A.4 of these proceedings and will therefore not be listed here again. But it should be added that, combined with the center on transition probabilities, a data center is also operated on the subject of spectral line shapes. This center has published a general bibliography on atomic line shapes and shifts with two supplements. (NBS Spec. Publ. 366 (1972); Suppl. 1 (1974); Suppl. 2 (1975)). These bibliographies may be of interest for the diagnostics of very dense plasmas as encountered in the laser fusion approach.

A critical problem in magnetic fusion research, as frequently cited in this meeting, is the very detrimental effects of heavy ion impurities, especially the large radiation losses which may drastically influence the energy balance. An overview of the heavy ions of importance from the viewpoint of required atomic structure data may be conveniently obtained from Fig. 1. In this graph the elements are plotted in order of nuclear charge versus the stage of ionization. The heavier elements used as wall materials in Tokamak machines (including limiters and divertors), as well as those under active consideration, are singled out as the vertical lines. Specified are Cr, Fe, Ni, Zr, Nb, Mo, Ta, W, Re, Pt, Au--and this list is probably not complete. Ions of lighter elements are not included, mainly because they become fully stripped in the larger machines. (Among these elements, Al, Si, and Ti are of special importance.) The upper limits for the range of ions encountered in various Tokamak devices are very approximately indicated by the broken lines; i.e., the broken lines represent estimates of the highest stages of ionization attainable in the central parts of the plasmas.

A few selected isoelectronic sequences are shown as the diagonal lines. These sequences are especially important as far as atomic data are concerned for the following two reasons:

(a) The spectra of ions belonging to these sequences (e.g., alkalis, alkaline earths) are relatively simple since their atomic structure is simple. These spectra are thus especially attractive for diagnostic purposes.

(b) The excitation rates for the principal resonance lines are very large so that the subsequent resonance radiation represents a large part of the total radiative loss rate. For estimates of radiation losses and plasma modelling, the knowledge of the excitation rate into a single excited level may therefore often be sufficient for such species.

Since the central, hot parts of plasmas are usually of principal importance, the areas where the vertical (element) lines intersect the broken lines are presently of the highest interest, and the cases where diagonal lines are involved are most important. Usually, these areas involve highly ionized species for which very few atomic structure data are available, and those known are furthermore often rather unreliable. On a relative scale, the largest amount of atomic data (and the most reliable) for such highly ionized species may be found among atomic energy levels and wavelengths, while the available body of data for atomic transition probabilities (oscillator strengths) is substantially smaller and much more unreliable. The situation is even worse with respect to cross sections.

In view of the existence of a number of different centers compiling literature references or data on atomic processes, it appears important to stress the particular nature of the data centers at NBS.

The term "data center" is often rather broadly used and is applied to (at least) three distinctly different aspects of data compilation activities: (1) the compilation of literature references and their arrangement into bibliographies organized according to subject, specific atomic process, element, spectrum, etc.; (2) critically evaluated tabulations of numerical data--i.e., the principal output is a general table of best selected data with an indication of their accuracy (this may also be in the form of a critical review); (3) the rearrangement of previously compiled data into a new format, which usually involves "computerization".

Accordingly, one may thus divide data centers into (1) information centers on literature references, (2) critical data evaluation centers, and (3) "reformatting" centers. The NBS centers fall into categories (1) as well as (2), but are structured in such a way as to primarily fulfill the second function,

which takes the largest amount of time and effort of the people involved. For the critical evaluation of numerical data, the staffing of a data center with scientists experienced in the respective field is an absolute necessity. Furthermore, it is very advantageous to have associated with the data center an active research group, involved in the respective experimental and theoretical methods. The NBS data centers have thus all been designed to be intregal parts of research groups in their respective fields.

The critical evaluation of original papers is normally pursued on the following basis: a judgment is made as to (a) whether the critical factors (see below) involved in a method are adequately taken into account, (b) whether the data agree within the stated error limits with other data and (c) whether the data fit into regularities and systematic trends.

For example, on the subject of atomic transition probabilities the critical factors for all the major experimental and theoretical techniques have been listed in detail in the general introduction to the 2nd volume of the NBS transition probability tables (NSRDS - NBS 22 (1969)). These critical factors have been the result of detailed prior studies of the original literature with the strong participation of NBS researchers with firsthand experience in the respective technique. Thus, to quote as a specific example the "atomic lifetime" techniques, the literature is examined for discussions of possible radiative cascading effects, collisional depopulation, radiation trapping, and line blending.

The NBS centers on atomic data have up to this date presented the numerical body of data in books or review chapters, which is the way of presenting the data that seems to be most preferred by the users. (Apparently, in a typical case very few specific numbers are needed by the user). Quotations of the NBS books in the open literature are numerous (of the order of 200 per

year in the area of atomic transition probabilities), and requests for numerical data and literature information come in at the rate of several per week.

The major goal for the NBS data centers are either systematic data compilations for a group of spectra comprising one or several elements, or critical reviews of all results for a particular atomic process. However, in specific demand situations the data centers have been flexible and responsive even to extensive requests. For example, in response to demands by fusion researchers on atomic transition probability data for the Li sequence, a special new compilation cited by C. F. Barnett in his review paper was recently prepared (G. A. Martin and W. L. Wiese, J. Phys. Chem. Ref. Data 5, 537 (1976)).

Returning finally to the categorization of data centers mentioned earlier, one may state that critical reviews and evaluations and tabulations of data constitute the most involved and therefore slowest processes in a data center operation. They are, however, also the most valuable ones, since they provide the user with definitive numerical values. A usually much faster data center service is the publication of literature references in bibliographies, which may be more readily updated. In this case, however, the user must search through the original literature himself and make the data choice (which, due to his inexperience in the field, may often not be the optimum one). Efforts to computerize or re-format the data appear to be reasonable only when an extensive, critically evaluated body of data is available.

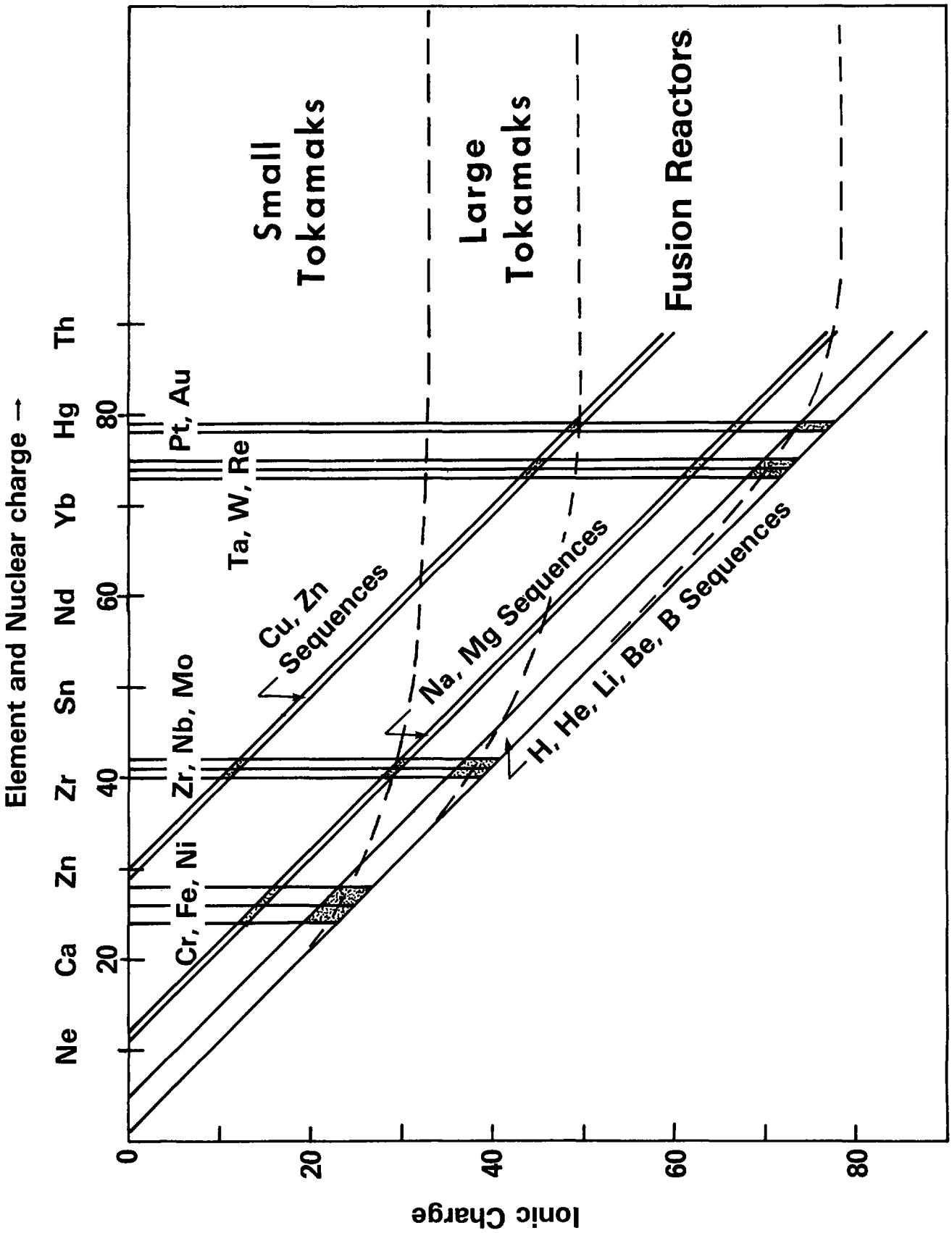

Figure 1: Overview of atomic structure data needs for magnetic fusion research devices.

Contributed Paper to Topic B6

PREPRINT UCRL-79286

Lawrence Livermore Laboratory

THE TIME FOR ATOMIC AND MOLECULAR DATA BASES IS NOW!

(AN OVERVIEW OF DATA MANAGEMENT RESEARCH AT LLL)

Viktor E. Hampel and Eugene A. Henry

February 1, 1977

This paper was prepared for submission to the Proceedings of the IAEA Advisory Group Conference on Atomic and Molecular Data for Fusion at the UKAEA Culham Laboratory, 1-5 November, 1976.

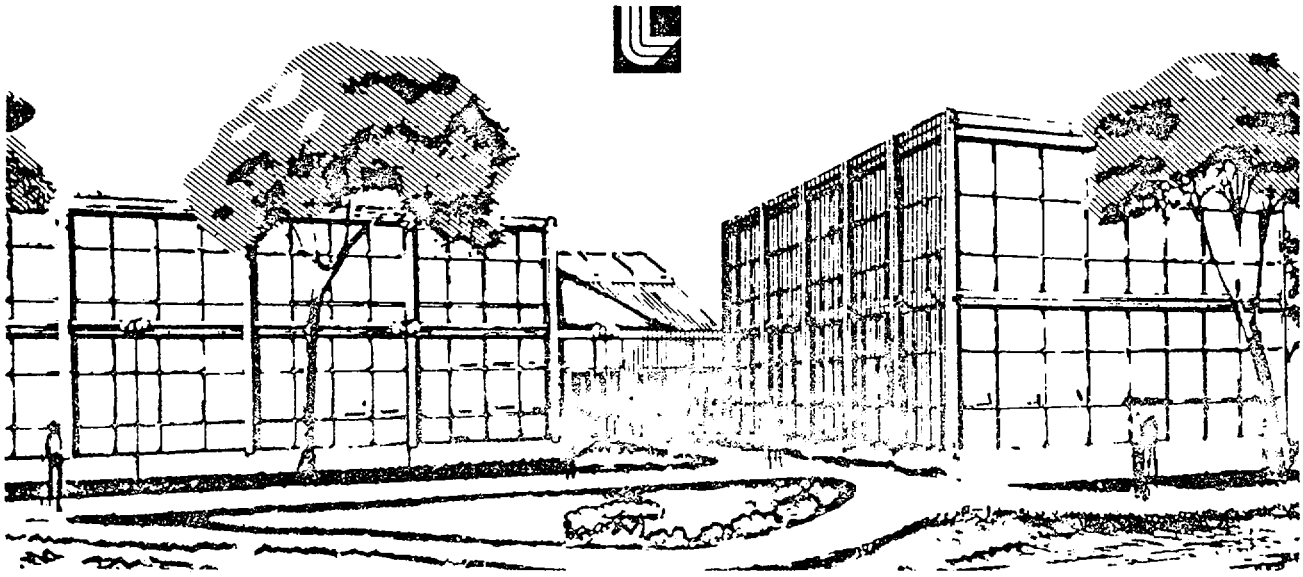

THE TIME FOR ATOMIC AND MOLECULAR DATA BASES IS NOW!

(AN OVERVIEW OF DATA MANAGEMENT RESEARCH AT LLL)

Abstract

We have created two numerical data bases of atomic and molecular (A&M) data required for laser induced fusion studies. One file contains primarily atomic energy levels and atomic transition data released by *Charlotte E. Moore* in NBS publications. The second file is based on the spectroscopic constants for more than 1000 molecular levels of approximately 160 heteronuclear diatomic molecules prepared by *S. N. Suchard.* Additional data bases are contemplated in support of the accelerating research activities in these fields. The present paucity of authenticated, computer-readable A&M data is not unlike that observed two decades ago in nuclear fission research. At that time, emphasis was also given to the accurate measurement of physical parameters and to reaction rates which eventually led to the ENDF/B series of evaluated neutron cross sections. Today, powerful computers have a more dominant role in modeling and predicting the results of promising experiments. Their effective use, however, depends more than ever before upon the availability of comprehensive and accurate files of A&M data. At the Lawrence Livermore Laboratory (LLL), these requirements are accentuated by the heavy reliance on computers. Also, trends are presently becoming apparent among users of the national computer network for Magnetic Fusion Energy (MFE), with its center at LLL, to coalesce organization-dependent data files into central data bases containing bibliographic information and numerical data as a common resource. The Data Management Research Project (LLL/DMRP) is collaborating with the National Bureau of Standards (NBS/NSRDS) to be able to respond to the emerging requirements. This should contribute to a *"Public Well"* of atomic and molecular data, unencumbered by legal or monetary constraints.

Work performed under the auspices of the U.S. Energy Research & Development Administration under contract No. W-7405-Eng-48.

1. Introduction

We would like to start by recalling the introductory remarks prepared for the *Advisory Group on Atomic and Molecular Data for Fusion* at the UKAEA Culham Laboratory, 1st-5th November, 1976:

> Experience with present-day fusion devices has shown a critical need for numerical data for the detailed understanding of the physical processes which occur in these devices. As the fusion research programmes progress toward the design and construction of larger experimental devices, serving as prototype facilities for full-scale fusion reactors, the data requirements will become more severe as other physical processes become important and the required level of understanding becomes more advanced.
>
> This meeting on atomic and molecular data for fusion, convened by the International Atomic Energy Agency (IAEA) will be the first international meeting on this topic. The goals of the meeting are to identify specific data requirements, review the national programs, and agree on an international cooperative effort to compile and disseminate atomic and molecular data needed in fusion research and technology. The advisory group meeting will recommend guidelines for international collaboration and specify IAEA's role in this effort.

Bibliographic data bases of citations to the scientific literature provide a powerful means of finding pertinent publications. Computer-aided retrieval today is fast, and the volume of computerized information is large, so that requestors of a literature search readily become deluged with high-speed printouts of pertinent reports and articles. To manage this "successful" retrieval, specialized and user-tailored bibliographies are needed and are beginning to appear in different fields. An example is a *Multiphoton Bibliography* now in preparation for the laser induced fusion program in collaboration with *Dr. J. H. Eberly* of the University of Rochester. This collection and that of *Dr. C. F. Barnett* in the general area of fusion research should probably be made available to the fusion research community on the MFE computer.

But this is not enough. In general, what the requestor of a literature search really needs in most cases are not bibliographic citations, or full-text reports, but rather their numerical contents and validity domains for which the text is merely the means of communication. Presently, the requestor is thus obliged to obtain hard copies of the reports, to read and note the significance of measurements, to extract the desired numerical values, to evaluate them by comparison with other measurements, and to keyboard the data perhaps for ultimate use in his modeling program. This is a time-consuming and costly procedure, repeated over and over whenever and wherever someone wishes to use the data. In addition, depending upon the thoroughness of the individual reviewer, the conclusions and evaluations may still be different from case to case.

Numerical, scientific data bases are needed now! This refers to both experimental and evaluated data, and to A&M measurements in particular. Nevertheless, the research community of this country, and their supporting federal agencies, are still content with only the Gutenberg printing method of communication which served so well prior to the advent of the computer: You do the research and describe the results in books. Then, the results are gradually filtered back into the forefront of research. The major federal research organizations are spending today rather large funds on experimental and materials research. The National Bureau of Standards evaluates data for selected fields, but it also stops in most cases with the printing of evaluated information and data in monographs and circulars. Although type is being set for these publications with the assistance of instructions stored on magnetic tape, the number of corresponding computer-readable data bases is small.* Data evaluation centers throughout the country are still operating on subsistence funding.

---

* *We are told that even these few magnetic tapes are not in high demand. We suspect that this is due to their little-known availability, and due to the absence of a standard exchange format, requiring the recipient to take each file as a special case and to translate it to the local data base management system - if one is available.*

With regard to computer-readable A&M data, we find that individual research efforts develop and maintain their own data files. The calculational programs of the national laboratories, universities and industry appear to favor their time-proven sets, often directly embedded in their computer programs. These collections are thus not open to the scrutiny of the scientific community and can be shared only with difficulty.

Experience with the MFE computer network tends to improve this situation. As students and professionals change their working location, but continue to work on the MFE net, the mutual awareness of data files and calculational algorithms for A&M data grows and contributes to the refinement and extension of numerical data sets. This evolution is being sped up by the rapidly increasing R&D activities in magnetic and laser induced fusion energy research. However, to direct these developments here and elsewhere into desirable, practical and cost-effective paths, timely and innovative solutions are needed and steady and appropriate funding for the aggregation, evaluation and dissemination of numerical data. The design and development of systems to manage the complex scientific data is also required and requires a lead time of several years.

The situation today in the field of atomic and molecular data is reminiscent of events several decades ago when the U.S. Atomic Energy Commission was charged with the responsibility of harnessing fission energy. At that time, data banks of neutron cross sections and their processing codes were urgently needed to predict by machine the energy release and time behavior of nuclear reactors. Whatever the forthcoming solutions might be for fusion under the aegis of the present U.S. Energy Research and Development Administration, or a future Department of Energy, they will depend upon the availability of comprehensive and accurate sets of evaluated computer-readable data.

2. Overview of Data Management Research at LLL

Data Bases are becoming an exceedingly important part of computer utilization. They provide the input to calculations and do the bookkeeping and comparing of results. Intimately associated are *Data Base Management Systems* that provide the desired rapid access and manipulative power for the growing volume of scientific textual information and numerical data. Finally, data bases and their management systems are relatively useless unless they are shared with others in a controlled manner, e.g., as *Geographically Distributed Resources over Computer Networks.*

DATA BASES

We are presently funded to establish a number of technological and scientific data bases. These demands arise primarily from energy and environmentally related research, where the expanding use of computers in application programs and in modeling is placing increasing demands upon the availability of authenticated, evaluated data of physical and chemical properties. Without these primary sources of factual data it is progressively more difficult to intercompare calculated results and to judge the efficiency claims of energy conversion and energy storage systems now under development.

There is a profound difference between scientific data and the customary numerical data now necessarily used in technological and scientific work. In fact, the difference is sufficiently pronounced to have discouraged the production of *'scientific'* data bases because of their complexity: Physicists, chemists and biologists are accustomed to about two dozen attributes by which a numerical value is necessarily qualified:

ATTRIBUTES OF SCIENTIFIC DATA:

1. *Value*
2. *Uncertainty (symmetric or assymetric)*
3. *Units of Measurement*
4. *Normalization*
5. *Validity Domain*
6. *Method of Measurement*
7. *Conditions & Constraints*
8. *Type of Data (vector, matrix, array...)*
9. *Source of Data*
10. *Bibliographic References*
11. *Comments of experimenter or evaluator*
12. *Proprietary Status, Classification, etc.*

Without these and additional attributes, the numerical value, or datum, is often without meaning. And, because of the difficulty to retain and to display these attributes by conventional and business-like data base management systems, truly *scientific* numerical data bases are infrequent and comparatively small in size.*

At the Lawrence Livermore Laboratory, we have interdisciplinary requirements for the creation and use of scientific data bases. These range from the data contained in *The Table of Isotopes*,[1] gamma-ray [2-5] transitions, properties of atomic and molecular data for potential use in laser research,[6-7] and biomedical data quantifying human organs and tissues.[8-9] Material properties of energy storage materials and the ecological study of the San Bernardino Forest in the Los Angeles area pose similar problems of complexity, requiring in the latter case some 600 different data descriptors to store biological and environmental variables.

---

* *An exception are the immense collections of measured and evaluated data neutron cross sections, reaction rates of charged particles, and similar data aggregated during the past three decades by the international community in support of nuclear research and fission reactors. However, in context, we would classify these as technological data bases, being narrow in scope and hence requiring fewer attributes.*

DATA BASE MANAGEMENT SYSTEMS

The primary charter of the *DATA MANAGEMENT RESEARCH PROJECT* at LLL, formerly known as the *INFORMATION RESEARCH GROUP*, is the design and development of data base management systems that can cope with the different types of data required in support of LLL and ERDA programs. We have thus been designers, implementors and users of the MASTER CONTROL Program (MCP), a generalized data base management system,[10-14] and are presently laying the foundation for an advanced system for scientific data. To gain experience with state-of-the-art systems and to judge their potential relevance for scientific needs, we are also working with the ADBMS[15-18] system based on *CODASYL* specifications, and with INGRES,[19-23] an advanced relational system. Finally, we have studied the SET-THEORETIC[24-26] approach to data management.

Of these systems, MASTER CONTROL is written in LRLTRAN,[27] an advanced version of FORTRAN, and depends upon the Livermore Time Sharing System (LTSS),[28] developed at LLL for the *OCTOPUS* network of CDC-6600/7600[29-30] computers shown in Fig. 2-1. ADBMS, under development at the University of Michigan, is written in FORTRAN and has been installed on several mainframe computers. INGRES is written in "C" and is used in combination with UNIX, an operating system under ongoing development by Bell Telephone Laboratories for the Digital Equipment Corporation PDP-11/40/45/70 minicomputers. INGRES is a rather sophsiticated research system of the Electronics Research Laboratory of the College of Engineering at the University of California, Berkeley. We have experimented with it on a PDP-11/45 at LLL and are going to use it with the PDP-11/70 machine, which is one of the host computers of the ARPAnet node at LLL. The SET-THEORETIC system is proprietary and is being marketed by the Set-Theoretic Information System Corporation (STIS) at Ann Arbor, Michigan. It has been available to us by contractual arrangements at Wayne State Univ.

Most of our experience to date has been with the MASTER CONTROL system. It has been in use at LLL since 1969 and at the Los Alamos Scientific Laboratory (LASL) since 1973, when the Livermore Time Sharing System was transferred to become the secure computer network at LASL.

MASTER CONTROL is used now at LLL by 17 Divisions and a much larger number of users for highly diversified programmatic tasks. A total of more than 250 hours of CDC-7600 equivalent time was expended last year. The program has been substantially improved in recent years through segmentation and dynamic dimensioning. New features were added that permit a variety of arithmetic and functional operations. In addition to FORTRAN relations, the user may use any of 50 different functions in an interactive manner. These range from conventional trigonometric and exponential relations, to functions that permit unique operations, e.g., the conversion of units, identifications of the smallest or largest arguments of a set, replacement of vector elements, and the translation of character strings into numerals and vice versa. The user may define a relation from his terminal and in the very next command he may already employ this newly defined variable as a search criterion for editing. All functions may be multiply subscripted and may be embedded within each other to 58 levels. We have really just begun to explore the flexibility and power of this functional, virtual capability. We have also added improved features for the creation of multi-term concordances and user-definable dictionary options for the compaction of scientific data and their attributes.[31] Refer to Fig. 2-2.

The system is presently used with more than 200 different data bases. These range from personnel-related administrative files to the large bibliographic holdings of the scientific literature, and with programmatic numerical data files. Some 1,500 interest profiles are processed each month against an influx of ca. 35,000 citations from different sources to alert researchers about new work being done in their field. This Selective Dissemination of Information (SDI) covers the major large bibliographic data bases of the professional literature. Retrospective searching, in contrast to SDI, is being carried out at LLL under contract from remote terminals at LLL by the Staff of the Technical Information Department with access to the large data banks of Lockheed, SDC, Medline, Toxline, DDC, and others. Some bibliographic and numerical, scientific data bases available through MASTER CONTROL at LLL are shown in Fig. 2-3.

The ADBMS data base management system, operational at LLL on the CDC-7600 since October 1976, is being used primarily for the *Safeguards* program of the Nuclear Regulatory Commission (NRC) at LLL.

The INGRES relational system with its innate hierarchial capabilities is being tested against personnel related data bases of the Data Processing Services Division (DPS). Here, a PDP-11/45 is being used. When the PDP-11/70 computer on the LLL ARPAnet node becomes operational in 1977, we intend to use INGRES for the technological data bases of the ERDA Energy Storage Systems Division and for scientific data.

The SET-THEORETIC data base system has been used for the processing of the large CAB Flight Segment data base of nearly two million records at Wayne State University where each commercial flight of U.S. carriers during the past four years is described by some 97 parameters. This work is being done under contract with the Information Division of the Transportation Systems Center for the U.S. Department of Transportation, DOT/TSC. The Set-Theoretic system was investigated as a potential solution to handling their large data bases.

The source programs of MASTER CONTROL, ADBMS and INGRES are available to us. By themselves, none of these programs are adequate to meet the near-term and/or far-term programmatic requirements for the manipulation of technological and scientific data. However, our experience with these systems and their unique concepts is proving valuable in defining and implementing an advanced system for interdisciplinary, scientific work. Here, of course, we are mindful of the availability of commercial systems. To date, those that we did examine are strongly business oriented and do not lend themselves readily for adaptation to scientific work. There would also be the difficulty of responding quickly to ever-changing demands in research when the availability of the software, and its dissemination, are controlled by commercial interests. If we postulate that the sharing of numerical, scientific data should be unencumbered by monetary or legal constraints, we must necessarily also conclude that the computer programs for managing the data should be in the public domain. The precedent exists in neutron cross section data and their computer programs.

The design and development of a *Scientific Data Base Management System (SDBMS)*, capable of handling the more complex atomic and molecular data and their customary notations, for example, is a challenging task. Fortunatelly, there exist already advanced routines and graphical and statistical capabilities that do not have to be reinvented but should rather be linked in an integrated manner with the SDBMS to provide the user with a total capability, in place of separate programs with their own peculiarities and requirements. This does not diminish the challenge of the task but defines more clearly where the emphasis has to lie, namely in data structures, their interpretation, and primary manipulative powers. The evolution of data base management systems at LLL, leading toward the SDBMS, is shown below:

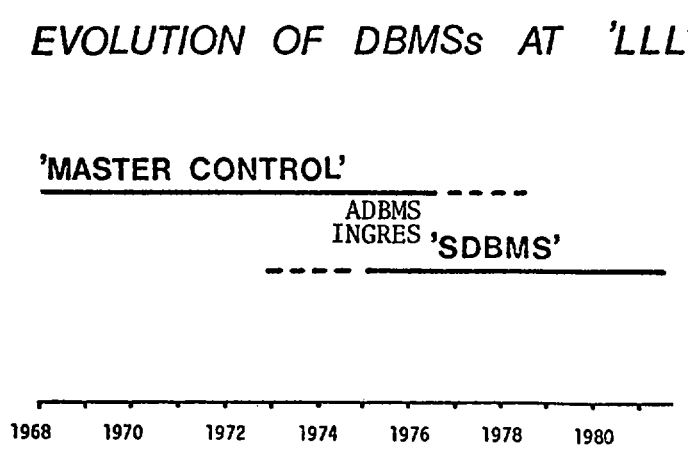

Some of the unique features to be made part of the SDBMS are listed in Fig. 2-4. Here we wish to point out especially that the Hershey character sets are probably indispensable for the display of customary scientific notation, especially in A&M data.[32] In addition, immediate access to tables of the fundamental constants of nature, and to conversion coefficients for units of measurement, has to be provided to permit the degree of freedom expected for professional use in the sciences. Some of these have been prepared by us and were released to the public domain. [33]

Aside from using a data management system to create direct input to application programs and to calculational models, we find it most desirable to give the user the option to store the results of his calculations in the data base as well:

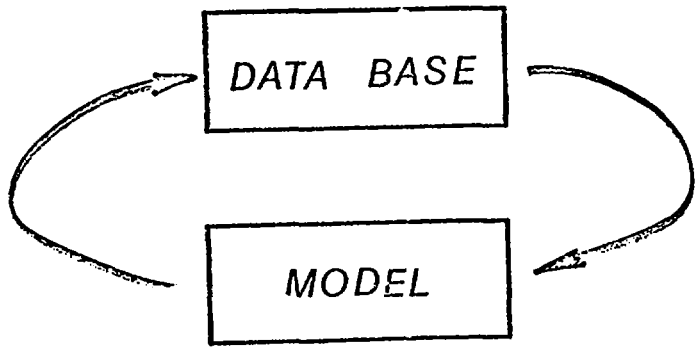

INPUT & OUTPUT

The effectiveness of this technique has been demonstrated when we could store the succinct results of Monte Carlo calculations in the same data base that provided the input to calculations. In this manner direct feedback was established between input and output. By storing only the essential calculated results, we could demonstrate the power of the technique to automate perturbation and sensitivity studies, to process much larger volumes of production calculations in a rigorous and dependable manner, and to subject the results and their input to graphical interpretation and display without manual intervening steps. This procedure proved to be a considerable cost and time saving by removing the tedium of keeping track of voluminous computer printouts and the manual slow extraction of crucial parameters. The totality of the calculated output file was actually sent into secondary storage, but could be called back for careful and detailed examination whenever warranted by the inspection of the more succinct data. The savings in time and paper were considerable.

There exists a universal need for efficient, cost-effective and user-oriented systems that can support the growing demands for the manipulation of scientific data. Fig. 2-5.

Here we are not referring to the mammoth collections of air- and water-quality data, or that communicated by earth observation satellites. These will always probably be best served by specialized systems uniquely adapted to the large tasks. We find it necessary to respond to the emergence of medium-sized files of complex technological and scientific data required by the inter-disciplinary end-user for interactive aggregation of data, and for his personal or programmatic research.[34]

The situation faced today with numerical data bases is similar to that of a decade ago with bibliographic information files. At that time the need arose from engineers and scientists *to find* quickly from the growing literature pertinent publications. The development of highly-efficient bibliographic storage and retrieval systems were the result. Today, the same requestors would like to have the option *to use* the corresponding data just as effectively, and directly, by computer. The development of numerical systems is now a growing concern.

The design and implementation of an adequate system for the manipulation of scientific data has been under development at LLL for some time. We have assembled a staff of 4-5 complementary professionals with considerable experience in information science and data management.* Talent and know-how is also available elsewhere in the Laboratory where similar requirements have fostered the development of specialized systems in support of programmatic requirements. This pertains especially to graphics, statistics, pattern recognition and system analysis.

** The staff of the Data Management Research Project numbers 16 today.*

At last, with regard to the *computer hardware for data management*, there seems to exist now a universal concensus that a small, dedicated computer of the PDP-11/70 class would serve well for data acquisition, interrogation and most I/O operations. Major numerical analyses, and the preparation of integrated look-up tables, should best be carried out on a larger machine, under direct control of the mini-computer, and fully transparent to the user.

This approach is proving very useful in several existing and planned computer networks. A cogent example is the Magnetic Fusion Energy computer network and its ongoing development. Our present work with the PDP-11/70 node at LLL on the ARPAnet, and an additional PDP-11/70 expected later this year for the National Uranium Resources Evaluation Program (NURE) all have in common a mini-maxi computer combination. Considerable work is required to fully develop and automate these concepts and to cause them to function reliably in the research environment.

NETWORKING AND THE SHARING OF RESOURCES

We are going to limit our discussions only to the research in networking and the use of distributed resources as it pertains to the work being done by the *DATA MANAGEMENT RESEARCH PROJECT (DMRP)* with the PDP-11/45/70 computers on the LLL ARPAnet node, Fig.2-6 . The LLL *OCTOPUS* operating system has been described conceptually in the literature.[29-30] An up-to-date summary of the Magnetic Fusions Energy (MFE) computer and its national network (cf. Fig. 2-7) is contained in Appendix-I of this report as an extract from the forthcoming December issue of Energy and Technology Review with permission of its author *John M. Fitzgerald.*[35] Suffice it to say at this time that the throughput of bits for the MFE computer network is expected to exceed that of the whole ARPA net[36] in February, 1977.*

---

* *Note added during proofreading of this report: The MFE national computer network has indeed exceeded in late February, 1977, the total number of bits transmitted on the average by the ARPAnet.*

A major breakthrough in computer resource sharing has been accomplished by the novel techniques of the Distributed Capability Computing System (DCCS). The DCCS system permits the sharing of resources between computer systems regardless of the resource type. It accomplishes in *one* extendable mechanism the tasks performed by the emerging plethora of computer resource sharing protocols.

The concepts of the DCCS have been reported in the literature [37-39] and discussed with experts familiar with the issues involved. A prototype system, embodying some of the principal techniques, is operational and is undergoing development for the U.S.Department of Transportation (DOT/TSC). The DCCS is innately suitable for the standardization and utilization of such diverse processes as:

* *Hierarchical display of available resources, local and remote.*
* *Access to distributed data bases.*
* *Access to distributed calculational resources, e.g., models.*
* *Monitoring of secure and controlled access.*
* *Interconnection of computer networks.*
* *Automatic dial-up and execution of remote processes.*
* *Accounting of transactions.*

Previous work that most closely resembles the DCCS is the Resource Sharing Executive System (RSEXEC), developed by Bolt, Beranek and Neuman for the TENEX operating system. Both systems, DCCS and RSEXEC, address themselves to the problem of making available resources on remote systems to local programs exactly as if they were local resources. The major differences are:

1. The RSEXEC can share only files. *The DCCS can share resources, e.g. files, directories, terminals, processes, etc.*
2. The RSEXEC mechanism must monitor and interpret specific operating system calls. *The DCCS is entered through a single invocation mechanism and is, therefore, much simpler in its function.*
3. The RSEXEC protocol is very specific to TENEX. *The DCCS is system independent!*

Development and prototyping of the Distributed Capability Computing System (DCCS) are currently funded by the Information Division of DOT/TSC at Cambridge, Mass. It is anticipated that the DCCS concept will alleviate substantially the tedium now faced by DOT/TSC analysts in accessing a multitude of DOT data bases for statistical purposes and prognosis. Unlike ERDA, DOT collects and interprets by congressional mandate a large number of geographically distributed data bases that document the movement of people and freight by ship, barge, aircraft, trains and trucks, in addition to the accounting of interstate transfers of oil and gas. Presently, the analysts are obliged to familiarize themselves with each data base and calculational resource to be used, they must learn the peculiarities of computer centers and operating systems on which these resources reside, and have to employ from their offices separate voice and data telephones in making and maintaining viable connections with remote computer networks. All of the steps must be executed as a variety of dissimilar processes *manually*.

To automate these routine and tedious operations, we have extended the RATS operating system,[40] developed at LLL under a two-year ARPA contract to advance the Research In Secure Operating Systems (RISOS), by inclusion of the DCCS concepts in the prototyping of a *Monitor Of Distributed Data Systems (MODDS)* for DOT/TSC. During a demonstration in June of 1976 it took only 15-45 seconds to establish direct terminal connection with a number of remote computer centers, down to the execution level, by specifying simply the objective to be reached, e.g.:

@ WAYNE	*Indiana University*
@ DOT	*DOT/TSC Center at Cambridge, Mass.*
@ CTR	*CTR-Computer at LLL, California. (Now known as MFE)*
@ TYMNET	*Connection to open net, different hosts.*
@ ARPA	*Connection to open net, different hosts.*
@ INFONET	*Chicago computer facility.*

The rest was done by the MODDS, *automatically*.[41] Fig. 2-8 through 2-11.

Differences in connect time resulted due to automated dial-up of computer link requirements when the optimum path was selected by the prototype MODDS, establishing the access by giving all required entry information, inclusive of commands and passwords. This permitted the transfer of files from one net to another with subsequent processing elsewhere. Crossover among computer networks today is generally not encouraged by commercial networks. The ramifications of this capability are still to be explored.

At some future date, we envision the requirement to translate protocols and data bases, as well as computational resources, from computer net to computer net. Generalized Software for translating data has been under development for some time.[18]

Our research to work effectively with technological data for DOT/TSC as distributed resources will become especially pertinent for ERDA in 1-3 years when scientific data and scientific computational programs will necessarily have to be shared in larger measure than today.

Here it is pertinent to note that the *ERDA Interlaboratory Working Group for Data Exchange (IWGDE)*, under sponsorship of the ERDA Division of Biological and Environmental Research (ERDA/DBER), has formulated an exchange standard for numerical data on magnetic tape[42] that is expected to be adopted as a natural extension and utilization of the following American National Standards:

* *American National Standard Code for Information Interchange, X3.4-1968.*
* *American National Standard Recorded Magnetic Tape for Information Exchange (800 CPI, NRZI) X3.22-1967.*
* *American National Standard Magnetic Tape Labels for Information Interchange, X3.27-1969, including its proposal revision, X3L5/506T (9-18-75), if adopted.*

3. Programmatic Applications

The San Francisco Bay Area Pollution Model emloys MASTER CONTROL (MCP) as the central depository of information and data from a dozen different sources and organizations.[43-44] The integrated data is then subjected to analytical models for simulation and prediction. Fig. 3-1,2. The National Uranium Resources Evaluation Program (NURE) employs MCP for the aggregation and manipulation of a historic data bank that is expected to contain some 100,000,000 data items in time.[45] The present data base, considerably smaller in size after two years of operation, has contributed to the discovery of potential uranium deposits in the Walker Lake region in Utah. NURE is a 5-year program involving other ERDA Laboratories und universities and is expected to alleviate the shortage of fissile materials by 1980. A PDP-11/70 dedicated computer complex will be used later in 1977 for the acquisition and manipulation of the data. Some of the data bases in MCP are coupled PATTER,[46] a pattern recognition program of powerful algorithms capable of establishing correlations among large sets of phenomenological data.[47] The Laser Fusion Programs at LLL employ MCP for the storage of experimental data, and for the orderly accounting and scheduling of their multimillion dollar inventory of expensive laser components.[48] MCP is also used as the primary data base system for the aggregation of specialized bibliographies and numerical data of physical and chemical properties for materials of interest to the ERDA Energy Storage System research and development projects. LLL has been designated as the Lead Laboratory and collaborates with the National Bureau of Standards (NBS/NSRDS) in establishing the data bases and preparing them for transfer into the public domain.[49] For the ERDA Division of Biological and Environmental Research, we are using MCP for the aggregation of *The National Index of Energy and Environmentally Related Data Bases and Models*. The 1976 Edition of this Index contains some 4,000 data bases and approximately the same number of models. This unique collection of holdings from the major federal agencies is now being updated for transfer to the public domain.[50] It is already accessible over the ERDA/RECON national information network.

With reference to the production of numerical data bases, we are collaborating with NBS/NSRDS and have transferred funds for the evaluation of material properties by recognized data evaluation centers under their auspices. *Drs. David Lide* and *Lew Gevantman* are monitoring the progress of this collaborative venture. The resultant data bases of properties on molten salts for batteries and thermal storage systems, for fiber composits of flywheels, and many others, will be made available on the PDP-11/70 computer over the ARPAnet, by telephone dial-up and on magnetic tape from the Argonne Code Center. Succinct results will also be published in the NBS journals of standard reference data. NBS is presently providing this assistance free to LLL and ERDA. *Fig. 3-3.*

Here we are glad to announce that we have reached apparent agreement with some of the evaluation centers to provide ERDA and the public with evaluated material properties data free of subsequent monetary or legal constraints. This is in contrast to earlier requests where royalties were asked for the use of numerical data and where dissemination to non-ERDA users was prohibited or severely constrained by demands for royalties. The procedure by which we believe that data can be obtained in general for free and unencumbered use is:

> *Evaluation centers are asked to evaluate properties in light of the up-to-date literature. For some materials and properties this may have to be carried out ab initio;*
>
> *for others, the examination of the recent literature may not affect a previous evaluation. In either case, the evaluation process is being carried out under full government support, causing the resultant data to be in the public domain.*

We are mindful, that the evaluation costs may necessarily have to be somewhat higher under these arrangements to provide evaluation centers with some surplus of funds to sustain their research posture and professional competence.

In a related activity, supported by programmatic work at LLL in laser-induced fusion research, we have created scientific data bases of atomic and molecular parameters, as mentioned earlier. The release procedures of these data bases through the ANL Code Center, the National Technical Information Service (NTIS), the normalization of units of measurement and standard notations are presently being discussed and prepared with NBS/NSRDS.

Earlier last year, the power of interactive access to numerical scientific data bases was demonstrated when we searched interactively some 30,000 gamma-ray transitions by machine, employing Boolean logic on their numerical values and qualifying attributes, to identify only some 20 potential transitions as candidates for a gently-pumped X-ray laser device. The results were published at the recent laser conference at Coral Gables and at Novosibirsk.[51-52]

In collaboration with *Dr. Mike Lederer* of the Lawrence Berkeley Laboratory (LBL), we have written processors and translators that should permit the creation of a numerical data base next year as a machine-readable analogue to the forthcoming 1977 Edition of the *Table of Isotopes*.

Clearly, these are only beginnings and will require endorsement and support for timely completion of a small font of public knowledge.

4. Let us Create a *"Public Well"* of Scientific Data.

Programmatic requirements for accurate data in the physical sciences and in engineering are clearly apparent from the increasing number of requests received, a diversity of specific national and international efforts, and from the preponderance of committees that try to cope with the escalating situation.

These demands are a direct consequence to the decreasing costs of computing, data storage and communication. Equally important as a driving motive is the growing emphasis on interdisciplinary programs, a greater social awareness in our work, and the requirement for optimization of complex solutions in a highly competitive research community. The scarcity of pure research funds and long lead times of major national programs all contribute to the necessity for the use of the *best* data in an *open* manner for cost/risk/benefit analyses and decision making.

These demands are difficult to meet. Authenticated bodies of accurate data often do not exist for new materials or new operating conditions. Where they do exist, they are not computer-readable. Even data for traditional materials and operating conditions are locked in tables of printed books, or are contained in data files that are an innate part of some computer program and thus inaccessible for scrutiny and sharing. Finally, in the absence of a well funded national program for numerical, evaluated data we observe the emergence of a growing number of individual commercial efforts which offer unqualified data of material properties for sale with legal constraints on their use under the copyright umbrella.

We seem to forget that most of the research in physical and chemical properties of nature has been supported, in the United States and abroad, by public funds and should be available for free and unencumbered use. Progress in our civilization has been based on this tenet.

What then has changed? As long as researchers copied numbers by hand from journals and books, as long as they assembled them laboriously in orderly tables, and keyboarded them perhaps as input to their computer programs - nobody objected. When the monetary value of computer-readable data became apparent, and when the efficiency and time-saving of identifying, extracting and displaying dat by machine be demonstrated - unexpected difficulties arose. Originators of data files started to attach legal and/or monetary constraints upon their use. Recipients or buyers of such data could then no longer freely combine these data with other data, not even their own, especially if they intended to transmit the integrated files to coworkers or students outside the physical and/or legal constraints of their research organization.

There are those who argue that the commercialization of the measured and evaluated properties of nature is not different from the time-tested analogue of the public water well: *"Anyone, lifting water from a public well, placing it into containers and carrying it to places of demand, can charge for the water whatever the market can bear."*

We submit that it is in the interest of the scientific community to establish a "Public Well" for technological and scientific data, for anyone to use as he sees fit.[*]

Most of us will agree that users of data in universities, at national laboratories and at research centers, should have the freedom of choice to draw needed data from the public domain, if possible, or from commercial vendors.

The National Bureau of Standards (NBS/NSRDS) is mandated to aggregate and evaluate physical and chemical properties, especially also atomic and molecular data. It would seem appropriate that NSRDS have a key role in the computerization and dissemination of these data to assure their validity and consistency.

---

[*] *Some refer to a well as a hole in the ground. We prefer to call it a spring.*

References

1. C. M. Lederer, J. M. Hollander, and I. Perlman, *Table of Isotopes*, Sixth Edition (1967). The next edition is expected in 1977.

2. R. N. Rao and K. B. Lai, *Nuclear Level Half-lives (10^{-20}sec) for Alpha, Beta, Gamma Decay, Covering the Literature through 1972.* Department of Physics, Indian Institute of Physics, Indian Institute of Technology, Kanpur, India. In MASTER CONTROL at LLL and also at LBL, to be published in the Atomic Data and Nuclear Data Tables. (13,297 values of measured levels)

3. Ibid, *Weighted Averages of Experimental Data*, Recommended by G. N. Rao. (2,337 evaluated levels).

4. Ibid. *Bibliography in Support of the Above Two Quantitative Data Bases.*

5. W. W. Bowman and K. W. Macmurdo, *Radioactive Decay Gammas*, Atomic Data and Nuclear Data Tables, Vol. 13, No. 2-3, February 1974. (19,415 levels)

6. Eugene A. Henry, *Computerization of Atomic Level and Transition Data for the First and Second Ionization States of the Elements Hydrogen Through Phosphorus.* UCRL-52148, October 6 (1976).

7. Eugene A. Henry and Viktor E. Hampel, *Computerization of Spectroscopic Constants for Selected Heteronuclear Diatomic Molecules*, UCRL-52149, October 6 (1976).

8. L. R. Anspaugh, W. L. Robison, W. H. Martin, O. A. Lowe, *Compilation of Published Information on Elemental Concentrations in Human Organs in Both Normal and Diseased States*, 1. Raw Data Ordered by Atomic Number, Subordered by Organ and Suborgan, Listing Method of Analysis, Geographical Source, Age, Sex, Number of Individuals. Parts 2 & 3 show the same data ordered by different criteria, TID-4500, UC-48 (1971).

9. Arthur R. Tamplin, *Estimation of the Maximum Dose to Man from the Contamination of an Aquatic Ecosystem with Radionuclides*, UCRL-71865 and UCRL-50163 Pt. V. (1969).

10. Viktor E. Hampel and John A. Wade, *MASTER CONTROL - A Unifying Free-Form Data Storage and Data Retrieval System for Dissimilar Data Bases*, UCRL-71686 (1968), also published in the Proceedings of the Am. Soc. for Inform. Sc., San Francisco (1969).

11. Staff of the Information Research Group at LLL, *MASTER CONTROL User's Manual*, Rev.-8, M-066 (1975).

12. V. E. Hampel and J. A. Wade, *Utilization of Scientific Data Bases at LLL Using the MASTER CONTROL Data Base Management System*, UCRL-74259 (1972).

13. V. E. Hampel, *Problems and Some Solutions for the Creation and Utilization of Large Interdisciplinary Computerized Data Banks*, UCRL-74685, CODATA Symposium on Man-Machine Communication for Scientific Data Handling, Freiburg, Federal Republic of Germany, July 22-27 (1973).

14. V. E. Hampel, Eugene A. Henry, Robert W. Kuhn, Leonard Lyles, *Acquisition, Storage, Retrieval, Display and Utilization of Computerized Data in the LLL Data Bank of Physical and Chemical Properties*, UCRL-78372 (Rev.2) (1976), Presented at the 5th Biennial International Conference at Boulder, Colorado, June 28-July 2, 1976.

15. Edward W. Birss, *ADBMS Installation Guide*, UCID-17418 (1977).

16. Edward W. Birss, *ADBMS Users Guide*, UCID-17417 (1977).

17. The basic design consideration of ADBMS was to produce a data base management system for a Problem Statement Analyzer developed by the ISDOS project at the University of Michigan. It has since been modified by the Data Translation Project at the University of Michigan for internal DBMS support for their Data Translator; See Ref. 18, below. Although developed for internal use, it can be used independently as a data base management system. It is attractive because of its small memory requirements, its ability to use FORTRAN or COBOL as the host language, and the ability to define and use network structures. References 16 and 17, above, pertain to its installation on the CDC-7600s at the Lawrence Livermore Laboratory.

18. Edward W. Birss and James P. Fry, *Generalized Software for Translating Data*, AFIPS Conference Proceedings, Volume 45, presented as the technically outstanding and award winning paper at the National Computer Conference in New York, 1976.

19. G. Held, M. Stonebraker, E. Wong, *INGRES - A Relational Data Base System*, Proceedings of the 1975 National Computer Conference, Anaheim, Ca., May 1975.

20. W. Zook, et al. *INGRES Reference Manual, University of California*, Electronics Research Laboratory, Memorandum ERL-M519, (1975)

21. M. Stonebraker, E. Wong, *Access Control in a Relational Data Base System by Query Modification*, Proc. 1974 ACM National Conference, San Diego, Ca., (1974)

22. G. Held, M. Stonebraker, E. Wong, *Access Methods in the Relational Data Base Management System - INGRES*, Proceedings of ACM-Pacific-75, San Francisco (1975)

23. M. Stonebraker, *Implementation of Views and Integrity Constraints in Relational Data Base Systems by Query Modification*, Proc. 1975 SIGMOD Workshop on Management of Data, San Jose, Ca., (1975)

24. D. L. Childs, *Feasibility of a Set-Theoretic Data Structure Based on a Reconstructed Definition of Relation*, IFIP Congress, pp.420-430, (1968)

25. D. L. Childs, *Description of a Set-Theoretic Data Structure*, AFIPS Conference Proceedings, Vo. 33, Part-1, AFIPS Press, Montvale, NJ, pp-557-564 (1968)

    Also, D. L. Childs, *Extended Set Theory: A Formalism for the Design, Implementation and Operation of an Information System, CURRENT TRENDS on PROGRAMMING METHODOLOGY, Vol. 4*, edited by R. T. Yeh,m Prentice Hall, to be published in 1977.

26. Edward W. Birss, Jeffry W. Yeh., *Set-Theoretic Data Structures (STDS) An Illustrative Example*, Lawrence Livermore Laboratory, UCID-17378 (1977).

27. Jeanne T Martin, Richard G. Zwakenberg, Stanley V. Solbeck, M-026, *LTSS - Livermore Time Sharing System, Part-III: Problem Program Production*, Chapter 207: LRLTRAN Language Used with the CHAT and STAR Compilers, Edition-4 (1974)

28. Series of Publications by Computation Department, Lawrence Livermore Laboratory, M-026 (1976).

29. J. G. Fletcher, *The OCTOPUS Computer Network*, Datamation (1973)

30. D. L. Pehrson, *A Look at the LLL OCTOPUS System*, UCRL-76317, (1974)

31. Robert W. Kuhn, *A Numeric Processor and Text Manipulator for the MASTER CONTROL Data Management System*, UCRL-52015 (1976)

32. A. V. Hershey, *FORTRAN-IV Programming for Cartography and Typography*, Dahlgren U.S.Naval Weapons Laboratory, (1967-1971)

33. Eugene E. Henry and Viktor E. Hampel, *A Computerized Data Base of the Fundamental Constants of Nature*, UCRL-51969 (1975)

34. V. E. Hampel, R. A. Wiley, *Integrating Text and Data for Energy Research*, Lawrence Livermore Laboratory and Los Alamos Scientific Laboratory, UCRL-76991, also published in abbreviated form in the Proceedings of the ERDA-wide Conference on Computer Support of Environmental Science and Analysis, Albuquerque, NM, July 9-11, 1975.

35. J. M. Fitzgerald, *National MFE Computer Center: 1976 Update*, pp.18-23 in Energy and Technology Review, Lawrence Livermore Laboratory, *Laser Implosion Dynamics*, UCRL-52000-76-12, December (1976).

36. *ARPANET DIRECTORY 1976*, Produced and published by the Network Information Center of the Stanford Research Institute, Menlo Park, CA., 94025, for the Defense Communications Agency, Washington, D.C., NIC-36437 (1976).

37. J. E. Donnelley, *Extendable Information Formats*, UCRL-78211, Proceedings of the Berkeley Workshop on Distributed Data Management, May 25-26, Berkeley, CA., (1976)

38. J. E. Donnelley, *Controlling Transactions Between Distributed Computer Resources*, UCRL-78282 Rev.-1, Proceedings of the Fifth Texas Conference on Computing Systems, Austin, Texas, October 18, 1976.

39. J. E. Donnelley, *A Distributed Capability Computing System*, UCRL-77800, Proceedings of the Third International Conference on Computer Communications, August 3, 1976, Toronto, Canada.

40. Charles Landau, *The RATS Operating System*, UCRL-77378, October 13, 1975

Charles Landau, *An Introduction to RATS - (RISOS/ARPA Terminal System): An Operating System for the DEC PDP-11/45*, UCRL-51582, March 1, 1974.

William G. Frickel et al., *RISOS Analytic Tool Description Manual.* Part-1: Program Description, Part-2: Program Source Listings, UCRL-51810, Pt.-1,2, (1975)

41. E. W. Birss, J. E. Donnelley, J. W. Yeh, *A Monitor of Distributed Data Systems (MODDS): Part-1: Digest of Functional Specifications & Part-2: Detailed Functional Specifications*, UCRL-17314. (1976)

42. Deane Merril and Donald Austin, *ERDA Interlaboratory Working Group for Data Exchange (IWGDE)*, LBL-5329 (1976)

43. M. C. MacCracken, G. D. Sauter, *Development of an Airpollution Model for the San Francisco Bay Area*, Final Report to the National Science Foundation, Volumes 1 & 2, UCRL-51920. See also especially the Second Semiannual Report, UCRL-51537 (1974-1975).

44. M. C. MacCracken, *User's Guide to the LIRAQ Model: An Air Pollution Model for the San Francisco Bay Area*, UCRL-51983 (1975)

45. *The National Uranium Resource Evaluation Program (NURE) - Preliminary Report*, U.S. Energy Research and Development Administration (ERDA), Grand Junction Office, Grand Junction, Colorado, GJO-111-(76) (1976).

46. L. A. Cox, Jr. and C. F. Bender, *PATTER: A Polyalgorithm for the Analysis of Generalized Data Sets. Principles & Practice.* UCID-16915 (1975)

47. C. F. Bender, B. R. Kowalski, *Pattern Recognition - I: A Powerful Approach to Interpreting Chemical Data*, J. Am. Chem. Soc., Vol. 94, P. 5632 (1972)

C. F. Bender, B. R. Kowalski, *PATTERN RECOGNITION - II: Linear and Non-Linear Methods for Displaying Chemical Data*, J. Am. Chem. Soc., Vol. 95, P. 686 (also published as UCRL-74027) (1973)

cf. also *Chemical Engineering News*, August 28, 1972, pp. 14-15.

48. Alexander J. Glass, Kent L. Cummings, *Laser Program Annual Rerport - 1975*, Lawrence Livermore Laboratory, UCRL-50021-75 (1975)

cf. also earlier progress reports for different years, same Number.

49. E. A. Henry, *Research Leading to the Production and Early Use of Numerical Data Banks of Material Properties and System Analyses*, Quarterly Progress Reports, UCRL-1,2,3,4 (1976).

50. Viktor E. Hampel, Howard C. Martin, David A. Seberger, Alfredo Despy, *Preliminary Results of the ERDA/DBER Nationwide Survey of Energy & Environmentally Related Data Bases and Models*, UCRL-76777 Summary (1975).

51. Patrick L. Sommerville, Lowell Wood and Viktor E. Hampel, *Prospective Nuclear Transitions for a Gently-Pumped Gamma-Ray Laser, Identified by use of the MASTER CONTROL data base management system and manually*, UCRL-76442 (1974)

52. George Chapline and Lowell Wood, *X-Ray and Gamma-Ray Lasers*, UCRL-76530. Presented at the Orbis Scientiae II Conference in Coral Gables, January 21, 1975, and revised at the Vavilov Conference in Novosibirsk, in May 1975.

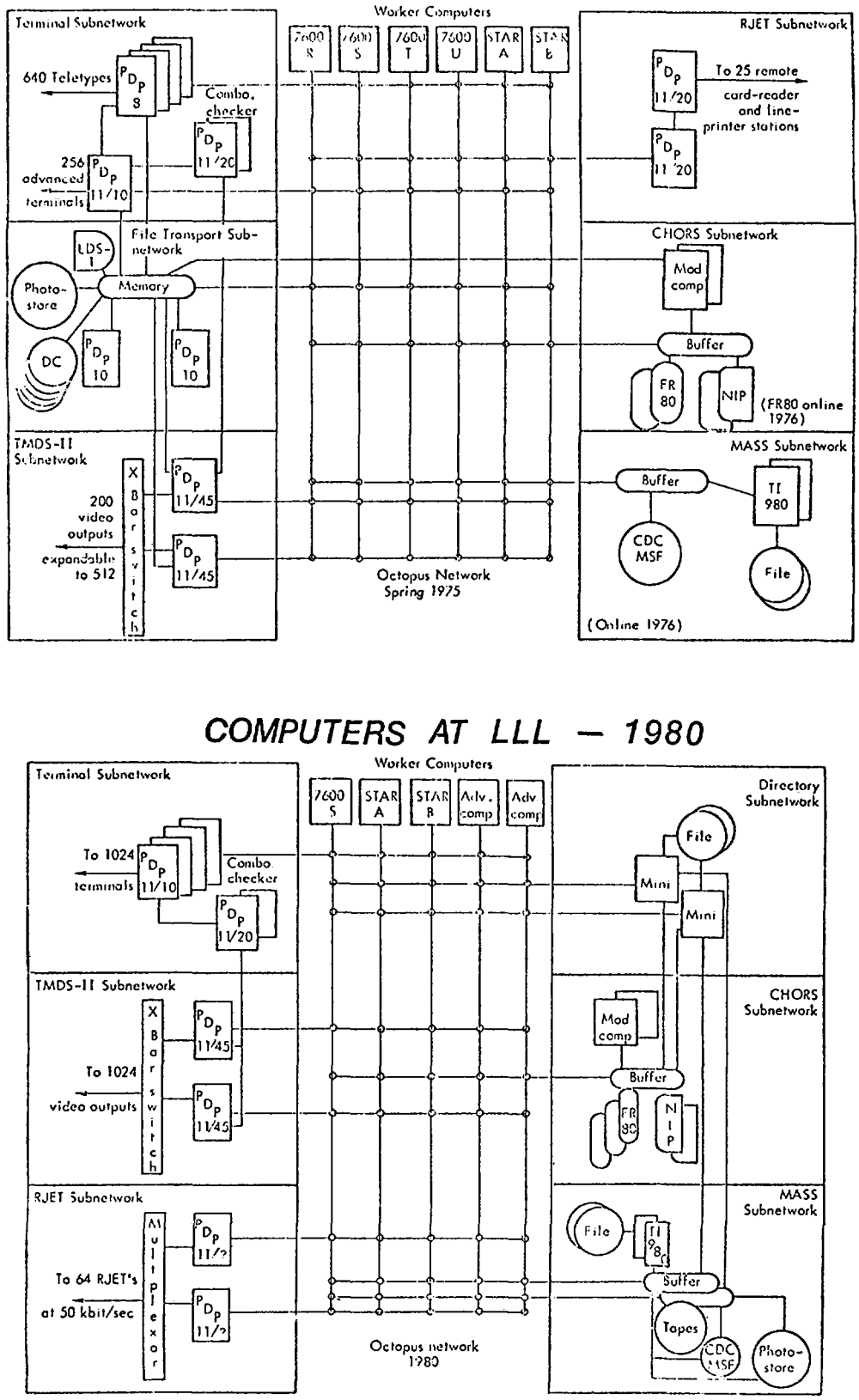

Fig. 2-1: The *OCTOPUS* Computer Network at LLL, 1975 & 1980.

EXTRACT FROM COMPUTER-GENERATED FLYWHEEL BIBLIOGRAPHY

			Accession Number Lookup:
BATTERY, BATTERIES			
1974	Battery-Powered Vehicle Drive	Deane, C. T.	142
1974	Superflywheel; The Battery that Spins	Lampe, D.	1136
1975	Energy Storage for Wind Energy Conversion Systems	Zlotnick, M.	101
1975	Energy Storage	Kalhammer, F. R.; Cooper, V. R.	102
1975	AC/DC Power Conditioning and Control Equipment for Advanced Conversion and Storage Technology	Wood, P.; Pelly, B. R.	1199
1975	An Evaluation of the Future Role of Energy Storage Techniques in Electric Power Technology	Pezdirtz, G. F.	103
1976	Energy Storage - Summaries, Feb-29 March 1 Meeting	American Nuclear Society Mtg.	1198
1976	Energy Storage	Casazza, J. A.; Schneider, T.R.	1196
1976	Energy Storage	Kalhammer, F. R.; Schneider,	1198
BATTERY CHARGING			
1971	Electric Road Vehicle	Union Carbide Corporation	144
BATTERY POWERED VEHICLE			
1974	Battery-Powered Vehicle Drive	Deane, C. T.	142
BATTERY-FLYWHEEL			
1976	Battery-Flywheel Hybrid Electric Power System for Near-Term Applications, Vol. 1 (System Description), Vol. 2 (System Design)	Davis, D. D.	1182/83
BATTERY-STORED ENERGY			
1974	Mechanical and Batter-Stored Energy Systems for Meeting Uninterruptable and Buffered Electric Power Needs	Comeau, G. E.	134
BAXTER, J. W.			
1974	Kinetic Energy Systems for Moving People	Baxter, J. W., Lawson, L. J.	1123
BEACHLEY, N. H.			
1969	Wobble-Spin Technique for Spacecraft Inversion and Earth Photography	Beachley, N. H.; Uicker, C. W.	1175
1975	Increased Fuel Economy in Transportation Systems by Use of Energy Management	Beachley, N. H.; Frank, A. A.	159

Fig. 2-2: Multi-term Concordance created with MASTER CONTROL for the ERDA Division of Energy Storage.

SCIENTIFIC BIBLIOGRAPHIC DATA BASES

1. Nuclear Science Abstracts
2. Chemical Titles
3. Engineering Index
4. Searchable Physics Information Notices
5. Nuclear Constants
6. Integral Neutron Experiments
7. Lasers
8. Computer Science
9. Thermophysical Properties (TPRC)
10. Gamma-Ray Transitions
11. Geothermal Phenomena
12. INSPEC, BIOSIS, Atomic & Molecular Data, etc.

SCIENTIFIC NUMERIC DATA BASES

1. 8-Peak Mass Spectroscopic Data
2. Low Resolution Mass Spectroscopic Data
3. Nuclear Constants
4. Atmospheric Kinetic Data,
5. Solar System Position Vectors
6. Gamma-Ray Transitions
7. Atomic Masses, Q-Values, etc.
8. Radio-active Decay Gammas
9. Table of Isotopes Data
10. Atomic & Molecular Transitions, Lasers
11. Properties of Materials for Energy Research

Fig. 2-3: Bibliographic and Numeric Scientific Data Bases at LLL in the MASTER CONTROL data base management system.

Unique Features of the 'SDBMS'

1. SCIENTIFIC, FUNCTIONAL ANALYSIS BY INTEGRATING *GRAPHICS*
   STATISTICS
   PATTERN RECOGNITION
   SYSTEMS ANALYSIS
2. SCIENTIFIC NOTATION & HERSHEY CHARACTER SETS: U_3O_8 NOT *U308*
3. SCIENTIFIC ATTRIBUTES TO DATA: *Value, Uncertainty, Units, Normalization, etc.*
4. BUILT-IN LOOKUP TABLES OF FUNDAMENTAL CONSTANTS & PROPERTIES
5. AUTOMATIC CONVERSION OF UNITS OF MEASUREMENT, *Yours, SI, or both.*
6. FLOATING POINT, COMPLEX & DOUBLE PRECISION
7. INTERFACE TO APPLICATION PROGRAMS
8. INTERFACE TO PROGRAMMING LANGUAGES, *e.g. FORTRAN, LLLTRAN*
9. RELATIONAL & NETWORK VIEW OF DATA
10. AUTOMATIC VALIDATION, RECOVERY, SECURITY & AUDIT TRAILS
11. USER-ORIENTED, SIMPLE & EXTENDABLE COMMAND LANGUAGE
12. EASY & EFFICIENT TO USE

Fig. 2-4: Unique Features of a Scientific Data Base Management System. MASTER CONTROL, ADBMS & INGRES do not meet all of these requirements.

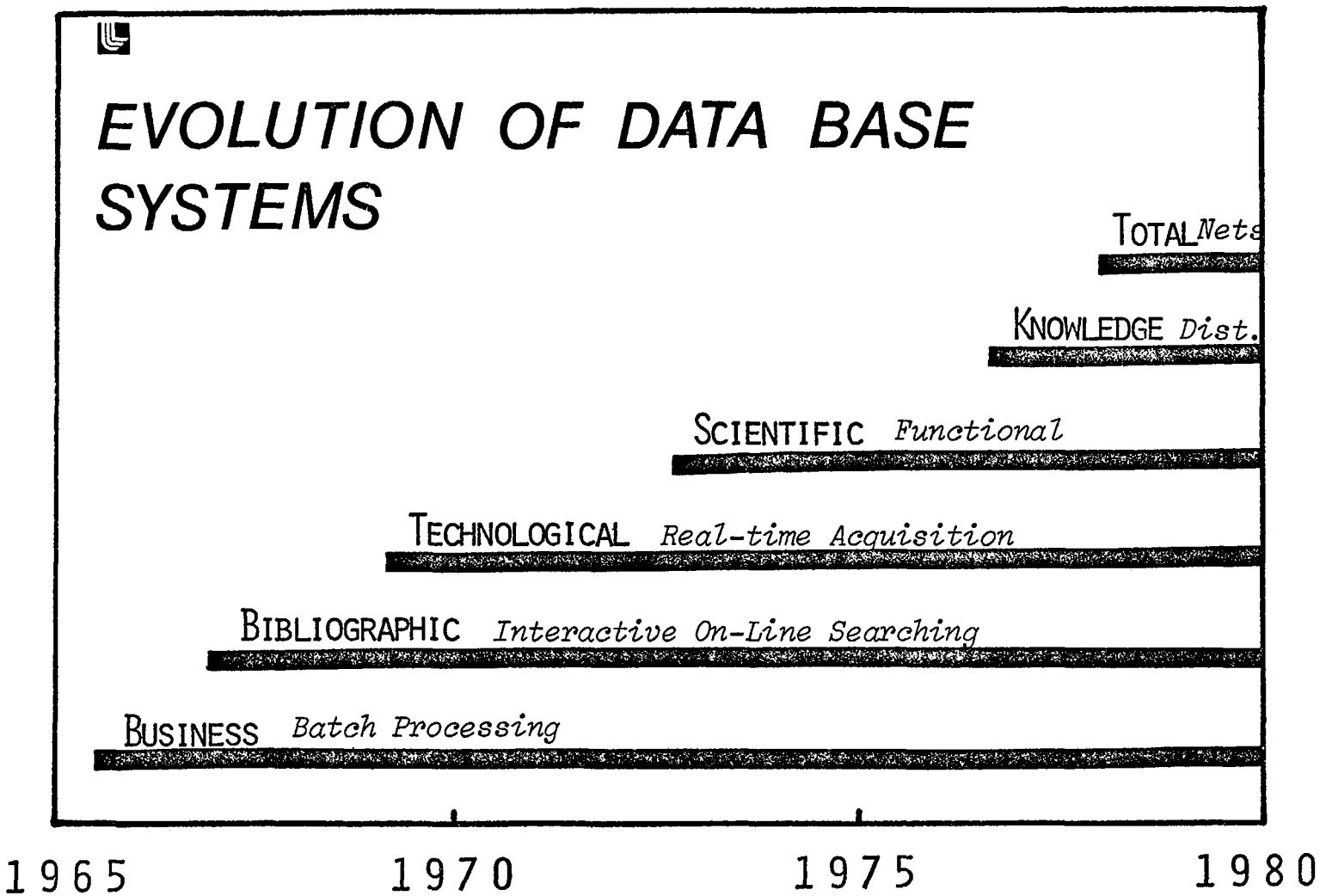

Fig. 2-5: Conceptual Evolution of Data Base Management Systems.

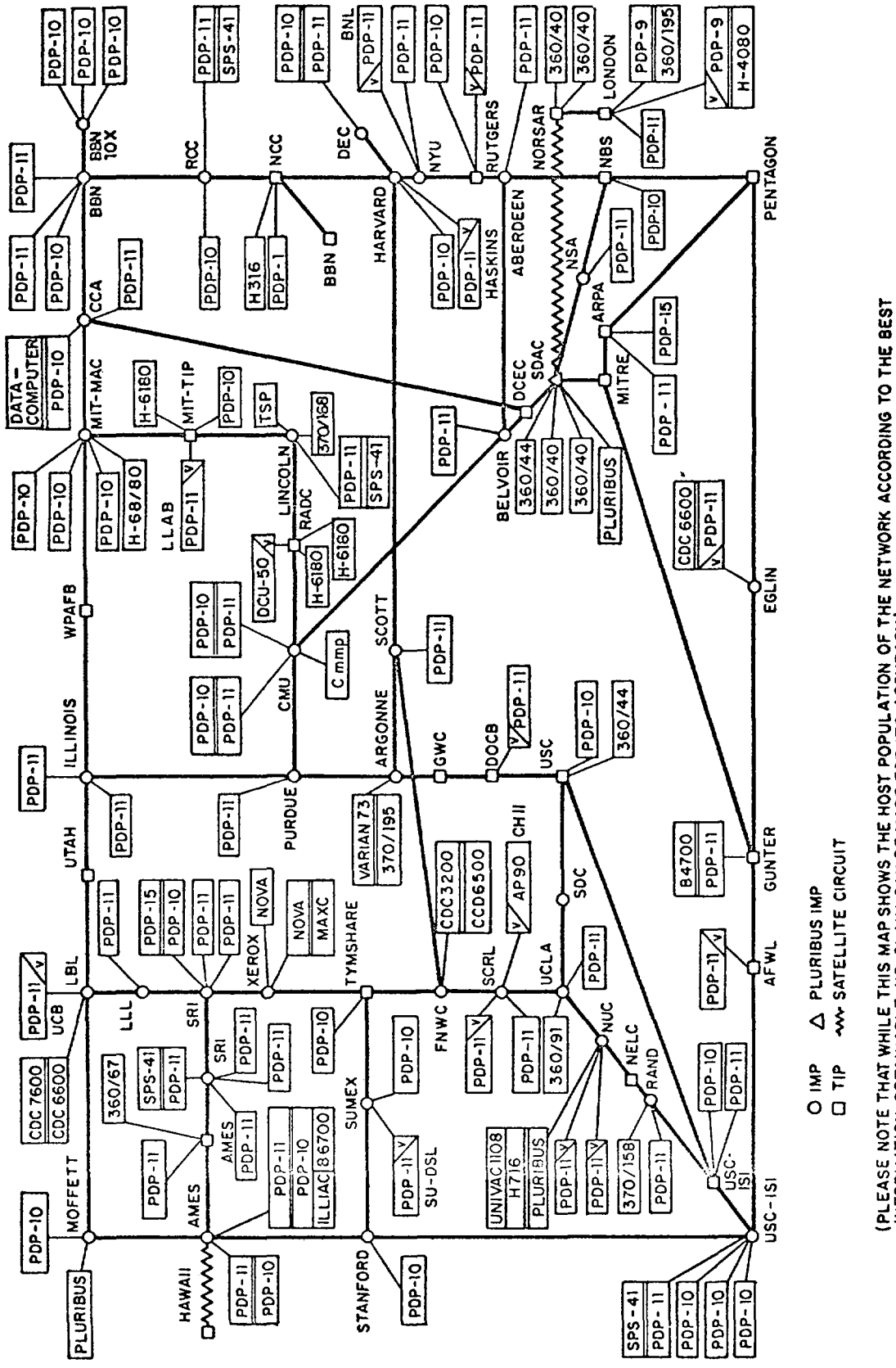

Fig. 2-6: The Logical Map of the ARPA network, taken from Ref. 36.

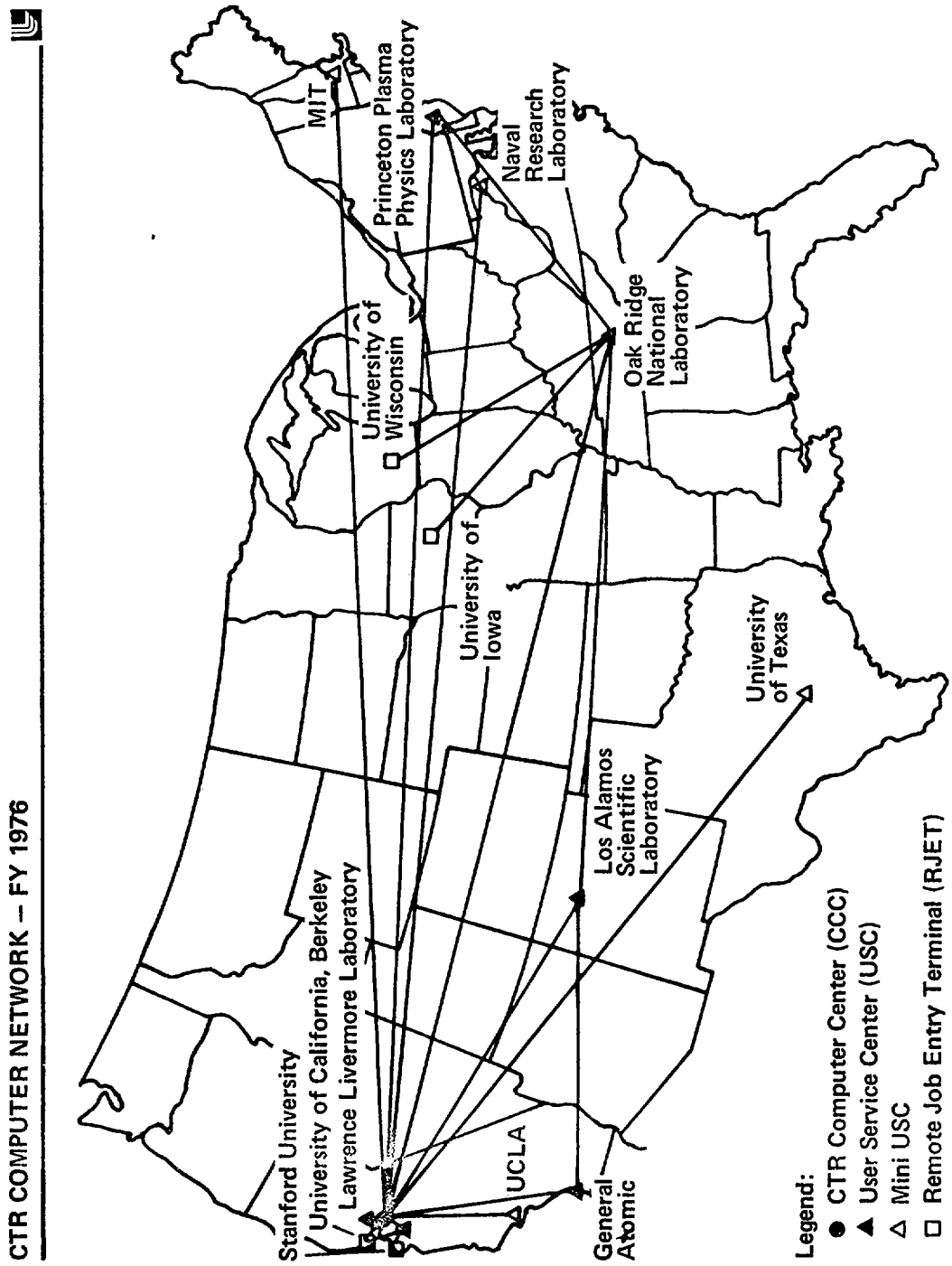

Fig. 2-7: The Magnetic Fusion Energy (MFE) Computer Network, formerly the Controlled Thermonuclear Research (CTR) network.

NETWORKING AT LLL

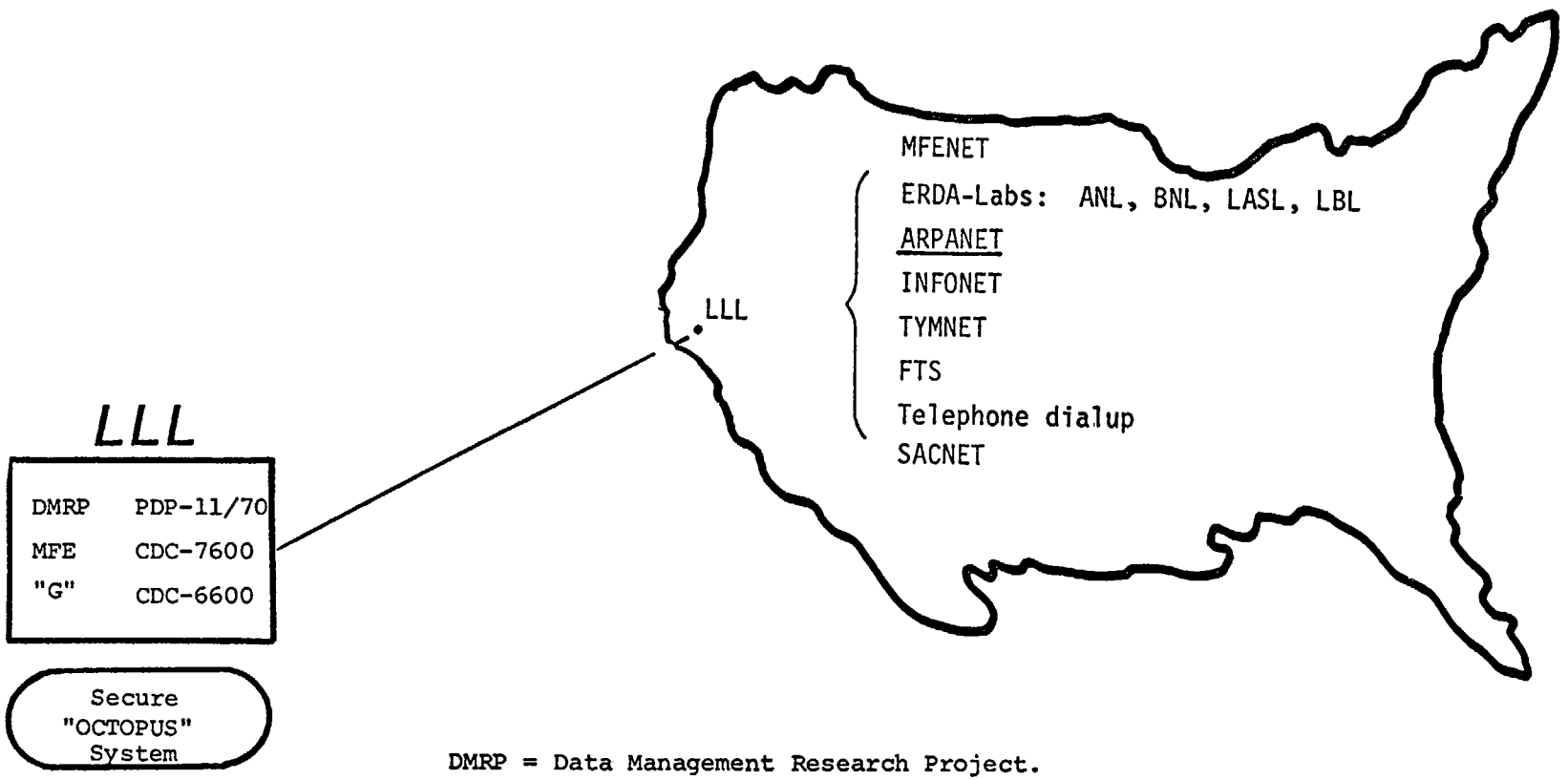

DMRP = Data Management Research Project.
PDP-11/70 is the primary host on the ARPAnet, with connections to the MFE and "G" machines.

MFE = Magnetic Fusion Energy program.
CDC-7600 is the primary host on the MFEnet.

Fig. 2-8

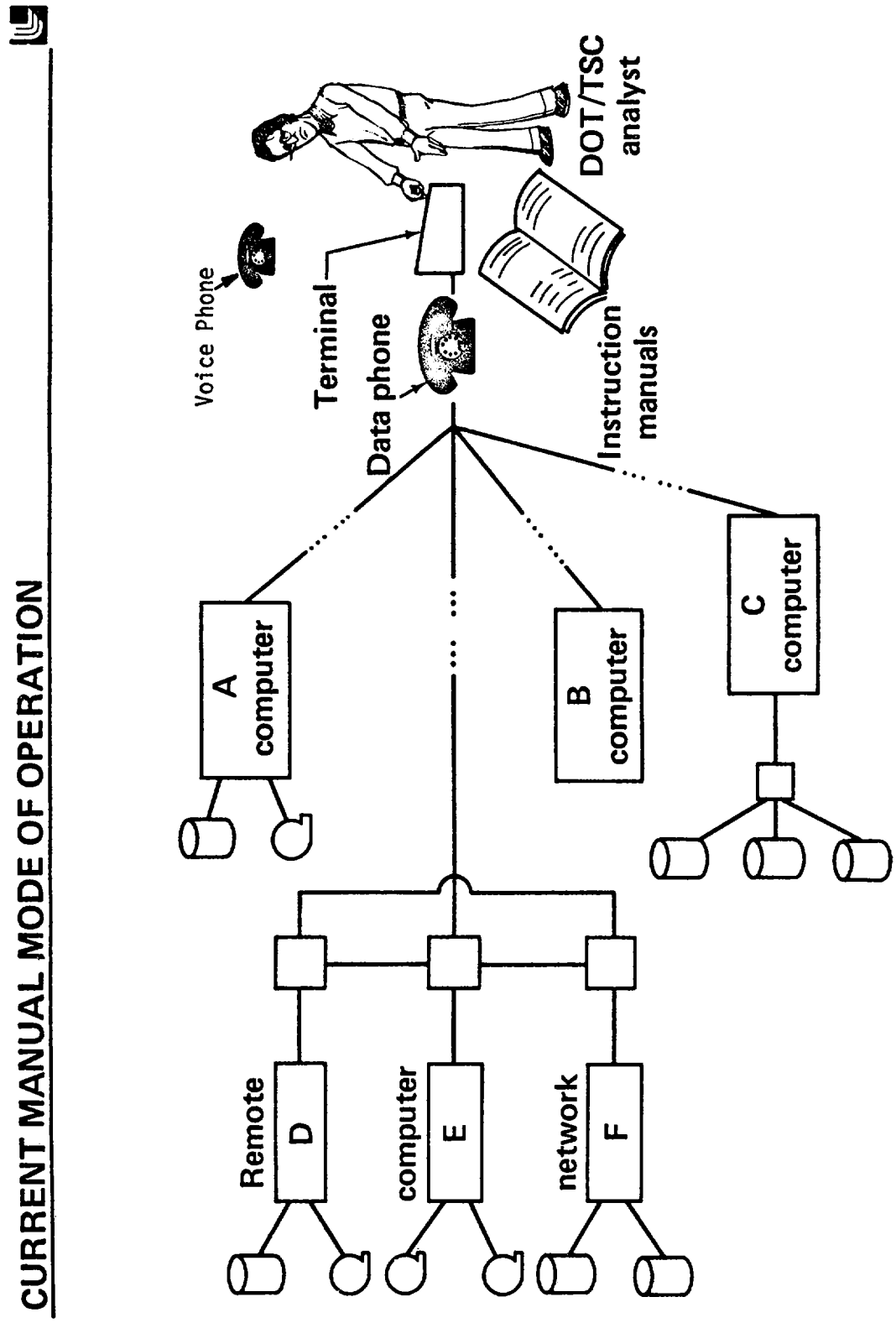
CURRENT MANUAL MODE OF OPERATION
DOT/TSC analyst
Voice Phone
Terminal
Data phone
Instruction manuals
A computer
B computer
C computer
Remote computer network
D
E
F

Fig. 2-9

SOLUTIONS TO CURRENT PROBLEMS

Problem	Solution
1. Difficult to identify available resources	Directory of available resources
2. Cumbersome to use	Automated, standard operating procedures
3. Difficult to control and monitor use	Access control through central monitor
4. Difficult to account for usage	Central monitor keeps log and statistics
5. Inefficient, non-optimum use of resources	Optimization based on resources and usage

⇩

"Monitor of Distributed Data Systems"

(MODDS) *

*Under Development for the Department of Transportation, (DOT/TSC).

Fig. 2-10

CONCEPTUAL USER VIEW SUPPORTED BY THE "MODDS"

(The complex distributed computers appear to analyst as ONE powerful machine)

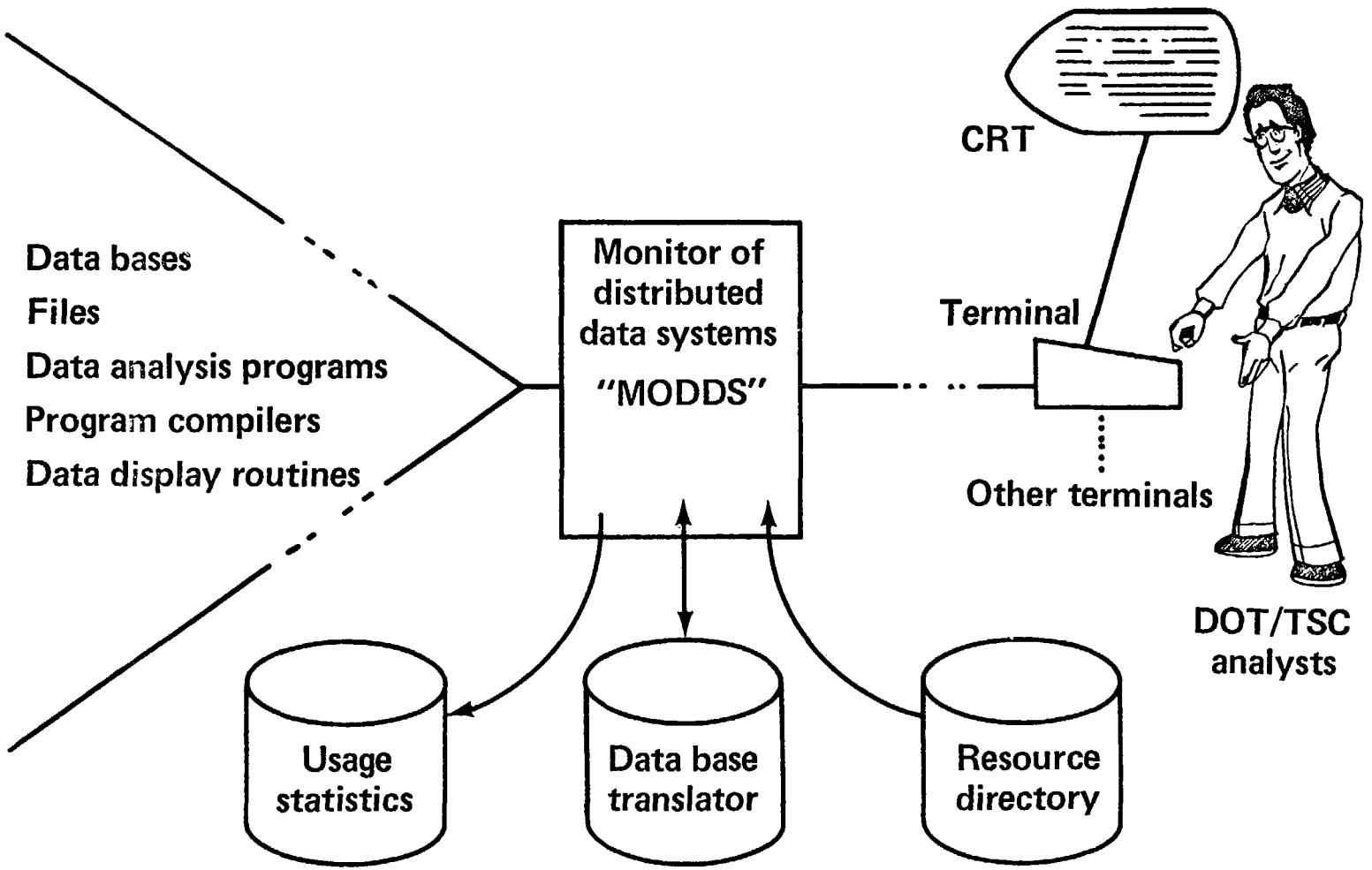

Fig. 2-11

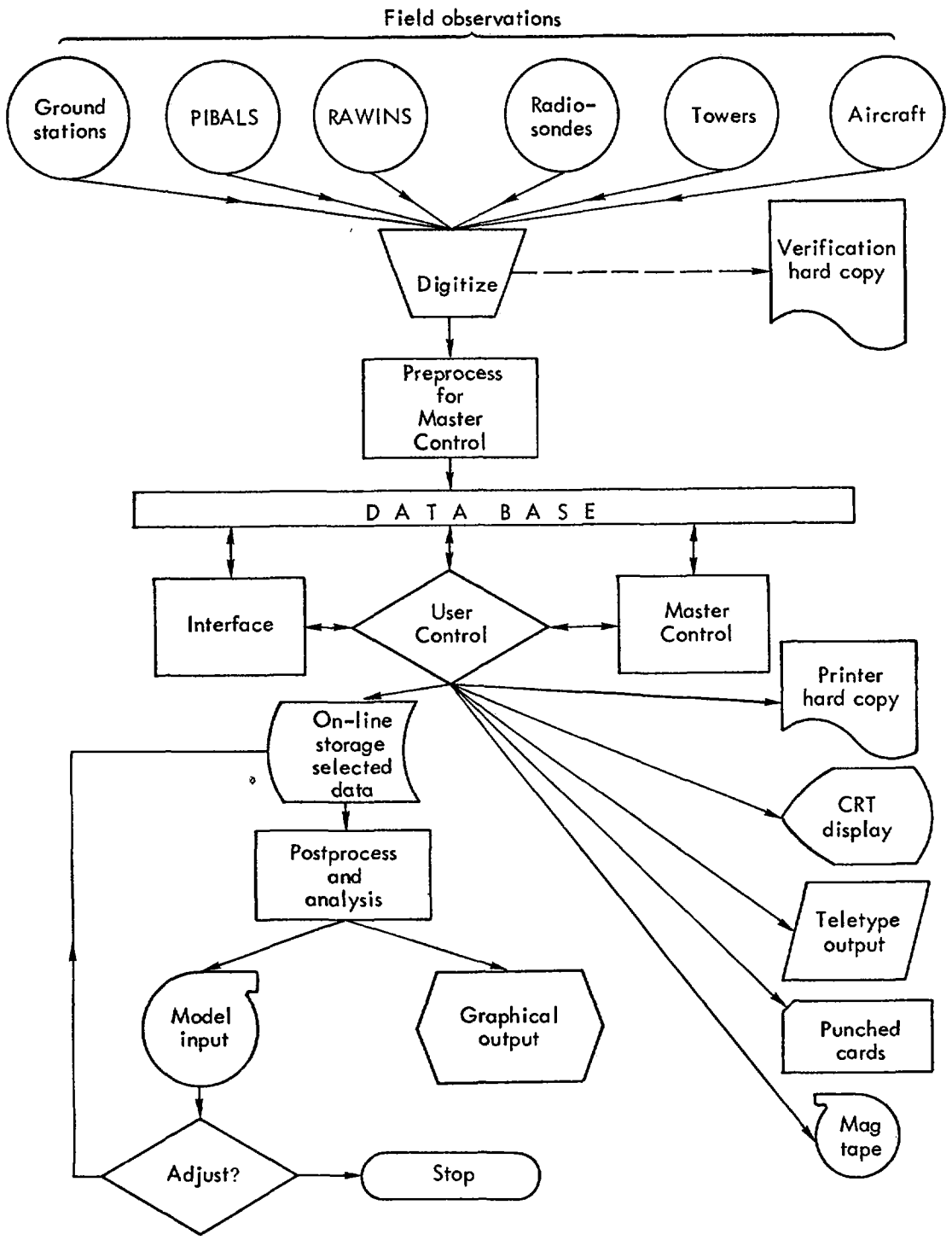

Fig. 3-1: Flow Chart of Data Processing Techniques for the San Francisco Bay Area Pollution Model carried out by the Atmospheric and Geophysics Research Division at LLL. Cf Ref. 43.

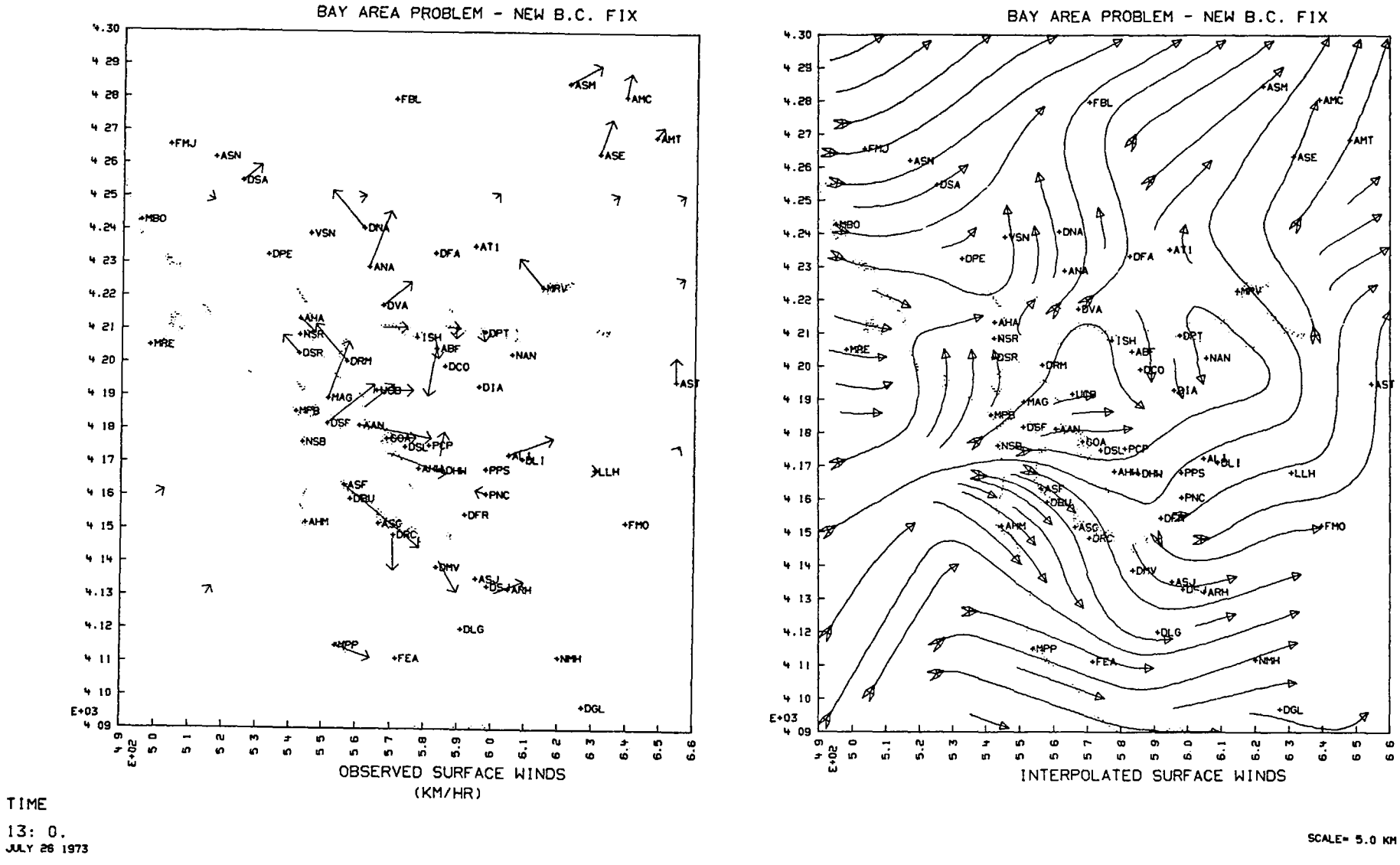

Fig. 3-2: Comparison of observed and interpolated surface winds from the San Francisco Bay Area Pollution Model, employing a MASTER CONTROL data base.

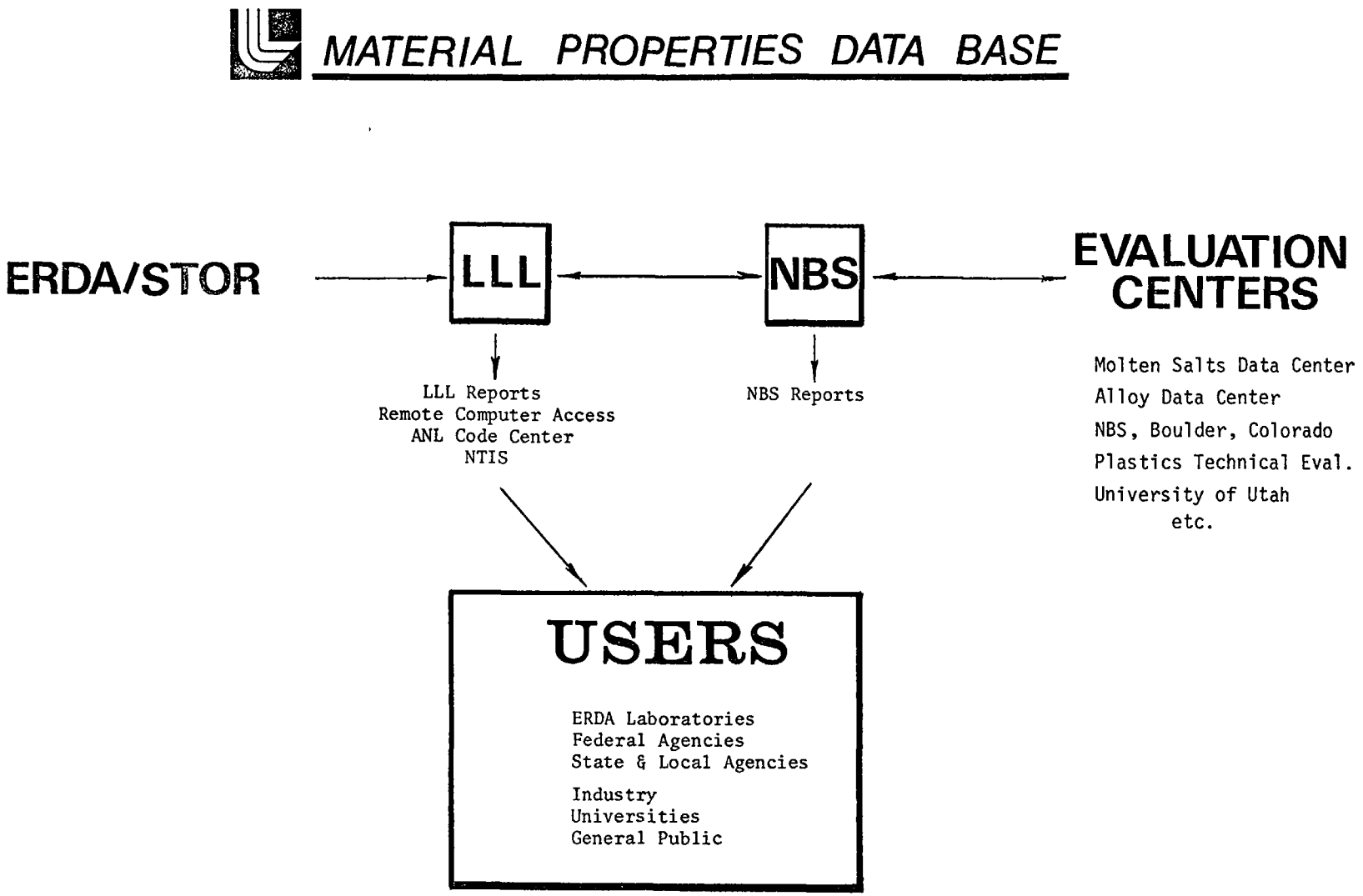

Fig. 3-3: Production of Material Properties Data Bases.

A P P E N D I X - I

ADVANCED ENERGY SYSTEMS

NATIONAL MFE COMPUTER CENTER: 1976 UPDATE

The national magnetic-fusion-energy (MFE) computer center at Livermore, operational since the fall of 1974, expanded its data communication network and improved its software and hardware during 1976. The network now includes seven user service centers across the country (including two at LLL) connected by 50 000-bit/s transmission lines to the MFE center. The most recent addition is a service center at Science Applications, Inc. in La Jolla, California. Among the major developments this past year is a high-speed channel that standardizes the process of interfacing computers of various manufacturers. FILEM, a versatile file-management system for remote users, was also significantly improved and will include a 500-billion-bit mass storage facility later this year. Demand for computational support in the MFE community continues to outstrip the center's capacity, requiring us to plan for a second CDC 7600 at Livermore and spurring interest in a next-generation computer as a third processing unit.

In 1974, LLL was selected as the site for a national magnetic-fusion-energy computer center (MFECC). Computional studies at the center were to be keyed to the research needs of the three principal MFE confinement schemes: low-density closed systems (mainly tokamaks), high-β systems (mainly the theta pinch), and open systems (magnetic mirrors). Major MFE research sites and scientists at universities with ERDA-sponsored MFE projects were to have access to the national center.

In the fall of 1974, the center went online to users via voice-grade telephone lines with a CDC 6600 as the central computer and a remote job entry terminal at the Princeton Plasma Physics Laboratory. One year later, a CDC 7600 replaced the 6600, inaugurating large-scale computational support to the MFE community. High-speed (50 000-bit/s) transmission lines were operational by mid-1976 to four user service centers: Los Alamos Scientific Laboratory, Princeton Plasma Physics Laboratory, Oak Ridge National Laboratory, and General Atomic Co., San Diego, California. The advent of these transmission lines marked the start of a national wideband communications network.

The idea behind a national MFE computer center is to provide large-scale computer capability in addition to local capability at various remote locations according to research priorities and anticipated computational demand. The CDC 7600 central computer, available to the entire MFE community, has 64 000 words of small semiconductor memory, 500 000 words of large-core memory, and disk storage. The national center also has a PDP-11/50 central communications control processor, a PDP-11/50 network control station, and a CDC 6400 file management computer that stores files and maintains indices for information retrieval.

The user service centers have PDP-10 computers systems with direct high-speed access to the national center through PDP-11/40 remote communications control processors. Seven service centers are now operational: one for the MFE program at LLL, one at the MFE computer center, and one each at Princeton, Oak Ridge, LASL, General Atomic, and Science Applications Inc. (SAI), La Jolla, California. The SAI service center, our latest addition, is connected to the 50 000-bit/s transmission line that terminates at General Atomic.

Small computation problems are handled locally at the user service centers. Large-scale problems are routed to the national center and then returned to the service centers for final processing. For offnet users, the ultimate intent is to provide either mini-service centers or remote job entry terminals. Access for these users to the national center is currently via leased telephone lines. Figure 14 shows the present configuration of the MFE computer network.

1976 Update

At the time of our initial article on the computer center in December 1975,[12] user access to the CDC 7600 was via dial-up voice-grade lines, and the 50 000-bit/s lines were in the process of being installed and checked out. Even at this early stage it was evident that the forecasts of MFE demand for large-scale computing were not exaggerated. With the help of the center's programming staff, users quickly converted their codes for operation on the national system, and

Contact John M. Fitzgerald (Ext. 3961) for further information on this article.

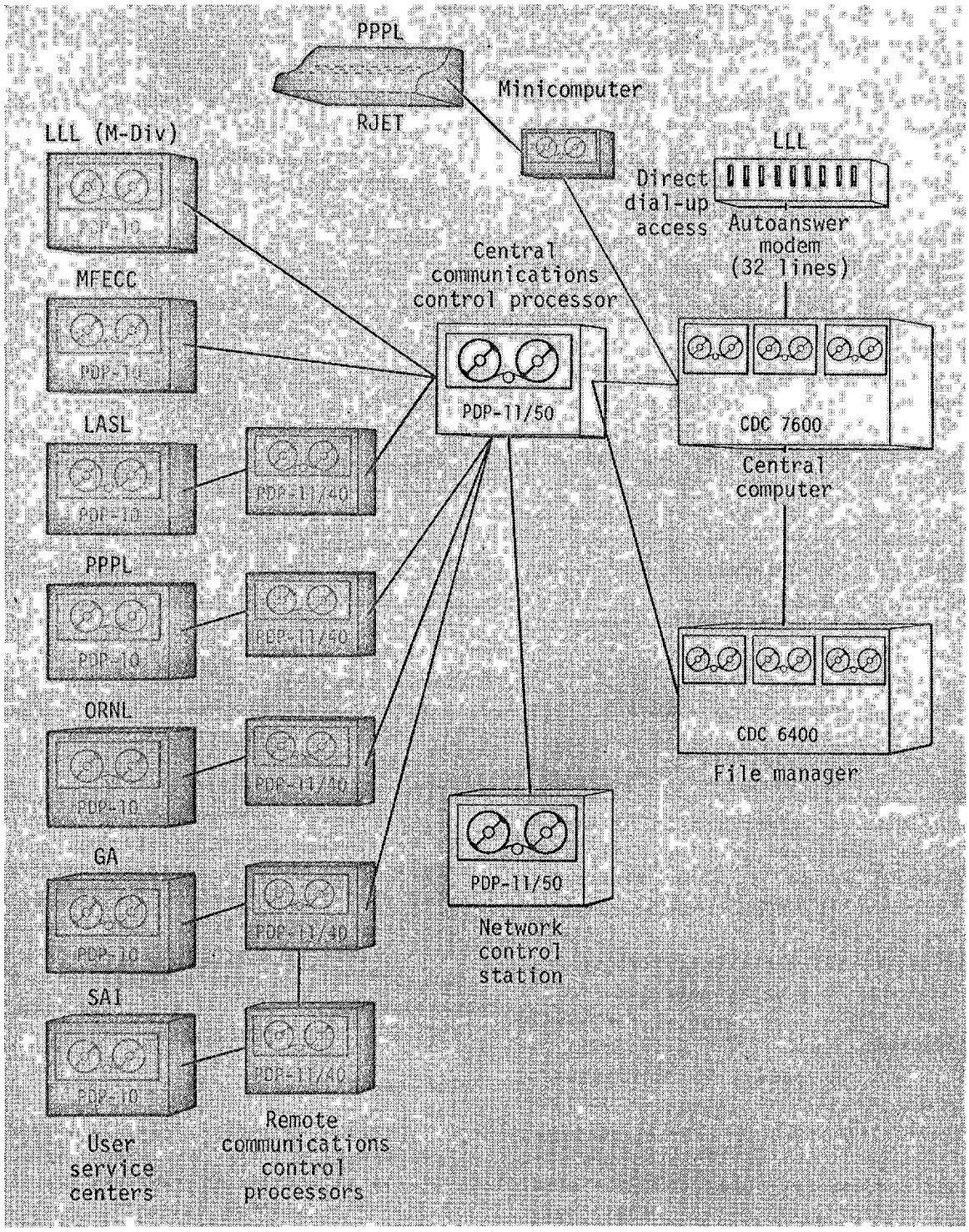

Fig. 14. General arrangement and connections between user service centers and the national MFE computer center (MFECC). The network includes seven user service centers: two at LLL (one for the MFE program and one at the computer center), and one each at Los Alamos Scientific Laboratory (LASL), Princeton Plasma Physics Laboratory (PPPL), Oak Ridge National Laboratory (ORNL), General Atomic (GA), and Science Applications Inc. (SAI). Princeton also has a remote job entry terminal (RJET). A 32-line autoanswer modem (shown at upper right) provides offnet users with voice-grade dial-up access to the central computer facilities. All unshaded equipment is part of the central computing facility at Livermore.

the capacity of the 7600-A machine was saturated early in 1976.

During this past year, we have concentrated on software and hardware refinements of the central computing system at Livermore and on developing improved user access via the data communication network.

Software and Hardware. In February, the capability of the CDC 7600 was enhanced by installing four high-performance CDC 819 disk drives and associated controllers. Software and hardware integration of these units into the system was accomplished to permit their use in early March.

Another need recognized early by the center's staff was a standardized high-speed channel (10 to 40 million bits/s) to be used for interprocessor communication. A large computer center needs to interconnect many varieties of computers of different manufacturers and models. Interconnecting channels are sometimes available between models of the same manufacturer but rarely between competitors' models, such as a CDC 6400 and a DEC PDP-11. At best, one would end up with a large array of interconnecting channels, each unique and incompatible with the others, with special designs required when no channel was available. Standardization would replace this with channels that allow total freedom of choice of interconnected computer pairs and could be structured to minimize custom hardware and software design.

A computer standard interface channel for computer intercommunication has been designed. Interfaces currently nearing completion include those for a CDC 7600, CDC 6400, DEC PDP-10, and DEC PDP-11. The interface channels will connect any of these machines to any other. Additionally, an interface to an HP 2100 minicomputer has been designed to allow connection to the LLL M-Division PDP-10, which will also have the standard channel interface.

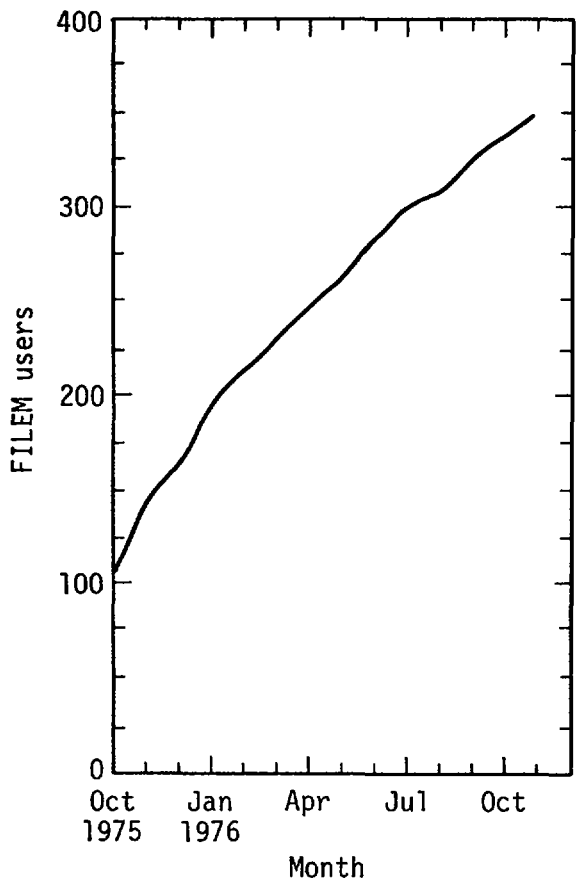

Fig. 15. Growth in user demand for central file storage in FILEM, a versatile file-management system enabling remote users to store and retrieve programs and files at the MFE computer center.

Data Communication Network. The ability to move files (first alpha-numeric, next graphic, and then binary) from the CDC 7600 to our user service centers through the 50 000-bit/s transmission lines was accomplished in March and April. In May we inaugurated input file traffic from the service centers to the 7600, and in July we implemented file traffic between service centers. Interactive terminal traffic over the transmission lines became operational in September. Interactive terminal access for nearly all sites not served by a user service center has remained available via autoanswer modem, which handles 28 dial-up users at 300 bits/s and 4 users at 1200 bits/s.

Development continued this past year on FILEM, a highly versatile file-management system that allows remote users to store and retrieve programs and data files at Livermore for an indefinite time. FILEM was designed to accommodate the special needs of users at remote sites, and the system has enjoyed excellent customer acceptance (Fig. 15). To enhance the FILEM system, we also selected a 500-billion-bit mass storage facility – Control Data model 38500 – which was approved by ERDA in August; estimated delivery of the storage facility is December 1977.

Currently FILEM uses rotating storage (CDC 844 disk packs) for medium-term file storage. When the mass storage facility is online, a file to be stored will be transferred to the facility with a copy also written onto the FILEM disk system for short-term rapid access. The urgent need for such a system has required the computer center to temporarily simulate the mass storage facility by transferring the data onto

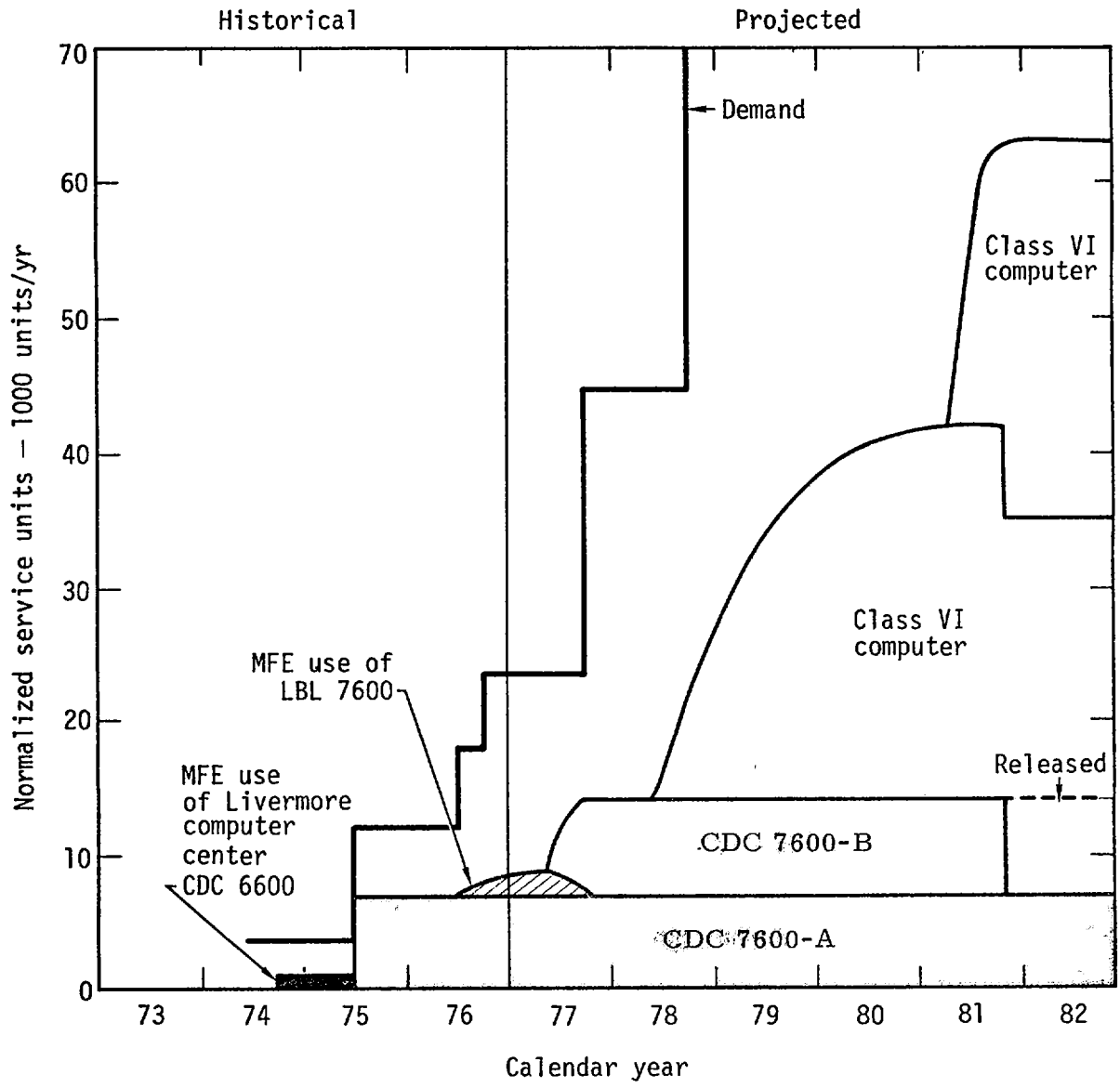

Fig. 16. Projected demand and anticipated hardware needed to keep pace with that demand at the MFE computer center. Projected demand comes from a 1976 survey in which users were asked to estimate their requirements by fiscal years. Immediate plans call for adding another CDC 7600 in 1977. We are also studying the possibility of adding a class VI (next-generation) computer as a third central processing unit in 1978.

conventional magnetic tape. However, these tapes must be manually retrieved, mounted, demounted, indexed, and stored.

A FILEM software effort under way during the past year has been programming the CDC 6400 to assume virtually all of the tasks associated with file custodianship, including indexing, storage, retrieval, and efficient management and allocation of the file storage media

Future Growth

The immediate problem facing the MFE computer center is that the ever-increasing demand for more computing time has oversubscribed the capacity of a single 7600. We need at least one more 7600 and are also planning to add a class VI (next-generation) processor as a third major central processing unit in FY 1978. As an interim stop-gap measure, the center is currently acquiring blocks of computer time from

the 7600 at the Lawrence Berkeley Laboratory for MFE users. Figure 16 shows anticipated future computational demand for the computer center.

A related development this year was establishing the design criteria and selecting an architect-engineering firm for our new $5 million computer facility. Construction is scheduled to begin in October 1977; complete occupancy is slated for December 1978. The 3700-m^2 facility is designed to accommodate three major computing mainframes and offices for about 87 people, including center staff and visitors.

Key Words: fusion research; MFECC; magnetic fusion energy.